209p.

NASA TECHNICAL MEMORANDUM

NASA TM X-53029

April 6, 1964

N64-22464

NASA TMX-53029

Code 1 — Cat. 33

NASA TM X-53029

# DYNAMIC TEST RESULTS OF SAD-6

by GALE R. ERNSBERGER
Aero-Astrodynamics Laboratory
NASA

*George C. Marshall Space Flight Center, Huntsville, Alabama*

OTS PRICE

XEROX $ 14.00 ph

MICROFILM $ 7.00

NASA-GEORGE C. MARSHALL SPACE FLIGHT CENTER

TECHNICAL MEMORANDUM X-53029

# DYNAMIC TEST RESULTS OF SAD-6

By Gale R. Ernsberger

## ABSTRACT

22464

The purpose of these vibration tests is to determine the body bending and torsional dynamic behavior of a full scale prototype of the Saturn SA-6 flight vehicle. A full scale prototype was vertically suspended in the test tower and excited by shakers mounted at the engine gimbal planes. The vehicle's dynamic response at various applied forcing frequencies was recorded by vibration pickups. Since the Saturn is stabilized and controlled by a servo loop, response measurements are needed to properly design the control system filter circuits, thus preventing vehicle dynamic instability. The SAD-6 vehicle was tested for both the boost flight with the S-I booster stage and for the S-IV powered flight with the S-I stage removed. AUTHOR author

NASA-GEORGE C. MARSHALL SPACE FLIGHT CENTER

TECHNICAL MEMORANDUM X-53029

April 6, 1964

# DYNAMIC TEST RESULTS OF SAD-6

By

Gale R. Ernsberger

DYNAMICS AND CONTROL SECTION
FLIGHT EVALUATION BRANCH
FLIGHT EVALUATION AND OPERATIONS STUDIES DIVISION
AERO-ASTRODYNAMICS LABORATORY

TABLE OF CONTENTS


| | | Page |
|---|---|---|
| I. | Introduction | 2 |
| II. | Description | |
| | A. Test Program | 3 |
| | B. Dynamic Test Setup | 4 |
| | C. Recording Instrumentation | 6 |
| | D. Data Reduction Program | 7 |
| III. | Test Results | |
| | A. General | 7 |
| | B. Lateral Vibrations During Boost Phase | 8 |
| | C. Torsional Vibrations During Boost Phase | 11 |
| | D. Longitudinal Vibrations During Boost Phase | 11 |
| | E. Lateral Vibrations During Powered S-IV Phase | 11 |
| | F. Torsional Vibrations During Powered S-IV Phase | 12 |
| IV. | Conclusions and Recommendations | 12 |

## LIST OF ILLUSTRATIONS


| Figure | Title | Page |
|---|---|---|
| 1 | SAD-6 Vehicle Suspended in Test Tower | 31 |
| 2 | Command Module With LES Being Attached | 32 |
| 3 | Command Module With Service Module and Adapter Assembly | 33 |
| 4 | Apollo Payload Being Assembled to S-IV Stage | 34 |
| 5 | Shaker Positioned for S-I Booster Phase Torsional Tests | 35 |
| 6 | Typical Attachment of Strain Bridge Type Accelerometer | 36 |
| 7 | Dynamic Test Tower With Wind Screens Attached | 37 |
| 8 | Typical Spring Cluster Used for Boost Phase Tests | 38 |
| 9 | Typical Spring Cluster Used for S-IV Phase Tests | 39 |
| 10 | Resonant Frequency Profile During Boost (Pitch Excitation) | 40 |
| 11 | Pitch Response at Nose for Hard Suspension (Pitch Excitation) | 41 |
| 12 | Pitch Response at Nose for Medium Suspension (Pitch Excitation) | 42 |
| 13 | Pitch Response at Nose for Soft Suspension (Pitch Excitation) | 43 |
| 14 | Pitch Response at IU for Hard Suspension (Pitch Excitation) | 44 |
| 15 | Pitch Response at IU for Hard Suspension (Pitch Excitation) | 45 |
| 16 | Pitch Response at IU for Soft Suspension (Pitch Excitation) | 46 |
| 17 | Phase Angle at Nose for Hard Suspension (Pitch Excitation) | 47 |
| 18 | Phase Angle at Nose for Medium Suspension (Pitch Excitation) | 48 |
| 19 | Phase Angle at Nose for Soft Suspension (Pitch Excitation) | 49 |

LIST OF ILLUSTRATIONS (Cont'd)


| Figure | Title | Page |
|---|---|---|
| 20 | Phase Angle at IU for Hard Suspension (Pitch Excitation) | 50 |
| 21 | Phase Angle at IU for Medium Suspension (Pitch Excitation) | 51 |
| 22 | Phase Angle at IU for Soft Suspension (Pitch Excitation) | 52 |
| 23 | 1st Outer Tank Mode at Liftoff (Pitch) | 53 |
| 24 | 1st Bending Mode at Liftoff (Pitch) | 54 |
| 25 | 2nd Outer Tank Mode at Liftoff (Pitch) | 55 |
| 26 | 3rd Outer Tank Mode at Liftoff (Pitch) | 56 |
| 27 | 4th Outer Tank Mode at Liftoff (Pitch) | 57 |
| 28 | 2nd Bending Mode at Liftoff (Pitch) | 58 |
| 29 | 5th Outer Tank Mode at Liftoff (Pitch) | 59 |
| 30 | 3rd Bending Mode at Liftoff (Pitch) | 60 |
| 31 | 6th Outer Tank Mode at Liftoff (Pitch) | 61 |
| 32 | 4th Bending Mode at Liftoff (Pitch) | 62 |
| 33 | Coupled Mode at Liftoff (Pitch) | 63 |
| 34 | 7th Outer Tank Mode at Liftoff (Pitch) | 64 |
| 35 | S-I Engine Mode at Liftoff (Pitch) | 65 |
| 36 | 8th Outer Tank Mode at Liftoff (Pitch) | 66 |
| 37 | 5th Bending Mode at Liftoff (Pitch) | 67 |
| 38 | 1st Bending Mode at 10 Sec (Pitch) | 68 |
| 39 | 2nd Outer Tank Mode at 10 Sec (Pitch) | 69 |
| 40 | 3rd Outer Tank Mode at 10 Sec (Pitch) | 70 |
| 41 | 4th Outer Tank Mode at 10 Sec (Pitch) | 71 |
| 42 | 2nd Bending Mode at 10 Sec (Pitch) | 72 |
| 43 | 5th Outer Tank Mode at 10 Sec (Pitch) | 73 |
| 44 | 3rd Bending Mode at 10 Sec (Pitch) | 74 |
| 45 | 6th Outer Tank Mode at 10 Sec (Pitch) | 75 |
| 46 | 4th Bending Mode at 10 Sec (Pitch) | 76 |
| 47 | S-I Engine Mode at 10 Sec (Pitch) | 77 |
| 48 | 7th Outer Tank Mode at 10 Sec (Pitch) | 78 |
| 49 | 8th Outer Tank Mode at 10 Sec (Pitch) | 79 |
| 50 | 5th Bending Mode at 10 Sec (Pitch) | 80 |
| 51 | 9th Outer Tank Mode at 10 Sec (Pitch) | 81 |
| 52 | 1st Bending Mode at 35 Sec (Pitch) | 82 |

LIST OF ILLUSTRATIONS (Cont'd)


| Figure | Title | Page |
|---|---|---|
| 53 | 1st Outer Tank Mode at 35 Sec (Pitch) | 83 |
| 54 | 2nd Outer Tank Mode at 35 Sec (Pitch) | 84 |
| 55 | 3rd Outer Tank Mode at 35 Sec (Pitch) | 85 |
| 56 | 4th Outer Tank Mode at 35 Sec (Pitch) | 86 |
| 57 | 2nd Bending Mode at 35 Sec (Pitch) | 87 |
| 58 | 5th Outer Tank Mode at 35 Sec (Pitch) | 88 |
| 59 | 3rd Bending Mode at 35 Sec (Pitch) | 89 |
| 60 | 6th Outer Tank Mode at 35 Sec (Pitch) | 90 |
| 61 | 4th Bending Mode at 35 Sec (Pitch) | 91 |
| 62 | 7th Outer Tank Mode at 35 Sec (Pitch) | 92 |
| 63 | Coupled Mode at 35 Sec (Pitch) | 93 |
| 64 | 8th Outer Tank Mode at 35 Sec (Pitch) | 94 |
| 65 | 5th Bending Mode at 35 Sec (Pitch) | 95 |
| 66 | 9th Outer Tank Mode at 35 Sec (Pitch) | 96 |
| 67 | 1st Bending Mode at 68 Sec (Pitch) | 97 |
| 68 | 1st Outer Tank Mode at 68 Sec (Pitch) | 98 |
| 69 | 2nd Outer Tank Mode at 68 Sec (Pitch) | 99 |
| 70 | 3rd Outer Tank Mode at 68 Sec (Pitch) | 100 |
| 71 | Tower Mode Coupled With 2nd Bending Mode at 68 Sec (Pitch) | 101 |
| 72 | 2nd Bending Mode at 68 Sec (Pitch) | 102 |
| 73 | 3rd Bending Mode at 68 Sec (Pitch) | 103 |
| 74 | 6th Outer Tank Mode at 68 Sec (Pitch) | 104 |
| 75 | 4th Bending Mode at 68 Sec (Pitch) | 105 |
| 76 | 7th Outer Tank Mode at 68 Sec (Pitch) | 106 |
| 77 | 5th Bending Mode at 68 Sec (Pitch) | 107 |
| 78 | Higher Mode at 68 Sec (Pitch) | 108 |
| 79 | 1st Bending Mode (1.91 cps) and Tower Mode Coupled With 2nd Bending (4.00 cps) at 110 Sec (Pitch) | 109 |
| 80 | 2nd Bending Mode (4.24 cps) and 1st Outer Tank Mode (4.73 cps) at 110 Sec (Pitch) | 110 |
| 81 | 2nd Outer Tank Mode (5.59 cps) and 3rd Outer Tank Mode (6.52 cps at 110 Sec (Pitch) | 111 |
| 82 | 3rd Outer Tank Mode (7.16 cps) and 4th Bending Mode (8.66 cps) at 110 Sec (Pitch) | 112 |

LIST OF ILLUSTRATIONS (Cont'd)


| Figure | Title | Page |
|---|---|---|
| 83 | Higher Mode Coupled With 5th Bending Mode at 110 Sec (Pitch) | 113 |
| 84 | 1st Bending Mode at 147 Sec (Pitch) | 114 |
| 85 | Tower Mode Coupled With 2nd Bending Mode at 147 Sec (Pitch) | 115 |
| 86 | 2nd Bending Mode at 147 Sec (Pitch) | 116 |
| 87 | 6th Outer Tank Mode at 147 Sec (Pitch) | 117 |
| 88 | 1st Outer Tank Mode at 147 Sec (Pitch) | 118 |
| 89 | 2nd and 3rd Outer Tank Modes at 147 Sec (Pitch) | 119 |
| 90 | 5th Bending Mode at 147 Sec (Pitch) | 120 |
| 91 | 1st Outer Tank Mode (1.59 cps) and 1st Bending Mode (1.74 cps)for Liftoff Reruns (Pitch) | 121 |
| 92 | 2nd Outer Tank Mode (2.15 cps) and 3rd Outer Tank Mode (2.39 cps) for Liftoff Reruns (Pitch) | 122 |
| 93 | 4th Outer Tank Mode (3.10 cps) and 2nd Bending Mode (3.31 cps) for Liftoff Reruns (Pitch) | 123 |
| 94 | 3rd Bending Mode (3.83 cps) and 6th Outer Tank Mode (4.31 cps) for Liftoff Reruns (Pitch) | 124 |
| 95 | 4th Bending Mode (5.14 cps) and Coupled Tank Mode (5.81 cps) for Liftoff Reruns (Pitch) | 125 |
| 96 | S-I Engine Mode (7.41 cps) and 7th Outer Tank Mode (9.54 cps) for Liftoff Reruns (Pitch) | 126 |
| 97 | 5th Bending Mode (10.44 cps) and Higher Vehicle Mode (13.81 cps) for Liftoff Reruns (Pitch) | 127 |
| 98 | 1st Bending Mode (1.99 cps) and 2nd Bending Mode (4.21 cps) for 147 Sec Reruns (Pitch) | 128 |
| 99 | 6th Outer Tank Mode (8.12 cps) and 1st Outer Tank Mode (10.39 cps) for 147 Sec Reruns (Pitch) | 129 |

LIST OF ILLUSTRATIONS (Cont'd)


| Figure | Title | Page |
|---|---|---|
| 100 | 2nd Outer Tank Mode (11.43 cps) and 5th Bending Mode (13.29 cps) for 147 Sec Reruns (Pitch) | 130 |
| 101 | Resonant Frequency Profile During Boost (Yaw Excitation) | 131 |
| 102 | Yaw Response at Nose for Soft Suspension (Yaw Excitation) | 132 |
| 103 | Yaw Response at IU for Soft Suspension (Yaw Excitation) | 133 |
| 104 | Phase Angle at Nose for Soft Suspension (Yaw Excitation) | 134 |
| 105 | Phase Angle at IU for Soft Suspension (Yaw Excitation) | 135 |
| 106 | 1st Outer Tank Mode at Liftoff (Yaw) | 136 |
| 107 | 1st Bending Mode at Liftoff (Yaw) | 137 |
| 108 | 2nd Outer Tank Mode at Liftoff (Yaw) | 138 |
| 109 | 3rd Outer Tank Mode at Liftoff (Yaw) | 139 |
| 110 | 4th Outer Tank Mode at Liftoff (Yaw) | 140 |
| 111 | 2nd Bending Mode at Liftoff (Yaw) | 141 |
| 112 | 3rd Bending Mode at Liftoff (Yaw) | 142 |
| 113 | 6th Outer Tank Mode at Liftoff (Yaw) | 143 |
| 114 | 4th Bending Mode at Liftoff (Yaw) | 144 |
| 115 | Cluster Mode Coupled With Torsion at Liftoff (Yaw) | 145 |
| 116 | 7th Outer Tank Mode at Liftoff (Yaw) | 146 |
| 117 | 8th Outer Tank Mode at Liftoff (Yaw) | 147 |
| 118 | 5th Bending Mode at Liftoff (Yaw) | 148 |
| 119 | Higher Cluster Mode at Liftoff (Yaw) | 149 |
| 120 | 1st Bending Mode (2.01 cps) and 1st Outer Tank Mode (2.55 cps) at 68 Sec (Yaw) | 150 |
| 121 | 2nd Outer Tank Mode (2.86 cps) and 3rd Outer Tank Mode (3.80 cps) at 68 Sec (Yaw) | 151 |
| 122 | Tower Mode (4.01 cps) and 2nd Bending Mode (4.12 cps) at 68 Sec (Yaw) | 152 |

LIST OF ILLUSTRATIONS (Cont'd)


| Figure | Title | Page |
|---|---|---|
| 123 | 3rd Bending Mode (4.78 cps) and 6th Outer Tank Mode (5.41 cps) at 68 Sec (Yaw) | 153 |
| 124 | 4th Bending Mode (7.62 cps) and 7th Outer Tank Mode (10.30 cps) at 68 Sec (Yaw) | 154 |
| 125 | 1st Bending Mode at 147 Sec (Yaw) | 155 |
| 126 | Tower Mode at 147 Sec (Yaw) | 156 |
| 127 | 2nd Bending Mode at 147 Sec (Yaw) | 157 |
| 128 | 6th Outer Tank Mode at 147 Sec (Yaw) | 158 |
| 129 | 1st Outer Tank Mode at 147 Sec (Yaw) | 159 |
| 130 | 5th Bending Mode at 147 Sec (Yaw) | 160 |
| 131 | Resonant Frequency Profile During Boost (Torsional and Longitudinal Excitation) | 161 |
| 132 | Torsional Response at Command Module (Sta. 1800) (Torsional Excitation) | 162 |
| 133 | Phase Angle at Command Module (Sta. 1800) (Torsional Excitation) | 163 |
| 134 | 1st Cluster Mode (2.38 cps) and 1st Torsional Mode (3.69 cps) at Liftoff (Torsion) | 164 |
| 135 | 2nd Cluster Mode (5.63 cps) and 3rd Cluster Mode (6.67 cps) at Liftoff (Torsion) | 165 |
| 136 | Tower Coupled With 4th Cluster Mode (10.00 cps) at Liftoff (Torsion) | 166 |
| 137 | Fuel Tank Mode (3.70 cps) and 1st Cluster Mode (3.85 cps) at 68 Sec (Torsion) | 167 |
| 138 | Cluster Mode Coupled With 2nd Bending (4.10 cps) and 1st Torsional Mode (5.15 cps) at 68 Sec (Torsion) | 168 |
| 139 | Fuel Tank Resonance (6.59 cps) and Cluster Resonance (6.92 cps) for 2nd Cluster Mode at 68 Sec (Torsion) | 169 |
| 140 | Center Tank Resonance (7.04 cps) for 2nd Cluster Mode and Tower Coupled With 4th Cluster Mode (12.34 cps) at 68 Sec (Torsion) | 170 |
| 141 | 1st Torsional Mode (5.51 cps) and 1st Cluster Mode (12.34 cps) at 147 Sec (Torsion) | 171 |
| 142 | Rigid Body Mode (1.54 cps) and Cluster Mode (7.52 cps) at Liftoff (Longitudinal) | 172 |

LIST OF ILLUSTRATIONS (Cont'd)


| Figure | Title | Page |
|---|---|---|
| 143 | 1st Longitudinal Mode (10.29 cps) and Cluster Mode (16.53 cps) at Liftoff (Longitudinal) | 173 |
| 144 | Rigid Body Mode (1.75 cps) and 1st Longitudinal Mode (11.59 cps) at 147 Sec (Longitudinal) | 174 |
| 145 | Cluster Modes (15.45 cps and 19.57 cps) at 147 Sec (Longitudinal) | 175 |
| 146 | Response for Pitch Excitation, S-IV Ignition (Phase II) | 176 |
| 147 | Response for Yaw Excitation, S-IV Ignition (Phase II) | 177 |
| 148 | Phase Angle for Pitch Excitation, S-IV Ignition (Phase II) | 178 |
| 149 | Phase Angle for Yaw Excitation, S-IV Ignition (Phase II) | 179 |
| 150 | Pitch and Yaw 1st Bending Modes, S-IV Ignition (Phase II) | 180 |
| 151 | Pitch and Yaw 2nd Bending Modes, S-IV Ignition (Phase II) | 181 |
| 152 | Pitch and Yaw 3rd Bending Modes, S-IV Ignition (Phase II) | 182 |
| 153 | Engine Mode at 26.40 cps, S-IV Ignition (Phase II) | 183 |
| 154 | Response for Pitch Excitation at 20 Sec and 290 Sec (Phase II) | 184 |
| 155 | Phase Angle for Pitch Excitation at 20 Sec and 290 Sec (Phase II) | 185 |
| 156 | 1st Bending Mode at 20 Sec and 290 Sec (Phase II) | 186 |
| 157 | Response for Torsional Excitation, S-IV Ignition (Phase II) | 187 |
| 158 | Torsional Modes at 14.11 cps and 15.01 cps, S-IV Ignition (Phase II) | 188 |
| 159 | Torsional Modes at 20.40 cps and 26.25 cps, S-IV Ignition (Phase II) | 189 |
| 160 | Torsional Mode at 28.94 cps, S-IV Ignition (Phase II) | 190 |

## LIST OF TABLES


| Number | | Page |
|---|---|---|
| I | Comparision of SA-6 and SAD-6 Mass Characteristics | 13 |
| II | Summary of Boost Phase Resonant Frequencies and Damping Coefficients for Lateral Tests | 14 |
| III | Summary of Boost Phase Lateral Response Characteristics - Liftoff Pitch | 16 |
| IV | Summary of Boost Phase Lateral Response Characteristics - 10 Sec Pitch | 18 |
| V | Summary of Boost Phase Lateral Response Characteristics - 35 Sec Pitch | 19 |
| VI | Summary of Boost Phase Lateral Response Characteristics - 68 Sec Pitch | 20 |
| VII | Summary of Boost Phase Lateral Response Characteristics - 110 Sec Pitch | 21 |
| VIII | Summary of Boost Phase Lateral Response Characteristics - 147 Sec Pitch | 22 |
| IX | Summary of Boost Phase Lateral Response Characteristics - Liftoff Yaw | 23 |
| X | Summary of Boost Phase Lateral Response Characteristics - 68 Sec Yaw | 25 |
| XI | Summary of Boost Phase Lateral Response Characteristics - 147 Sec Yaw | 26 |
| XII | Summary of Torsional and Longitudinal Resonant Frequencies and Damping Coefficients | 27 |

LIST OF TABLES (Cont'd)


| Number | | Page |
|---|---|---|
| XIII | Summary of Boost Phase Response Characteristics for Torsional Tests | 28 |
| XIV | Summary of S-IV Phase Resonant Frequencies and Damping Coefficients | 29 |
| XV | Summary of S-IV Phase Response Characteristics for Lateral Tests | 30 |

## LIST OF SYMBOLS

| | |
|---|---|
| $A_a$ | Bias shift of measuring instruments, units are g's for accelerometers and lbf for shakers |
| $A_o$ | Harmonic amplitude of measuring instruments, units are g's for accelerometers and lbf for shakers |
| $f$ | Frequency, cps |
| $F_s$ | Harmonic forcing function, Newtons |
| $F$ | Amplitude of the shaker force, Newtons |
| $I'_\varphi$ | Generalized torsional inertia computed by a complex curve fit, kg-m$^2$ |
| $K_T$ | Suspension system longitudinal stiffness, N/m |
| $K_\theta$ | Suspension system rotational stiffness, N-m/rad |
| $K_\phi$ | Suspension system torsional (roll) stiffness, N-m/rad |
| $M_B$ | Generalized lateral bending mass, kg |
| $M'_B$ | Generalized lateral bending mass computed by a complex curve fit, kg |
| $t$ | Time, sec |
| $X_{2278}$ | Lateral displacement at Station 2278 (extrapolated), cm |
| $Y_E$ | Gimbal station displacement normalized by nose displacement (Station 2278), cm/cm |
| $\alpha_T$ | Total phase angle (measured) at any $\omega$, rad |
| $\zeta$ | Viscous damping coefficient |
| $\frac{\eta}{F_s}$ | Total amplitude response (measured) divided by shaker force at any $\omega$, cm/N |

LIST OF SYMBOLS (Cont'd)

| | |
|---|---|
| $\theta$ | Accelerometer phase angle with respect to the exciting shaker, rad |
| $\phi_{1800}$ | Torsional displacement at Station 1800 (measured), deg |
| $\phi_E$ | Torsional displacement at gimbal station normalized by displacement at Station 1800, deg/deg |
| $\omega$ | Frequency, rad/sec |
| $\omega_B$ | Resonant frequency, rad/sec |

## ACKNOWLEDGEMENT

The SAD-6 dynamic tests were performed as a joint effort by the various MSFC Laboratories under the technical supervision of the Control Dynamics and Structural Feedback Working Group. The following MSFC organizations are especially acknowledged for their contributions in making this report possible.

Aero-Astrodynamics Laboratory

Dynamics and Flight Mechanics Division, Dynamic Analysis Branch, for theoretical resonant frequencies and mode shapes.

Flight Evaluation and Operational Studies Division, Flight Evaluation Branch for data analysis and documentation of the dynamic test results.

Astrionics Laboratory

Flight Dynamics Branch for recording and analyzing the rate gyro measurements.

Computation Laboratory

Research and Development Division, Data Reduction Branch for reducing the accelerometer test data.

Research and Development Division, Digital Projects Branch for generalized mass and torsional mode calculations.

Propulsion and Vehicle Engineering Laboratory

Structures Division, Experimental Structures Branch for conducting the dynamic tests and recording the accelerometer data.

Test Laboratory

Components Test Division, Fluid Mechanics and Environmental Branch for installing the dynamic vehicle in the test tower, providing facilities support, and loading the vehicle with simulated propellants.

ACKNOWLEDGEMENT (Cont'd)

The illustrations in this report were prepared with the assistance of Mr. J. Moore, Brown Engineering Company, Mr. J. Campbell and Mr. W. McFadden, NASA Co-op students, and Northrop personnel acting under Mission Support Services Contract NAS8-11111.

NASA-GEORGE C. MARSHALL SPACE FLIGHT CENTER

TECHNICAL MEMORANDUM X-53029

# DYNAMIC TEST RESULTS OF SAD-6

By Gale R. Ernsberger

## SUMMARY

SAD-6, which is a full scale dynamic model of SA-6, was dynamically tested while vertically suspended in the MSFC test tower. The elastic response characteristics of the model were excited with electrodynamic shakers applied at the engine gimbal plane. The resulting vehicle mode shapes were recorded by a network of accelerometers and rate gyros mounted throughout the vehicle. These dynamic tests determined the vehicle's frequency response, resonant frequencies, damping coefficients, and generalized masses for various propellant fill conditions. This information is used to design the electrical filters for the control system.

During the boost phase tests, pitch and yaw resonant frequencies from 1.6 to 13.9 cps were obtained at liftoff and 1.9 to 13.2 cps at cutoff. Torsional resonant frequencies of 2.4 to 10.0 cps and 5.5 to 12.3 cps were determined for the liftoff and cutoff conditions, respectively. Damping coefficients for the pitch modes varied from 0.6% to 1.4% of critical for the first two bending modes and from 0.6% to 1.0% of critical for the third bending mode. The first torsional mode has a damping rate of 1.2% to 4.2% of critical for various flight times during boost.

At S-IV ignition, pitch and yaw bending frequencies of 3.6 to 27.0 cps were obtained. When the launch escape tower (LES) was removed to simulate a flight time of S-IV ignition plus 20 seconds, the first bending frequency increased to 9.0 cps. At S-IV ignition

plus 290 seconds, the resonant frequencies varied from 10.1 to 28.8 cps. Torsional frequencies of 14.1 to 28.9 cps were determined at S-IV ignition. First bending mode damping coefficients for the S-IV phase varied from 0.7% to 5.6% of critical.

Values of generalized mass were computed at each resonant frequency from mode shape and mass distribution. These values of generalized mass compared well with values computed using a complex curve fit for the amplitude and phase angle response curve.

## I. INTRODUCTION

The SAD-6 Dynamic Test Vehicle (Figure 1) is a full scale prototype of Saturn SA-6, the second Block II flight vehicle. The dynamic test vehicle consists of the S-I Booster Stage, S-IV Stage, Instrument Unit, and Apollo Boilerplate Payload (Figures 2, 3, and 4).

The S-I Booster Stage consists of eight 70-inch diameter propellant tanks clustered about a center 105-inch diameter propellant tank. This tank cluster is attached at the forward end to a spider beam and at the aft end to a thrust structure. The thrust structure is composed of a cylindrical center with eight shear outriggers attached radially. Four stub fins and four large fins are alternately attached to the outriggers. Eight H-1 engines are mounted at the aft end of the thrust structure. The S-IV stage is basically a 220-inch diameter cylindrical container with hemispherical bulkheads. A common bulkhead divides the container into fuel and oxidizer compartments. Six RL10-A3 rocket engines are attached to a thrust structure on the aft hemispherical bulkhead. A cylindrical aft interstage attaches to the S-I stage and a forward interstage (truncated cone) attaches to the instrument unit.

The instrument unit consists of four 40-inch diameter tubes extending radially from a 70-inch diameter center tube to a 154-inch diameter exterior skin assembly. The hardware installation includes guidance and control, telemetry, tracking, electrical power sources, and distributors.

The Apollo Boilerplate Payload consists of a boilerplate command module, service module, adapter, and Launch Escape System (LES).

The SAD-6 vehicle was suspended vertically in the Dynamic Test Stand (Figure 1) by a spring-cable arrangement and excited by electrodynamic shakers positioned near the engine gimbal plane (Figure 5). The vehicle's dynamic response was measured by accelerometers (Figure 6) and rate gyros.

The propellant mass distributions for the boost flight conditions (see Table I for comparison of SA-6 and SAD-6 mass characteristics) were simulated by filling the booster tanks with deionized water on an equal weight basis. The propellant mass in the S-IV stage was simulated using deionized water in the LOX tank and styrofoam balls in the hydrogen tank. Mass distribution corresponding to S-IV flight times was varied by draining deionized water from the LOX tank. To compensate for the limited volume of the LOX tank, inner tubes filled with water were placed in the hydrogen tank on top of the LOX tank dome.

## II. DESCRIPTION

### A. Test Program

The dynamic response characteristics of the SAD-6 vehicle were obtained by inducing elastic vibrations in bending (pitch and yaw) and torsion as well as in the longitudinal direction. In the boost phase tests, the vehicle's response characteristics were investigated as follows:

| Test (S-I Phase) | Flight Time Simulated (Sec) |
|---|---|
| Pitch | Liftoff, 10, 35, 68, 110, 147 |
| Yaw | Liftoff, 68, 147 |
| Torsion | Liftoff, 68, 147 |
| Longitudinal | Liftoff, 147 |

Suspension effects were evaluated by use of two suspensions of different rotational stiffness for liftoff, 10, 35, 68 and 147 sec in the pitch shaker tests and for liftoff only in the yaw shaker tests.

All other tests utilized only one suspension. In the powered S-IV stage tests, vehicle response was evaluated as follows.

| Test (S-IV Phase) | Time from S-IV Ignition (Sec) |
|---|---|
| Pitch | Ignition, 20, 290 |
| Yaw | Ignition |
| Torsion | Ignition |

The Launch Escape System was removed from the vehicle for the 20 and 290 sec tests since it is jettisoned in flight after the main-stage (S-IV) motors are ignited. Since the rocking frequency was low, only one suspension was used in each series of tests.

A systematic test procedure was established by the test engineers for efficient test time. Resonant modes were detected by tuning the shaker frequency to maximize the gain of selected accelerometers (usually accelerometer # 20 at Station 2270) monitored on the control panel. Several files of steady state data were recorded at each resonant peak. Ringout damping was obtained by recording approximately 5 cycles of steady state data with the driving shaker at the resonant frequency, and then cutting the shaker off and recording approximately 10 additional cycles of damped free vibrations.

With the resonant frequency established, the vehicle's response characteristics were obtained by recording at incremental frequencies from 1.3 to 5.0 cps ($\Delta f$ = 0.05 cps) and from 5.0 to 10.0 cps ($\Delta f$ = 0.10 cps) with a nominal shaker force of 2224 N (500 lbf). Narrow bandwidth sweeps of approximately ten increments of $\Delta f$ = 0.01 cps for peaks below 10 cps and $\Delta f$ = 0.02 cps for peaks above 10 cps were also recorded about the resonant frequencies. During the S-IV phase tests, sweeps within a bandwidth of 0.6 to 2.5 cps were recorded around resonant peaks only.

B. Dynamic Test Setup

During the boost phase tests, the SAD-6 vehicle was suspended vertically in the dynamic test stand (Figure 7) by cables attached to its outriggers. These cables, approximately 60 feet in length including the spring clusters located at their upper ends, extended upward and radially outward from the vehicle at an angle of one-half degree. The spring clusters (Figure 8) are attached to hydraulic lifters mounted

on the test tower. These lifters were used to raise the vehicle from the ground supports to the suspended position.

These suspension cables produced a restraining moment at the aft end of the vehicle. To determine the effect of this restraint on natural frequencies, damping rates, etc., two suspensions were tested for each pitch condition (except 110 sec) and for liftoff yaw. The effective suspension stiffness was varied by changing the number of coils in the cluster (maximum of 12 springs) and by reducing the number of suspension cables employed. Suspension system stiffness based on experimental data (rocking frequencies) is presented in Table II. A detailed description of the various suspensions employed and their theoretical stiffnesses can be found in Reference 1.

The bending modes (pitch and yaw) in the S-I booster phase tests were excited by either a 2224 N (500 lbf) or a 6672 N (1500 lbf) electrodynamic shaker positioned perpendicular to the vehicle centerline at Station 118 on Fin I (Fin IV for yaw). The torsional modes were excited by a pair of 2224 N shakers positioned at Sta. 83 on the Stub Fins adjacent to S-I engines 2 and 4 at a radius of 4.394 meters (173 inches) from the vehicle centerline. In the longitudinal tests, two 2224 N shakers were positioned at the aft end (Station 71) of the same two Stub Fins.

In the S-IV powered flight phase tests, the vehicle was supported through an adapter ring located at the separation joint (Station 1146) by eight suspension cables. Each of these cables was attached at its upper end to a spring cluster (Figure 9) containing five coil springs. Suspension stiffness could be varied by removing coils from the clusters.

The S-IV vehicle's elastic modes were excited by a 2224 N shaker positioned perpendicular to the vehicle centerline at Station 1071 on the aft thrust structure for the pitch and yaw tests. The location corresponded to Fin I for the pitch tests and Fin IV for the yaw tests. The torsional elastic modes were excited by a pair of 2224 N shakers located at a position corresponding to Fins I and III at a radius of 2.286 meters (90 inches) in the aft thrust structure (Station 1069).

## C. Recording Instrumentation

The vehicle's response was measured by a series of strain bridge accelerometers mounted on the vehicle's outer surface (Figure 6). These accelerometers were oriented with their sensitive axis in either the pitch or yaw plane at 22 longitudinal locations along the center tank and upper stages. Pitch and yaw measurements were recorded for LOX tanks 1 and 2 and fuel tanks 1 and 2 at Stations 258, 497, 696, and 894; LOX tanks 3 and 4 and fuel tank 3 at Stations 497 and 696; and fuel tank 4 at Station 497.

Pitch and yaw instrumentation was also provided for S-I engine 4 and S-IV engine 4. Fins II and IV and one suspension cable was also instrumented to make a total of 78 accelerometer measurements.

The strain bridge accelerometers were viscous-damped (oil) with a natural frequency of 120 cps. At room temperature, these accelerometers recorded vibrations up to 12 cps with an amplification factor of 1.0 (flat response). The calibration varied with ambient temperature due to changes in the viscosity of the damping medium (oil). At a vibration level of 12 cps the amplification factor was 0.975 at 25°F and 0.95 at 0°F. Temperature caused a shift in angular phase angle which at 12 cps recording varied from 8 degrees at room temperature to 15 degrees at 25°F and to 20 degrees at 0°F.

The output signal from each accelerometer is recorded on magnetic tape by the SEL Data System. This system consists of two 48-channel low level multiplexers, an analog-to-digital converter, a digital-to-analog converter, a control unit, and an ampex TM4M tape recorder with a standard ampex 7-channel recording head for one-half inch width tape. An amplifier gain adjustment has been provided to supply 10.24 volts output for any full scale input in the range from 5 to 100 millivolts. Items recorded included accelerometer output voltage (amplified), shaker armature current, accelerometer supply voltage, shaker load cell output voltage, amplifier reference voltage, shaker excitation period, and reference file number. The amplifier reference voltage was recorded to provide a continuous calibration of system gain for the individual amplifiers. Each recorded item was digitized and commutatively recorded at a fixed rate of 306.3 samples per second.

Other measurements included a total of 16 rate gyros and 12 accelerometers which were recorded by Astrionics Laboratory on a separate data recording system.

### D. Data Reduction

The SEL Data System output data tape was reduced on the IBM 7094 computer using a modified Fourier analysis technique. The amplitude, bias, and phase angle for the individual shaker and accelerometer output recordings were determined by representing them as a harmonic function of the form:

$$\text{Function} = A_o \sin(2\pi ft + \theta) + A_a$$

where

$A_o$ = harmonic amplitude, units are g's for accelerometers and lbs for shakers

$A_a$ = bias shift, units are g's for accelerometers and lbs for shakers

$\theta$ = phase angle, radians

$f$ = frequency, cps

$t$ = time, seconds.

A detailed discussion of the program's features and output modes can be found in Reference 1.

## III. TEST RESULTS

### A. General

For each test run, the recorded data were reduced to shaker force amplitudes, accelerometer amplitudes and phase angles referenced to the shaker. Response curves were compiled for individual accelerometers by making plots of displacement/shaker force versus frequency. Similar curves were compiled for these accelerometers showing phase angle with respect to the shaker versus frequency. Resonant modes were determined by computing the energy content of the vehicle from the mass distribution and

accelerometer measurements. The ratio of energy computed using instantaneous accelerometer measurements ($90^{\circ}$ phase lag from shaker) to values using peak measurements indicates resonance when this ratio is equal to one. As this method involves the ratio of the squares of displacements, the resonant modes were readily identified. Mode shapes were obtained by plotting the peak acceleration (g's) at each accelerometer location.

Damping coefficients (Table II) were computed in terms of percent of critical damping based on a viscous damping approximation. Tabulated values represent an average of individual values found by three methods - ringout, frequency bandwidth, and phase angle - discussed in Reference 1. Ringout damping values were computed using at least eight accelerometer locations, while the bandwidth and phase angle methods were applied to the response curves of the nose and instrument unit accelerometers.

Generalized mass data (Reference 1) were computed using 117 equally spaced collocation points on the center tank and upper stages and 38 equally spaced collocation points on each of the eight outer tanks. Mode shape displacements and slopes were obtained by a linear interpolation between successive accelerometer locations.

B. Lateral Vibrations

A boost phase flight profile of resonant frequencies for pitch excitation is presented in Figure 10. Generally, changes in cable suspension had little effect on resonant frequencies. Bending modes were somewhat lower for SAD-6 than SAD-5 due to the LES and longer overall length of 2278 inches compared to 1967 inches for SAD-5.

Pitch response and corresponding phase angles for various flight times at Station 2270 and Station 1500 are shown in Figures 11 thru 22 for the hard, medium and soft suspensions. Generally the pitch resonant frequencies were 0.2% to 0.4% higher for the stiffer suspension used for the different flight conditions. Frequencies and damping coefficients determined for the principal pitch bending and cluster modes are listed in Table I.

Mode shapes are plotted in Figures 23 thru 100 for the resonant frequencies detected during pitch excitation. Slopes computed from

rate gyro measurements were also plotted on the figures to provide a comparison with the accelerometer data. A boost flight profile of yaw resonant frequencies is shown in Figure 101. Yaw responses and phase angles are shown in Figures 102 thru 105. Yaw resonant frequencies were 3 to 5% higher for the first and second bending modes than those recorded in the pitch plane. A comparison of the pitch and yaw resonant frequencies and measured damping coefficients is found in Table II. Yaw resonant mode shapes are plotted in Figures 106 thru 130.

Evaluation of test data obtained from the 68, 110, and 147 second tests indicated the presence of a strong second harmonic (4 cps) frequency when the shaker frequency was approximately 2 cps. This was caused by a loose bolt which secures the command module. This was corrected and reruns made for the liftoff pitch and 147 sec pitch and yaw conditions (Reference 3).

Results of the rerun tests indicated a 1% variation in resonant frequency and a 20% variation in system gain (accelerometer amplitude divided by shaker force). Frequencies and damping coefficients are presented in Table II for comparison purposes. No 4 cps resonant mode was found corresponding to the coupled tower mode at 68 sec thru 147 sec. Generalized mass, damping coefficients, and other response data for the lateral tests are found in Tables III thru XI.

The generalized mass was obtained (1) by integrating the product of mass distribution times the square of the normalized displacement and (2) by a complex curve-fit of the frequency response and phase angles. These generalized mass terms are indicated as $M_B$ and $M_B'$.

The complex curve-fit technique of determining generalized mass can be described briefly as follows. The component of each bending mode $\left(\frac{\eta}{F_s}\right)_i$ at any frequency $\omega$ can be evaluated in terms of its resonant frequency, $\omega_{B_i}$, damping coefficient, $\zeta_i$, and generalized mass $M_{B_i}'$ as

$$\left(\frac{\eta}{F_s}\right)_i = \frac{\dfrac{Y_E}{M_{B_i}' \, \omega_{B_i}^2}}{\sqrt{\left(1 - \dfrac{\omega^2}{\omega_{B_i}^2}\right)^2 + 4\zeta_i^2 \dfrac{\omega^2}{\omega_{B_i}^2}}} \tag{1}$$

and the associated phase angle is

$$\alpha_i = \tan^{-1}\left[\frac{2\zeta_i \dfrac{\omega}{\omega_{B_i}}}{1 - \left(\dfrac{\omega}{\omega_{B_i}}\right)^2}\right]. \tag{2}$$

The total response $\left(\frac{\eta}{F_s}\right)_T$ at any frequency is, therefore, a sum of components from all the resonant modes. Considering the first N resonant modes, then

$$\left(\frac{\eta}{F_s}\right) = \left\{\left[\sum_{i=1}^{N} \left(\frac{\eta}{F_s}\right)_i \sin \alpha_i\right]^2 + \left[\sum_{i=1}^{N} \left(\frac{\eta}{F_s}\right)_i \cos \alpha_i\right]^2\right\}^{\frac{1}{2}}. \tag{3}$$

The phase angle is

$$\alpha_T = \tan^{-1}\left[\frac{\sum_{i=1}^{N} \left(\frac{\eta}{F_s}\right)_i \sin \alpha_i}{\sum_{i=1}^{N} \left(\frac{\eta}{F_s}\right)_i \cos \alpha_i}\right]. \tag{4}$$

The system of equations (1) through (3) can now be solved in terms of $M_B'$ using the values of $\frac{\eta}{F_s}_T$, $\alpha_T$, $\zeta$ and $\omega_B$ obtained from test data. Resulting curve-fit values of $M_B'$ are compared

with values of $M_B$ obtained from the pitch mode shapes in Table III thru VII. This same procedure was used to obtain the generalized inertia $I'_\varphi$ from torsional test data (Table XIII).

C. Torsional Vibrations During Boost Phase

A flight profile of torsional and longitudinal resonant frequencies determined during the boost phase tests is presented in Figure 131. Torsional response and phase angle curves for Station 1800 are found in Figures 132 and 133 for the liftoff, 68, and 147 second flight time tests.

The 147 sec response curves indicate a higher response than expected from the suspension in the region of 1.3 to 5.0 cycles. A large percentage of this response may be due to sloshing in the tanks, as the slosh frequency at 147 sec is approximately 0.7 cps. Torsional resonant frequencies and damping rates are listed in Table XII. Response characteristics including generalized mass are included in Table XIII.

D. Longitudinal Vibrations During Boost Phase

Longitudinal mode shapes for the liftoff and 147 sec flight conditions are plotted in Figures 142 thru 145. Since no frequency sweeps were made, no response data was available for plotting purposes. The bouncing or rigid body frequencies occurred at 1.54 cps and 1.75 cps for liftoff and 147 sec, respectively. The first longitudinal modes (10.29 cps at liftoff and 11.59 cps at 147 sec) were very pronounced but insufficient instrumentation made identification of other modes difficult. Resonant frequencies are plotted in Figure 131 along with the torsional resonant frequencies.

E. Lateral Vibrations During Powered S-IV Phase

Resonant frequencies and damping coefficients for the lateral tests are summarized in Table XV for S-IV ignition and S-IV ignition plus 20 sec and plus 290 sec. Response and phase angle curves are contained in Figures 146 thru 149 for the S-IV ignition condition; corresponding pitch and yaw resonant modes are compared in Figures 150 thru 153. Response and phase angle curves for the S-IV ignition plus 20 sec and plus 290 sec conditions are found in Figures 154 and 155; corresponding first bending modes are compared in Figure 156.

## F. Torsional Vibrations During Powered S-IV Phase

Resonant frequencies and damping coefficients are summarized for the S-IV Ignition Conditional Torsional Tests in Table XIV. Response data was insufficient for tabulation, but most of the essential items can be found in the mode shape plots (Figures 158 thru 160). Response at Station 2259 is plotted in Figure 157.

# IV. CONCLUSIONS AND RECOMMENDATIONS

The SAD-6 exhibited five bending modes, one S-I engine mode, and nine cluster or outer tank modes below 13 cps during the boost phase lateral tests. The frequency sweep procedure utilized in the boost phase tests proved very beneficial in that weak modes not apparent in early flight times (liftoff thru 35 sec) were recorded.

Addition of the Launch Escape System (LES) and Apollo Payload lowered the first bending mode from 2.30 cps (SAD-5) to 1.73 cps (SAD-6) for the hard (8-12) suspension at liftoff. A corresponding reduction in second bending mode frequency of 4.80 cps (SAD-5) to 3.23 cps (SAD-6) was also noted for the hard suspension. Outer tank modes detected in SAD-5 tests remained essentially the same for SAD-6 with one additional outer tank mode being detected at 1.60 cps at liftoff. As expected, SAD-6 torsional modes did not vary appreciably from the previous SAD-5 tests. The first torsional mode detected had a frequency of 3.78 cps for SAD-5 and 3.69 cps for SAD-6.

The LES produced a large shift in resonant frequencies in the S-IV powered flight phase. The first bending frequency decreased from 9.98 cps (SAD-5) to 3.56 cps (SAD-6). Removal of the LES at S-IV ignition plus 20 seconds raised the first bending mode to 8.96 cps.

Damping coefficients obtained from SAD-6 tests averaged 17% lower for the 1st bending mode and 52% lower for the 2nd bending mode than those obtained for the SAD-5 tests. This difference is attributed to the change in configuration (LES and command module). Resonant frequencies detected for SAD-6 averaged 0.3% and 0.4% higher with the stiffer suspension for the 1st and 2nd bending modes, respectively. This compares with a corresponding 0.4% to 0.2% frequency increase for SAD-5.

TABLE I COMPARISON OF SA-6 AND SAD-6 MASS CHARACTERISTICS

| Component Description | SAD-6 Measured* | | | SA-6 Documented** | | | % Error | |
|---|---|---|---|---|---|---|---|---|
| | Mass (kg) | Mass (lbm) | C. G. (in) | Mass (kg) | Mass (lbm) | C. G. (in) | Mass (%) | C. G. (%) |
| S-I Booster (Dry) | 48,575 | 107,090 | 376.9 | 48,421 | 106,750 | 375.1 | 0.32 | 0.48 |
| S-I Propellant Ballast (Liftoff) | 398,484 | 878,507 | 553.0 | 397,269 | 875,828 | 549.4 | 0.31 | 0.66 |
| S-I/S-IV Interstage | 899 | 1,981 | 1056.9 | 1,081 | 2,383 | 1056.1 | 16.84 | 0.08 |
| S-IV Stage (Dry) | 6,276 | 13,836 | 1192.0 | 6,396 | 14,100 | 1195.6 | 1.88 | 0.30 |
| S-IV Propellant Ballast (Liftoff) | 45,652 | 100,645 | 1164.3 | 46,246 | 101,954 | 1165.6 | 1.28 | 0.11 |
| I. U. | 2,350 | 5,180 | 1482.0 | 2,778 | 6,125 | 1480.1 | 15.41 | 0.13 |
| Adapter and Insert | 1,466 | 3,231 | 1587.6 | 1,745 | 3,846 | 1578.9 | 15.99 | 1.20 |
| Service Module | 2,381 | 5,250 | 1725.3 | 2,490 | 5,489 | 1734.1 | 4.38 | 0.51 |
| Command Module | 3,971 | 8,755 | 1838.0 | 3,477 | 7,666 | 1836.2 | 14.21 | 0.10 |
| LES | 2,899 | 6,390 | 2095.0 | 3,004 | 6,623 | 2090.4 | 3.50 | 0.22 |
| Vehicle at Liftoff | 512,938 | 1,130,835 | 630.7 | 512,906 | 1,130,764 | 629.7 | 0.00 | 0.16 |
| Vehicle at 10 Sec | 479,516 | 1,057,151 | 618.6 | 486,067 | 1,071,596 | 618.1 | 1.35 | 0.08 |
| Vehicle at 35 Sec | 404,925 | 892,706 | 594.8 | 418,336 | 922,273 | 595.0 | 3.21 | 0.03 |
| Vehicle at 68 Sec | 324,796 | 716,052 | 581.3 | 328,677 | 724,610 | 582.1 | 1.18 | 0.14 |
| Vehicle at 110 Sec | 210,310 | 463,653 | 634.1 | 215,124 | 474,268 | 635.8 | 2.24 | 0.27 |
| Vehicle at 147 Sec | 122,603 | 270,294 | 855.7 | 124,948 | 275,464 | 859.9 | 1.88 | 0.49 |
| S-IV Stage at S-IV Ignition | 66,306 | 146,180 | 1291.2 | 65,894 | 145,271 | 1291.5 | 0.63 | 0.02 |
| S-IV Stage at S-IV Ignition + 20 Sec | 62,006 | 136,700 | ------ | 60,958 | 134,389 | 1254.5 | 1.72 | ---- |
| S-IV Stage at S-IV Ignition + 290 Sec | 36,673 | 80,850 | ------ | 35,513 | 78,292 | 1305.6 | 3.27 | ---- |

*Data obtained from R-P&VE-SE

** Memo No. R-P&VE-VAW-64-29, dated March 11, 1964

TABLE II SUMMARY OF BOOST PHASE RESONANT FREQUENCIES AND DAMPING COEFFICIENTS FOR LATERAL TESTS

| Condition | | LIFTOFF | | | | | 10 SEC | | 35 SEC | | 68 SEC | | | 110 SEC | 147 SEC | | | | |
|---|---|---|---|---|---|---|---|---|---|---|---|---|---|---|---|---|---|---|---|
| | | Pitch | | | Yaw | | Pitch | | Pitch | | Pitch | | Yaw | | Pitch | | | Yaw | |
| Suspension / Mode | | (8-12) | (8-8) | (8-8) (Rerun) | (8-12) | (8-8) | (8-12) | (8-8) | (8-12) | (8-6) | (8-12) | (8-6) | (8-6) | (8-4) | (4E-12) | (4E-4) | (4E-4) (Rerun) | (4E-4) | (4E-4) (Rerun) |
| 1st Outer Tank | f(cps) | 1.60 | 1.60 | 1.59 | - | 1.60 | - | - | 2.00 | 1.95 | 2.54 | 2.54 | 2.55 | 4.73 | 10.23 | 10.26 | 10.39 | 10.40 | 10.36 |
| | ζ | - | - | 1.0% | - | - | - | - | - | - | 0.6% | 0.6% | - | 1.7% | - | 2.0% | - | - | 1.7% |
| 1st Bending | f(cps) | 1.73 | 1.70 | 1.74 | 1.75 | 1.75 | 1.73 | 1.73 | 1.82 | 1.81 | 1.90 | 1.89 | 2.01 | 1.91 | 1.93 | 1.95 | 1.99 | 2.04 | 2.05 |
| | ζ | 1.2% | 1.0% | 1.1% | 0.9% | 1.1% | 1.4% | 1.3% | 1.2% | 1.2% | 1.2% | 1.0% | 1.0% | 1.1% | 1.1% | 2.7% | 0.9% | 0.9% | 0.7% |
| 2nd Outer Tank | f(cps) | - | 2.20 | 2.15 | - | 2.20 | 2.20 | 2.20 | 2.30 | 2.25 | 2.86 | 2.86 | 2.86 | 5.59 | - | 11.38 | 11.43 | - | - |
| | ζ | - | - | - | - | - | - | - | - | - | 3.0% | 1.9% | - | 1.1% | - | - | - | - | - |
| 3rd Outer Tank | f(cps) | 2.45 | 2.45 | 2.39 | 2.40 | 2.40 | 2.52 | 2.52 | 2.90 | 2.90 | 3.70 | 3.75 | 3.80 | 7.16 | 11.79 | - | - | - | - |
| | ζ | - | - | 1.3% | 1.3% | 1.3% | 1.5% | 1.0% | 1.0% | 1.2% | - | - | - | 1.4% | - | - | - | - | - |
| 4th Outer Tank | f(cps) | 3.10 | 3.10 | 3.10 | 3.24 | 3.25 | 3.10 | 3.10 | 3.15 | 3.20 | - | - | - | - | - | - | - | - | - |
| | ζ | - | - | - | - | - | - | - | - | - | - | - | - | - | - | - | - | - | - |
| Coupled Tower | f(cps) | - | - | - | - | - | - | - | - | - | 3.99 | 3.98 | 4.01 | 4.00 | 4.00 | 4.01 | - | 4.07 | - |
| | ζ | - | - | - | - | - | - | - | - | - | 0.9% | 1.3% | - | 0.7% | 0.7% | 0.6% | - | 0.9% | - |
| 2nd Bending | f(cps) | 3.23 | 3.22 | 3.31 | 3.33 | 3.33 | 3.27 | 3.27 | 3.50 | 3.47 | 4.15 | 4.15 | 4.12 | 4.24 | 4.25 | 4.25 | 4.21 | 4.24 | 4.25 |
| | ζ | 1.1% | 1.0% | 0.8% | 1.2% | 1.0% | 1.4% | 1.2% | 1.2% | 1.2% | - | - | - | 0.6% | 0.8% | 0.7% | 0.6% | 0.5% | 0.7% |
| 5th Outer Tank | f(cps) | 3.40 | 3.40 | - | - | - | 3.45 | 3.45 | 3.65 | 3.65 | - | - | - | - | - | - | - | - | - |
| | ζ | - | - | - | - | - | - | - | - | - | - | - | - | - | - | - | - | - | |
| 3rd Bending | f(cps) | 3.81 | 3.80 | 3.83 | 3.82 | 3.82 | 3.83 | 3.82 | 4.04 | 4.01 | 4.71 | 4.69 | 4.78 | - | - | - | - | - | - |
| | ζ | 0.6% | 0.7% | 1.0% | - | 0.6% | 0.8% | 0.6% | 1.0% | 1.0% | 0.7% | 1.0% | 1.4% | - | - | - | - | - | - |
| 6th Outer Tank | f(cps) | 4.37 | 4.29 | 4.31 | 4.36 | 4.31 | 4.68 | 4.66 | 4.83 | 4.80 | 5.48 | 5.44 | 5.41 | 6.52 | 8.01 | 7.99 | 8.12 | 8.12 | 8.17 |
| | ζ | 1.8% | 0.7% | 0.9% | - | 1.5% | 1.3% | 1.4% | 0.9% | 1.3% | 2.5% | 2.4% | 1.0% | - | 1.0% | 1.6% | 2.1% | 1.4% | 1.6% |
| 4th Bending | f(cps) | 5.02 | 5.02 | 5.14 | 5.15 | 5.16 | 5.34 | 5.33 | 6.04 | 6.00 | 7.58 | 7.55 | 7.62 | 8.66 | - | - | - | - | - |
| | ζ | 0.6% | 0.5% | 0.8% | 0.7% | 0.6% | 1.4% | 1.2% | 0.7% | 0.8% | 1.2% | 1.2% | 1.1% | 0.7% | - | - | - | - | - |
| Coupled | f(cps) | 5.81 | 5.80 | 5.81 | 5.81 | 5.81 | - | - | - | - | - | - | - | - | - | - | - | - | - |
| | ζ | 1.8% | 1.5% | 2.1% | 1.0% | 1.2% | - | - | - | - | - | - | - | - | - | - | - | - | - |
| 7th Outer Tank | f(cps) | 7.21 | 7.21 | - | - | 7.26 | 7.70 | 7.70 | 8.76 | 8.73 | 10.05 | 10.07 | 10.29 | - | - | - | - | - | - |
| | ζ | 0.8% | 1.2% | - | - | 1.8% | 1.6% | 1.7% | 1.5% | 1.5% | - | - | 1.8% | - | - | - | - | - | - |
| Coupled | f(cps) | - | - | - | - | - | - | - | 9.48 | 9.49 | - | - | - | - | - | - | - | - | - |
| | ζ | - | - | - | - | - | - | - | - | - | - | - | - | - | - | - | - | - | - |

TABLE II SUMMARY OF BOOST PHASE RESONANT FREQUENCIES AND DAMPING COEFFICIENTS FOR LATERAL TESTS (Cont'd)

| Condition | | LIFTOFF | | | | | 10 SEC | | 35 SEC | | 68 SEC | | | 110 SEC | 147 SEC | | | | |
|---|---|---|---|---|---|---|---|---|---|---|---|---|---|---|---|---|---|---|---|
| | | Pitch | | | Yaw | | Pitch | | Pitch | | Pitch | | Yaw | | Pitch | | | Yaw | |
| Suspension / Mode | | (8-12) | (8-8) | (8-8) (Rerun) | (8-12) | (8-8) | (8-12) | (8-8) | (8-12) | (8-6) | (8-12) | (8-6) | (8-6) | (8-4) | (4E-12) | (4E-4) | (4E-4) (Rerun) | (4E-4) | (4E-4) (Rerun) |
| S-I Engine | f(cps) | 7.51 | 7.40 | 7.41 | 7.39 | - | 7.49 | 7.30 | - | - | - | - | - | - | - | - | - | - | - |
| | ζ | - | - | 1.9% | - | - | - | - | - | - | - | - | - | - | - | - | - | - | - |
| Coupled | f(cps) | - | - | - | - | - | - | - | - | - | - | - | - | 12.06 | - | - | - | - | - |
| | ζ | - | - | - | - | - | - | - | - | - | - | - | - | - | - | - | - | - | - |
| 8th Outer Tank | f(cps) | 9.48 | 9.49 | 9.54 | 9.52 | 9.53 | 9.60 | 9.60 | 10.77 | 10.66 | - | - | - | - | - | - | - | - | - |
| | ζ | 0.7% | 0.8% | 0.8% | - | 2.0% | - | - | - | - | - | - | - | - | - | - | - | - | - |
| 5th Bending | f(cps) | 10.54 | 10.49 | 10.44 | 10.99 | 10.98 | 11.12 | 11.11 | 11.73 | 11.74 | - | - | 12.40 | - | 13.21 | 13.16 | 13.29 | 13.04 | 13.12 |
| | ζ | 1.6% | - | - | - | - | 3.3% | 3.5% | - | - | - | - | - | - | - | - | - | 3.7% | 3.2% |
| Higher Mode | f(cps) | - | - | - | - | - | 13.29 | 12.92 | 13.56 | 13.56 | 14.28 | 14.21 | - | - | - | - | - | - | - |
| | ζ | - | - | - | - | - | - | - | - | - | - | - | - | - | - | - | - | - | - |
| Higher Mode | f(cps) | 13.95 | 13.87 | 13.81 | 13.85 | 13.84 | - | - | - | - | - | - | - | - | - | - | - | - | - |
| | ζ | 1.4% | - | 0.9% | - | - | - | - | - | - | - | - | - | - | - | - | - | - | - |
| Rotational Stiffness - $K_\theta$ ($10^8$ N-m/rad) | | 3.42 | 2.90 | 3.08 | 3.42 | 2.90 | 3.42 | 2.90 | 3.42 | 2.66 | 3.42 | 2.66 | 2.46 | 2.25 | 2.70 | 1.74 | 1.74 | 1.31 | 1.31 |

TABLE III SUMMARY OF BOOST PHASE LATERAL RESPONSE CHARACTERISTICS - LIFTOFF PITCH

| Suspension | Freq. (cps) | $X_{2278}$ (cm) | $Y_E$ | Force (lbf) | Force (N) | $M_B$ (kg) | $M_B'$ (kg) | $\zeta$ (%) |
|---|---|---|---|---|---|---|---|---|
| 8-8 | 1.60 | .3465 | .1596 | 472 | 2100 | 32,470 | --- | --- |
| 8-12 | 1.60 | .3306 | .1643 | 480 | 2135 | 32,382 | --- | --- |
| 8-8* | 1.59 | .301 | .172 | 370 | 1646 | 40,727 | --- | 1.0 |
| 8-8 | 1.72 | 1.9072 | .0665 | 479 | 2131 | 3,295 | 3638 | 1.0 |
| 8-12 | 1.73 | 1.8142 | .0708 | 478 | 2126 | 3,305 | 2981 | 1.2 |
| 8-8* | 1.74 | 2.507 | .0768 | 489 | 2175 | 3,609 | ---- | 1.1 |
| 8-8 | 3.22 | .5718 | .0490 | 488 | 2171 | 1,893 | 2432 | 1.1 |
| 8-12 | 3.23 | .5717 | .0490 | 479 | 2131 | 1,952 | 2079 | 1.1 |
| 8-8* | 3.31 | .897 | .0539 | 514 | 2286 | 1,961 | ---- | 0.8 |
| 8-8 | 3.80 | .1109 | .0249 | 503 | 2375 | 6,208 | 6747 | 0.7 |
| 8-12 | 3.81 | .0894 | .0342 | 484 | 2153 | 9,208 | 1194 | 0.6 |
| 8-8* | 3.83 | .0646 | .0463 | 533 | 2371 | 6,384 | ---- | 1.0 |
| 8-8 | 4.29 | .0593 | .3394 | 503 | 2375 | 15,063 | ---- | 0.7 |
| 8-12 | 4.37 | .0339 | .4048 | 485 | 2157 | 18,642 | 7001 | 1.8 |
| 8-8* | 4.31 | .0446 | .444 | 469 | 2086 | 24,978 | ---- | 0.9 |
| 8-8 | 5.02 | .3528 | .0549 | 477 | 2122 | 2,393 | 3717 | 0.5 |
| 8-12 | 5.02 | .3521 | .0582 | 481 | 2140 | 2,481 | 3489 | 0.6 |
| 8-8* | 5.14 | .330 | .0655 | 446 | 1984 | 2,638 | ---- | 0.8 |
| 8-8 | 5.80 | .0392 | .3303 | 497 | 2211 | 18,839 | ---- | 1.5 |
| 8-12 | 5.81 | .0463 | .3230 | 479 | 2131 | 16,103 | ---- | 1.8 |
| 8-8* | 5.81 | .0561 | .274 | 492 | 2189 | 11,003 | ---- | 2.1 |
| 8-8 | 7.21 | .0201 | .3323 | 477 | 2122 | 25,890 | ---- | 1.2 |
| 8-12 | 7.21 | .0287 | .2965 | 485 | 2157 | 22,624 | ---- | 0.8 |
| 8-8* | 7.41 | .0194 | .359 | 483 | 2148 | 16,044 | ---- | 1.9 |
| 8-8 | 9.49 | .00937 | .0514 | 488 | 2171 | 40,855 | ---- | 0.8 |
| 8-12 | 9.48 | .00959 | .0990 | 491 | 2184 | 35,824 | ---- | 0.7 |
| 8-8* | 9.54 | .00311 | .0840 | 212 | 943 | 43,296 | ---- | 0.8 |

TABLE III (cont'd)

| Suspension | Freq. (cps) | $X_{2278}$ (cm) | $Y_E$ | Force (lbf) | Force (N) | $M_B$ (kg) | $M_{B'}$ (kg) | $\zeta$ (%) |
|---|---|---|---|---|---|---|---|---|
| 8-8 | 10.49 | .00390 | .2917 | 490 | 2180 | 28,204 | ---- | --- |
| 8-12 | 10.54 | .00354 | .3958 | 489 | 2175 | 34,931 | ---- | 1.6 |
| 8-8* | 10.44 | .00282 | .0389 | 444 | 1975 | 54,299 | ---- | --- |
| 8-8 | 13.87 | .00704 | .3609 | 431 | 1917 | 34,608 | ---- | ---- |
| 8-12 | 13.95 | .00629 | .4824 | 467 | 2077 | 44,797 | ---- | 1.4 |
| 8-8* | 13.81 | .00653 | .0771 | 168 | 747 | 8,983 | ---- | 0.9 |

* Files for rerun tests.

TABLE IV SUMMARY OF BOOST PHASE LATERAL RESPONSE CHARACTERISTICS - 10 SEC PITCH

| Suspension | Freq. (cps) | $X_{2278}$ (cm) | $Y_e$ | Force (lbf) | Force (N) | $M_B$ (kg) | $M'_B$ (kg) | $\zeta$ (%) |
|---|---|---|---|---|---|---|---|---|
| 8-8 | 1.73 | 1.794 | .0738 | 483 | 2148 | 3550 | 2844 | 1.3 |
| 8-12 | 1.73 | 1.939 | .0746 | 515 | 2291 | 3520 | 2775 | 1.4 |
| 8-8 | 2.52 | .0832 | .2140 | 495 | 2202 | 84190 | 54358 | 1.0 |
| 8-12 | 2.52 | .1081 | .2102 | 519 | 2309 | 64410 | 54692 | 1.5 |
| 8-8 | 3.27 | .6200 | .0618 | 502 | 2309 | 2069 | 2206 | 1.2 |
| 8-12 | 3.27 | .6150 | .0622 | 528 | 2349 | 2118 | 2020 | 1.4 |
| 8-8 | 3.82 | .0875 | .0377 | 491 | 2184 | 4717 | 13249 | 0.6 |
| 8-12 | 3.83 | .0736 | .0439 | 535 | 2380 | 6659 | 13582 | 0.8 |
| 8-8 | 4.66 | .2440 | .1531 | 504 | 2242 | 3981 | 6070 | 1.4 |
| 8-12 | 4.68 | .2540 | .1473 | 529 | 2353 | 3854 | 6365 | 1.3 |
| 8-8 | 5.33 | .0555 | .0776 | 478 | 2126 | 2658 | 7120 | 1.2 |
| 8-12 | 5.34 | .0840 | .0623 | 534 | 2375 | 2707 | 5835 | 1.4 |
| 8-8 | 7.30 | .0127 | .4200 | 465 | 2068 | 30165 | - | - |
| 8-12 | 7.49 | .00745 | .7200 | 528 | 2349 | 167478 | - | - |
| 8-8 | 7.70 | .0180 | .6338 | 478 | 2126 | 41168 | - | 1.7 |
| 8-12 | 7.70 | .0274 | .6068 | 536 | 2384 | 43846 | - | 1.6 |
| 8-8 | 9.60 | .00489 | .2013 | 464 | 2064 | 55633 | - | - |
| 8-12 | 9.60 | .00320 | .5125 | 532 | 2366 | 119455 | - | - |
| 8-8 | 11.11 | .0105 | .0683 | 476 | 2117 | 2716 | - | 3.5 |
| 8-12 | 11.12 | .0124 | .0715 | 532 | 2366 | 2834 | - | 3.3 |
| 8-8 | 12.92 | .00206 | 1.191 | 457 | 2033 | 108589 | - | - |
| 8-12 | 13.29 | .00206 | 1.001 | 515 | 2291 | 85367 | - | - |

TABLE V SUMMARY OF BOOST PHASE LATERAL RESPONSE CHARACTERISTICS - 35 SEC PITCH

| Suspension | Freq. (cps) | $X_{2278}$ (cm) | $Y_E$ | Force (lbf) | Force (N) | $M_B$ (kg) | $M_B'$ (kg) | $\zeta$ (%) |
|---|---|---|---|---|---|---|---|---|
| 8-6 | 1.81 | .1684 | .0624 | 476 | 2117 | 2540 | 2638 | 1.20 |
| 8-12 | 1.82 | .1851 | .0655 | 505 | 2246 | 2569 | 2628 | 1.22 |
| 8-6 | 2.88 | .1958 | .0791 | 974 | 4333 | 15259 | ---- | ---- |
| 8-6 | 2.90 | .0737 | .0793 | 447 | 1988 | 24252 | ---- | 1.19 |
| 8-12 | 2.90 | .0734 | .0795 | 523 | 2326 | 30705 | 25605 | 1.00 |
| 8-6 | 3.47 | .5598 | .0862 | 555 | 2469 | 2030 | 2825 | 1.20 |
| 8-12 | 3.50 | .6063 | .0879 | 527 | 2344 | 2108 | 2707 | 1.17 |
| 8-6 | 4.01 | .1176 | .0453 | 459 | 2042 | 4227 | ---- | 1.0 |
| 8-12 | 4.04 | .0907 | .0532 | 515 | 2291 | 5570 | 8561 | 1.0 |
| 8-6 | 4.80 | .2570 | .1245 | 430 | 1913 | 3050 | 3815 | 1.25 |
| 8-12 | 4.83 | .3449 | .1185 | 513 | 2282 | 2922 | 4903 | 0.89 |
| 8-6 | 6.00 | .0594 | .0940 | 432 | 1922 | 5011 | ---- | 0.81 |
| 8-12 | 6.04 | .0678 | .0936 | 518 | 2304 | 4697 | ---- | 0.68 |
| 8-6 | 8.73 | .0226 | .3258 | 466 | 2073 | 19917 | ---- | 1.53 |
| 8-12 | 8.76 | .0257 | .3267 | 517 | 2300 | 21555 | ---- | 1.54 |
| 8-6 | 9.49 | .0043 | .5294 | 458 | 2037 | 129448 | ---- | ---- |
| 8-12 | 9.48 | .0046 | .5555 | 532 | 2366 | 158456 | ---- | ---- |
| 8-6 | 10.66 | .0089 | .1142 | 446 | 1999 | 4511 | ---- | ---- |
| 8-12 | 10.77 | .0074 | .1724 | 523 | 2344 | 7924 | ---- | ---- |
| 8-6 | 11.74 | .0069 | .1481 | 445 | 1995 | 5560 | ---- | ---- |
| 8-12 | 11.73 | .0132 | .1730 | 526 | 2358 | 4717 | ---- | ---- |
| 8-6 | 13.56 | .0071 | .2142 | 428 | 1904 | 15210 | ---- | ---- |
| 8-12 | 13.56 | .0130 | .2156 | 529 | 2371 | 10993 | ---- | ---- |

TABLE VI SUMMARY OF BOOSTER PHASE LATERAL RESPONSE CHARACTERISTICS - 68 SEC PITCH

| Suspension | Freq. (cps) | $X_{2278}$ (cm) | $Y_E$ | Force (lbf) | Force (N) | $M_B$ (kg) | $M_B'$ (kg) | $\zeta$ (%) |
|---|---|---|---|---|---|---|---|---|
| 8-6 | 1.89 | 1.599 | .0498 | 478 | 2126 | 2275 | 2354 | 1.0 |
| 8-12 | 1.90 | 1.707 | .0483 | 479 | 2131 | 2148 | 1736 | 1.2 |
| 8-6 | 2.54 | .0572 | .0981 | 462 | 2055 | 84592 | ---- | 0.6 |
| 8-12 | 2.54 | .0606 | .0974 | 458 | 2037 | 63371 | ---- | 0.6 |
| 8-6 | 2.86 | .0592 | .2274 | 465 | 2068 | 92741 | ---- | 1.9 |
| 8-12 | 2.86 | .0668 | .2129 | 452 | 2011 | 55290 | ---- | 3.0 |
| 8-6 | 3.75 | .0940 | .0432 | 443 | 1967 | 4040 | ---- | --- |
| 8-12 | 3.70 | .1057 | .0395 | 459 | 2042 | 7277 | ---- | --- |
| 8-6 | 3.98 | .3950 | .0655 | 464 | 2064 | 3040 | 2099 | 1.3 |
| 8-12 | 3.99 | .4636 | .0613 | 464 | 2064 | 2285 | 2599 | 0.9 |
| 8-6 | 4.15 | .2129 | .0770 | 438 | 1948 | 2046 | ---- | 1.1 |
| 8-12 | 4.15 | .1916 | .0766 | 433 | 1926 | 2122 | ---- | 1.1 |
| 8-6 | 4.69 | .1750 | .2031 | 457 | 2033 | 8561 | ---- | 1.0 |
| 8-12 | 4.71 | .1725 | .2179 | 436 | 1939 | 8914 | 20133 | 0.7 |
| 8-6 | 5.44 | .0572 | .3155 | 460 | 2046 | 15416 | 21957 | 2.4 |
| 8-12 | 5.48 | .0610 | .3208 | 442 | 1966 | 14504 | ---- | 2.5 |
| 8-6 | 7.55 | .0122 | .1875 | 467 | 2077 | 17122 | ---- | 1.2 |
| 8-12 | 7.58 | .0147 | .1724 | 455 | 2024 | 12513 | ---- | 1.2 |
| 8-6 | 10.07 | .0109 | .0930 | 464 | 2064 | 5551 | ---- | --- |
| 8-12 | 10.05 | .0119 | .0638 | 479 | 2131 | 4815 | ---- | --- |
| 8-6 | 12.19 | .0180 | .0985 | 464 | 2064 | 4668 | ---- | 2.1 |
| 8-12 | 12.25 | .0193 | .0921 | 469 | 2086 | 5090 | ---- | 2.0 |
| 8-6 | 14.21 | .0053 | .3333 | 457 | 2033 | 28351 | ---- | --- |
| 8-12 | 14.28 | .0048 | .3684 | 447 | 1988 | 27321 | ---- | --- |

TABLE VII SUMMARY OF BOOST PHASE LATERAL RESPONSE CHARACTERISTICS - 110 SEC PITCH

| Suspension | Freq. (cps) | $X_{2278}$ (cm) | $Y_e$ | Force (lbf) | Force (N) | $M_B$ (kg) | $M'_B$ (kg) | $\zeta$ (%) |
|---|---|---|---|---|---|---|---|---|
| 8-4 | 1.91 | 1.1729 | .0459 | 477 | 2122 | 1952 | 2913 | 1.1 |
| 8-4 | 4.00 | .2139 | .0216 | 266 | 1183 | 1373 | 1451 | 0.7 |
| 8-4 | 4.24 | .0846 | .0277 | 422 | 2327 | 1549 | 4795 | 0.6 |
| 8-4 | 4.73 | .00767 | .2381 | 228 | 1014 | 93565 | - | 1.7 |
| 8-4 | 5.59 | .00947 | .3013 | 455 | 2024 | 83925 | - | 1.1 |
| 8-4 | 6.52 | .00665 | 1.7733 | 448 | 1993 | 198408 | - | - |
| 8-4 | 7.16 | .0110 | .5271 | 430 | 1913 | 57104 | - | 1.4 |
| 8-4 | 8.66 | .0122 | .1822 | 414 | 1842 | 9199 | - | 0.7 |
| 8-4 | 12.06 | .00371 | .2419 | 240 | 1068 | 6237 | - | - |

TABLE VIII SUMMARY OF BOOST PHASE LATERAL RESPONSE CHARACTERISTICS - 147 SEC PITCH

| Suspension | Freq. (cps) | $X_{2278}$ (cm) | $Y_e$ | Force (lbf) | Force (N) | $M_B$ (kg) | $M_B'$ (kg) | $\zeta$ (%) |
|---|---|---|---|---|---|---|---|---|
| 4E-4* | 1.99 | 2.5460 | .0860 | 425 | 1890 | 2589 | 3138 | 0.9 |
| 4E-4 | 1.95 | .7968 | .0994 | 415 | 1846 | 2295 | 4815 | 2.7 |
| 4E-12 | 1.93 | 1.2850 | .0771 | 476 | 2117 | 1961 | 1736 | 1.1 |
| 4E-4 | 4.01 | .3526 | .0337 | 389 | 1730 | 1275 | 2197 | 0.6 |
| 4E-12 | 4.00 | .3790 | .0384 | 463 | 2060 | 1314 | 2285 | 0.7 |
| 4E-4* | 4.21 | .5603 | .0311 | 467 | 2077 | 1353 | 1491 | 0.6 |
| 4E-4 | 4.25 | .2125 | .0521 | 466 | 2073 | 1373 | 5394 | 0.7 |
| 4E-12 | 4.25 | .1646 | .0521 | 458 | 2037 | 1492 | 5011 | 0.8 |
| 4E-4* | 8.12 | .0295 | .1211 | 448 | 1993 | 6296 | - | 2.1 |
| 4E-4 | 7.99 | .0275 | .1045 | 434 | 1931 | 6914 | - | 1.6 |
| 4E-12 | 8.01 | .0244 | .0997 | 409 | 1819 | 6835 | - | 1.9 |
| 4E-4* | 10.39 | .0041 | .2152 | 409 | 1819 | 11454 | - | - |
| 4E-4 | 10.26 | .0049 | .1528 | 335 | 1490 | 6845 | - | 2.0 |
| 4E-12 | 10.23 | .0073 | .1609 | 470 | 2091 | 7502 | - | - |
| 4E-4* | 11.43 | .0047 | .0849 | 171 | 761 | 4384 | - | - |
| 4E-4 | 11.38 | .0034 | .1218 | 254 | 1130 | 4335 | - | - |
| 4E-12 | 11.79 | .0088 | .0676 | 432 | 1922 | 2736 | - | - |
| 4E-4* | 13.29 | .0075 | .2089 | 459 | 2042 | 9915 | - | - |
| 4E-4 | 13.16 | .0096 | .1652 | 387 | 1721 | 6217 | - | - |
| 4E-12 | 13.21 | .0058 | .1417 | 213 | 948 | 5413 | - | - |

* Files for rerun tests.

TABLE IX SUMMARY OF BOOST PHASE LATERAL RESPONSE CHARACTERISTICS - LIFTOFF YAW

| Suspension | Freq. (cps) | $X_{2278}$ (cm) | $Y_E$ | FORCE (lbf) | FORCE (N) | $M_B$ (kg) | $M_B'$ (kg) | $\zeta$ (%) |
|---|---|---|---|---|---|---|---|---|
| 8-8 | 1.60 | .1604 | .1374 | 235 | 1045 | 3,961 | --- | --- |
| 8-8 | 1.75 | 2.3148 | .0724 | 502 | 2233 | 2,795 | --- | 1.1 |
| 8-12 | 1.75 | 2.0815 | .0745 | 457 | 2033 | 2,903 | --- | 0.90 |
| 8-8 | 1.75 | 1.2274 | .0736 | 273 | 1214 | 2,805 | --- | 1.1 |
| 8-12 | 1.75 | .9317 | .0752 | 209 | 930 | 2,942 | --- | 0.90 |
| 8-8 | 2.40 | .0790 | .2264 | 488 | 2171 | 18,044 | --- | 1.3 |
| 8-12 | 2.40 | .0785 | .2735 | 467 | 2077 | 19,437 | --- | 1.3 |
| 8-8 | 3.25 | .2295 | .0377 | 478 | 2126 | 1,569 | --- | --- |
| 8-12 | 3.24 | .1369 | .0383 | 298 | 1326 | 1,667 | --- | --- |
| 8-8 | 3.33 | .6644 | .0516 | 465 | 2068 | 1,491 | --- | 0.99 |
| 8-12 | 3.33 | .5507 | .0515 | 426 | 1895 | 1,579 | --- | 1.2 |
| 8-8 | 3.82 | .0838 | .0465 | 449 | 1997 | 3,697 | --- | 0.55 |
| 8-12 | 3.82 | .0764 | .0269 | 449 | 1997 | 4,648 | --- | ---- |
| 8-8 | 4.31 | .0135 | .3487 | 150 | 667 | 10,003 | --- | ---- |
| 8-8 | 4.34 | .0358 | .4164 | 471 | 2095 | 13,916 | --- | 1.5 |
| 8-12 | 4.36 | .0407 | .4131 | 510 | 2269 | 13,612 | --- | ---- |
| 8-8 | 5.16 | .3001 | .0619 | 446 | 1984 | 2,295 | --- | 0.56 |
| 8-12 | 5.15 | .2839 | .0617 | 435 | 1935 | 2,334 | --- | 0.68 |
| 8-8 | 5.81 | .0703 | .2340 | 400 | 1779 | 4,158 | --- | 1.2 |
| 8-12 | 5.81 | .0714 | .2301 | 392 | 1744 | 4,109 | --- | 1.0 |
| 8-8 | 7.26 | .0136 | .2709 | 412 | 1833 | 11,680 | --- | 1.8 |
| 8-12 | 7.39 | .0128 | .3617 | 337 | 1499 | 8,610 | --- | ---- |

TABLE IX (cont'd)

| Suspension | Freq. (cps) | $X_{2278}$ (cm) | $Y_E$ | Force (lbf) | Force (N) | $M_B$ (kg) | $M_B'$ (kg) | (%) |
|---|---|---|---|---|---|---|---|---|
| 8-8 | 9.53 | .0027 | .2010 | 408 | 1815 | 64,057 | --- | 2.0 |
| 8-12 | 9.52 | .0032 | .2696 | 407 | 1810 | 51,279 | --- | --- |
| 8-8 | 10.98 | .0016 | 1.0630 | 427 | 1899 | 165,389 | --- | --- |
| 8-12 | 10.99 | .0016 | .7374 | 325 | 1446 | 148,718 | --- | --- |
| 8-8 | 13.84 | .0039 | .1670 | 264 | 1174 | 9,012 | --- | --- |
| 8-12 | 13.85 | .0073 | .1699 | 374 | 1664 | 11,199 | --- | --- |

TABLE X SUMMARY OF BOOST PHASE LATERAL RESPONSE CHARACTERISTICS - 68 SEC YAW

| Suspension | Freq. (cps) | $X_{2278}$ (cm) | $Y_E$ | FORCE (lbf) | FORCE (N) | $M_B$ (kg) | $M_B'$ (kg) | $\zeta$ (%) |
|---|---|---|---|---|---|---|---|---|
| 8-6 | 2.01 | 1.6408 | .0564 | 455 | 2024 | 3,530 | --- | 1.0 |
| 8-6 | 2.01 | .7377 | .0648 | 231 | 1028 | 3,089 | --- | 1.0 |
| 8-6 | 2.86 | .0782 | .2287 | 417 | 1855 | 11,356 | --- | --- |
| 8-6 | 3.80 | .0606 | .0261 | 407 | 1810 | 1,372 | --- | --- |
| 8-6 | 4.01 | .2179 | .0836 | 400 | 1779 | 1,765 | --- | --- |
| 8-6 | 4.05 | .1944 | .0720 | 400 | 1779 | 1,442 | --- | --- |
| 8-6 | 4.12 | .5838 | .0695 | 468 | 2082 | 1,393 | --- | 1.1 |
| 8-6 | 4.78 | .1305 | .1983 | 423 | 1882 | 4,894 | --- | 1.4 |
| 8-6 | 5.41 | .0374 | .1319 | 446 | 1984 | 3,776 | --- | 1.0 |
| 8-6 | 5.40 | .0791 | .2539 | 369 | 1641 | 10,032 | --- | 1.0 |
| 8-6 | 7.62 | .0111 | .1980 | 458 | 2037 | 12,003 | --- | 1.1 |
| 8-6 | 10.29 | .0125 | .1042 | 379 | 1686 | 5,796 | --- | 1.8 |
| 8-6 | 12.40 | .0005 | 2,6025 | 491 | 2184 | 5,050 | --- | --- |

TABLE XI SUMMARY OF BOOST PHASE LATERAL RESPONSE CHARACTERISTICS - 147 SEC YAW

| Suspension | Freq. (cps) | $X_{2278}$ (cm) | $Y_E$ | FORCE (lbf) | FORCE (N) | $M_B$ (kg) | $M_B'$ (kg) | $\zeta$ (%) |
|---|---|---|---|---|---|---|---|---|
| 4E-4 | 2.04 | 2.0522 | .0748 | 423 | 1882 | 2,216 | --- | 0.85 |
| 4E-4* | 2.05 | 3.0097 | .0738 | 454 | 2019 | 2,187 | --- | 0.74 |
| 4E-4 | 4.07 | .0733 | .0829 | 247 | 1099 | 2,079 | --- | 0.87 |
| 4E-4 | 4.24 | .5365 | .0293 | 439 | 1953 | 1,167 | --- | 0.47 |
| 4E-4* | 4.28 | .5170 | .0271 | 447 | 1988 | 1,138 | --- | 0.65 |
| 4E-4 | 8.12 | .0275 | .1218 | 477 | 2122 | 6,894 | --- | 1.4 |
| 4E-4* | 8.17 | .0256 | .0876 | 451 | 2006 | 5,962 | --- | 1.6 |
| 4E-4 | 10.40 | .0049 | .2602 | 474 | 2108 | 10,817 | --- | --- |
| 4E-4* | 10.36 | .0050 | .0372 | 449 | 1997 | 7,688 | --- | 1.7 |
| 4E-4 | 13.04 | .0133 | .1287 | 497 | 2211 | 9,738 | --- | 3.7 |
| 4E-4* | 13.12 | .0112 | .1268 | 447 | 1988 | 9,277 | --- | 3.2 |

NOTE: $M_B'$ was not computed for yaw tests.

* Files for rerun tests.

TABLE XII SUMMARY OF TORSIONAL AND LONGITUDINAL RESONANT FREQUENCIES AND DAMPING COEFFICIENTS

| Condition | | LIFTOFF | | 68 SEC | 147 SEC | |
|---|---|---|---|---|---|---|
| | | Torsional | Longitudinal | Torsional | Torsional | Longitudinal |
| Suspension / Mode | | (8-8) | (8-8) | (8-6) | (4E-4) | (4E-4) |
| 1st Torsional Cluster | f (cps) | 2.38 | - | 3.85 | 12.34 | - |
| | $\zeta$ | 1.2% | - | - | - | - |
| 1st Torsional | f (cps) | 3.69 | - | 5.15 | 5.51 | - |
| | $\zeta$ | 2.7% | - | 2.2% | 4.2% | - |
| 2nd Torsional Cluster | f (cps) | 5.63 | - | 7.05 | - | - |
| | $\zeta$ | 3.6% | - | - | - | - |
| 3rd Torsional Cluster | f (cps) | 6.67 | - | - | - | - |
| | $\zeta$ | 1.5% | - | - | - | - |
| Tower Coupled Cluster | f (cps) | 10.00 | - | 12.34 | - | - |
| | $\zeta$ | - | - | - | - | - |
| 1st Longitudinal Cluster | f (cps) | - | 7.52 | - | - | - |
| | $\zeta$ | - | - | - | - | - |
| 1st Longitudinal | f (cps) | - | 10.29 | - | - | 11.59 |
| | $\zeta$ | - | - | - | - | - |
| Suspension-stiffness | | | | | | |
| Torsional Stiffness $K_{\phi}$ ($10^6$N-m/rad) | | 4.87 | - | 3.23 | 1.18 | - |
| Longitudinal Stiffness $K_T$ ($10^7$N/m) | | - | 4.71 | - | - | 1.48 |

TABLE XIII SUMMARY OF BOOST PHASE RESPONSE CHARACTERISTICS FOR TORSIONAL TESTS

| Suspension | Freq. (cps) | $\phi_{1800}$ ($10^{-3}$deg) | $\phi_E$ (deg/deg) | Torque (N-m) | $I'_\varphi$ ($10^7$kg-m$^2$) | $\zeta$ (%) |
|---|---|---|---|---|---|---|
| Liftoff | | | | | | |
| 8-8 | 2.38 | 6.413 | .6390 | 9989 | 1.2263 | 1.18 |
| 8-8 | 3.69 | 22.25 | .7972 | 9617 | .06832 | 2.66 |
| 8-8 | 5.63 | 4.817 | .3383 | 5721 | .02588 | 3.59 |
| 8-8 | 6.67 | 3.292 | .8556 | 9959 | .4017 | 1.52 |
| 8-8 | 10.00 | 4.601 | .5223 | 9703 | ----- | ----- |
| 68 SEC | | | | | | |
| 8-6 | 3.70 | 1.389 | .3556 | 8479 | ----- | ----- |
| 8-6 | 3.85 | 1.504 | .3329 | 8113 | ----- | ----- |
| 8-6 | 4.10 | 1.528 | .3647 | 8702 | ----- | ----- |
| 8-6 | 5.15 | 13.23 | .7053 | 8776 | .05844 | 2.20 |
| 8-6 | 6.59 | 3.147 | .8408 | 8784 | .1921 | 2.50 |
| 8-6 | 6.91 | 3.366 | 1.1997 | 9089 | .2958 | 2.50 |
| 8-6 | 7.05 | 2.938 | 1.3224 | 8871 | ----- | ----- |
| 8-6 | 12.34 | 1.356 | .6849 | 9230 | ----- | ----- |
| 147 SEC | | | | | | |
| 4E-4 | 5.51 | 13.21 | .4311 | 9632 | .01789 | 4.16 |
| 4E-4 | 12.34 | 1.056 | .1548 | 5834 | ----- | ----- |

NOTE:

$\phi_{1800}$ - Rotational displacement at Sta. 1800 (measured)

$\phi_E$ - Rotation at Sta. 118 normalized rotation at Sta. 1800 (deg/deg)

$I'_\varphi$ - Generalized torsional inertia (referenced to Sta. 1800) for SAD-6 Vehicle (kg-m$^2$)

TABLE XIV SUMMARY OF S-IV PHASE RESONANT FREQUENCIES AND DAMPING COEFFICIENTS

| Condition | | S-IV IGNITION Pitch | Yaw | Torsion | +20 SEC. Pitch | + 290 SEC. Pitch |
|---|---|---|---|---|---|---|
| Suspension / Mode | | (8-5) | (8-5) | (8-5) | (8-5) | (8-3) |
| 1st Bending | f(cps) | 3.56 | 3.63 | --- | 8.96 | 9.86 |
| | ζ | 0.6% | 0.6% | | 2.8% | 6.2% |
| 2nd Bending | f(cps) | 8.88 | 9.28 | --- | --- | --- |
| | ζ | 2.7% | 3.3% | | | |
| 3rd Bending | f(cps) | 14.44 | 14.40 | --- | --- | --- |
| | ζ | 1.8% | 2.9% | | | |
| Engine | f(cps) | 26.40 | --- | --- | --- | --- |
| | ζ | --- | | | | |
| 1st Torsional | f(cps) | --- | --- | 14.11 | --- | --- |
| | ζ | | | --- | | |
| Torsional | f(cps) | --- | --- | 15.01 | --- | --- |
| | ζ | | | --- | | |
| 2nd Torsional | f(cps) | --- | --- | 20.40 | --- | --- |
| | ζ | | | 0.7% | | |
| Engine | f(cps) | --- | --- | 26.25 | --- | --- |
| | ζ | | | --- | | |
| Engine | f(cps) | --- | --- | 28.94 | --- | --- |
| | ζ | | | --- | | |

TABLE XV SUMMARY OF S-IV PHASE RESPONSE CHARACTERISTICS FOR LATERAL TESTS

| Suspension | Freq. (cps) | $X_{2278}$ (cm) | $Y_E$ | Force (lbf) | Force (N) | $M_B$ (kg) | $\zeta$ (%) |
|---|---|---|---|---|---|---|---|
| S-IV Ignition (Pitch) | | | | | | | |
| 8-5 | 3.56 | 1.477 | .0811 | 481 | 2140 | 1510 | 0.6 |
| 8-5 | 8.88 | .0630 | .3412 | 473 | 2104 | 3246 | 2.7 |
| 8-5 | 14.44 | .0169 | .3421 | 253 | 1125 | 1226 | 1.8 |
| 8-5 | 26.40 | .00061 | 43.65 | 471 | 2095 | ---- | --- |
| S-IV Ignition (Yaw) | | | | | | | |
| 8-5 | 3.63 | 1.577 | .0750 | 330 | 1468 | 804 | 0.6 |
| 8-5 | 9.28 | .0559 | .4063 | 485 | 2157 | 2569 | 3.3 |
| 8-5 | 14.40 | .0012 | 7.714 | 252 | 1121 | 3579 | 2.9 |
| S-IV Ignition + 20 Sec. (Pitch) | | | | | | | |
| 8-5 | 8.96 | .0502 | .1118 | 486 | 2162 | 4707 | 2.8 |
| S-IV Ignition + 290 Sec (Pitch) | | | | | | | |
| 8-3 | 9.86 | .0374 | .1074 | 497 | 2211 | 5707 | 6.2 |

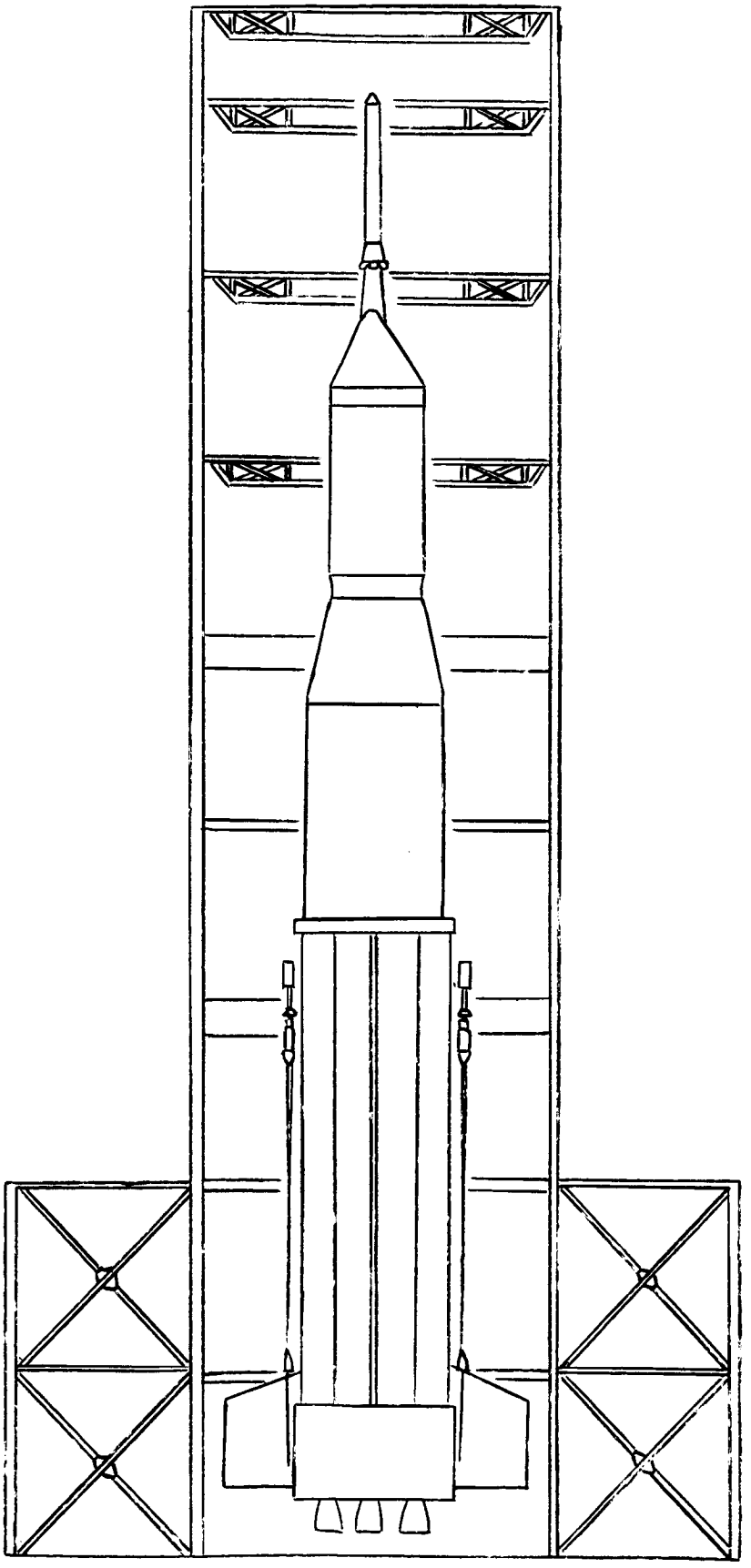

FIGURE 1 SAD-6 VEHICLE SUSPENDED IN TEST TOWER

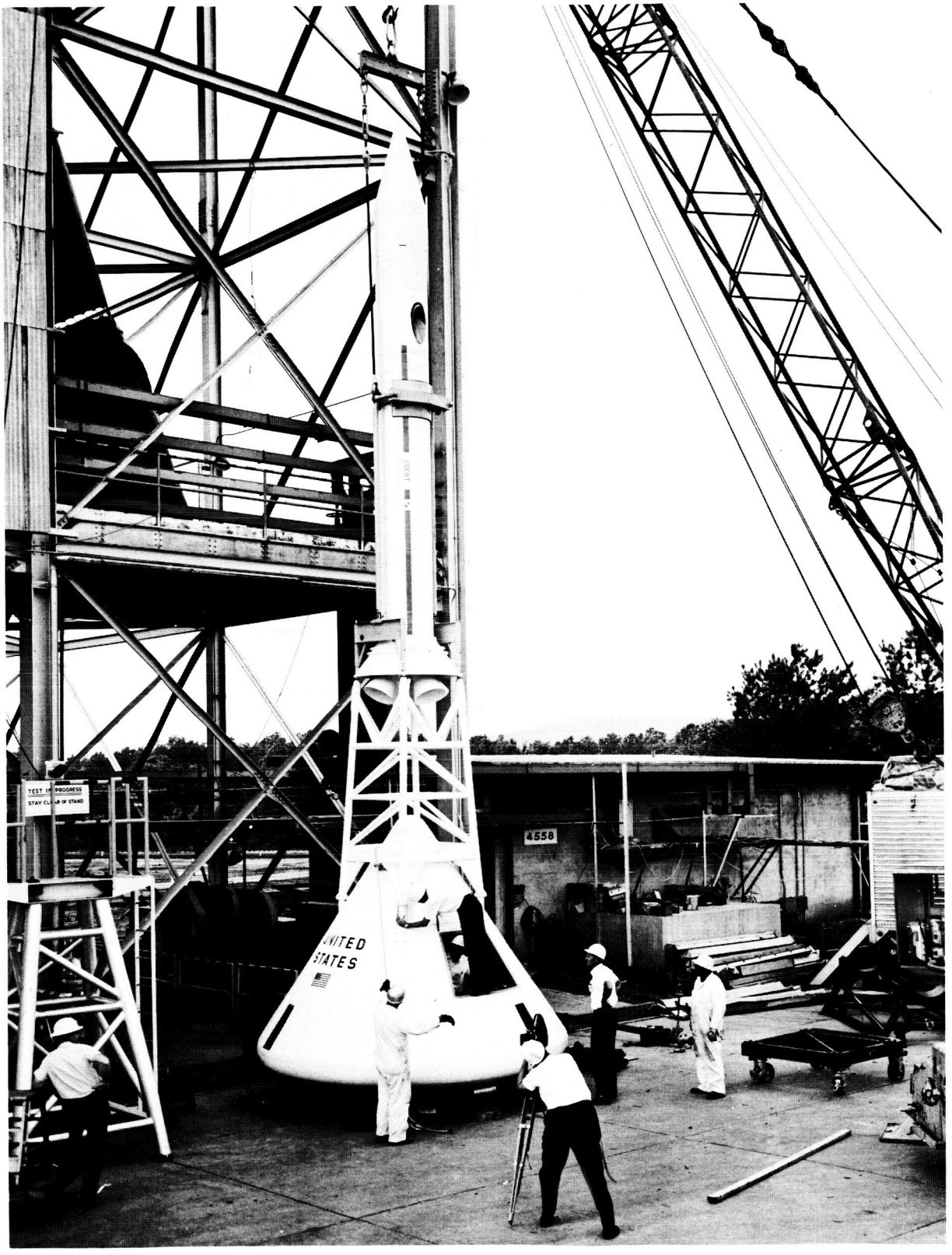


FIGURE 2 COMMAND MODULE WITH LES BEING ATTACHED

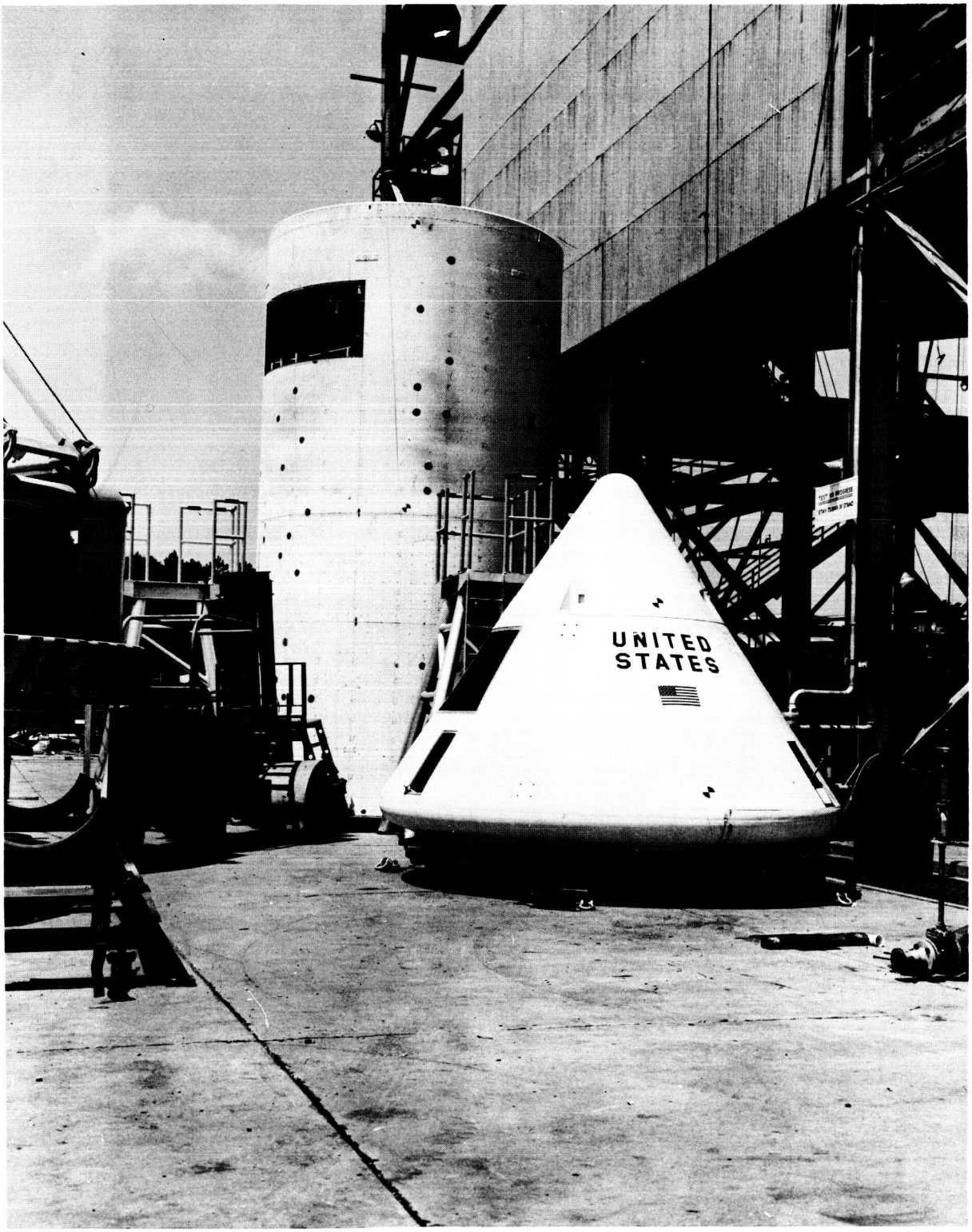


FIGURE 3 COMMAND MODULE WITH SERVICE MODULE AND ADAPTER ASSEMBLY

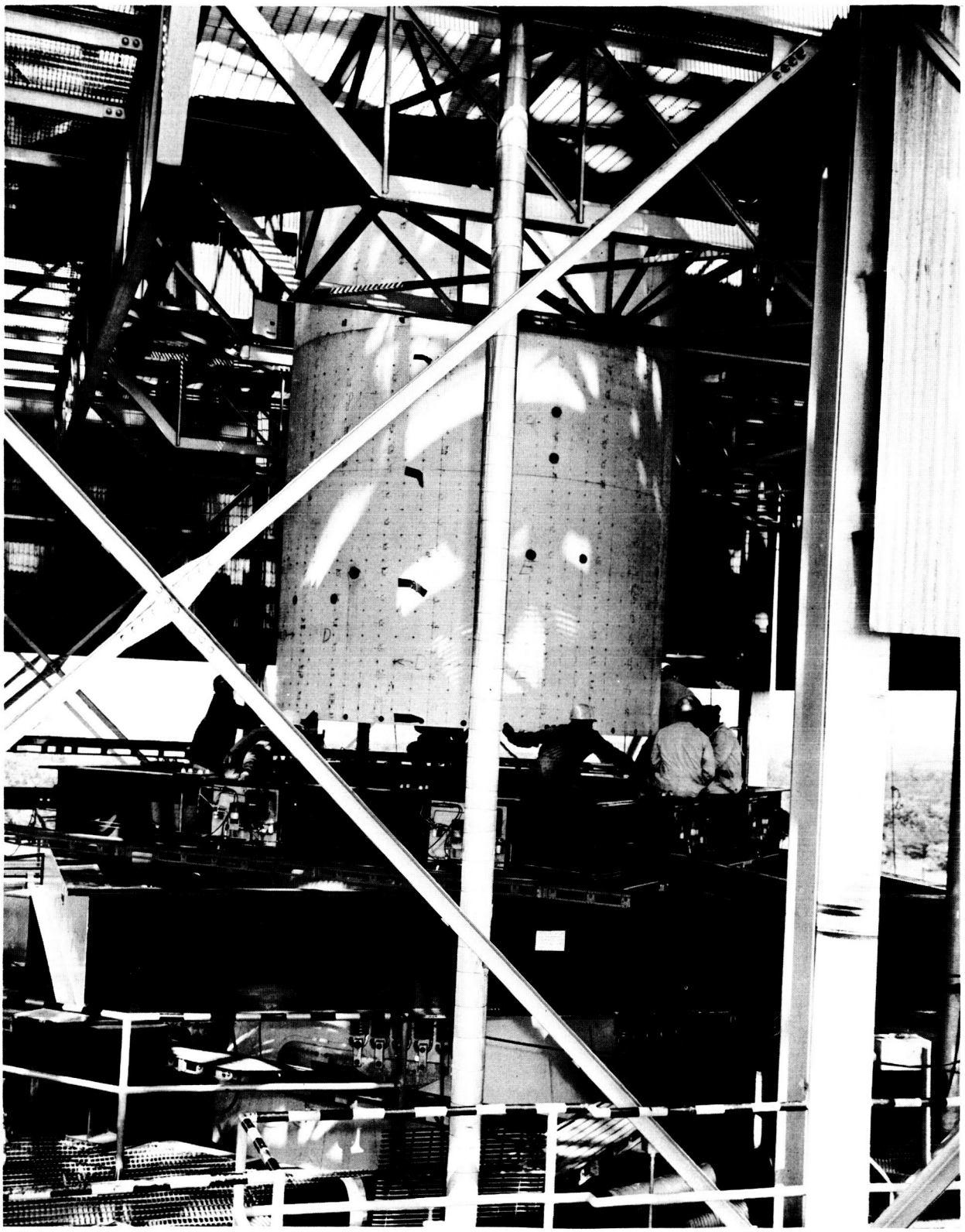

FIGURE 4 APOLLO PAYLOAD BEING ASSEMBLED TO S-IV STAGE

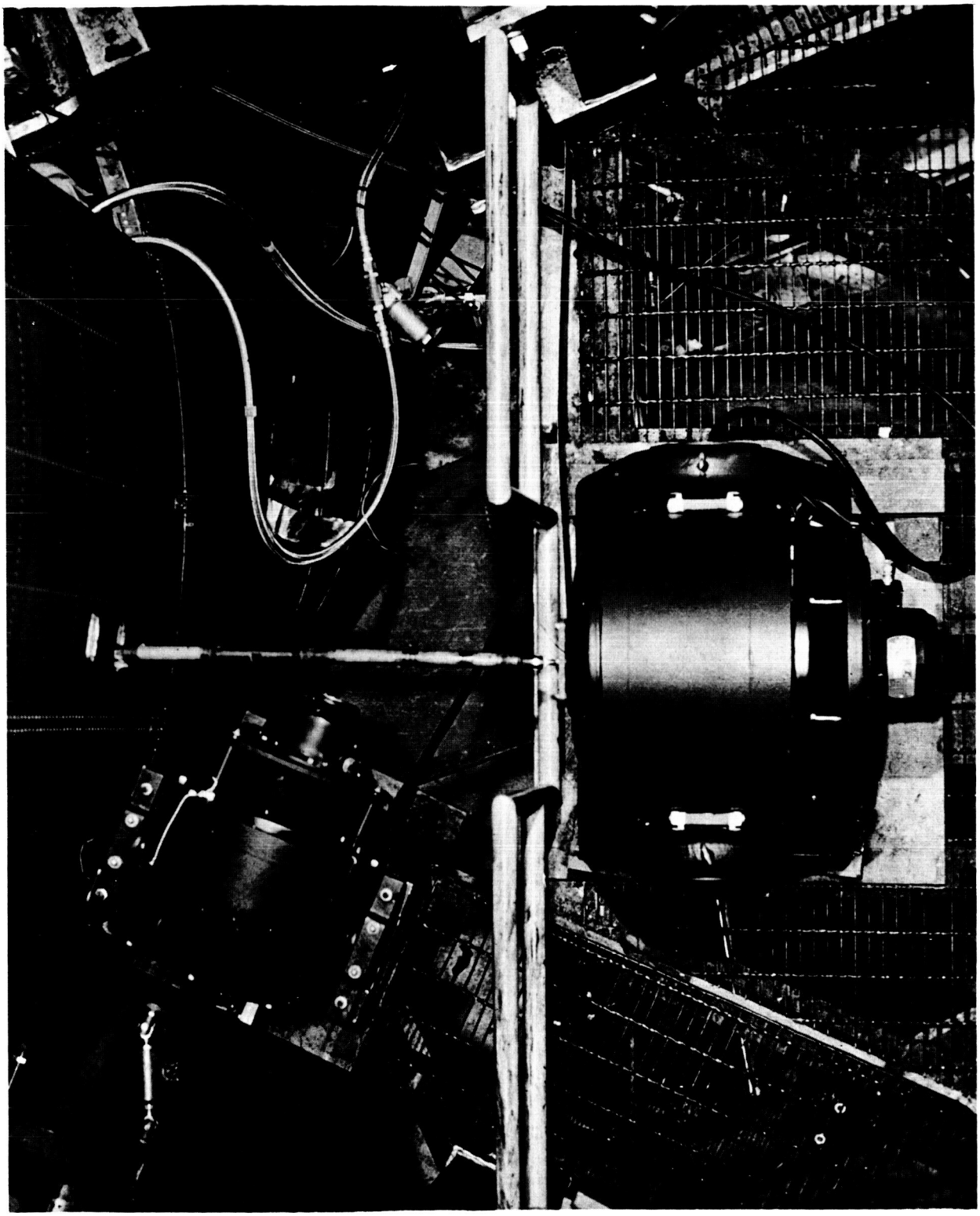

FIGURE 5 SHAKER POSITIONED FOR S-I BOOSTER PHASE TORSIONAL TESTS

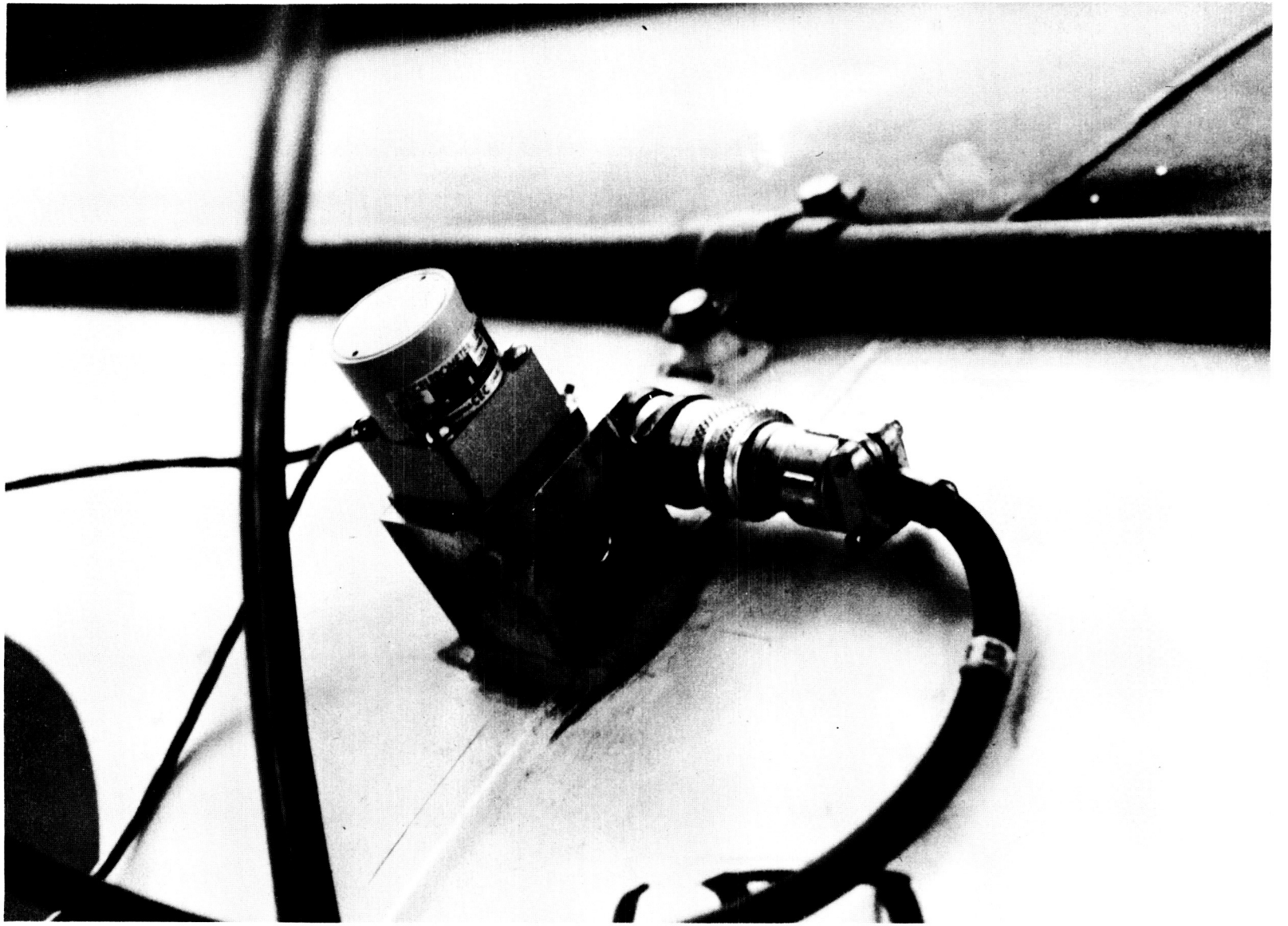

FIGURE 6 TYPICAL ATTACHMENT OF STRAIN BRIDGE TYPE ACCELEROMETER

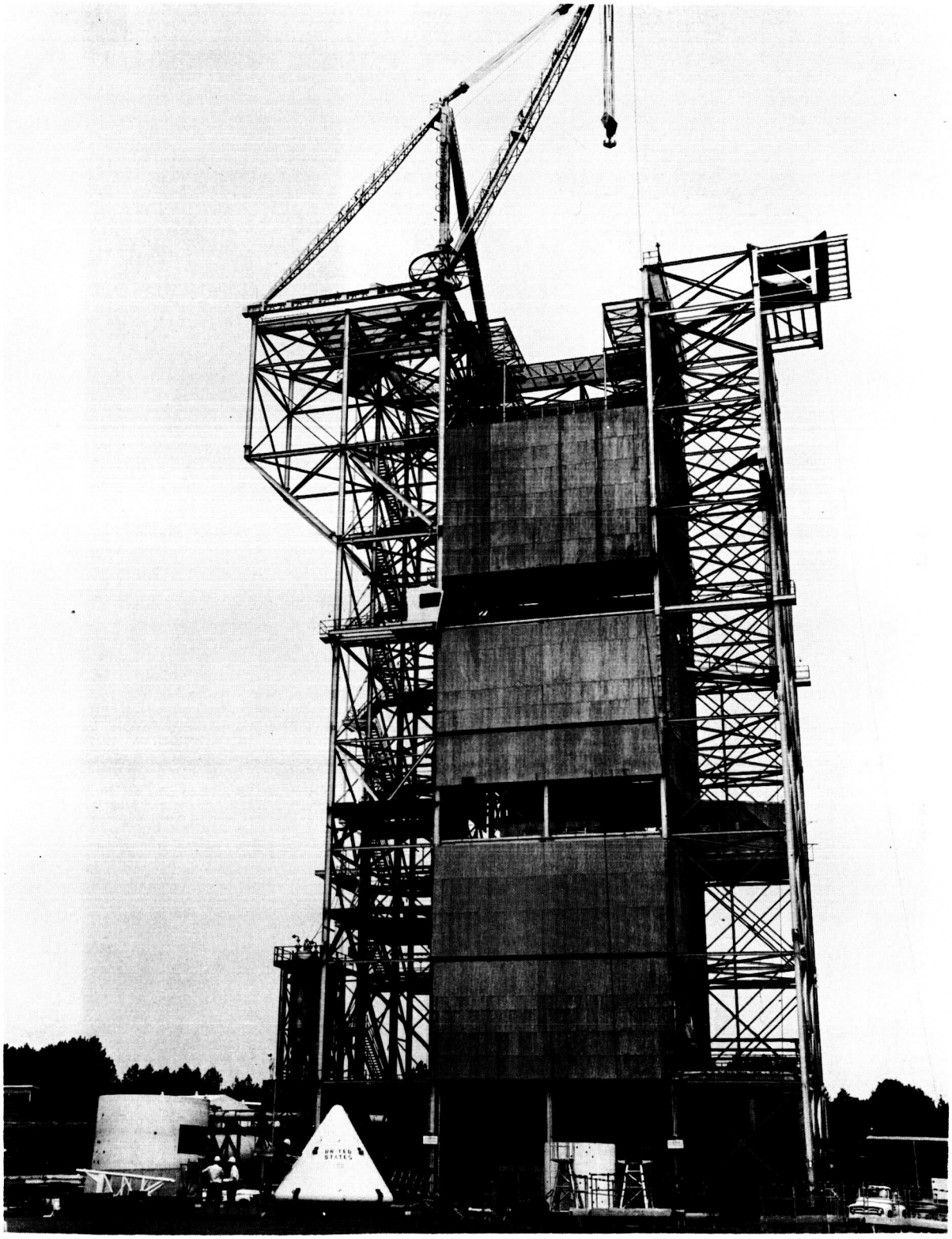


FIGURE 7 DYNAMIC TEST TOWER WITH WIND SCREENS ATTACHED

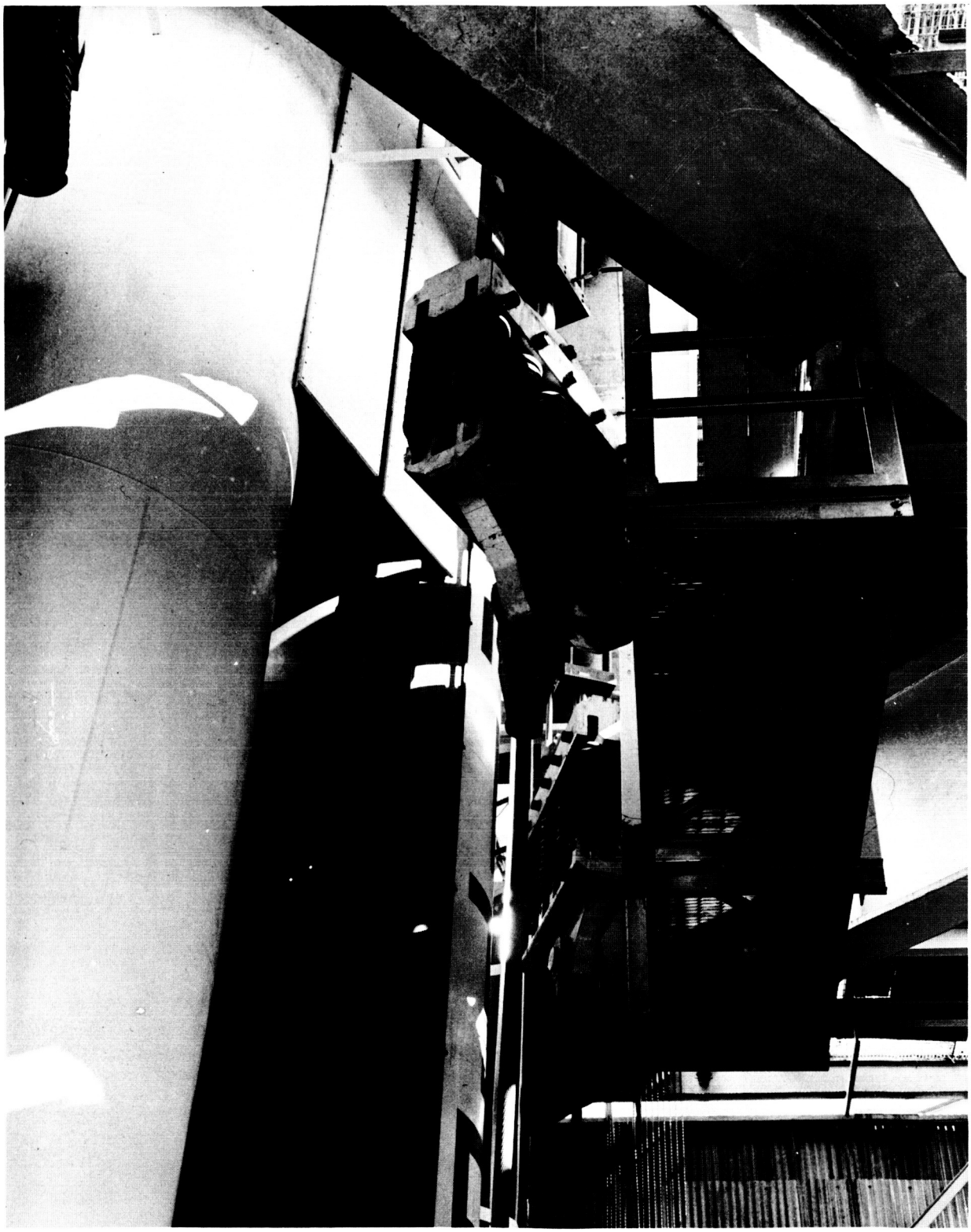

FIGURE 8 TYPICAL SPRING CLUSTER USED FOR BOOST PHASE TESTS

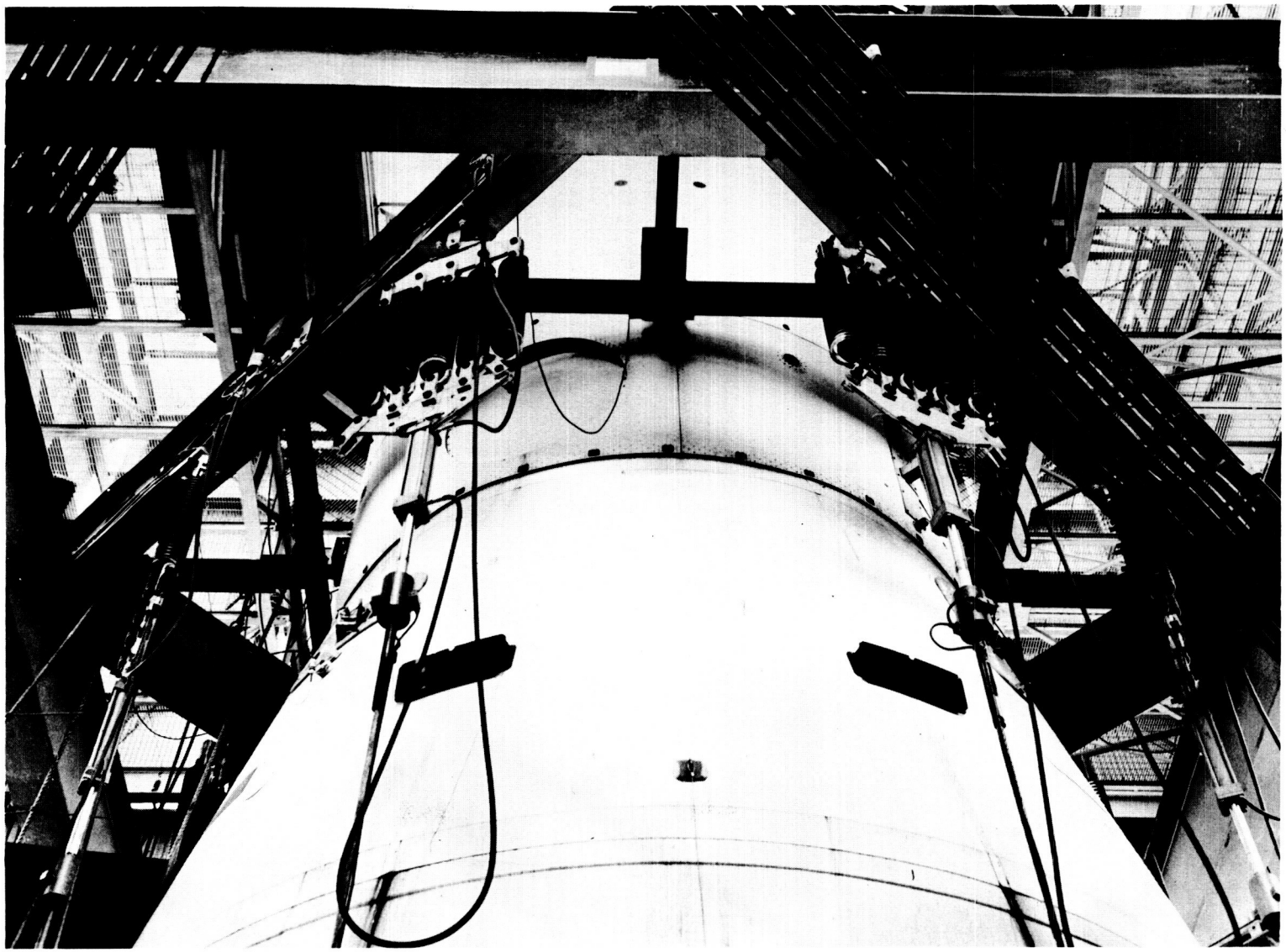

FIGURE 9 TYPICAL SPRING CLUSTER USED FOR S-IV PHASE TESTS

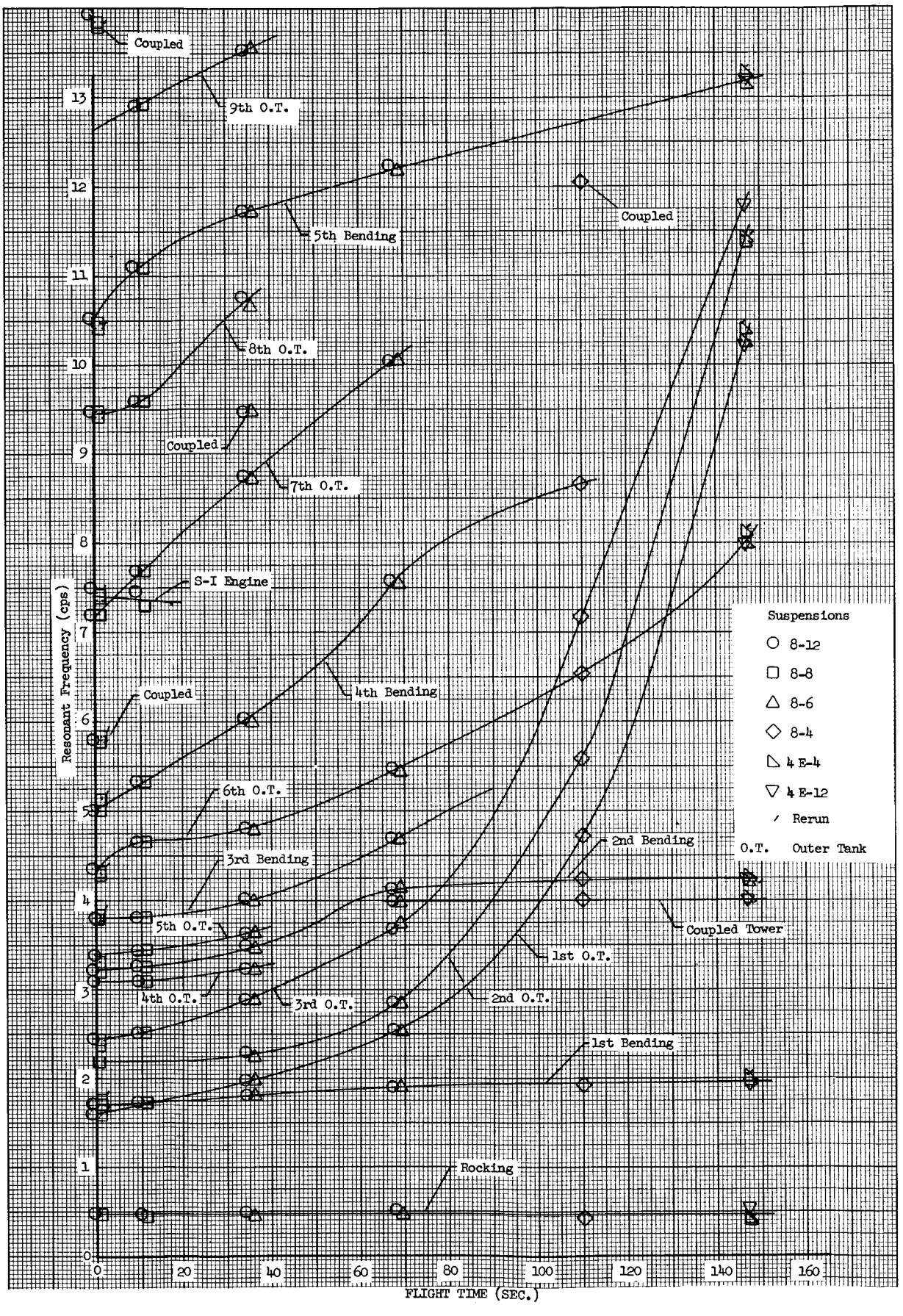


FIGURE 10 RESONANT FREQUENCY PROFILE DURING BOOST (PITCH EXCITATION)

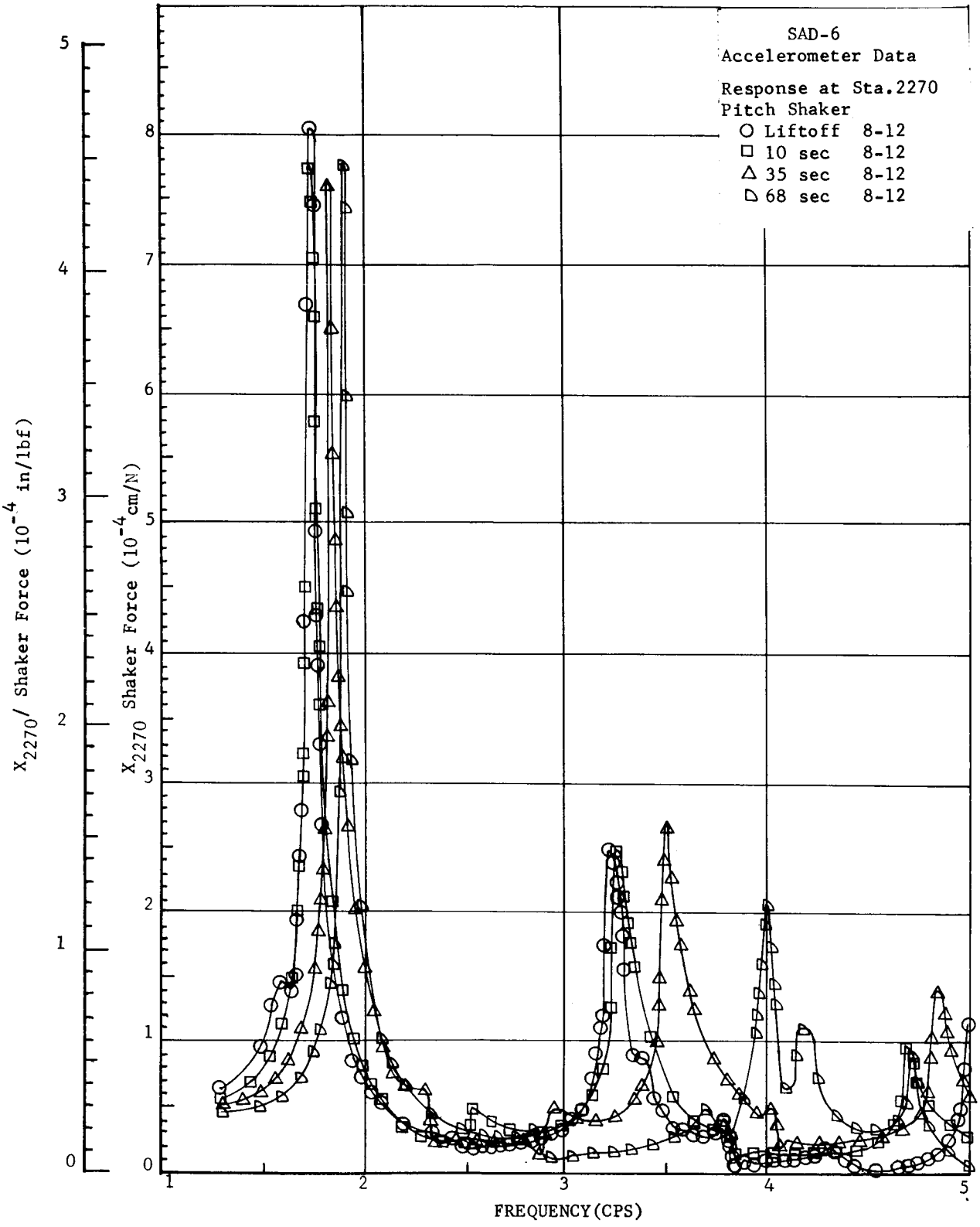


FIGURE 11 PITCH RESPONSE AT NOSE FOR HARD SUSPENSION (PITCH EXCITATION)

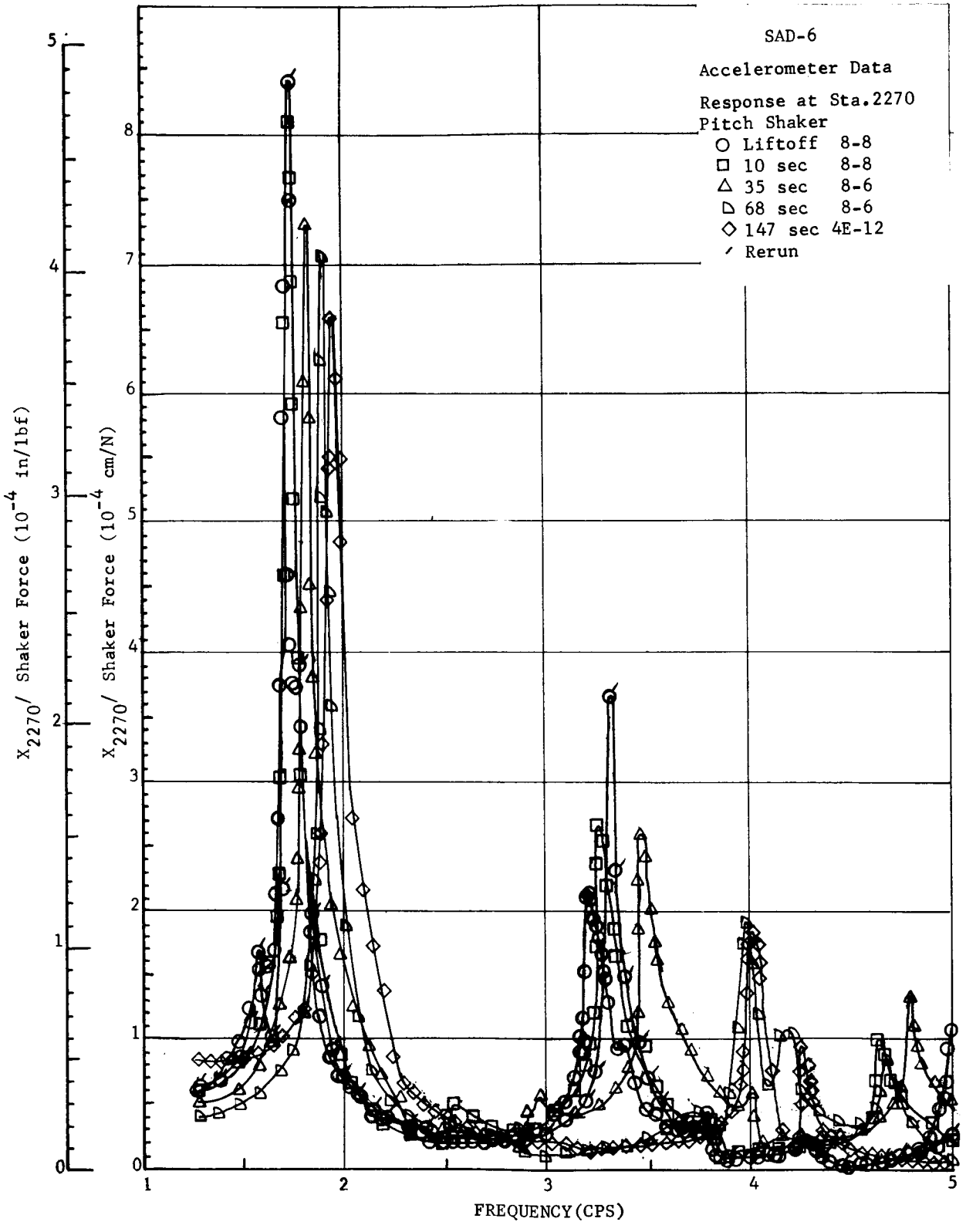


FIGURE 12 PITCH RESPONSE AT NOSE FOR MEDIUM SUSPENSION (PITCH EXCITATION)

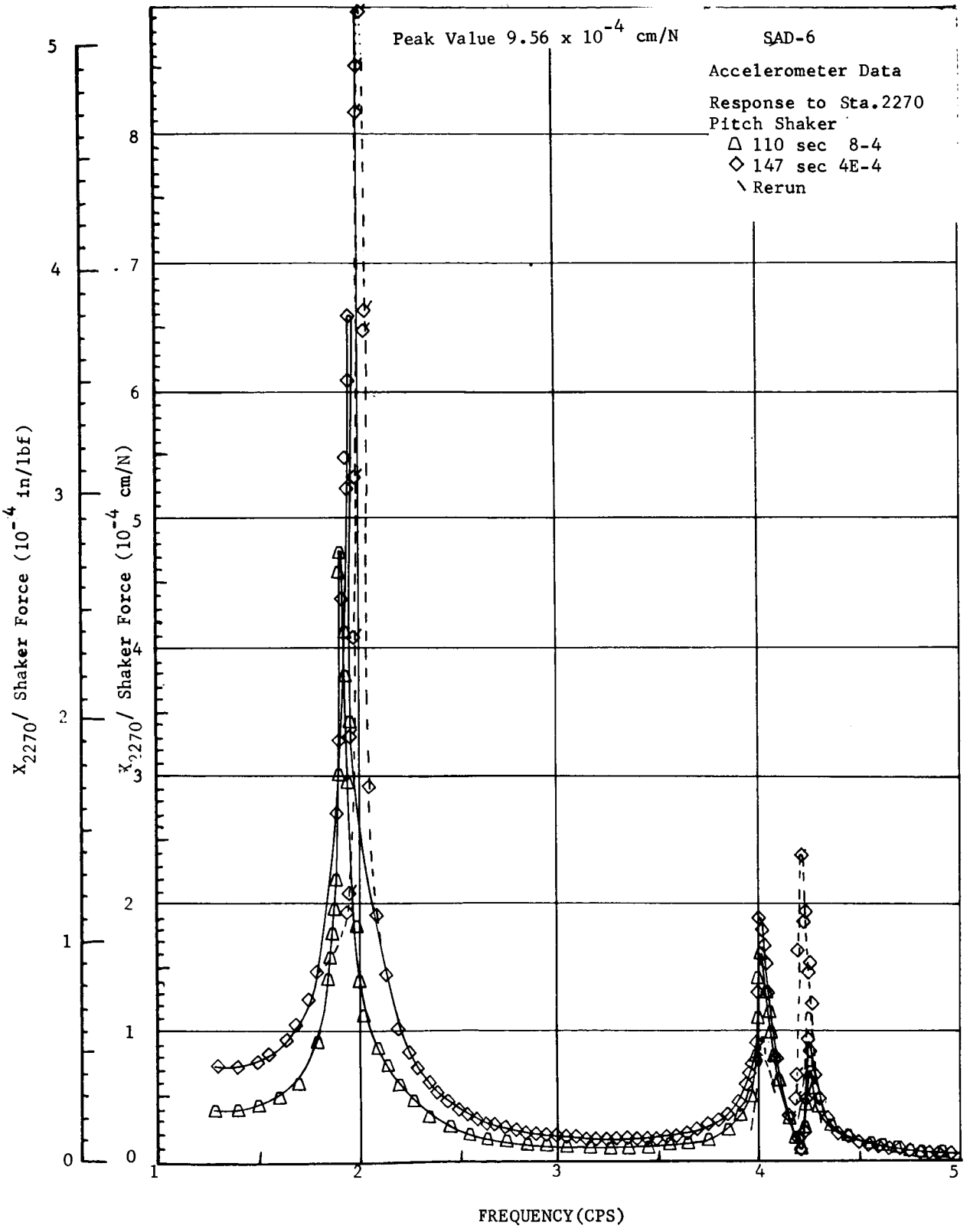


FIGURE 13 PITCH RESPONSE AT NOSE FOR SOFT SUSPENSION (PITCH EXCITATION)

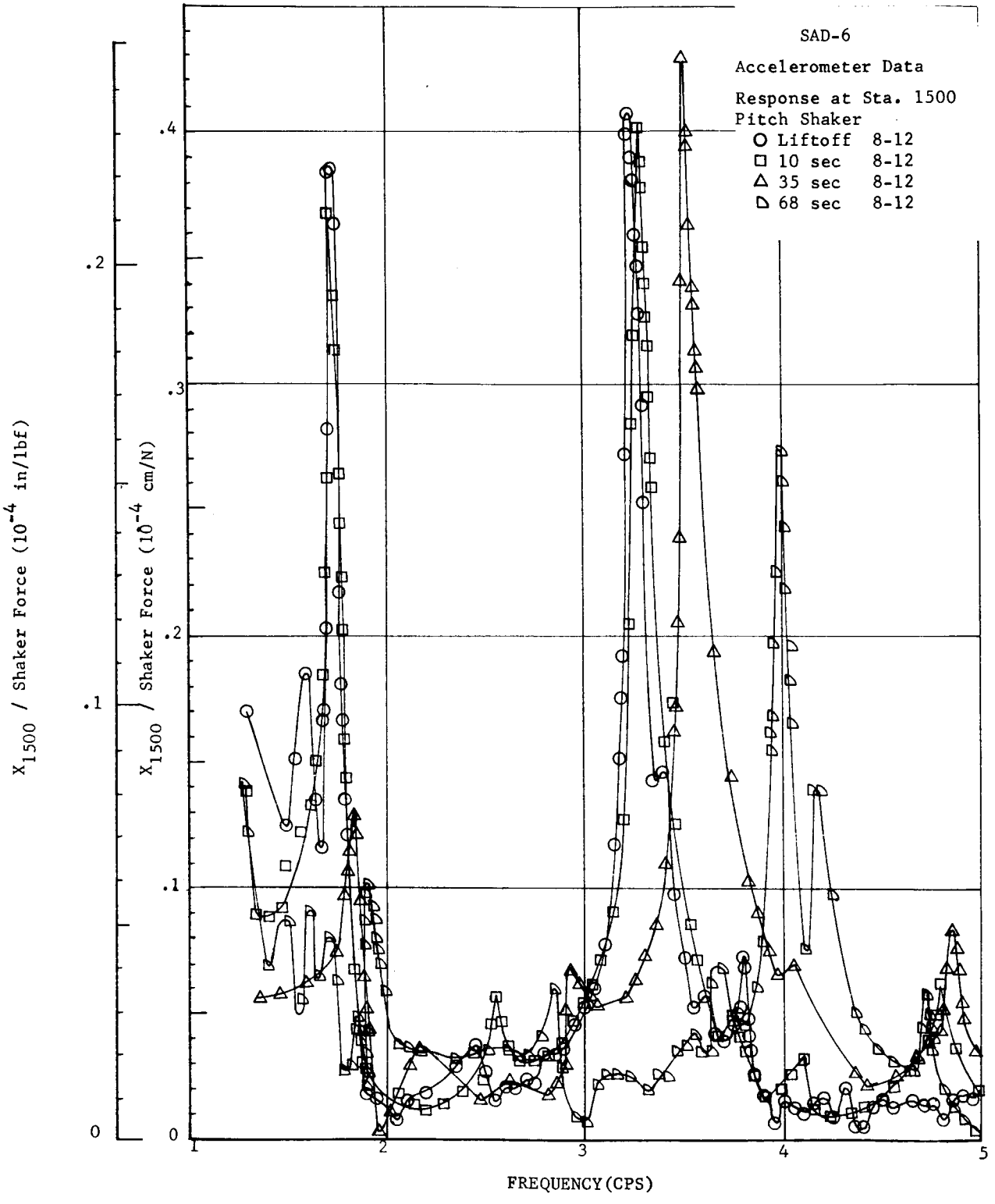


FIGURE 14 PITCH RESPONSE AT IU FOR HARD SUSPENSION (PITCH EXCITATION)

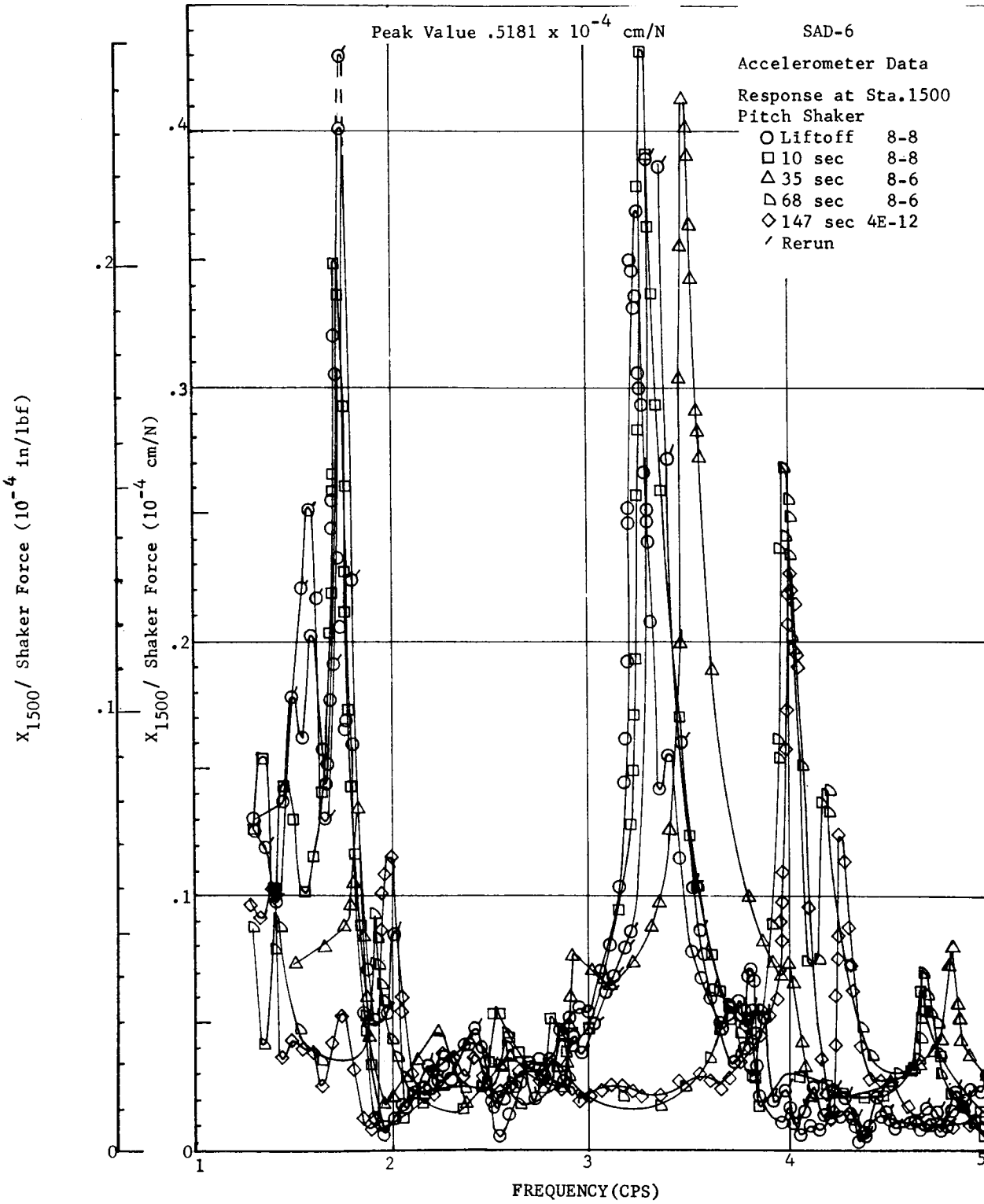


FIGURE 15 PITCH RESPONSE AT IU FOR MEDIUM SUSPENSION (PITCH EXCITATION)

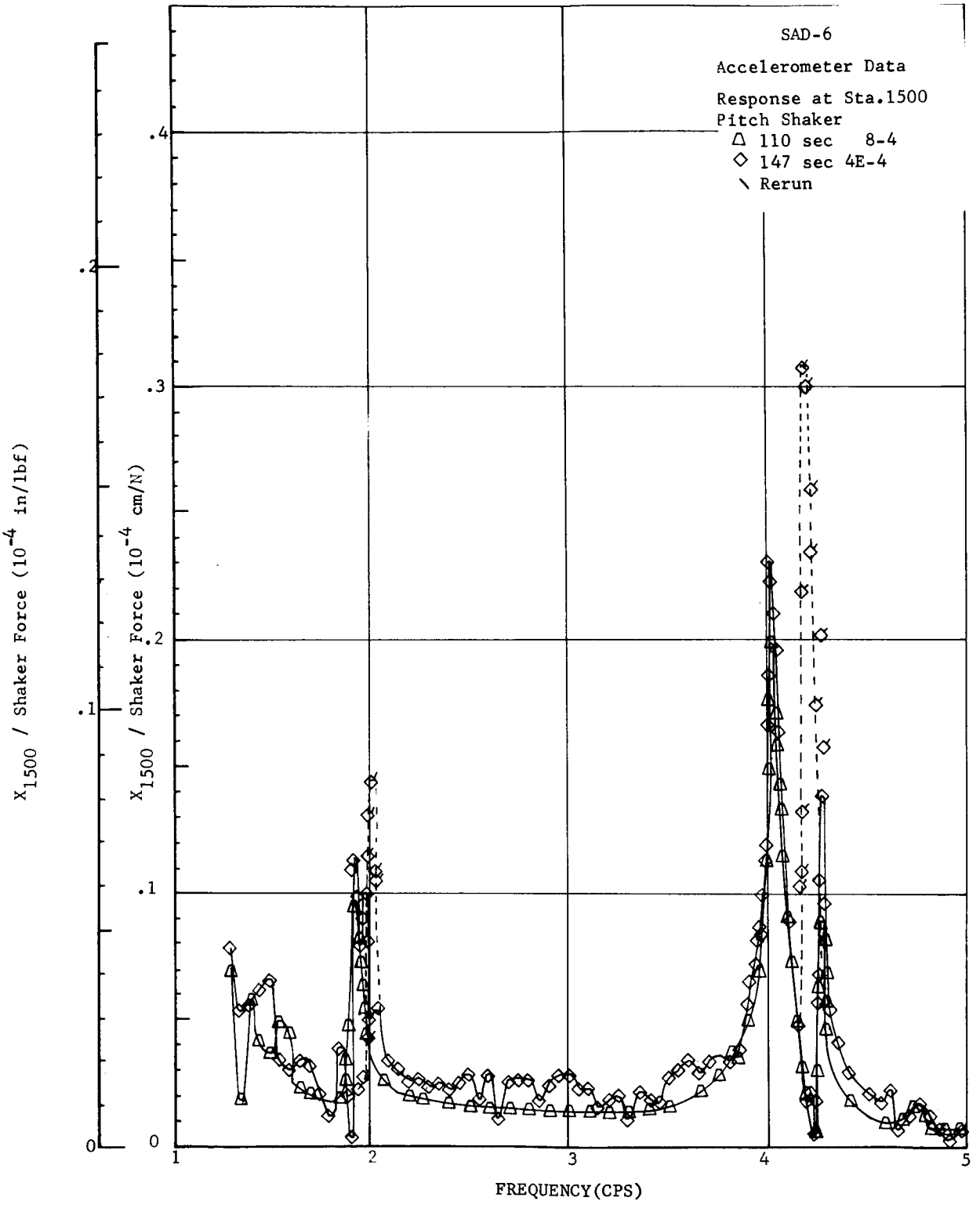


FIGURE 16 PITCH RESPONSE AT IU FOR SOFT SUSPENSION (PITCH EXCITATION)

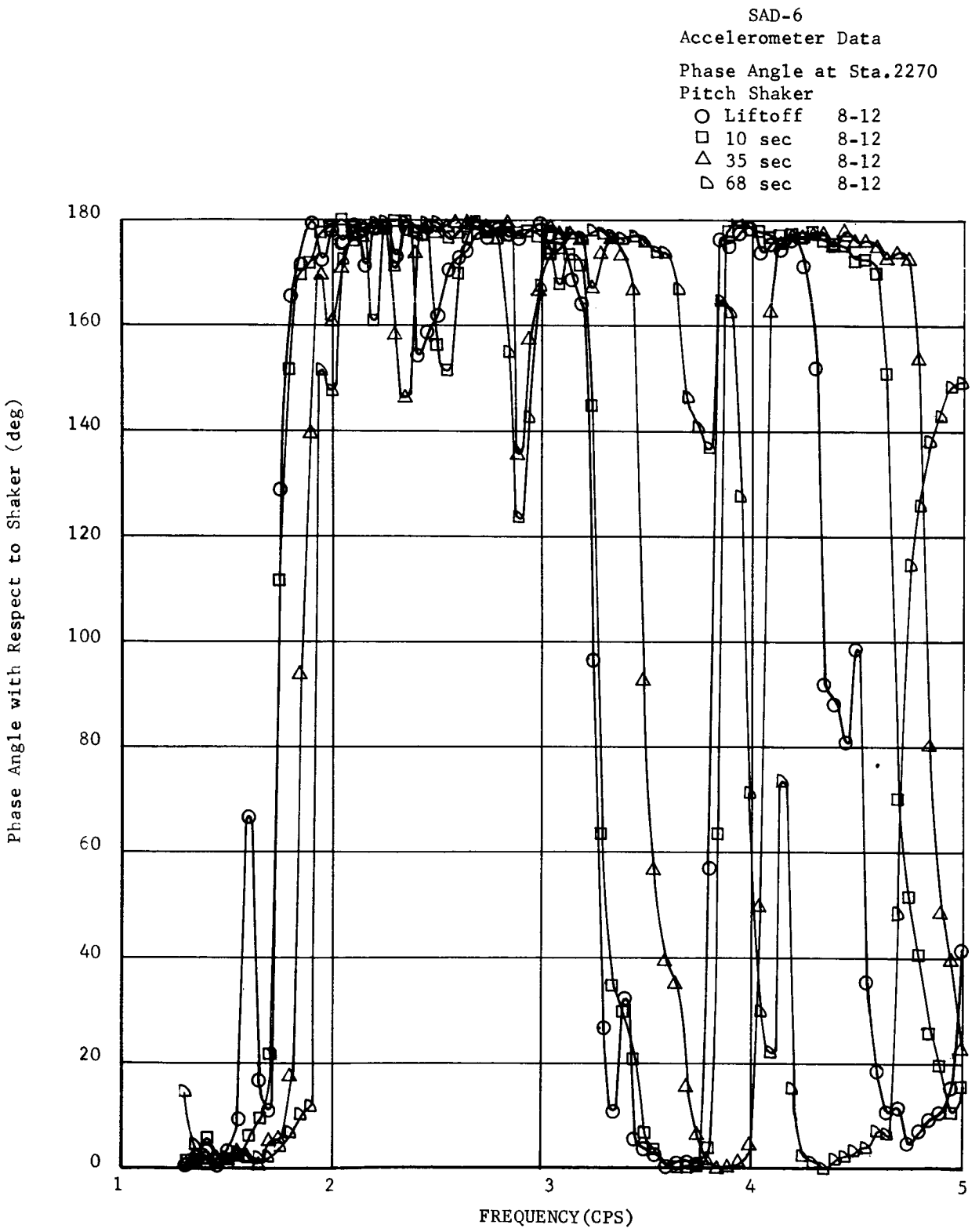


FIGURE 17 PHASE ANGLE AT NOSE FOR HARD SUSPENSION (PITCH EXCITATION)

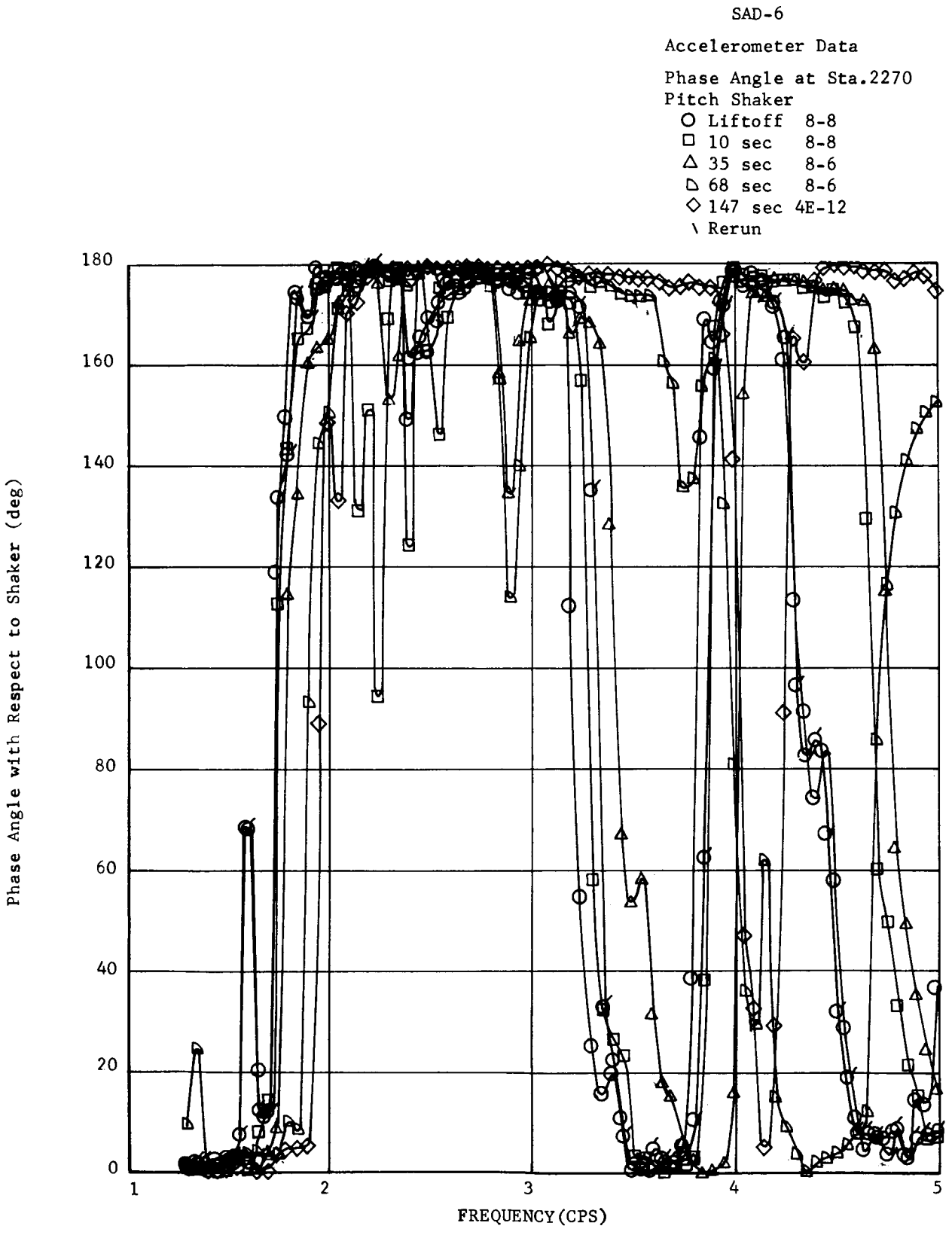


FIGURE 18 PHASE ANGLE AT NOSE FOR MEDIUM SUSPENSION (PITCH EXCITATION)

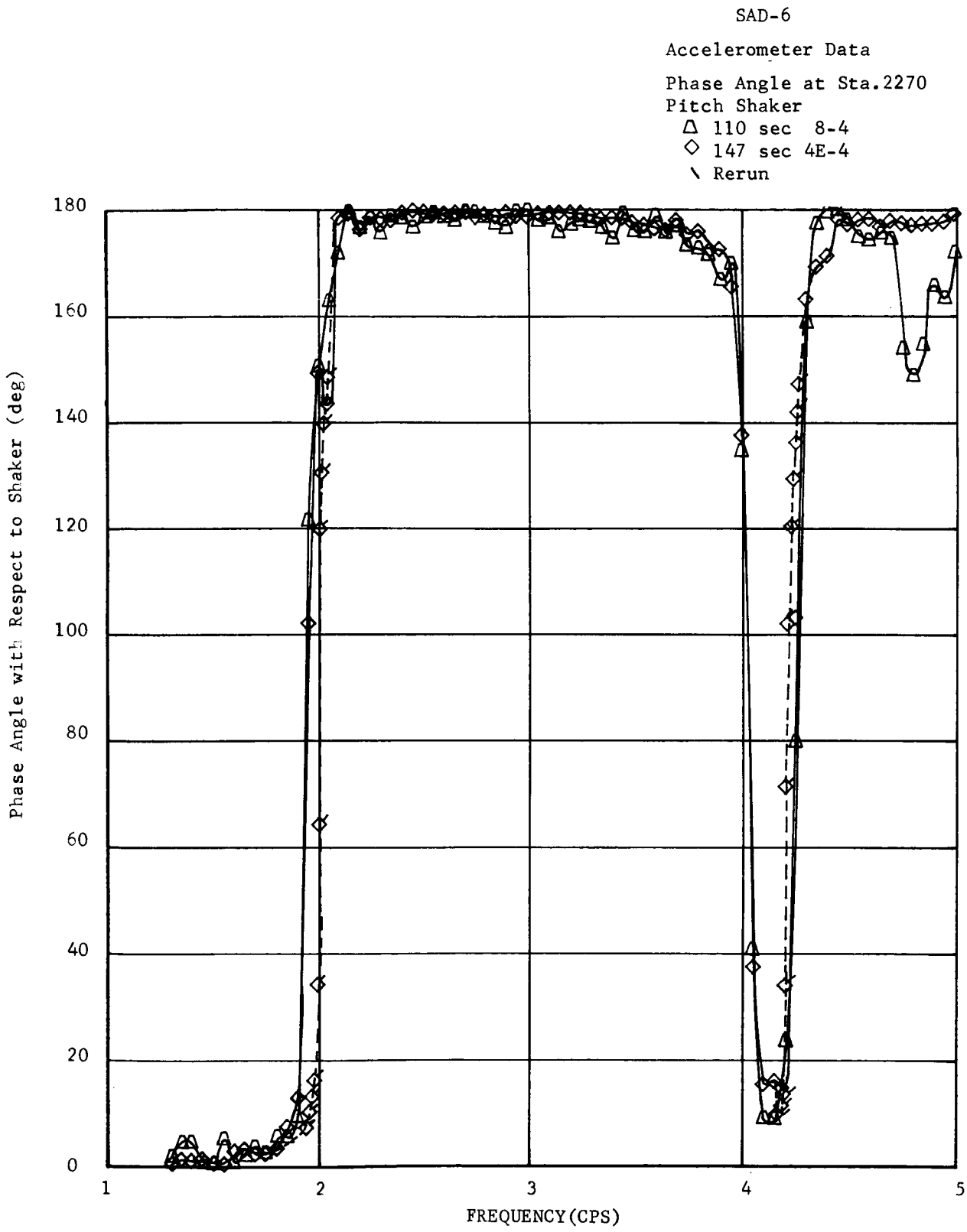


FIGURE 19 PHASE ANGLE AT NOSE FOR SOFT SUSPENSION (PITCH EXCITATION)

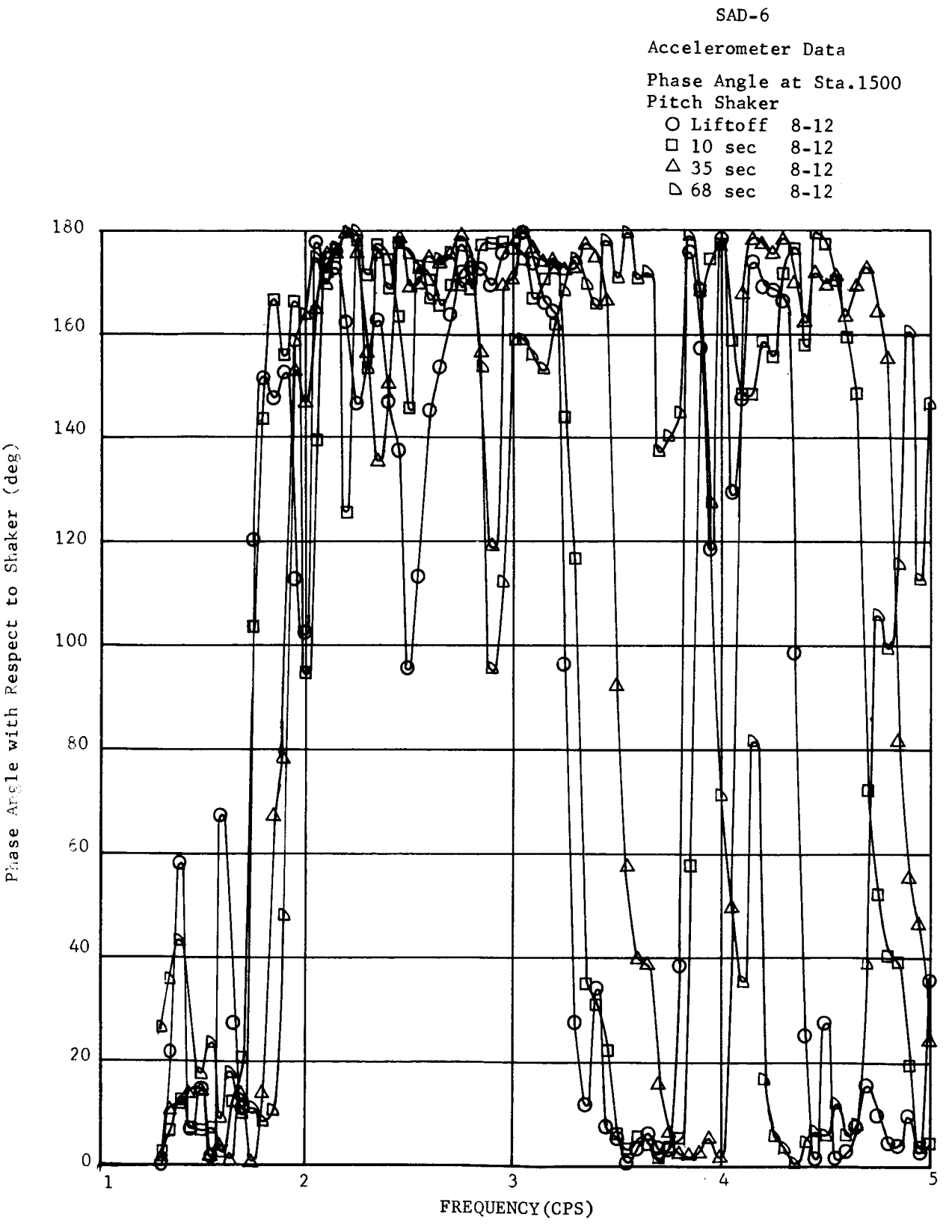


FIGURE 20 PHASE ANGLE AT IU FOR HARD SUSPENSION (PITCH EXCITATION)

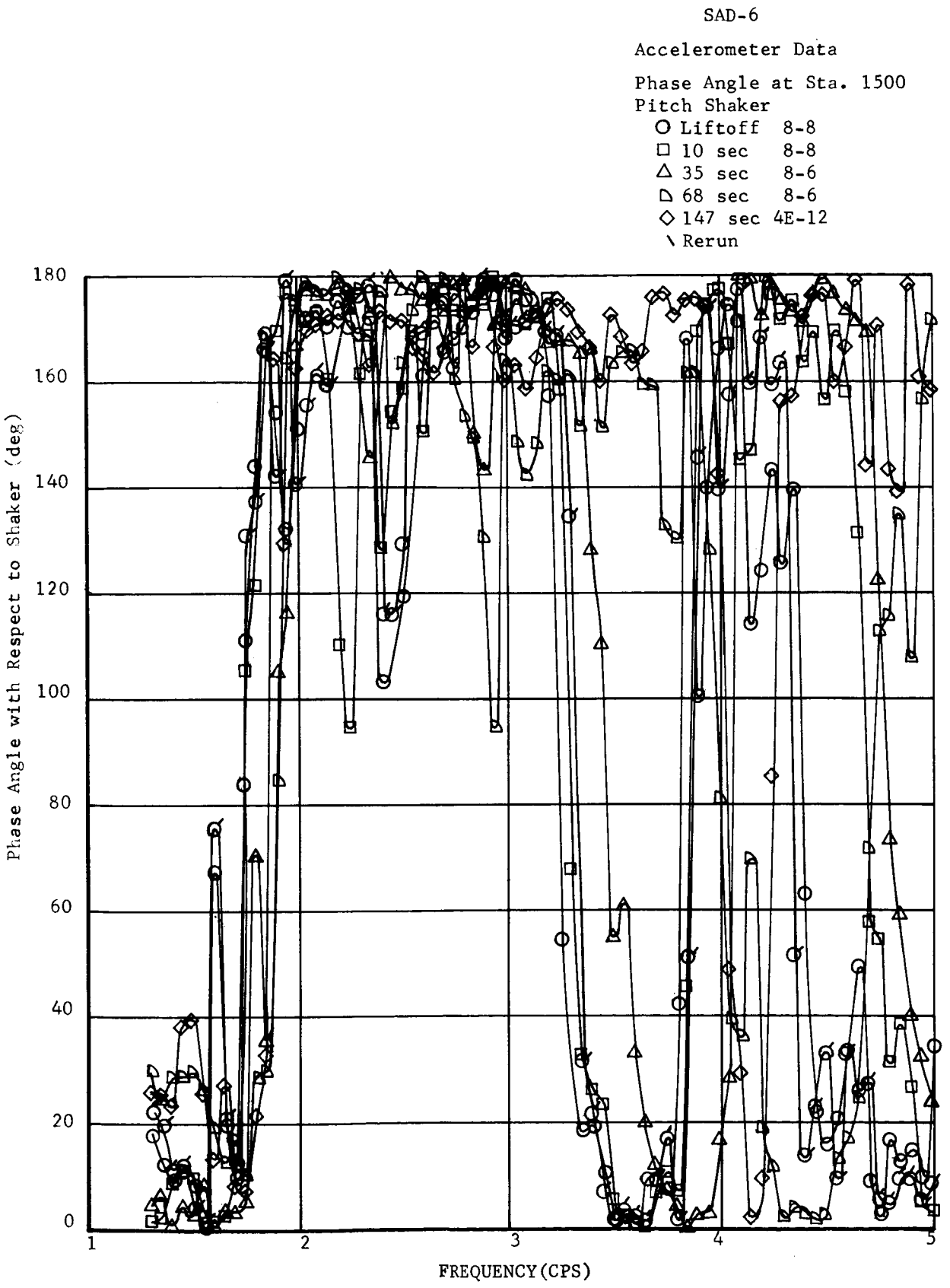


FIGURE 21 PHASE ANGLE AT IU FOR MEDIUM SUSPENSION (PITCH EXCITATION)

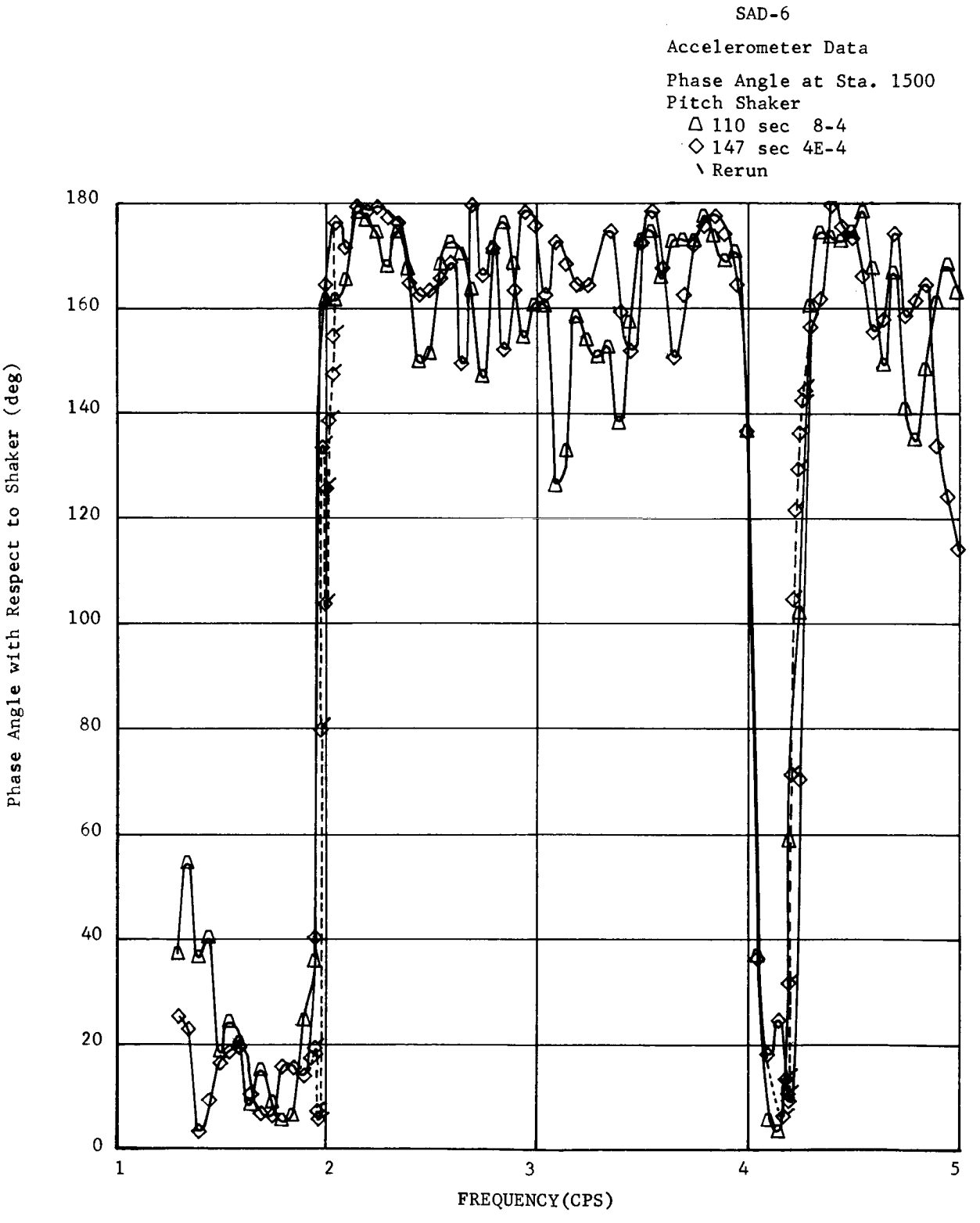


FIGURE 22 PHASE ANGLE AT IU FOR SOFT SUSPENSION (PITCH EXCITATION)

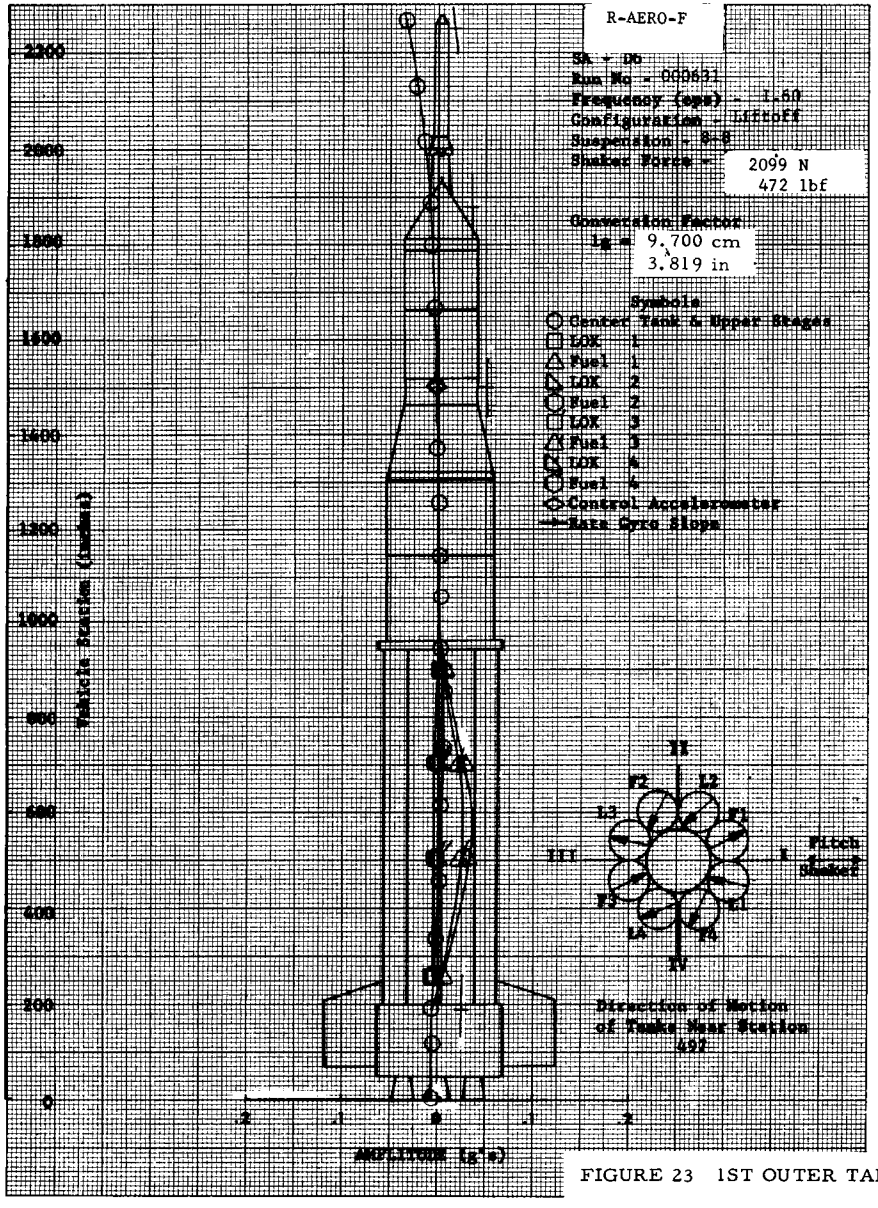


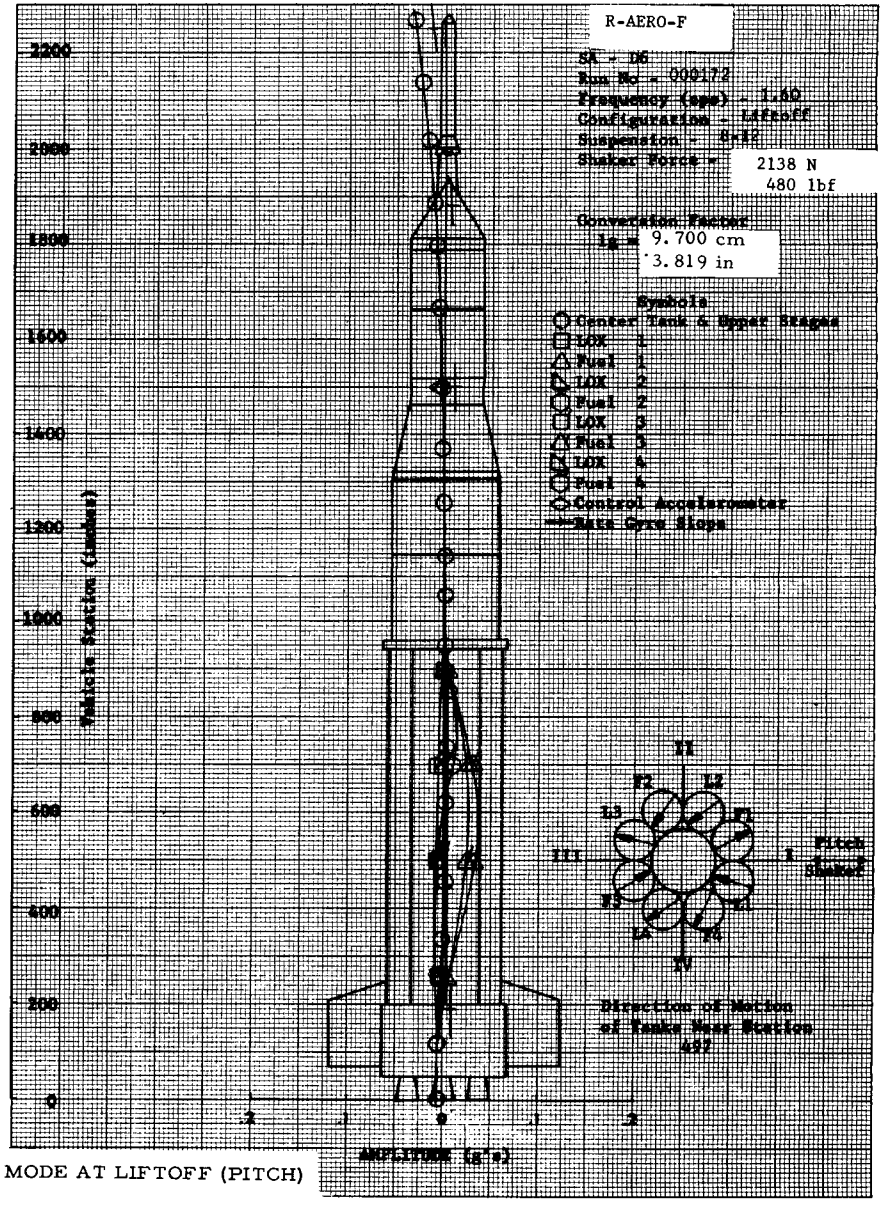


FIGURE 23 1ST OUTER TANK MODE AT LIFTOFF (PITCH)

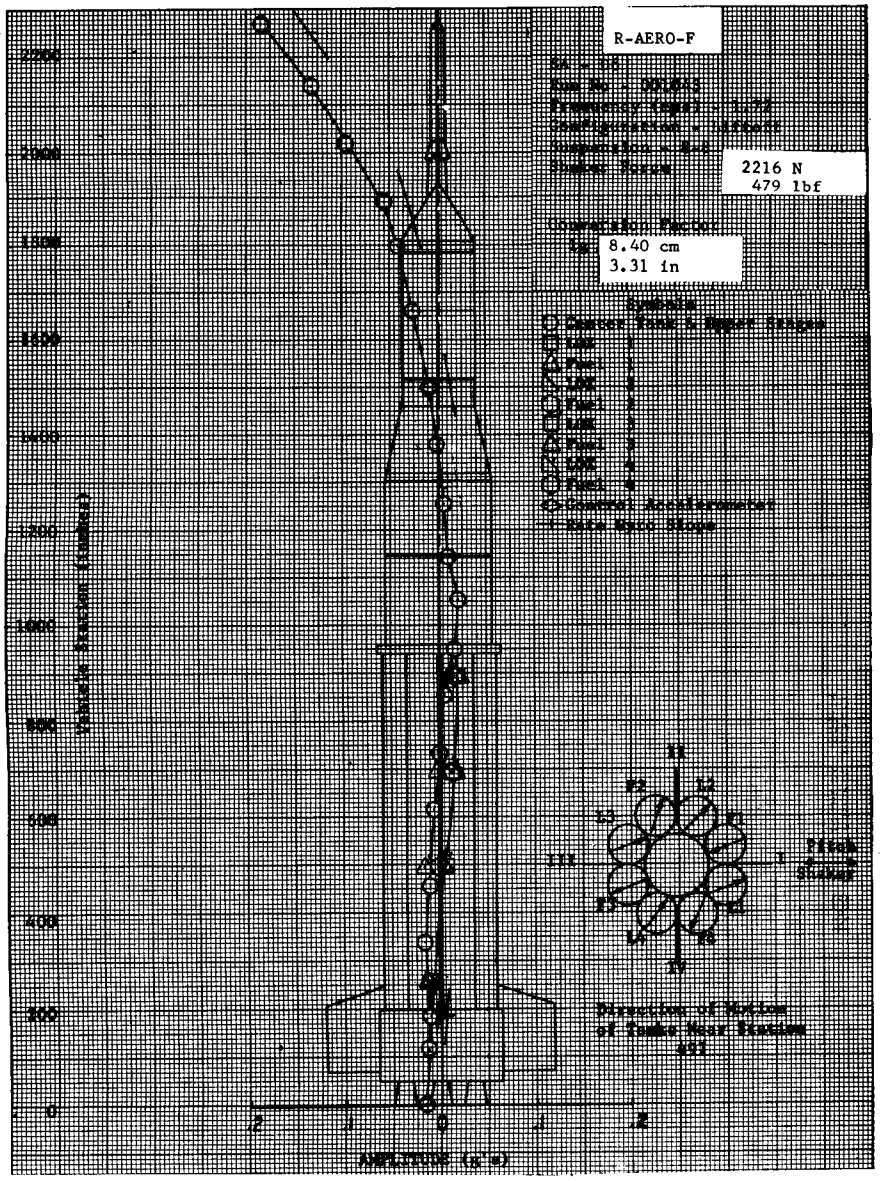


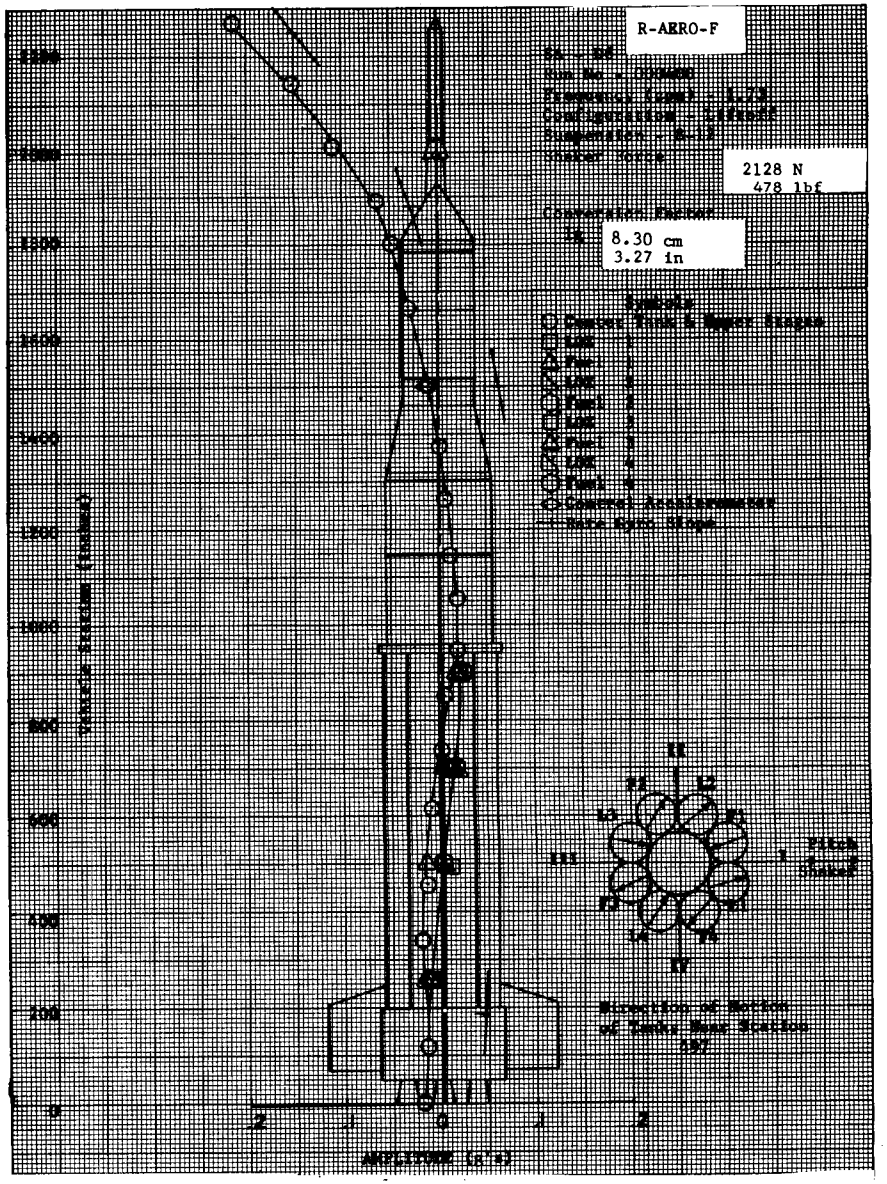


FIGURE 24 1ST BENDING MODE AT LIFTOFF (PITCH)

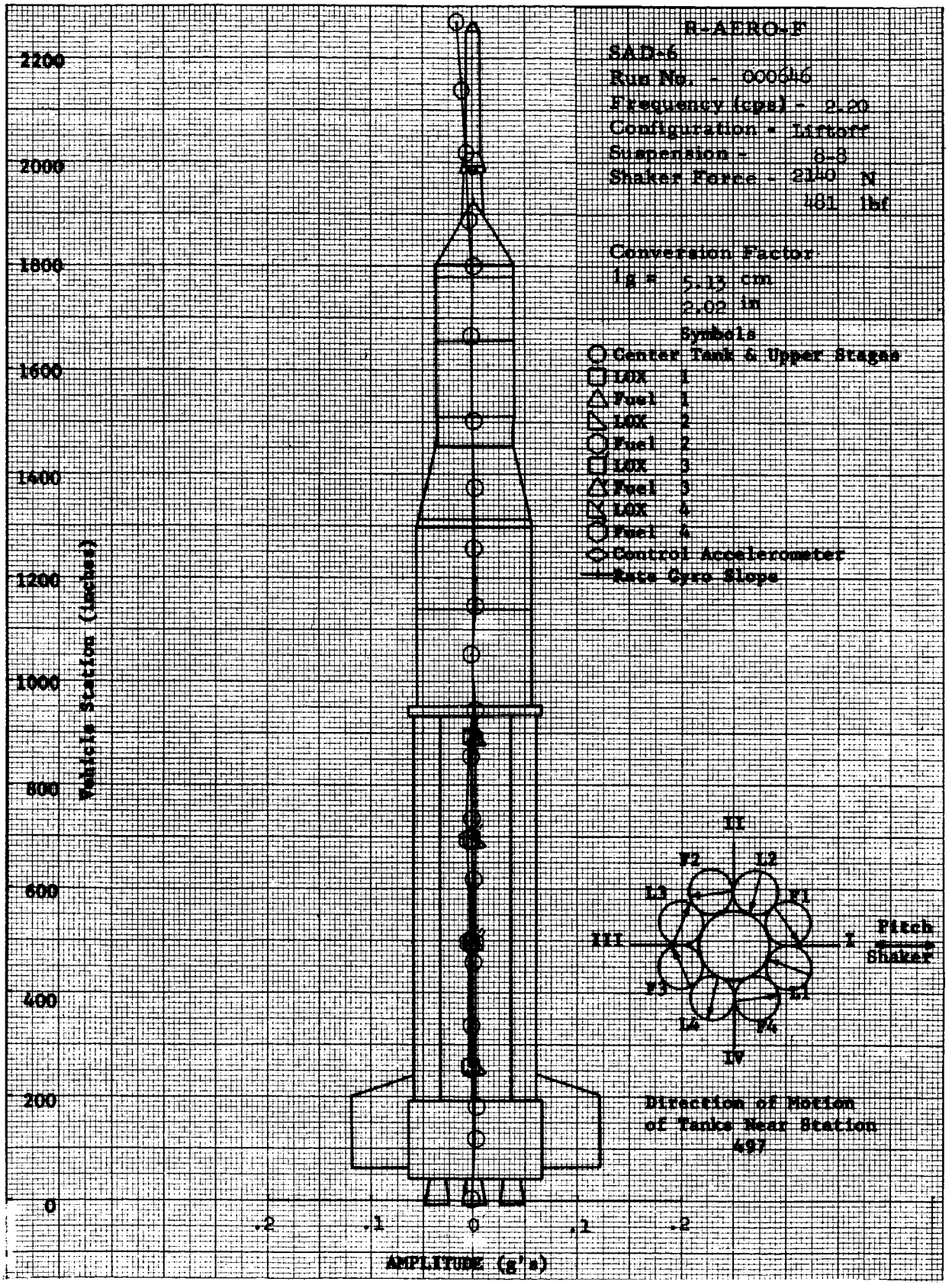


FIGURE 25 2ND OUTER TANK MODE AT LIFTOFF (PITCH)

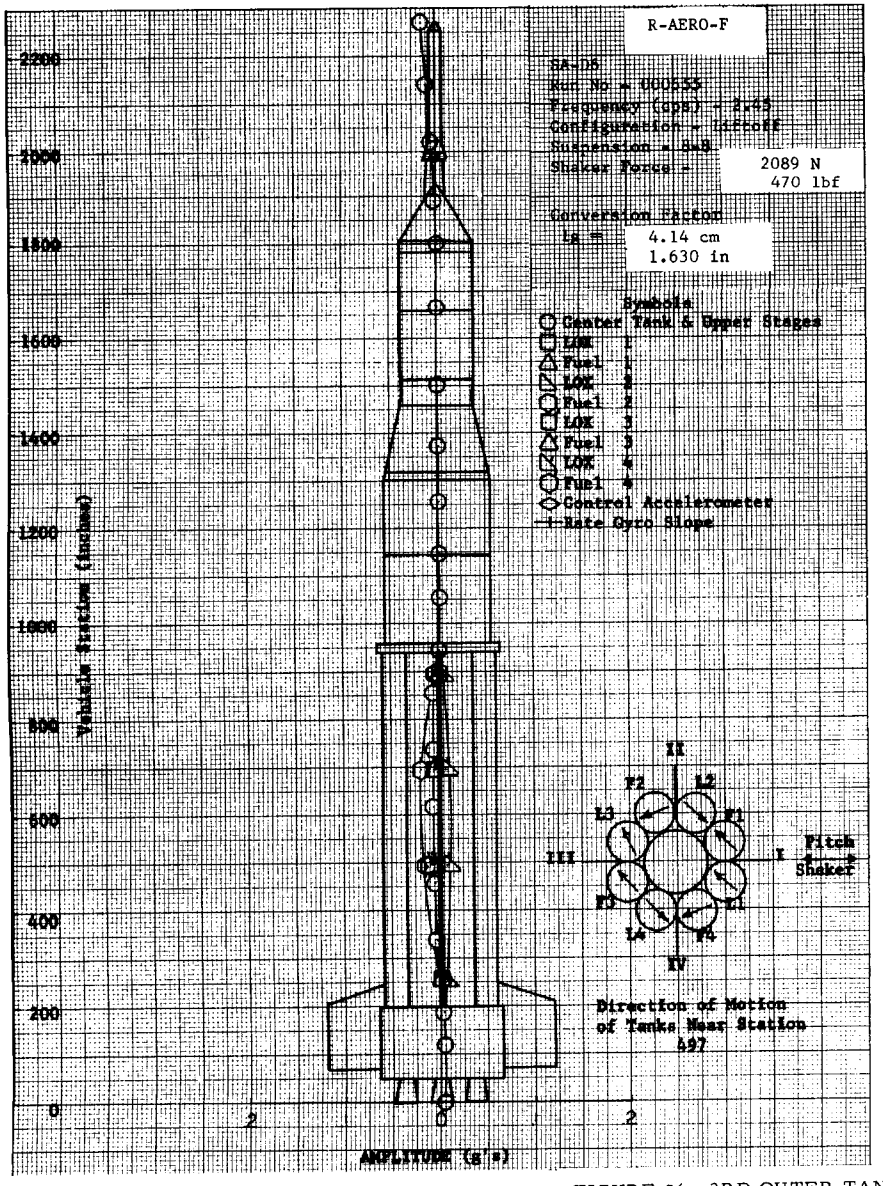


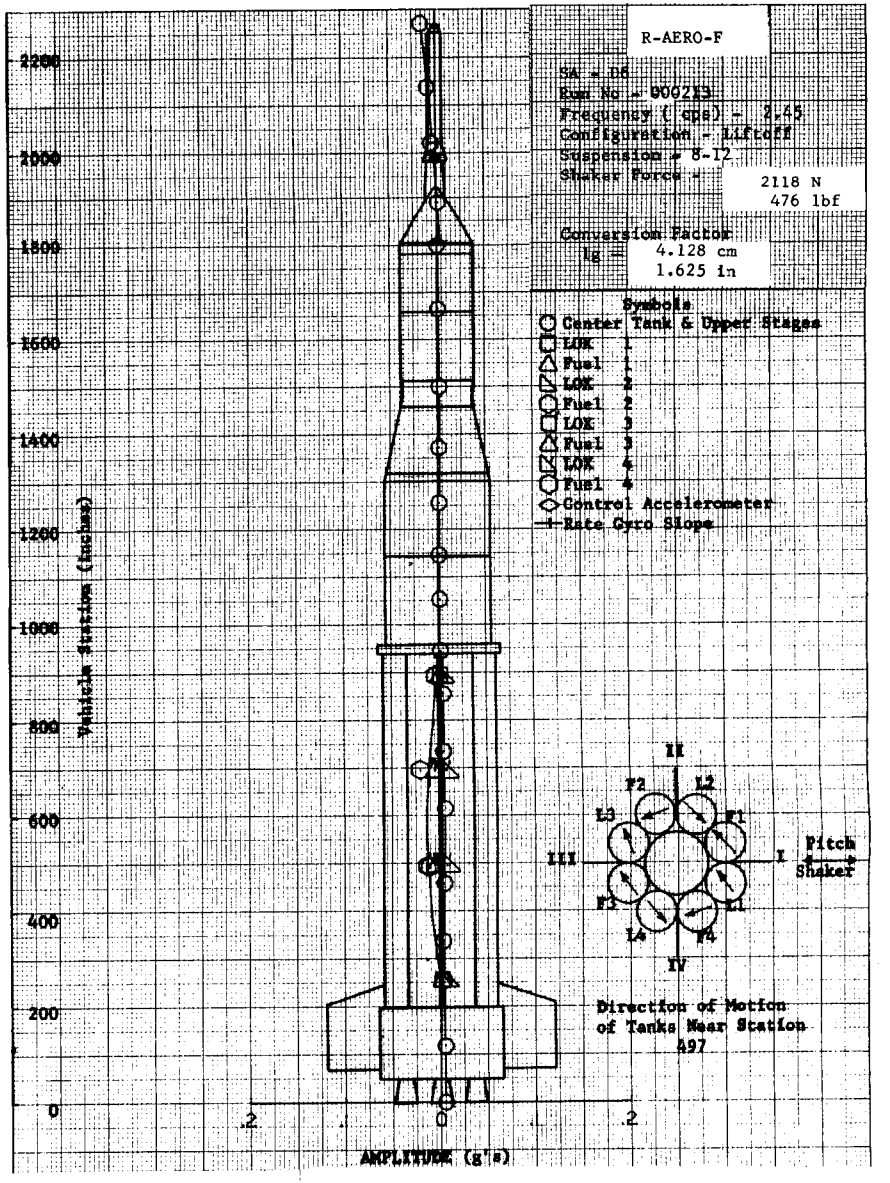


FIGURE 26 3RD OUTER TANK MODE AT LIFTOFF (PITCH)

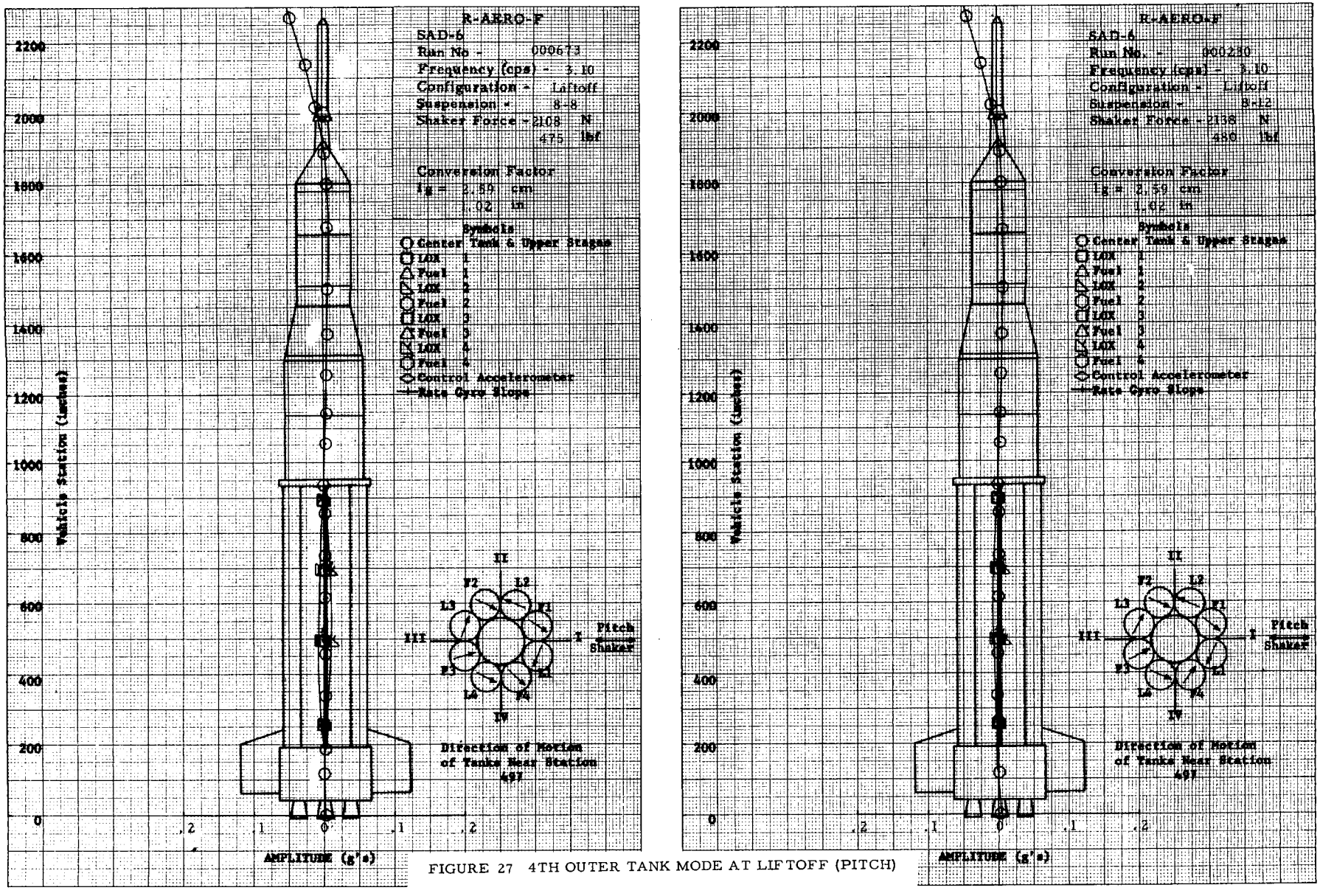


FIGURE 27 4TH OUTER TANK MODE AT LIFTOFF (PITCH)

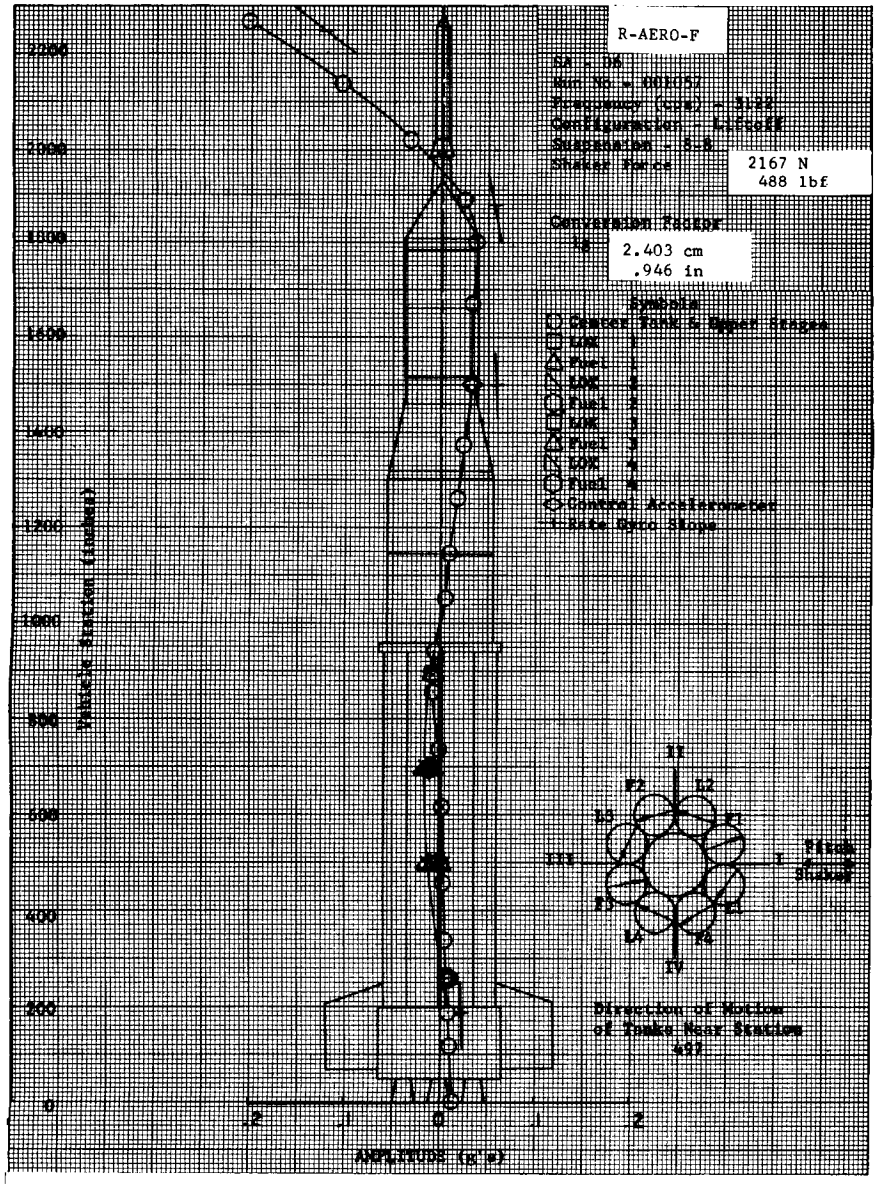


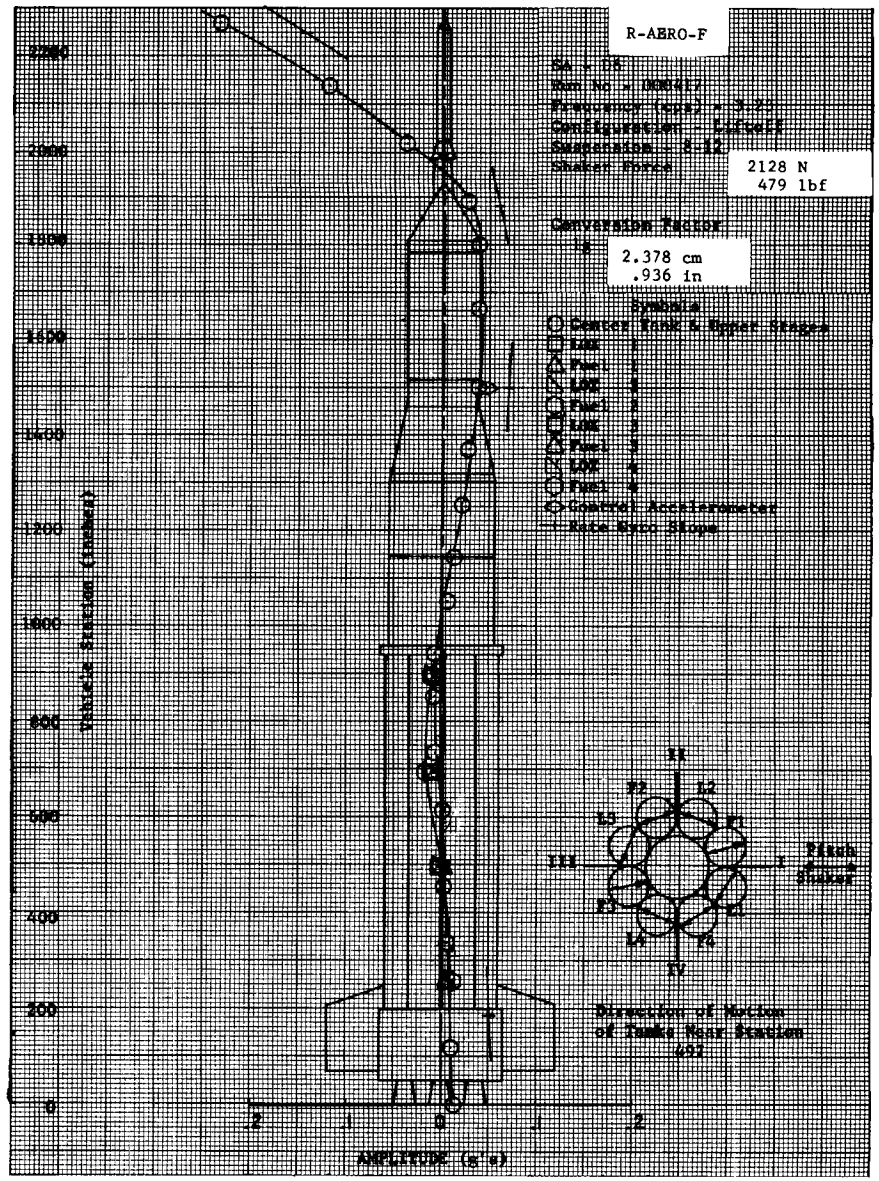


FIGURE 28 2ND BENDING MODE AT LIFTOFF (PITCH)

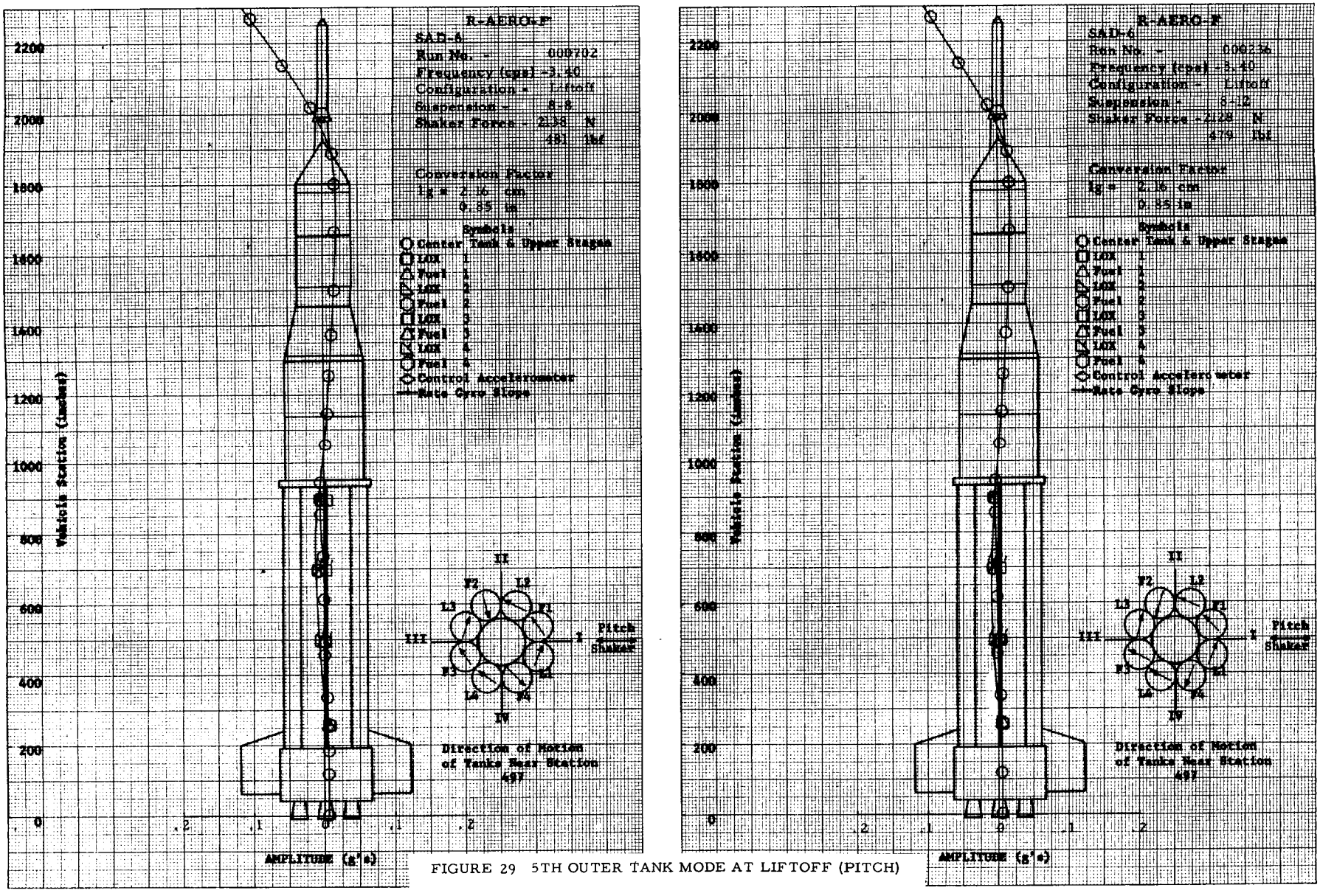


FIGURE 29 5TH OUTER TANK MODE AT LIFTOFF (PITCH)

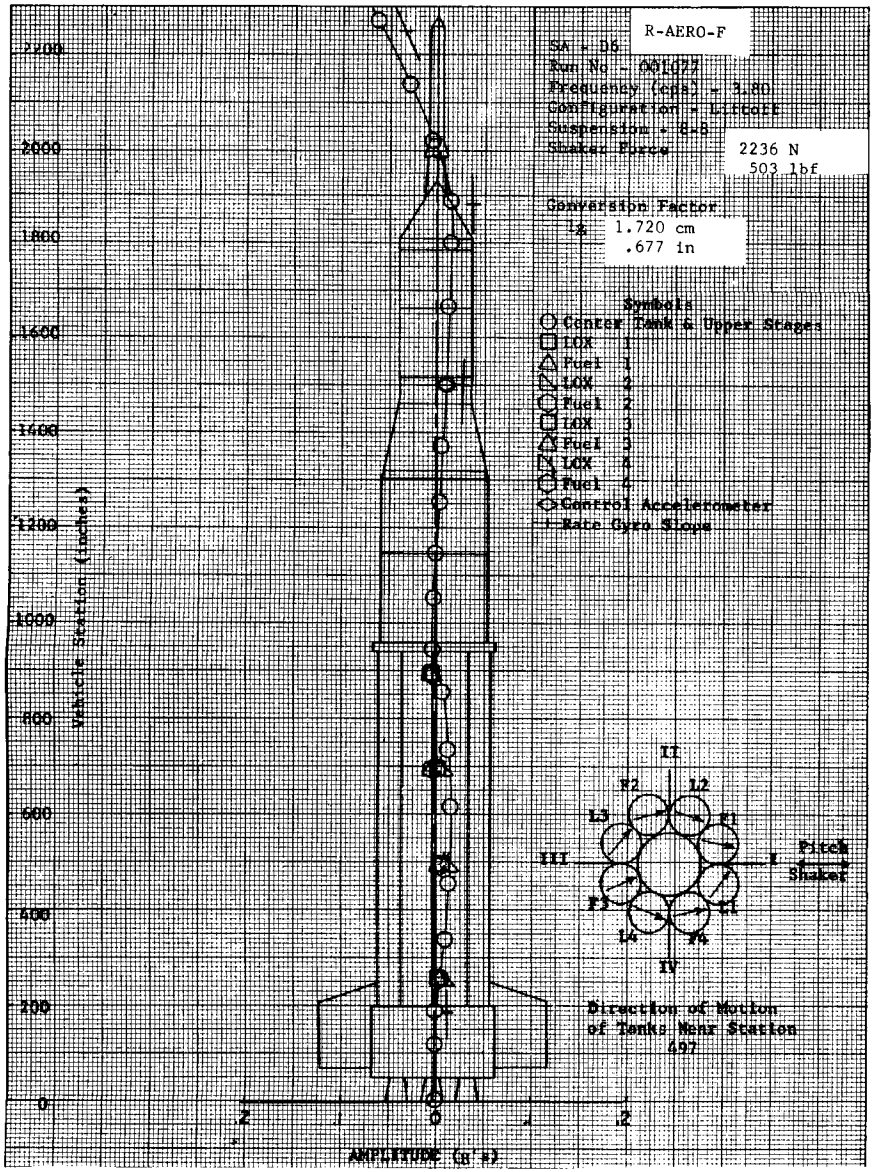


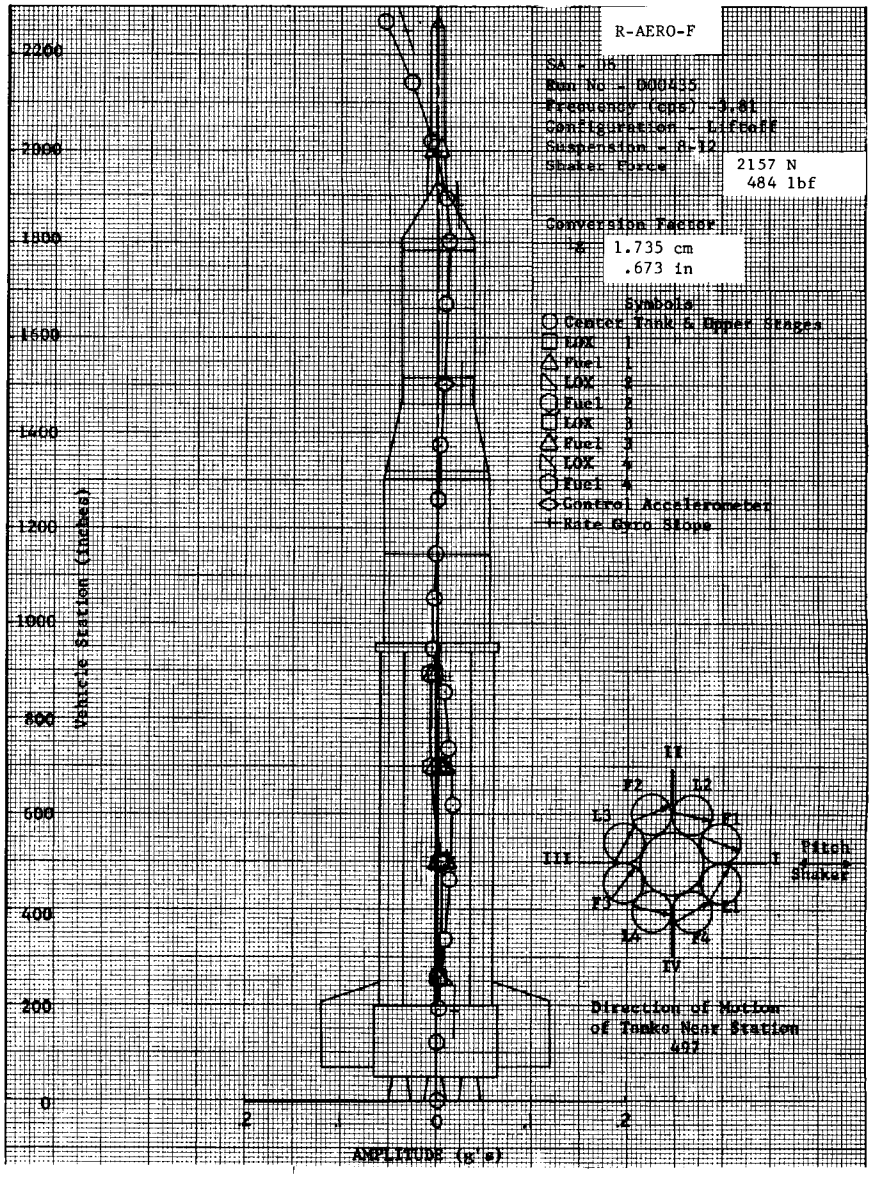


FIGURE 30 3RD BENDING MODE AT LIFTOFF (PITCH)

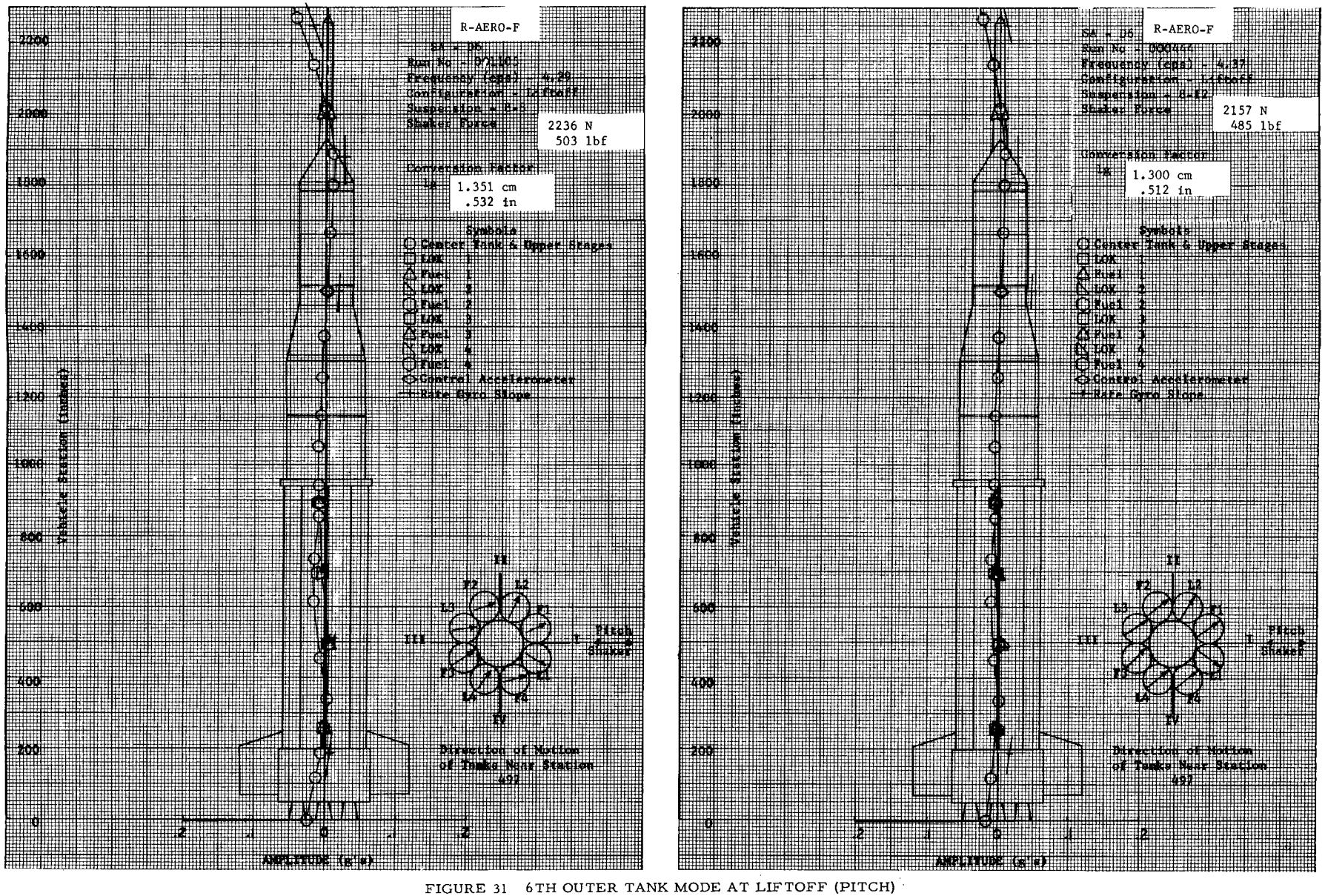


FIGURE 31 6TH OUTER TANK MODE AT LIFTOFF (PITCH)

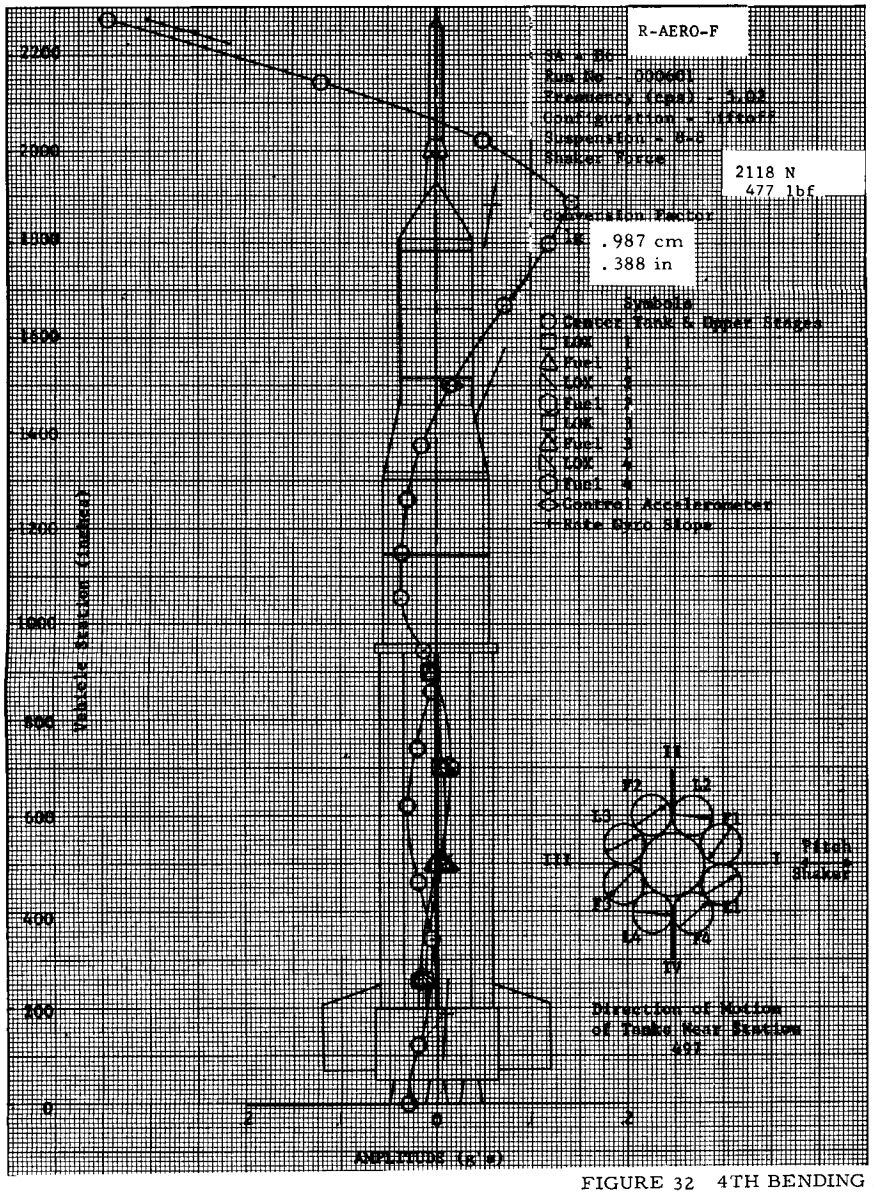


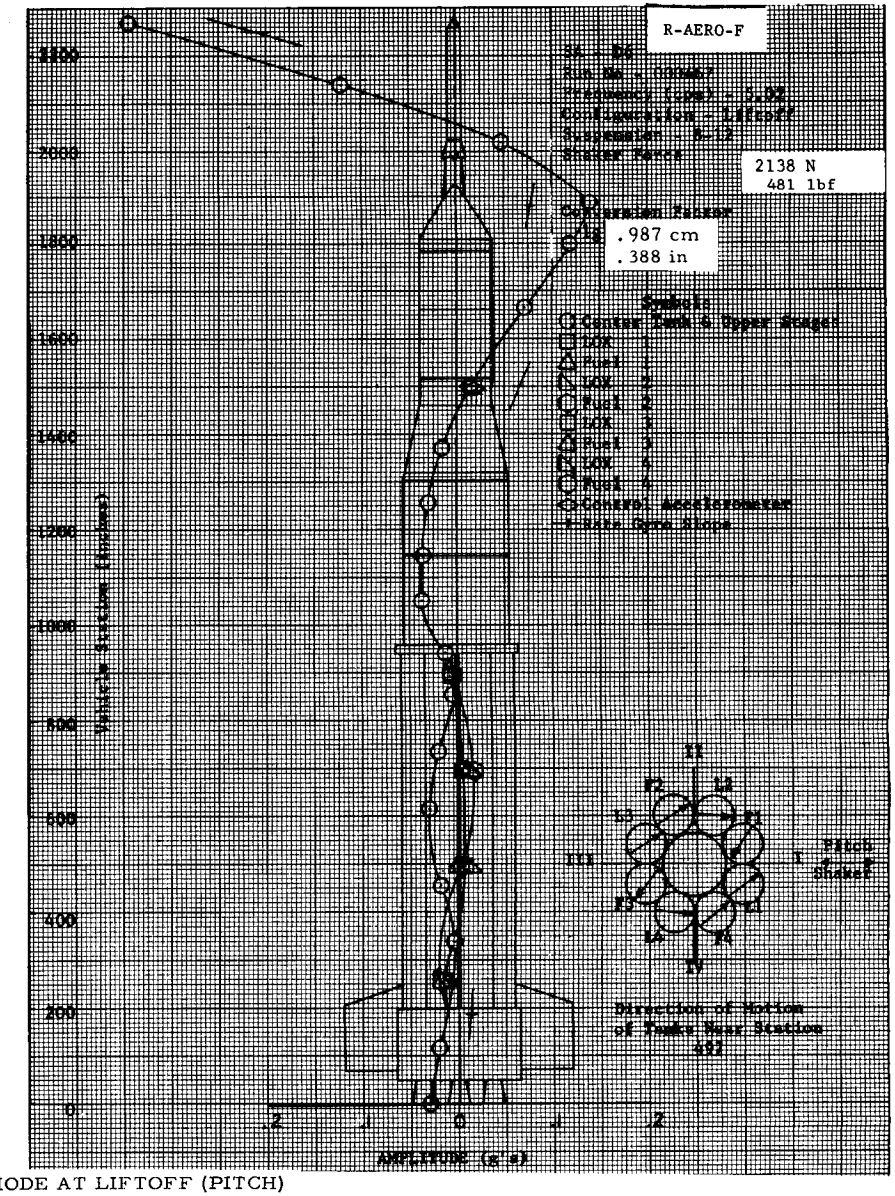


FIGURE 32 4TH BENDING MODE AT LIFTOFF (PITCH)

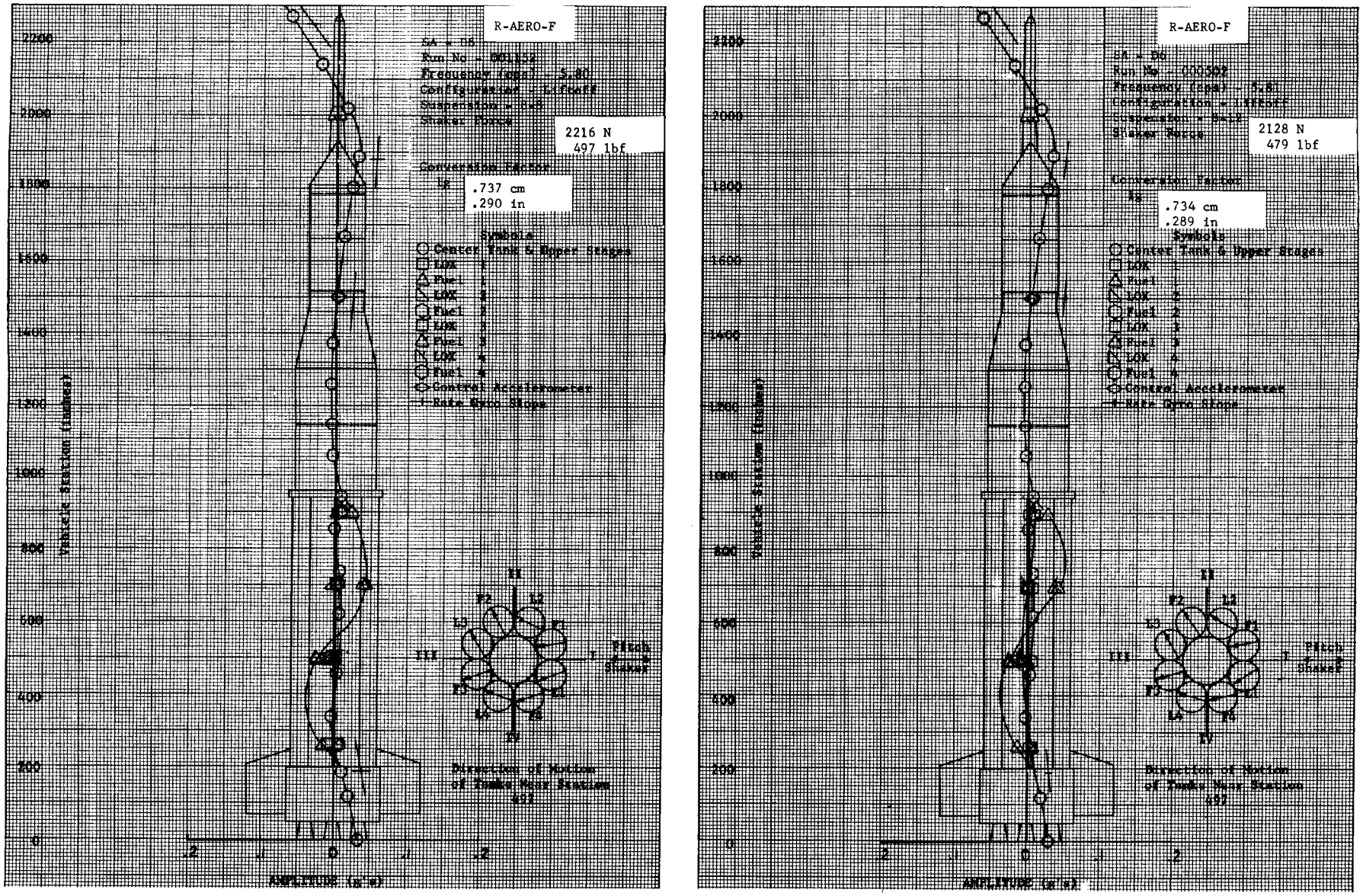


FIGURE 33 COUPLED MODE AT LIFTOFF (PITCH)

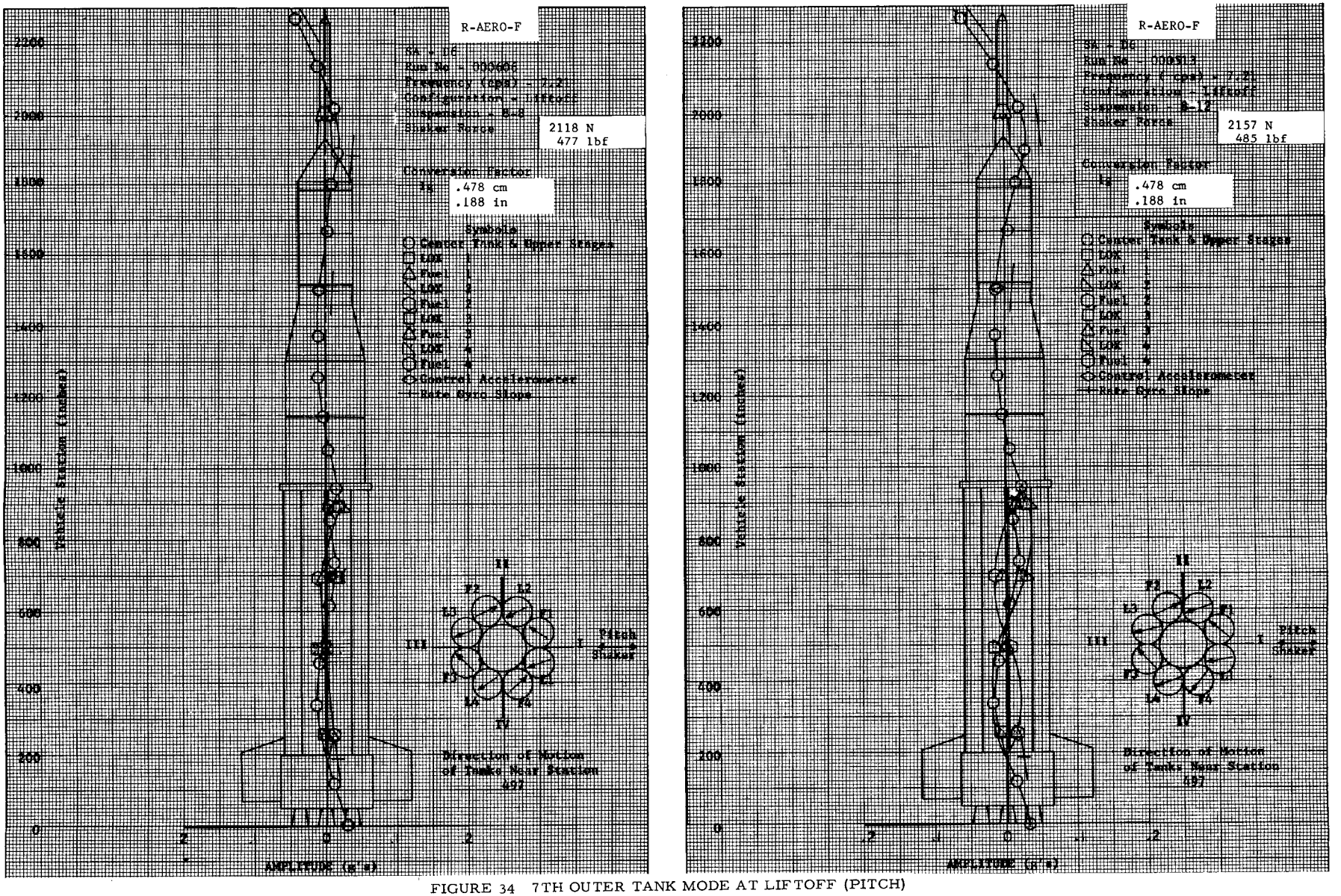


FIGURE 34 7TH OUTER TANK MODE AT LIFTOFF (PITCH)

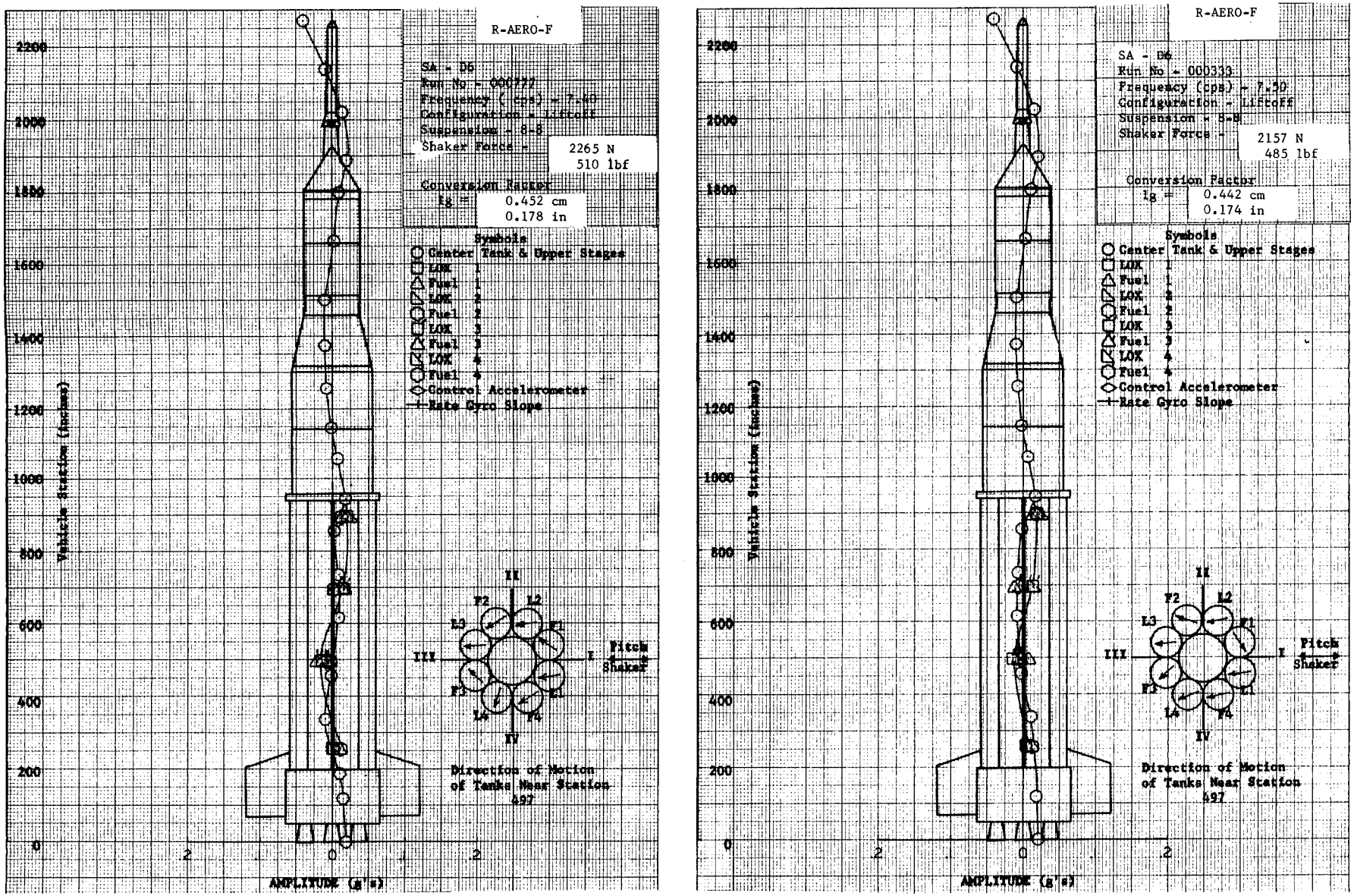


FIGURE 35 S-I ENGINE MODE AT LIFTOFF (PITCH)

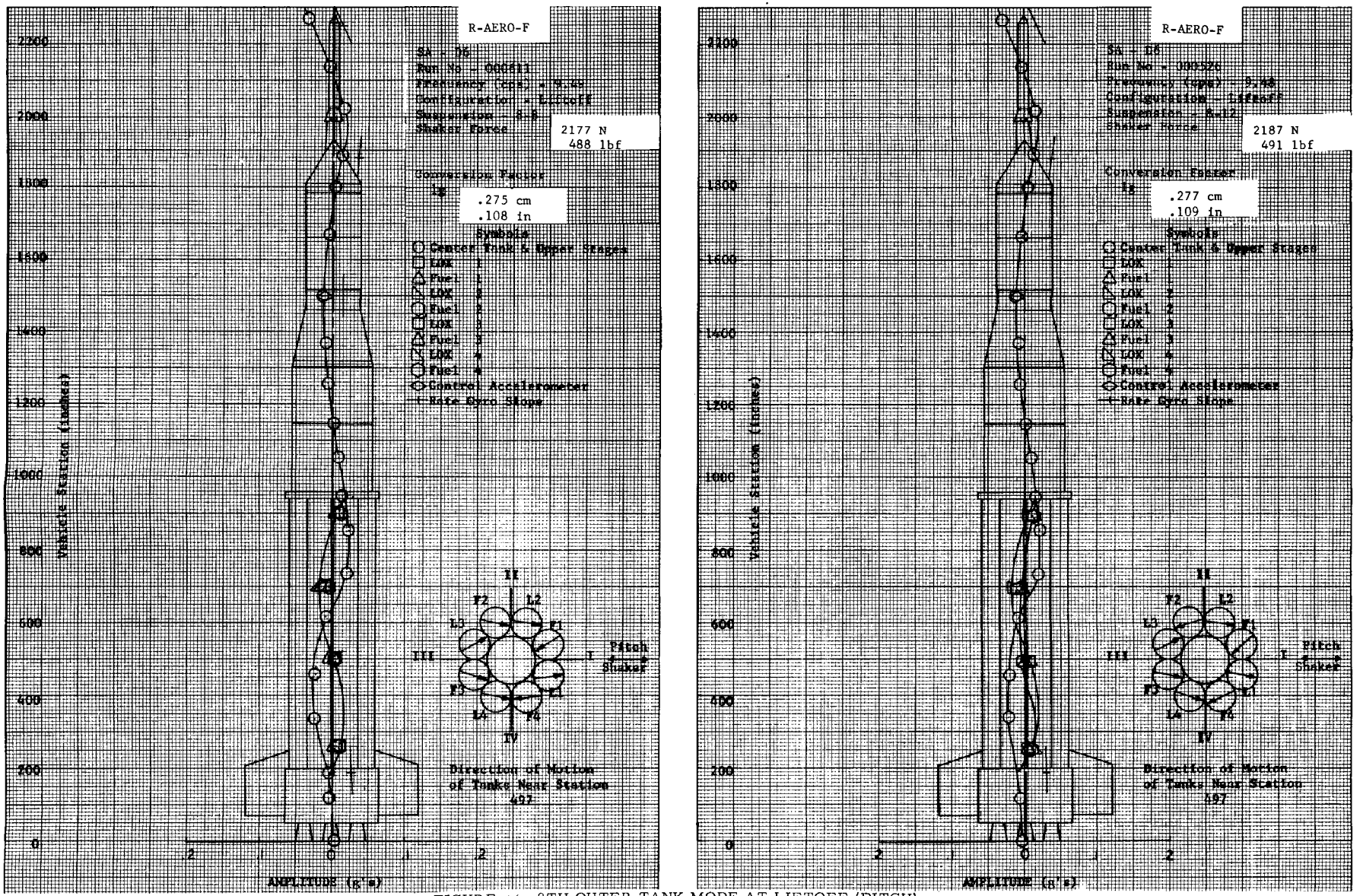


FIGURE 36 8TH OUTER TANK MODE AT LIFTOFF (PITCH)

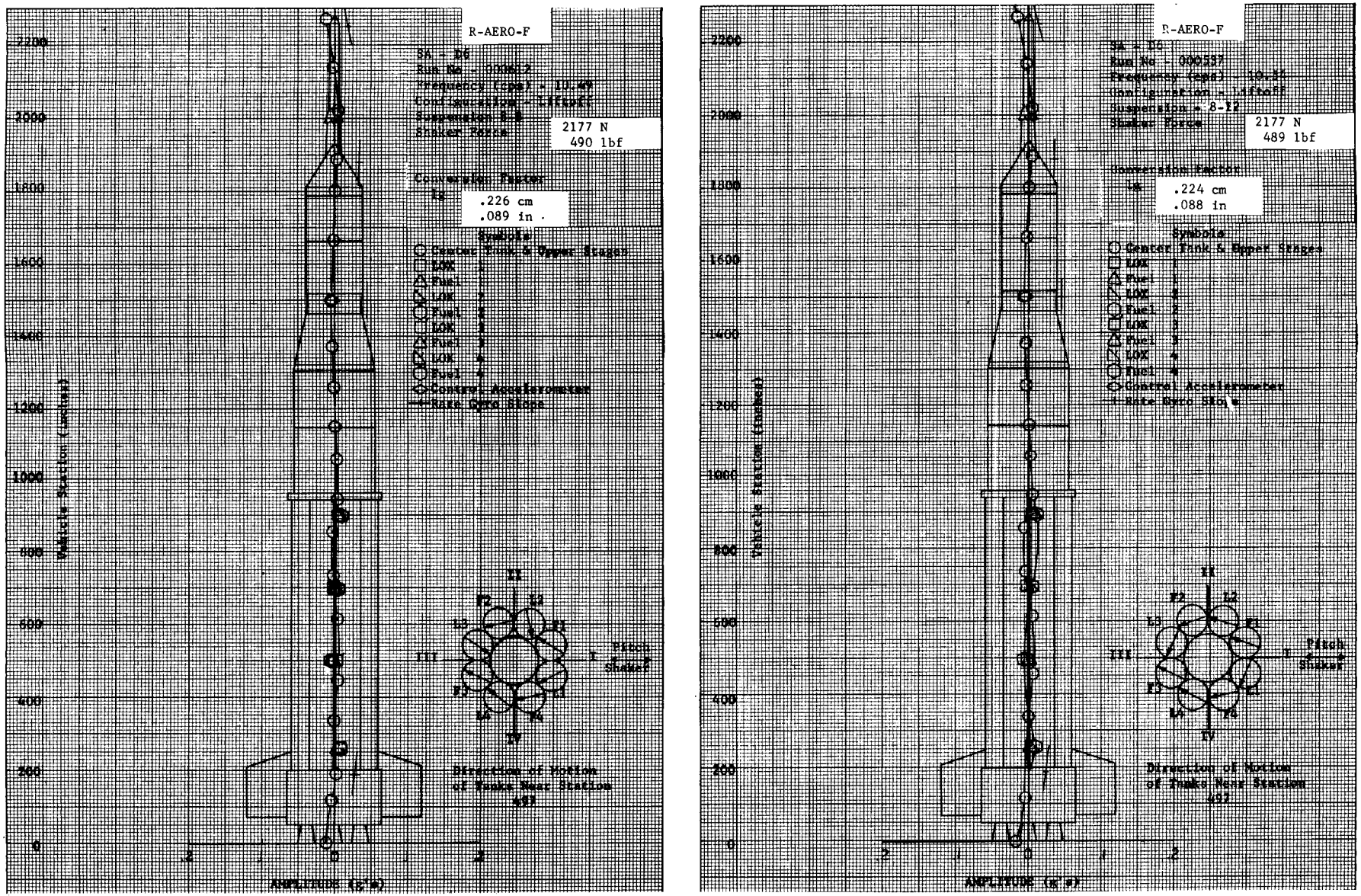


FIGURE 37 5TH BENDING MODE AT LIFTOFF (PITCH)

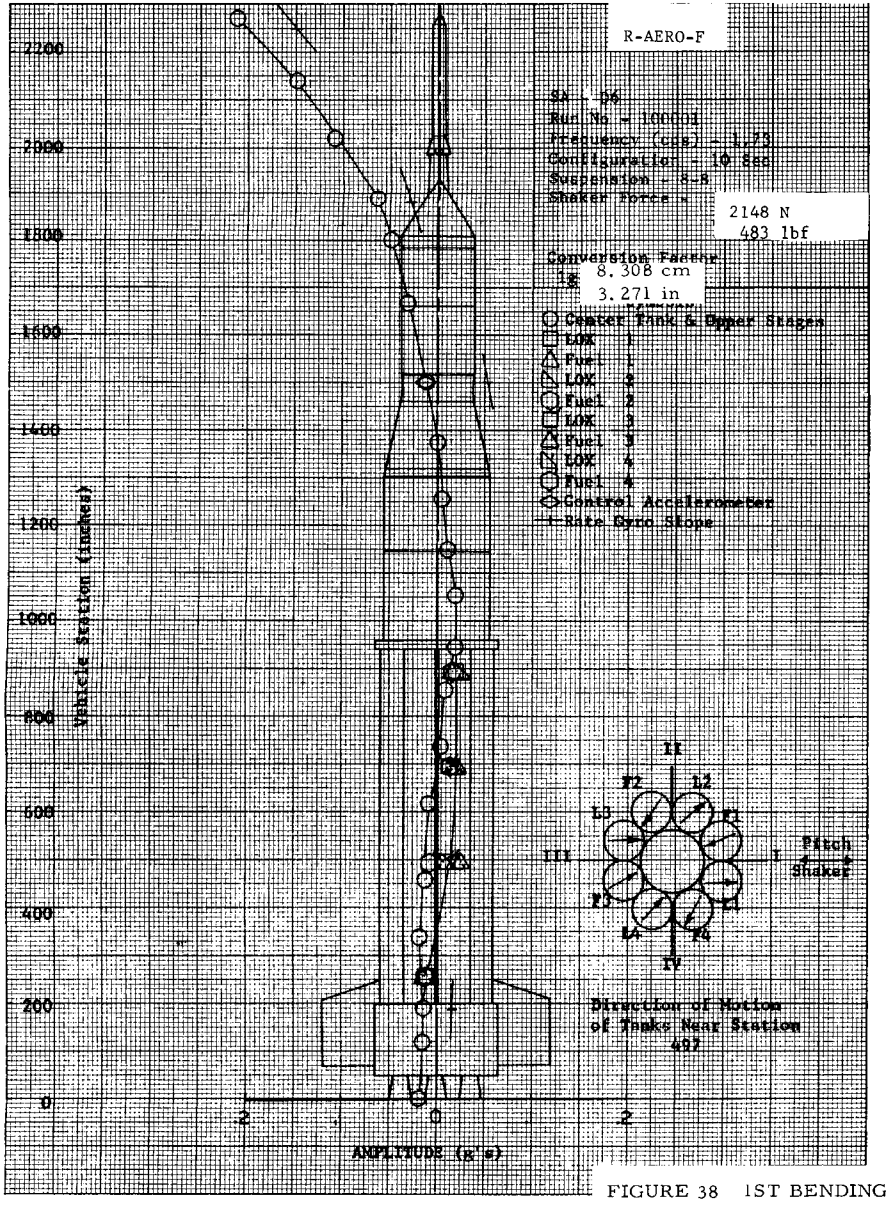


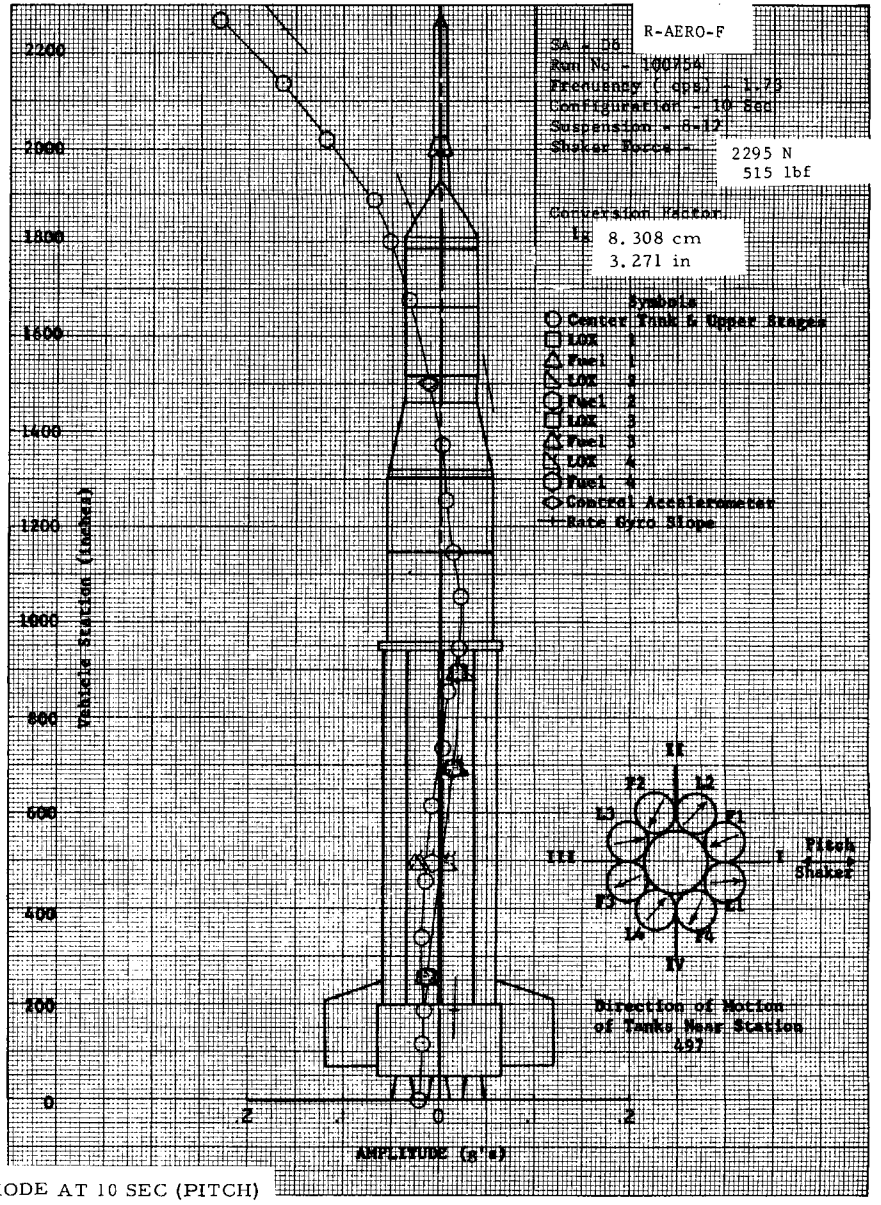


FIGURE 38 1ST BENDING MODE AT 10 SEC (PITCH)

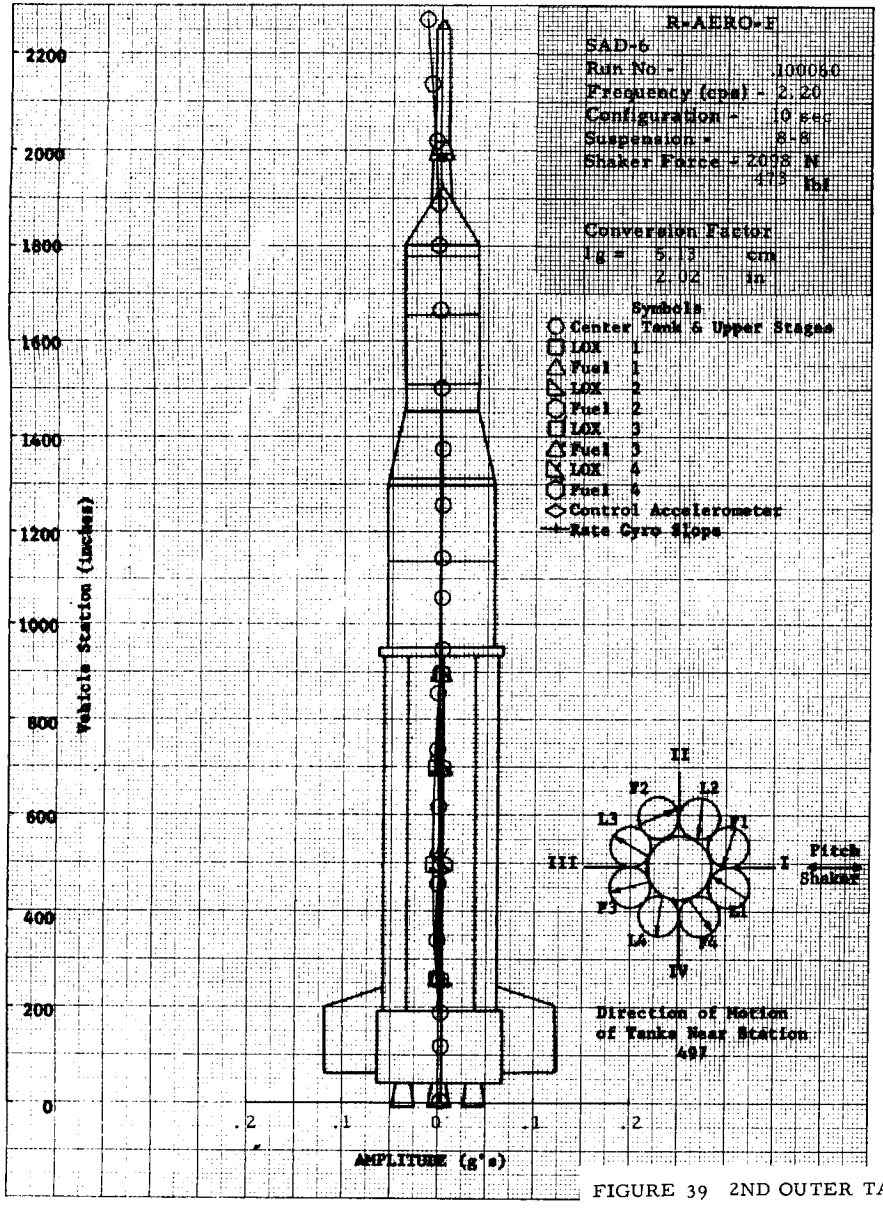


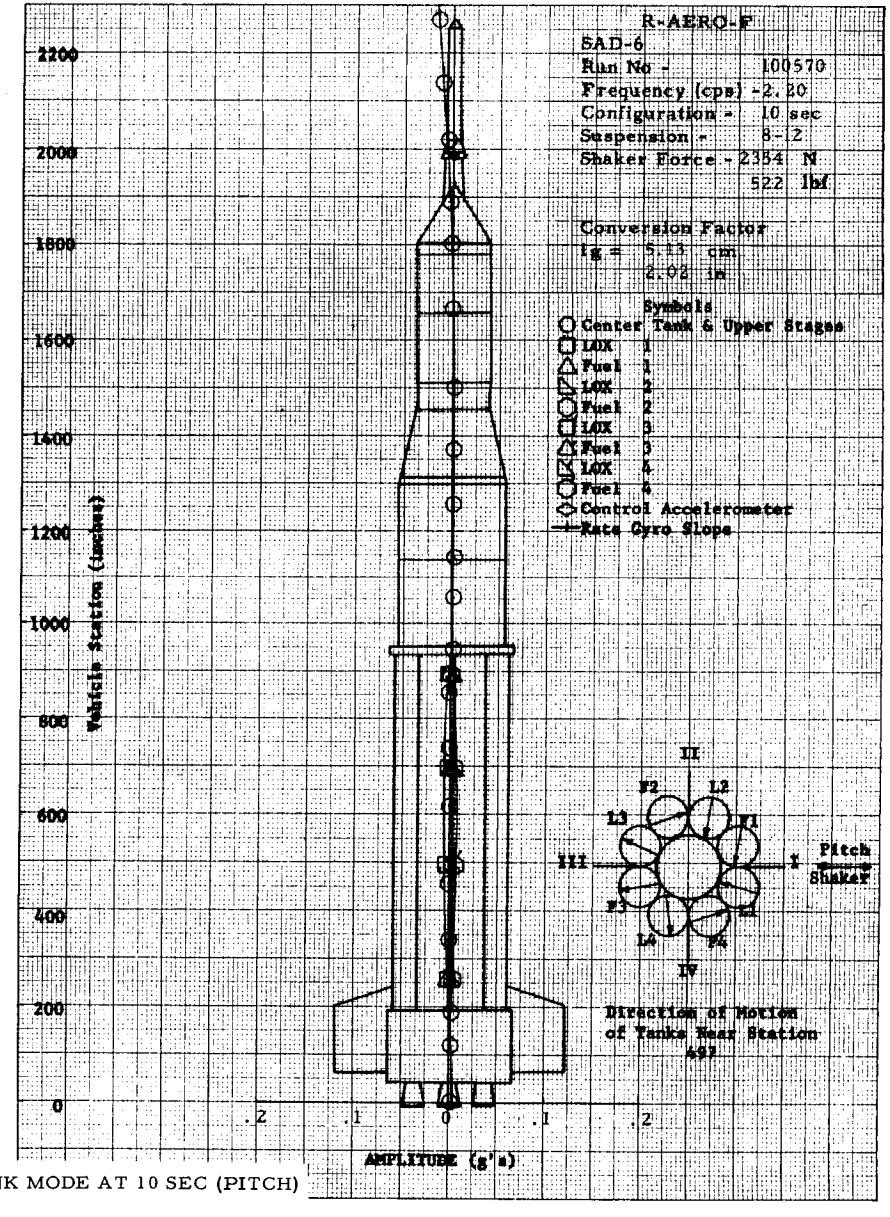


FIGURE 39 2ND OUTER TANK MODE AT 10 SEC (PITCH)

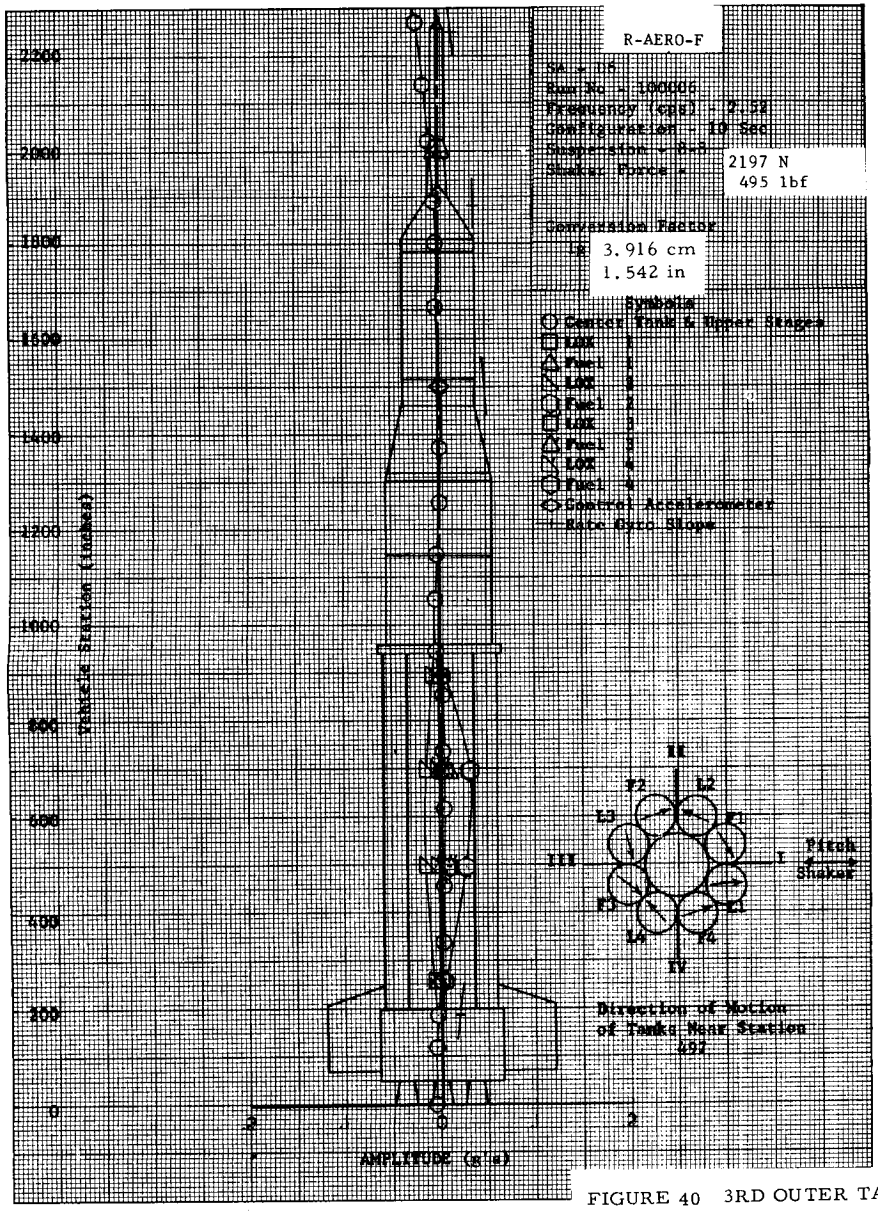


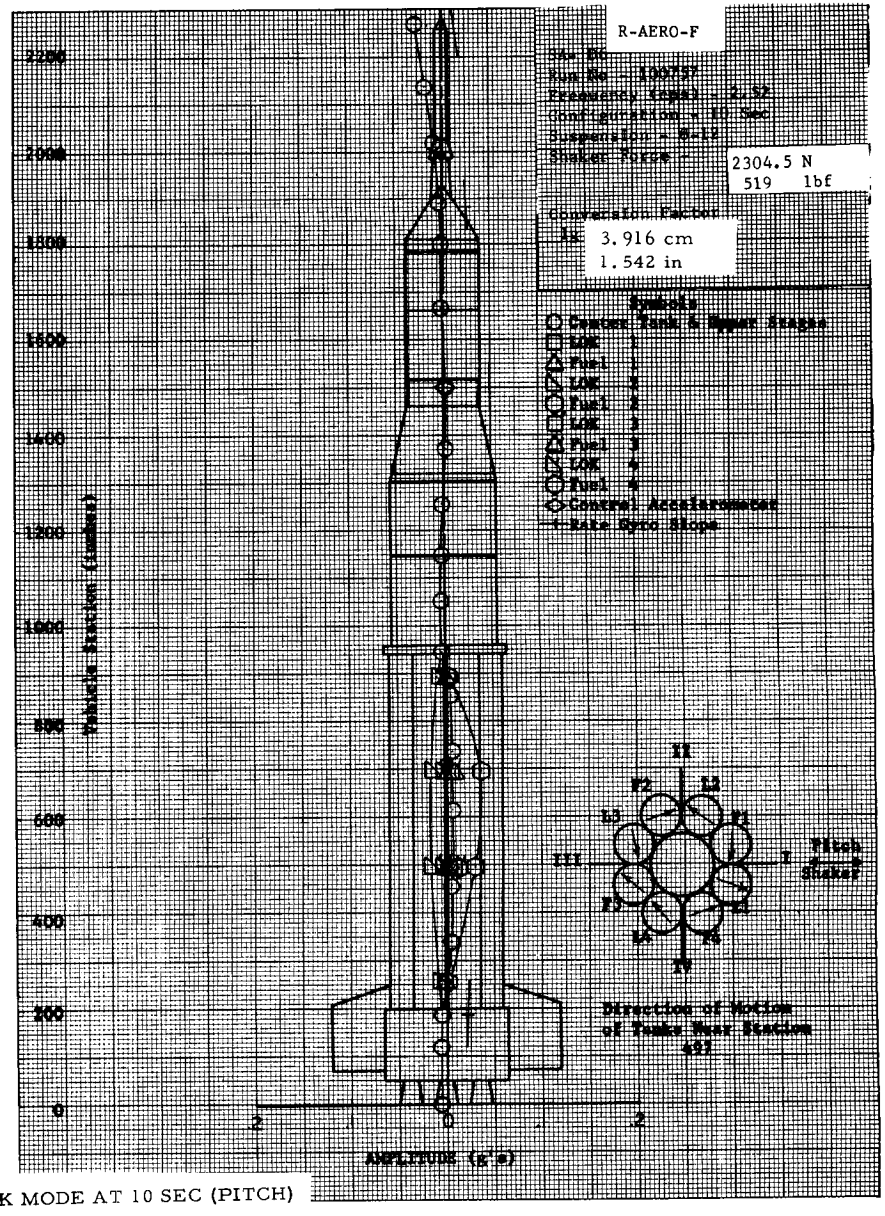


FIGURE 40 3RD OUTER TANK MODE AT 10 SEC (PITCH)

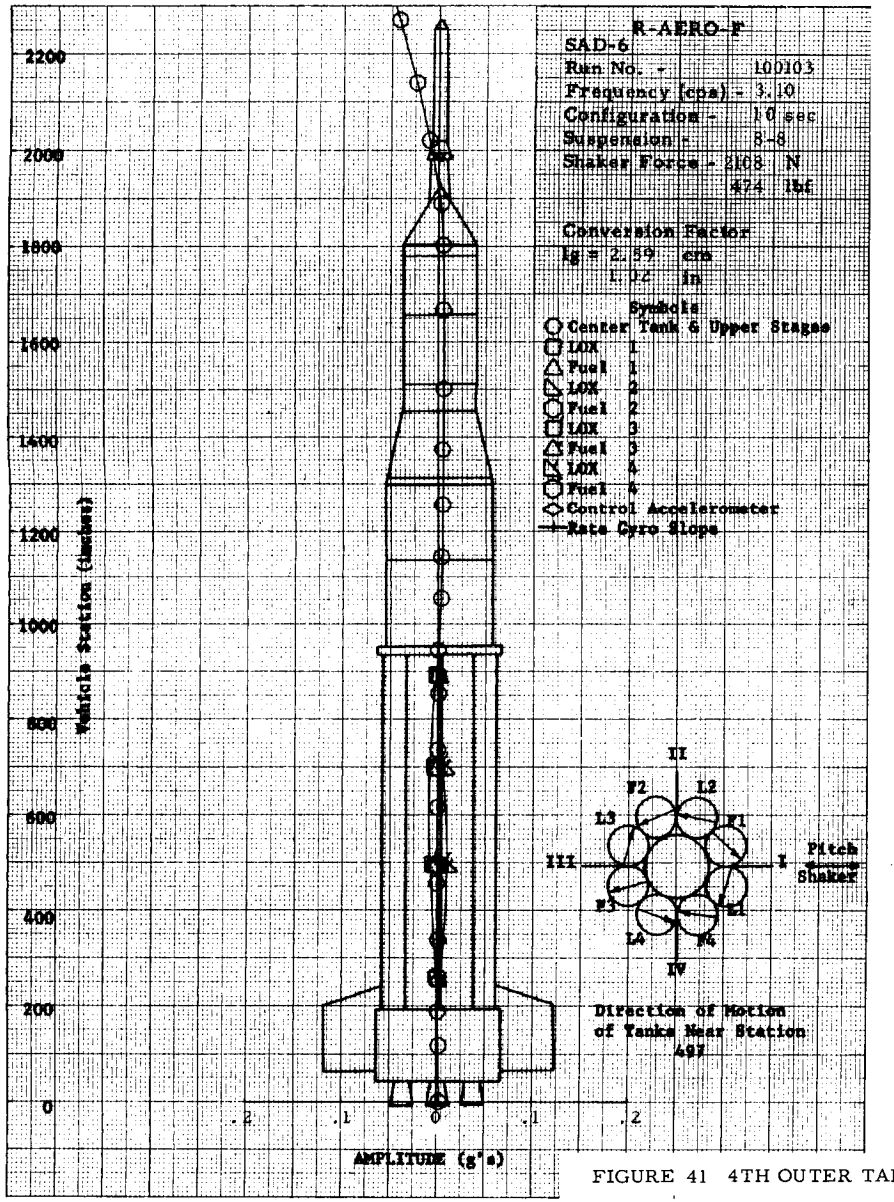


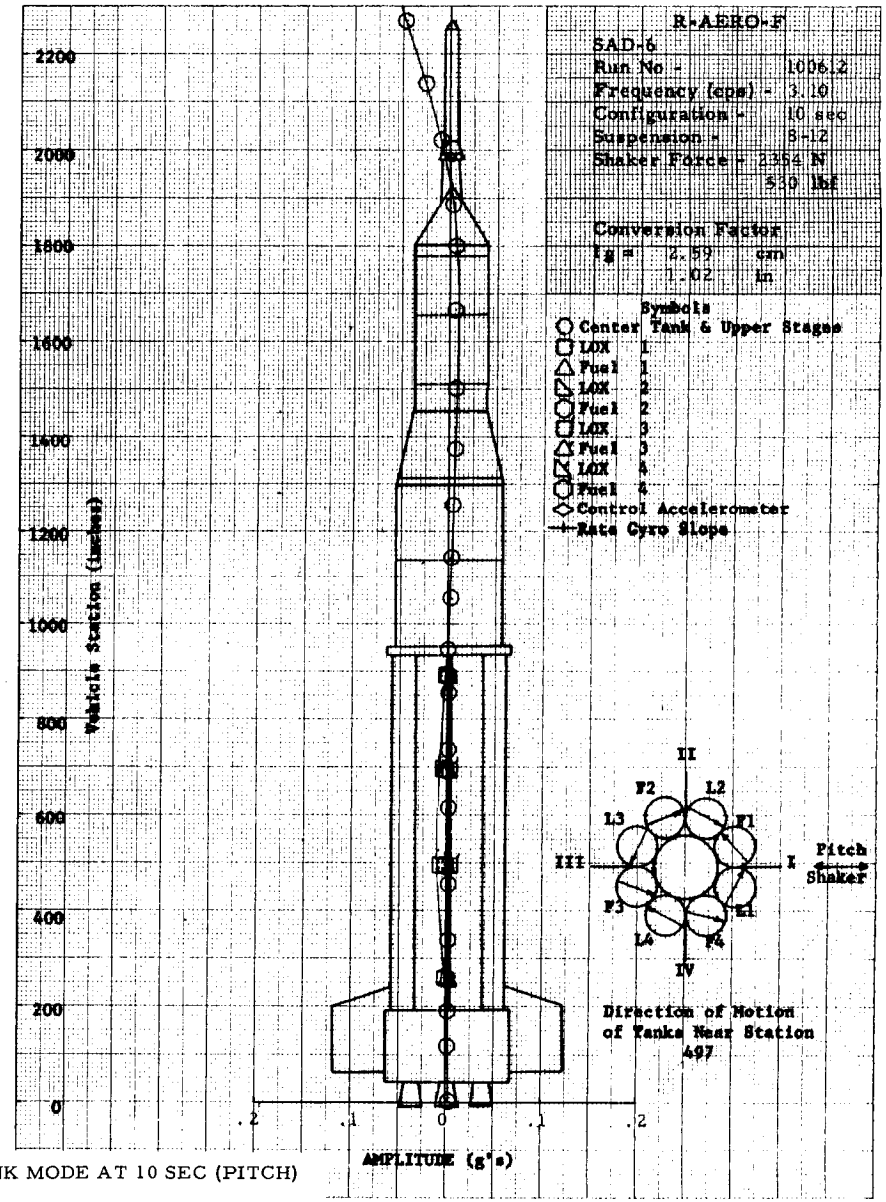


FIGURE 41 4TH OUTER TANK MODE AT 10 SEC (PITCH)

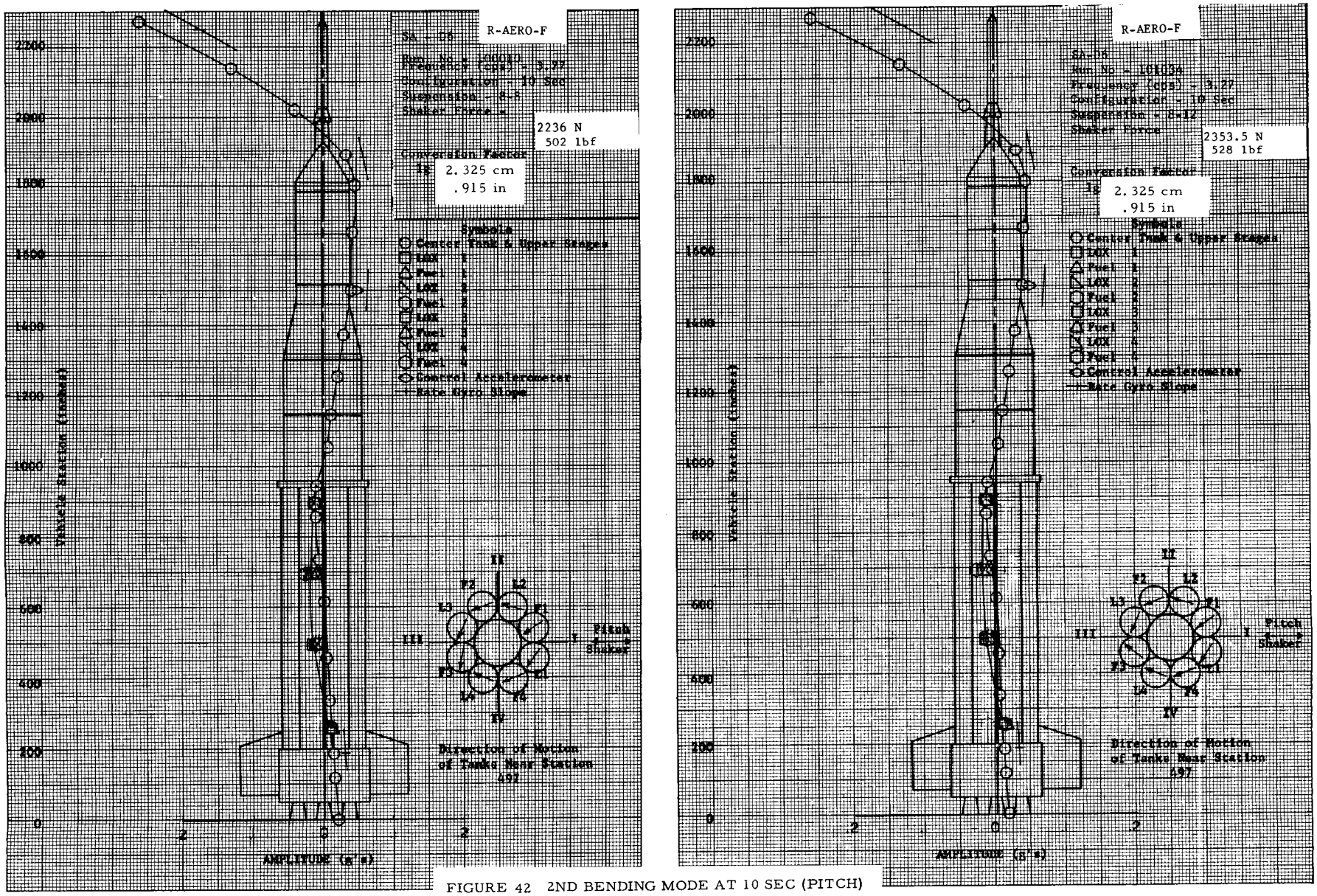


FIGURE 42 2ND BENDING MODE AT 10 SEC (PITCH)

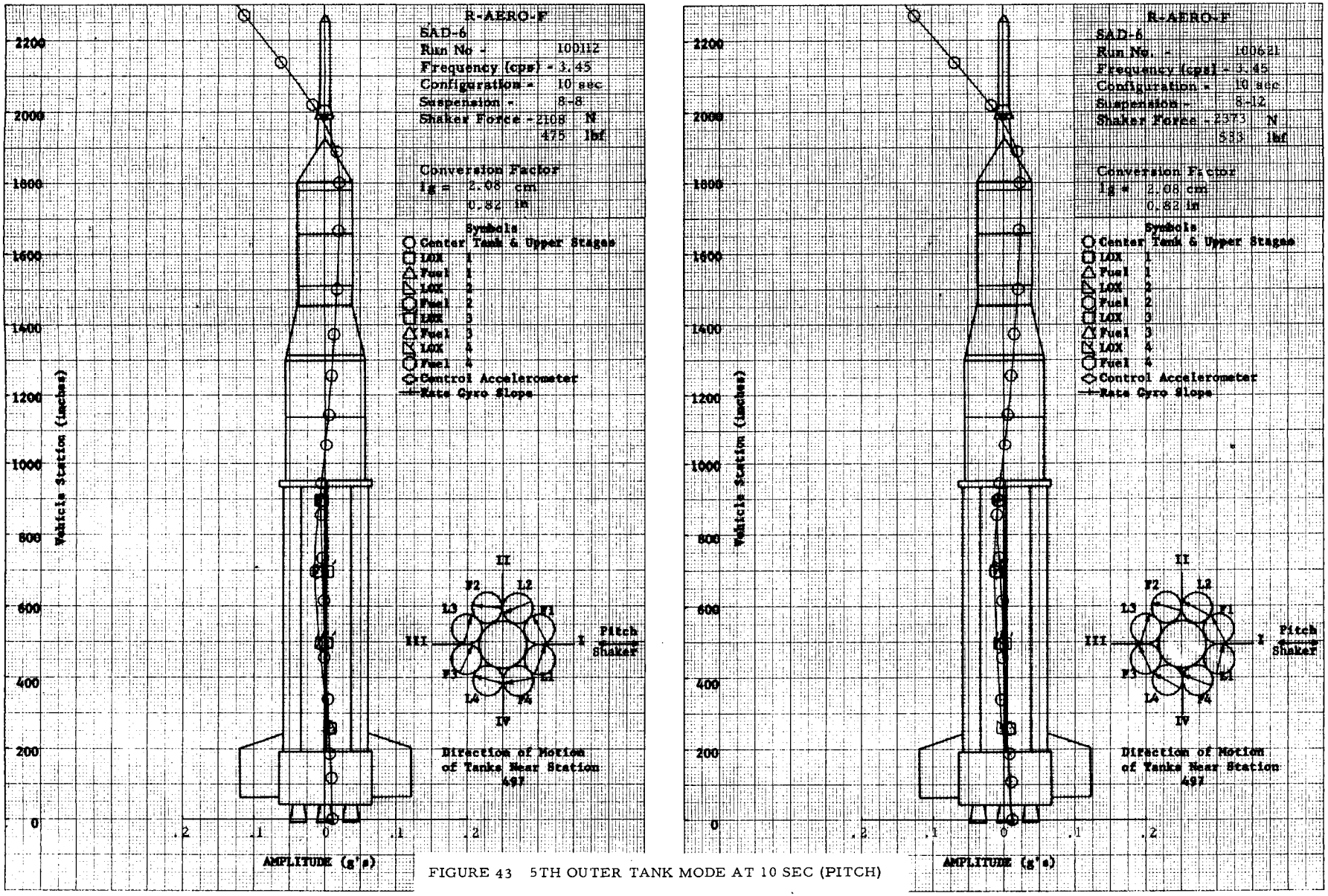


FIGURE 43 5TH OUTER TANK MODE AT 10 SEC (PITCH)

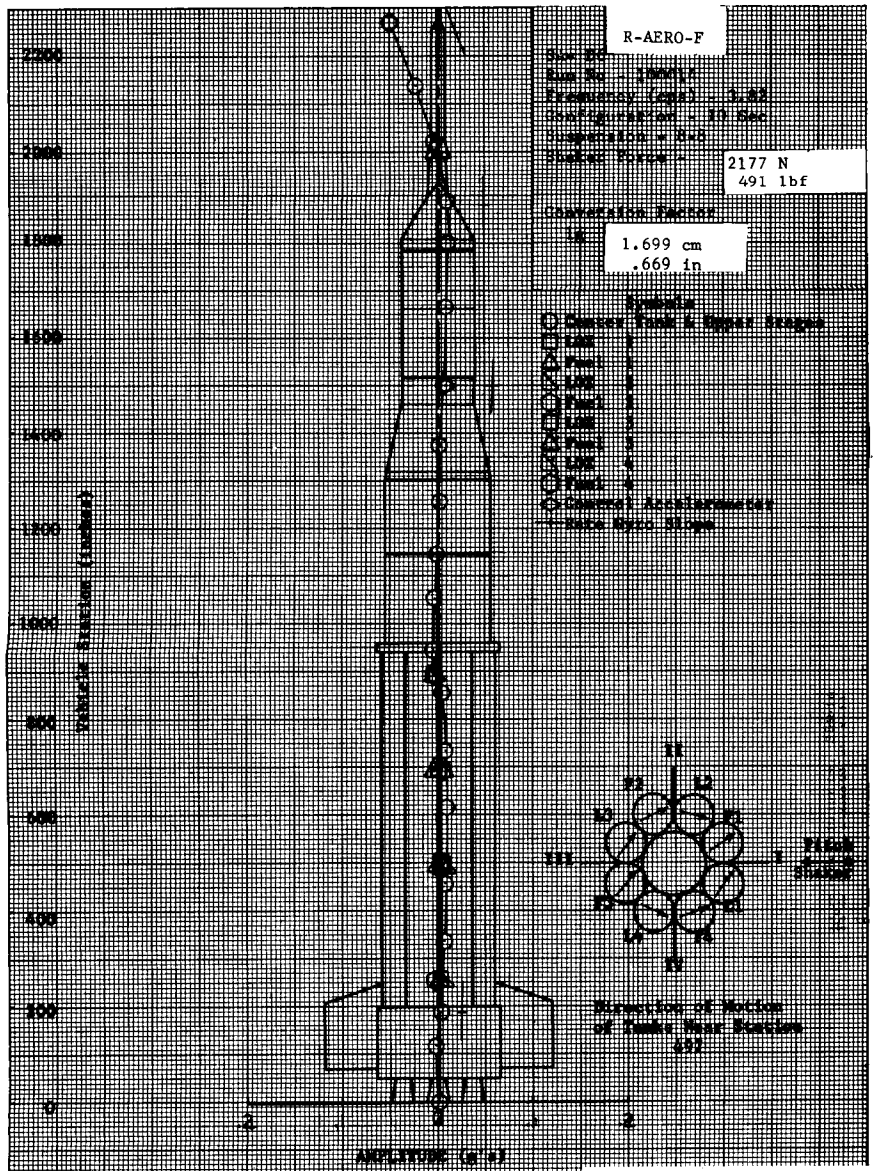


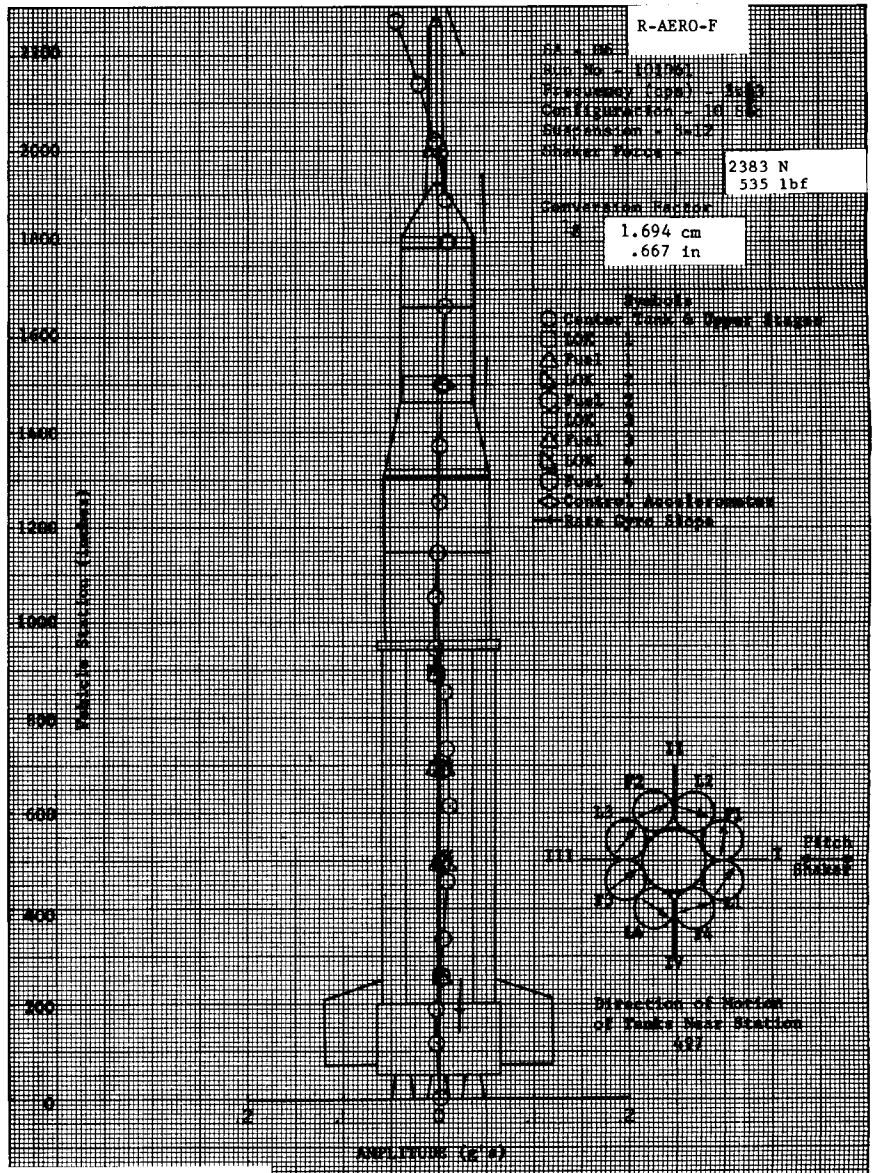


FIGURE 44 3RD BENDING MODE AT 10 SEC (PITCH)

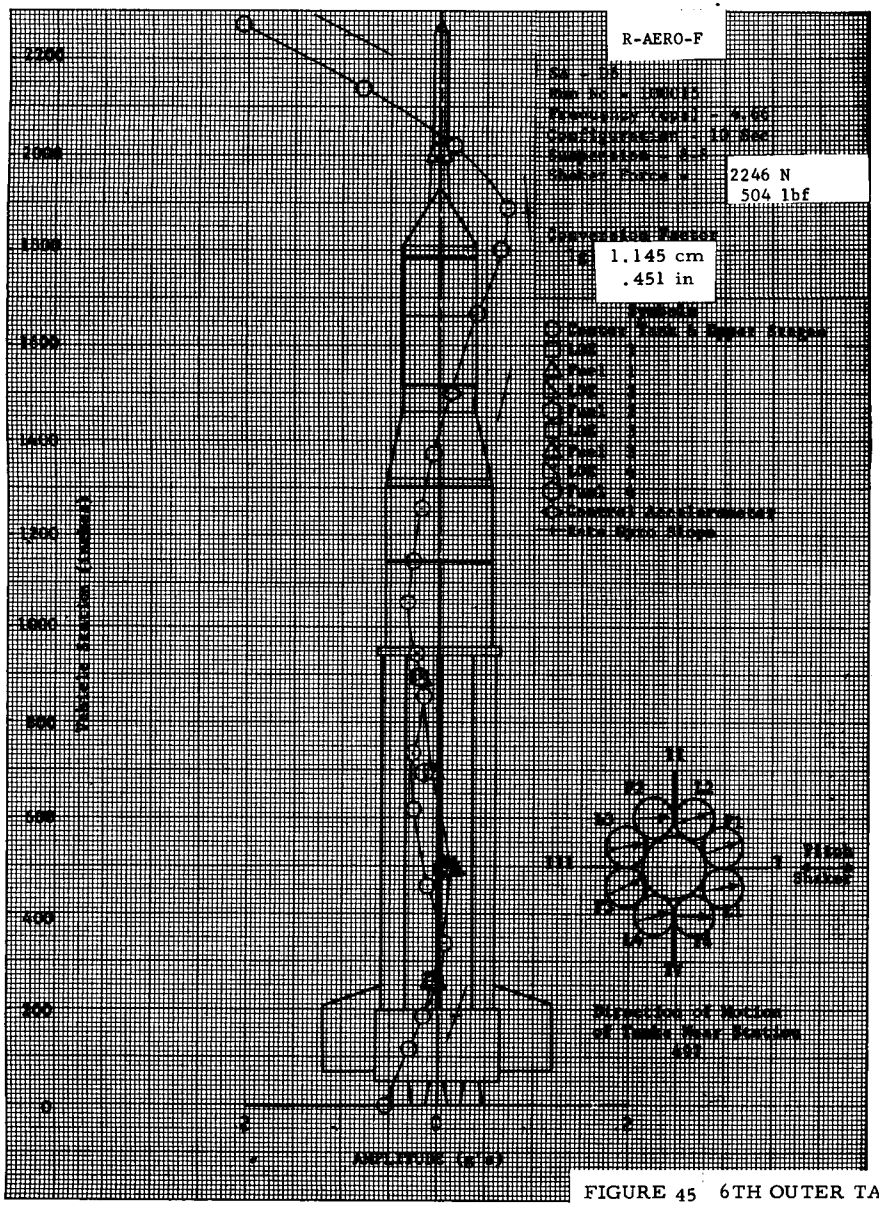


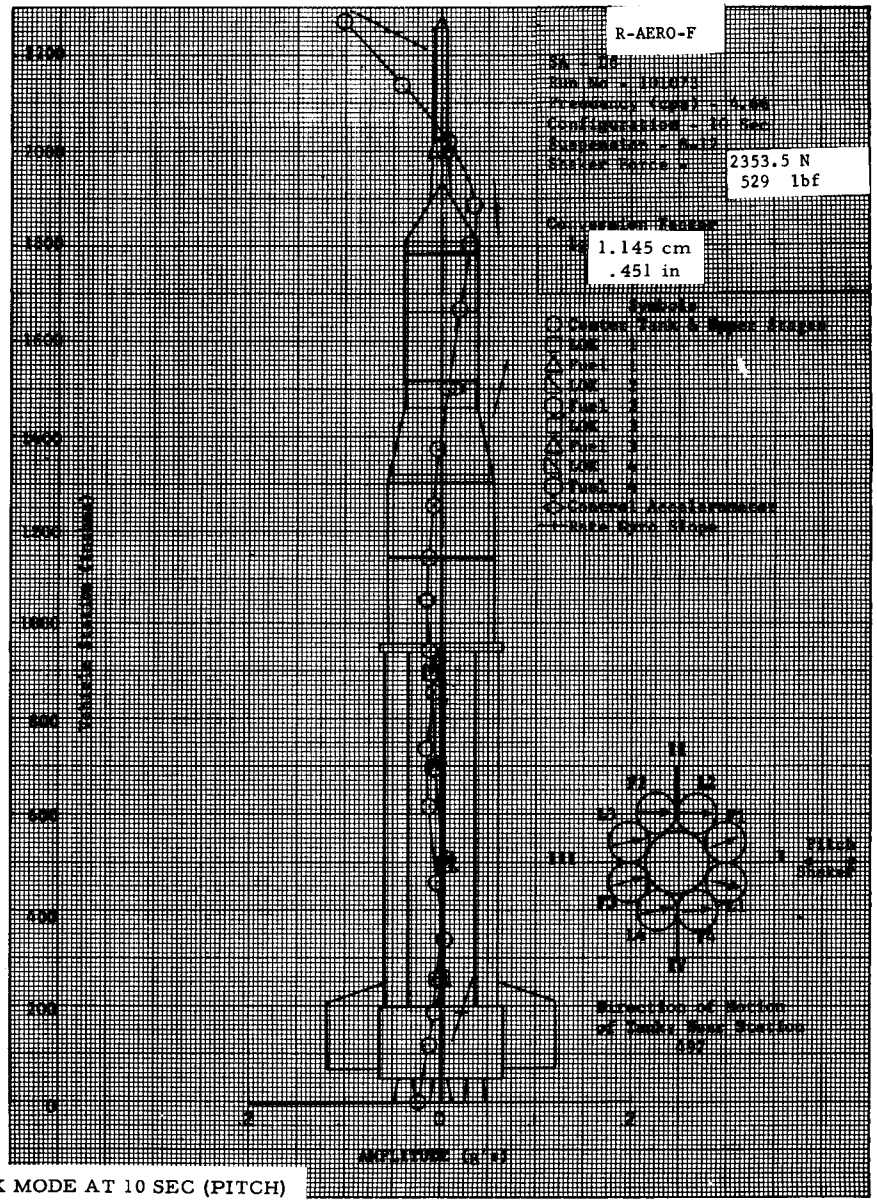


FIGURE 45 6TH OUTER TANK MODE AT 10 SEC (PITCH)

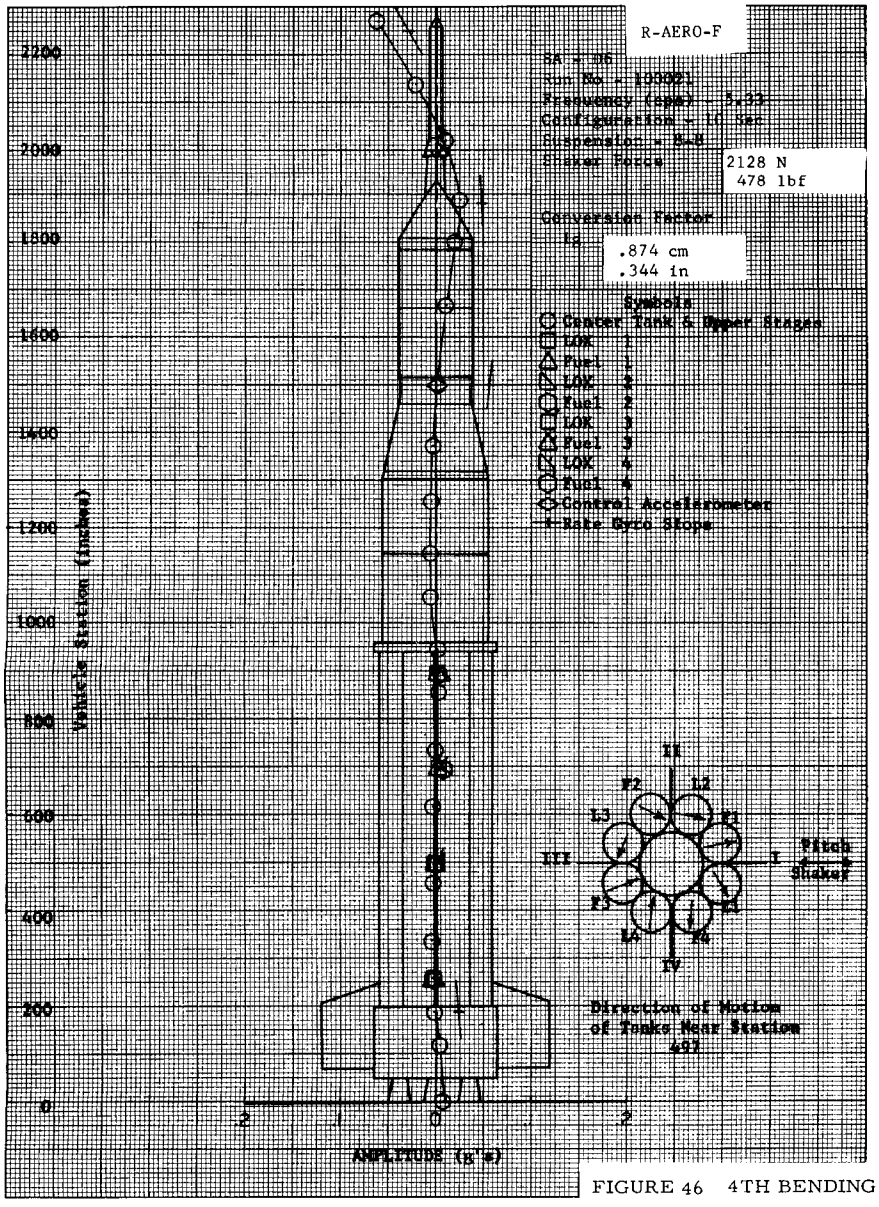


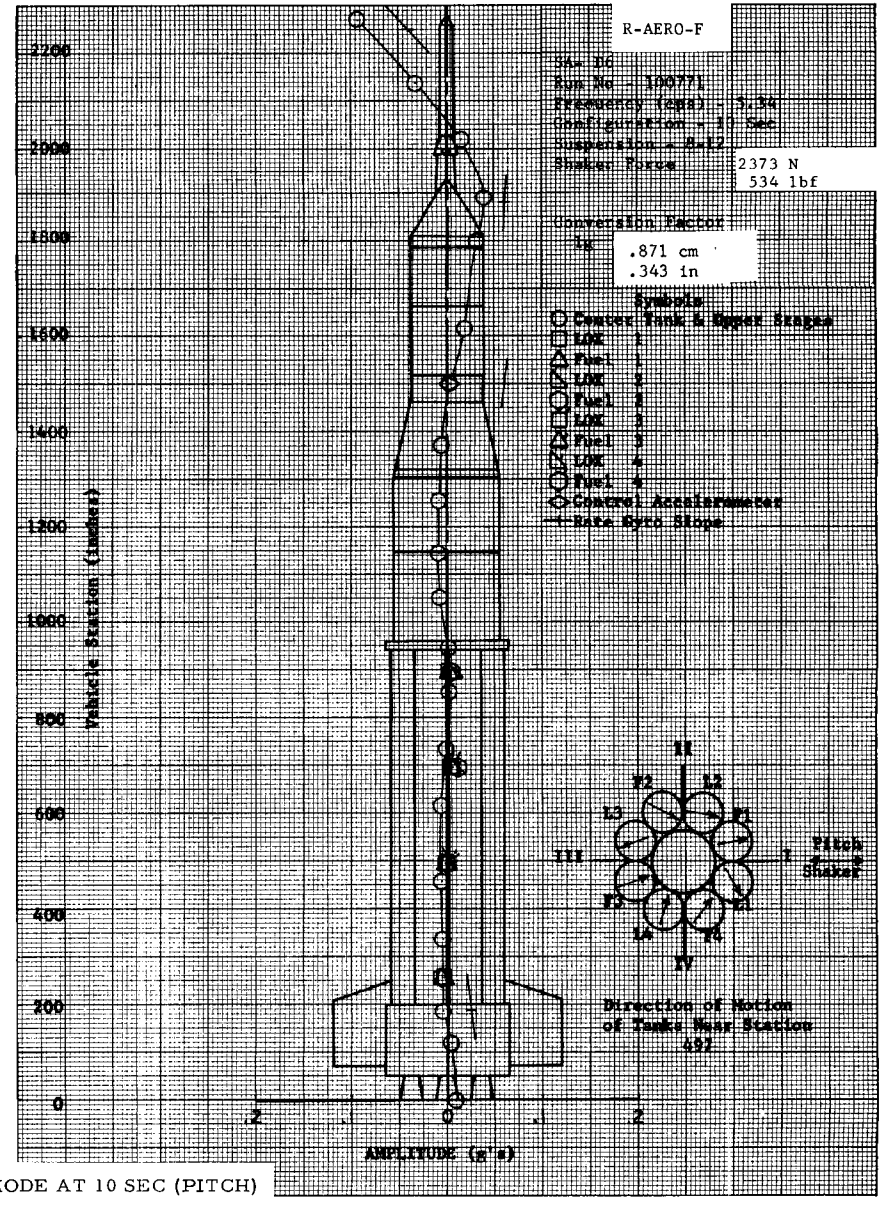


FIGURE 46 4TH BENDING MODE AT 10 SEC (PITCH)

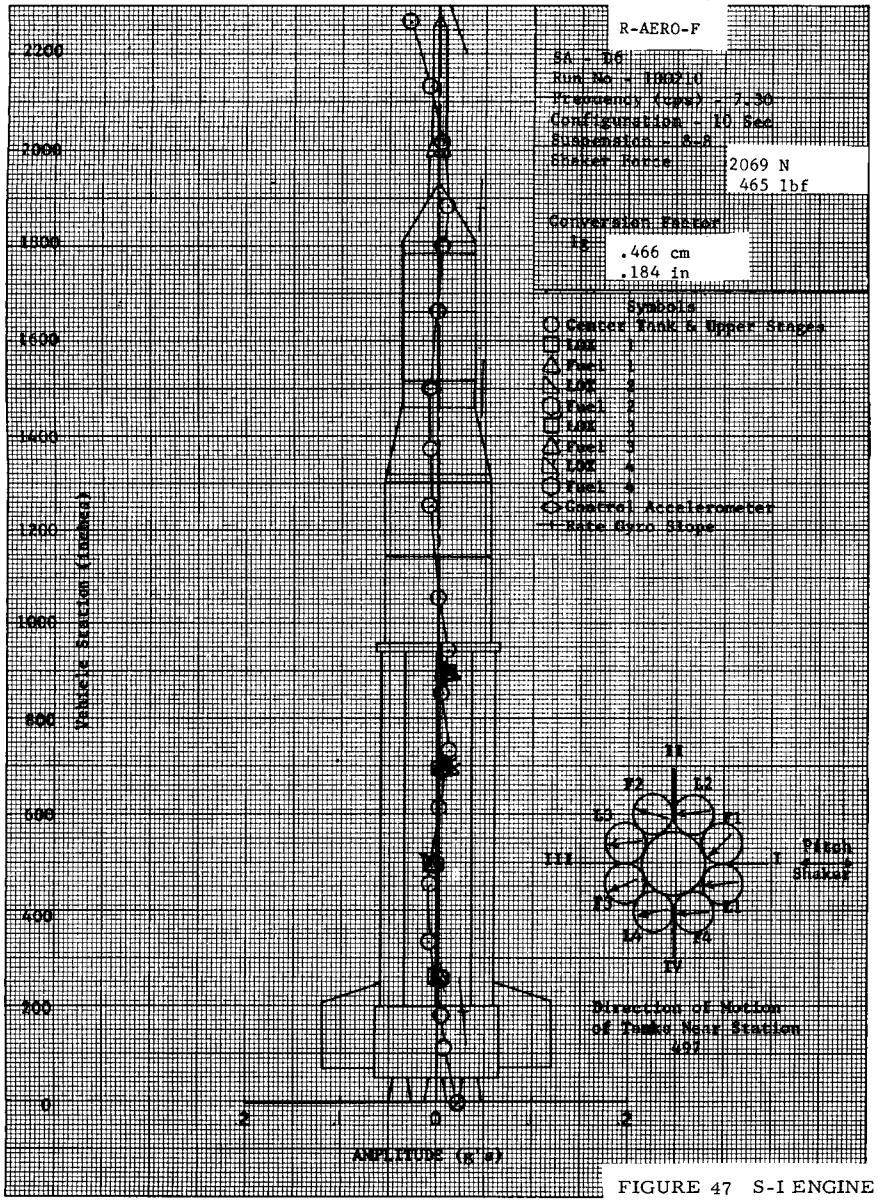


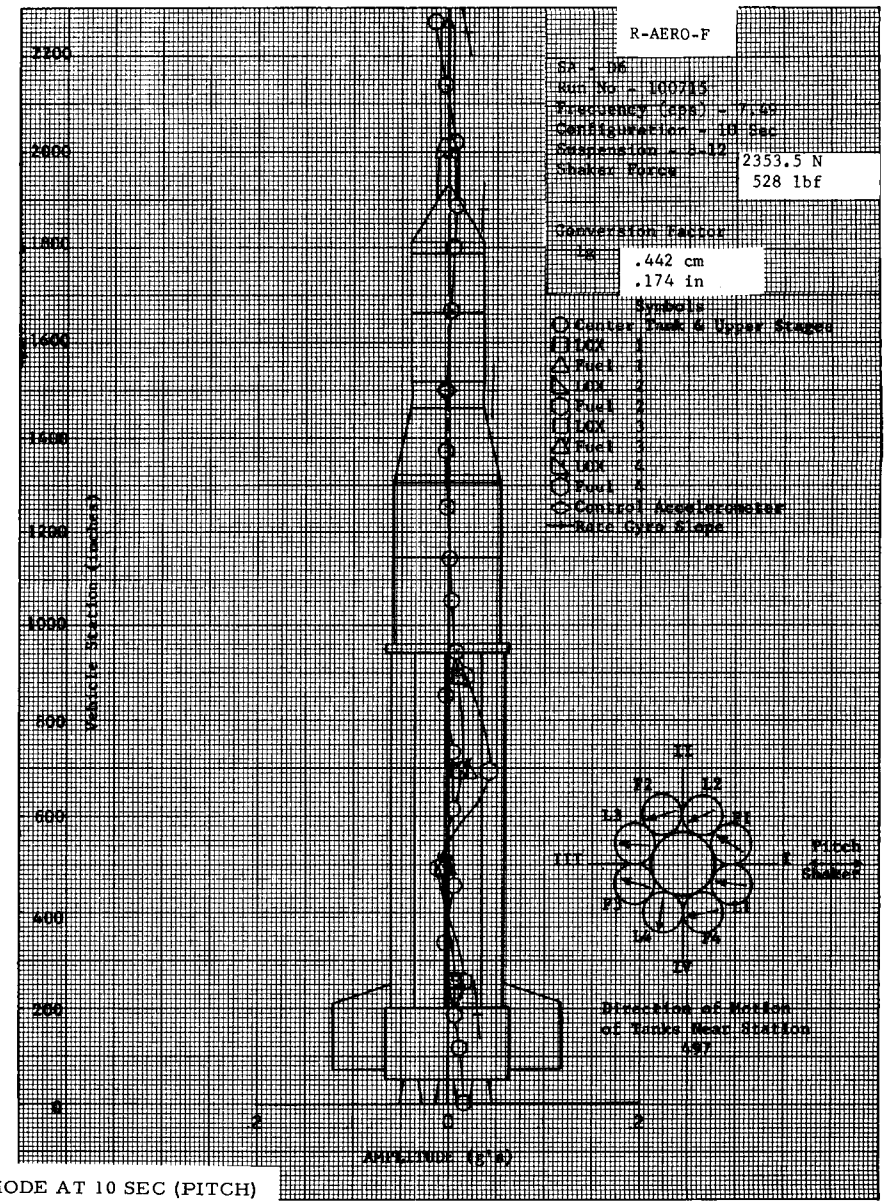


FIGURE 47 S-I ENGINE MODE AT 10 SEC (PITCH)

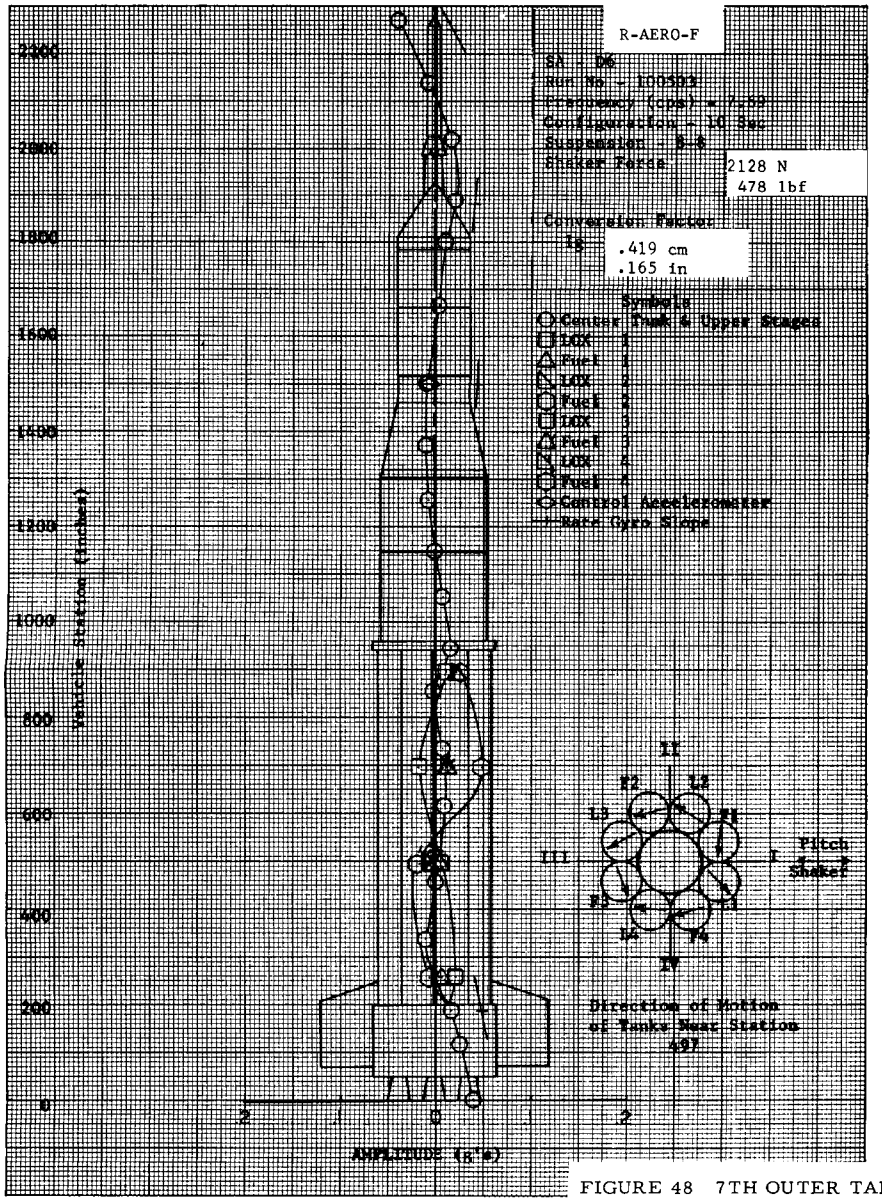


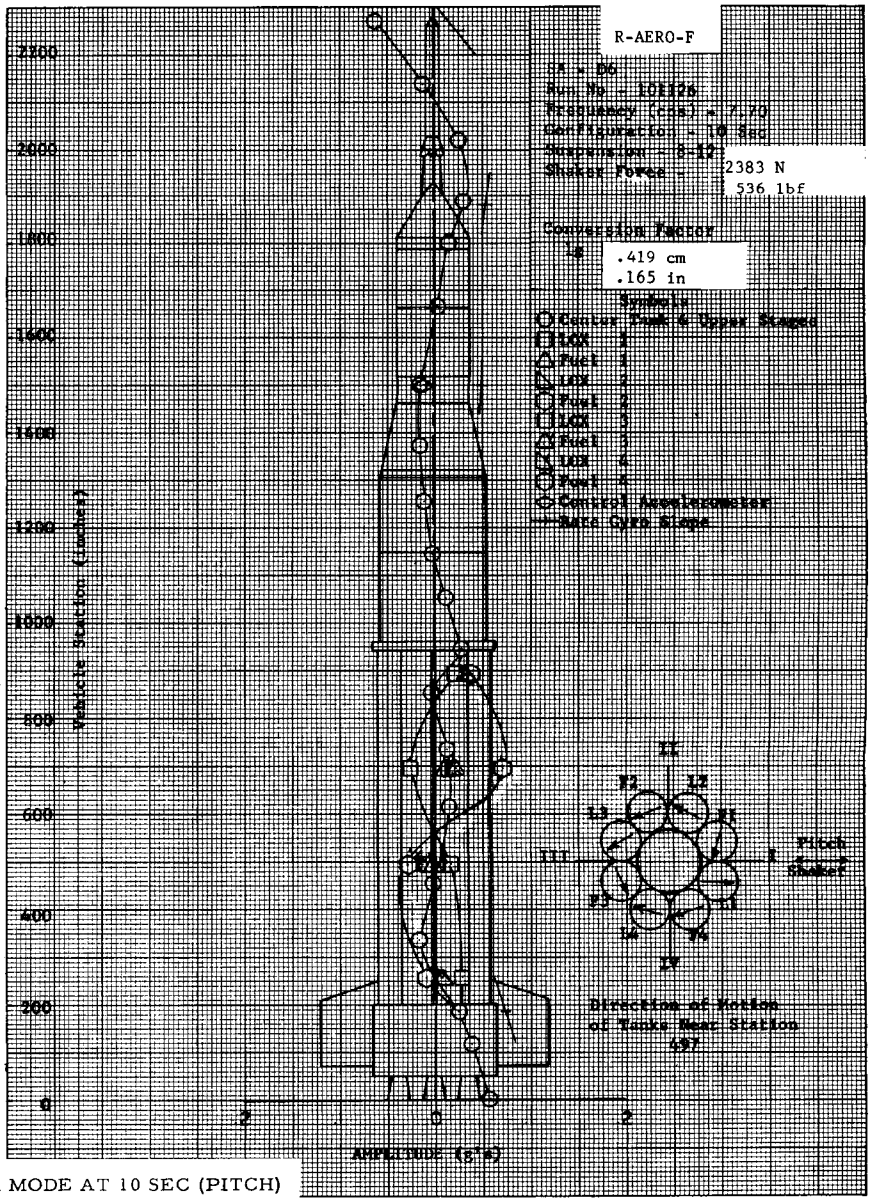


FIGURE 48 7TH OUTER TANK MODE AT 10 SEC (PITCH)

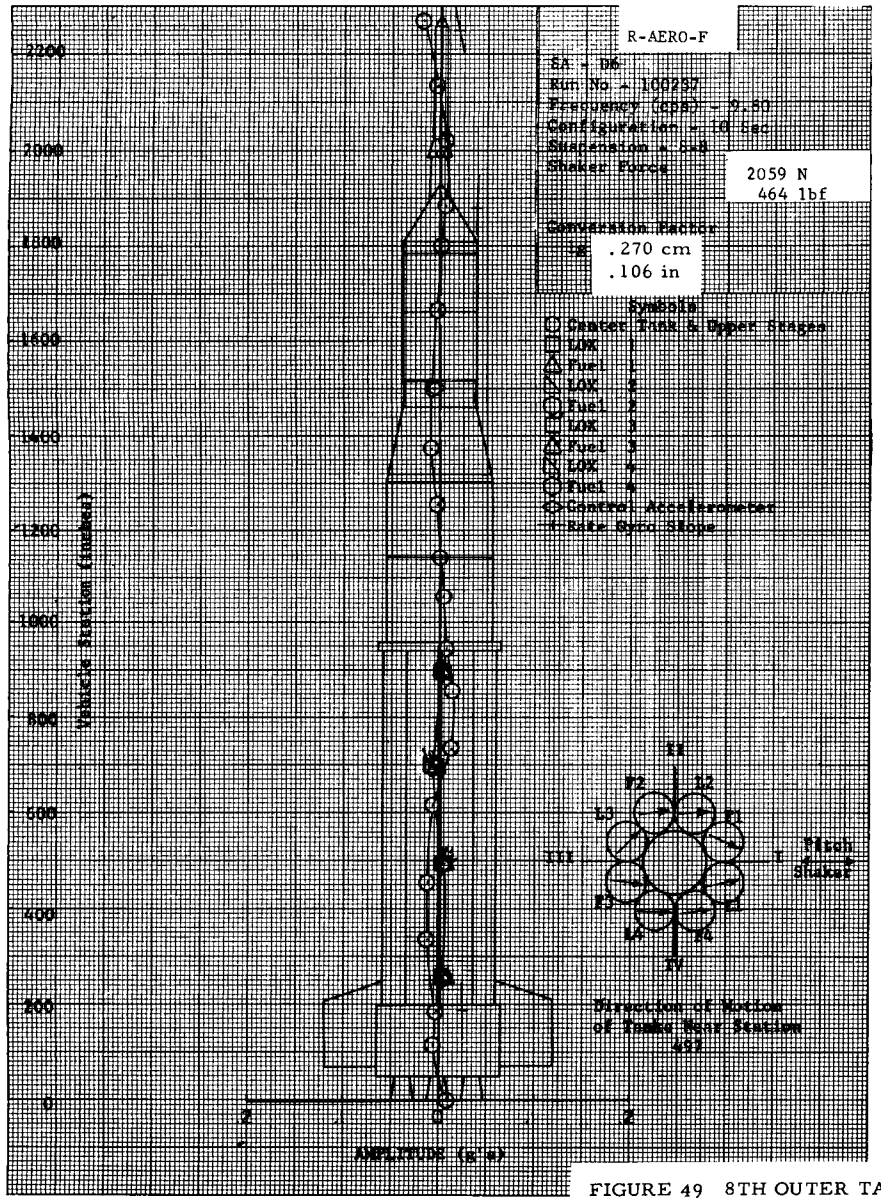


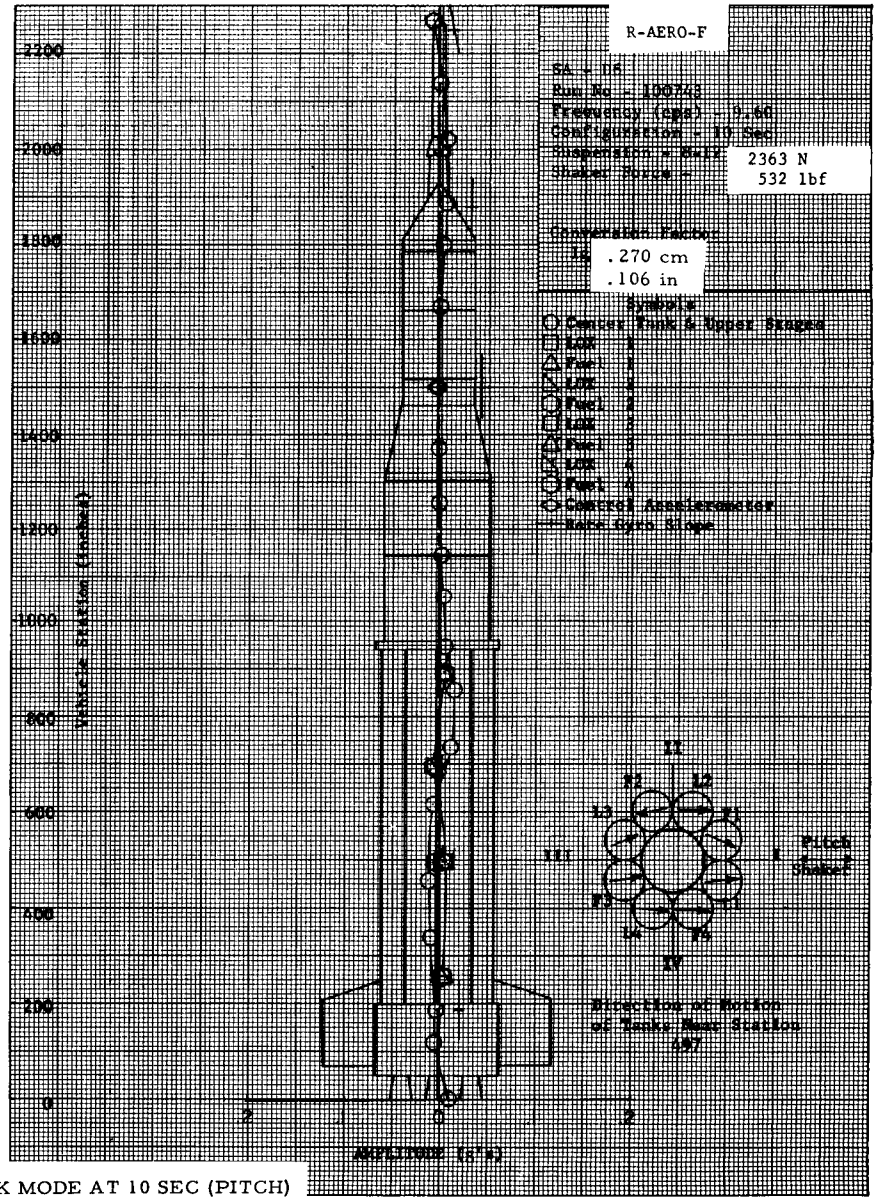


FIGURE 49 8TH OUTER TANK MODE AT 10 SEC (PITCH)

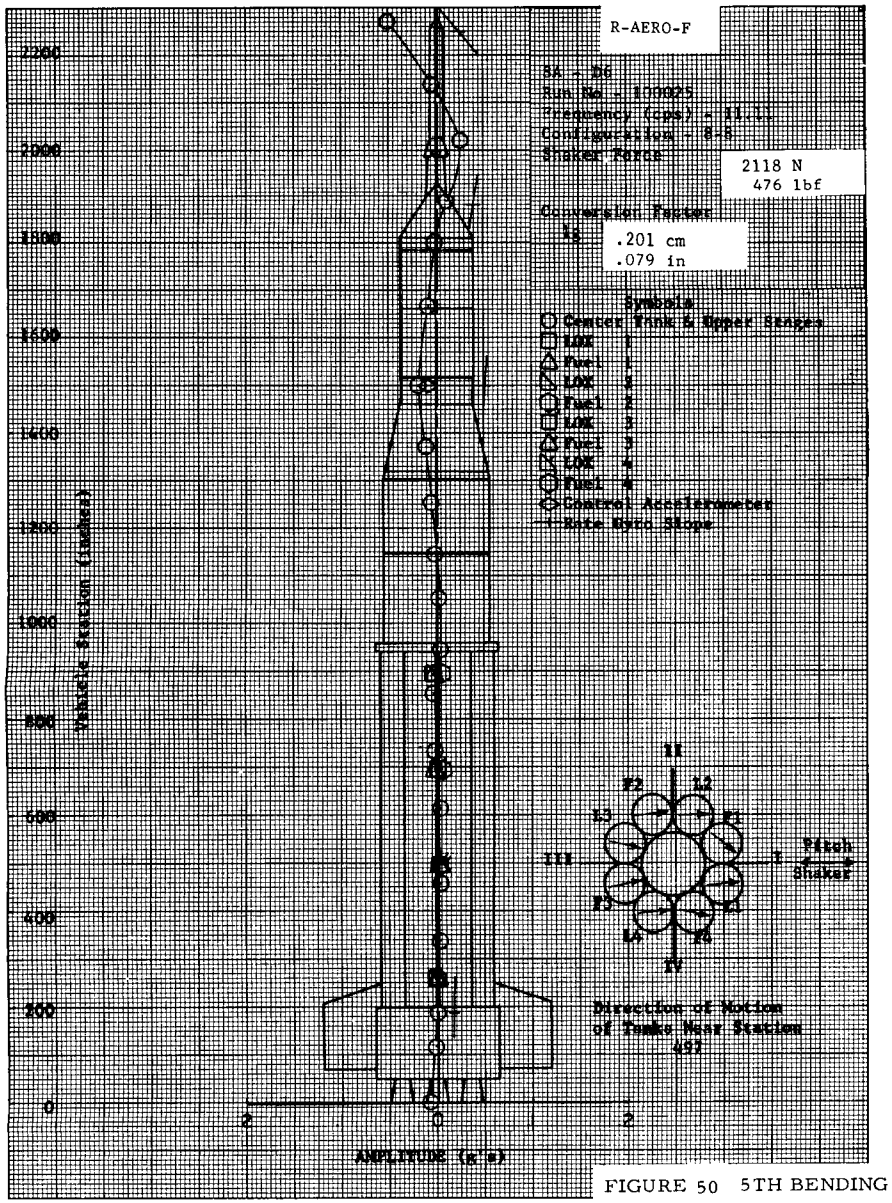


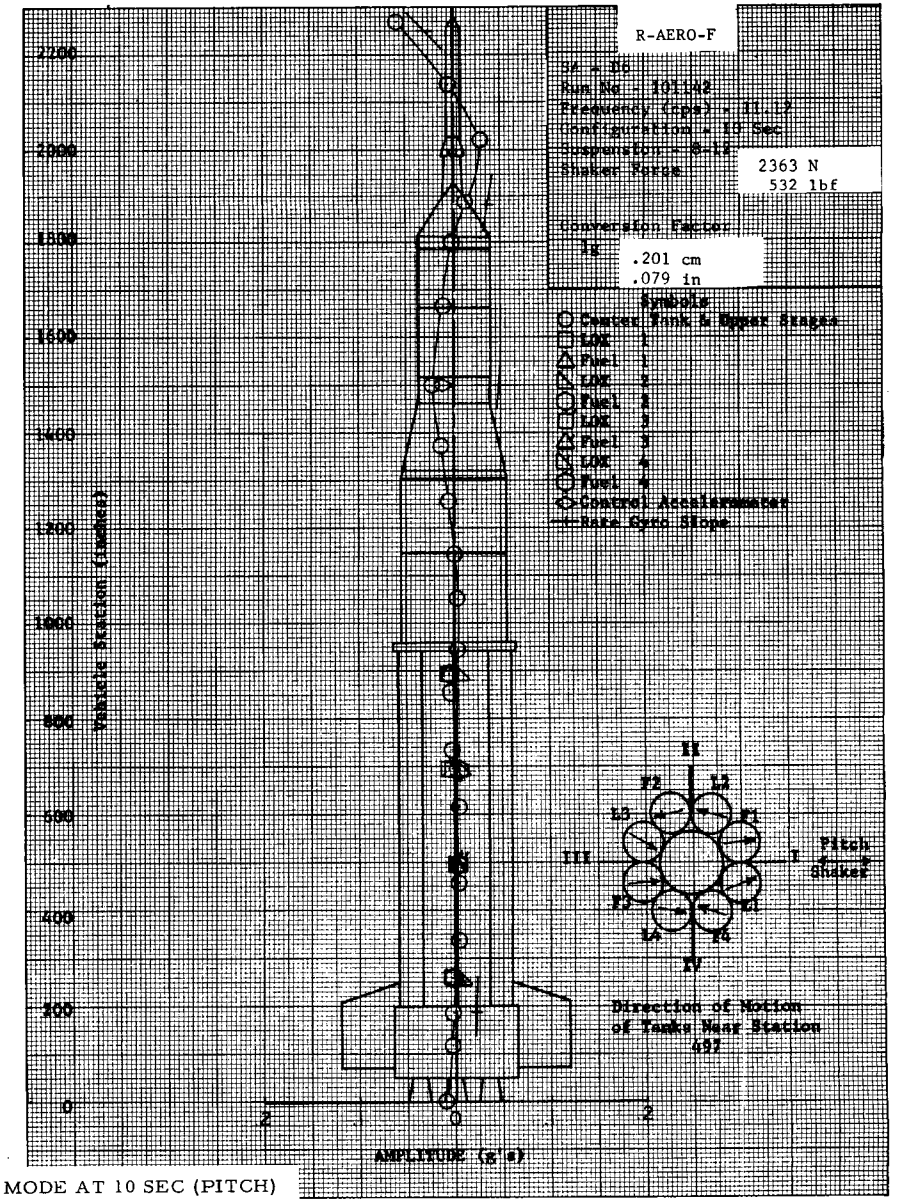


FIGURE 50 5TH BENDING MODE AT 10 SEC (PITCH)

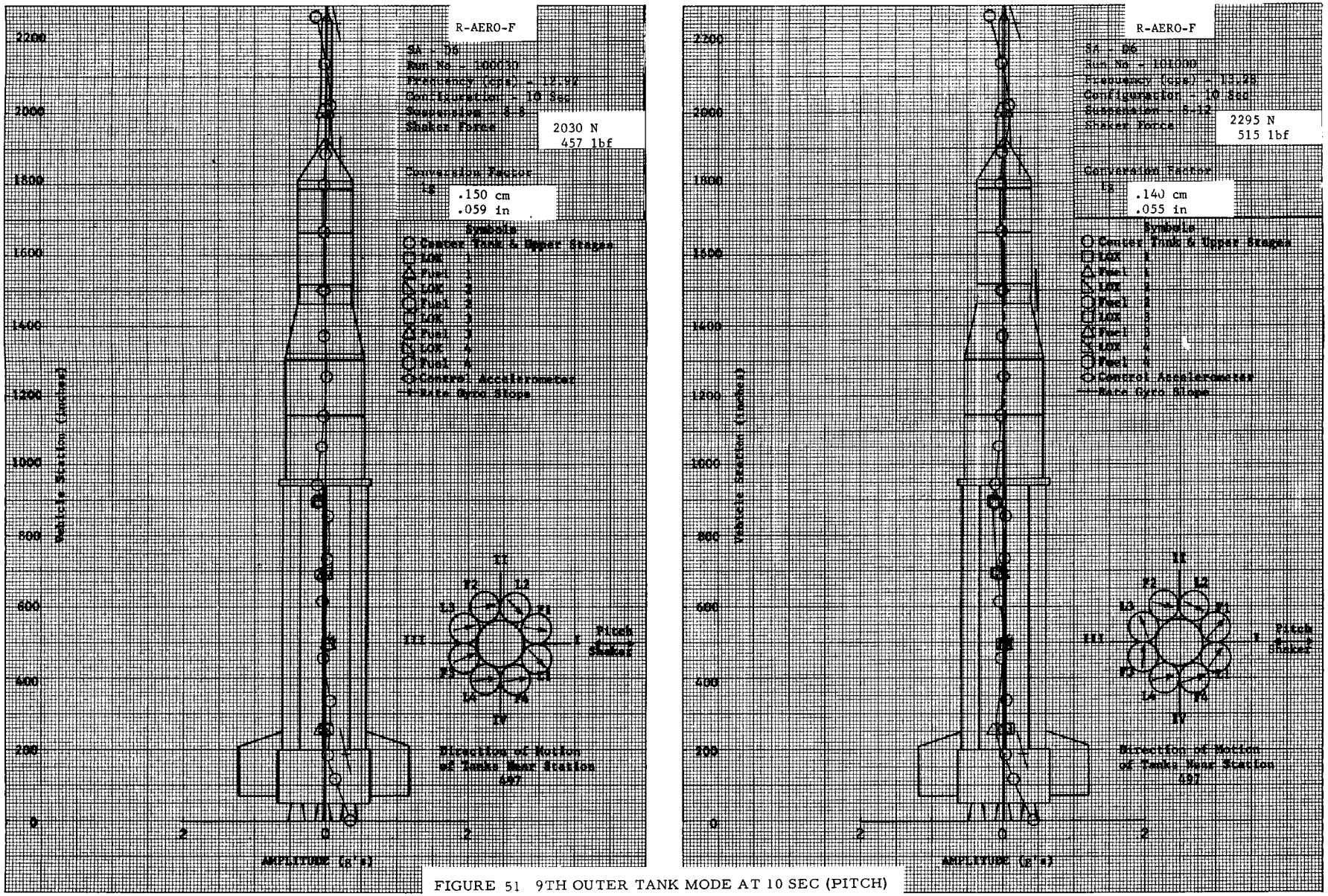


FIGURE 51 9TH OUTER TANK MODE AT 10 SEC (PITCH)

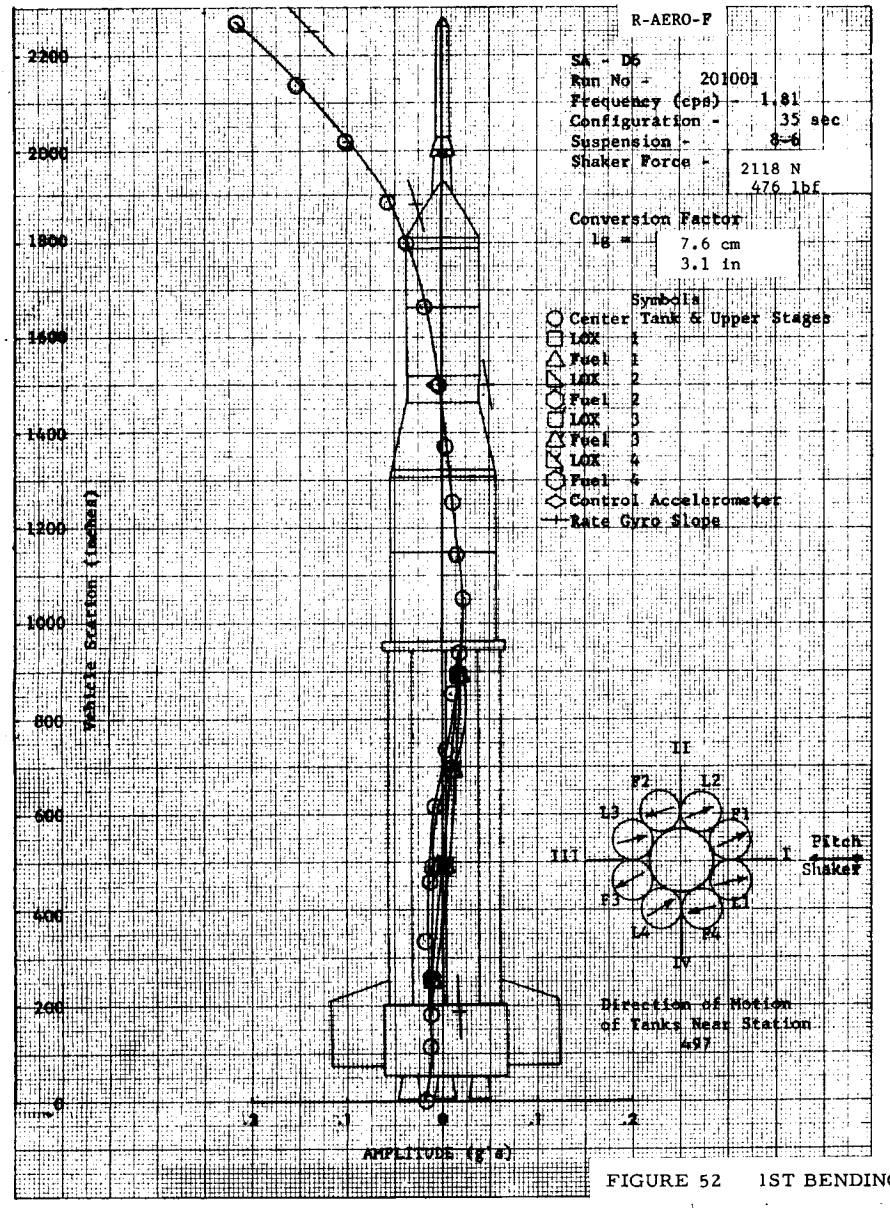


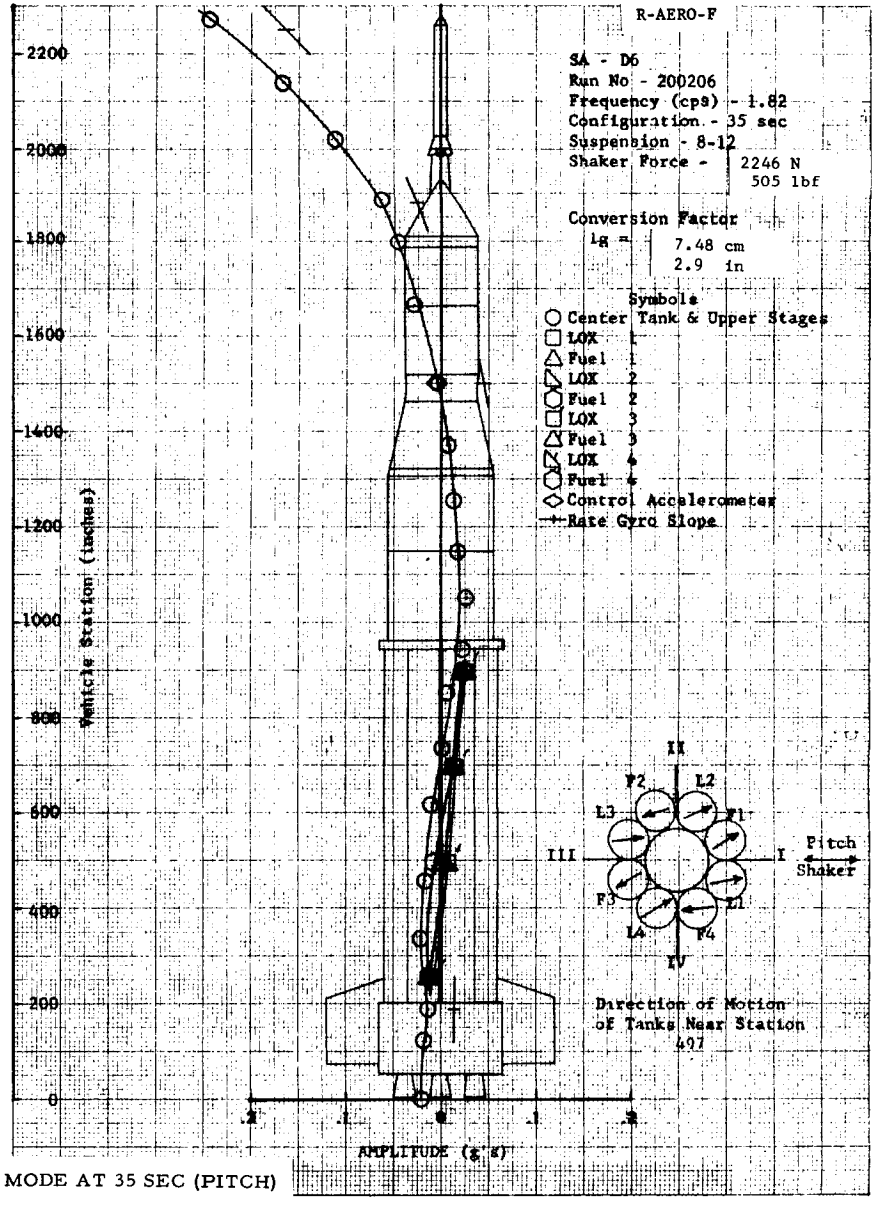


FIGURE 52 1ST BENDING MODE AT 35 SEC (PITCH)

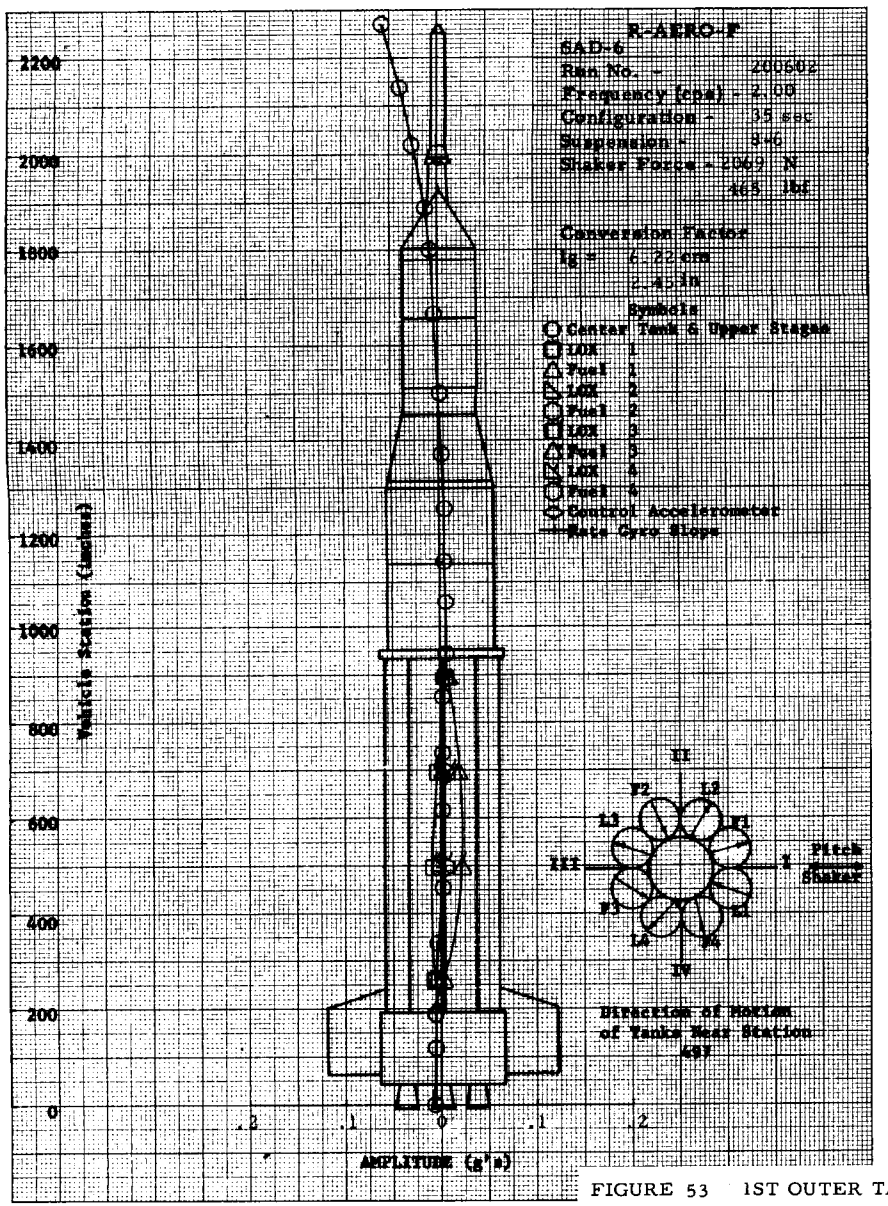


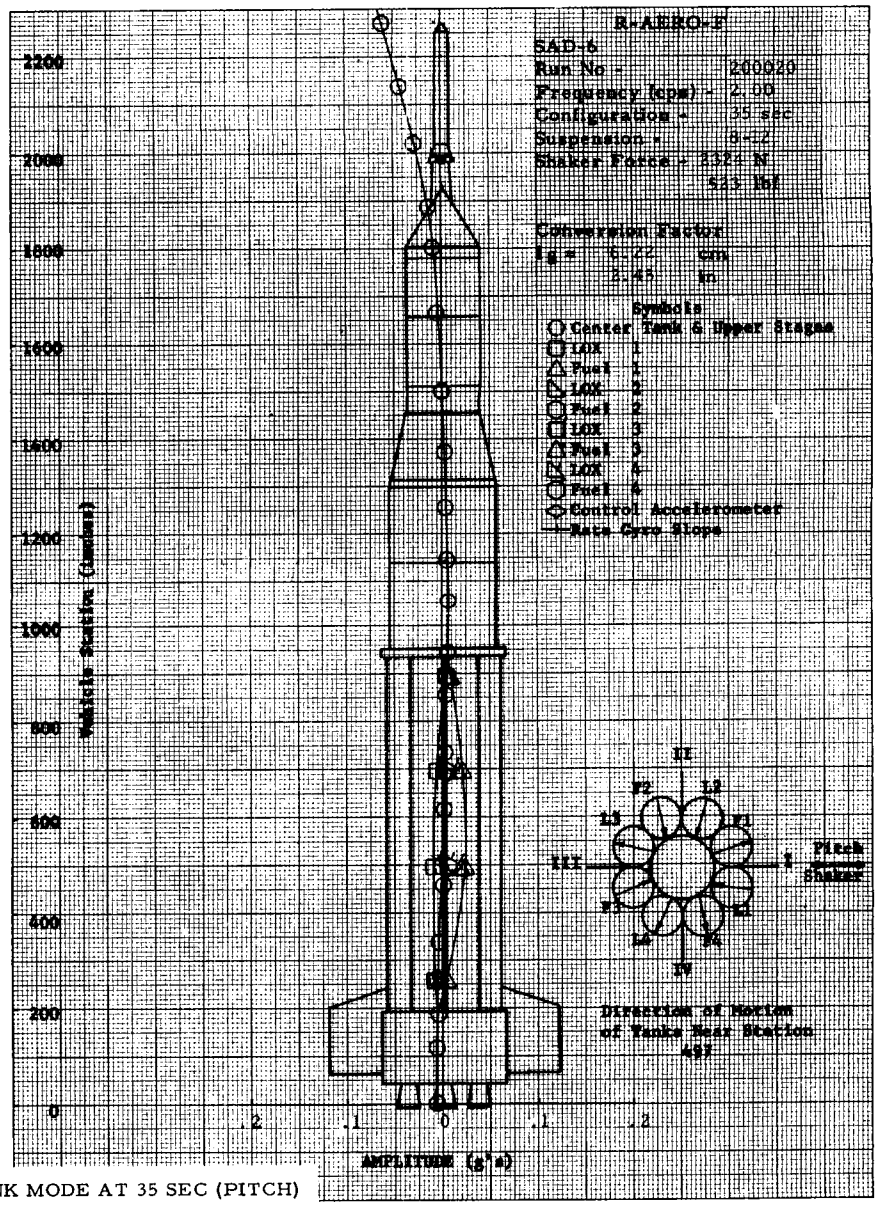


FIGURE 53 1ST OUTER TANK MODE AT 35 SEC (PITCH)

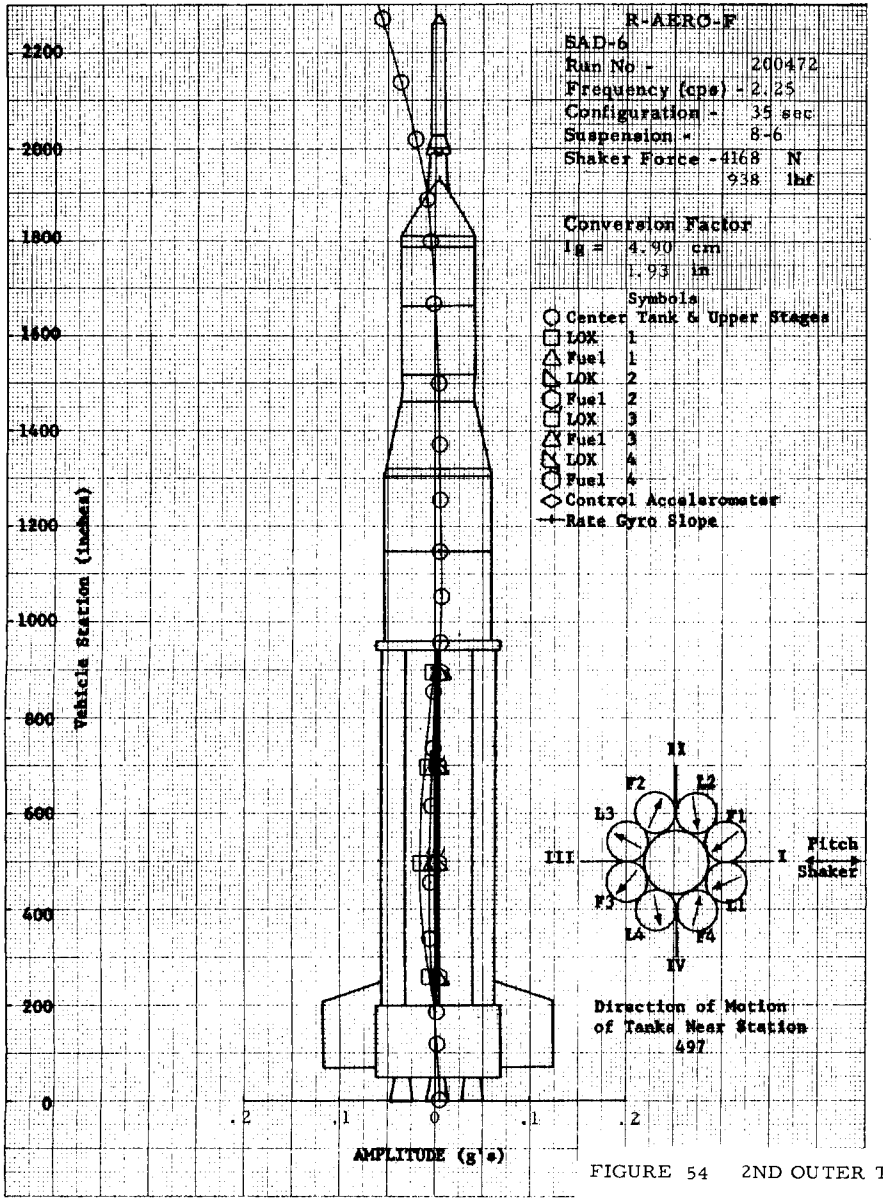


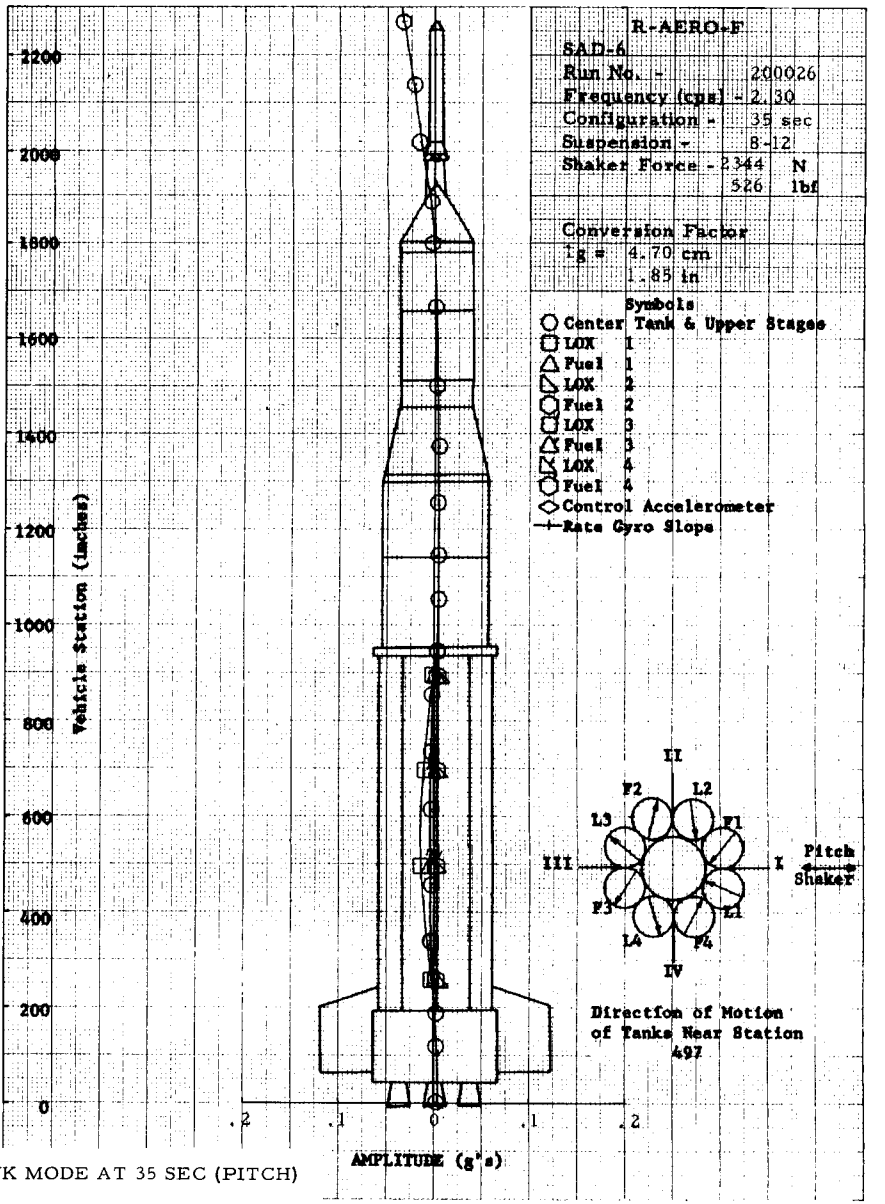


FIGURE 54 2ND OUTER TANK MODE AT 35 SEC (PITCH)

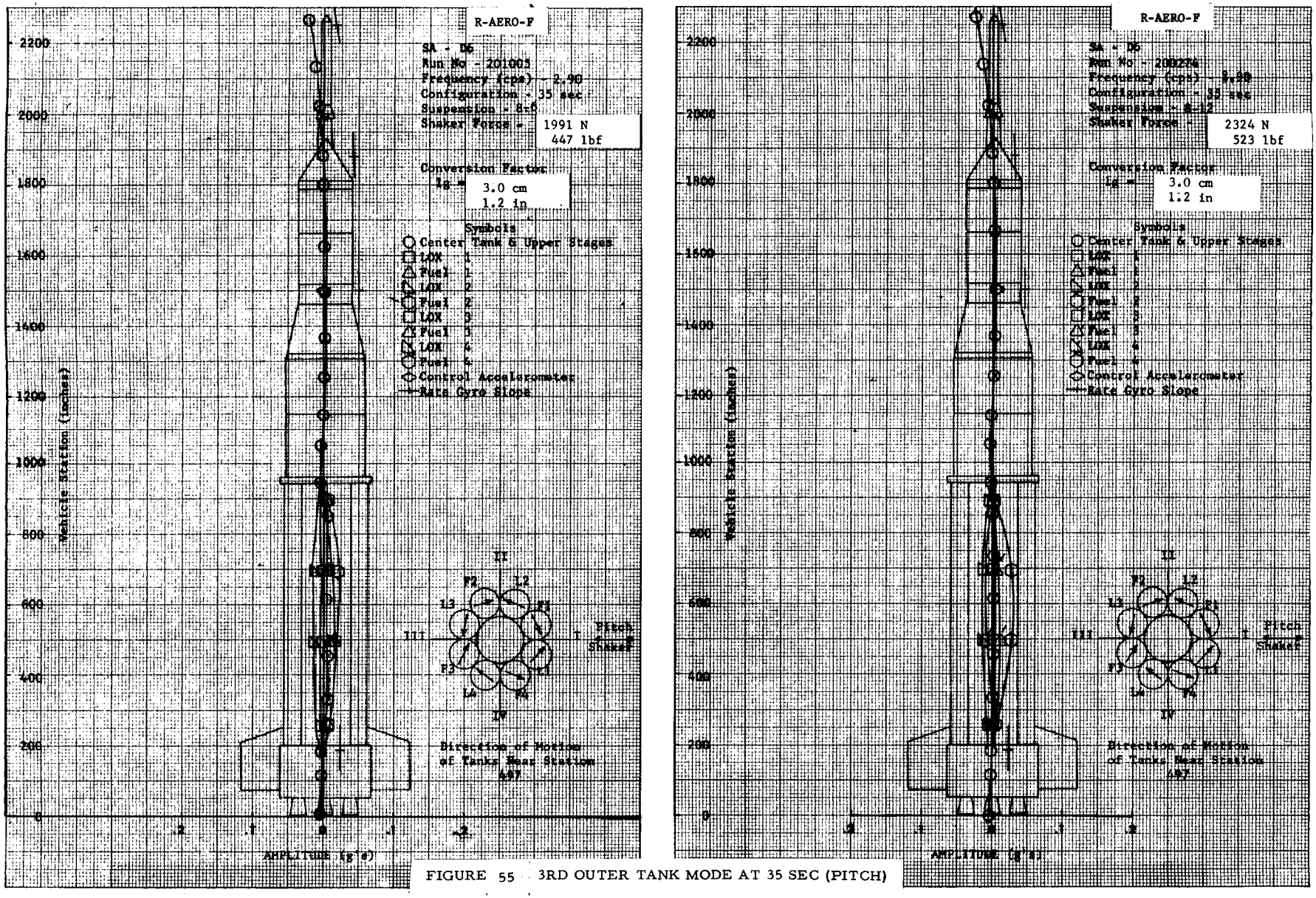


FIGURE 55 3RD OUTER TANK MODE AT 35 SEC (PITCH)

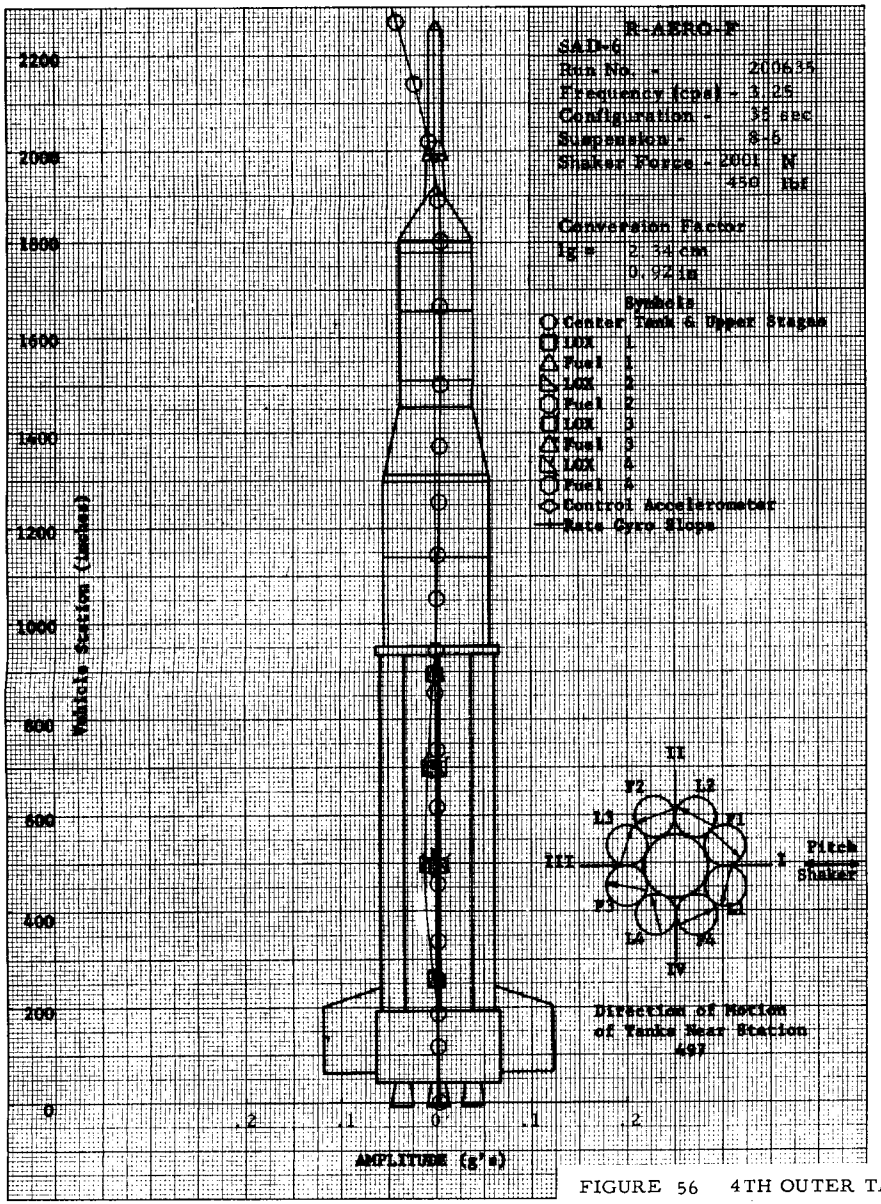


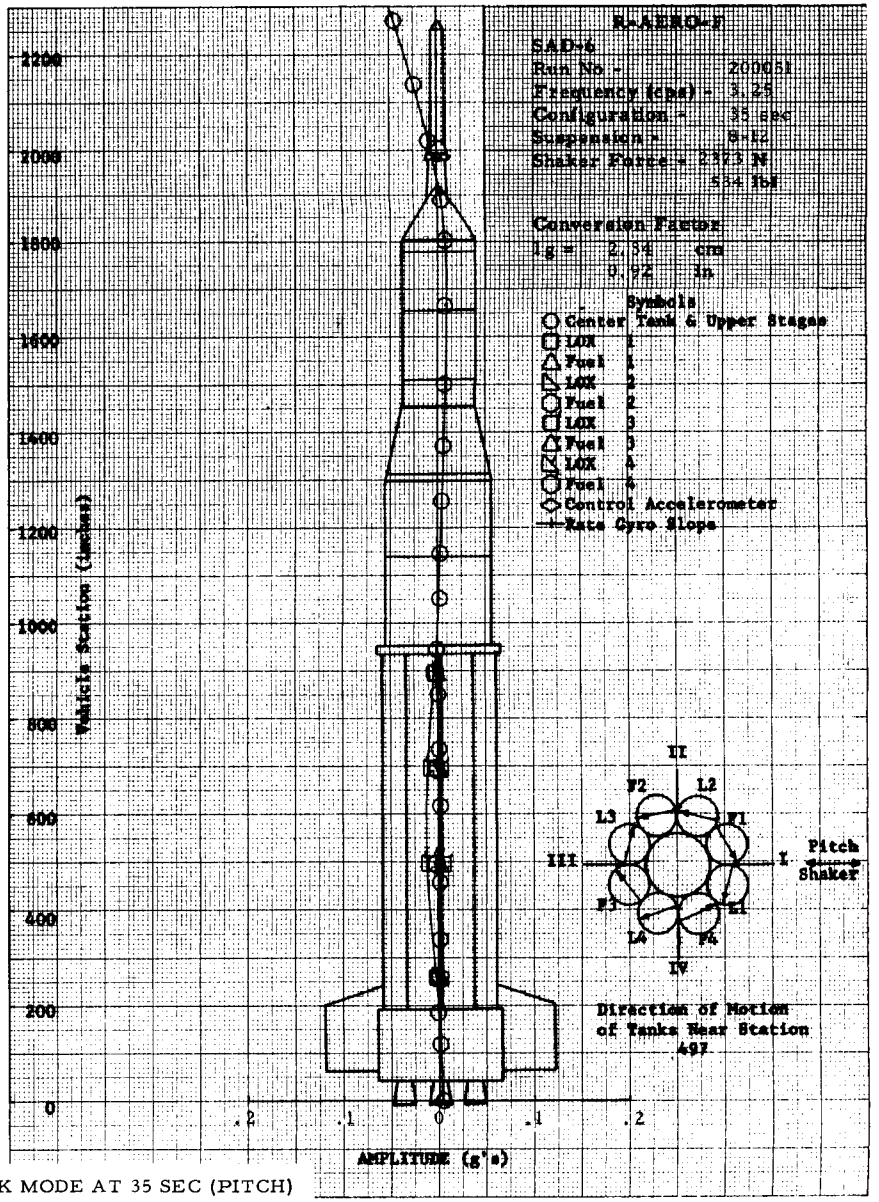


FIGURE 56 4TH OUTER TANK MODE AT 35 SEC (PITCH)

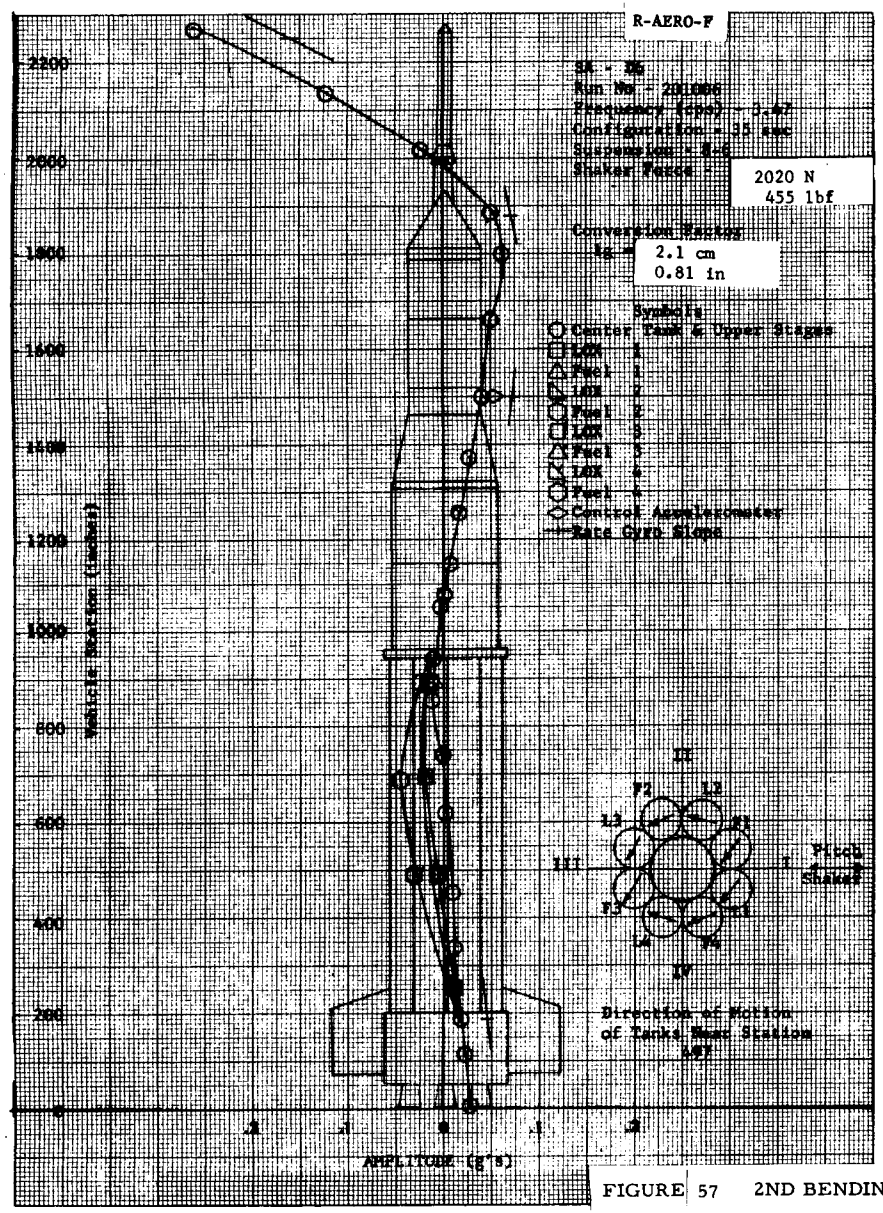


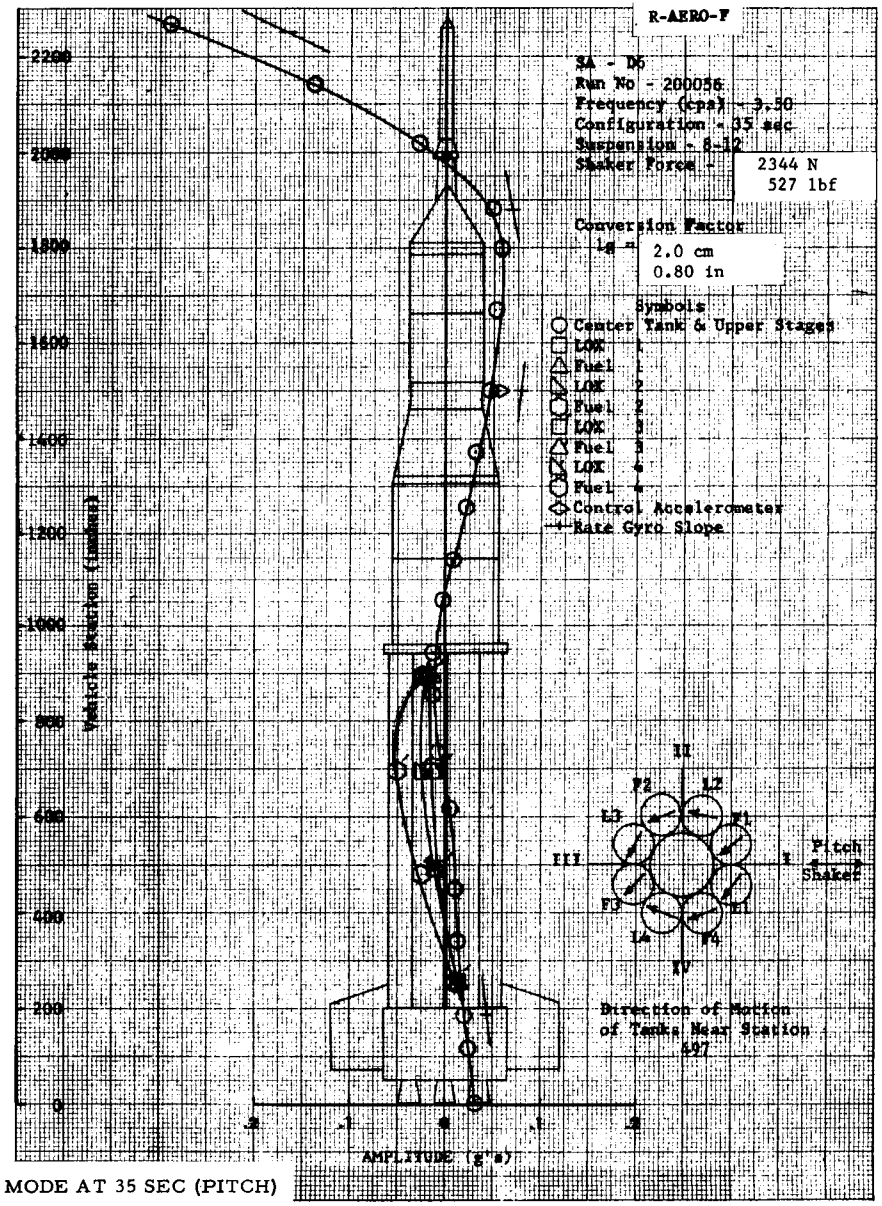


FIGURE 57 2ND BENDING MODE AT 35 SEC (PITCH)

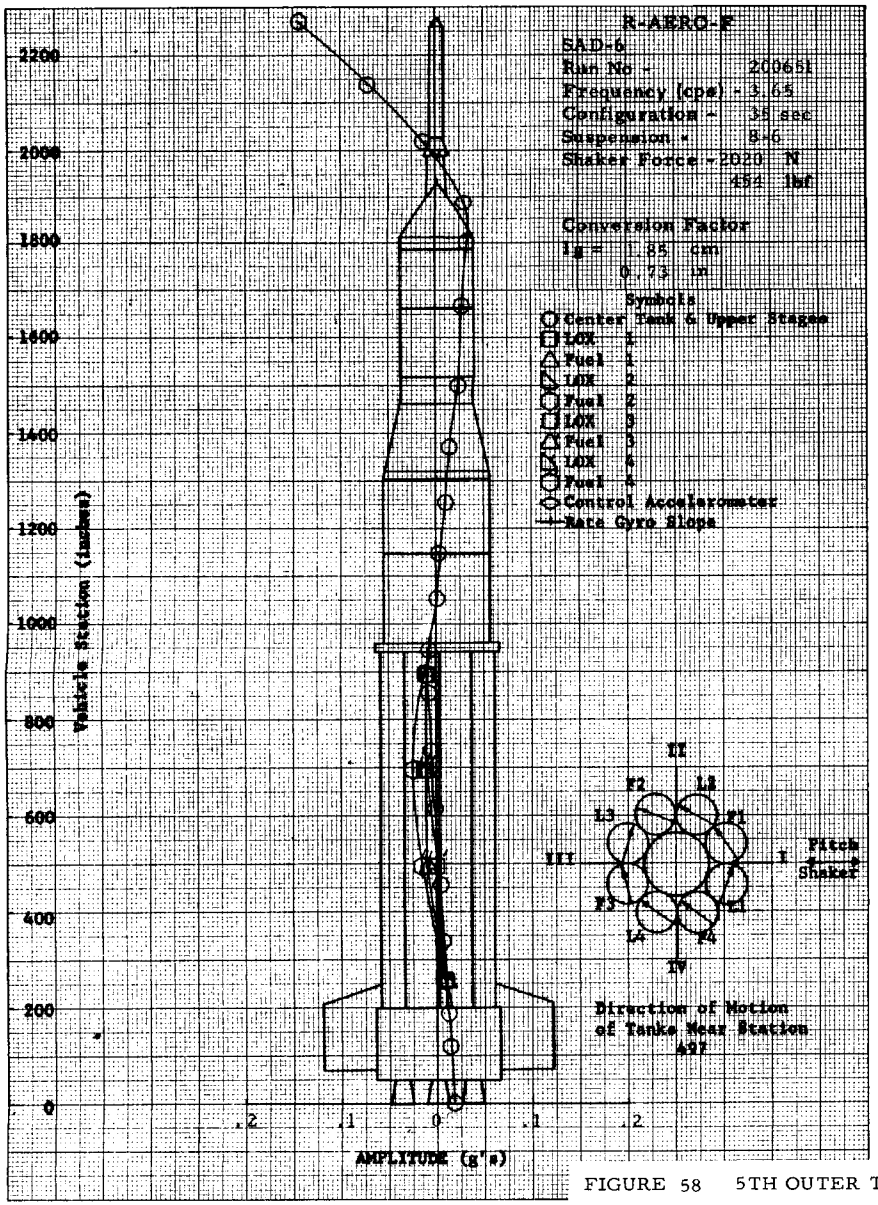


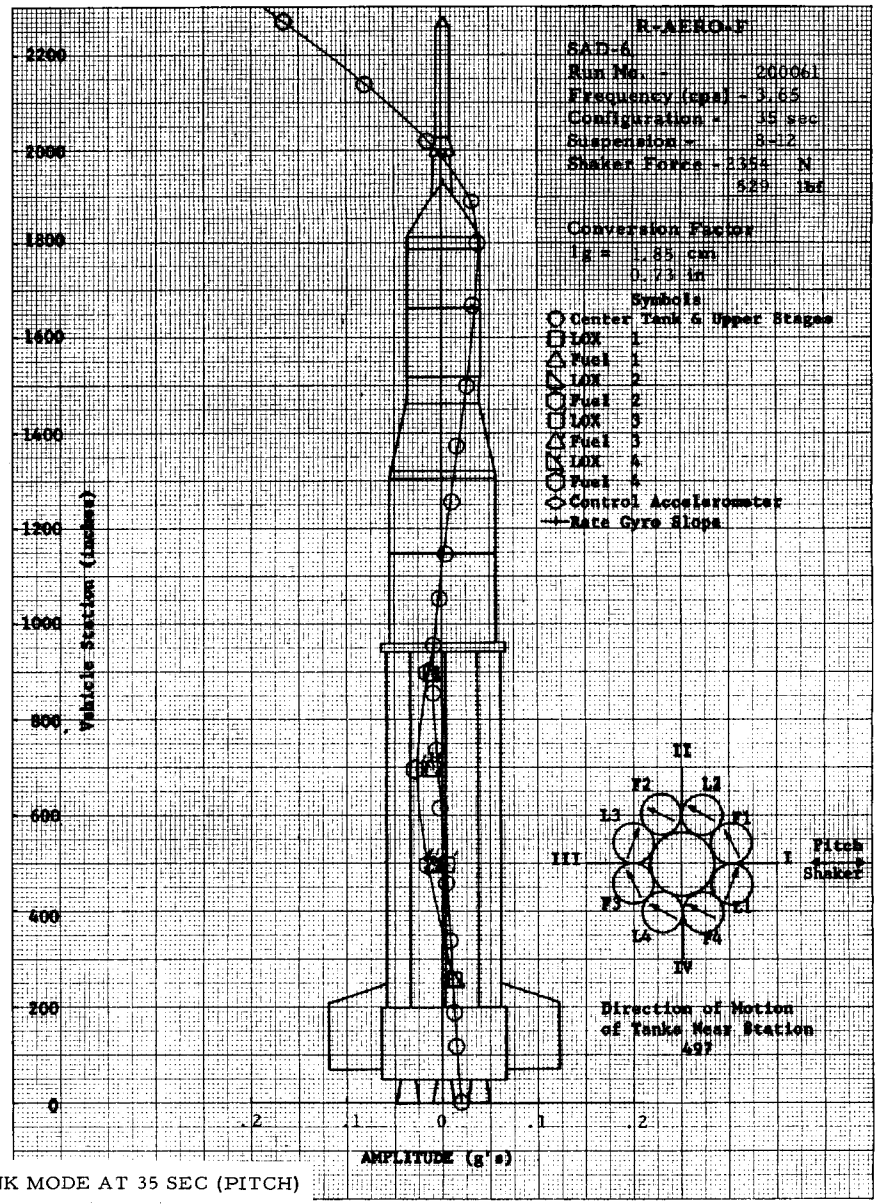


FIGURE 58 5TH OUTER TANK MODE AT 35 SEC (PITCH)

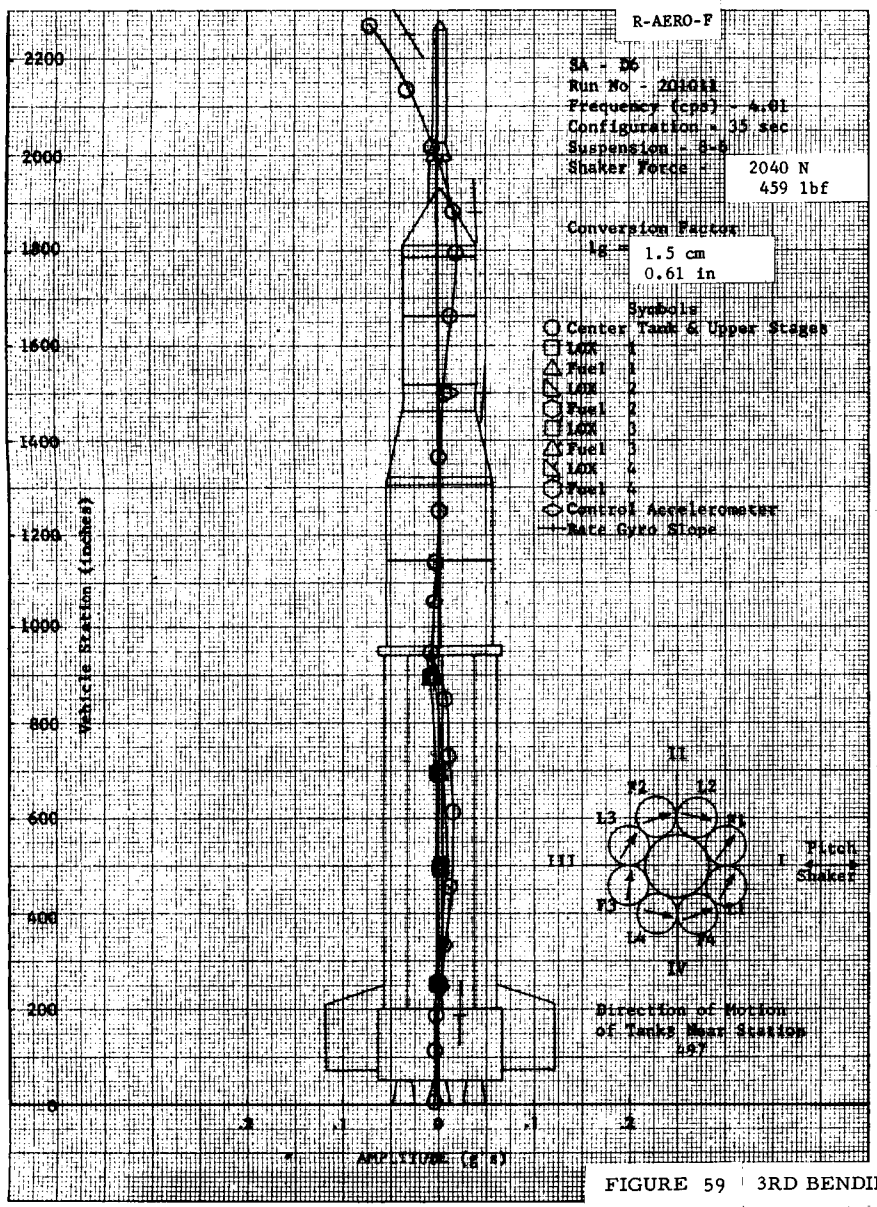


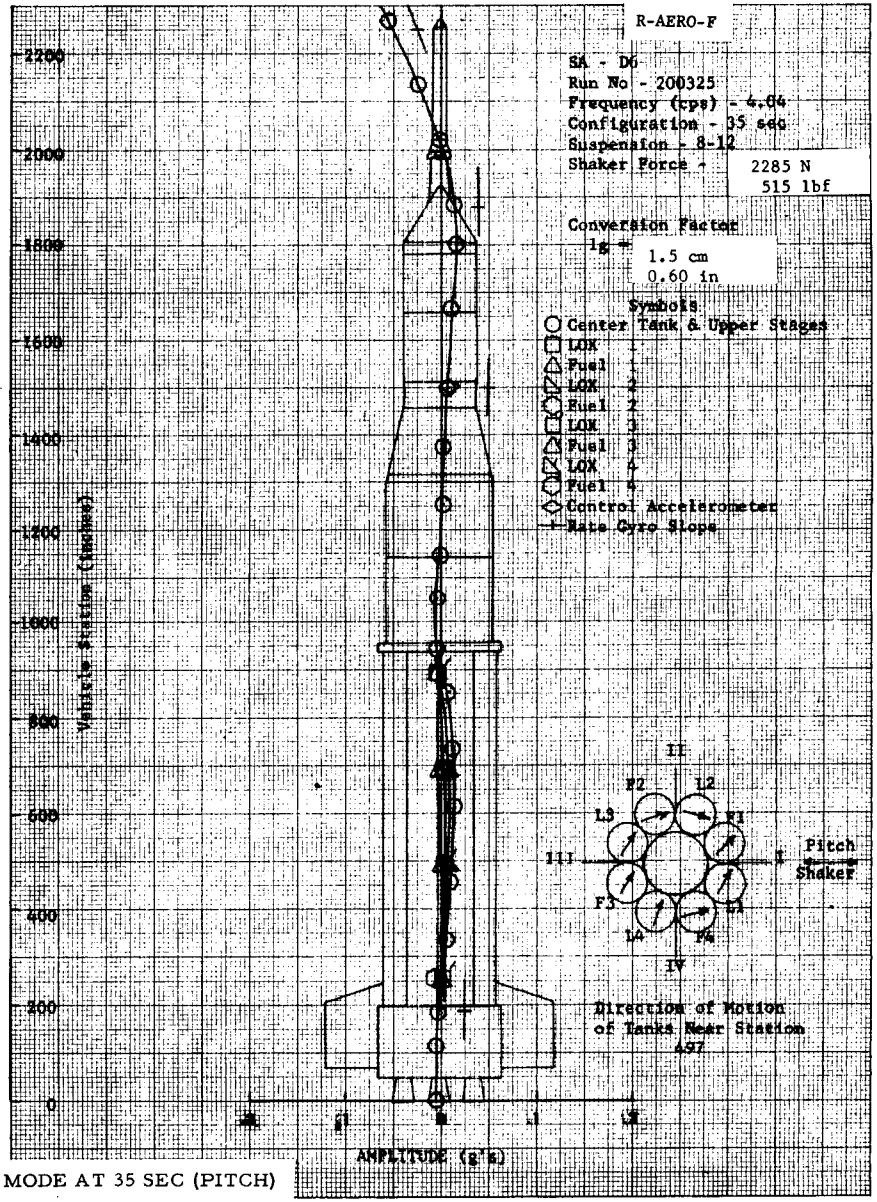


FIGURE 59 3RD BENDING MODE AT 35 SEC (PITCH)

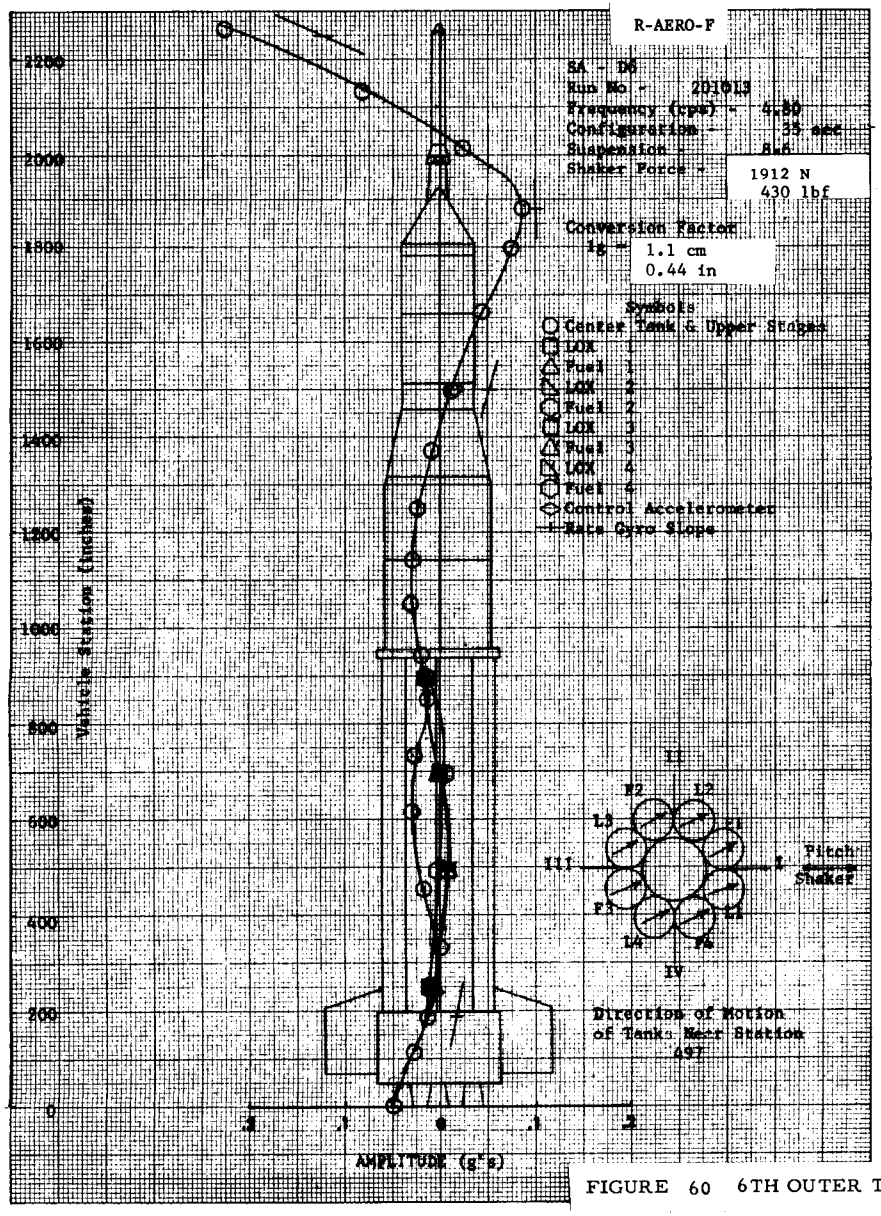


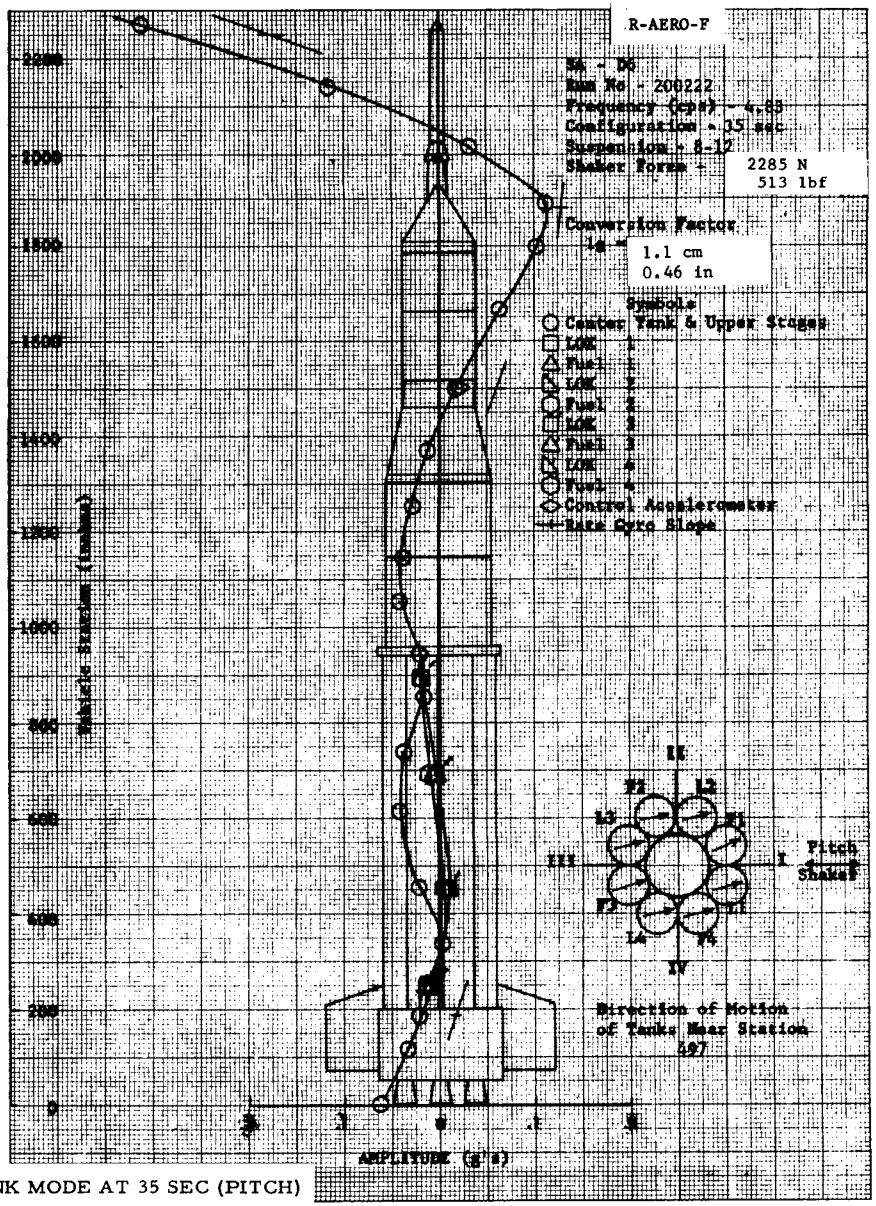


FIGURE 60 6TH OUTER TANK MODE AT 35 SEC (PITCH)

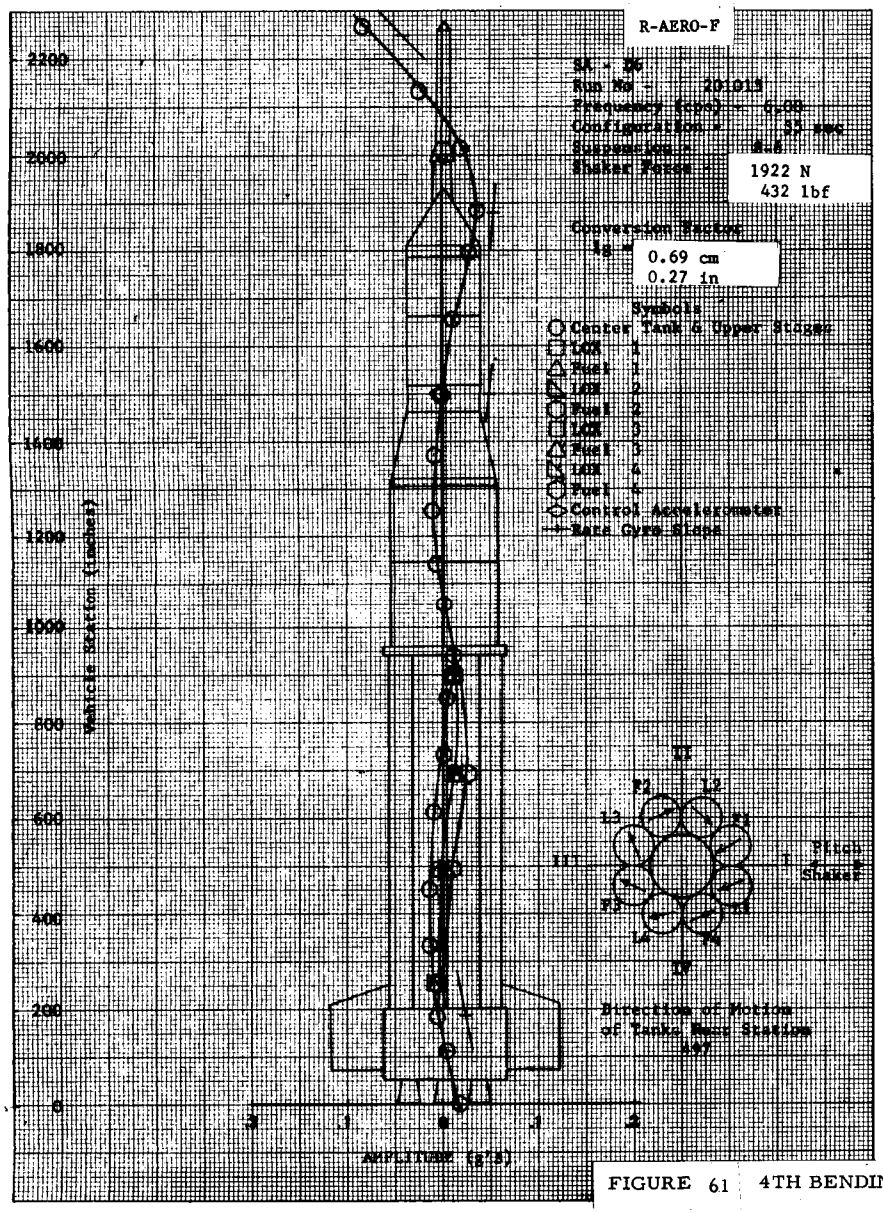


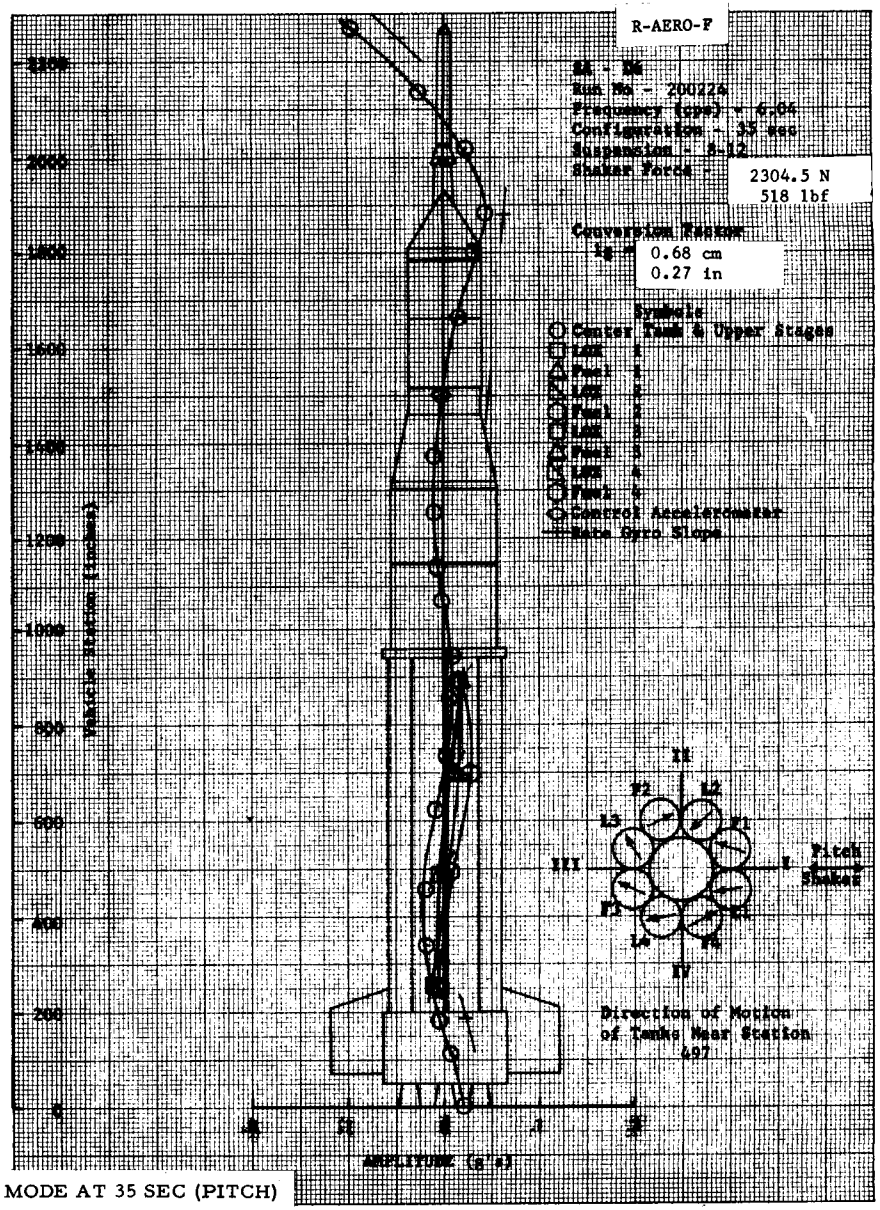


FIGURE 61 4TH BENDING MODE AT 35 SEC (PITCH)

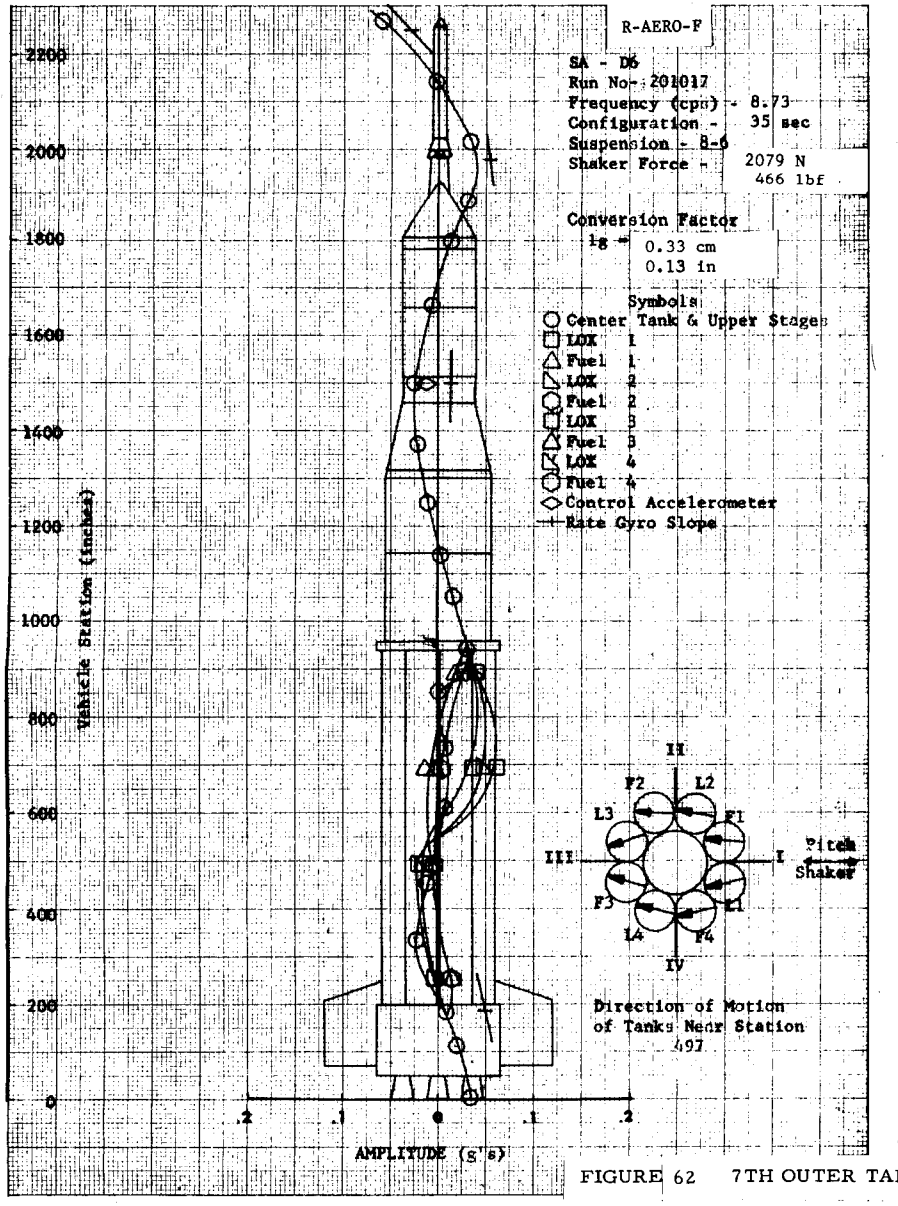


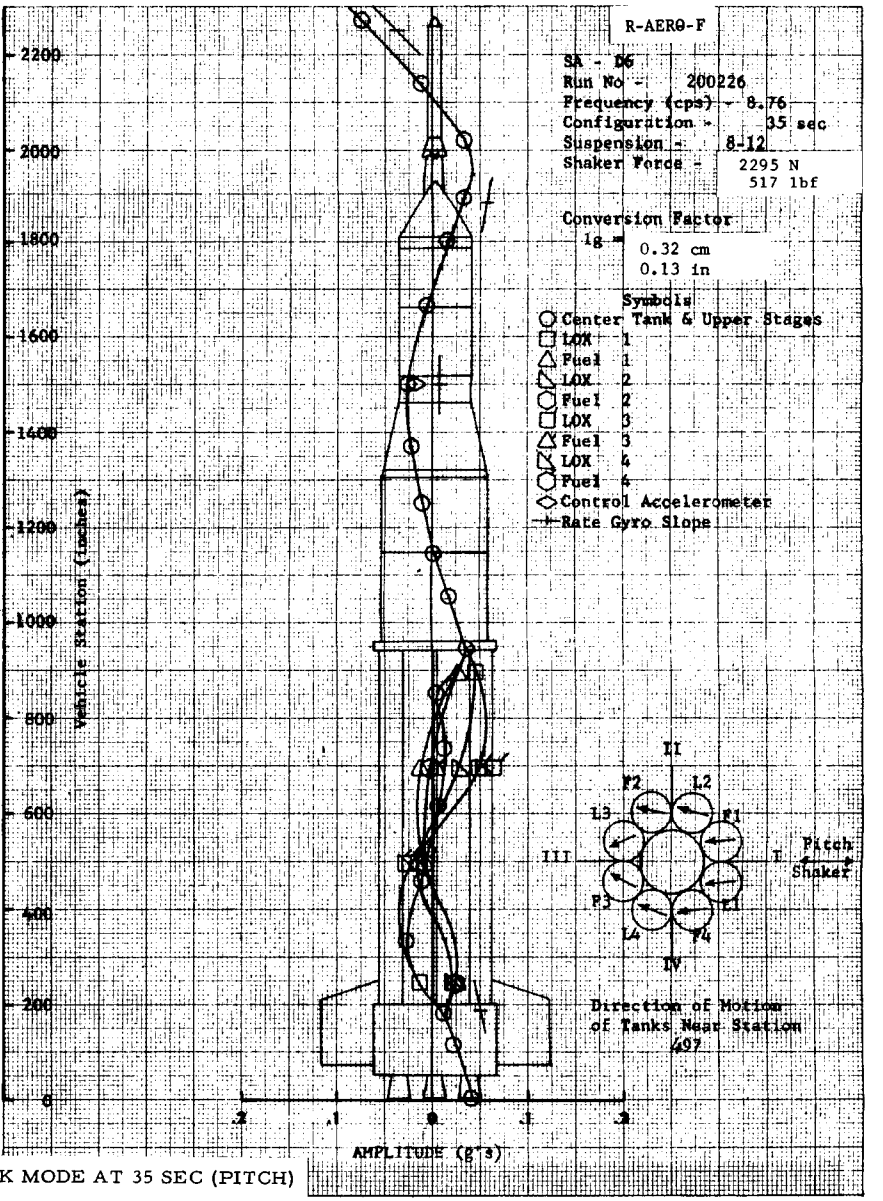


FIGURE 62 7TH OUTER TANK MODE AT 35 SEC (PITCH)

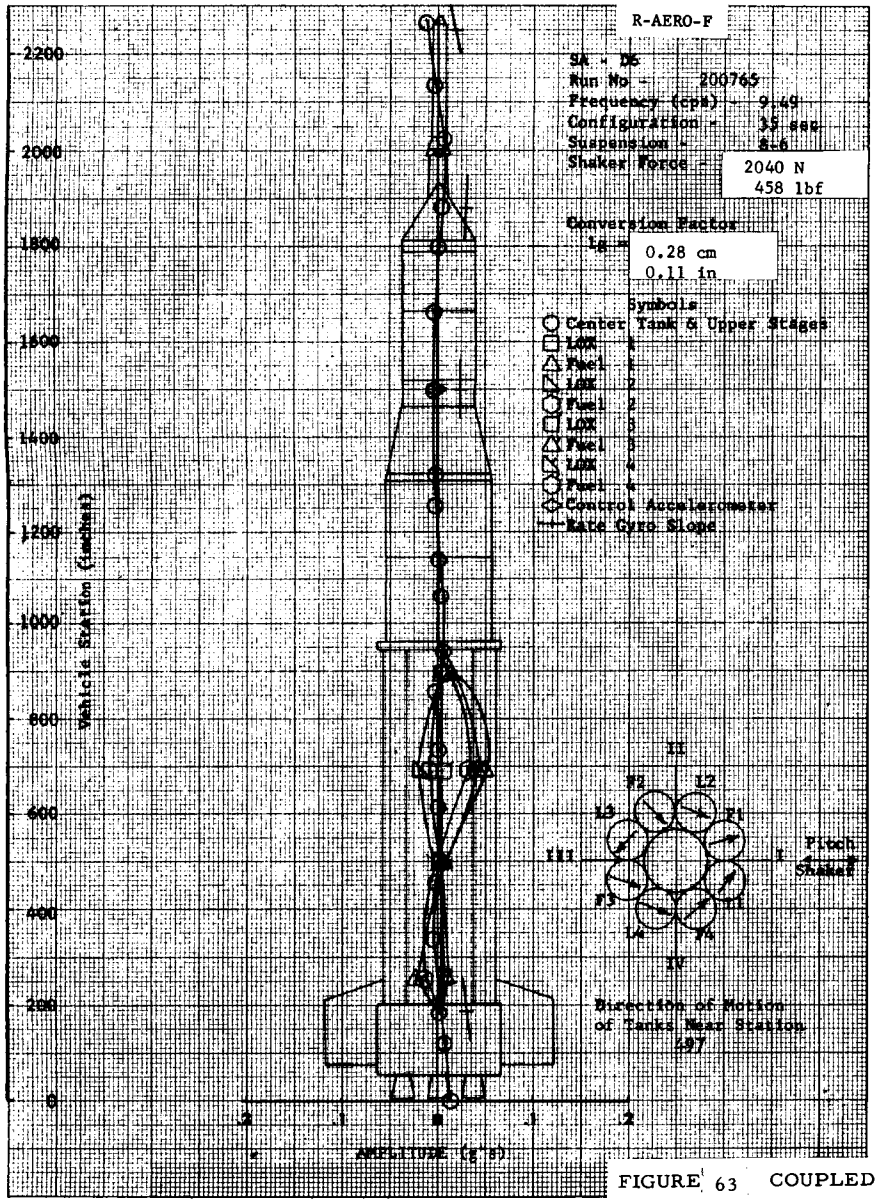


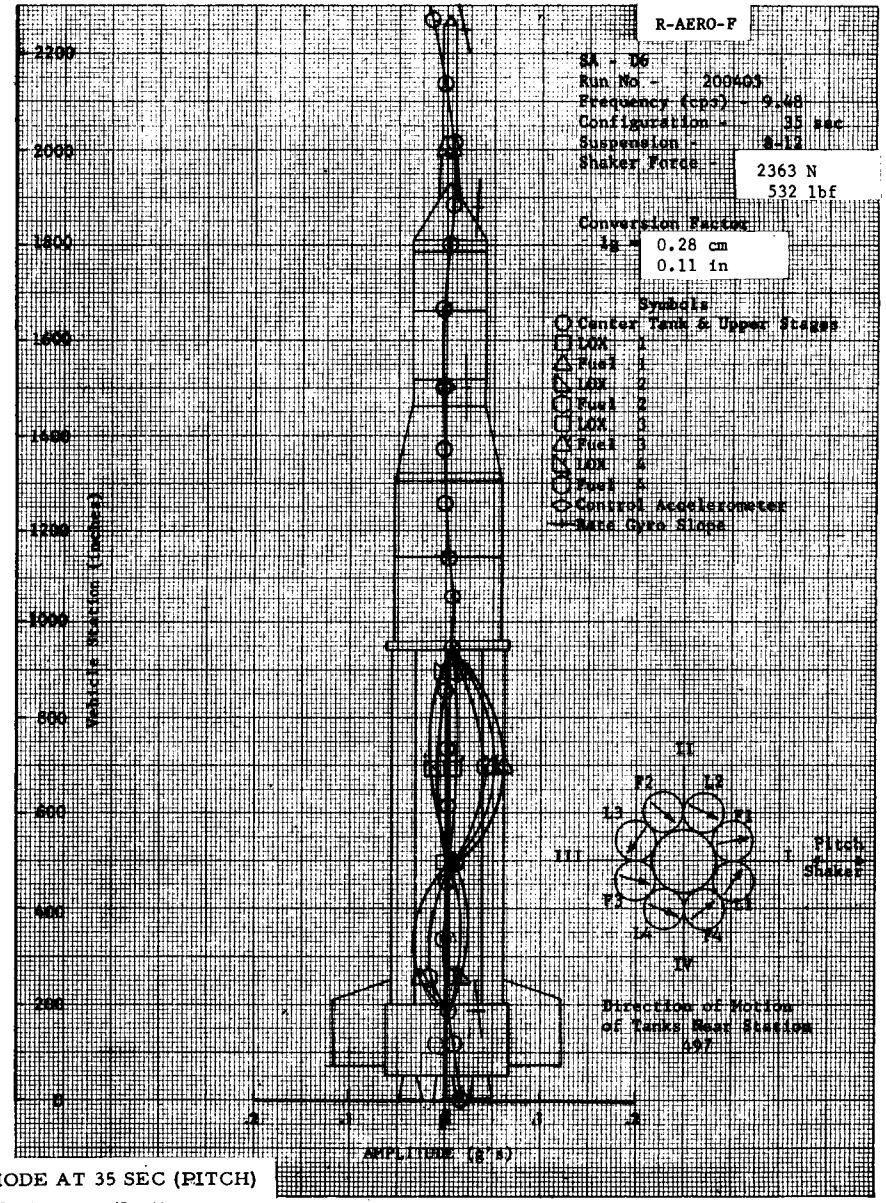


FIGURE 63 COUPLED MODE AT 35 SEC (PITCH)

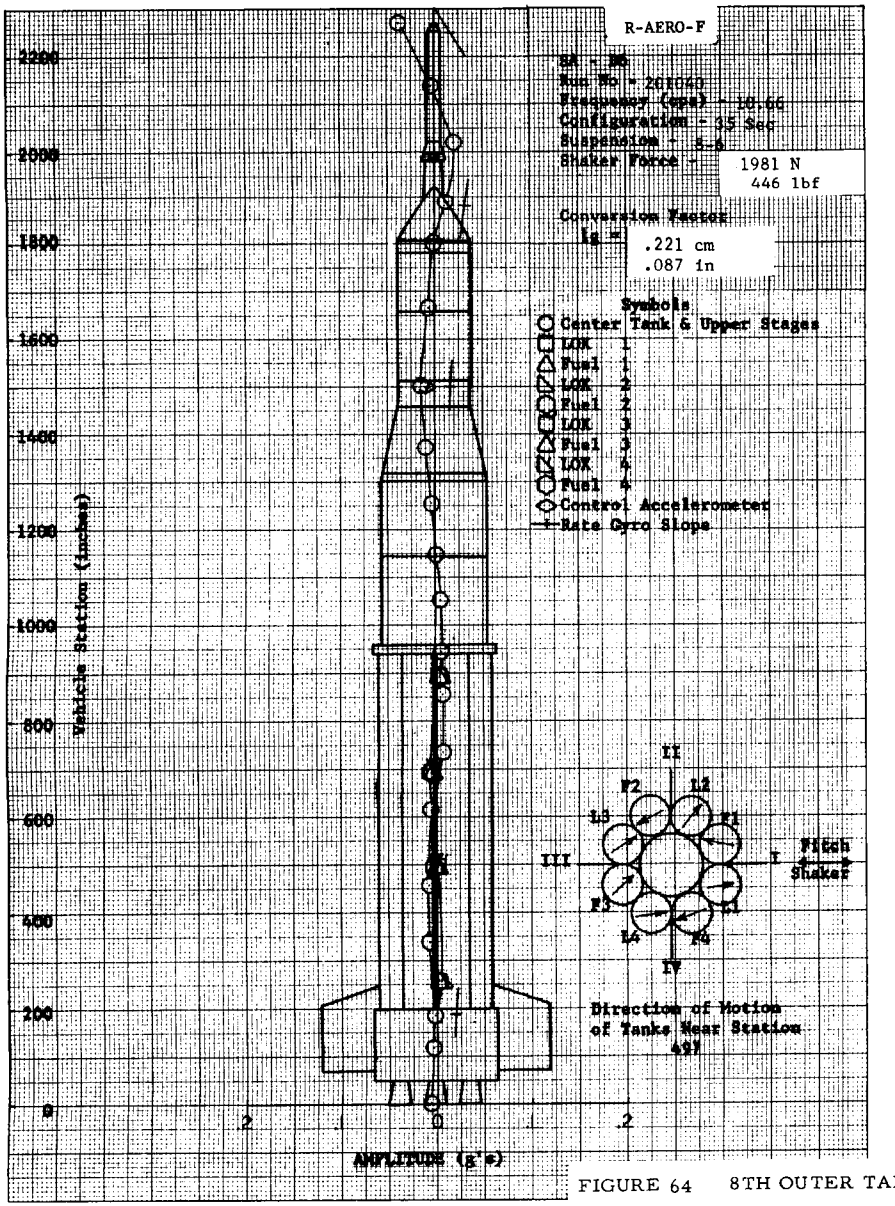


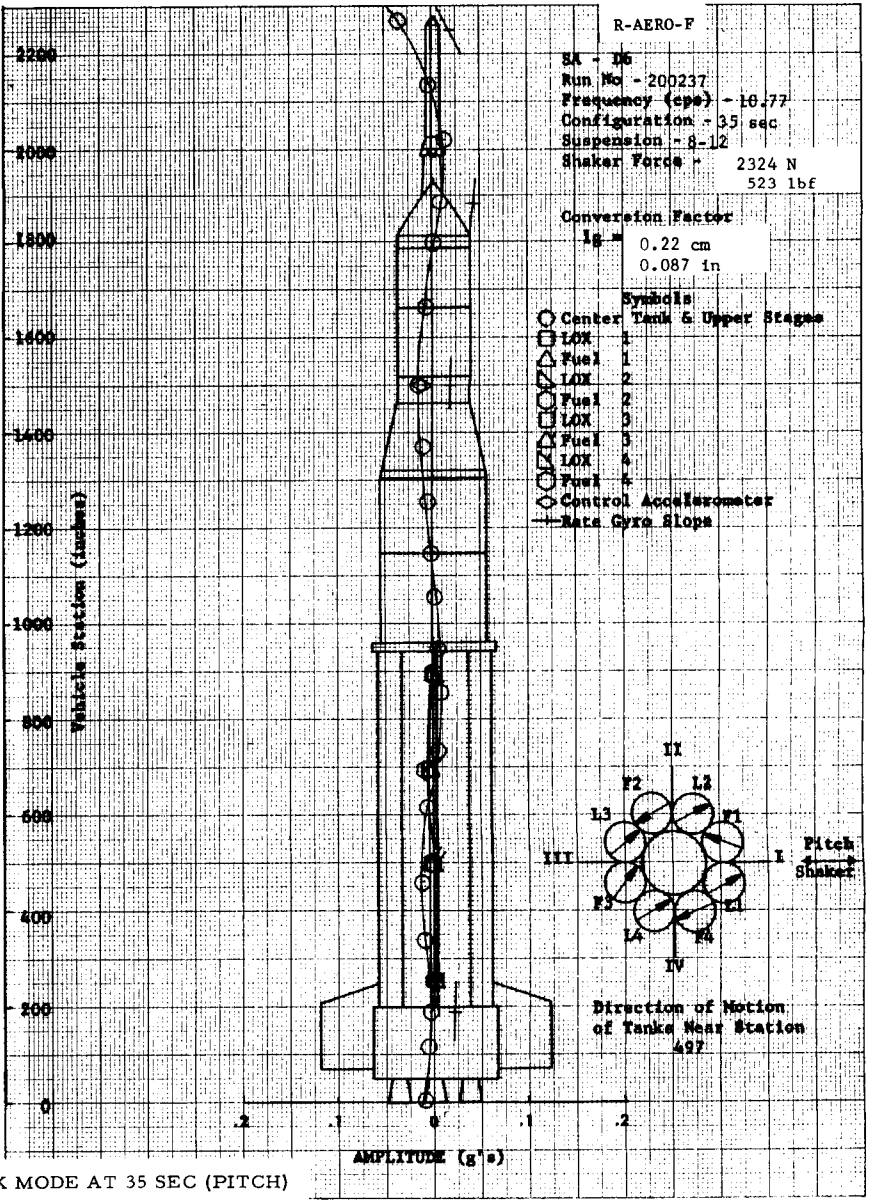


FIGURE 64 8TH OUTER TANK MODE AT 35 SEC (PITCH)

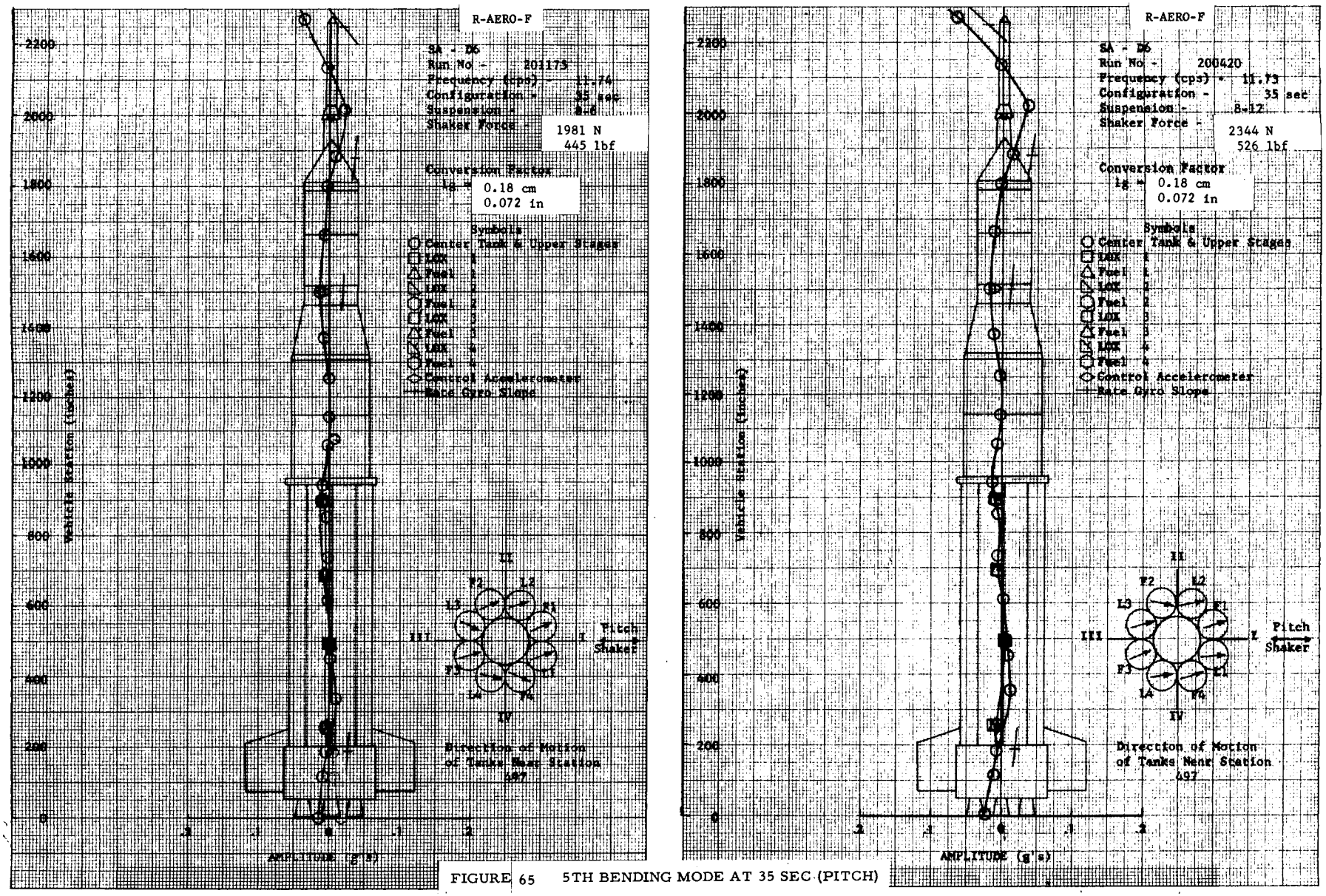


FIGURE 65 5TH BENDING MODE AT 35 SEC (PITCH)

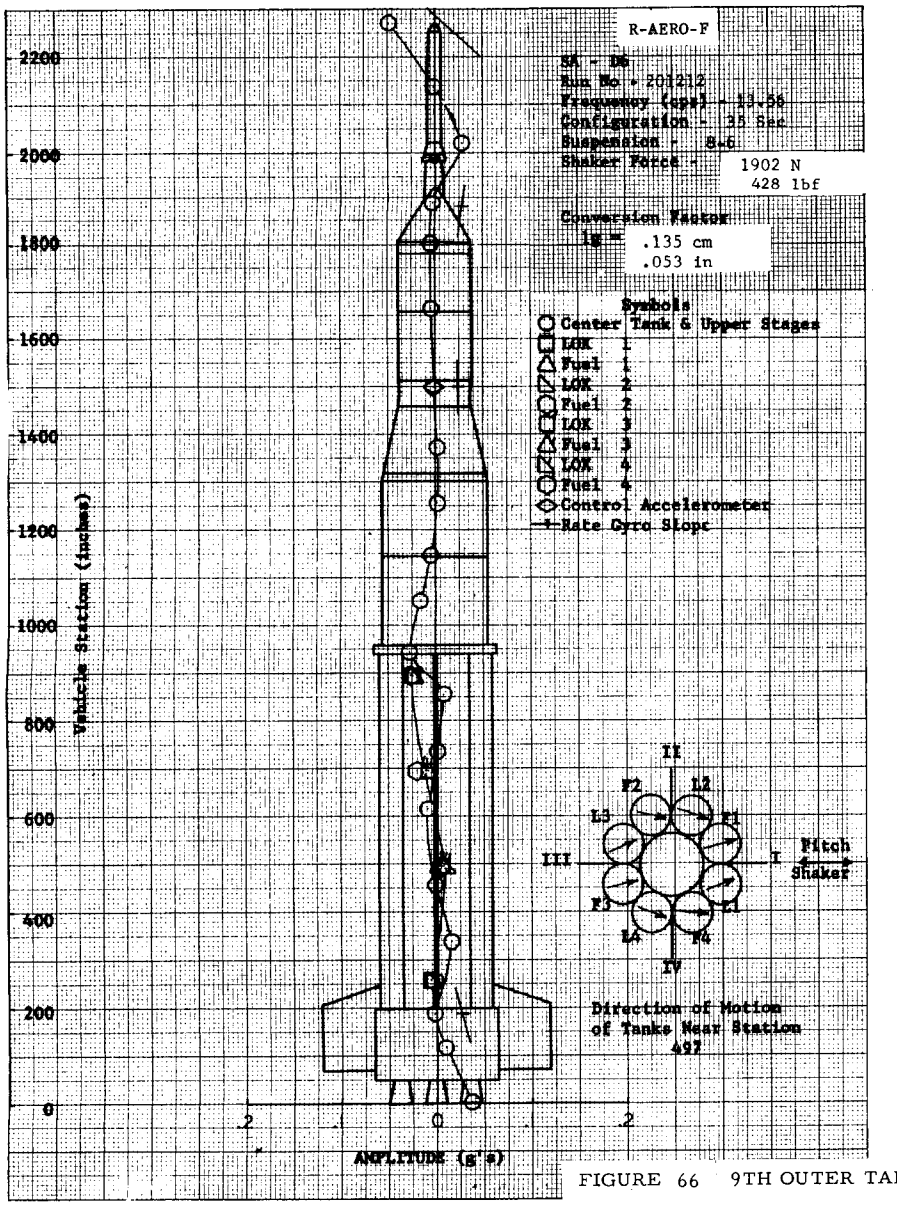


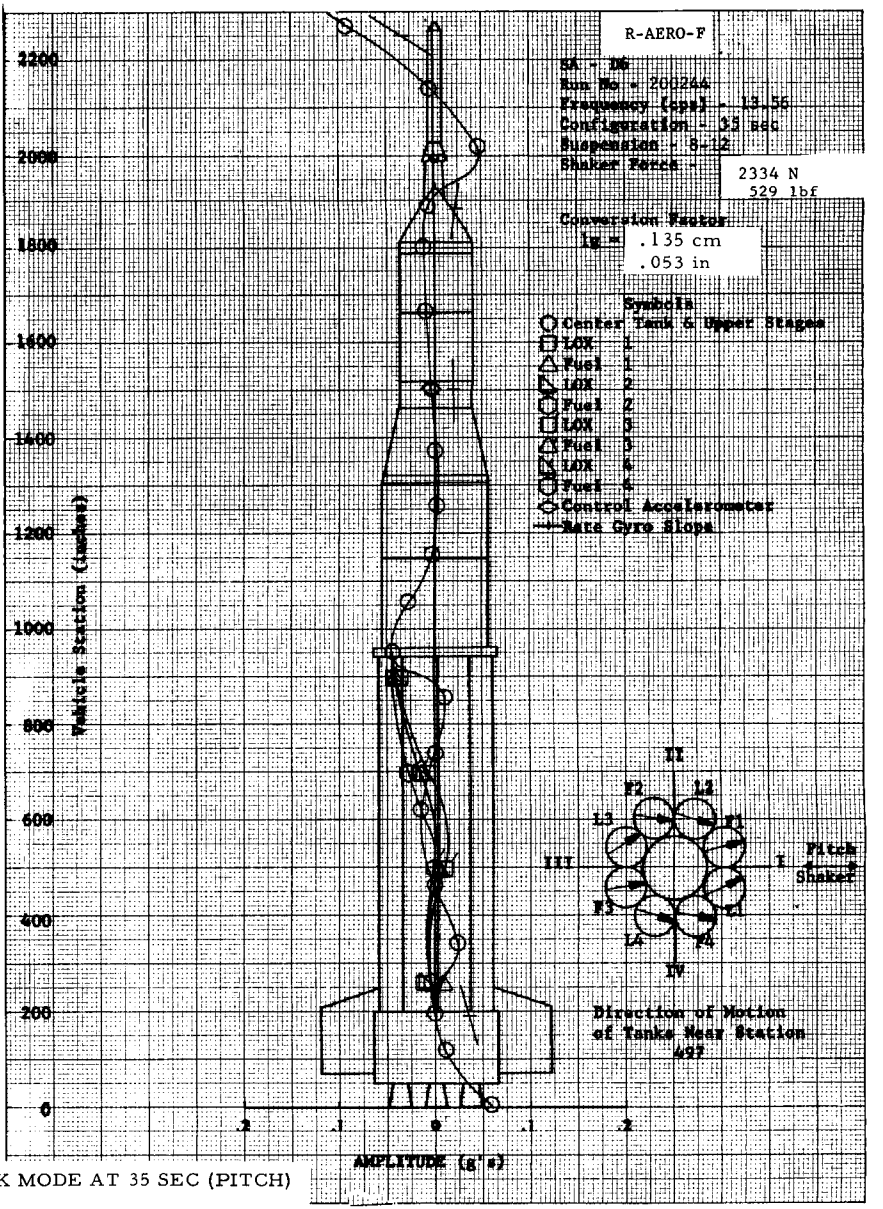


FIGURE 66 9TH OUTER TANK MODE AT 35 SEC (PITCH)

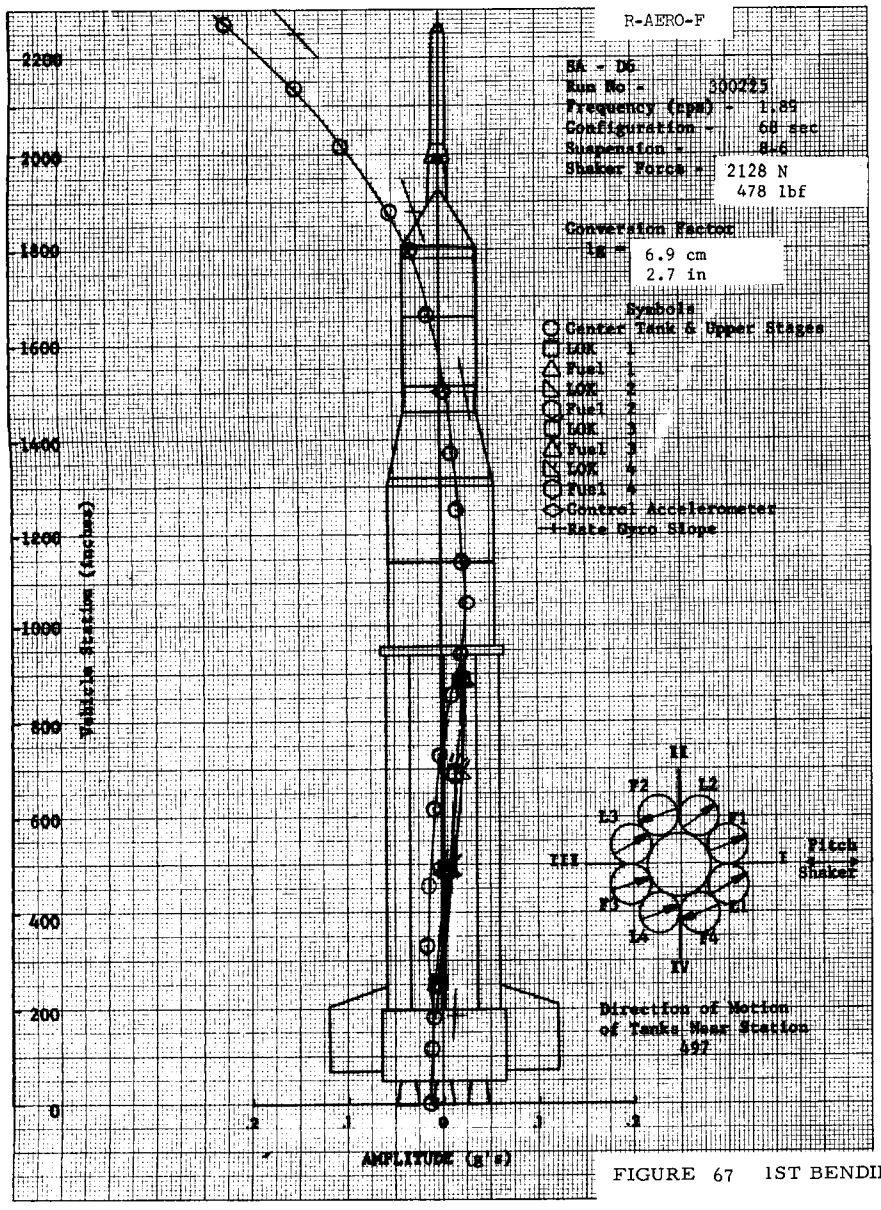


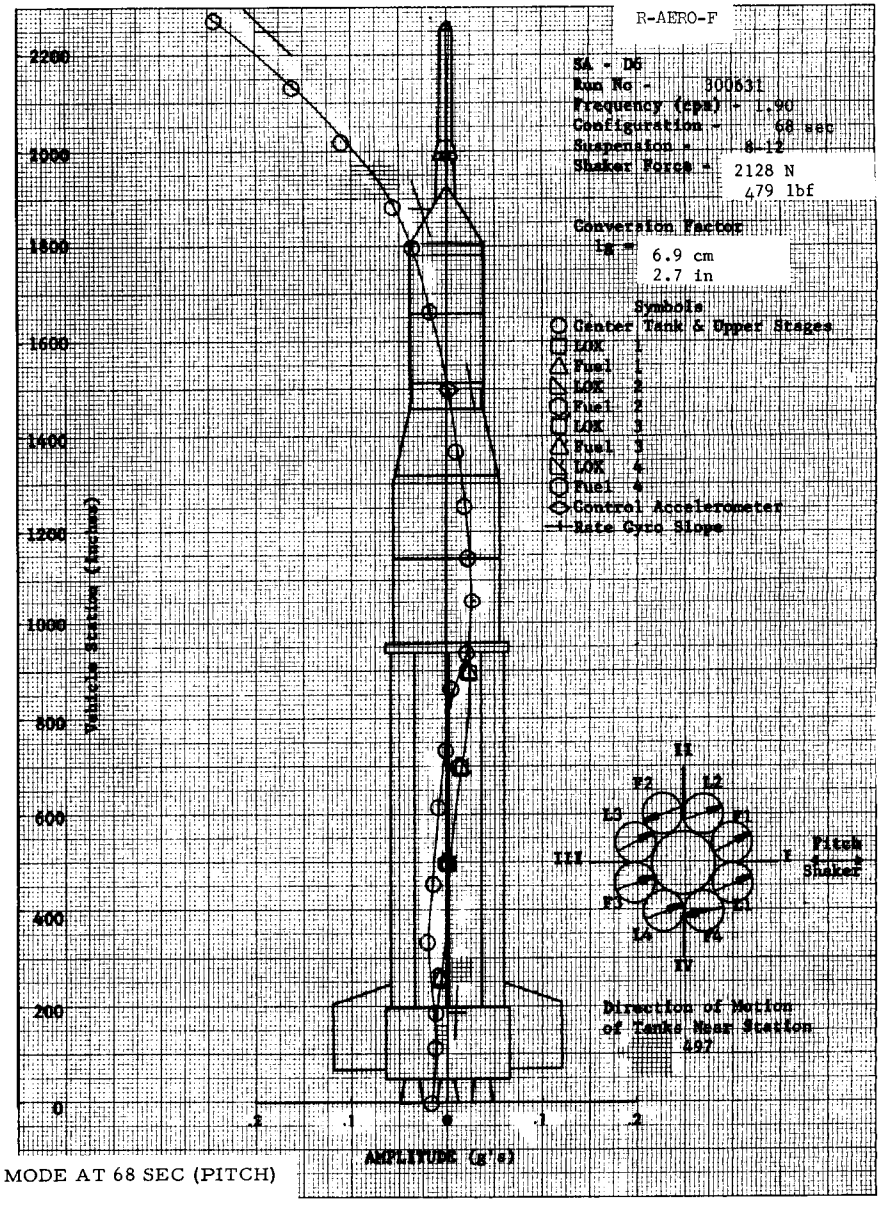


FIGURE 67 1ST BENDING MODE AT 68 SEC (PITCH)

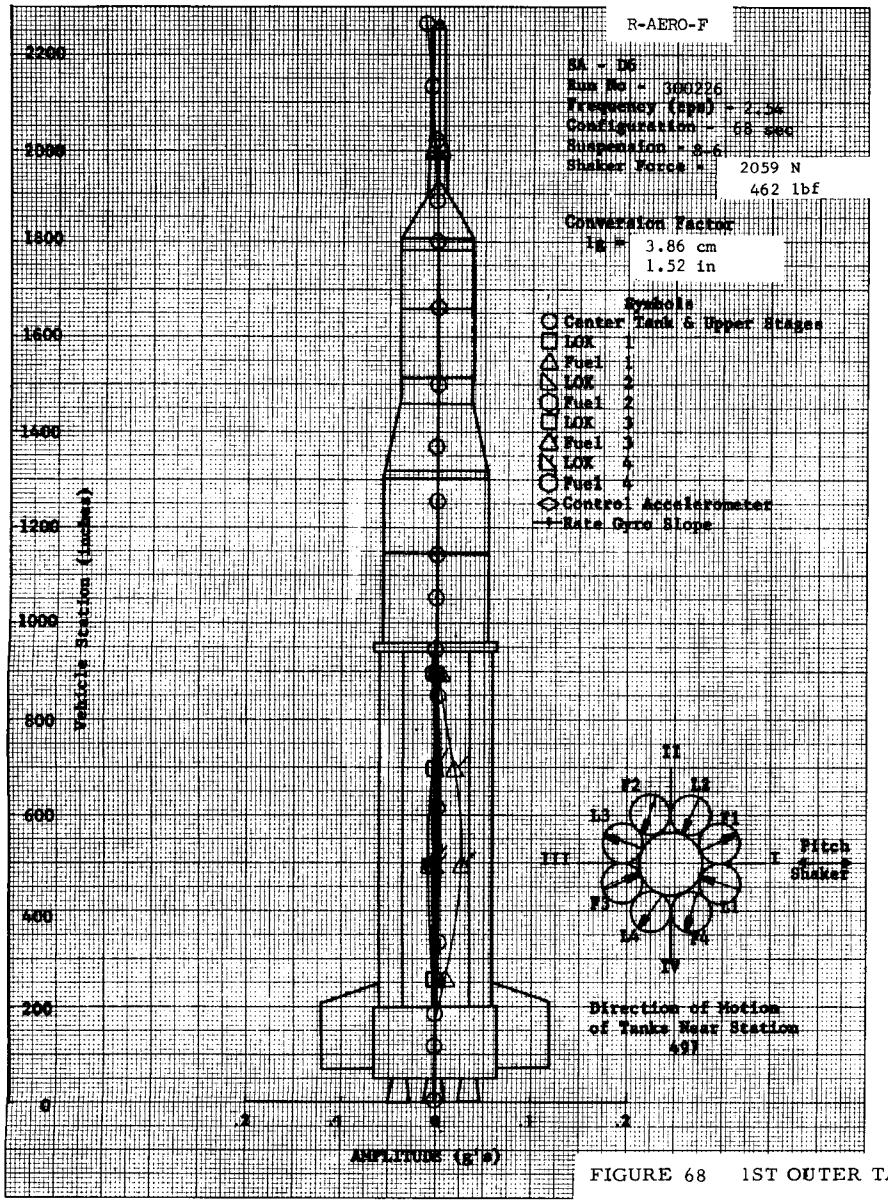


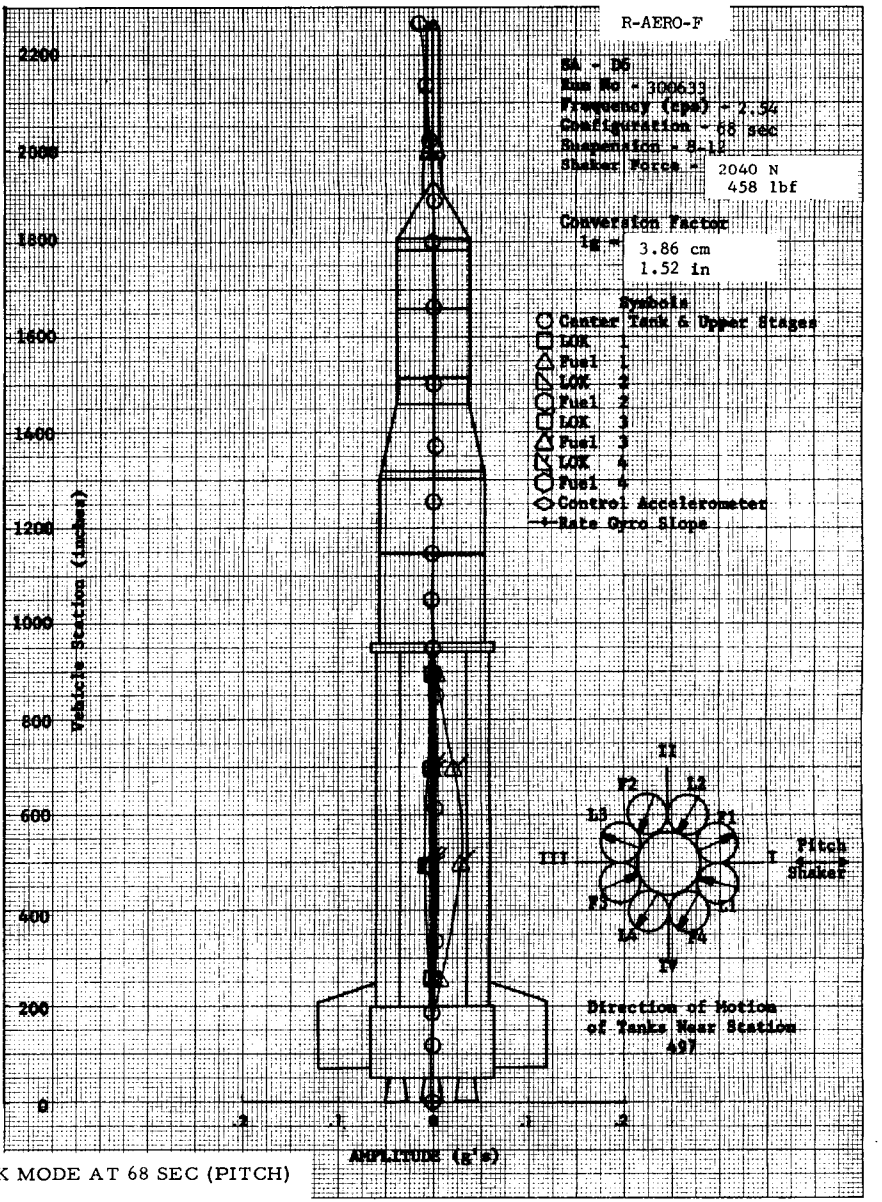


FIGURE 68 1ST OUTER TANK MODE AT 68 SEC (PITCH)

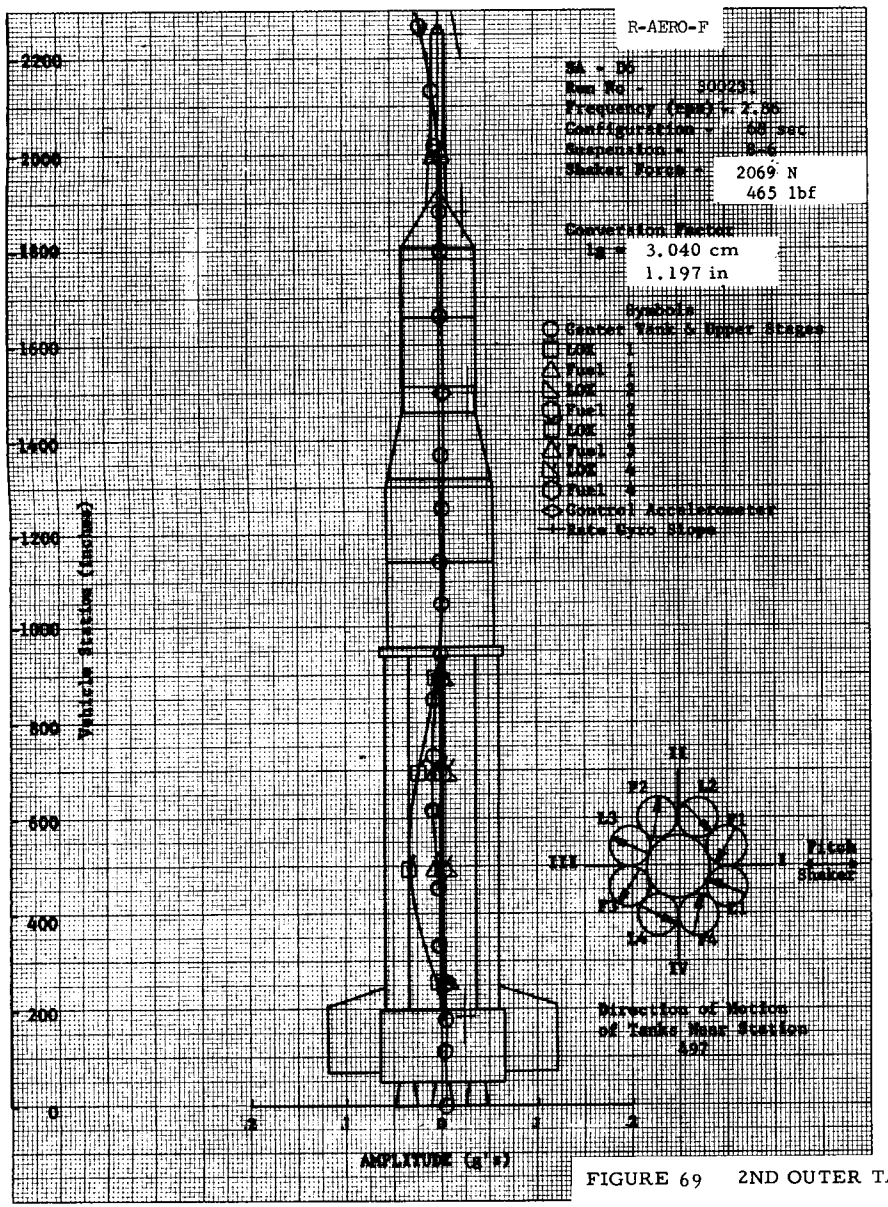


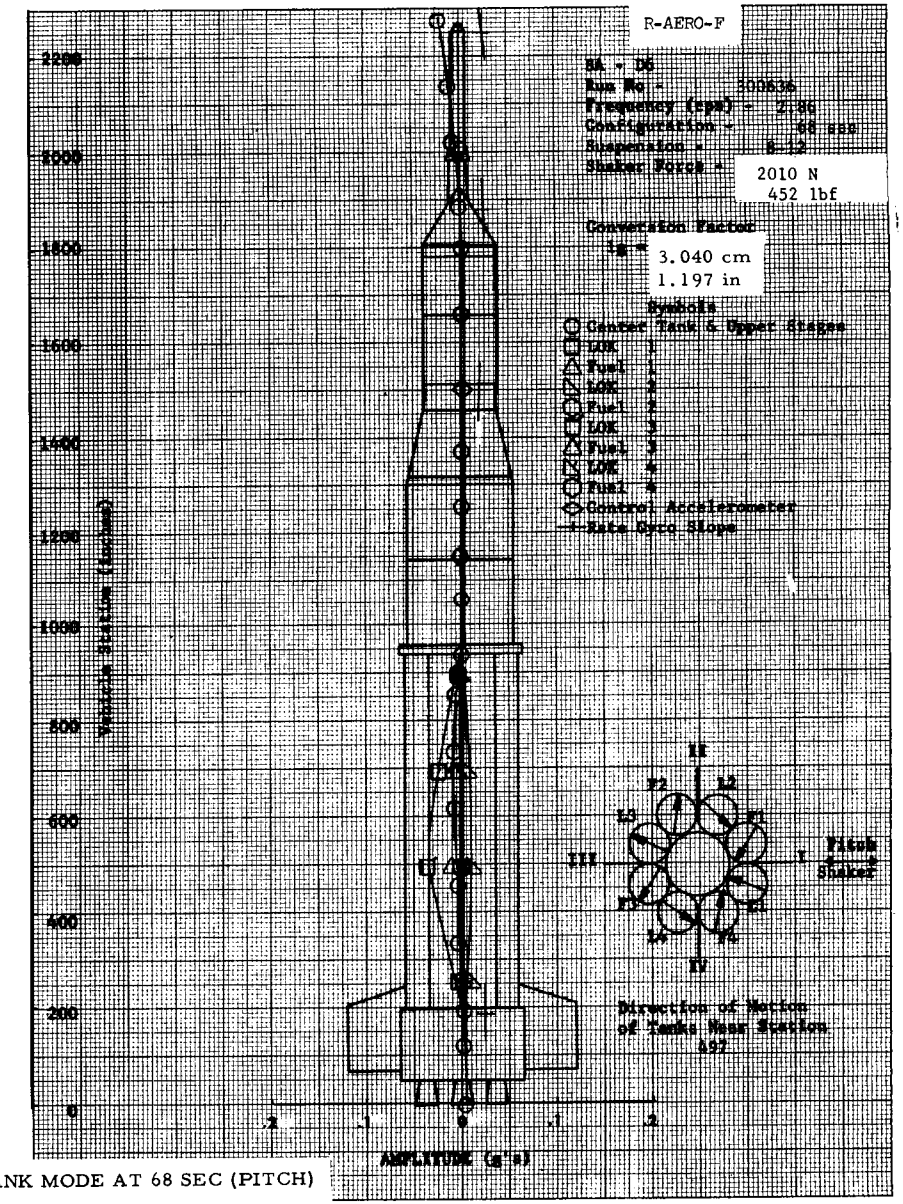


FIGURE 69 2ND OUTER TANK MODE AT 68 SEC (PITCH)

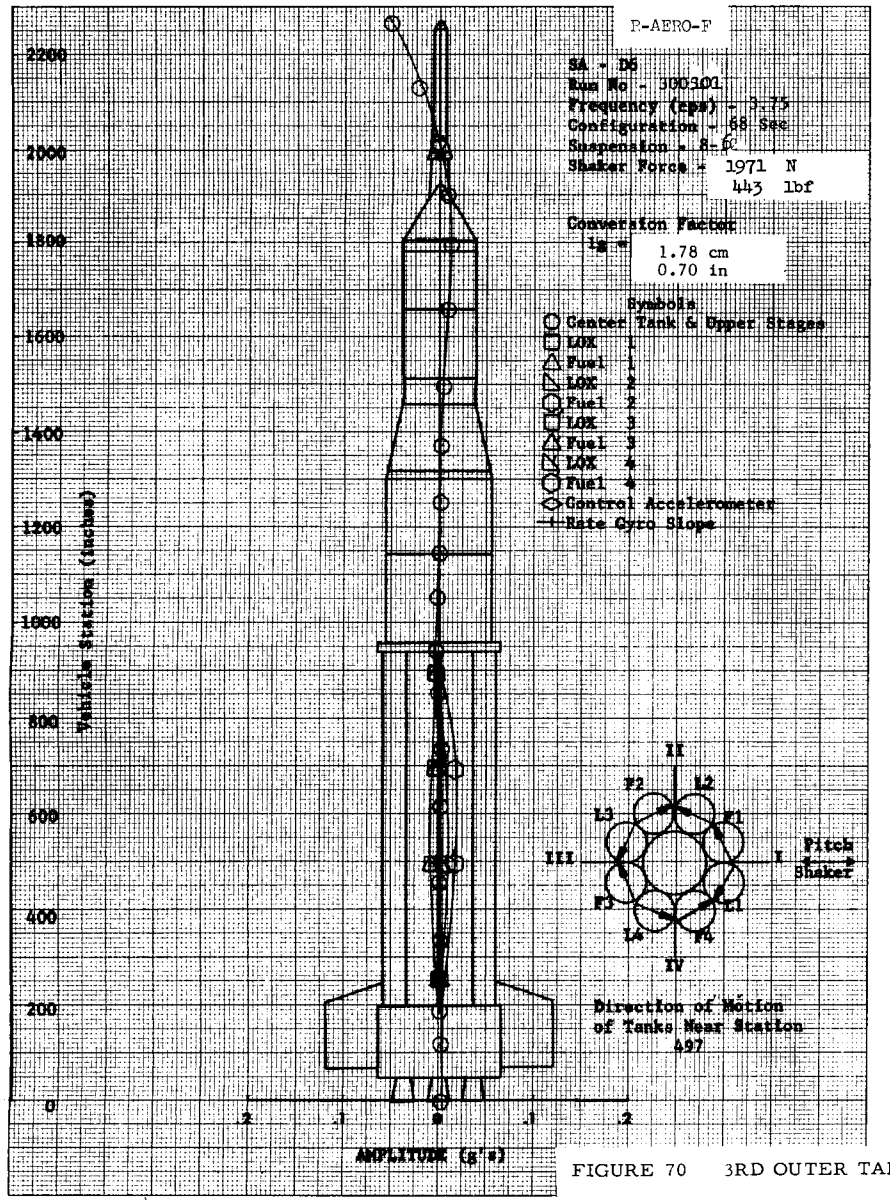


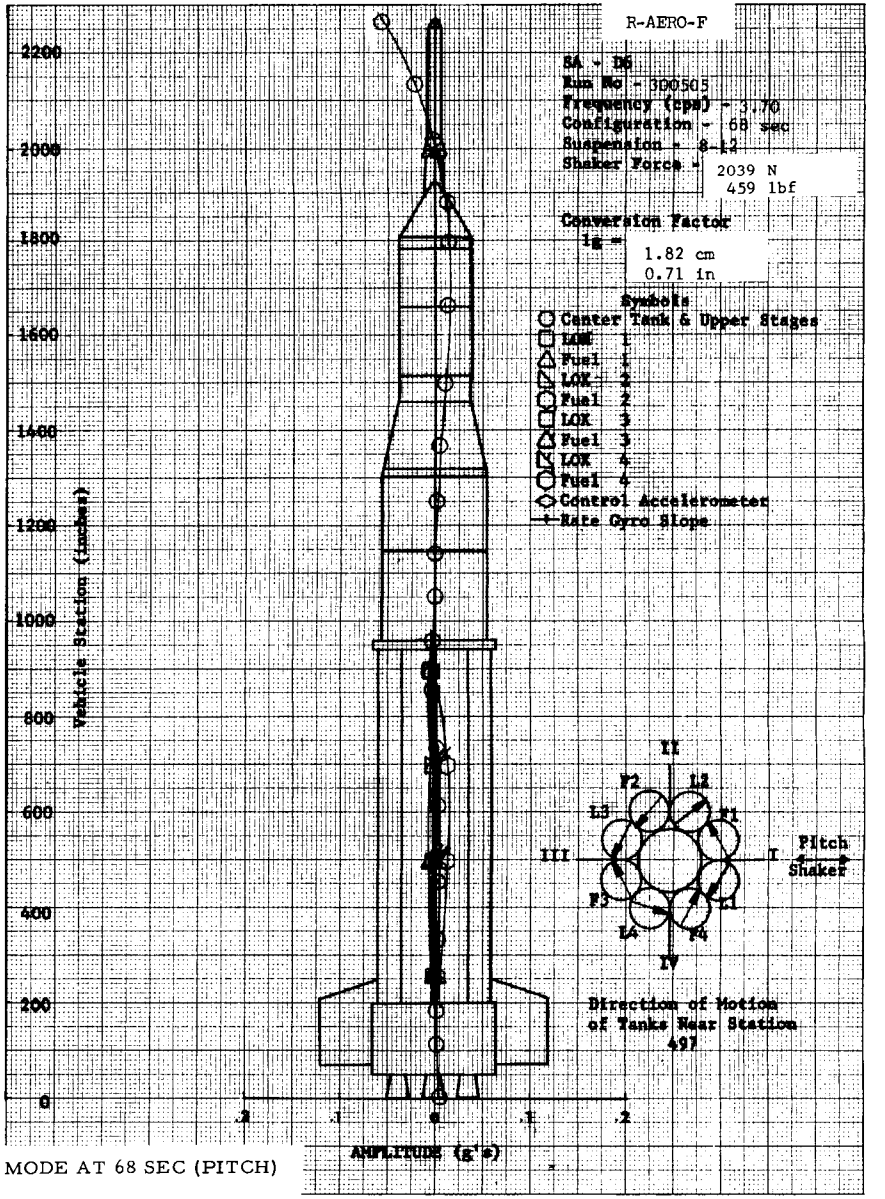


FIGURE 70 3RD OUTER TANK MODE AT 68 SEC (PITCH)

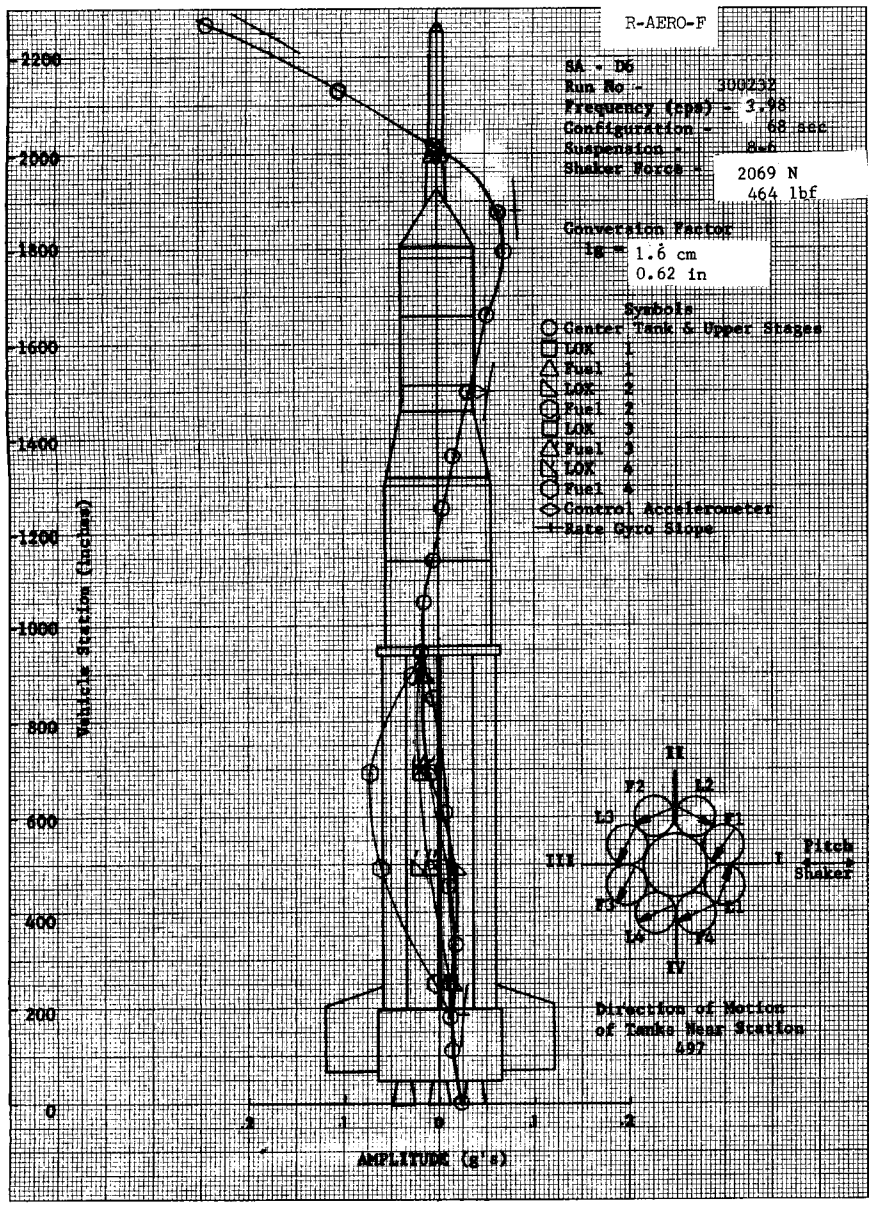


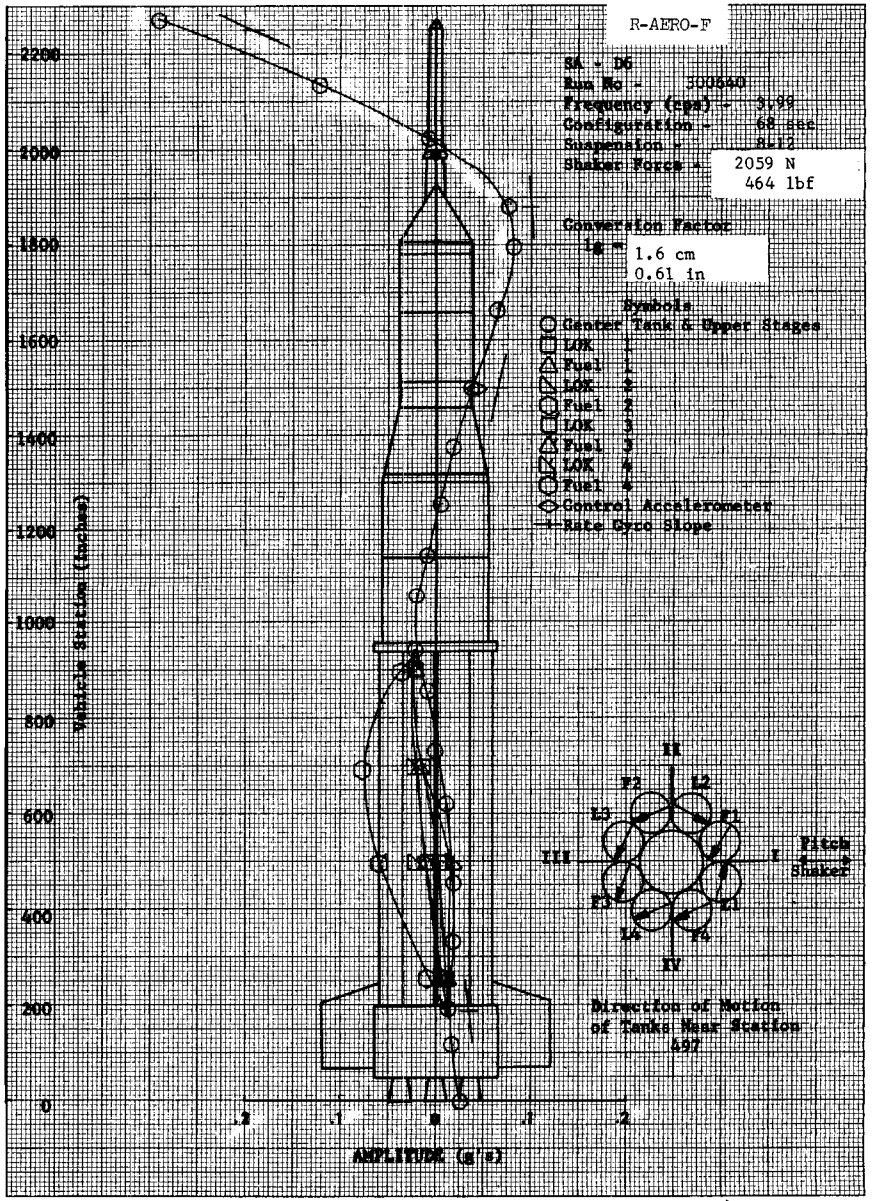


FIGURE 71 TOWER MODE COUPLED WITH 2ND BENDING MODE AT 68 SEC (PITCH)

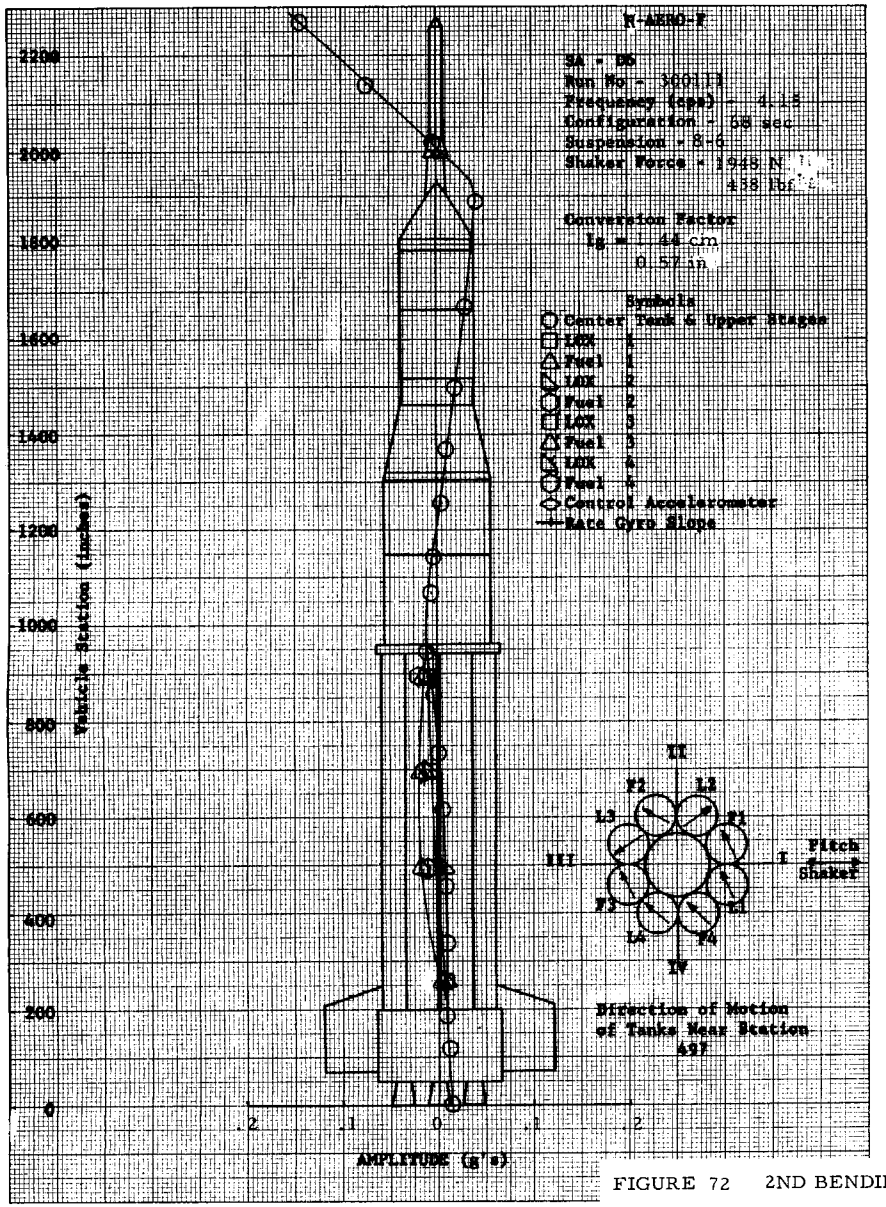


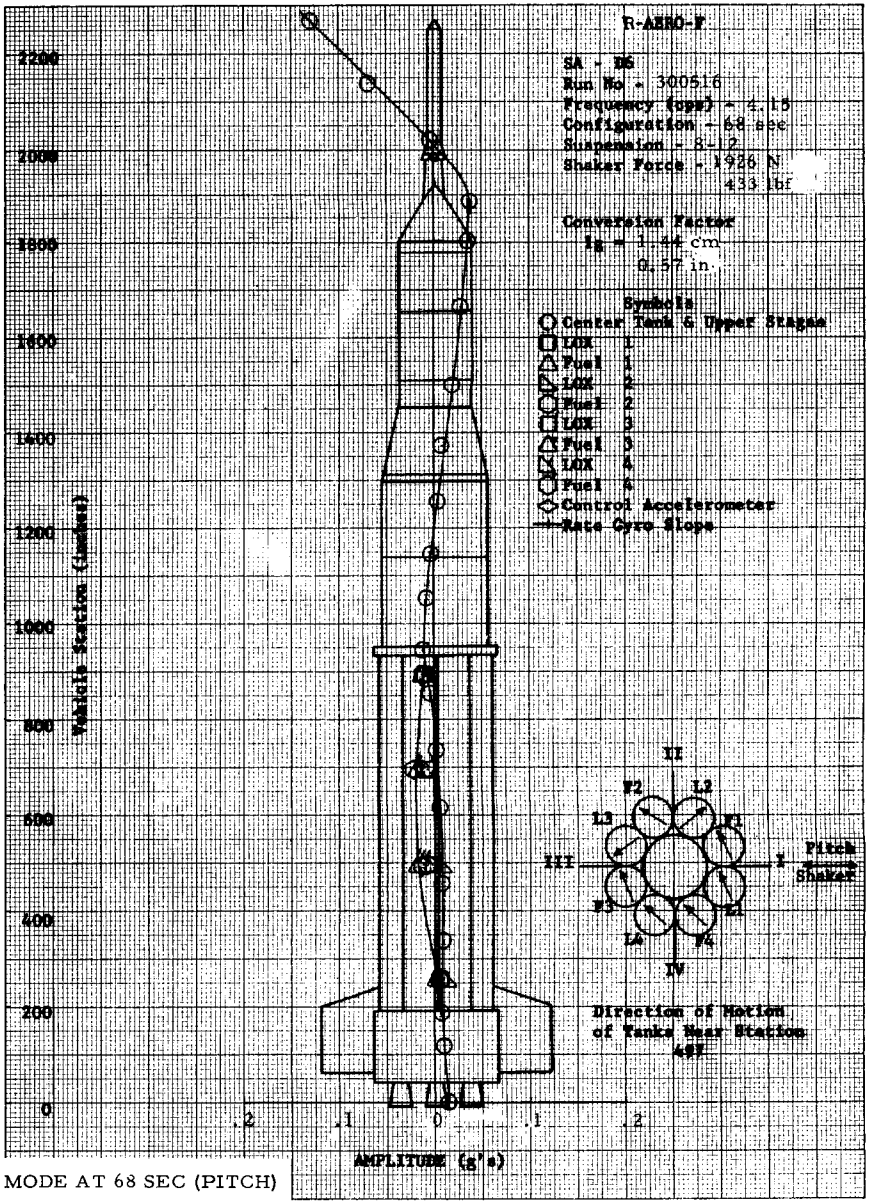


FIGURE 72 2ND BENDING MODE AT 68 SEC (PITCH)

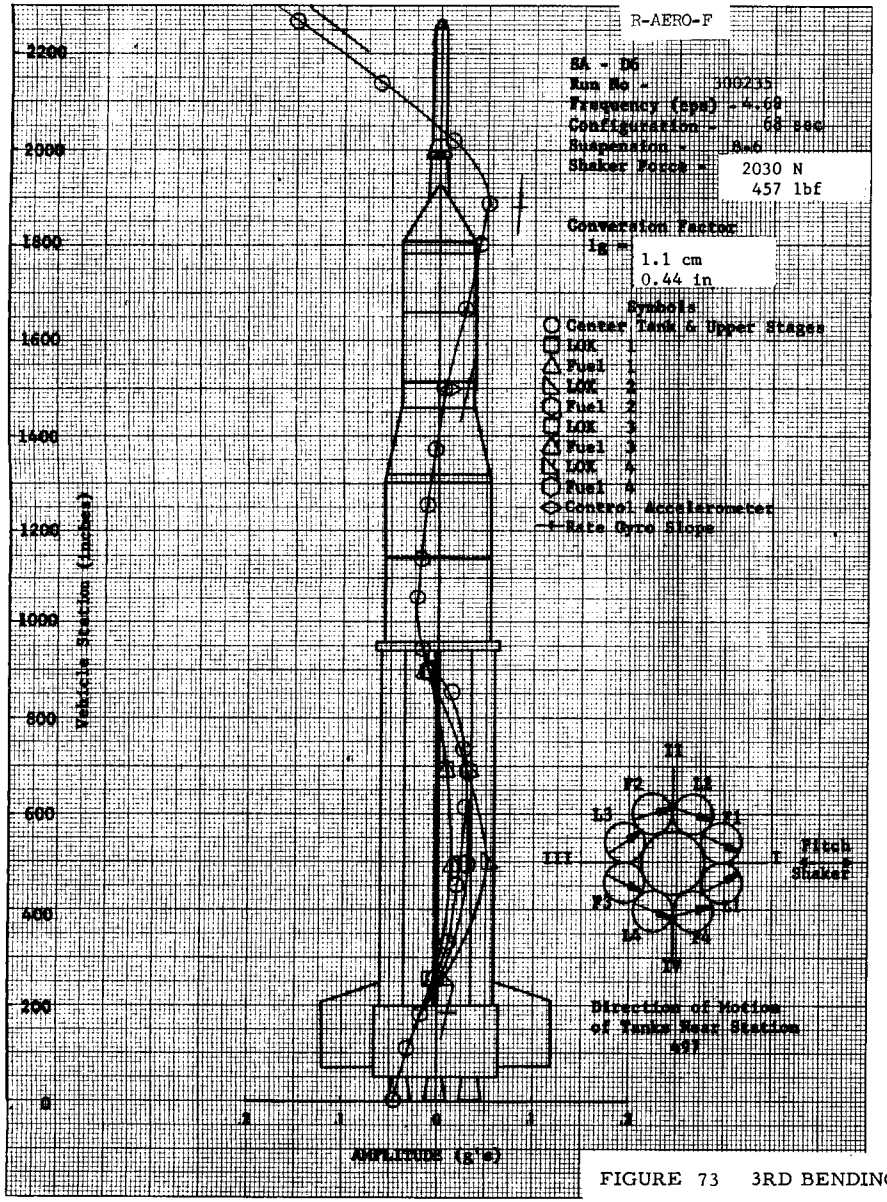


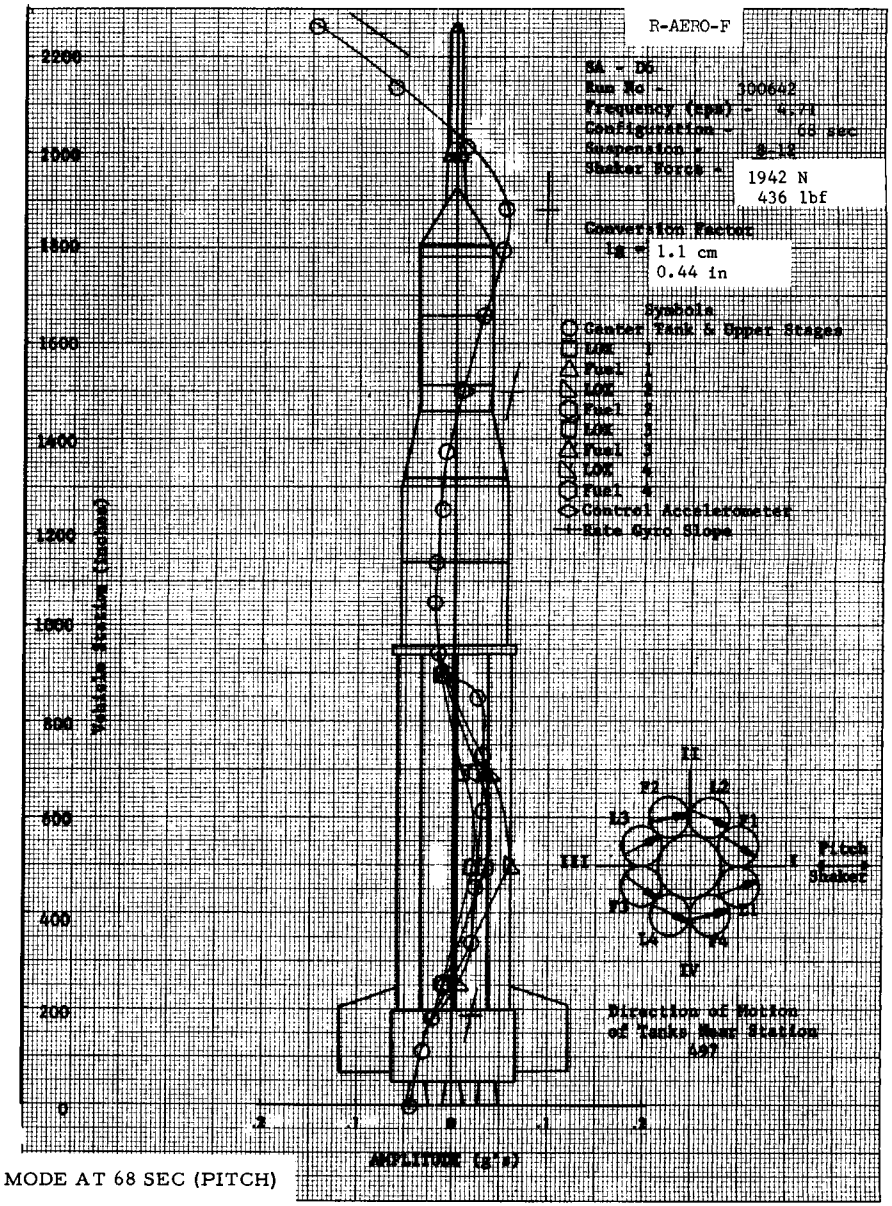


FIGURE 73 3RD BENDING MODE AT 68 SEC (PITCH)

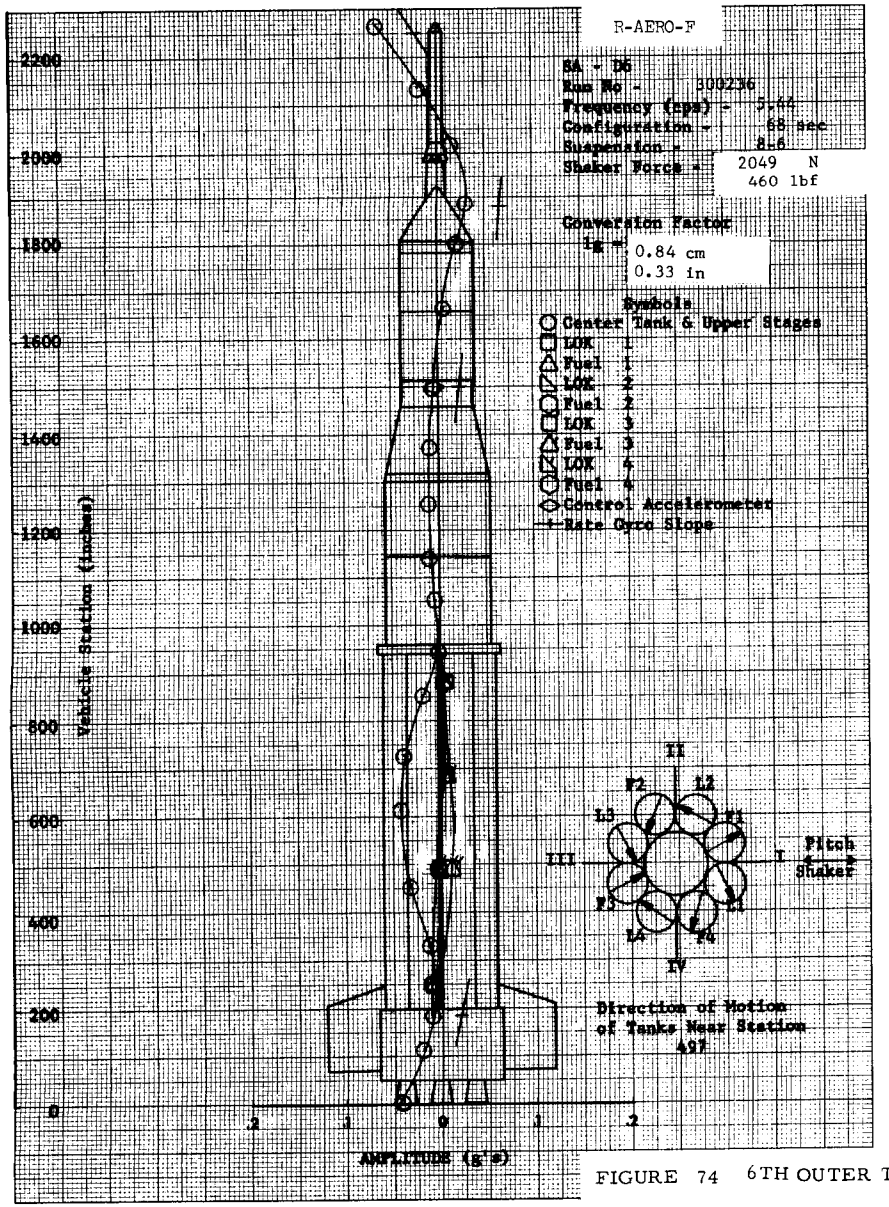


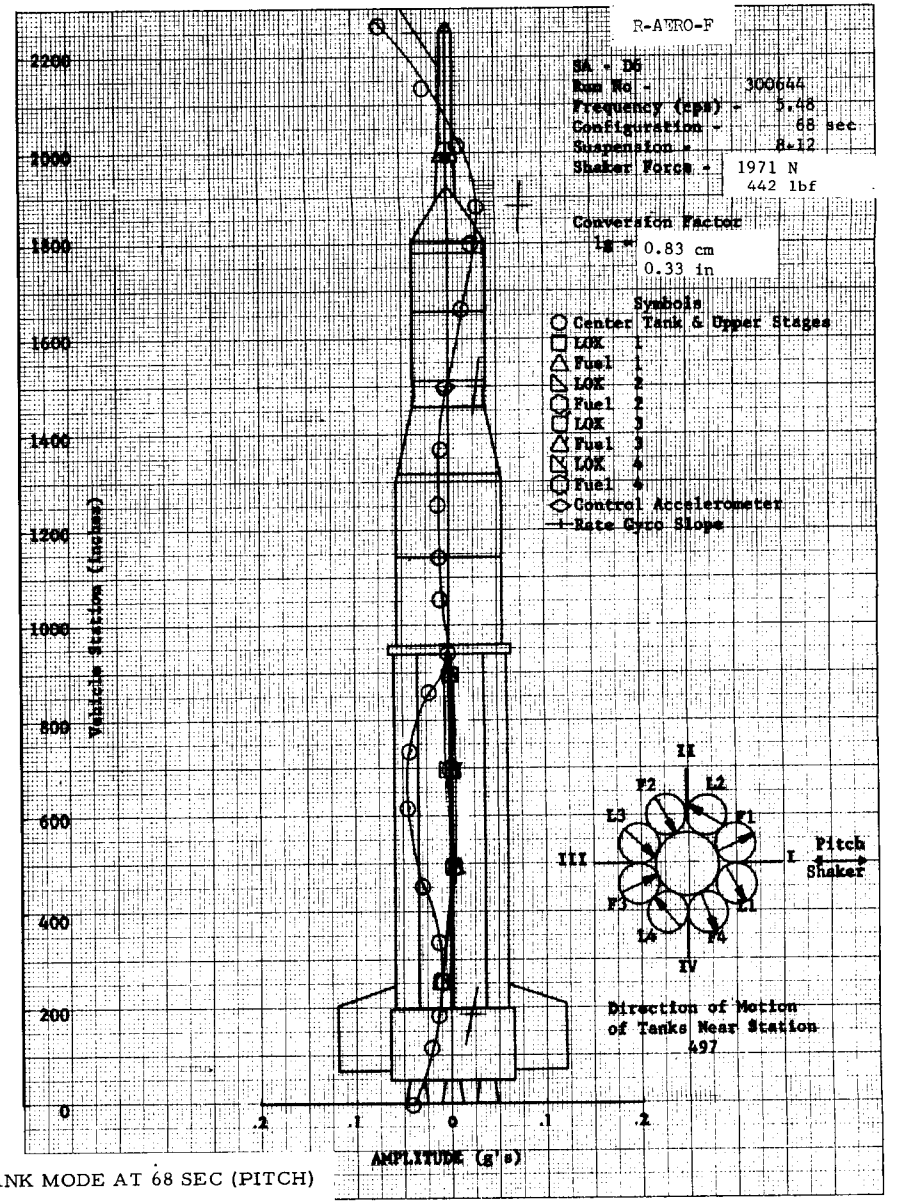


FIGURE 74 6TH OUTER TANK MODE AT 68 SEC (PITCH)

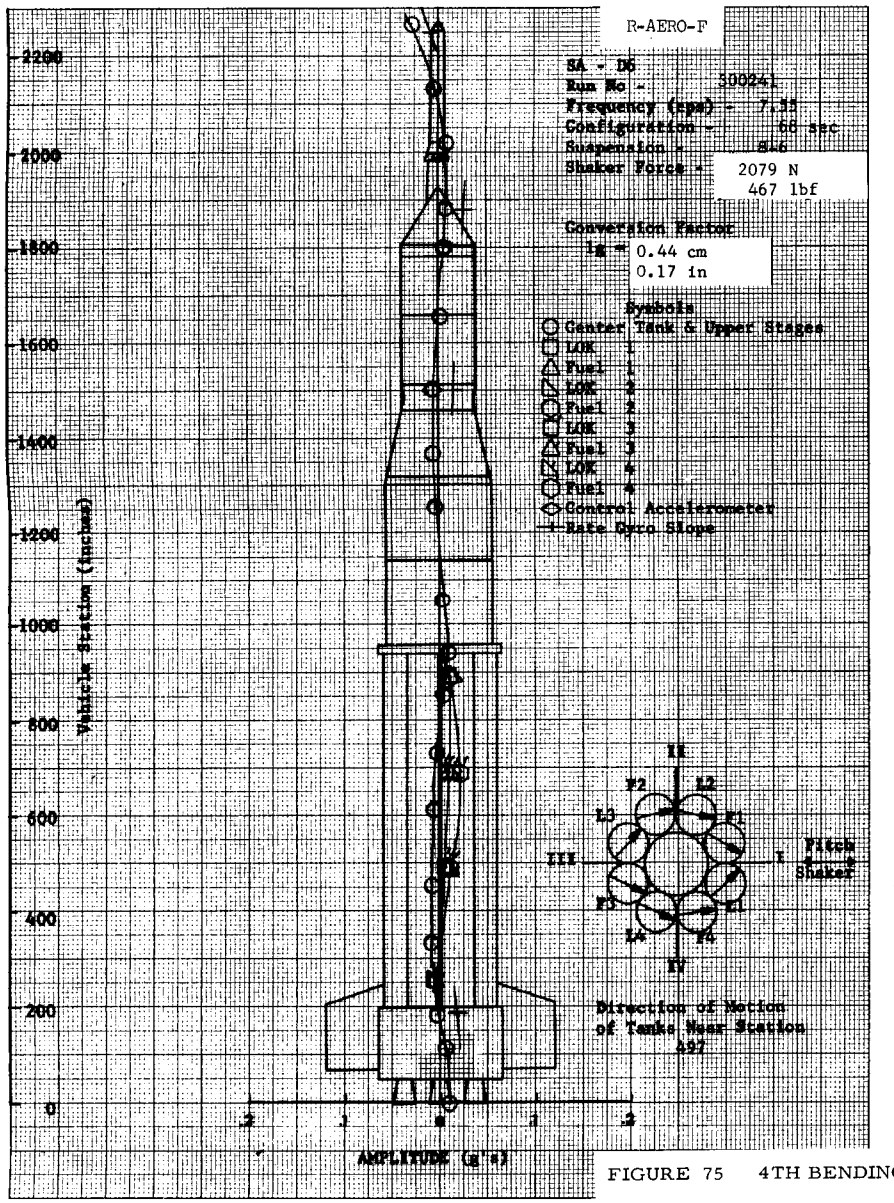


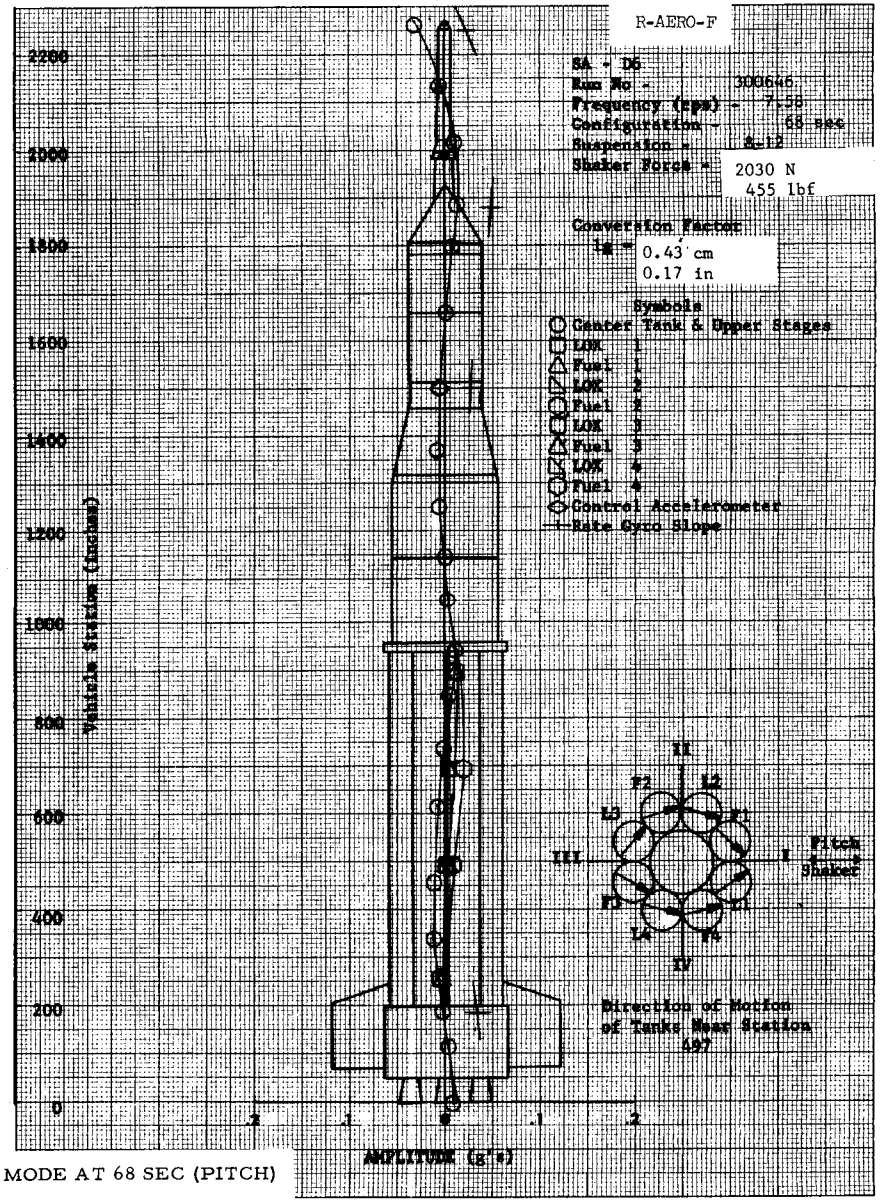


FIGURE 75 4TH BENDING MODE AT 68 SEC (PITCH)

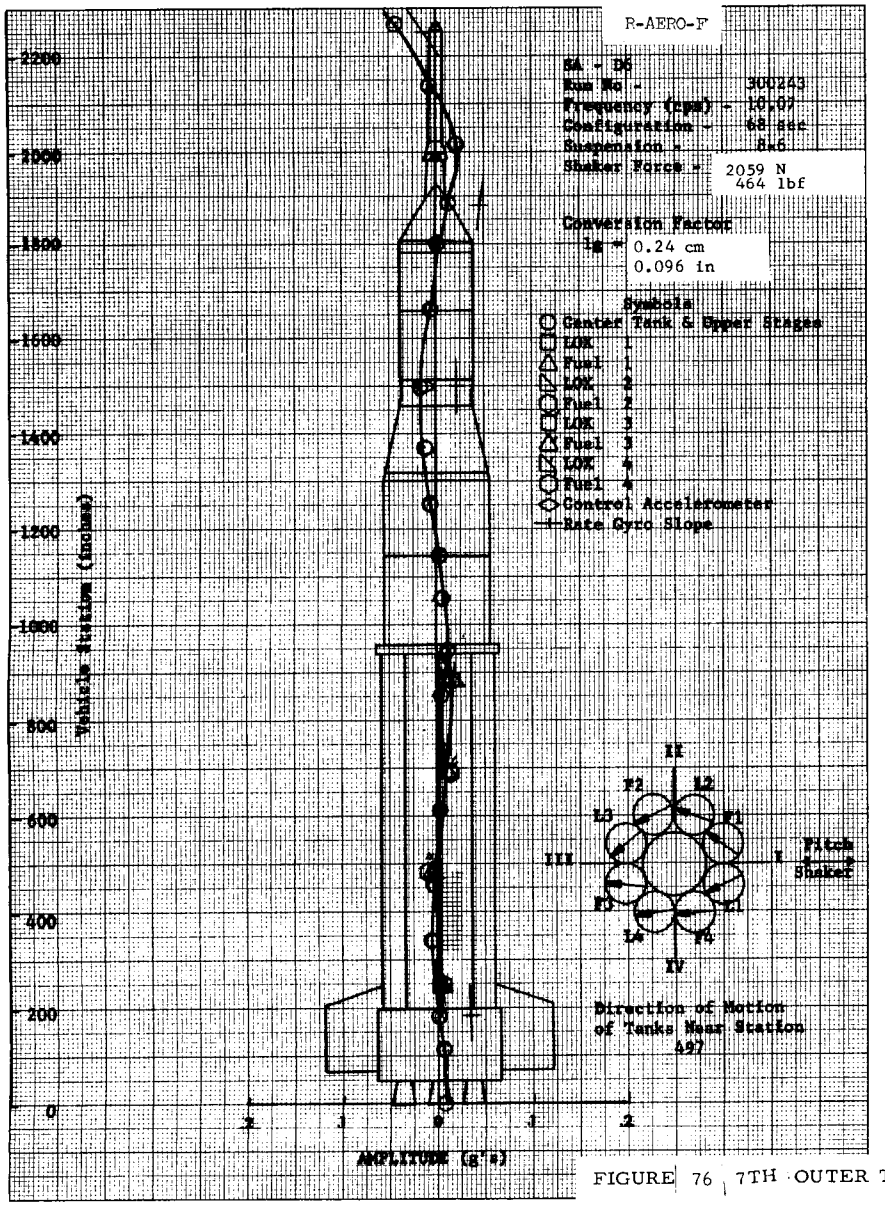


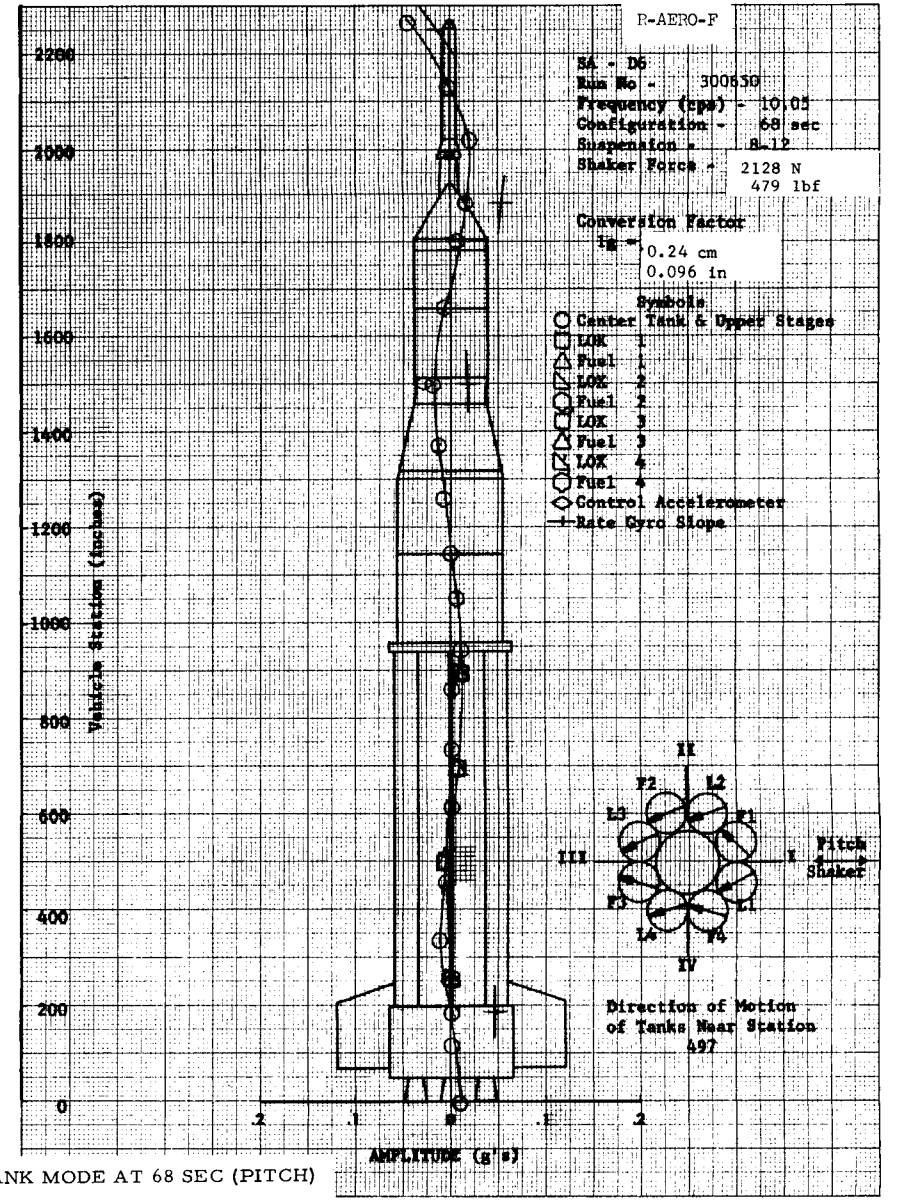


FIGURE 76 7TH OUTER TANK MODE AT 68 SEC (PITCH)

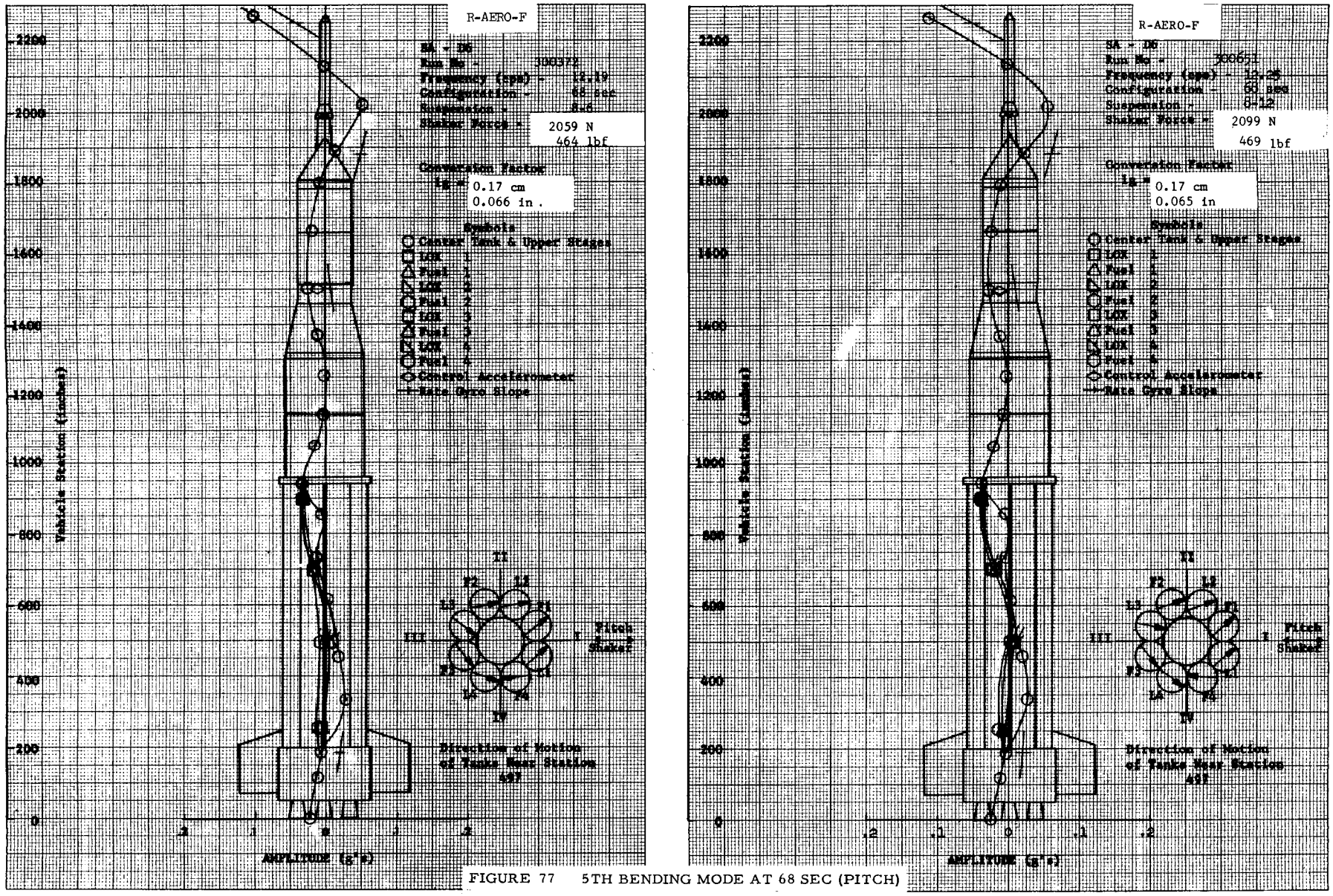


FIGURE 77 5TH BENDING MODE AT 68 SEC (PITCH)

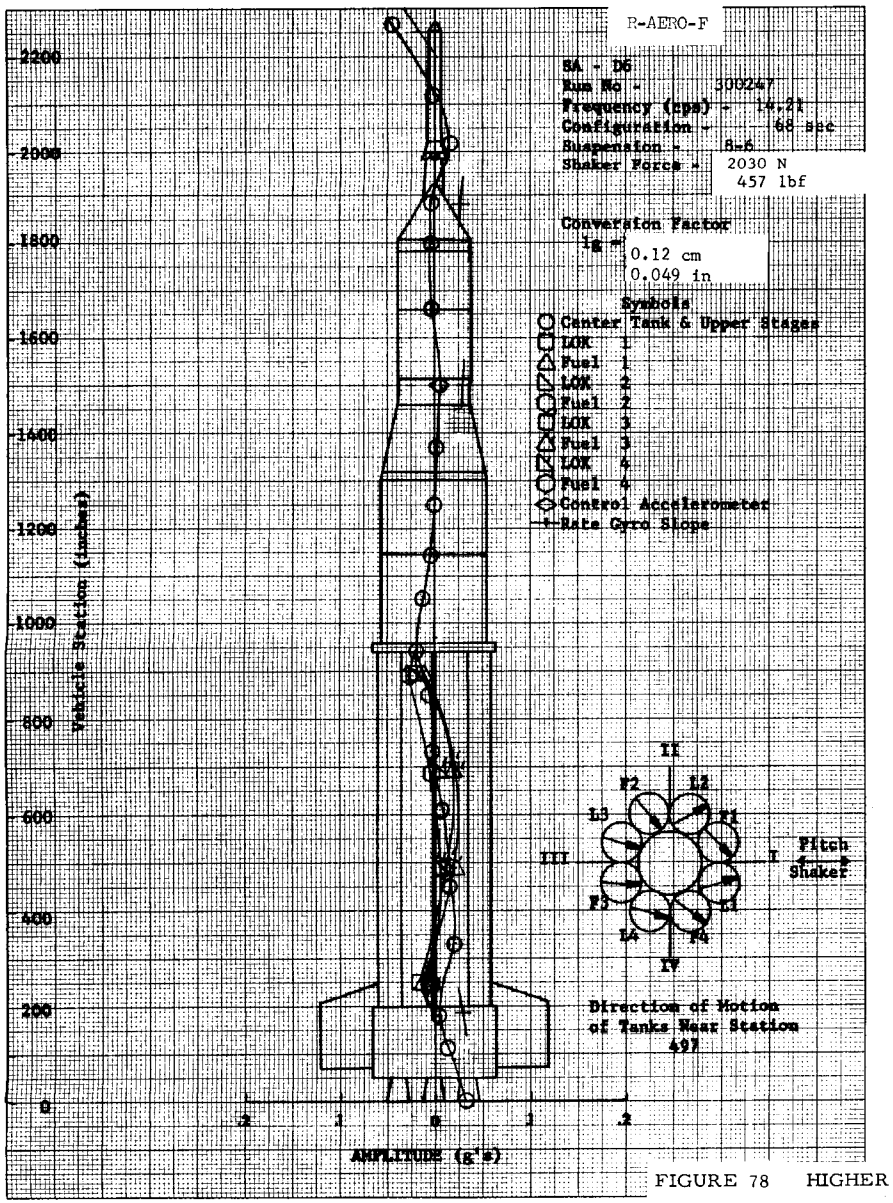


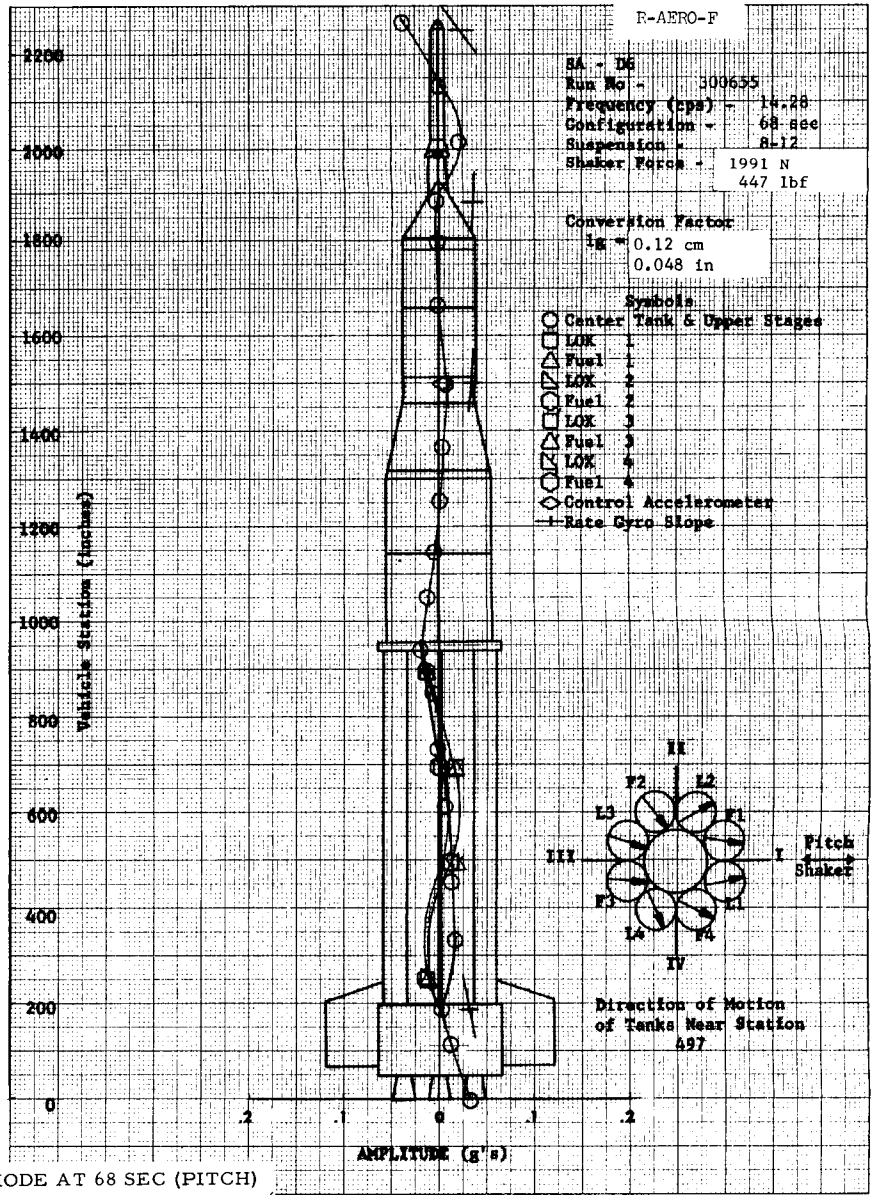


FIGURE 78 HIGHER MODE AT 68 SEC (PITCH)

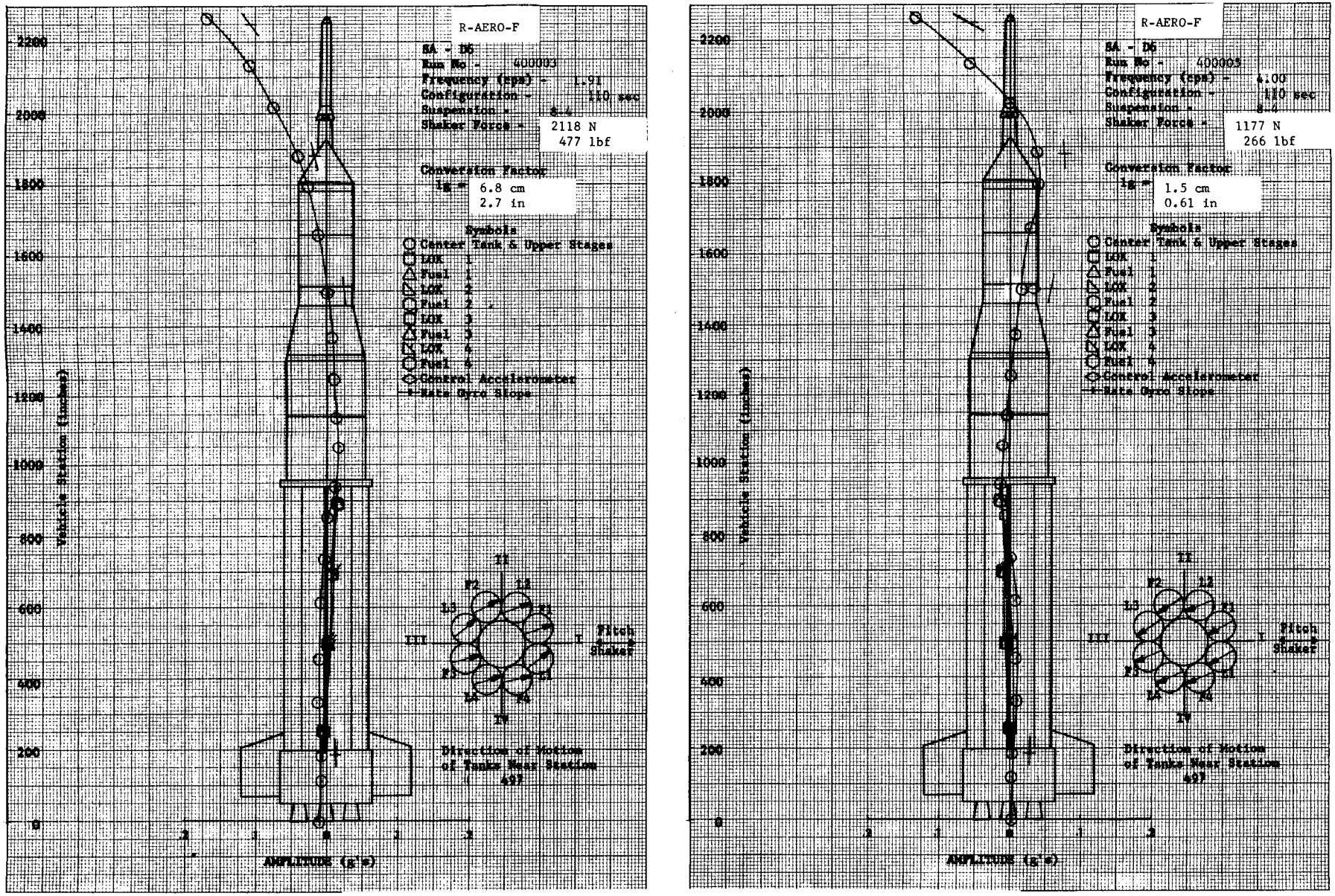


FIGURE 79 1ST BENDING MODE (1.91 CPS) AND TOWER MODE COUPLED WITH 2ND BENDING (4.00 CPS) AT 110 SEC (PITCH)

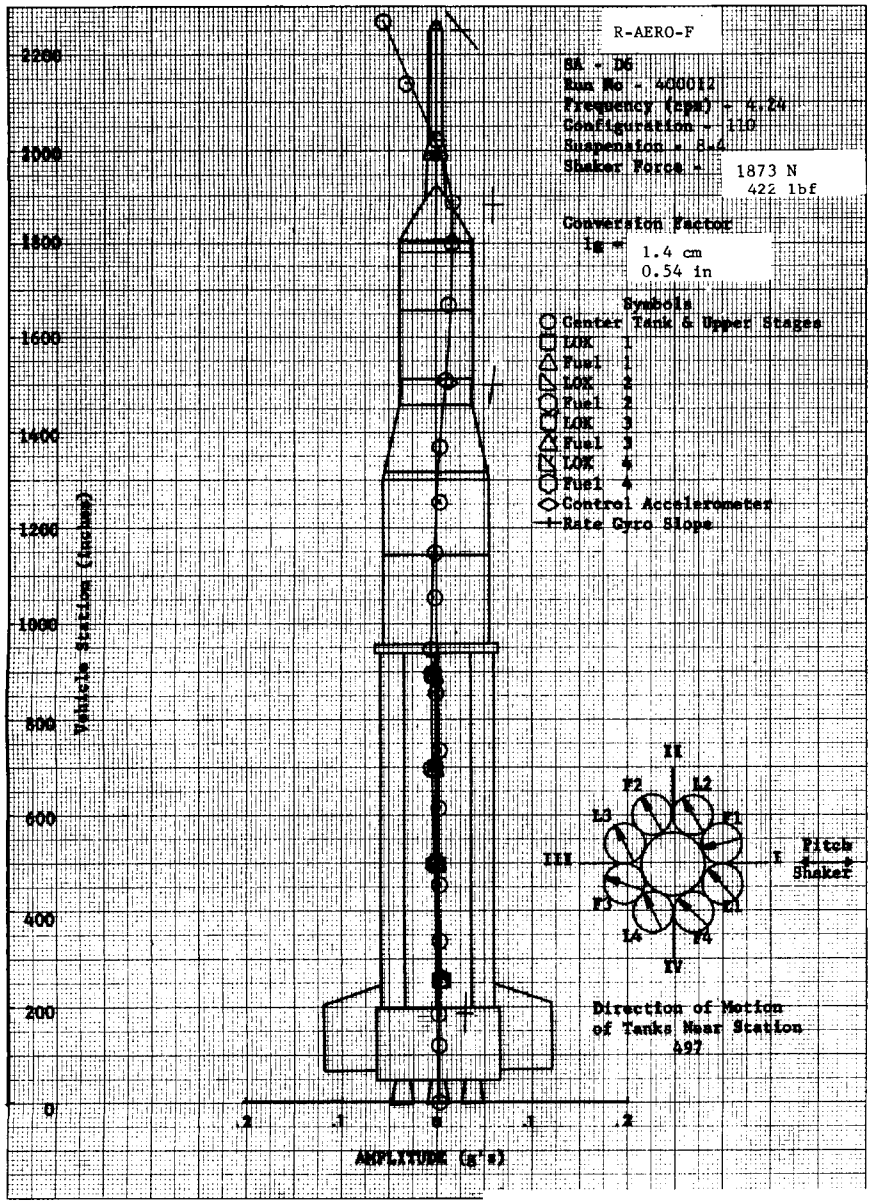


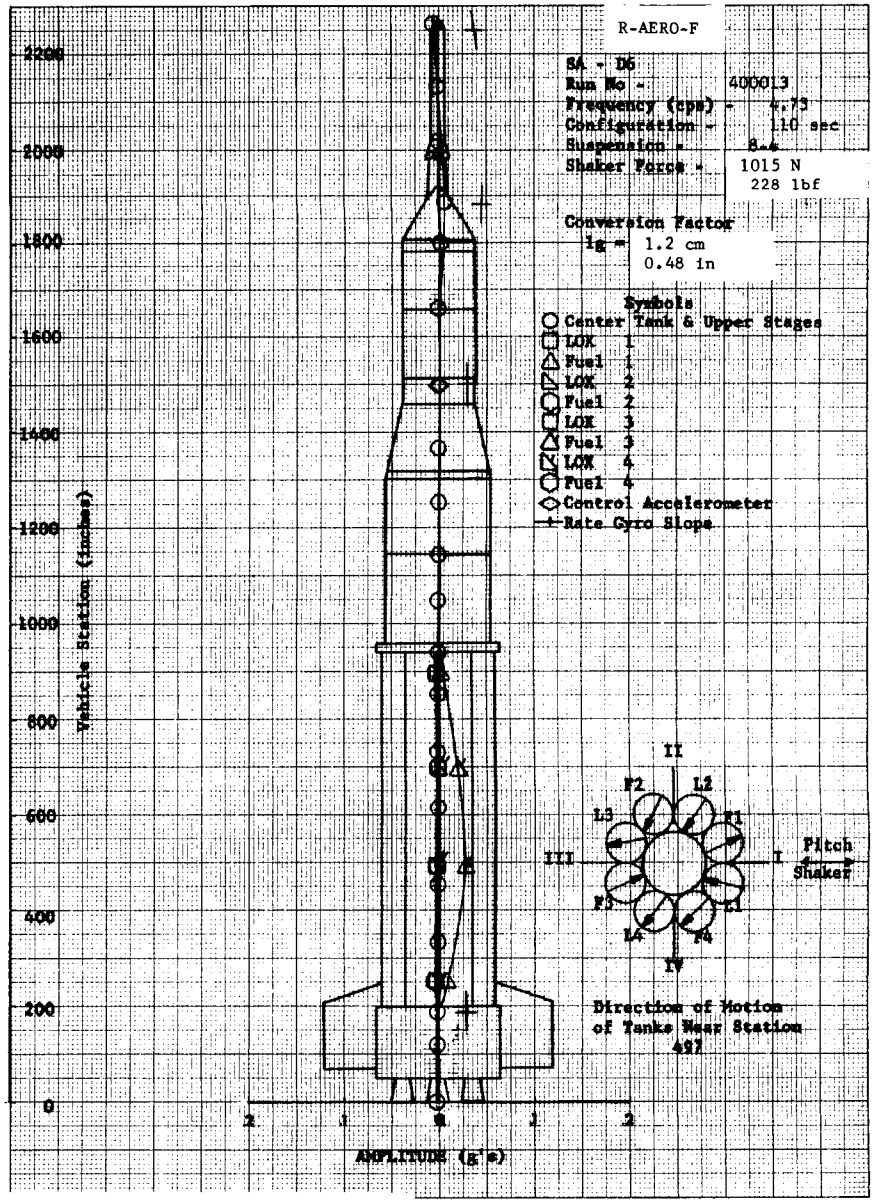


FIGURE 80 2ND BENDING MODE (4.24 CPS) AND 1ST OUTER TANK MODE (4.73 CPS) AT 110 SEC (PITCH)

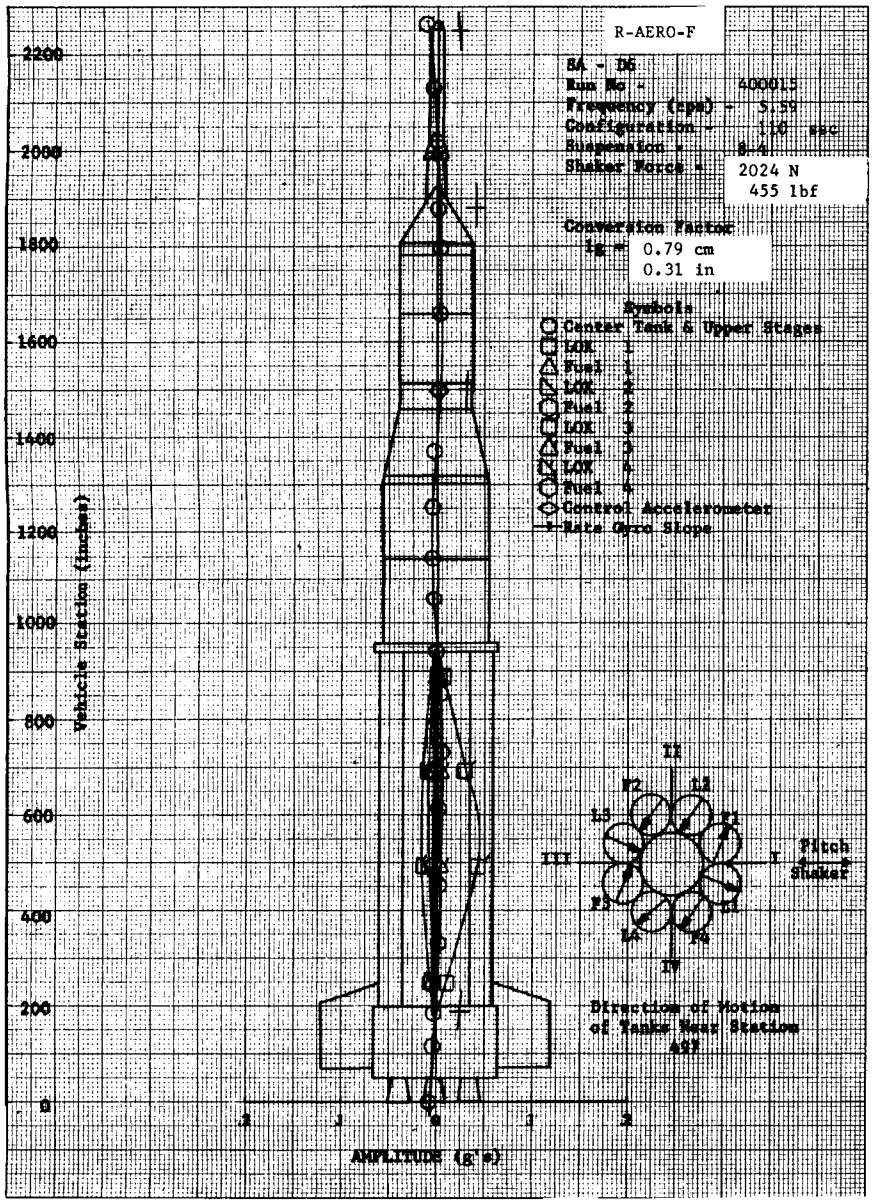


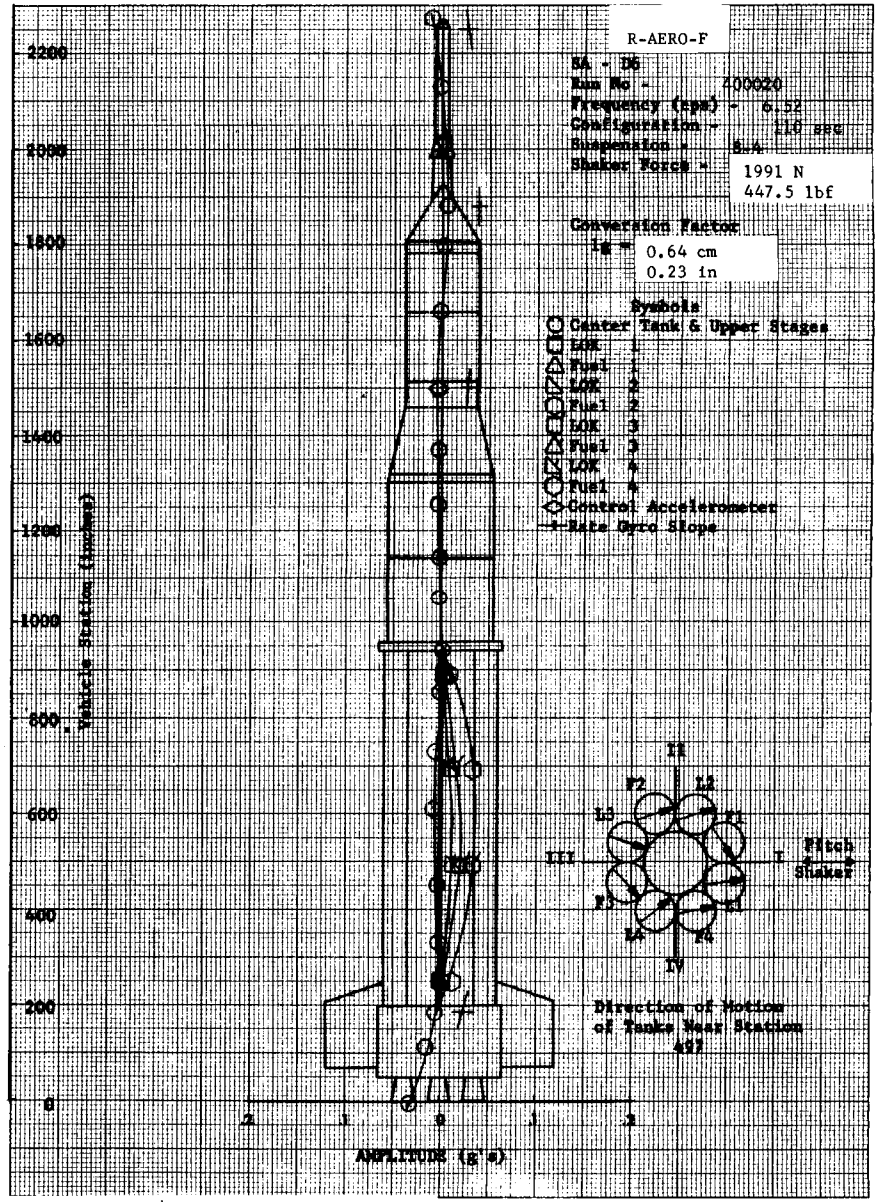


FIGURE 81 2ND OUTER TANK MODE (5.59 CPS) AND 6TH OUTER TANK MODE (6.52 CPS) AT 110 SEC (PITCH)

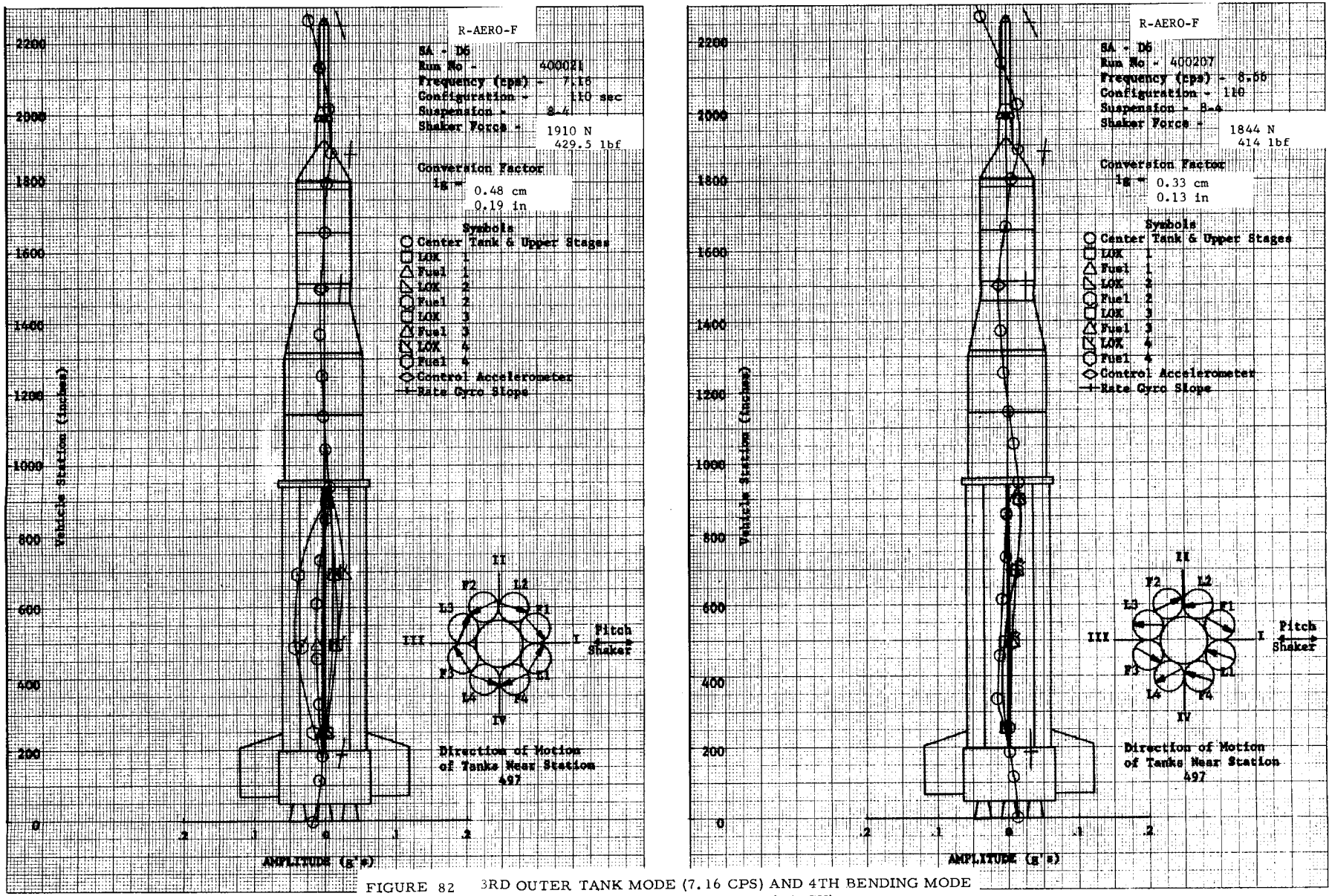


FIGURE 82 3RD OUTER TANK MODE (7.16 CPS) AND 4TH BENDING MODE (8.66 CPS) AT 110 SEC (PITCH)

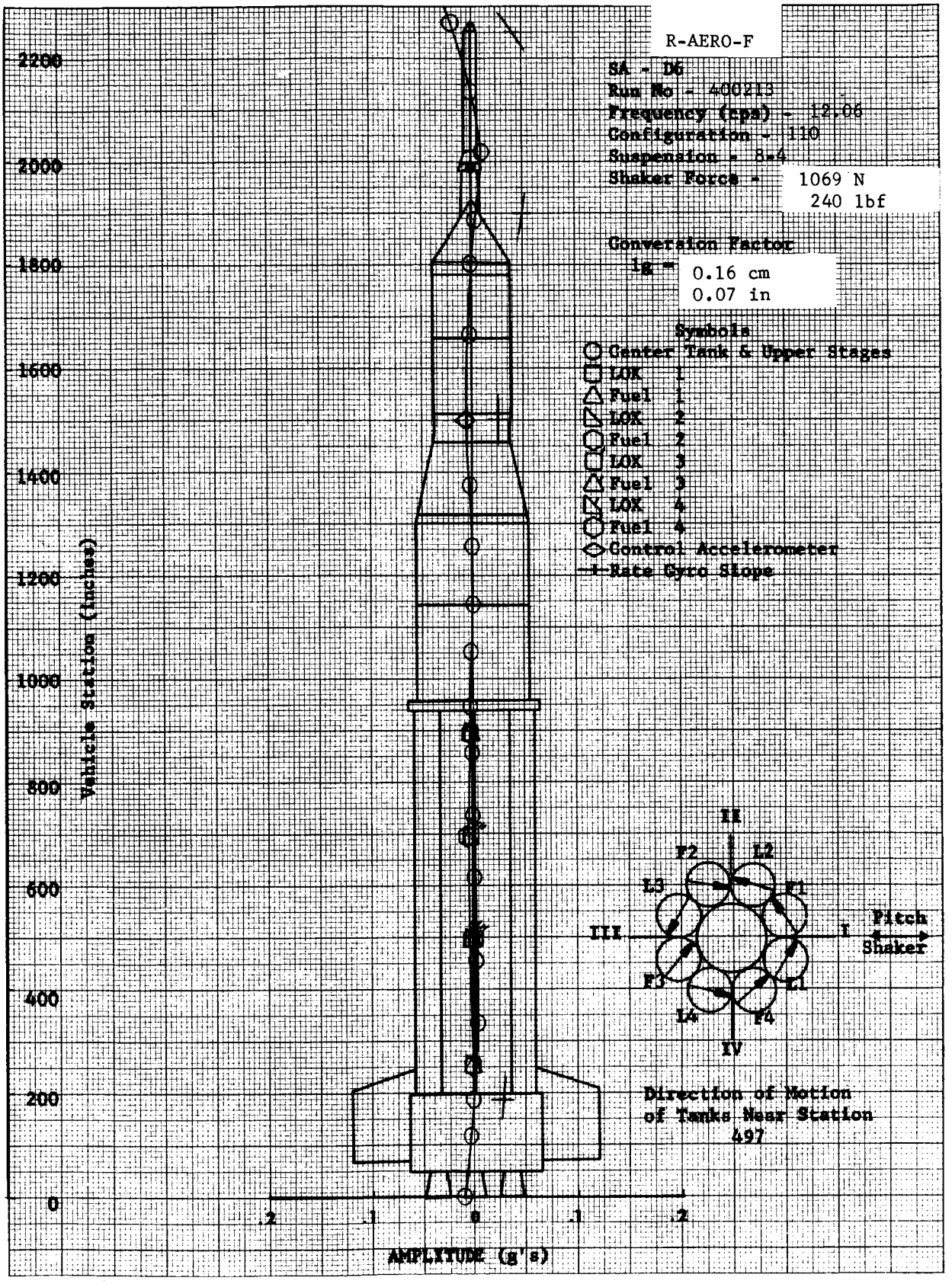


FIGURE 83 HIGHER MODE COUPLED WITH 5TH BENDING MODE AT 110 SEC (PITCH)

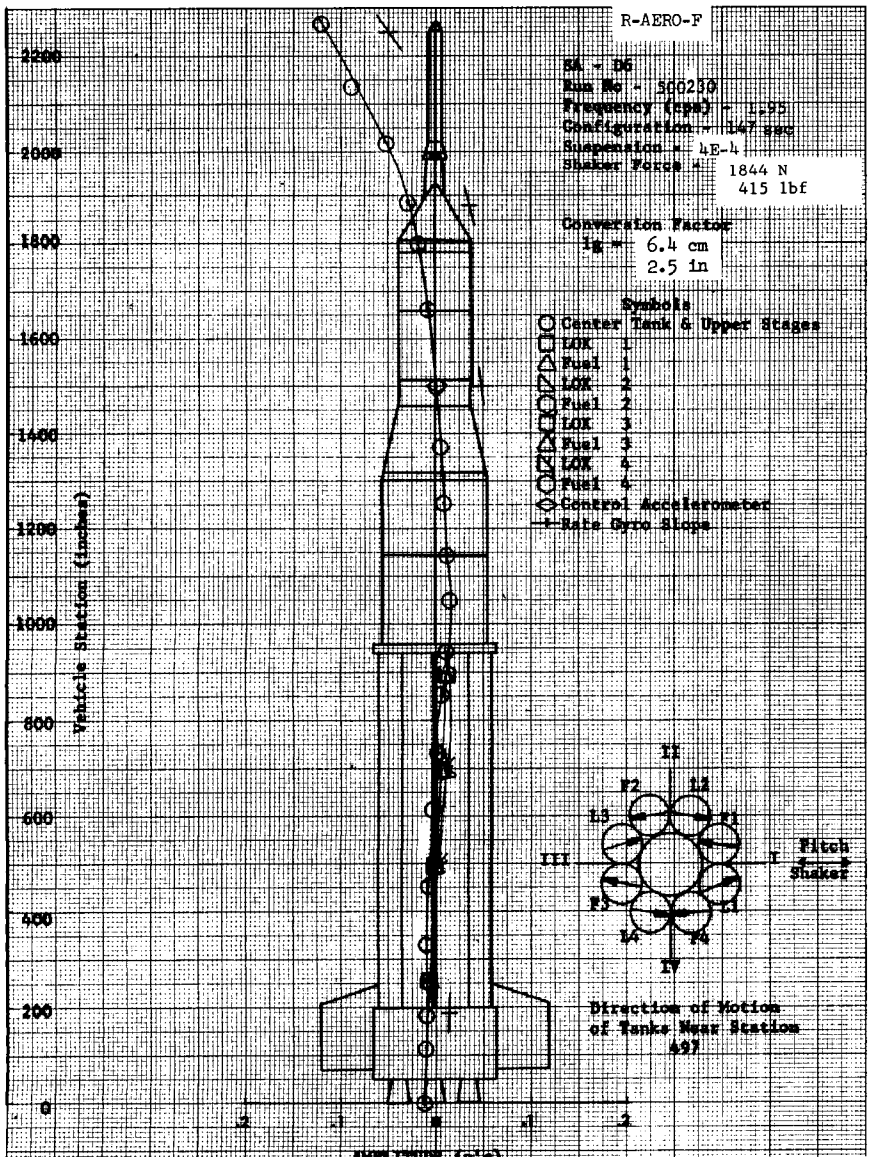


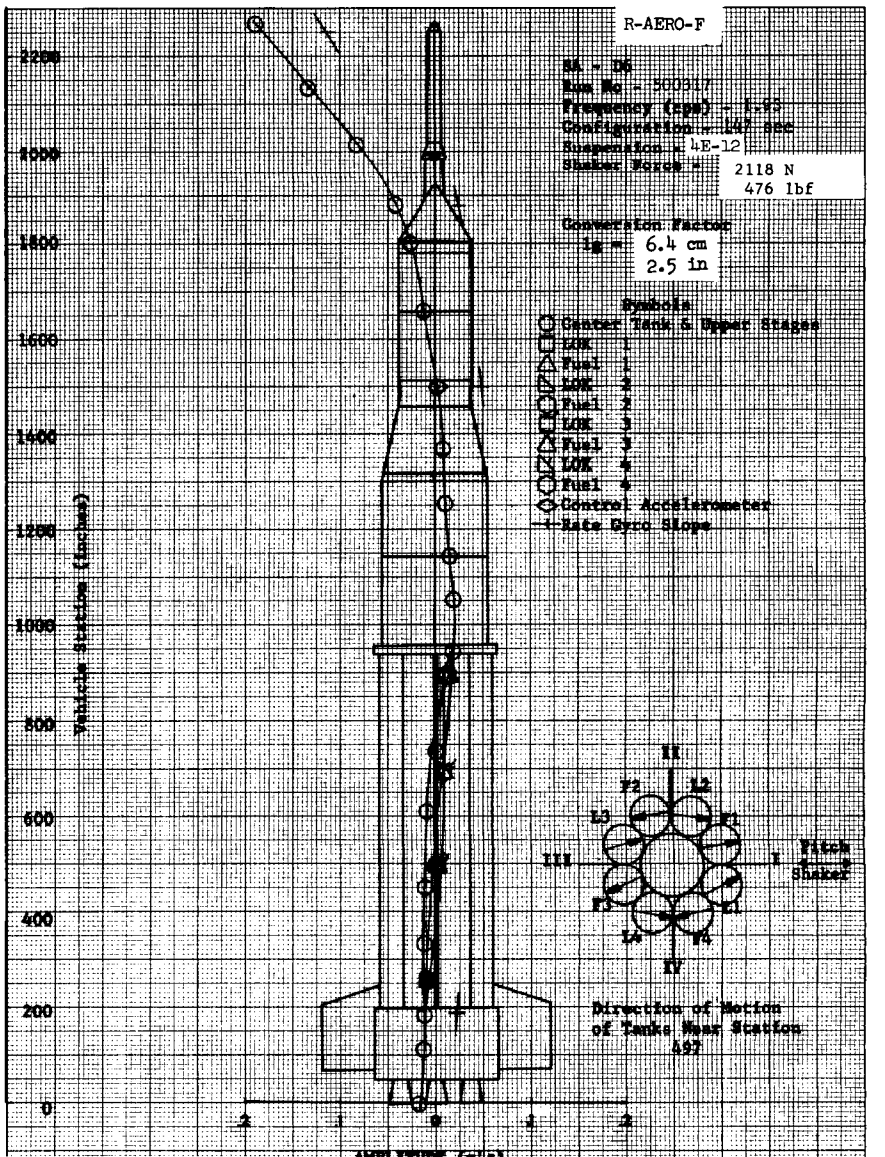


FIGURE 84 1ST BENDING MODE AT 147 SEC (PITCH)

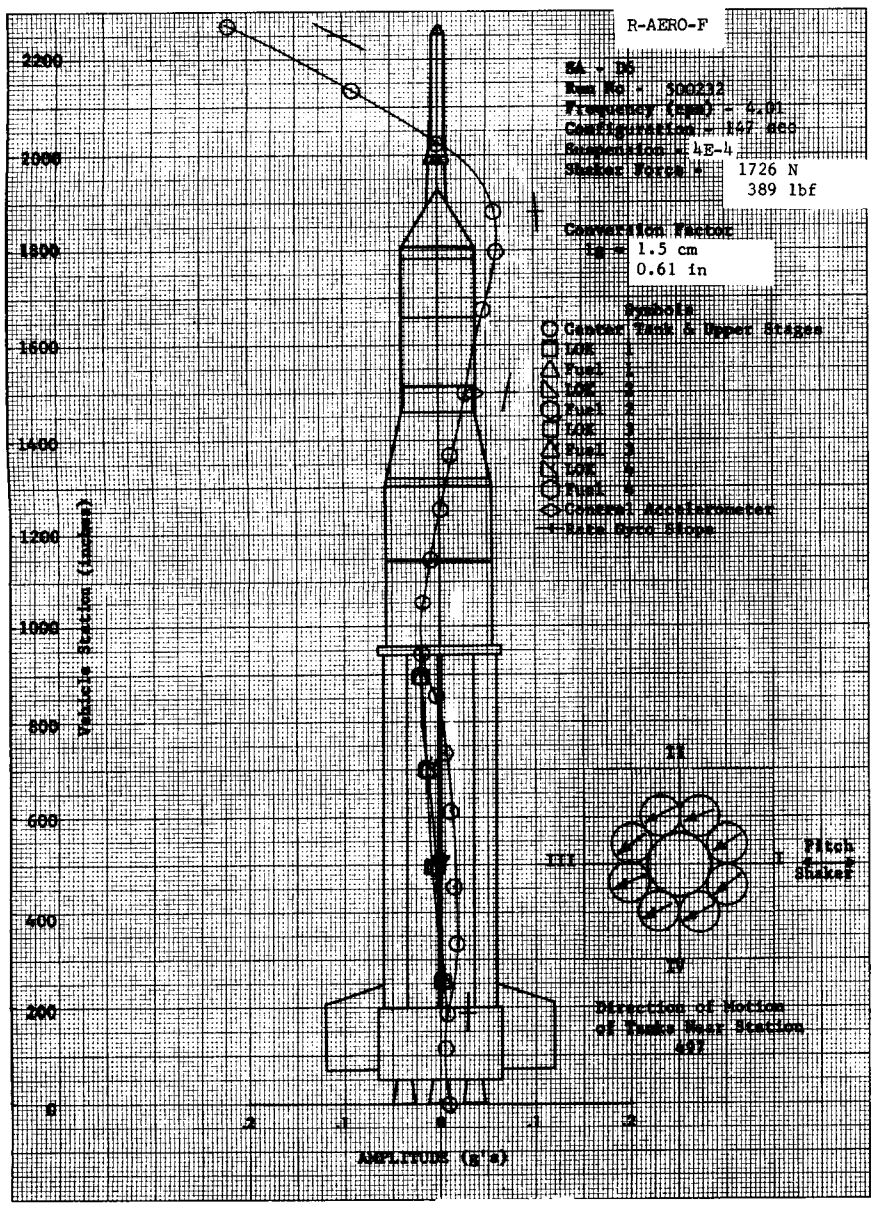


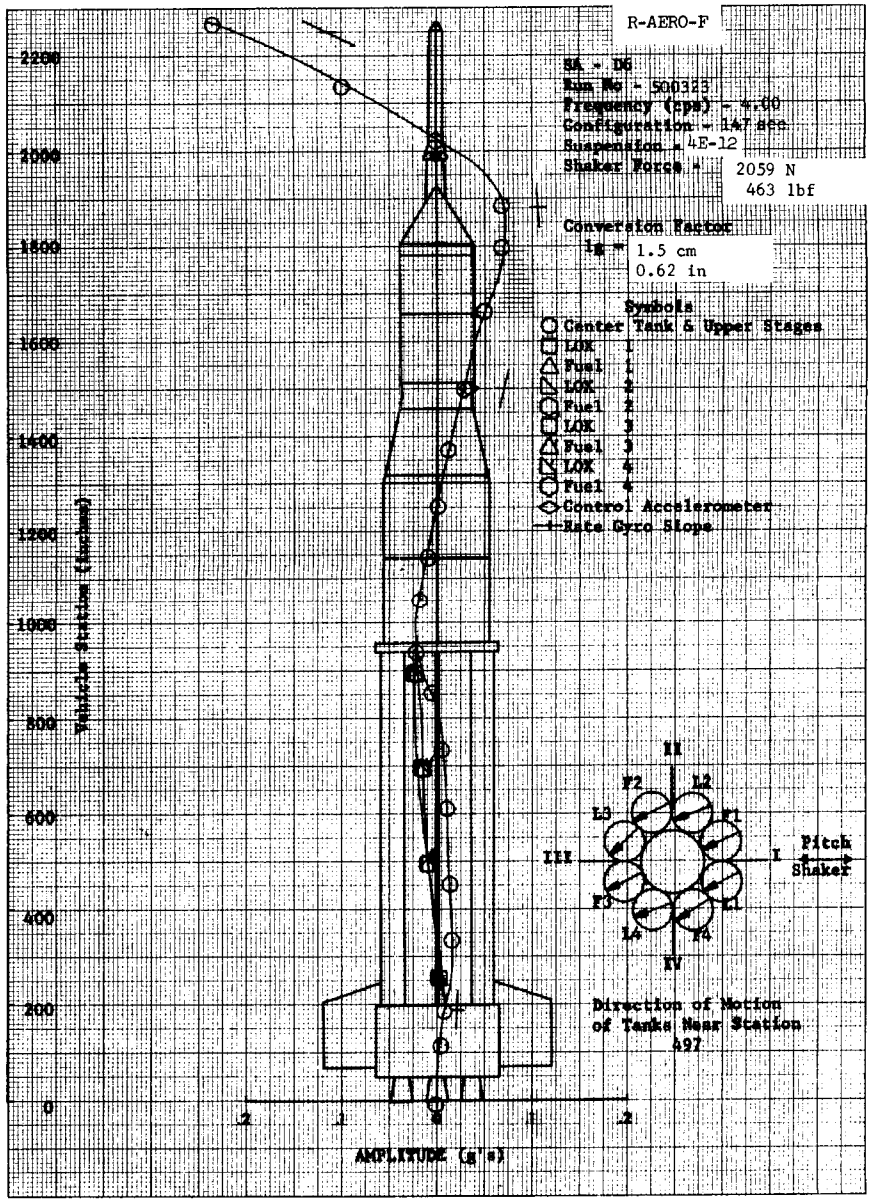


FIGURE 85 TOWER MODE COUPLED WITH 2ND BENDING MODE AT 147 SEC (PITCH)

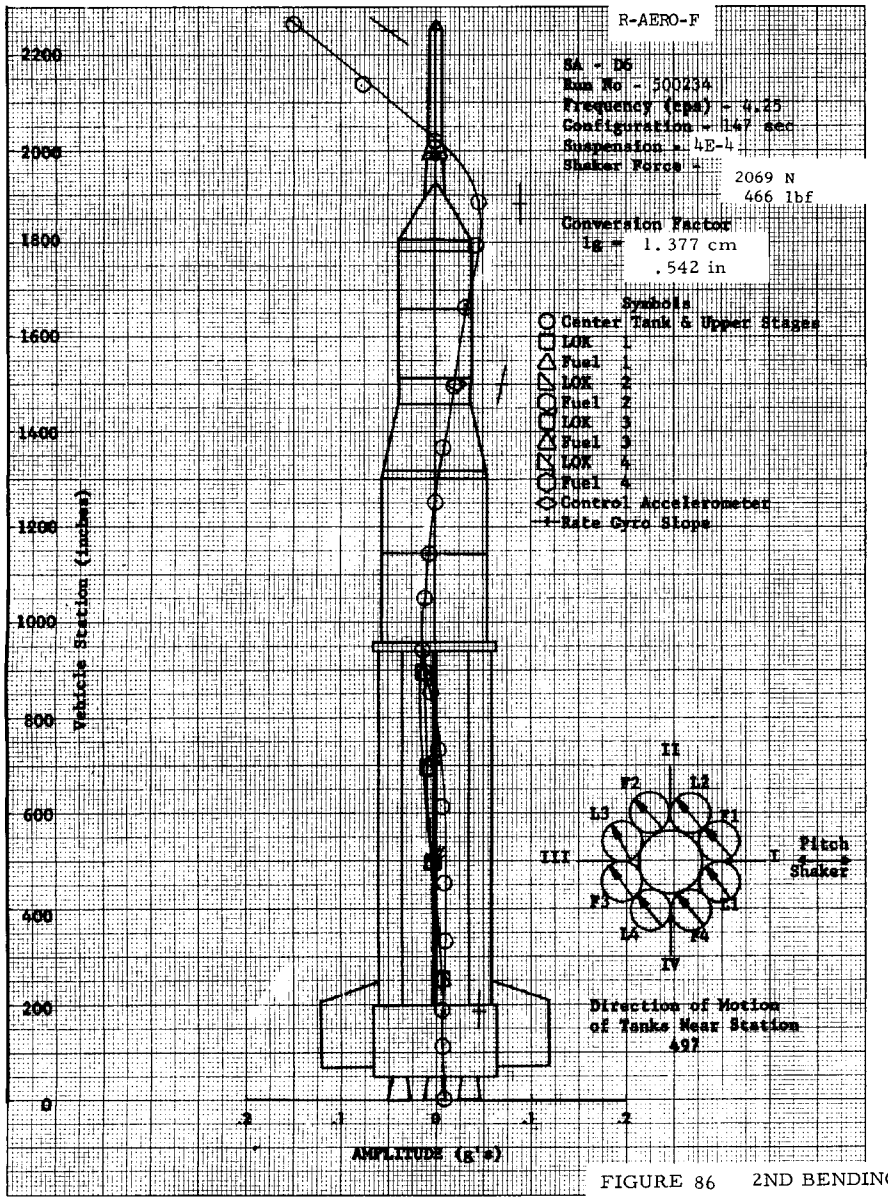


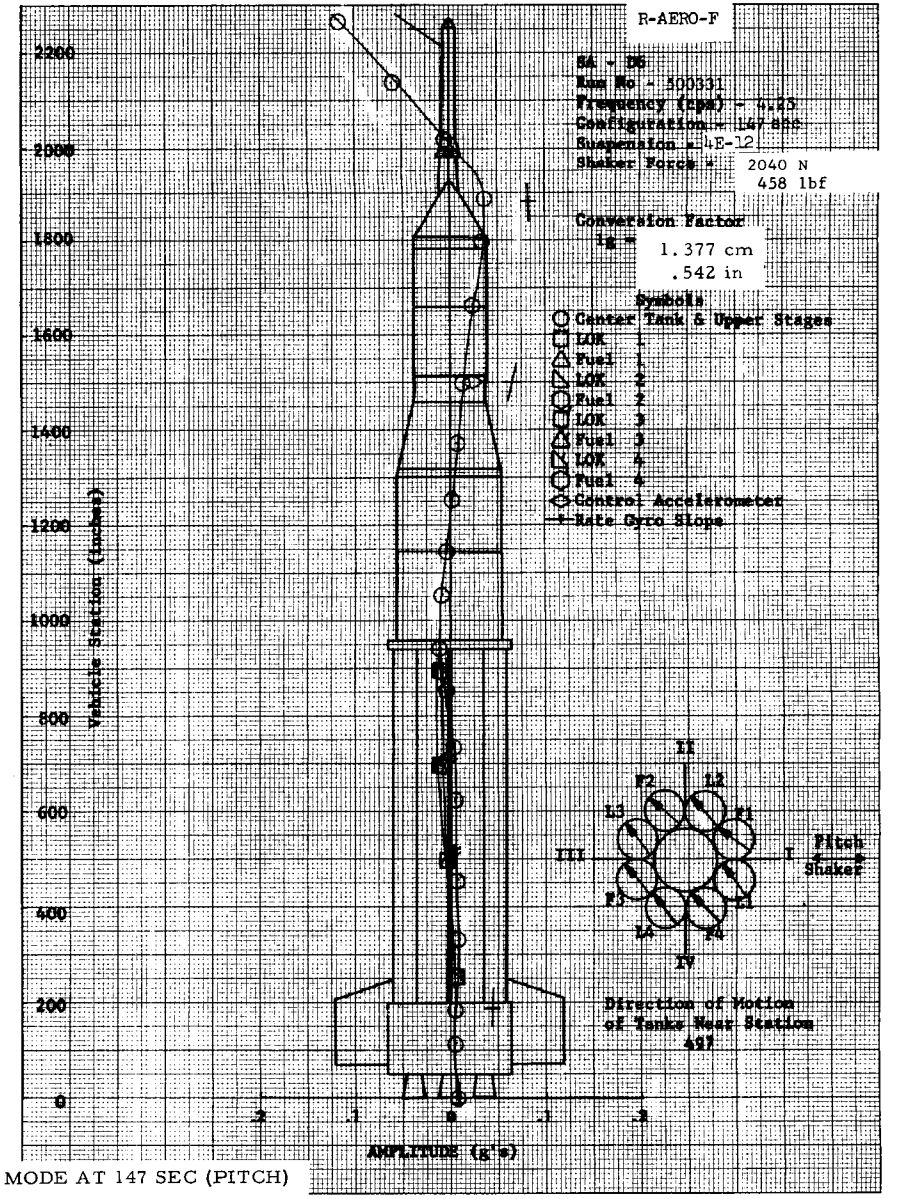


FIGURE 86 2ND BENDING MODE AT 147 SEC (PITCH)

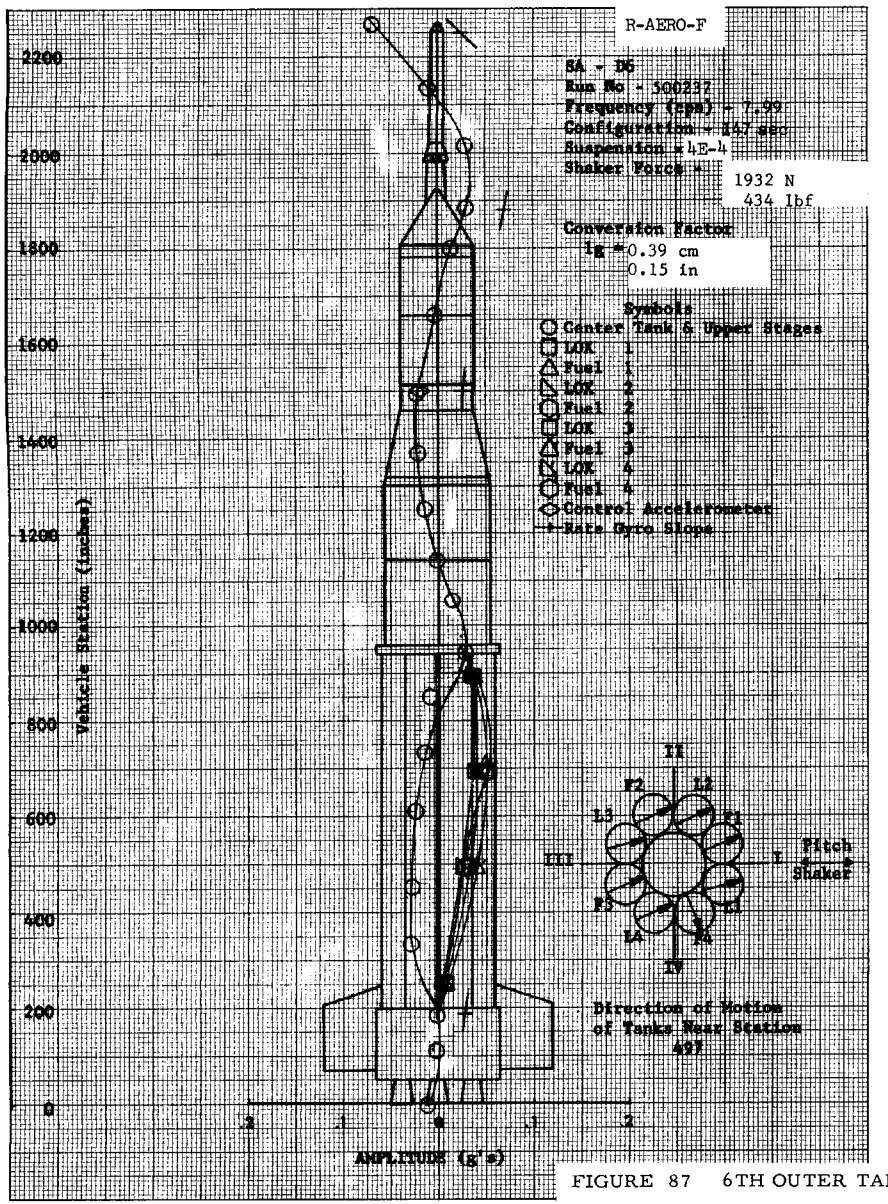


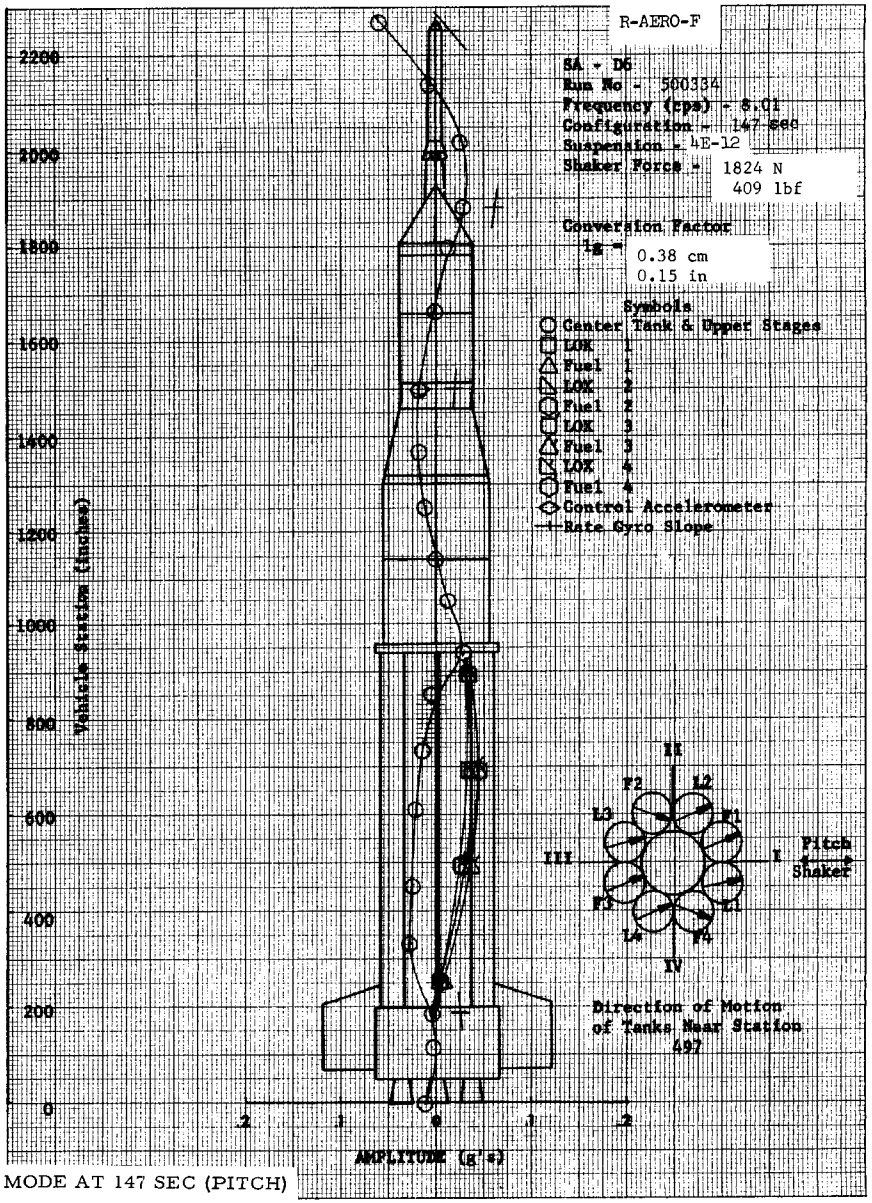


FIGURE 87 6TH OUTER TANK MODE AT 147 SEC (PITCH)

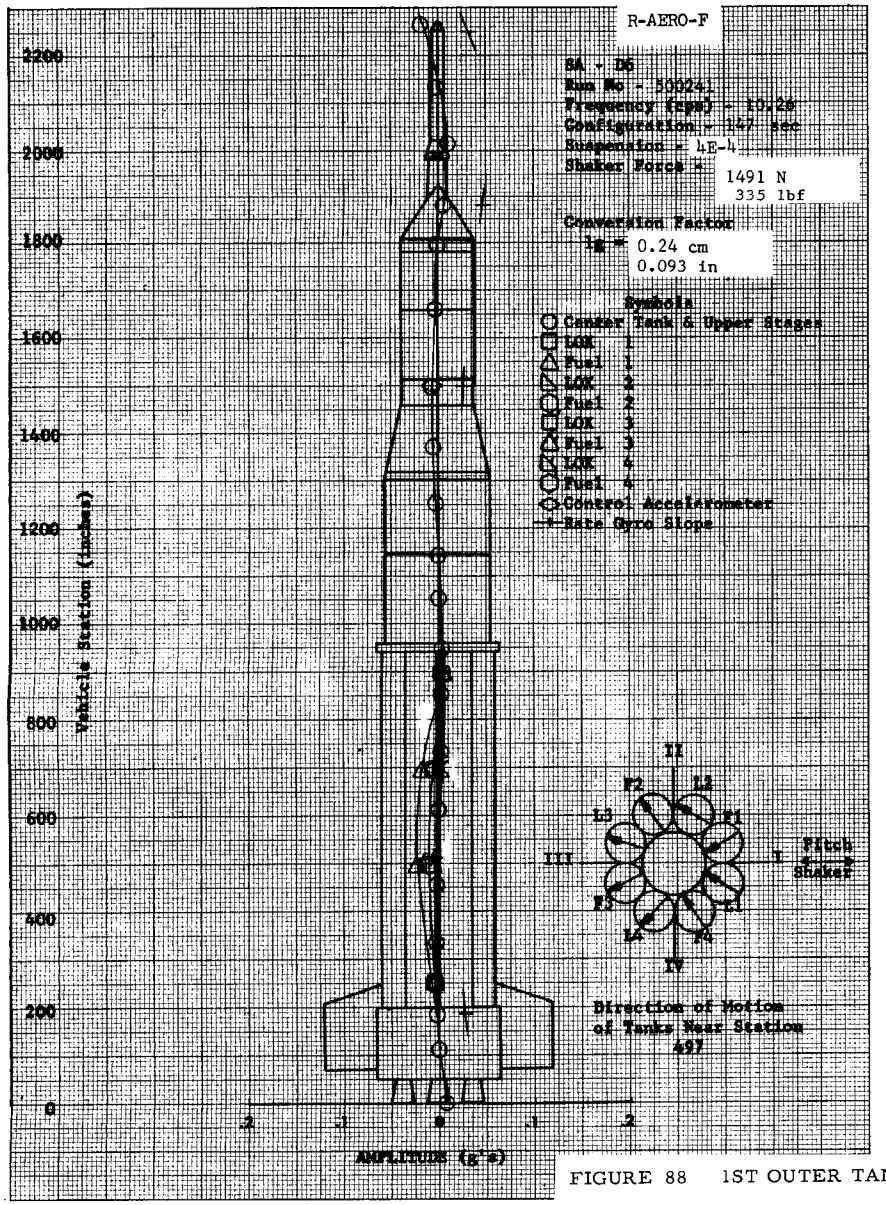


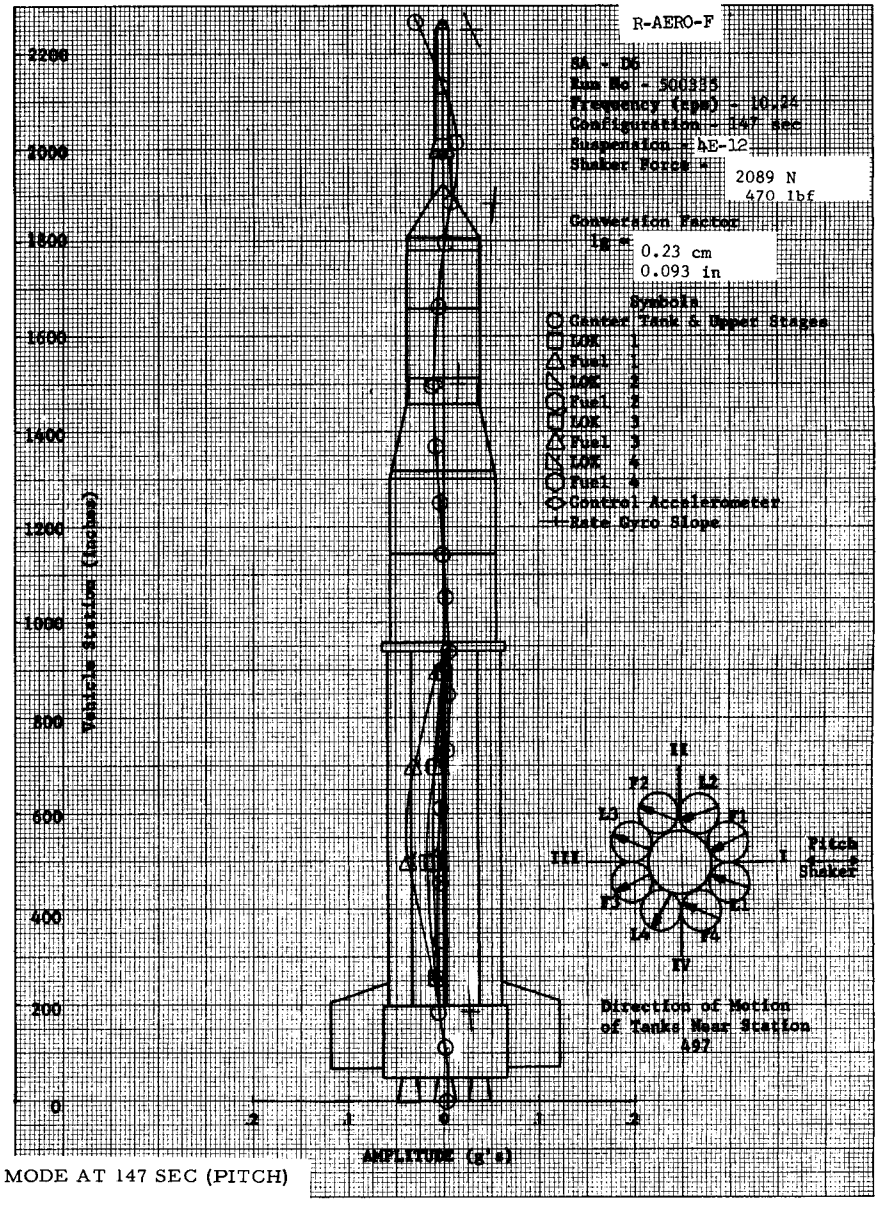


FIGURE 88 1ST OUTER TANK MODE AT 147 SEC (PITCH)

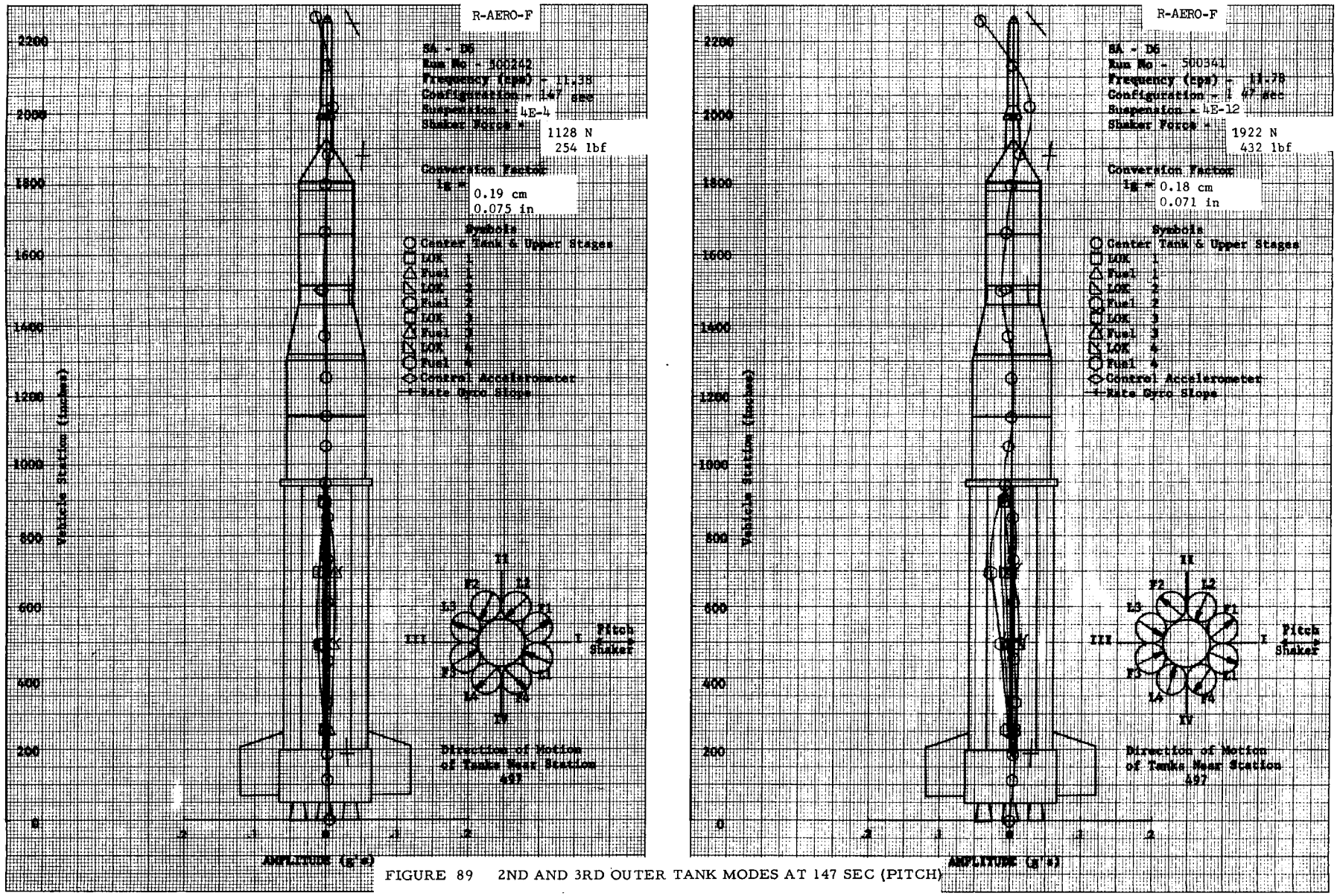


FIGURE 89 2ND AND 3RD OUTER TANK MODES AT 147 SEC (PITCH)

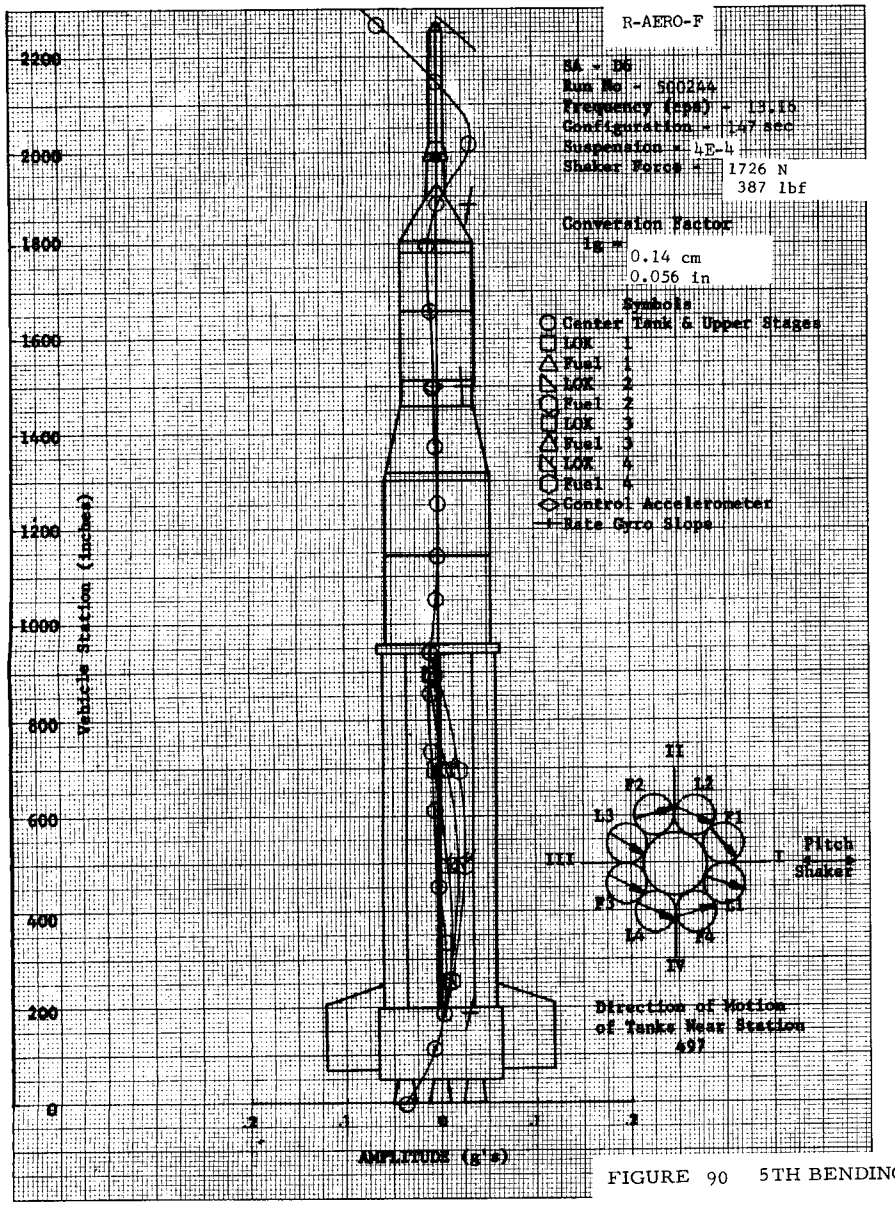


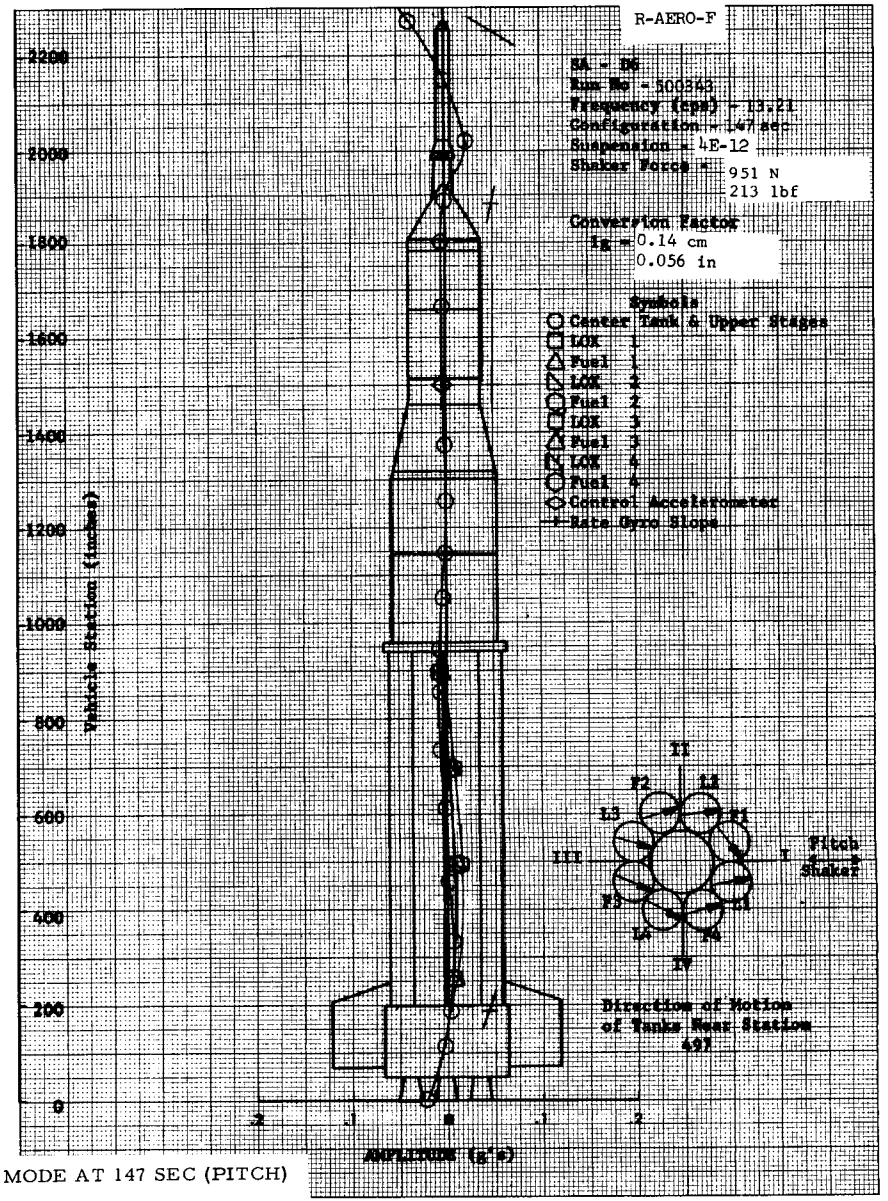


FIGURE 90 5TH BENDING MODE AT 147 SEC (PITCH)

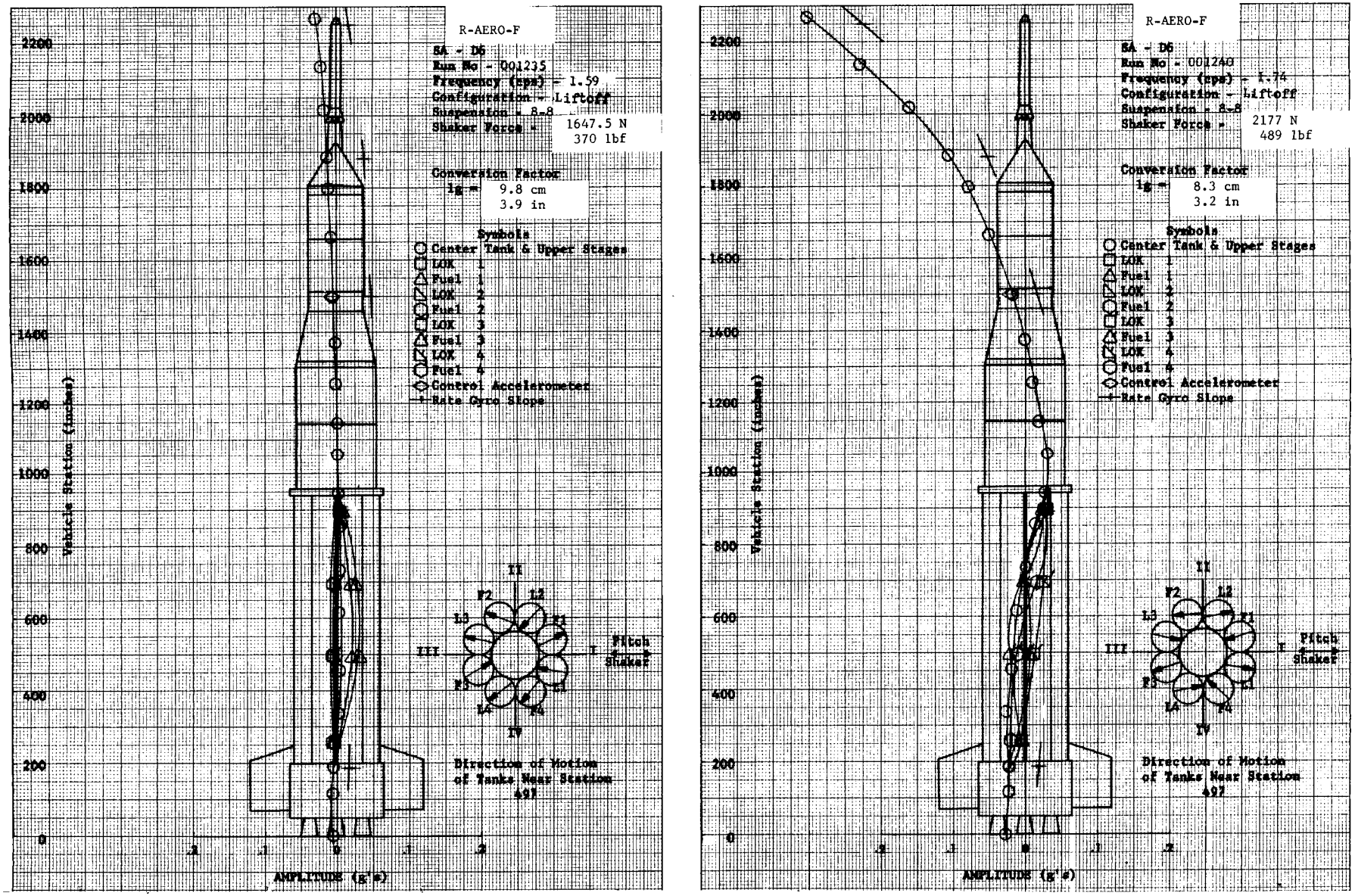


FIGURE 91 1ST OUTER TANK MODE (1.59 CPS) AND 1ST BENDING MODE (1.74 CPS) FOR LIFTOFF RERUNS (PITCH)

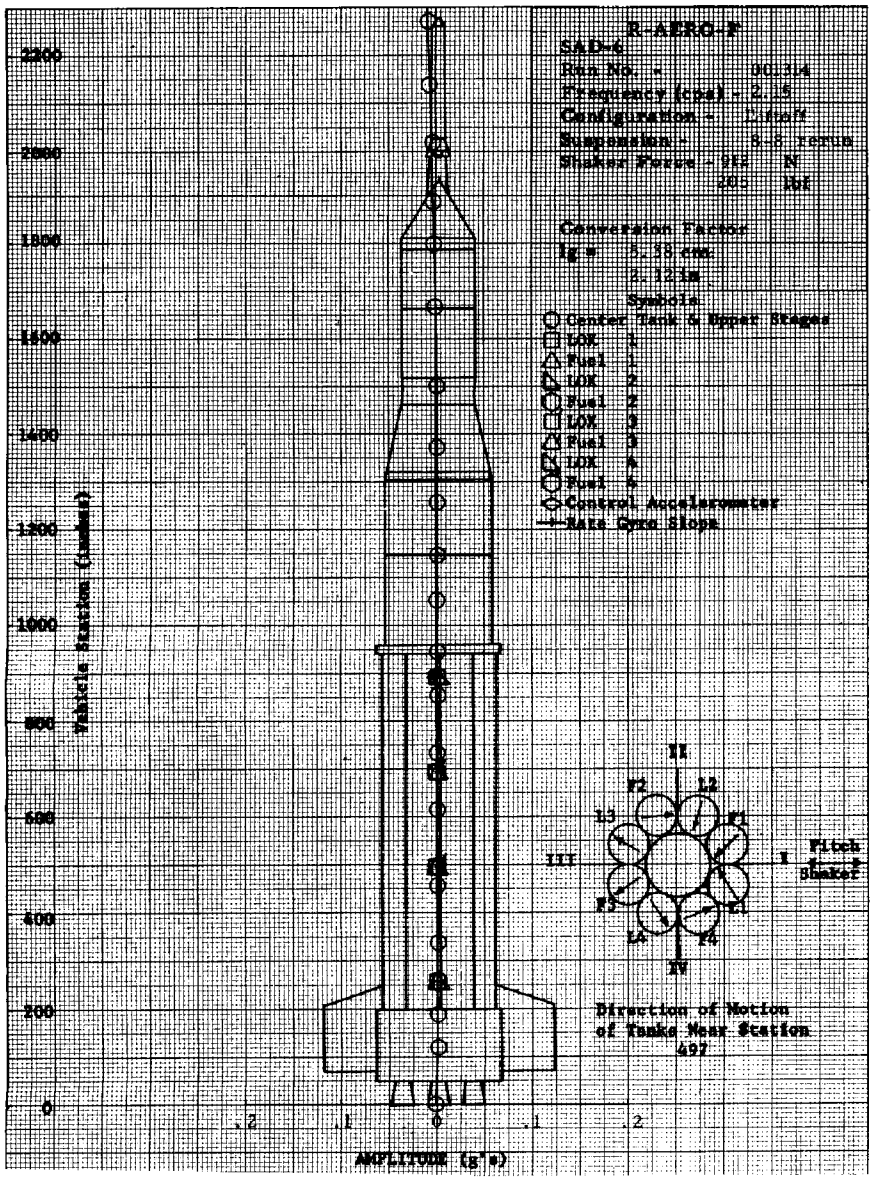


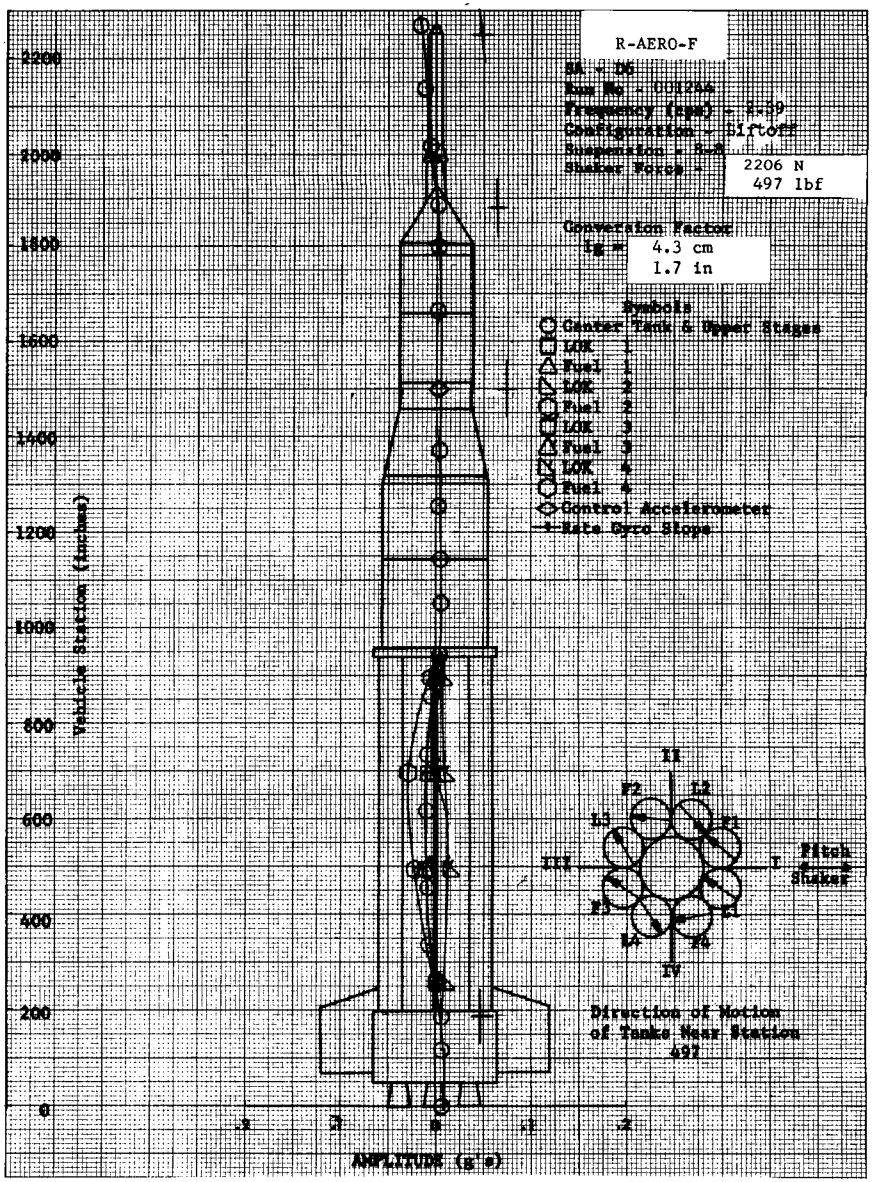


FIGURE 92 2ND OUTER TANK MODE (2.15 CPS) AND 3RD OUTER TANK MODE (2.39 CPS) FOR LIFTOFF RERUNS (PITCH)

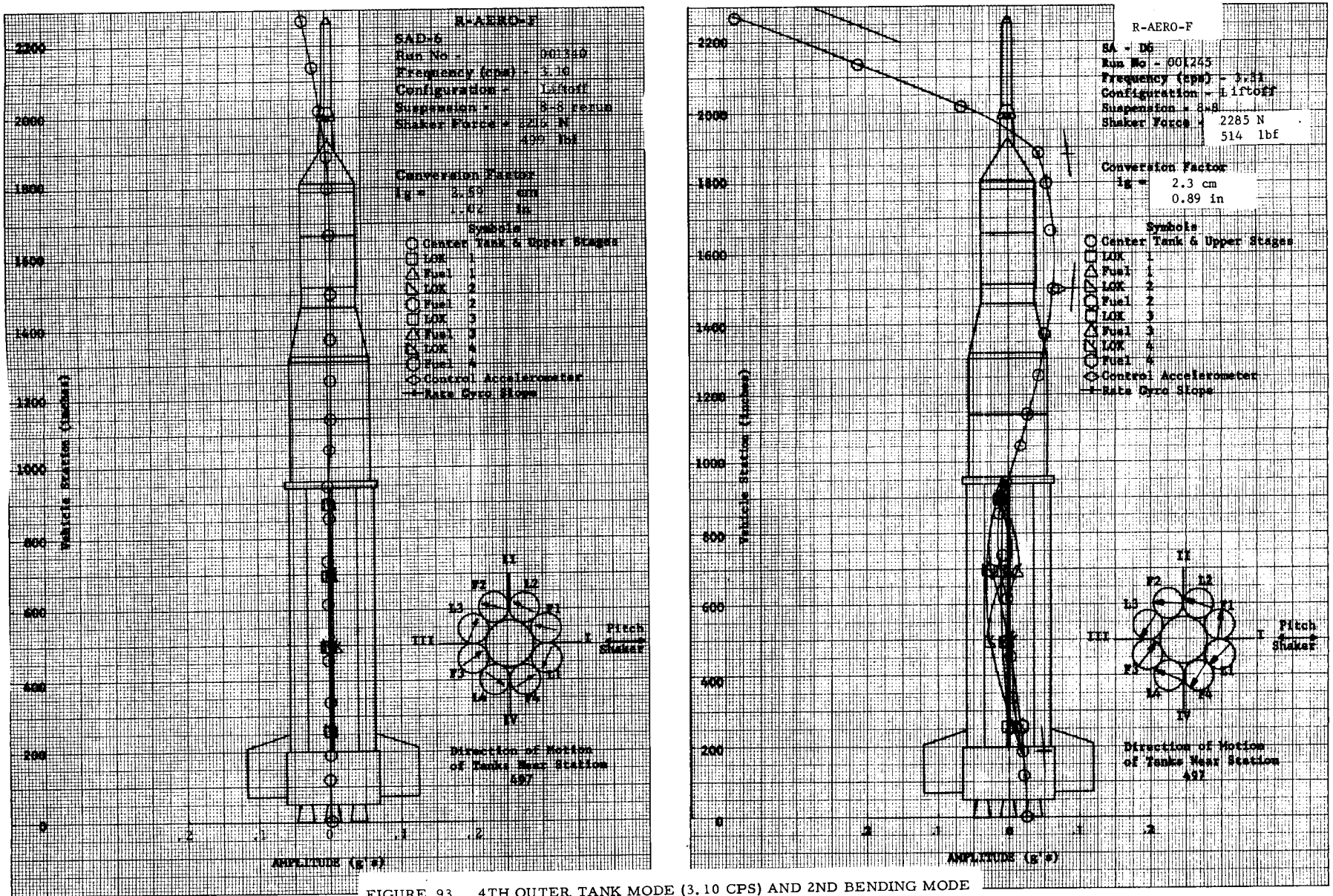


FIGURE 93 4TH OUTER TANK MODE (3.10 CPS) AND 2ND BENDING MODE (3.31 CPS) FOR LIFTOFF RERUNS (PITCH)

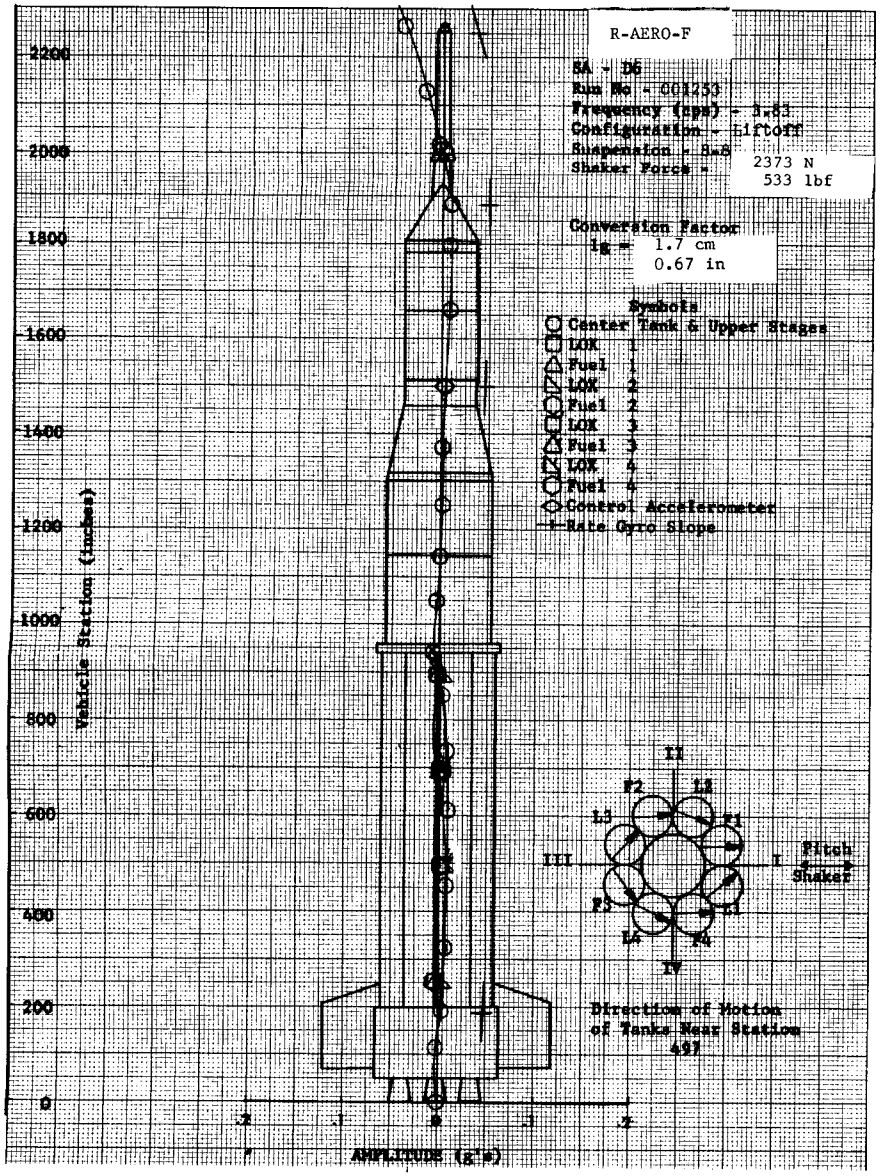


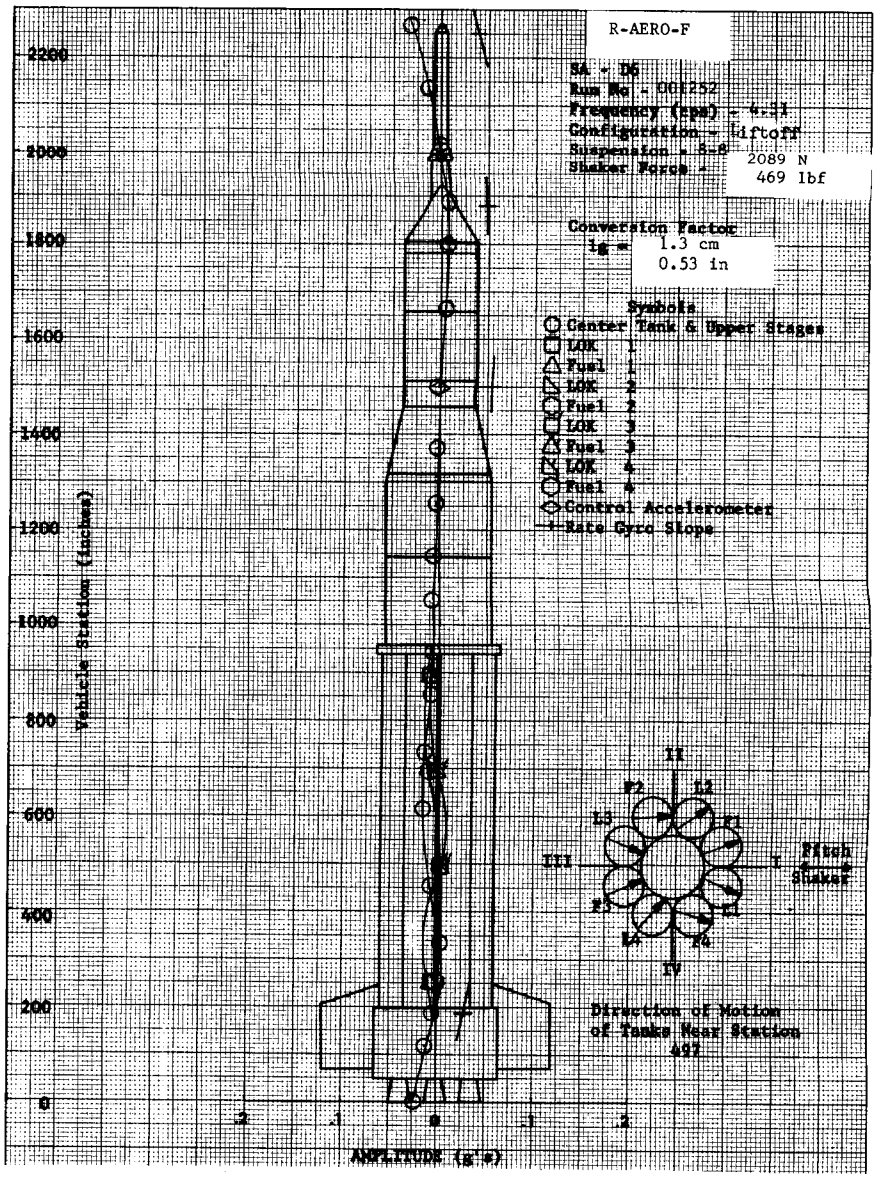


FIGURE 94 3RD BENDING MODE (3.83 CPS) AND 6TH OUTER TANK MODE (4.31 CPS) FOR LIFTOFF RERUNS (PITCH)

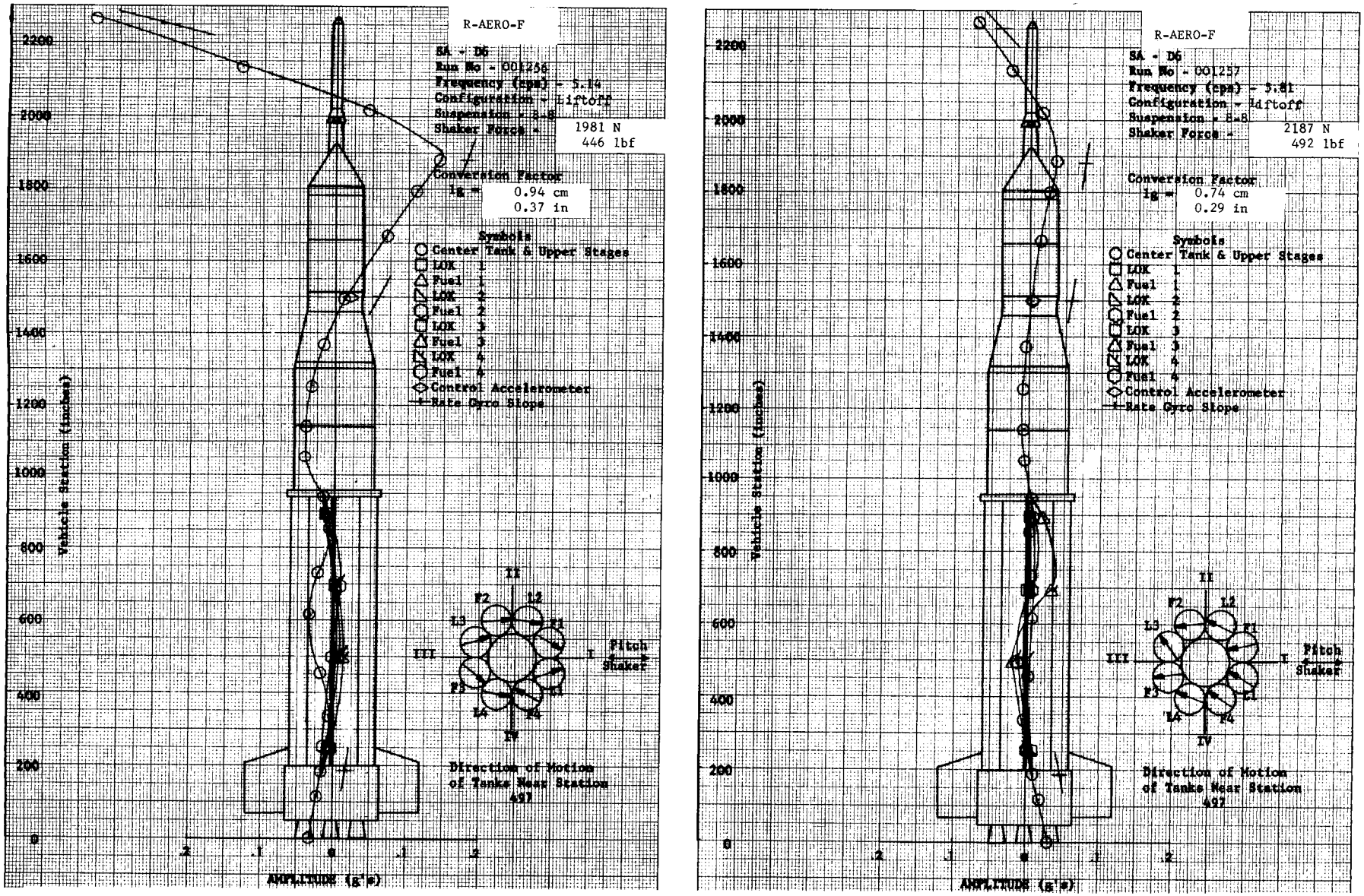


FIGURE 95 4TH BENDING MODE (5.14 CPS) AND COUPLED TANK MODE (5.81 CPS) FOR LIFTOFF RERUNS (PITCH)

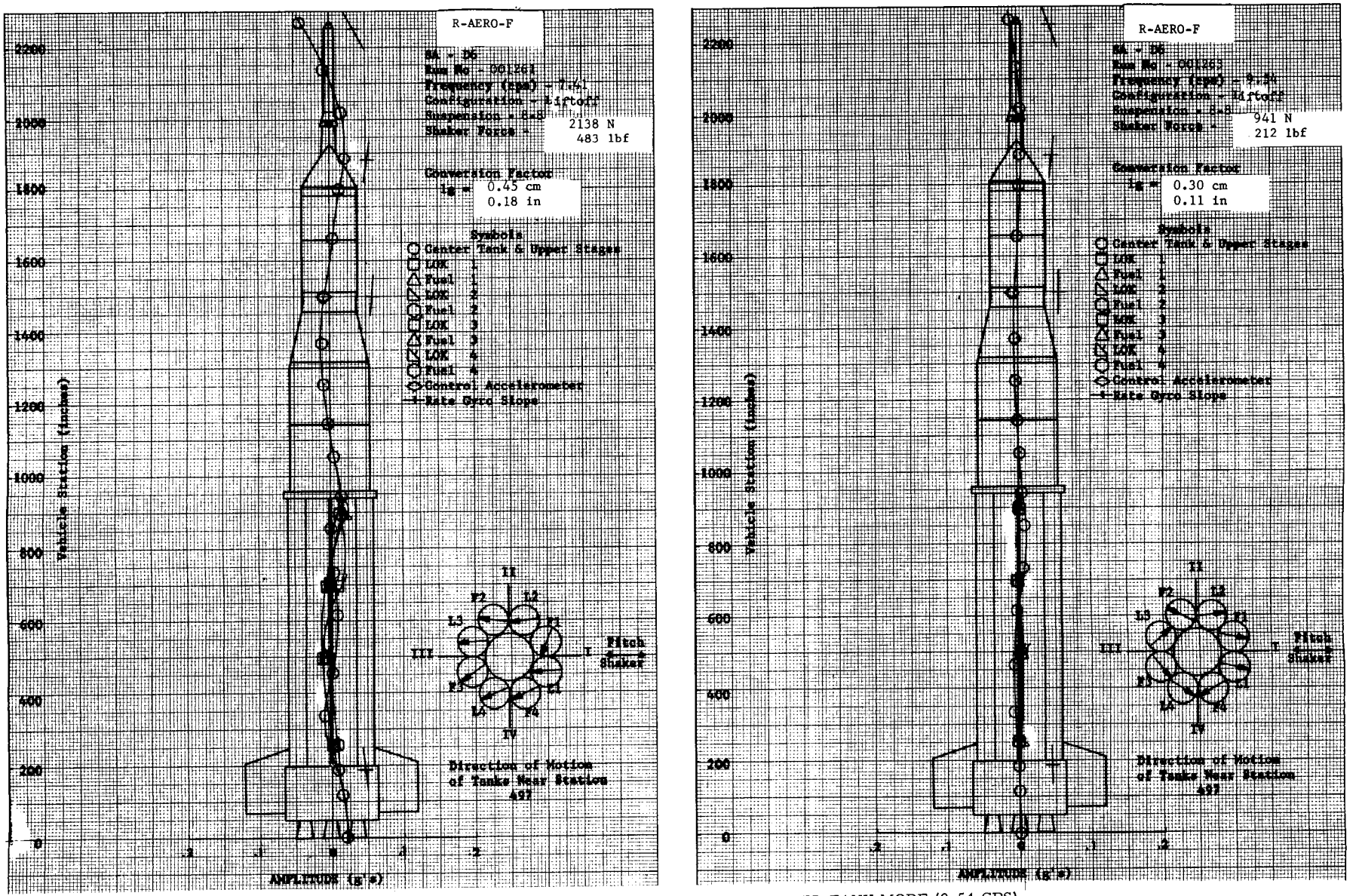


FIGURE 96 S-I ENGINE MODE (7.41 CPS) AND 8TH OUTER TANK MODE (9.54 CPS) FOR LIFTOFF RERUNS (PITCH)

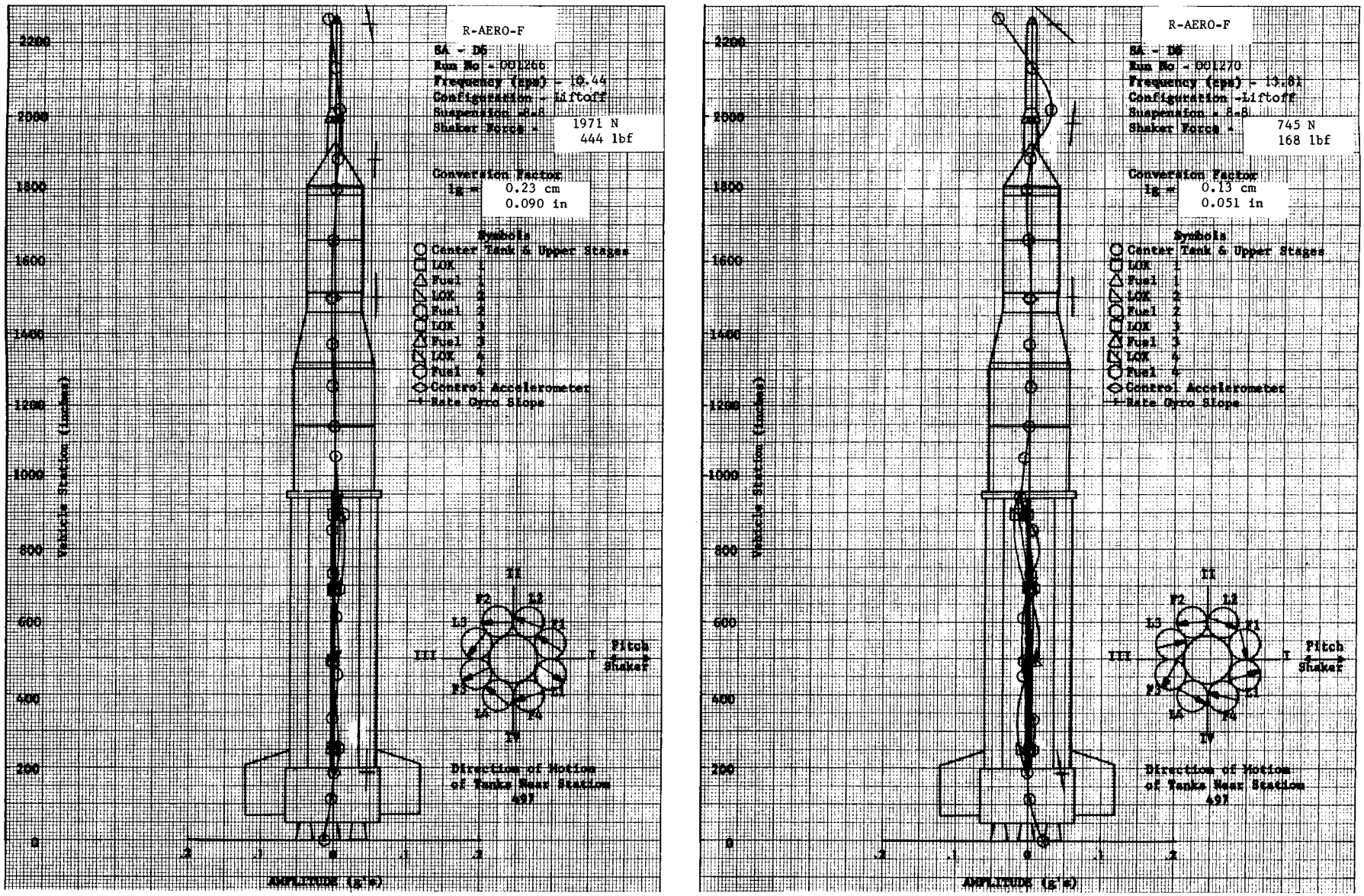


FIGURE 97 5TH BENDING MODE (10.44 CPS) AND HIGHER VEHICLE MODE (13.81 CPS) FOR LIFTOFF RERUNS (PITCH)

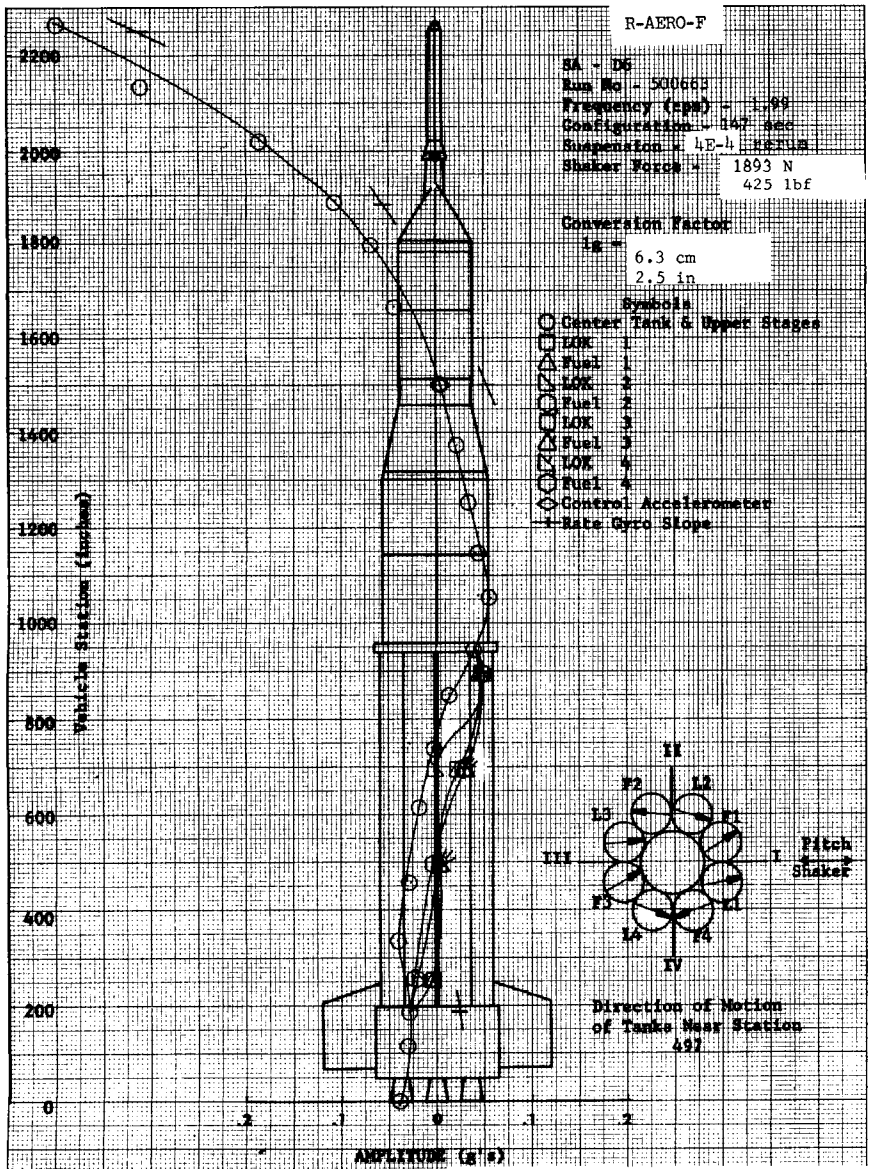


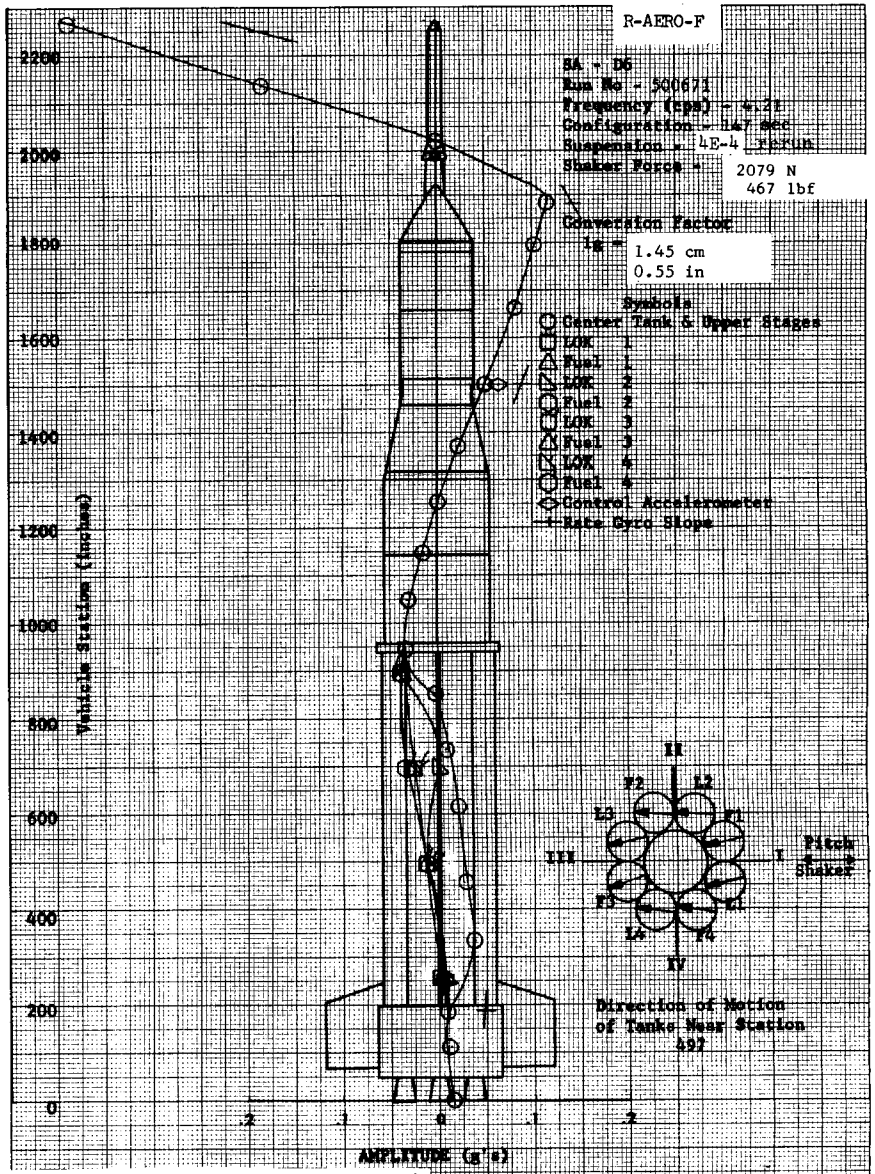


FIGURE 98 1ST BENDING MODE (1.99 CPS) AND 2ND BENDING MODE (4.21 CPS) FOR 147 SEC RERUNS (PITCH)

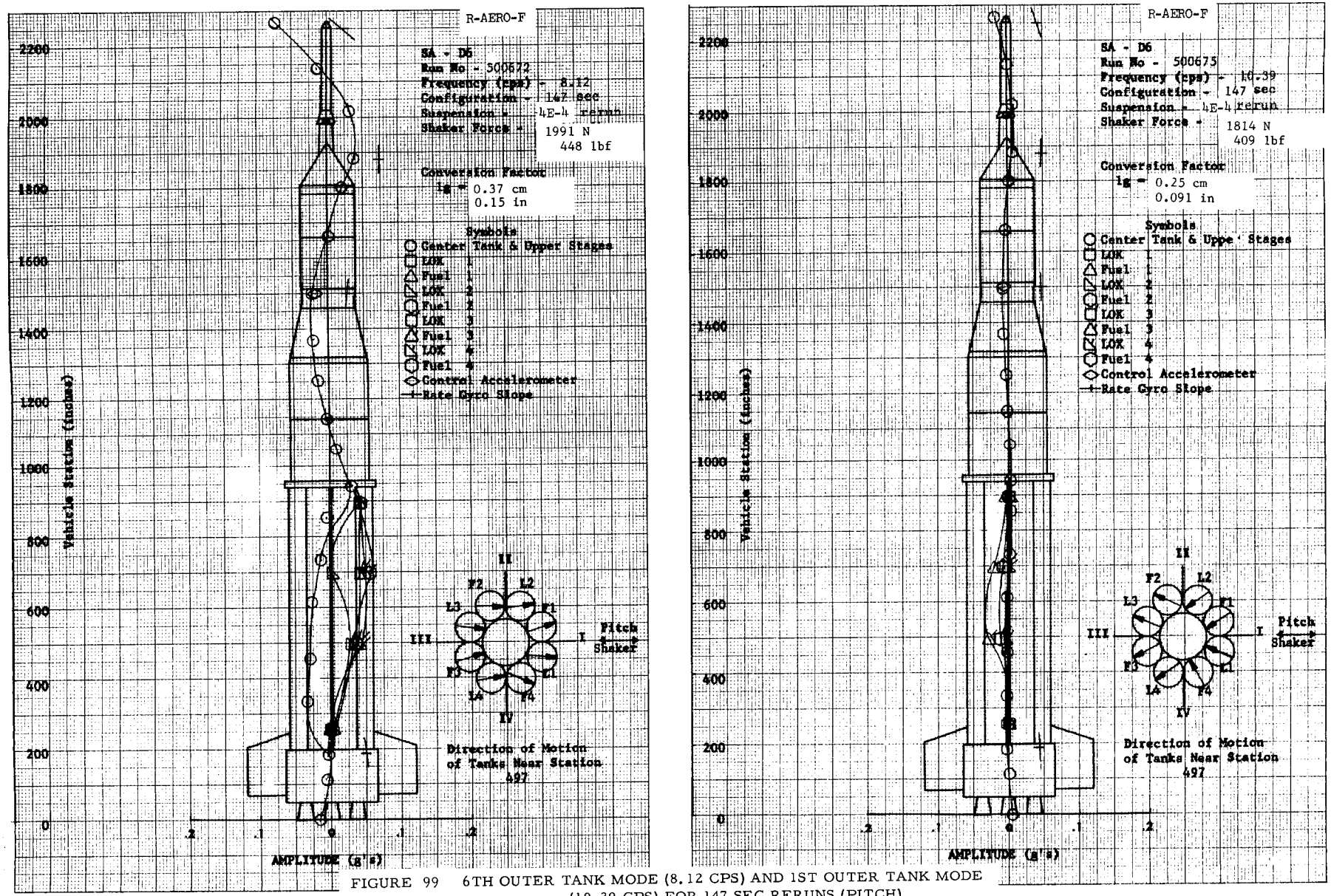


FIGURE 99 6TH OUTER TANK MODE (8.12 CPS) AND 1ST OUTER TANK MODE (10.39 CPS) FOR 147 SEC RERUNS (PITCH)

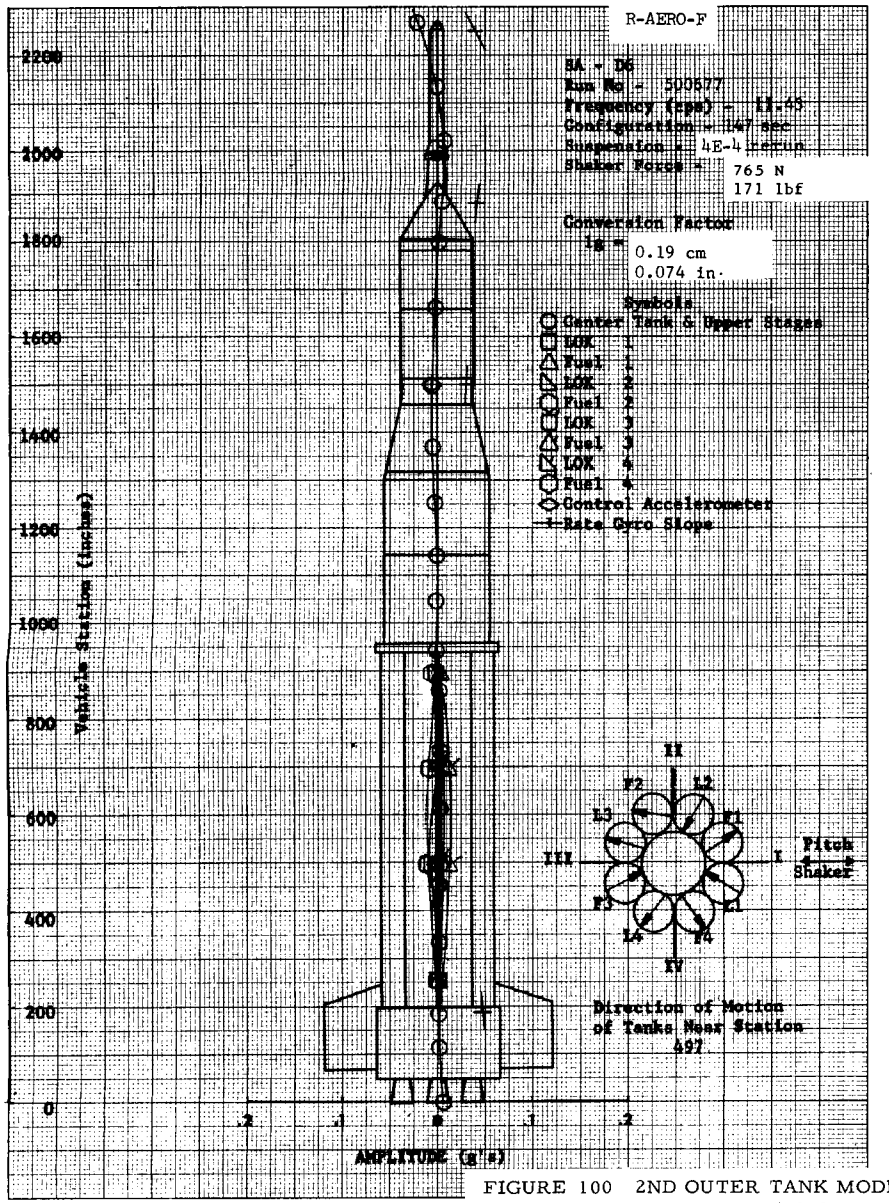


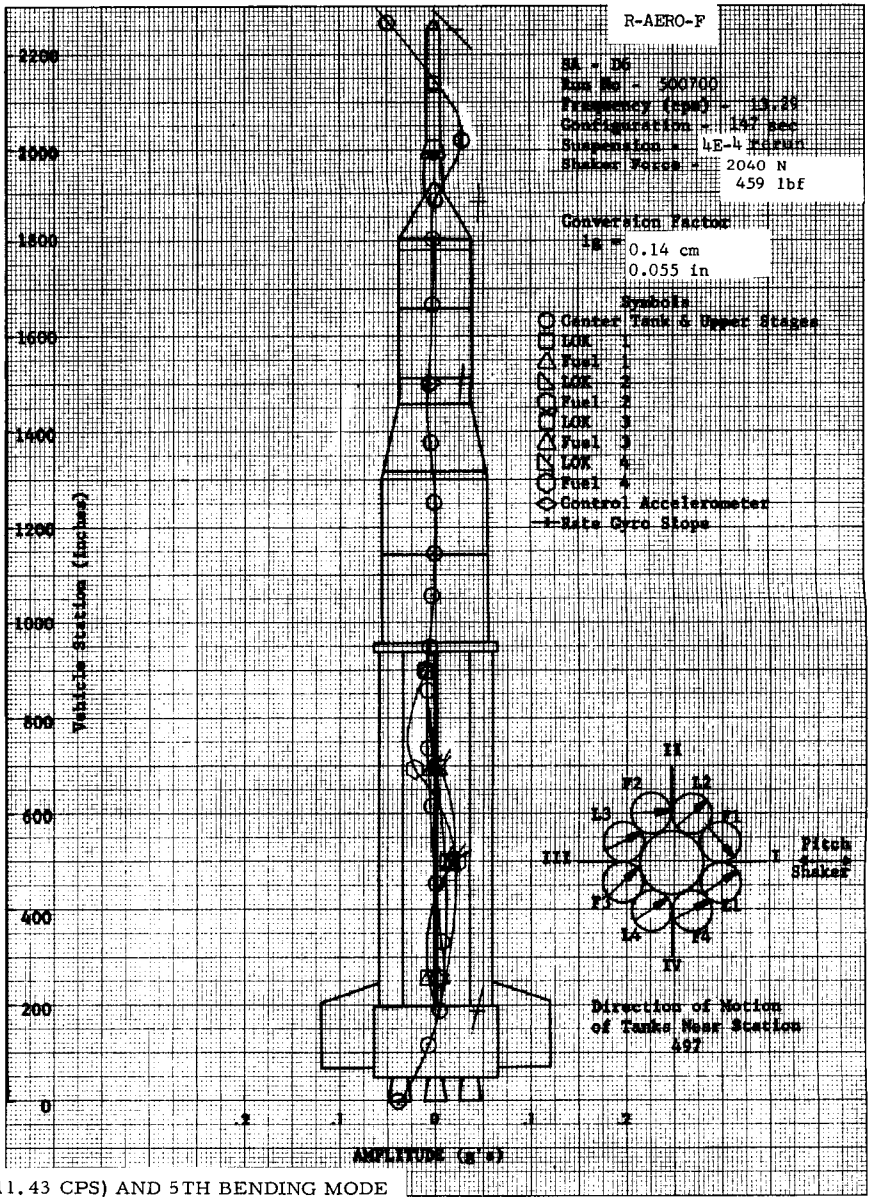


FIGURE 100 2ND OUTER TANK MODE (11.43 CPS) AND 5TH BENDING MODE (13.29 CPS) FOR 147 SEC RERUNS (PITCH)

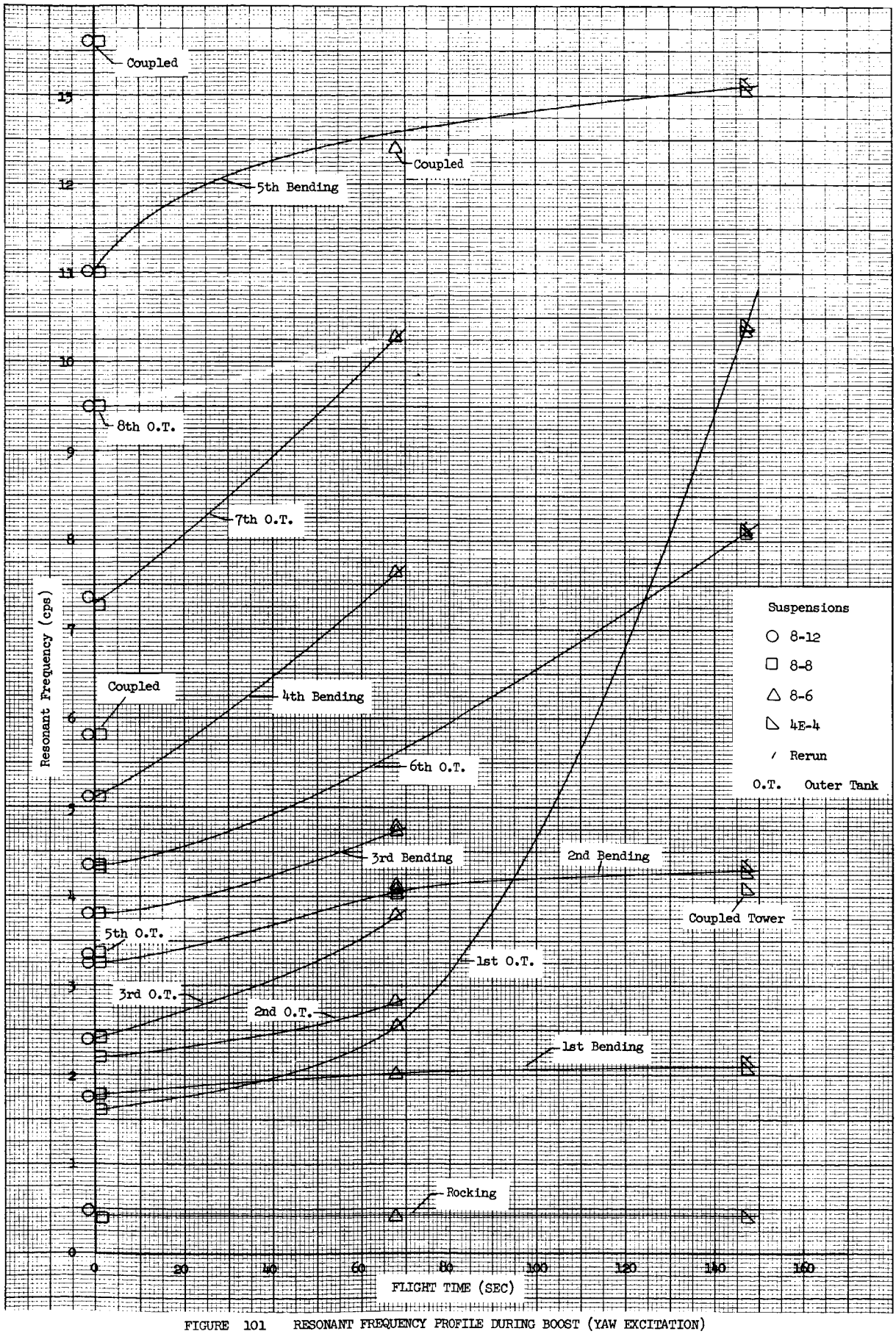


FIGURE 101 RESONANT FREQUENCY PROFILE DURING BOOST (YAW EXCITATION)

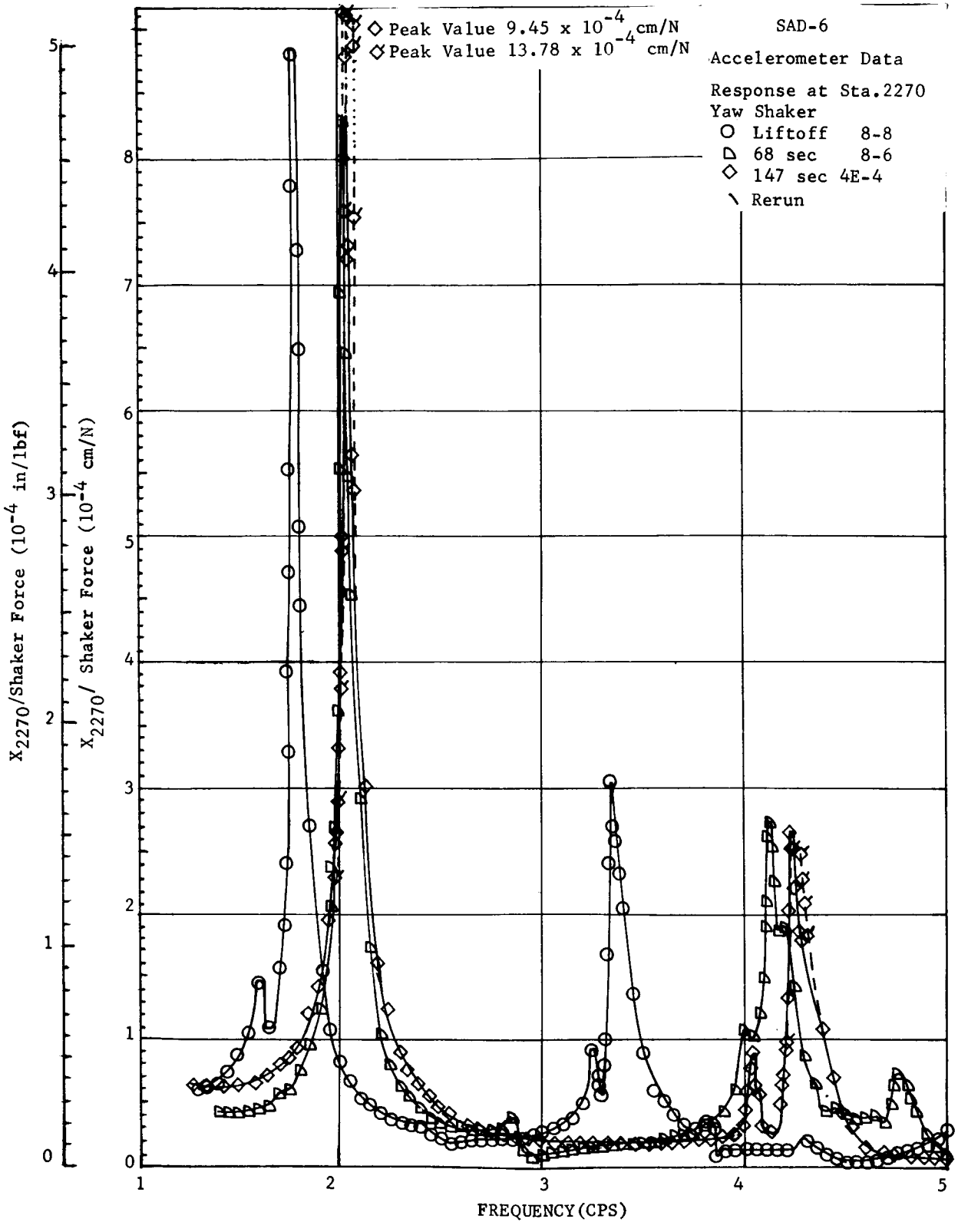


FIGURE 102 YAW RESPONSE AT NOSE FOR SOFT SUSPENSION (YAW EXCITATION)

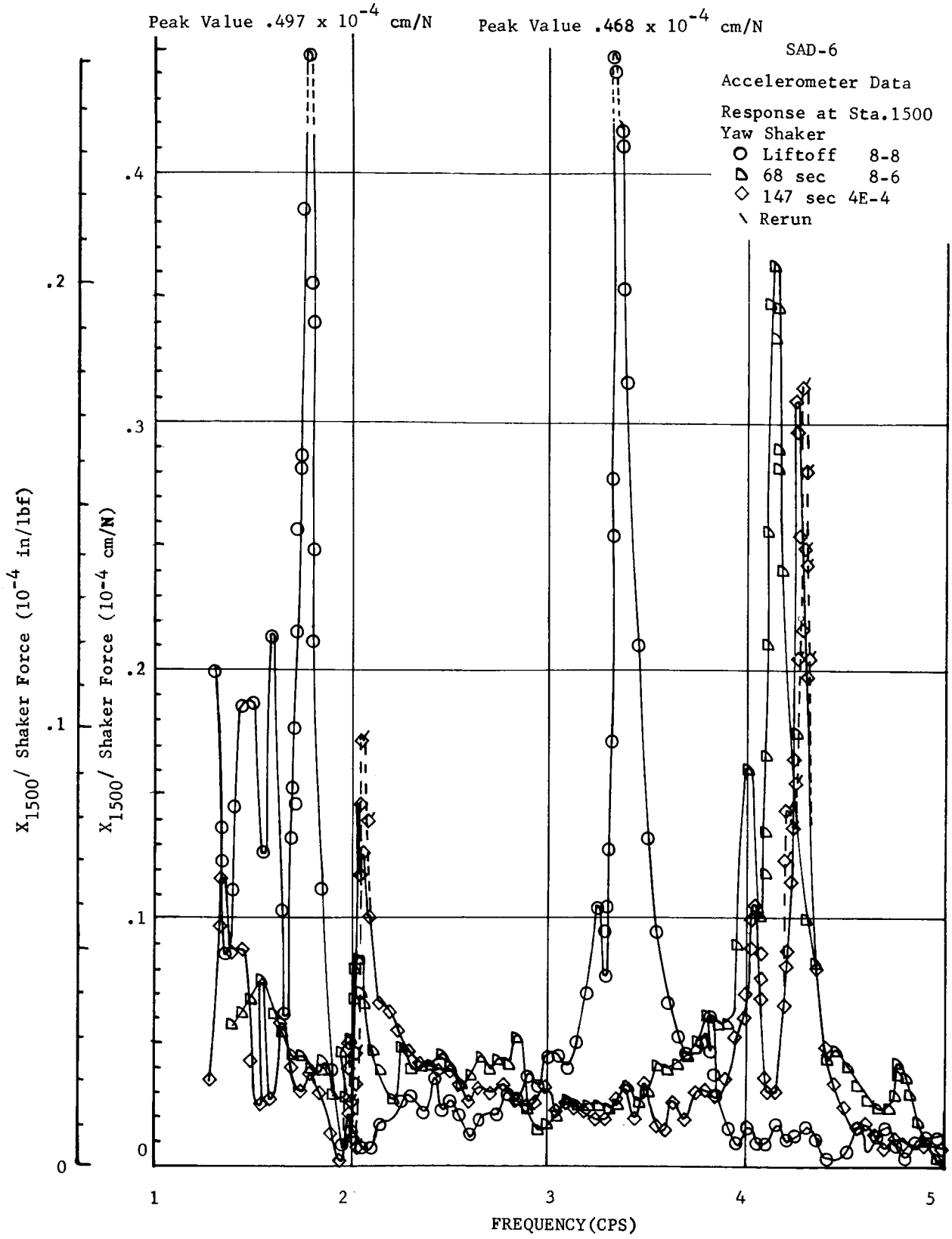


FIGURE 103 YAW RESPONSE AT IU FOR SOFT SUSPENSION (YAW EXCITATION)

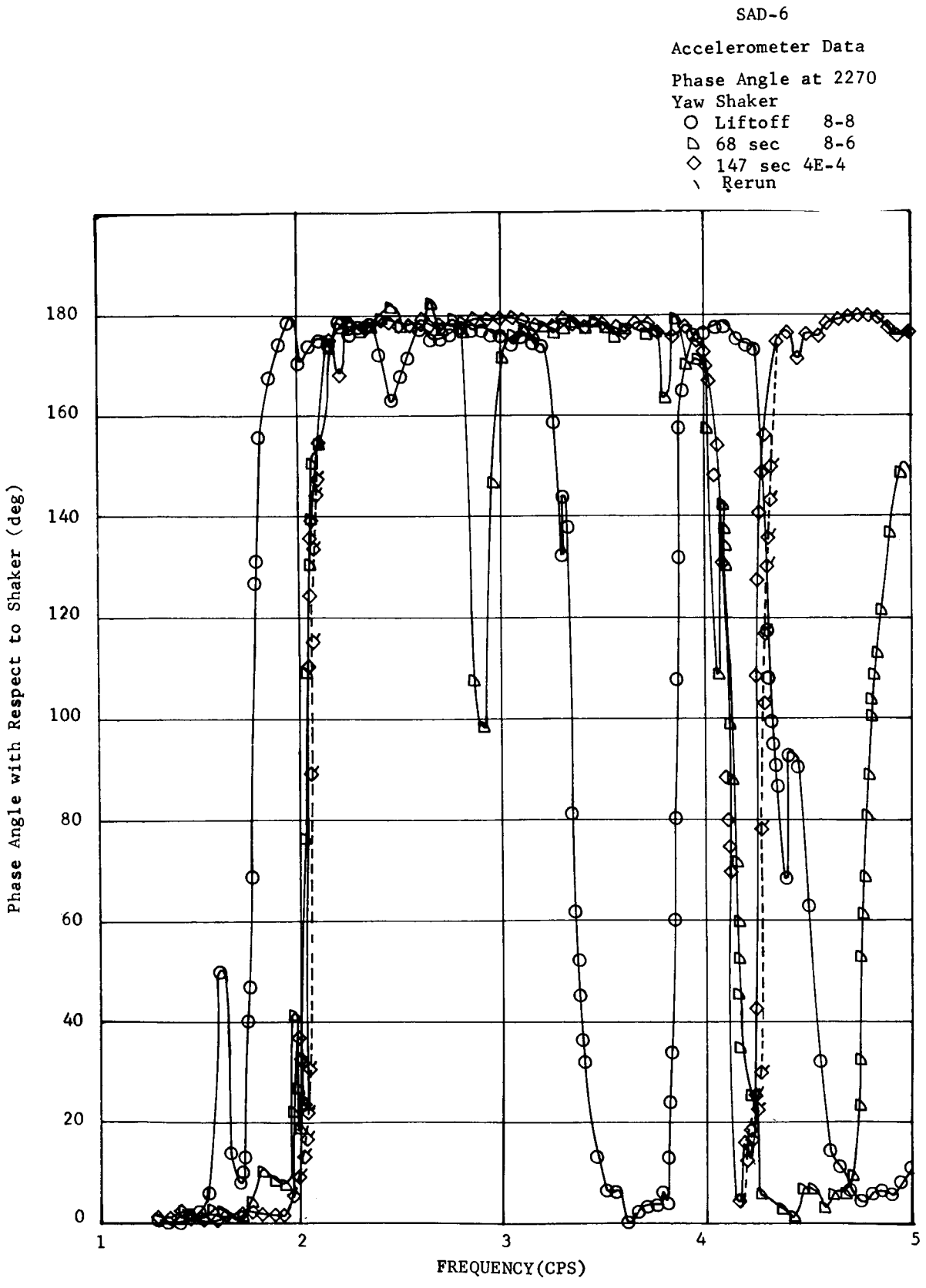


FIGURE 104 PHASE ANGLE AT NOSE FOR SOFT SUSPENSION (YAW EXCITATION)

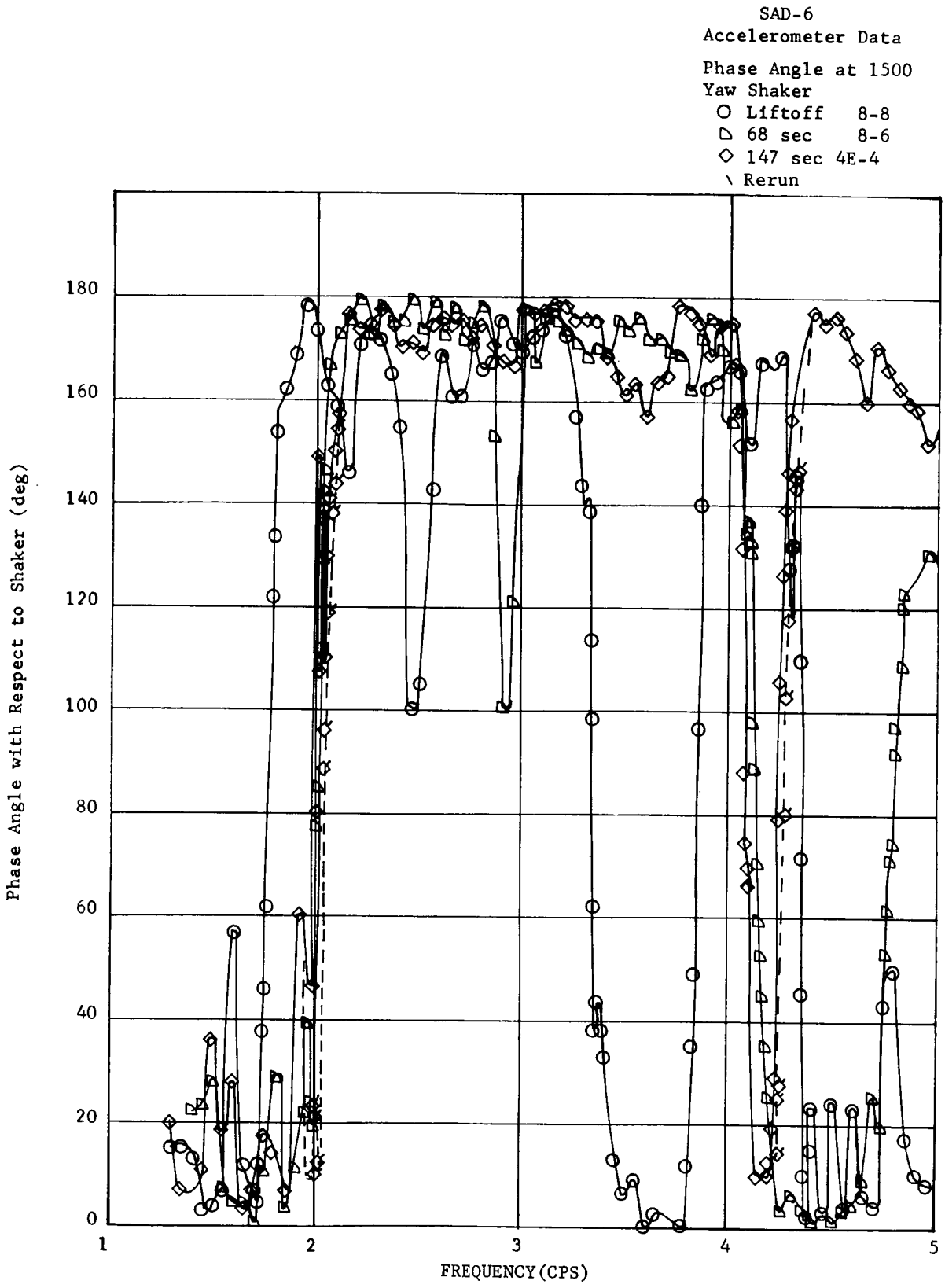


FIGURE 105 PHASE ANGLE AT IU FOR SOFT SUSPENSION (YAW EXCITATION)

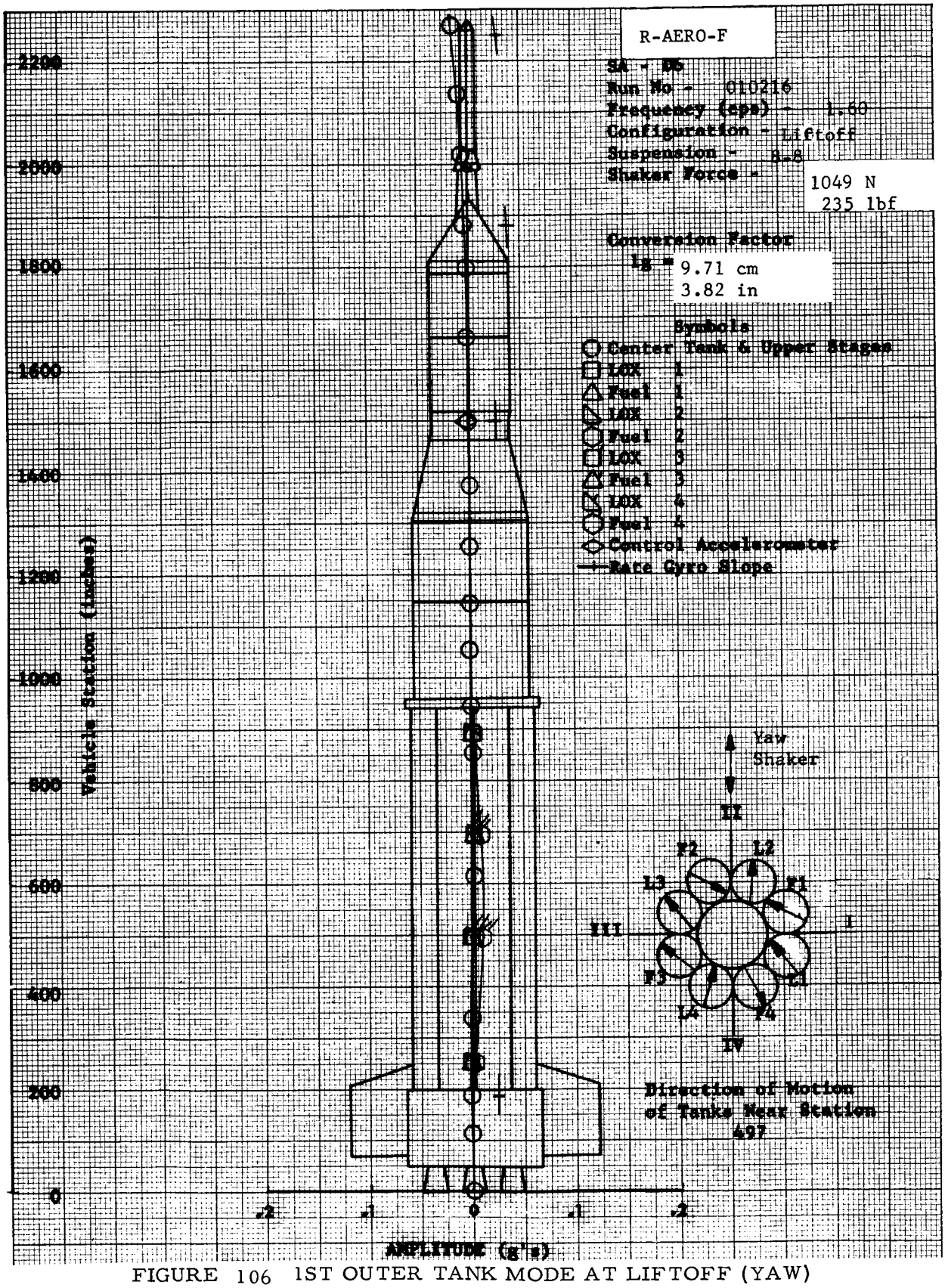


FIGURE 106 1ST OUTER TANK MODE AT LIFTOFF (YAW)

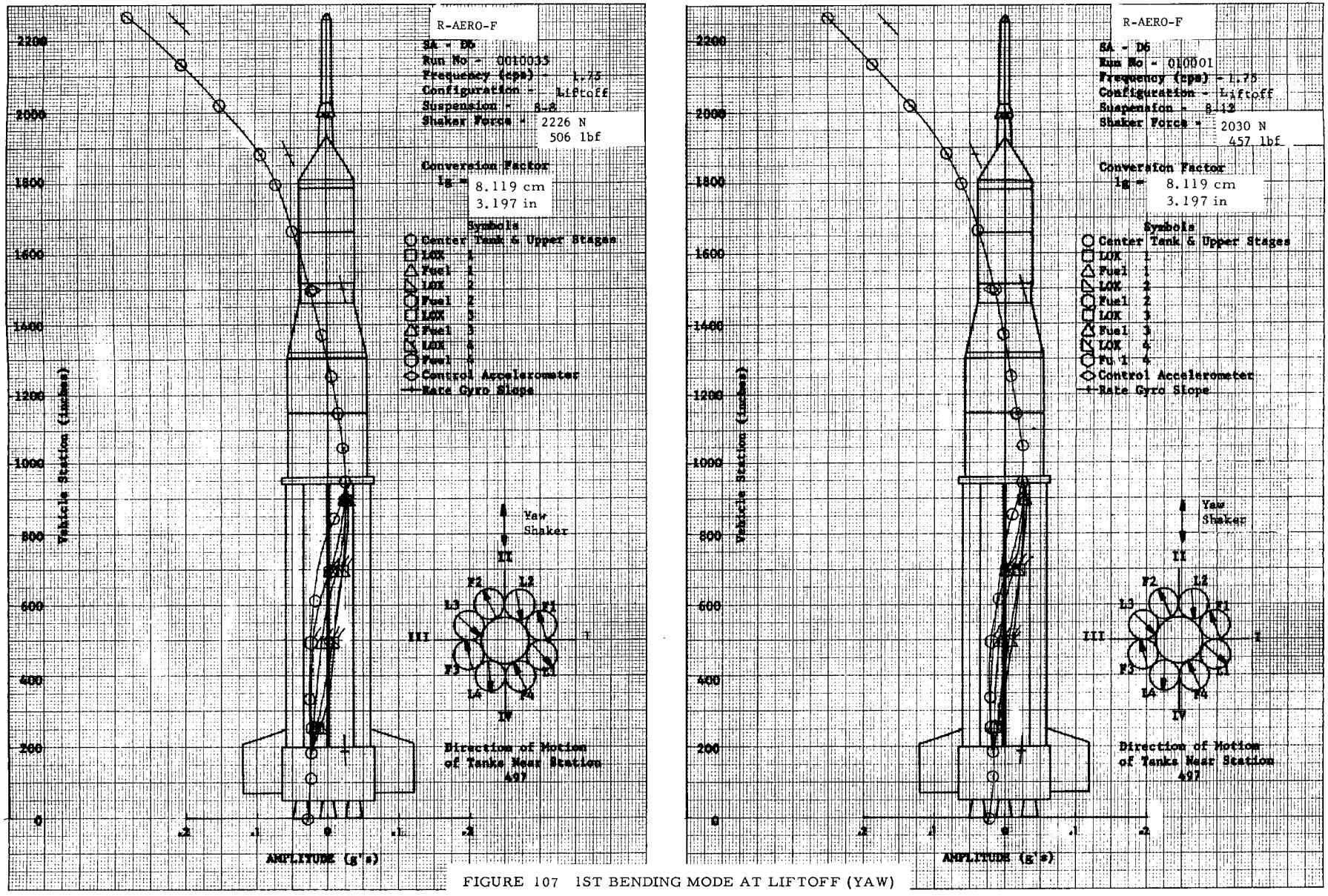


FIGURE 107 1ST BENDING MODE AT LIFTOFF (YAW)

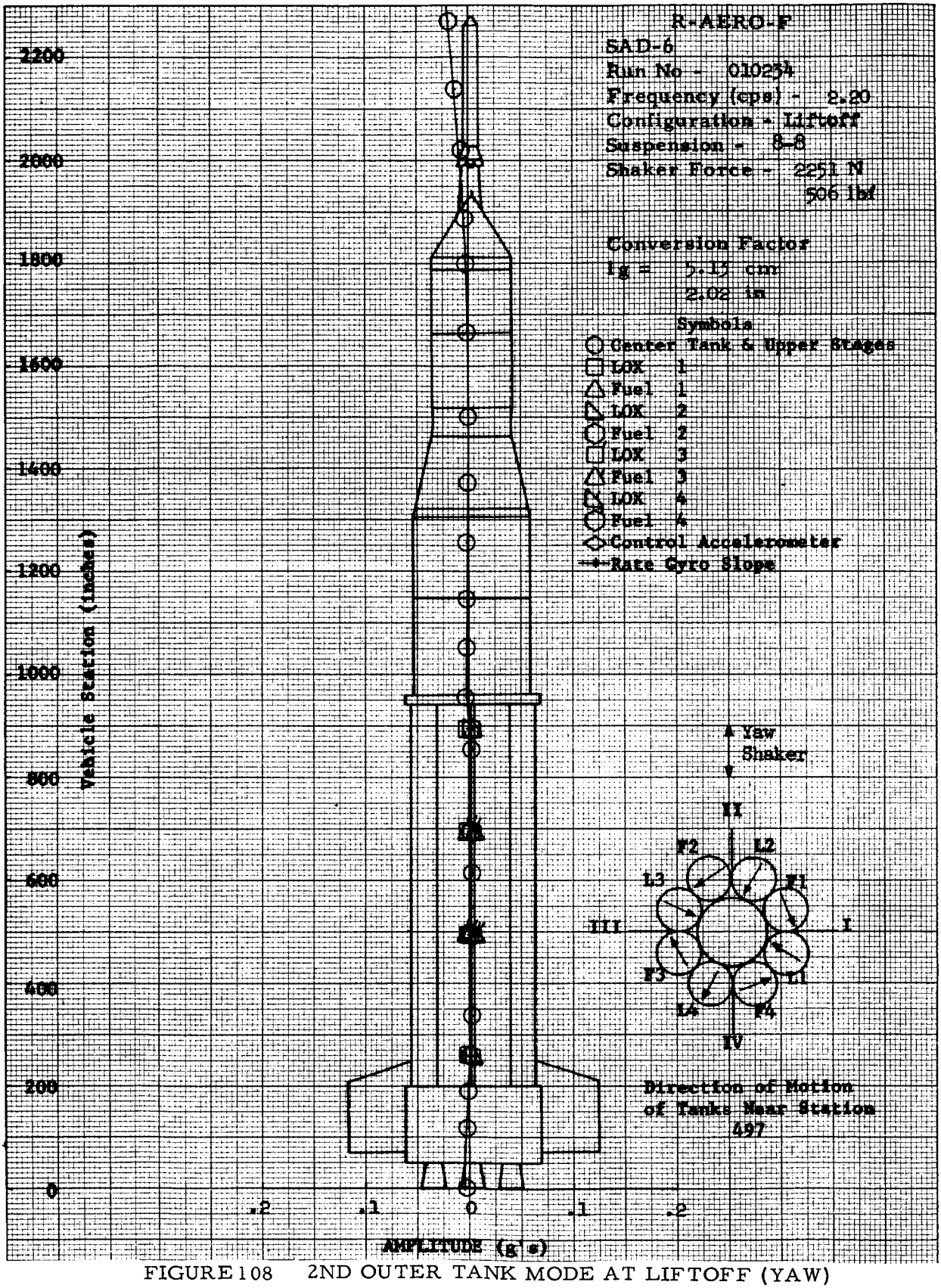


FIGURE 108 2ND OUTER TANK MODE AT LIFTOFF (YAW)

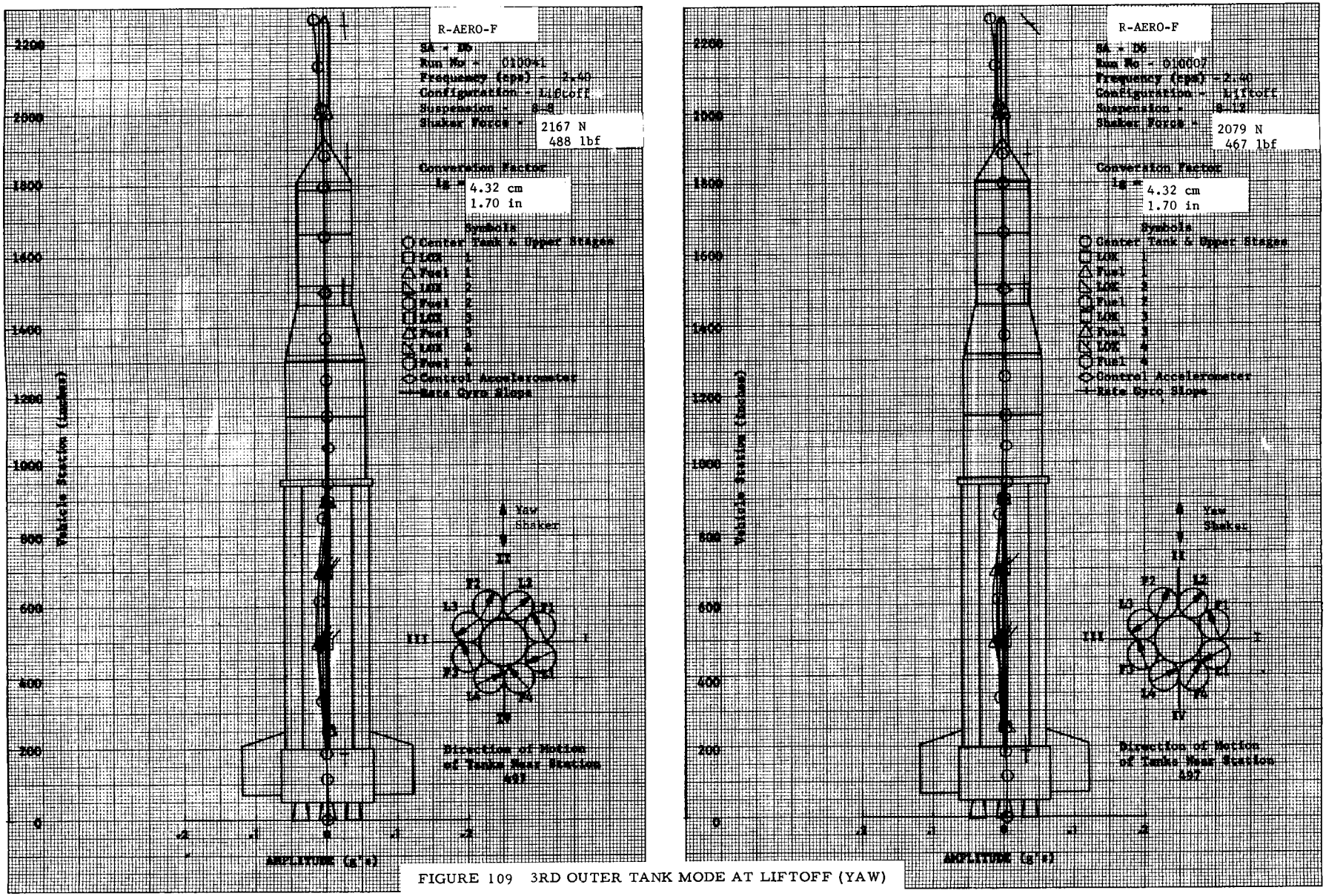


FIGURE 109 3RD OUTER TANK MODE AT LIFTOFF (YAW)

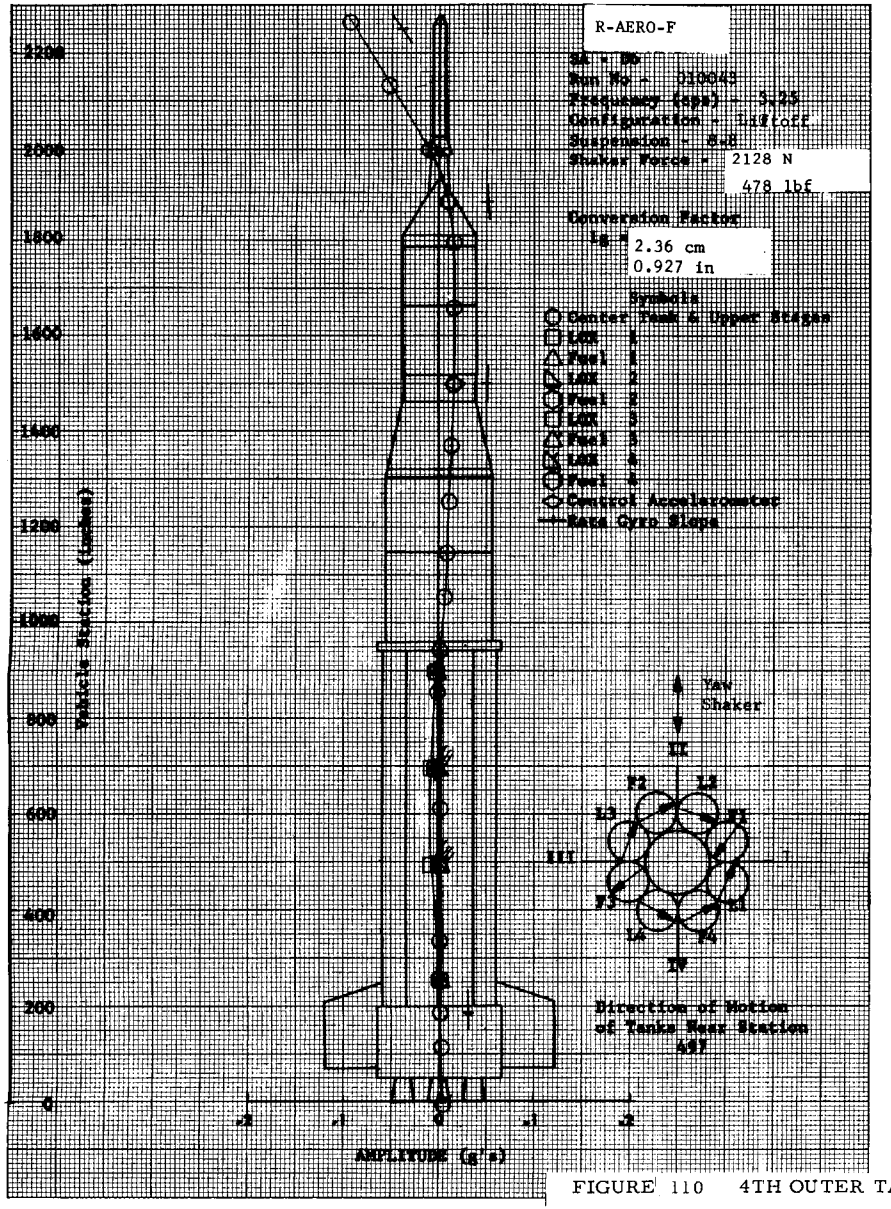


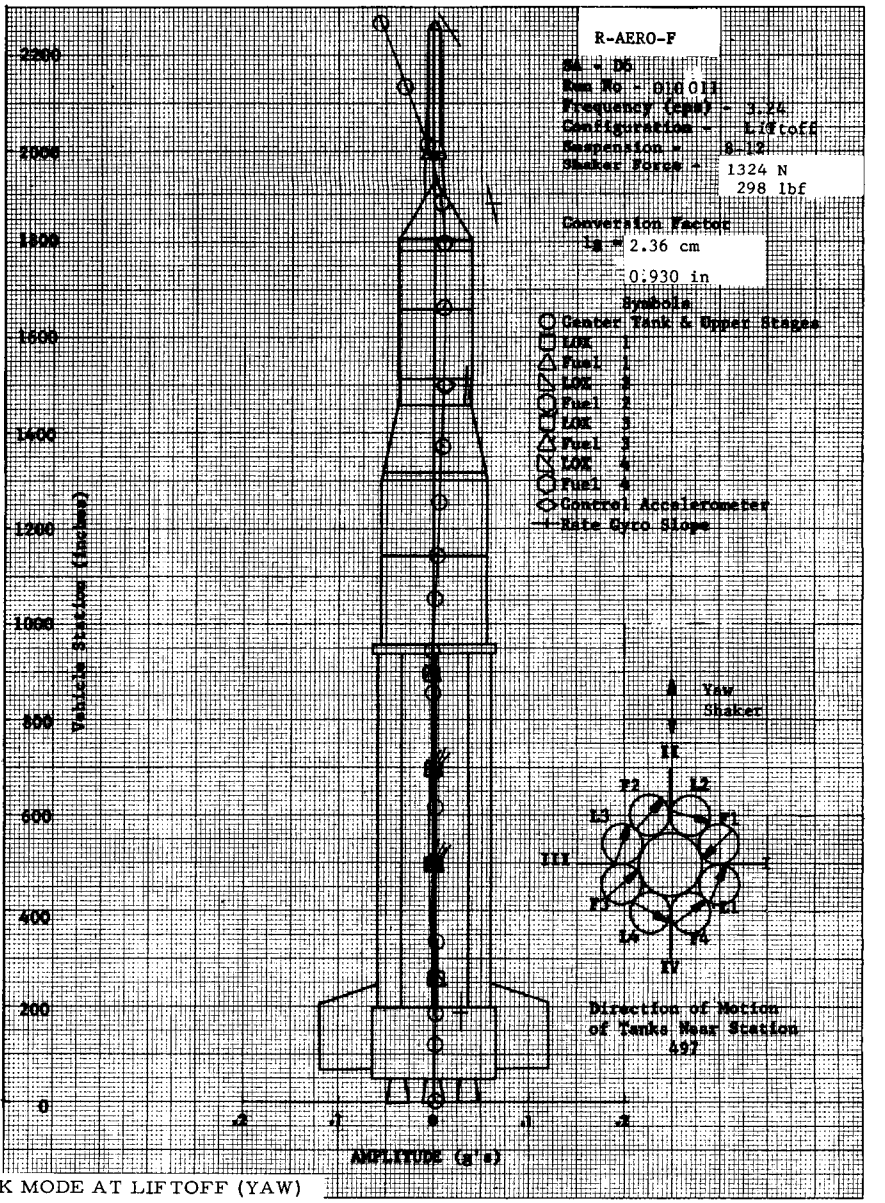


FIGURE 110 4TH OUTER TANK MODE AT LIFTOFF (YAW)

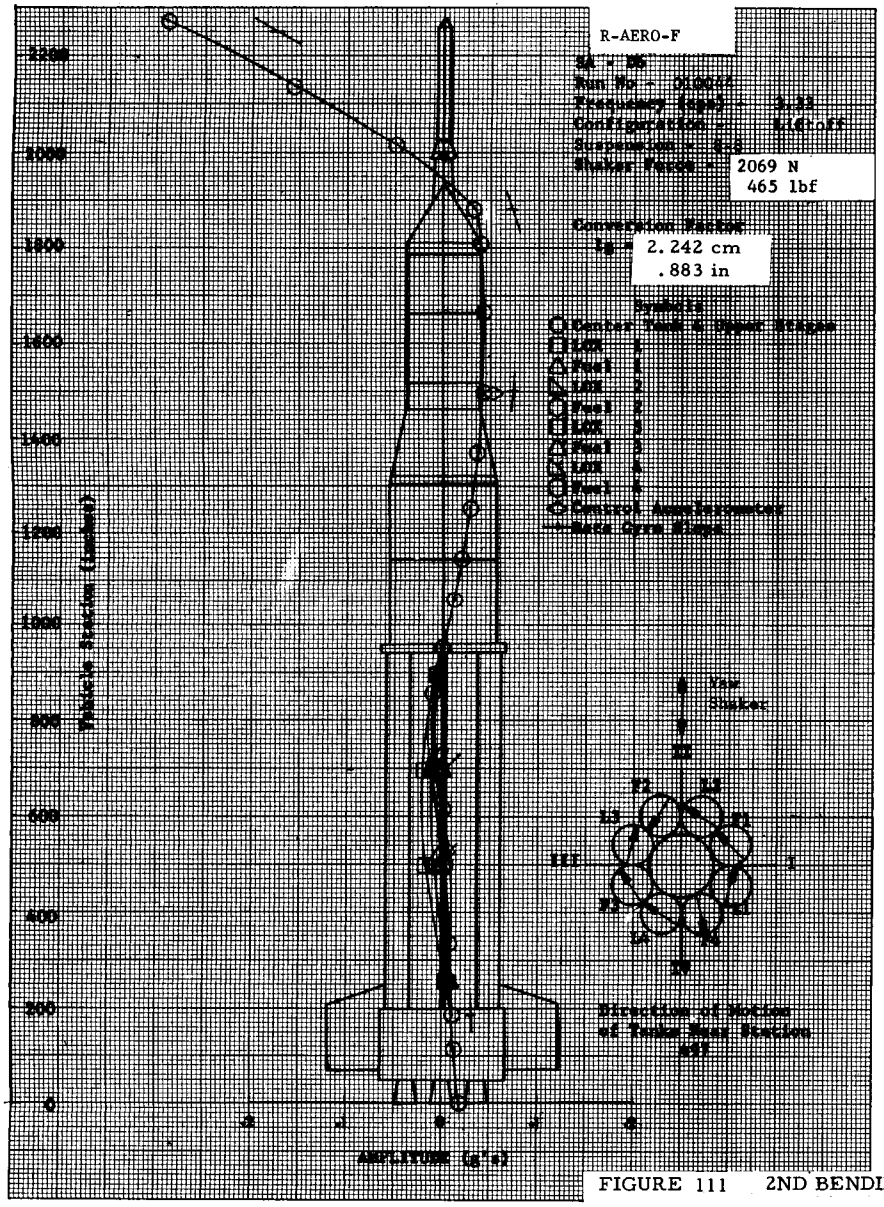


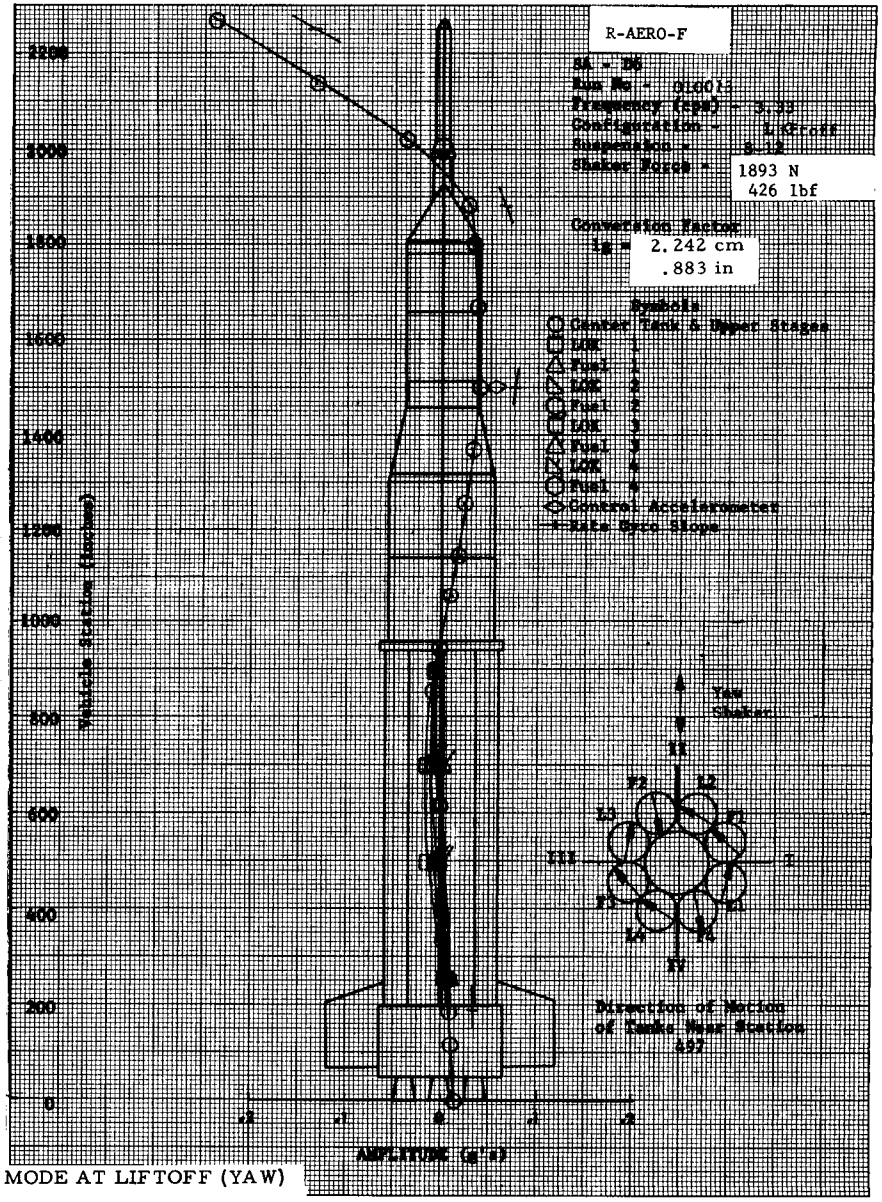


FIGURE 111 2ND BENDING MODE AT LIFTOFF (YAW)

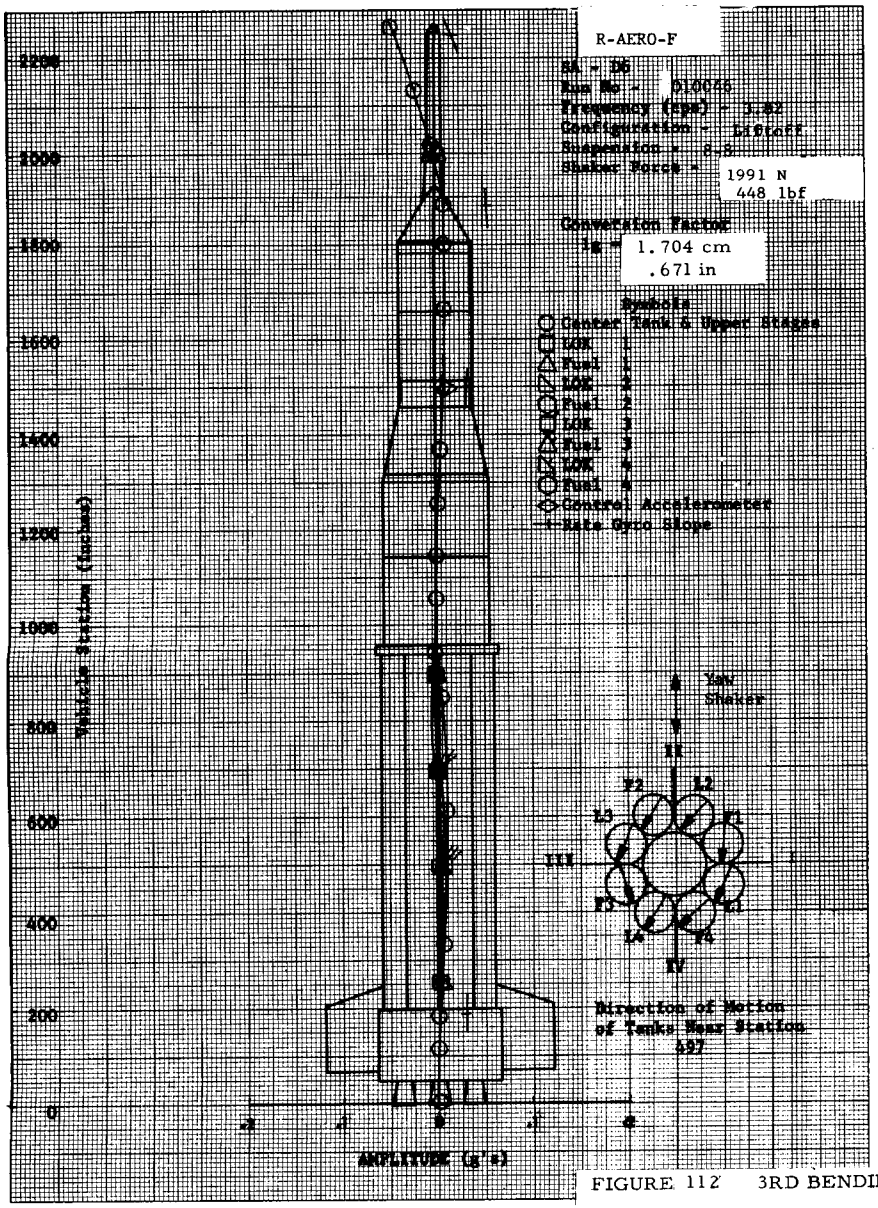


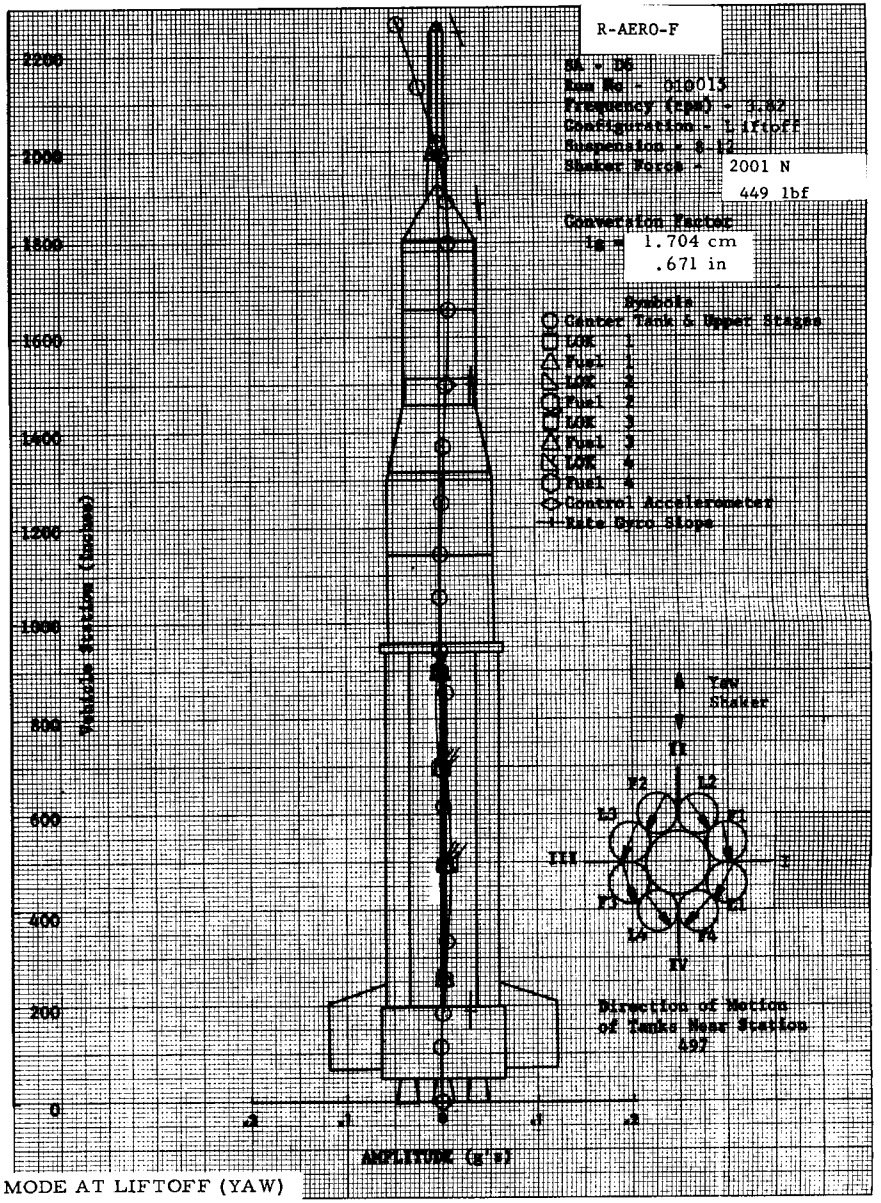


FIGURE 112 3RD BENDING MODE AT LIFTOFF (YAW)

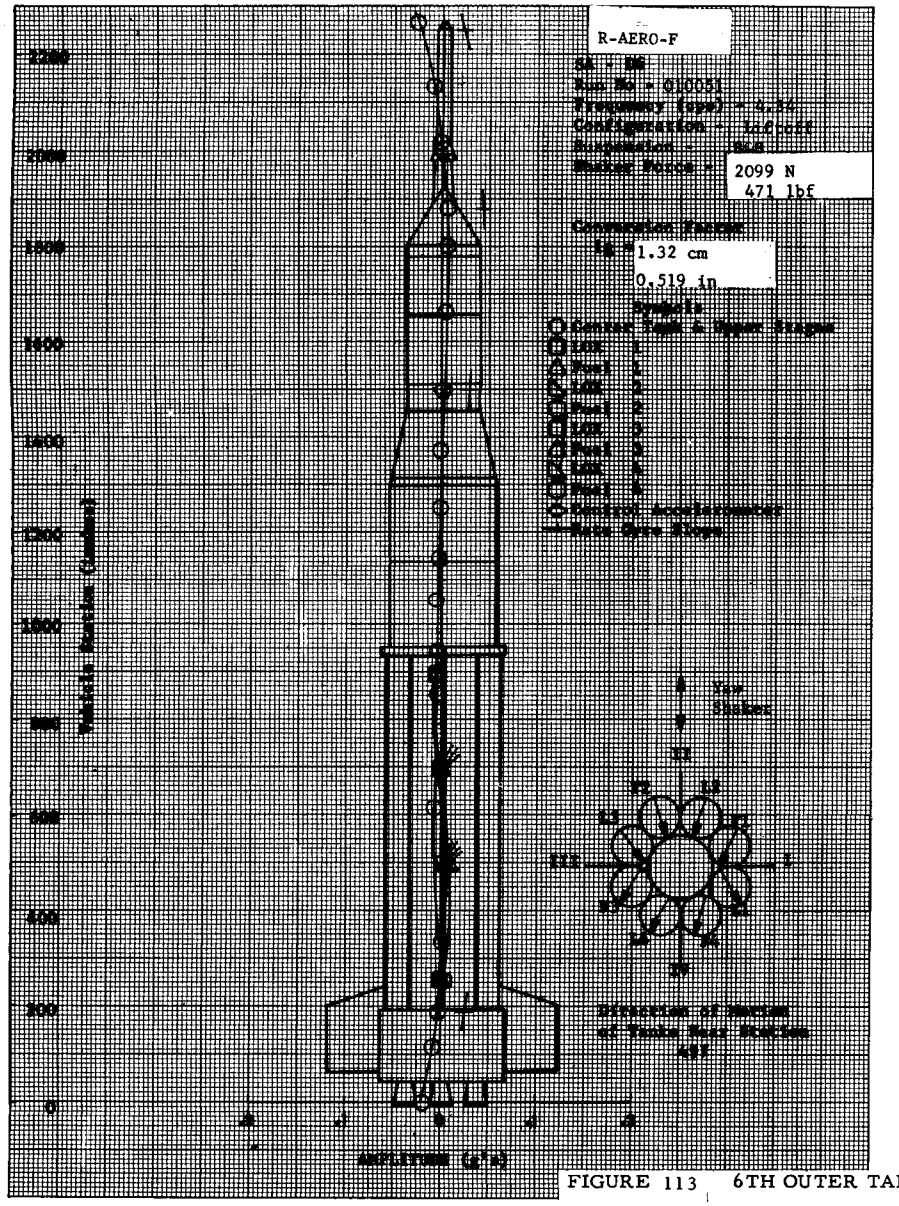


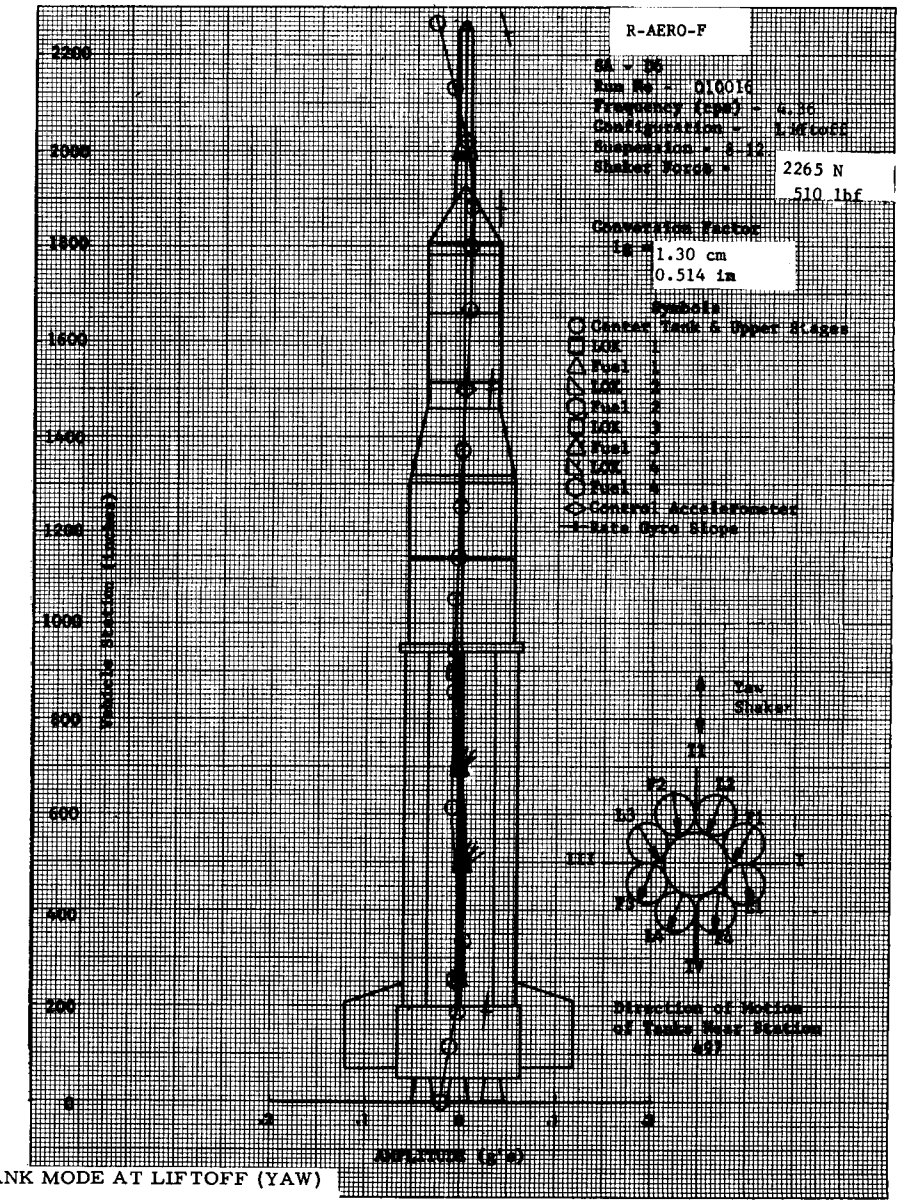


FIGURE 113 6TH OUTER TANK MODE AT LIFTOFF (YAW)

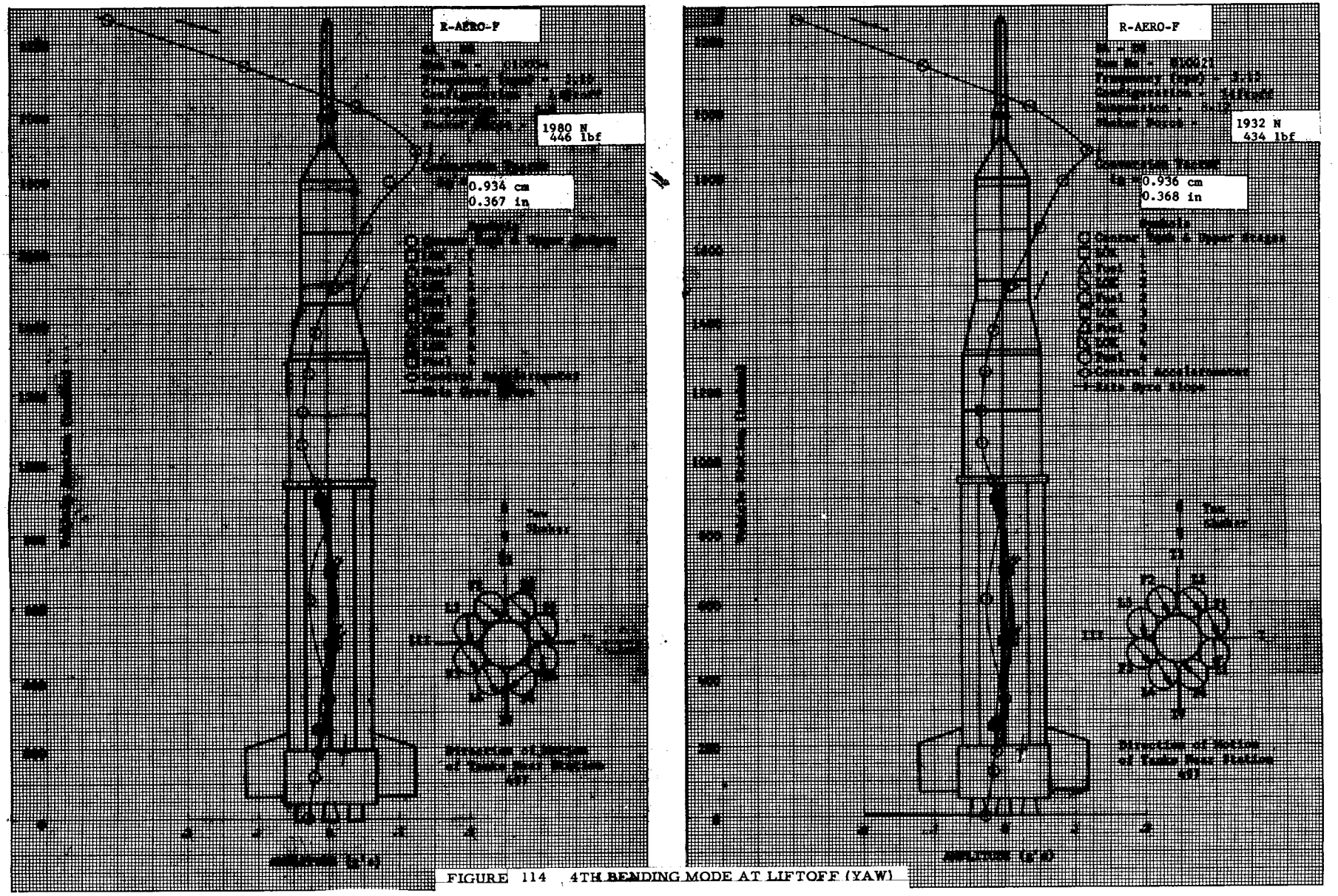


FIGURE 114 4TH BENDING MODE AT LIFTOFF (YAW)

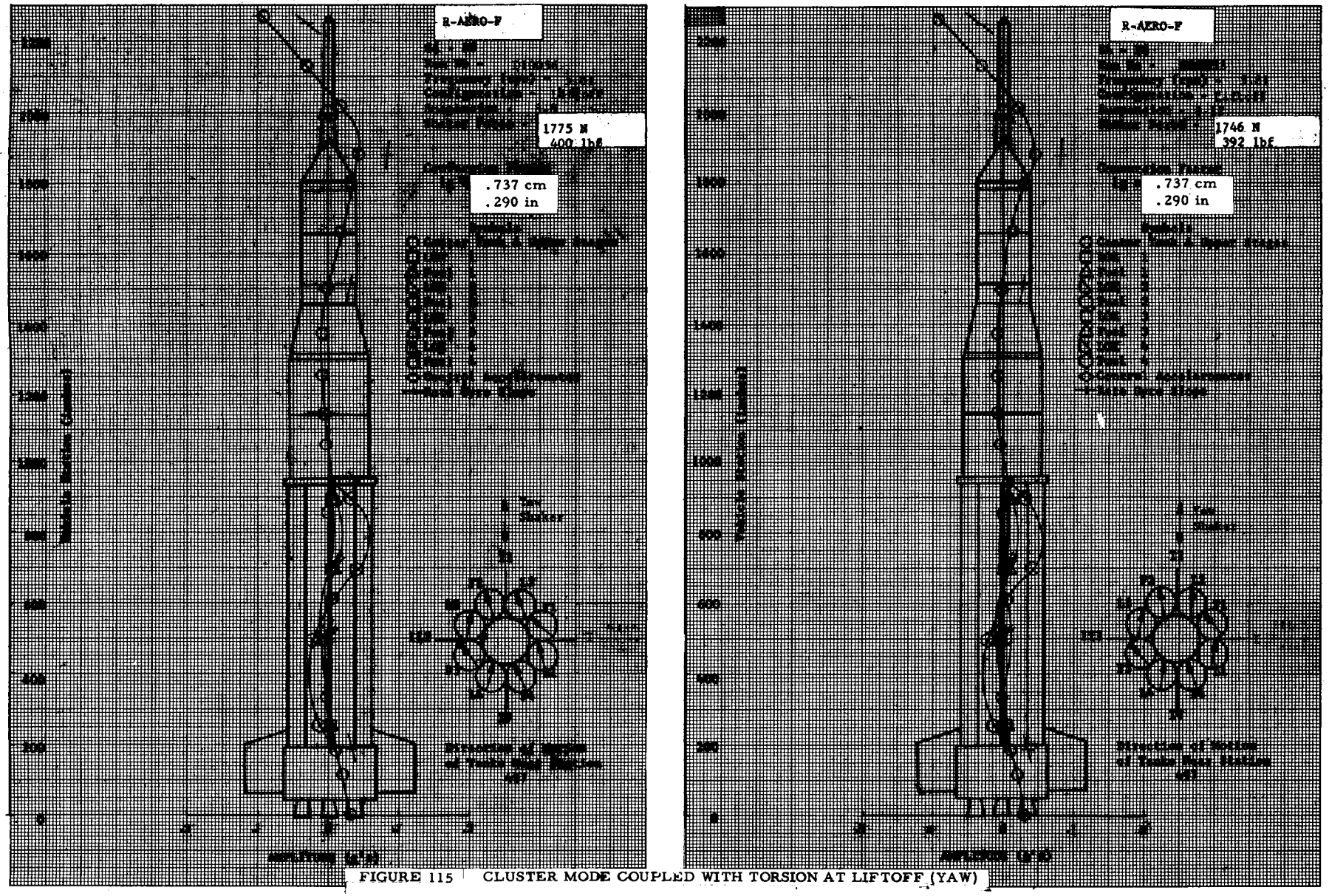


FIGURE 115 CLUSTER MODE COUPLED WITH TORSION AT LIFTOFF (YAW)

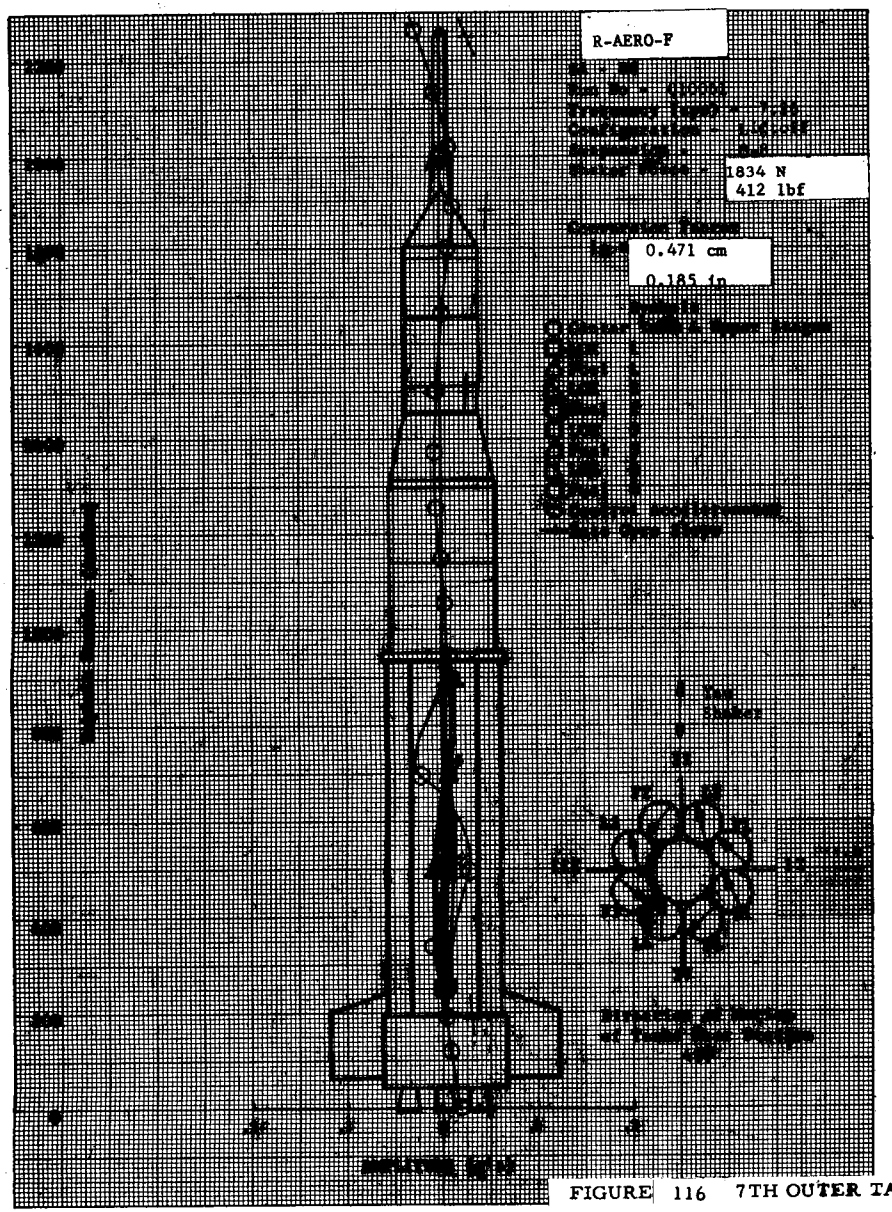


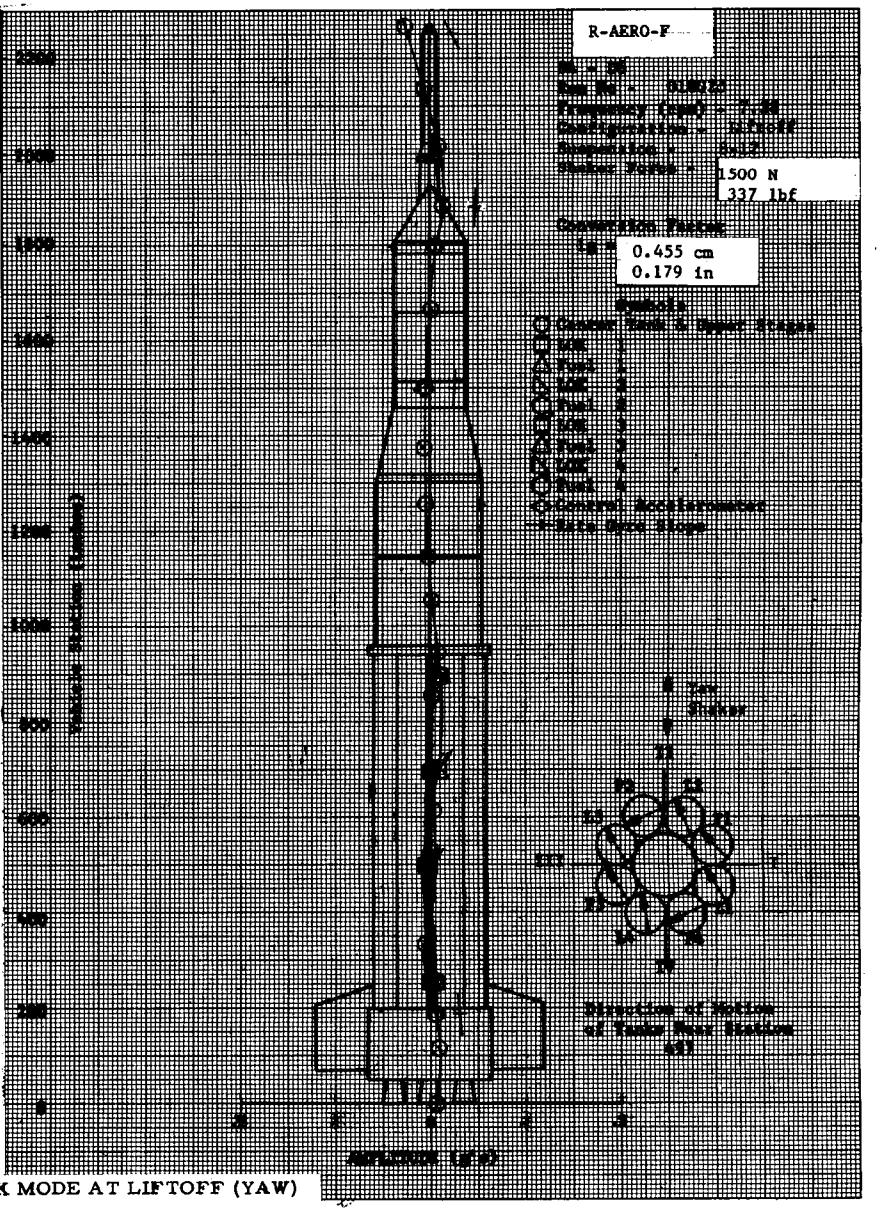


FIGURE 116 7TH OUTER TANK MODE AT LIFTOFF (YAW)

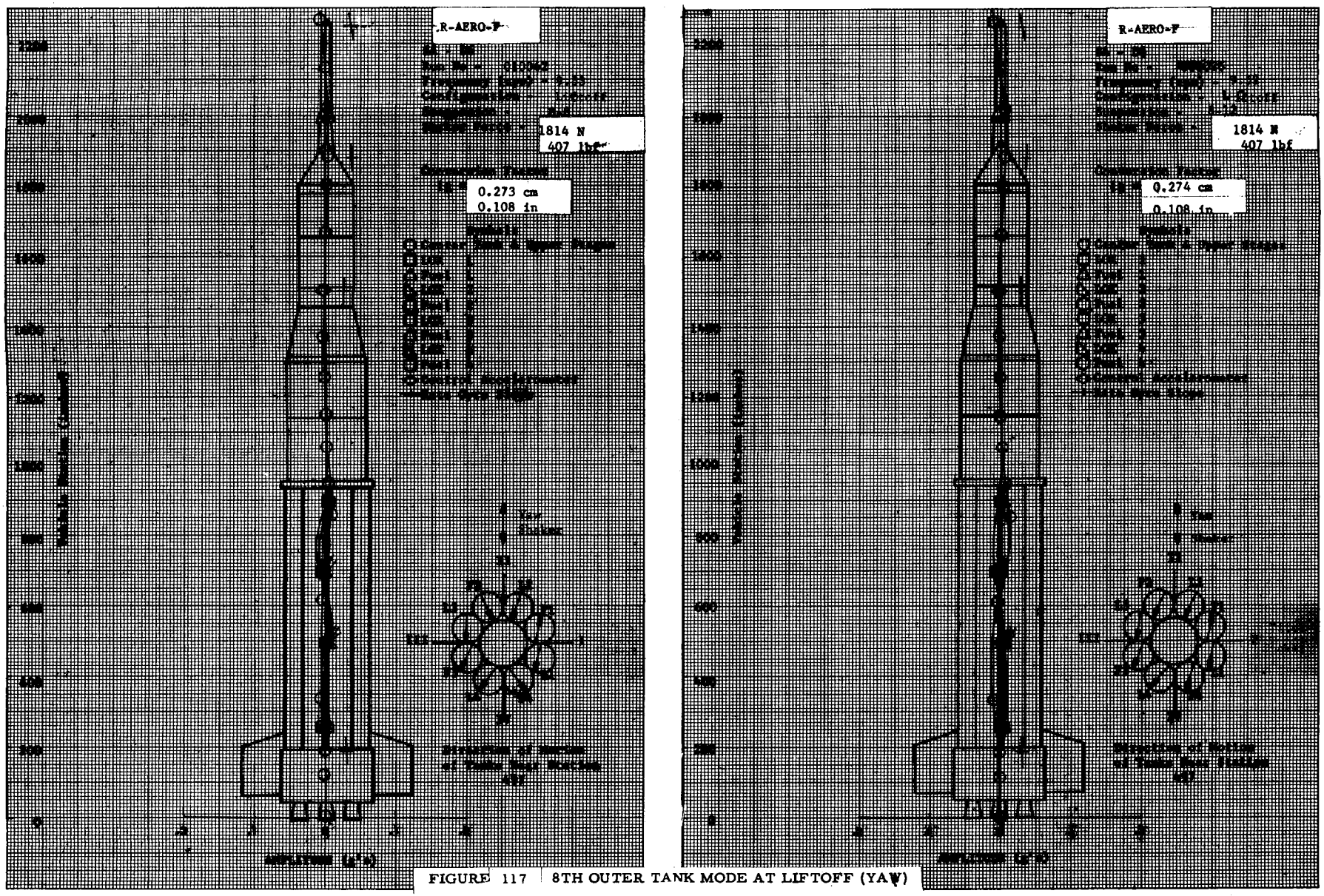


FIGURE 117 8TH OUTER TANK MODE AT LIFTOFF (YAW)

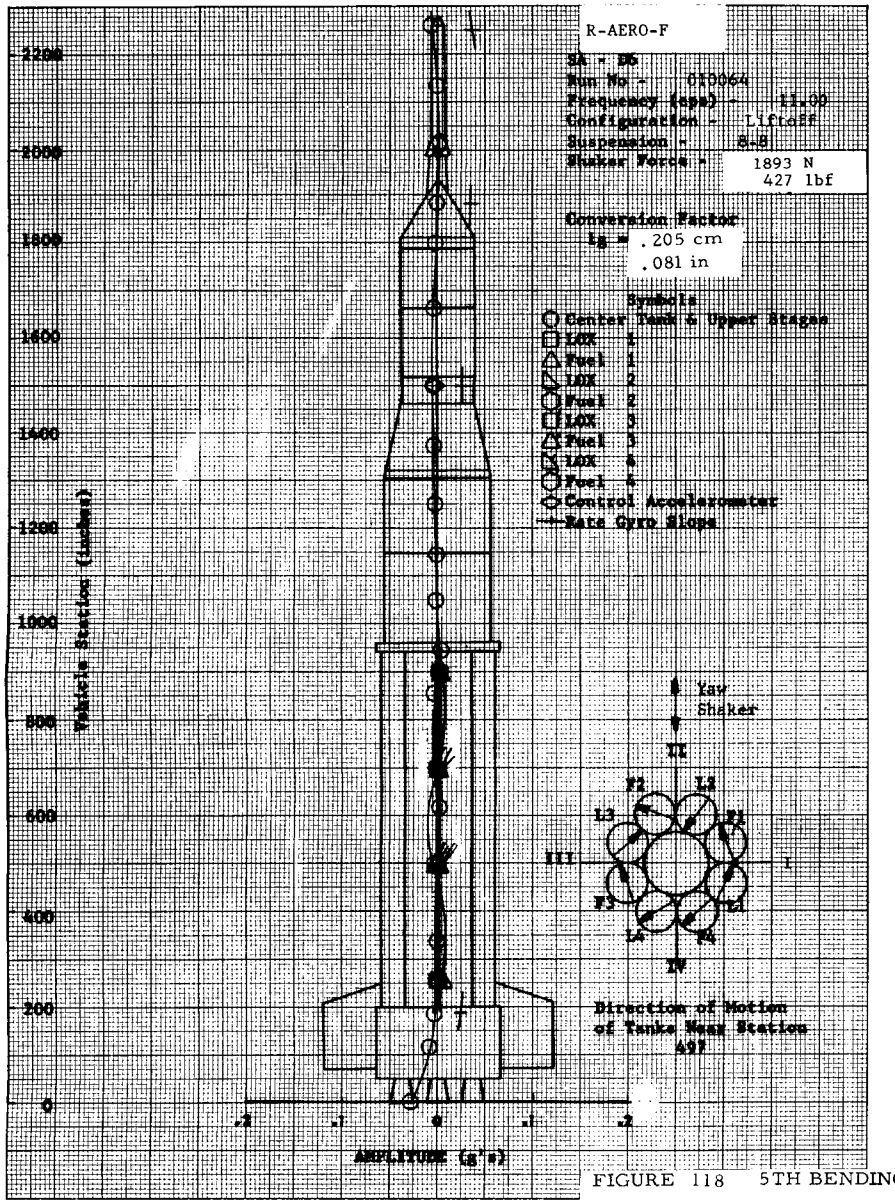


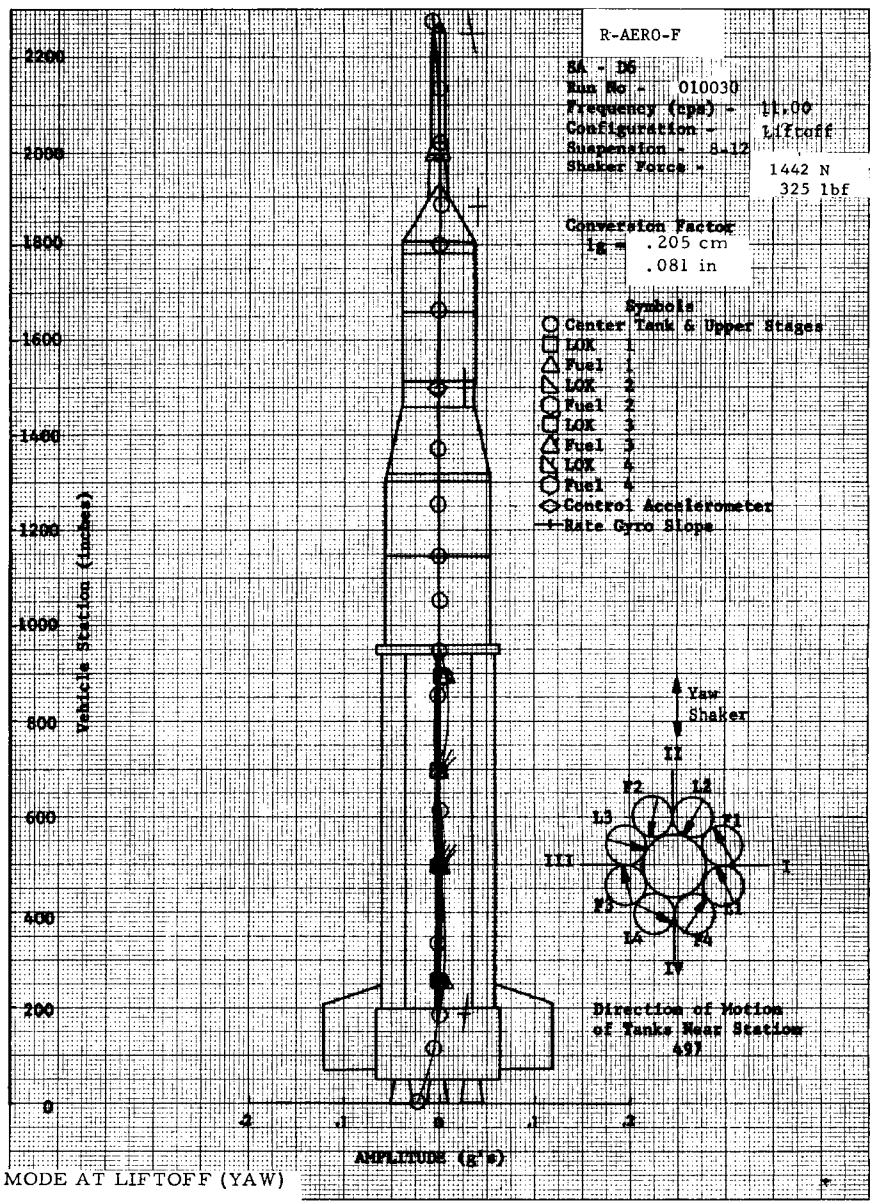


FIGURE 118 5TH BENDING MODE AT LIFTOFF (YAW)

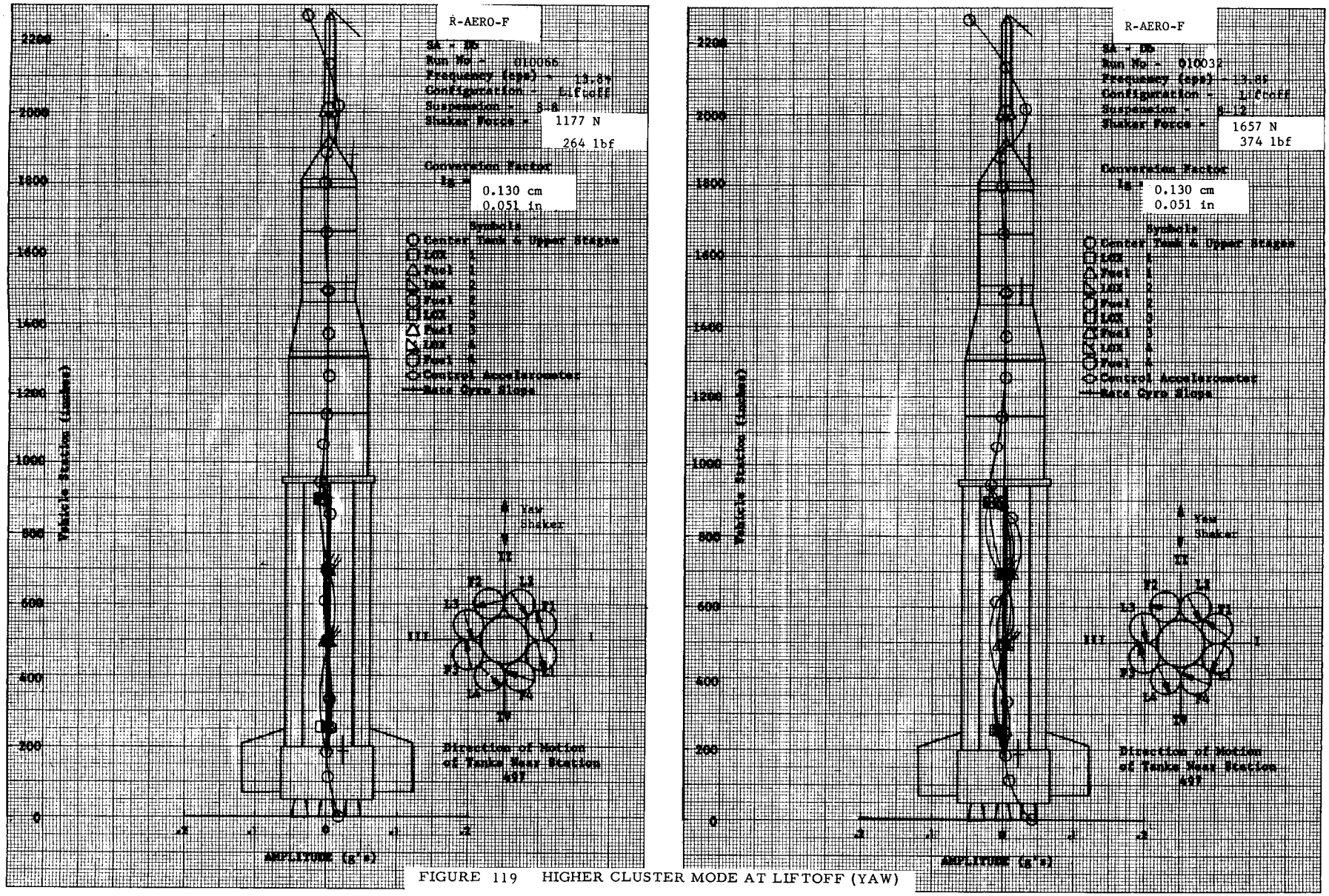


FIGURE 119 HIGHER CLUSTER MODE AT LIFTOFF (YAW)

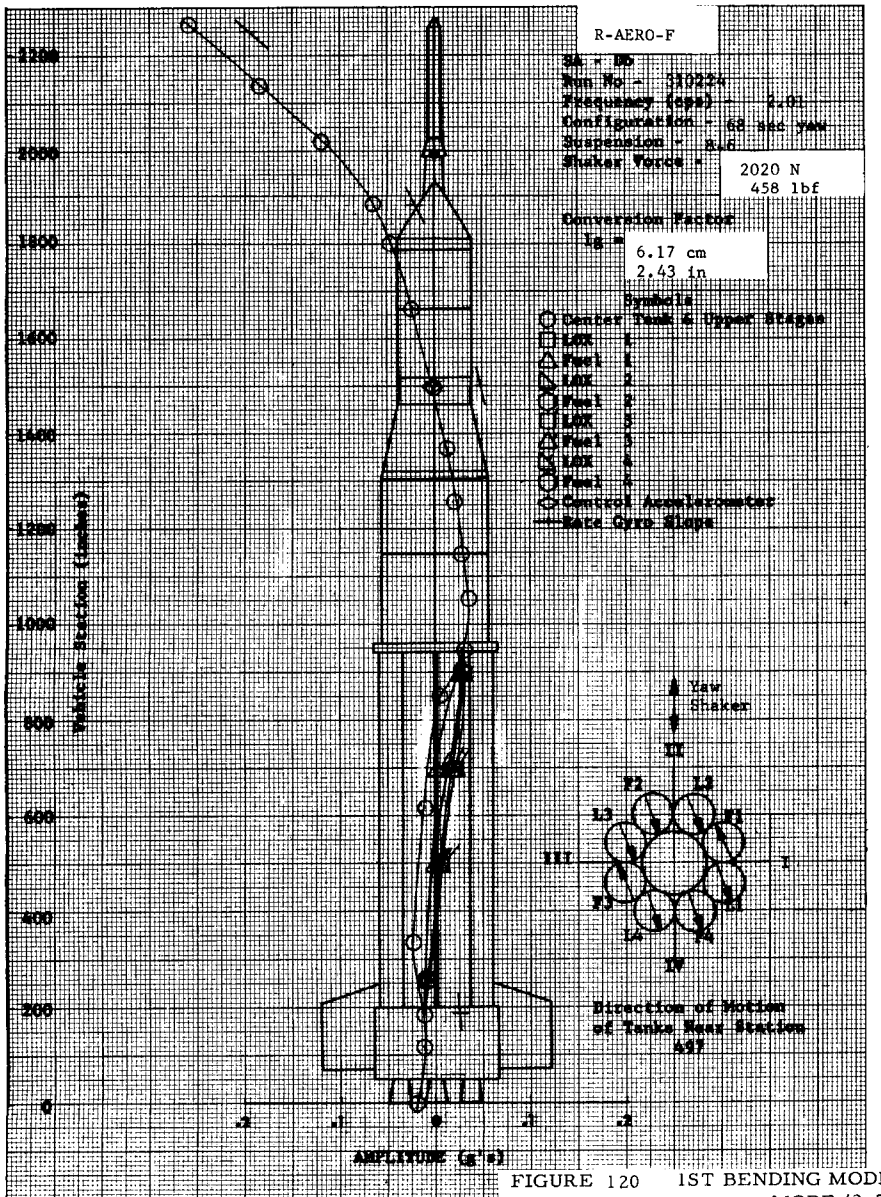


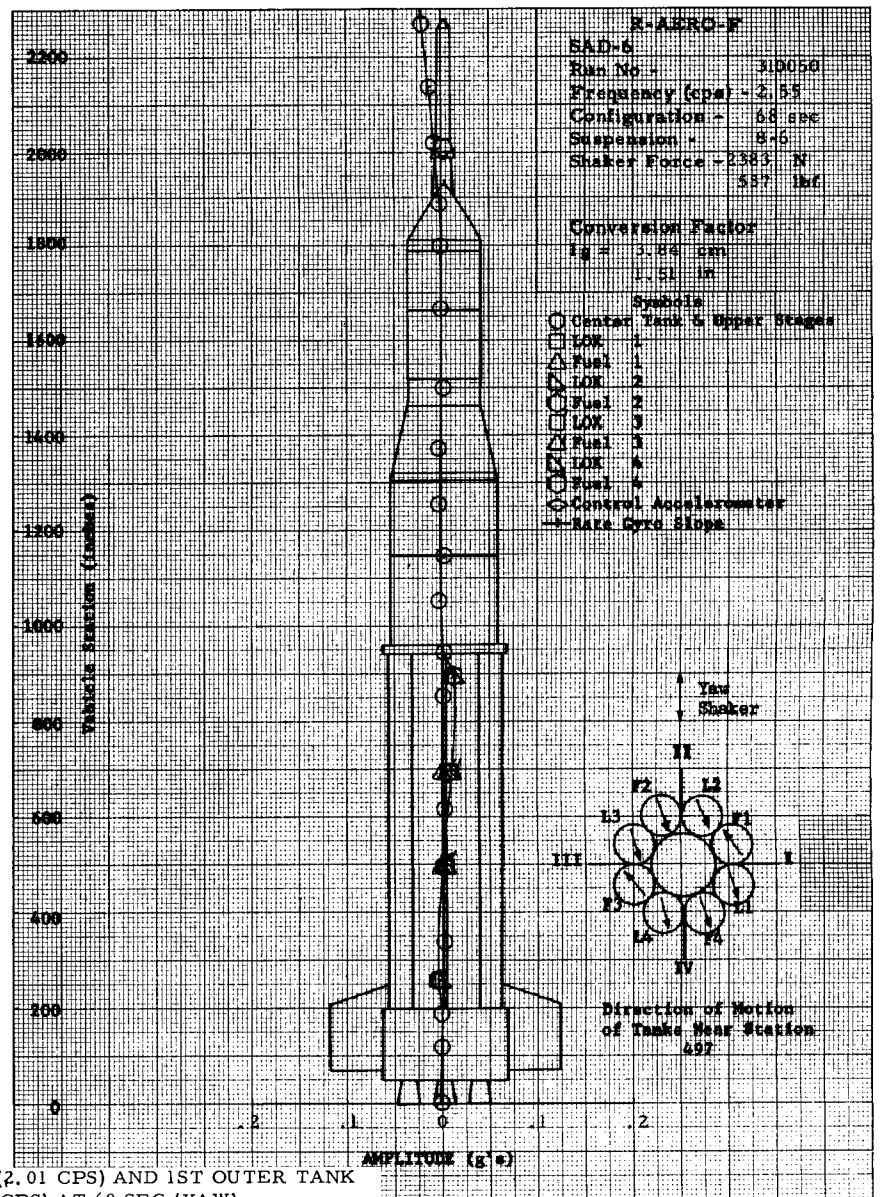


FIGURE 120 1ST BENDING MODE (2.01 CPS) AND 1ST OUTER TANK MODE (2.55 CPS) AT 68 SEC (YAW)

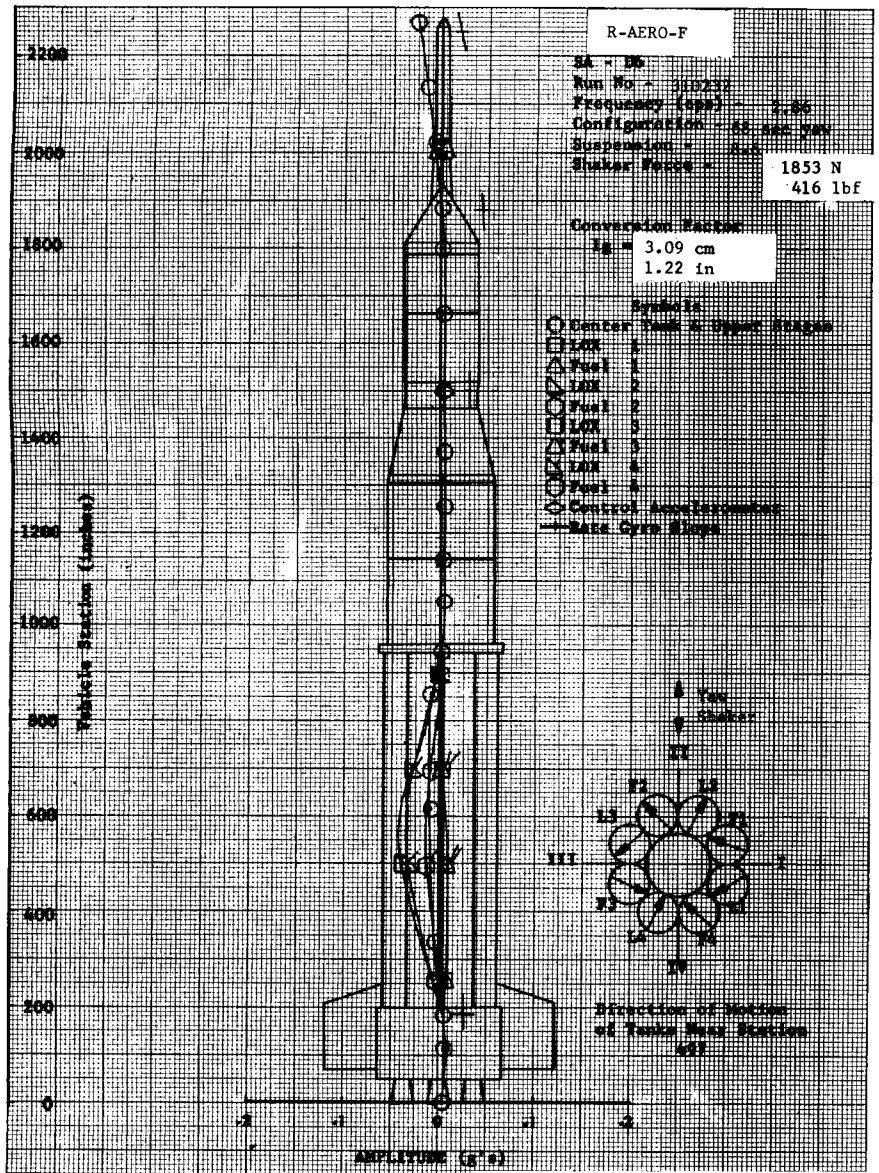


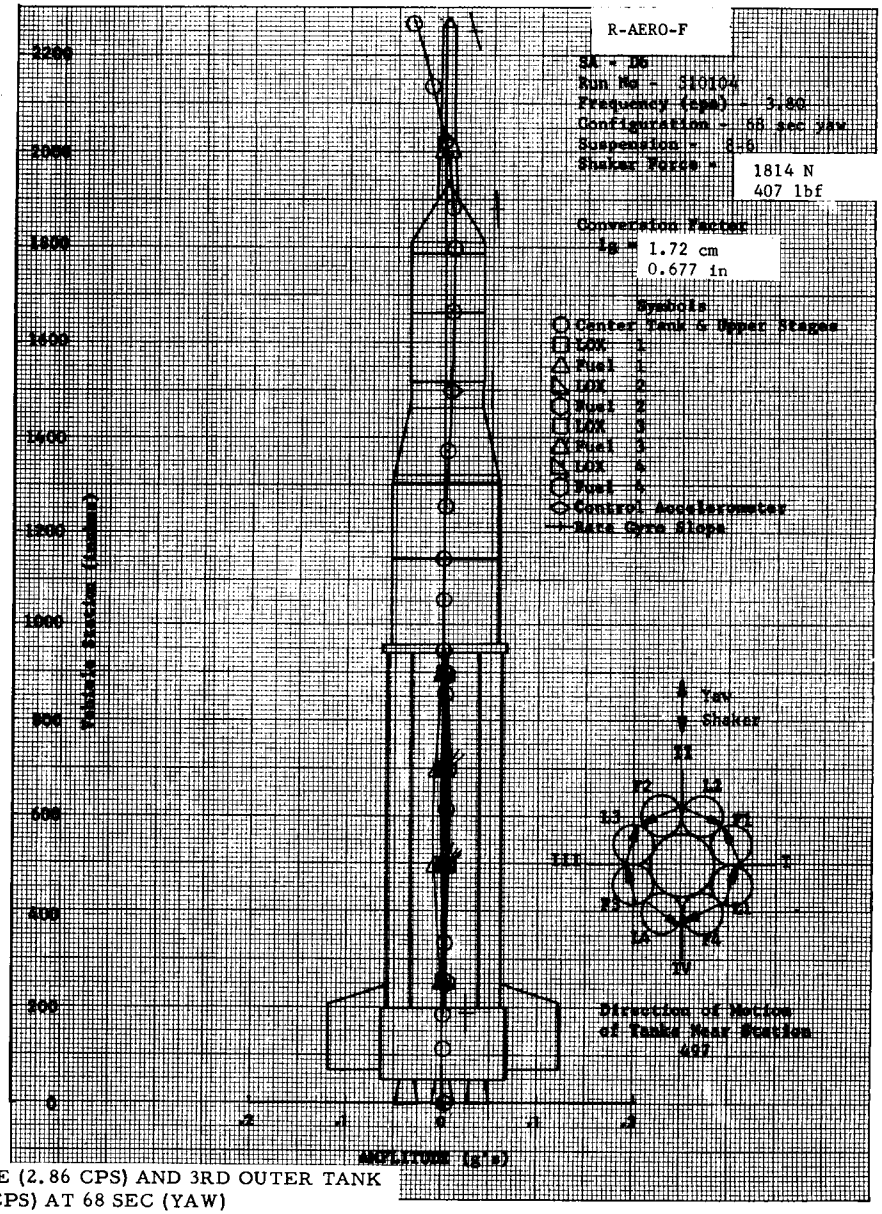


FIGURE 121 2ND OUTER TANK MODE (2.86 CPS) AND 3RD OUTER TANK MODE (3.80 CPS) AT 68 SEC (YAW)

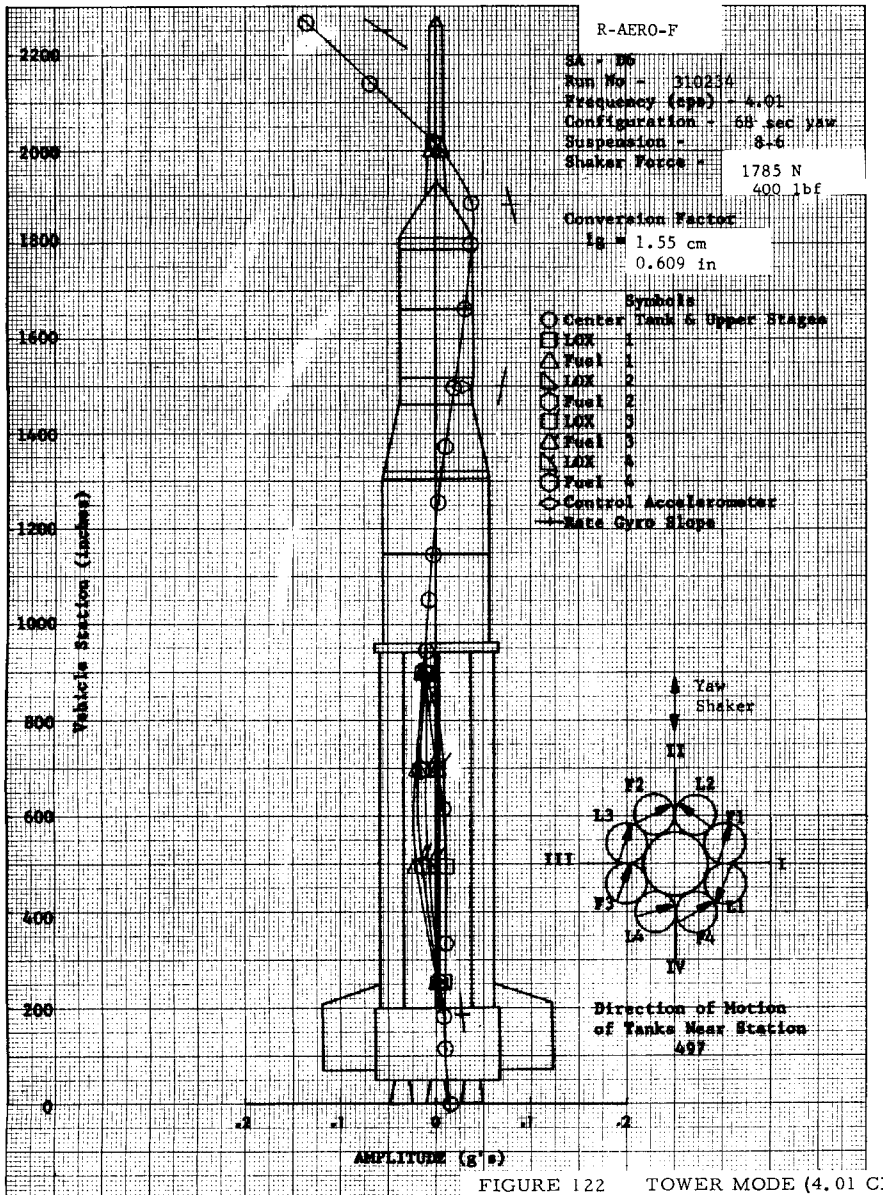


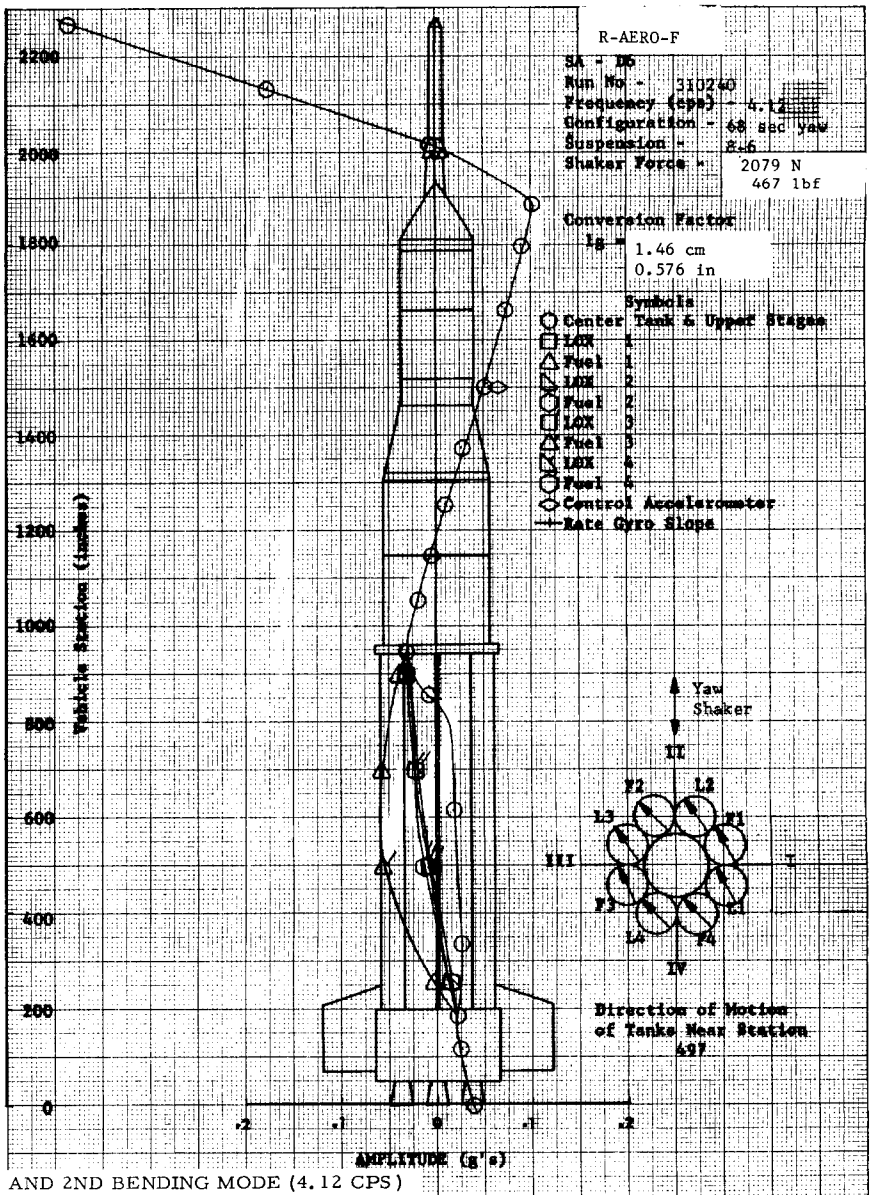


FIGURE 122 TOWER MODE (4.01 CPS) AND 2ND BENDING MODE (4.12 CPS) AT 68 SEC (YAW)

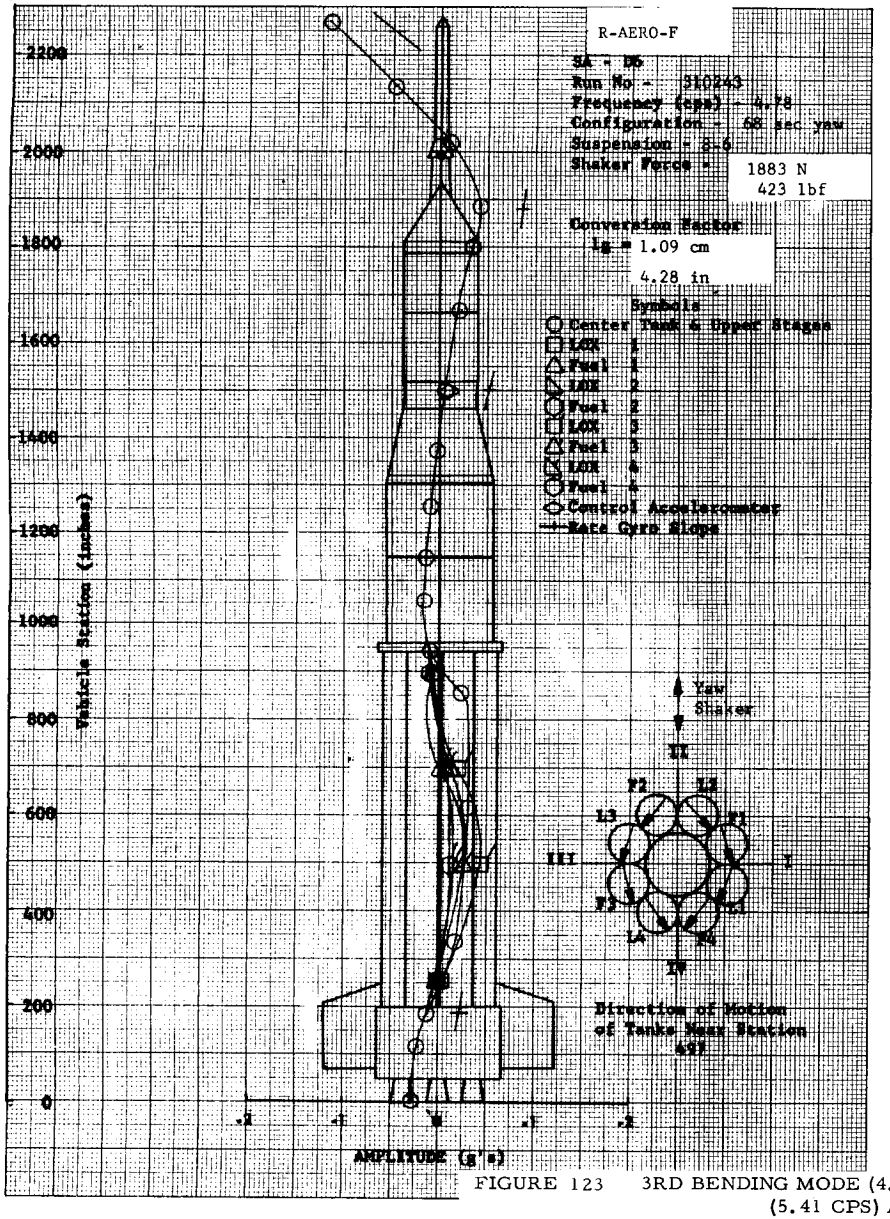


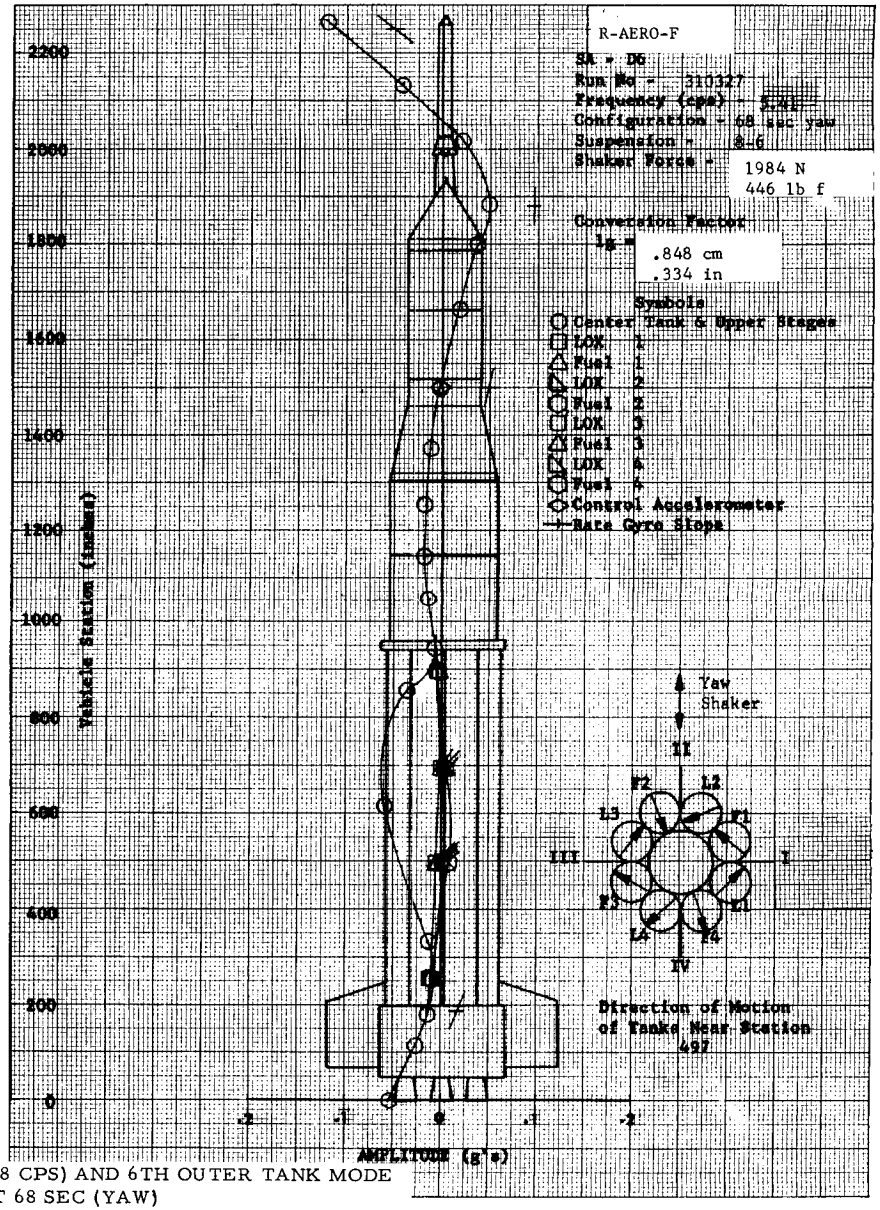


FIGURE 123 3RD BENDING MODE (4.78 CPS) AND 6TH OUTER TANK MODE (5.41 CPS) AT 68 SEC (YAW)

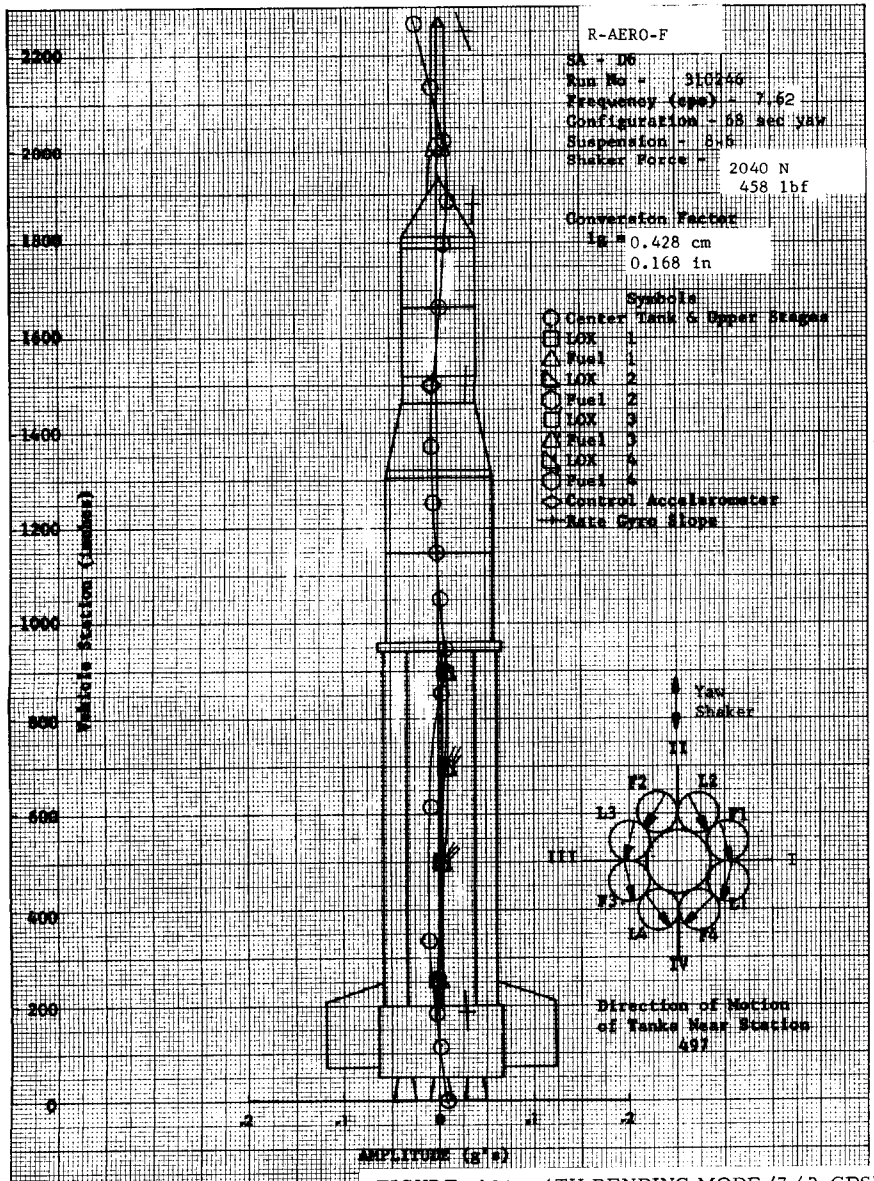


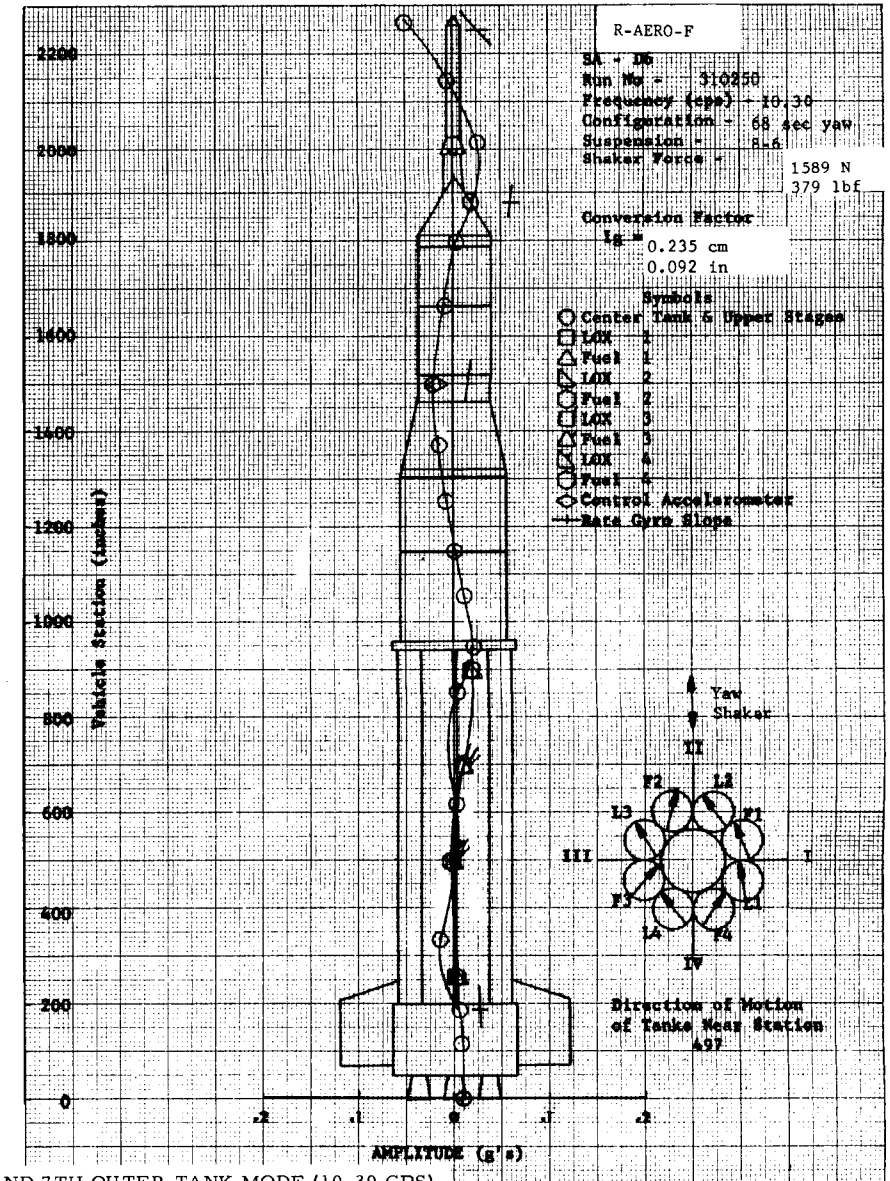


FIGURE 124 4TH BENDING MODE (7.62 CPS) AND 7TH OUTER TANK MODE (10.30 CPS) AT 68 SEC (YAW)

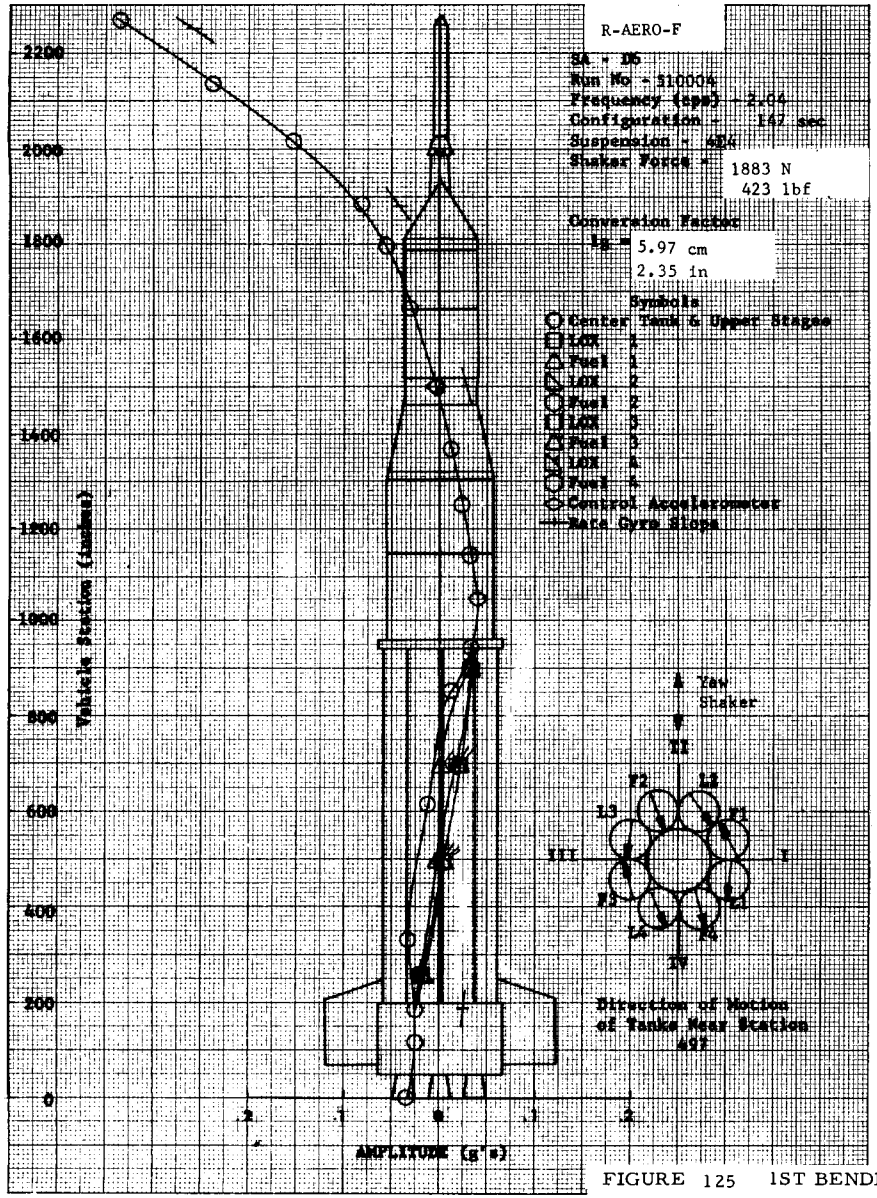


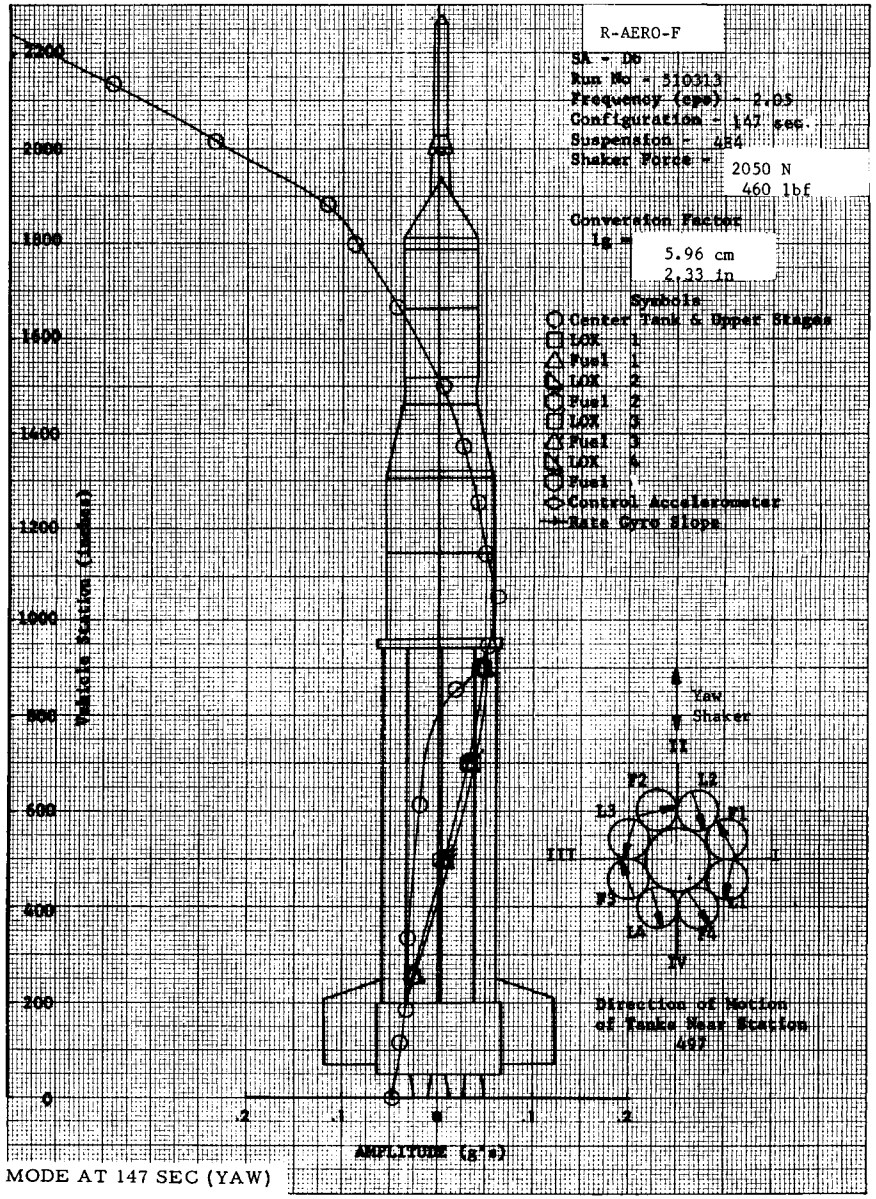


FIGURE 125 1ST BENDING MODE AT 147 SEC (YAW)

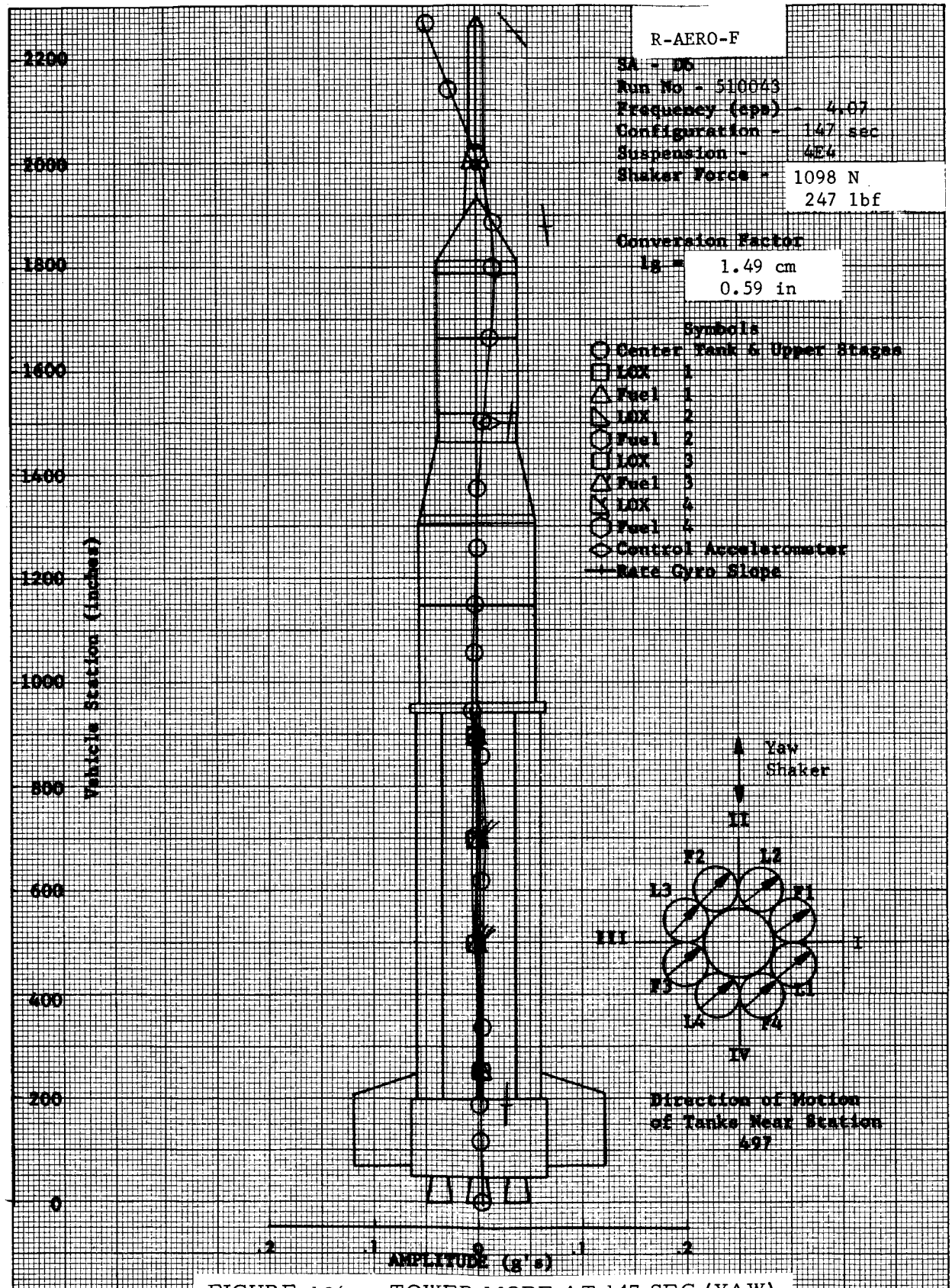


FIGURE 126 TOWER MODE AT 147 SEC (YAW)

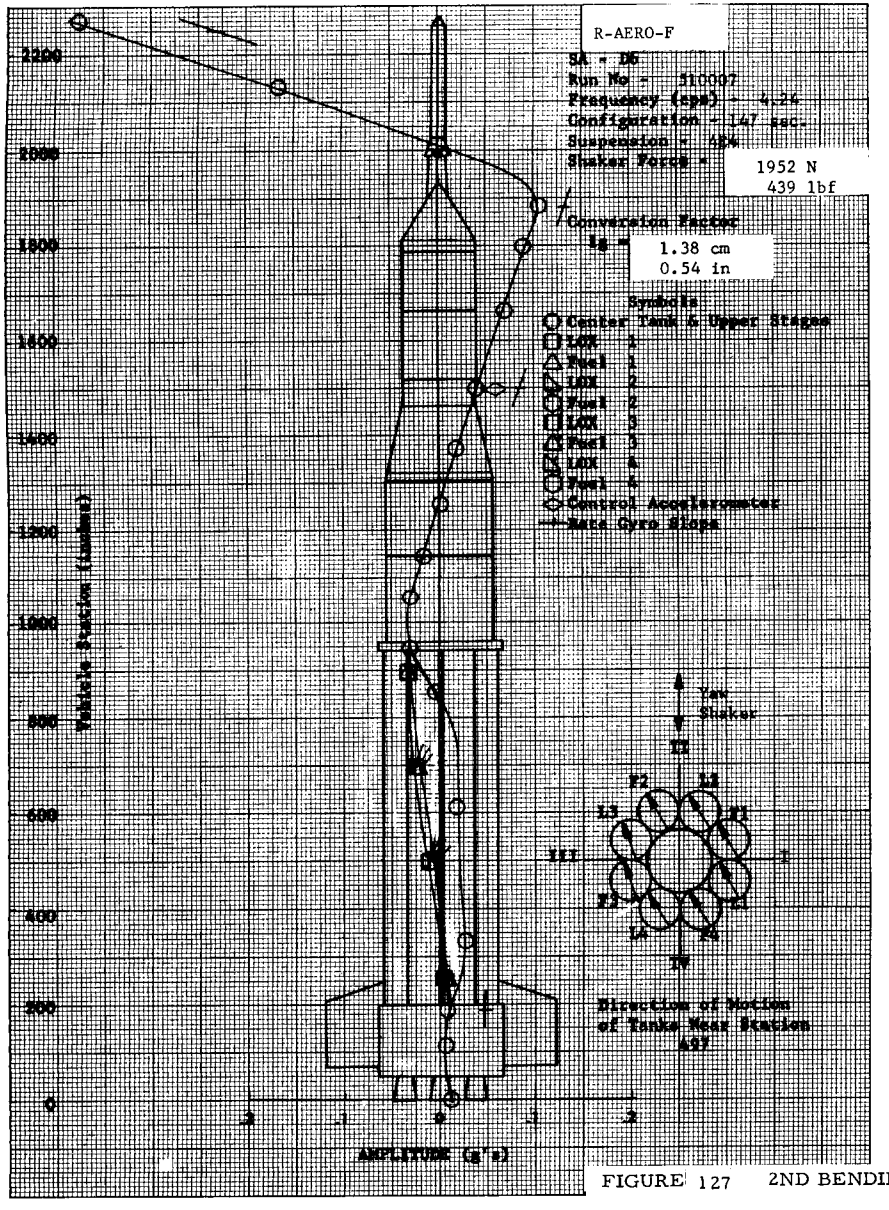


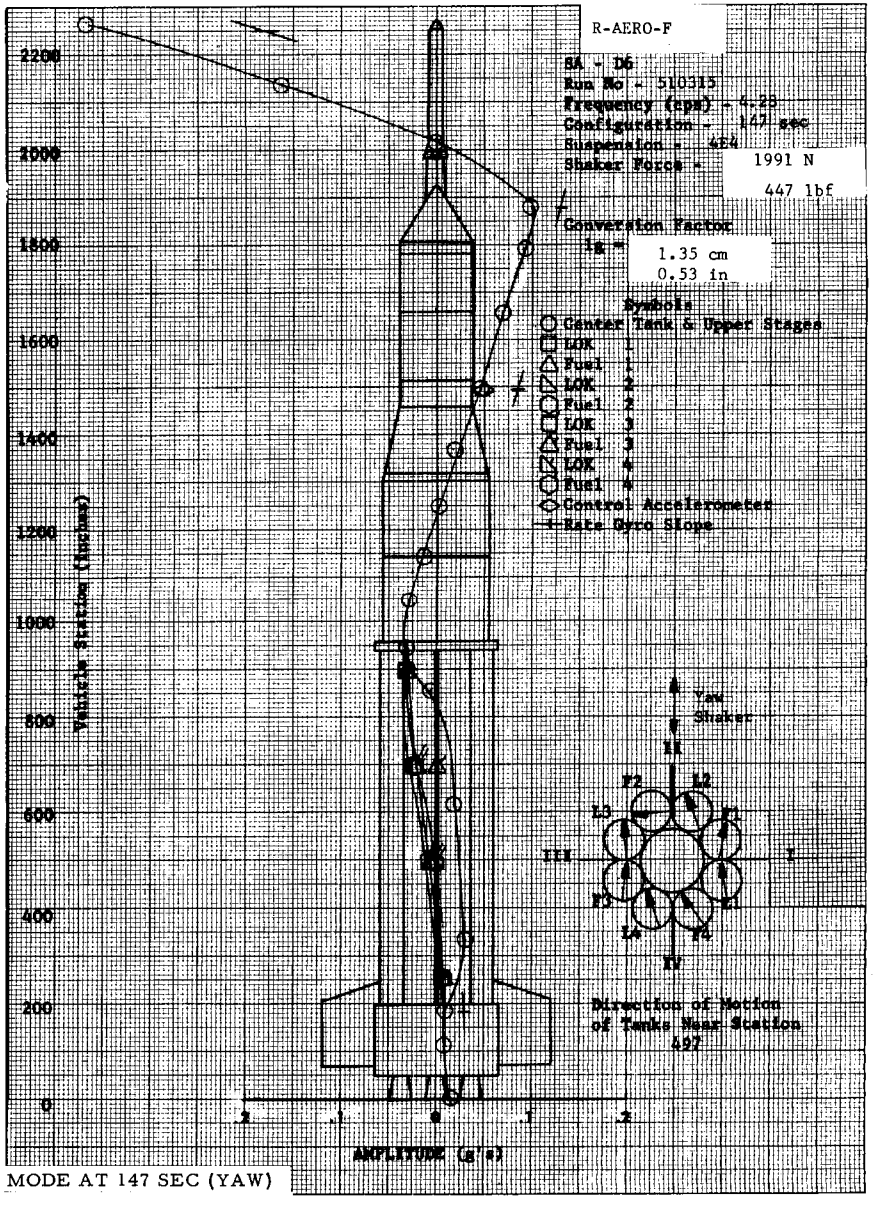


FIGURE 127 2ND BENDING MODE AT 147 SEC (YAW)

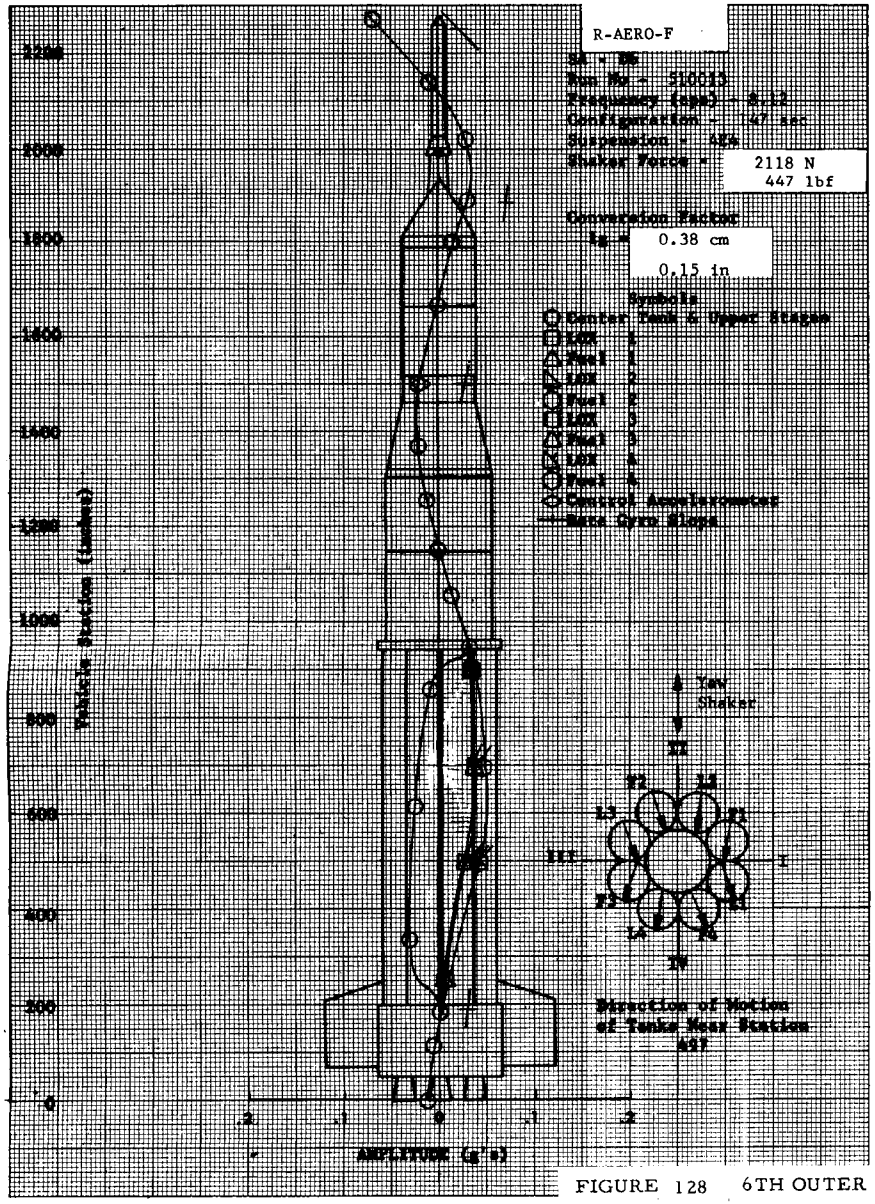


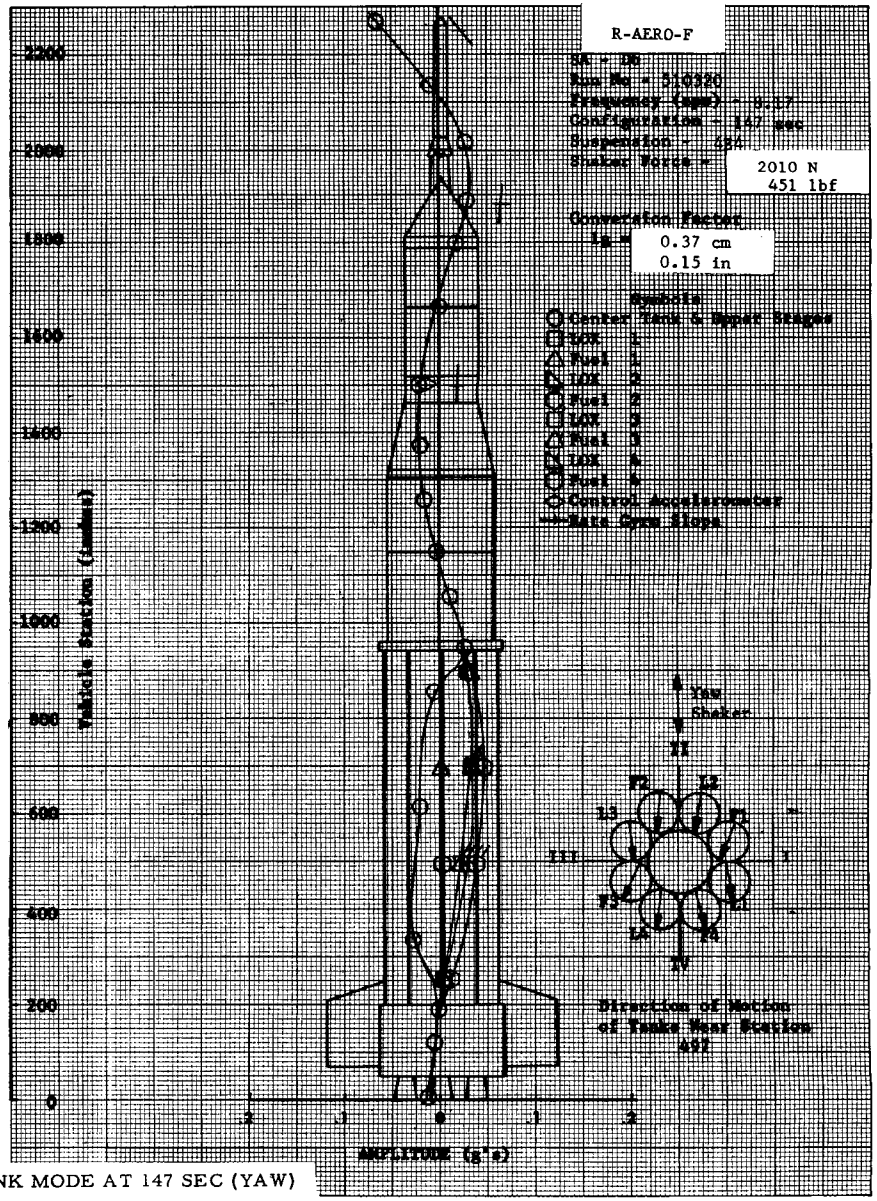


FIGURE 128 6TH OUTER TANK MODE AT 147 SEC (YAW)

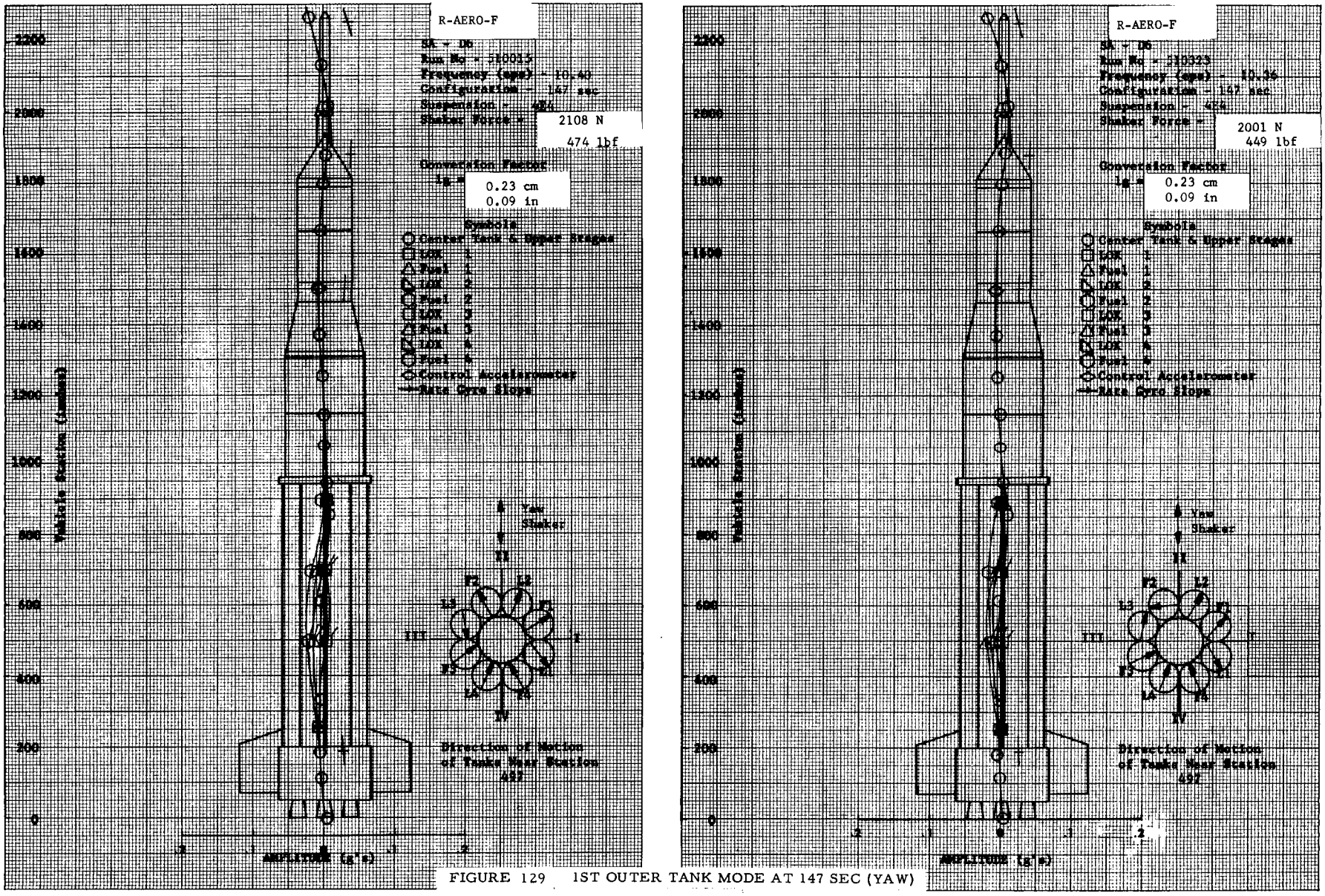


FIGURE 129 1ST OUTER TANK MODE AT 147 SEC (YAW)

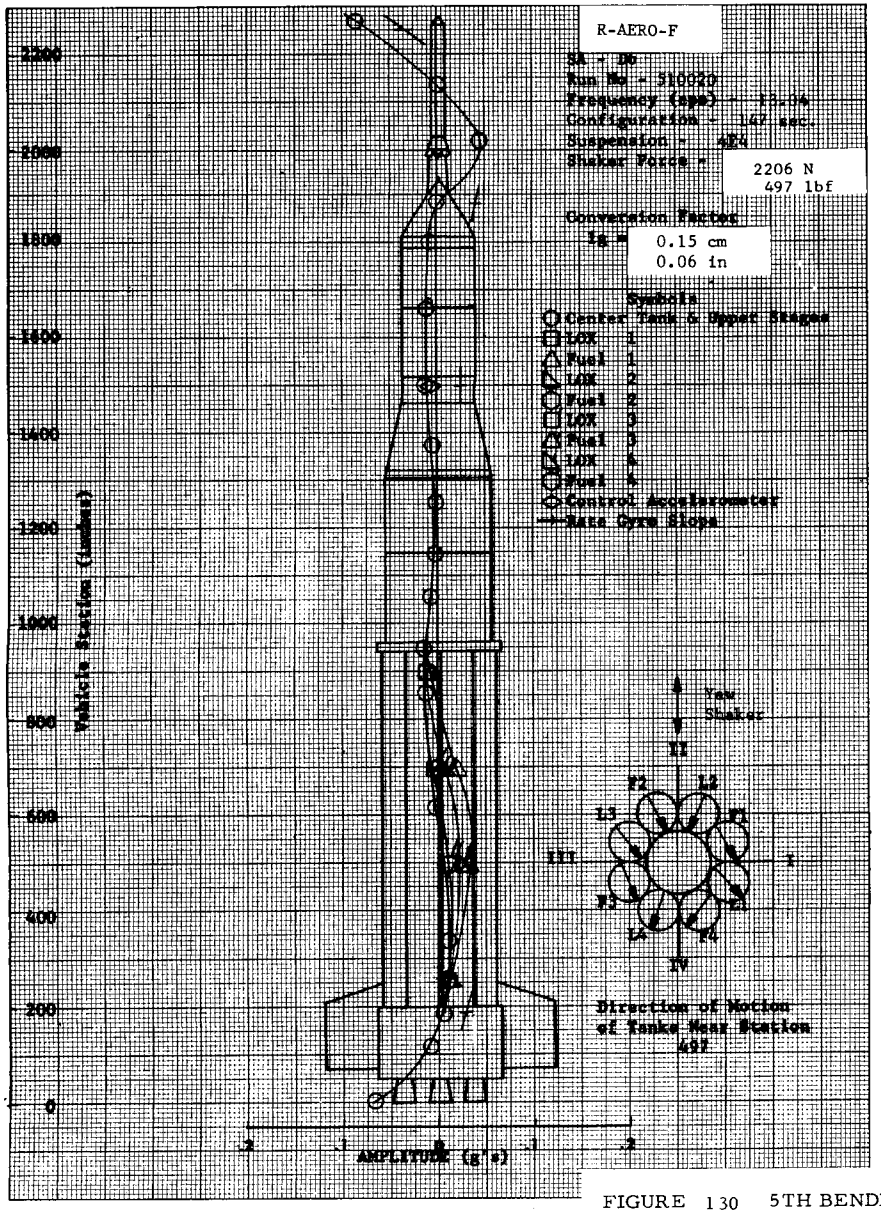


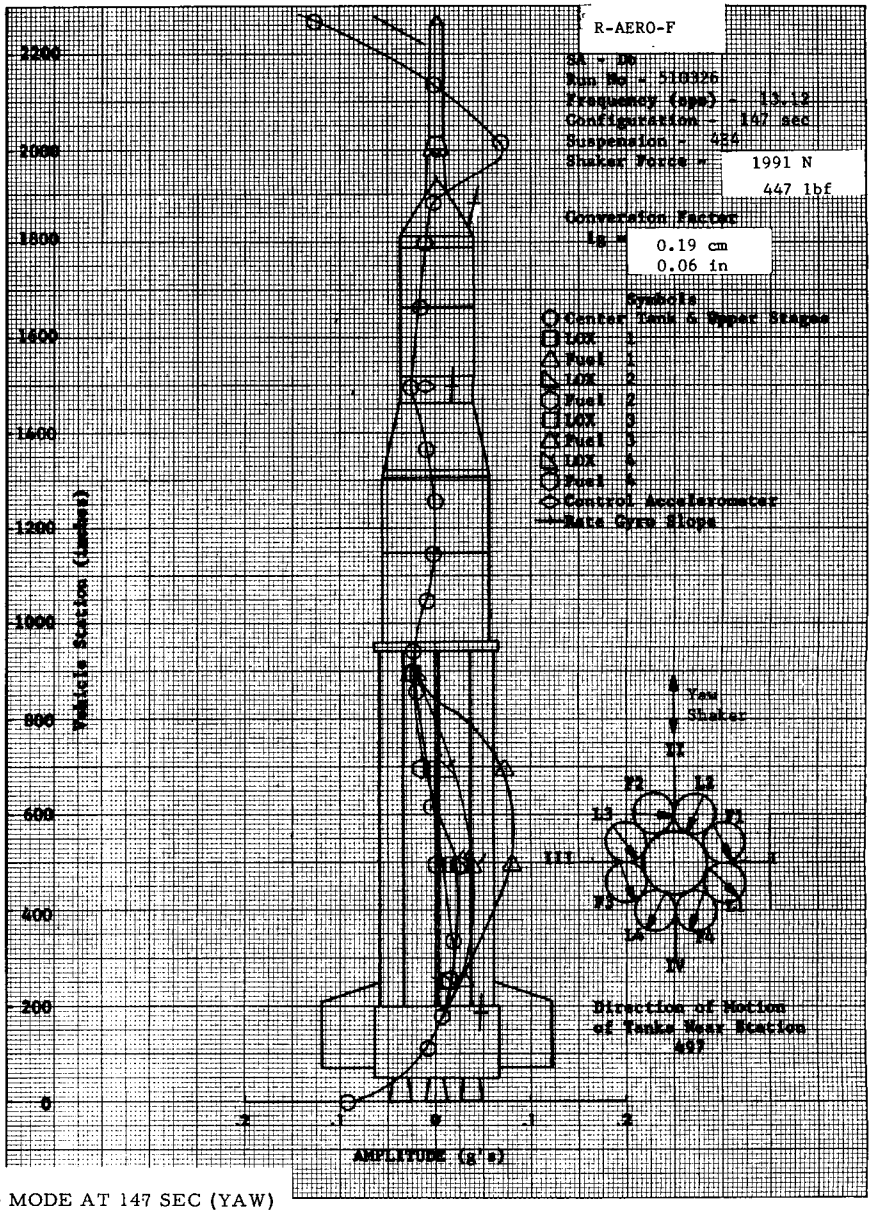


FIGURE 130 5TH BENDING MODE AT 147 SEC (YAW)

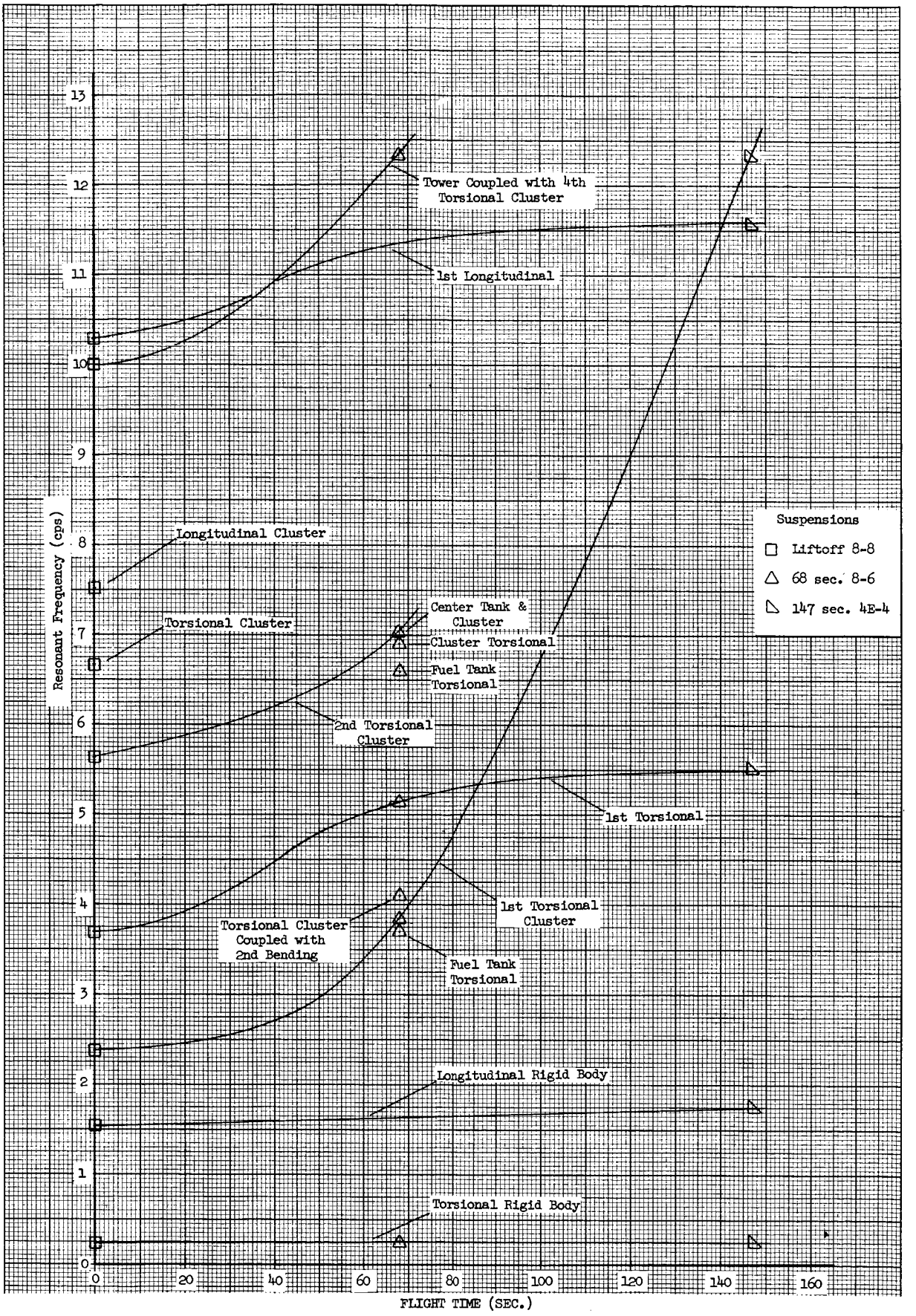


FIGURE 131 RESONANT FREQUENCY PROFILE DURING BOOST (TORSIONAL AND LONGITUDINAL EXCITATION)

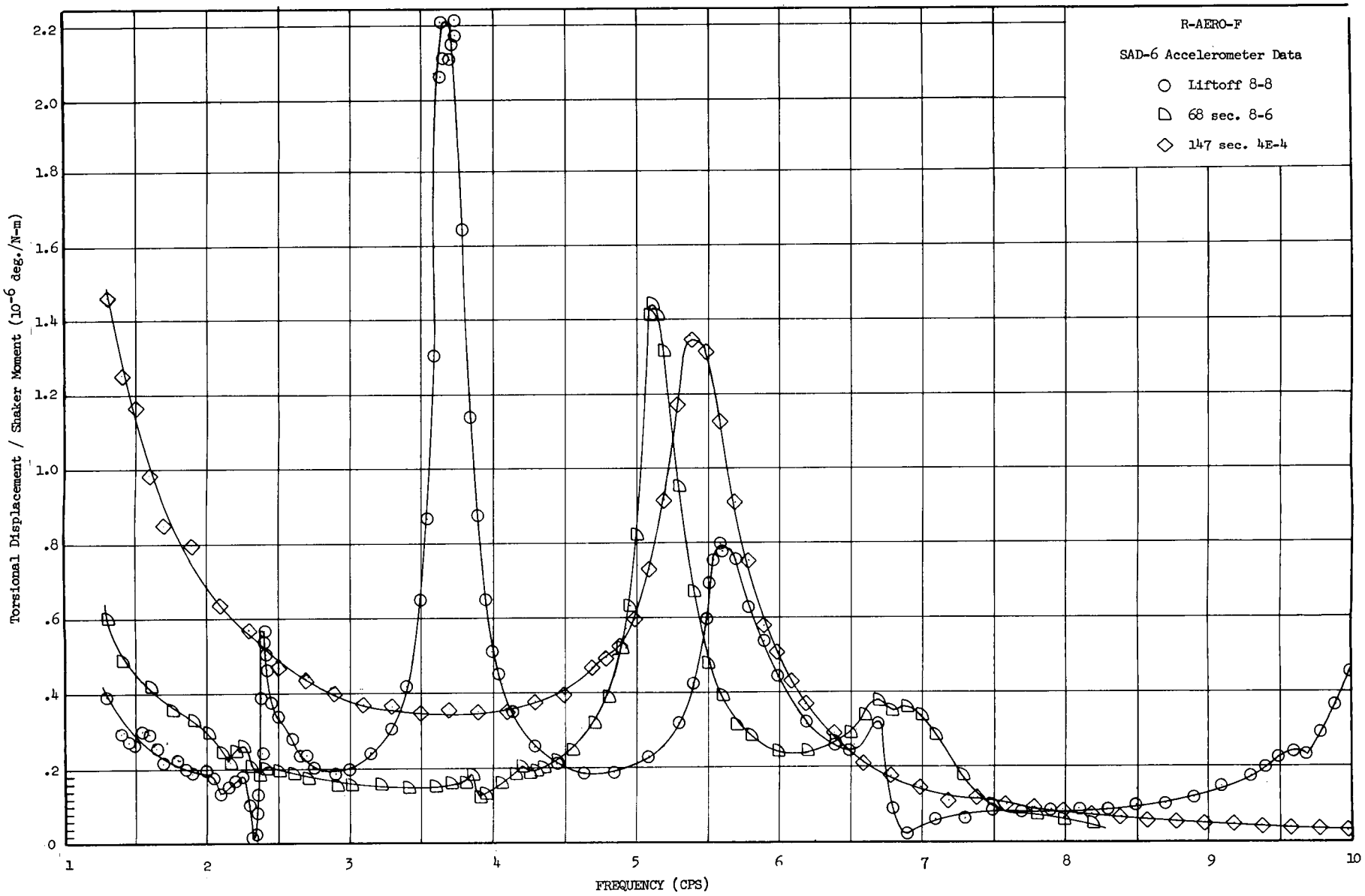


FIGURE 132 TORSIONAL RESPONSE AT COMMAND MODULE (STA. 1800)
(TORSIONAL EXCITATION)

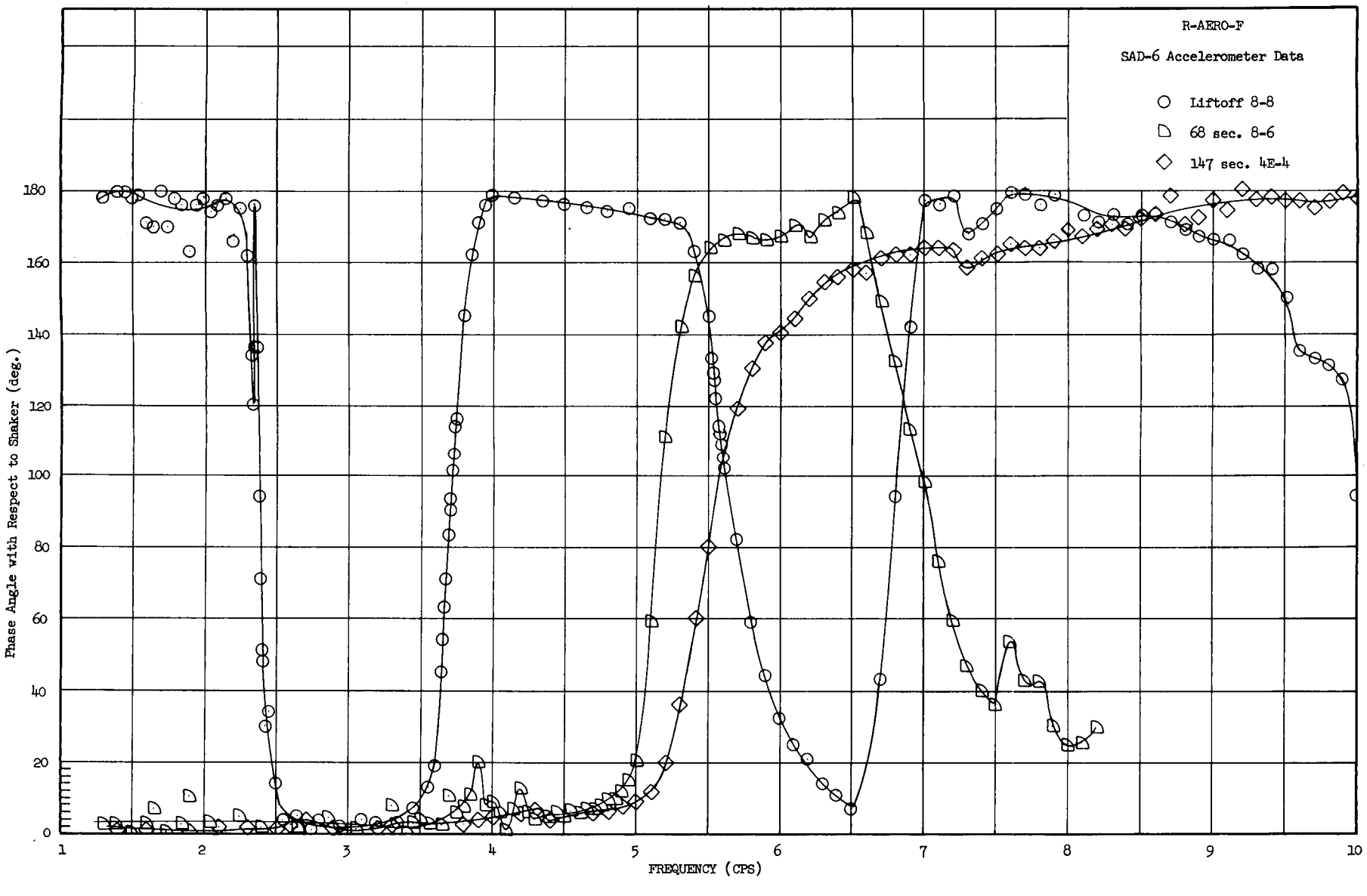


FIGURE 133 PHASE ANGLE AT COMMAND MODULE (STA. 1800)
(TORSIONAL EXCITATION)

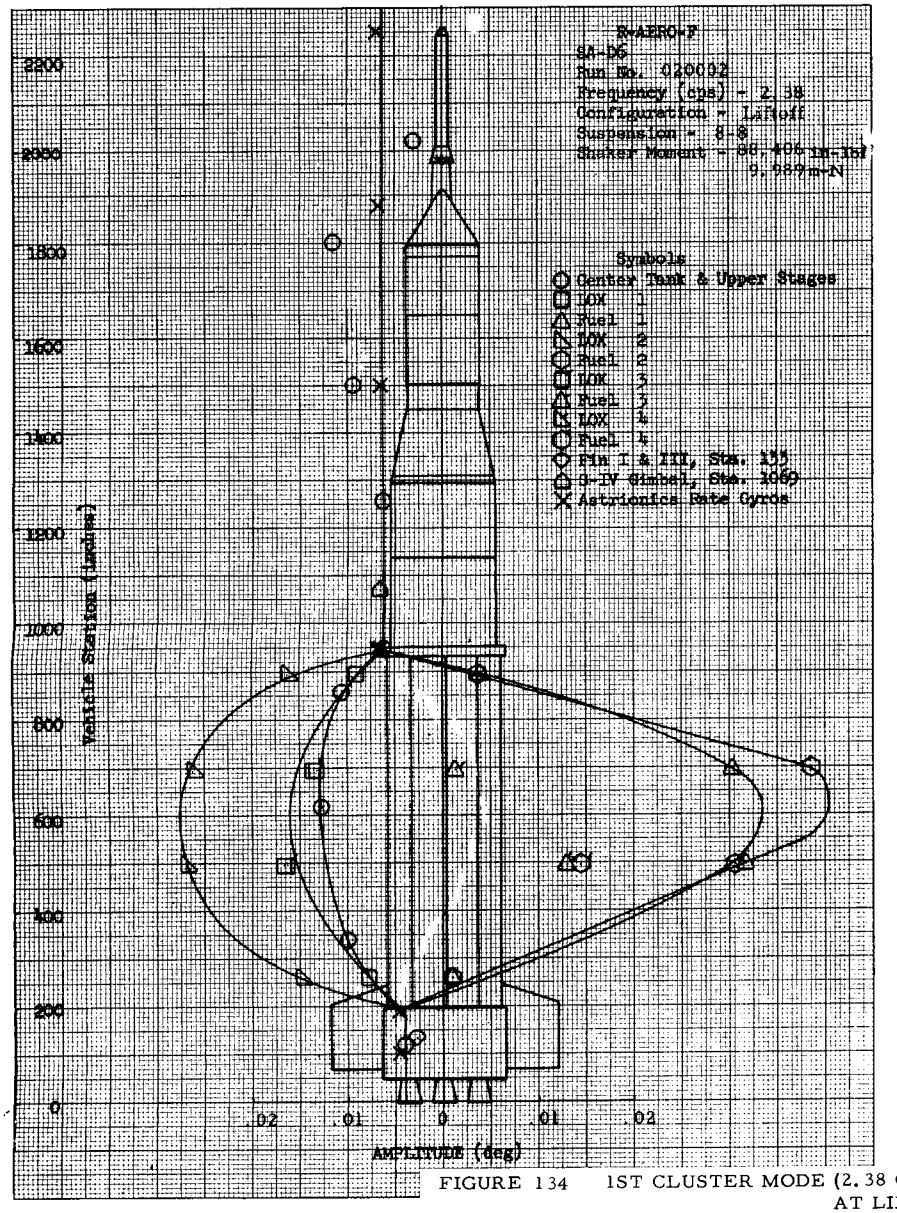


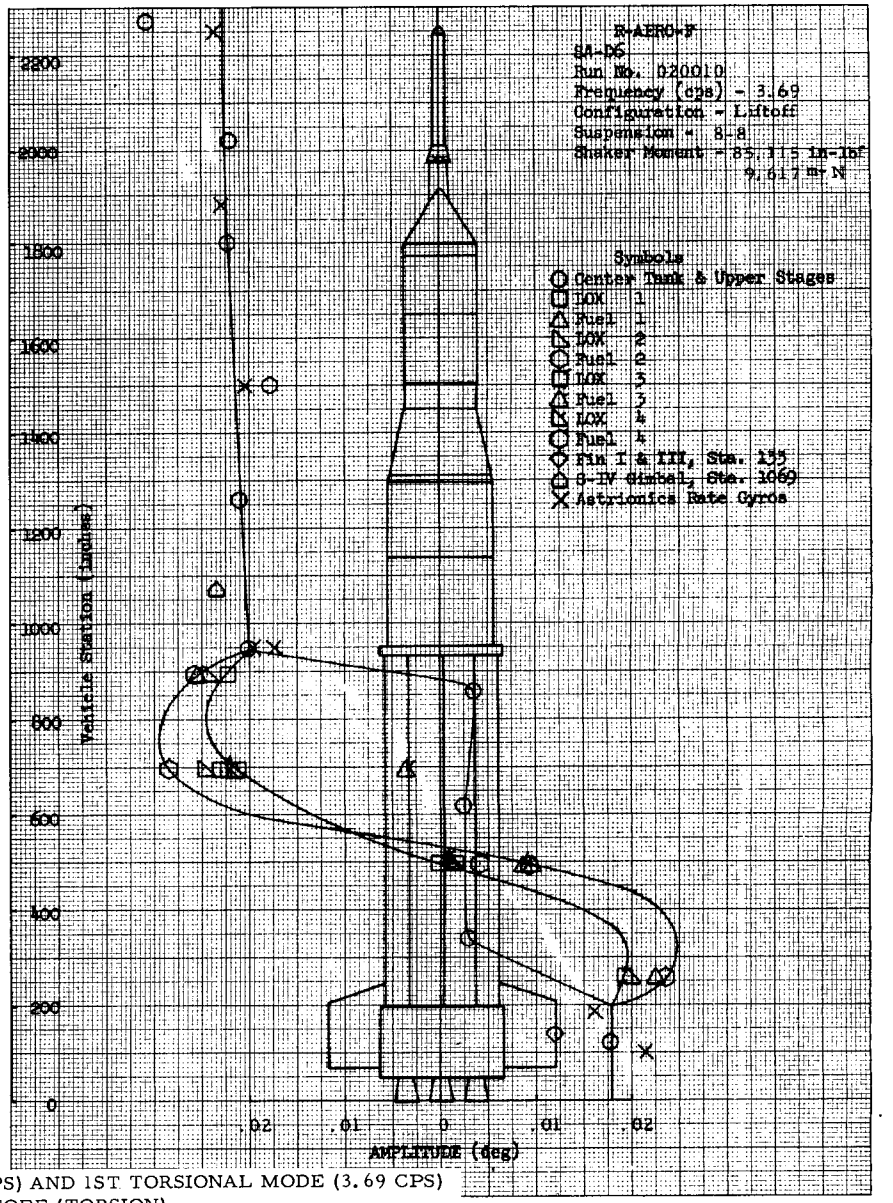


FIGURE 134 1ST CLUSTER MODE (2.38 CPS) AND 1ST TORSIONAL MODE (3.69 CPS) AT LIFTOFF (TORSION)

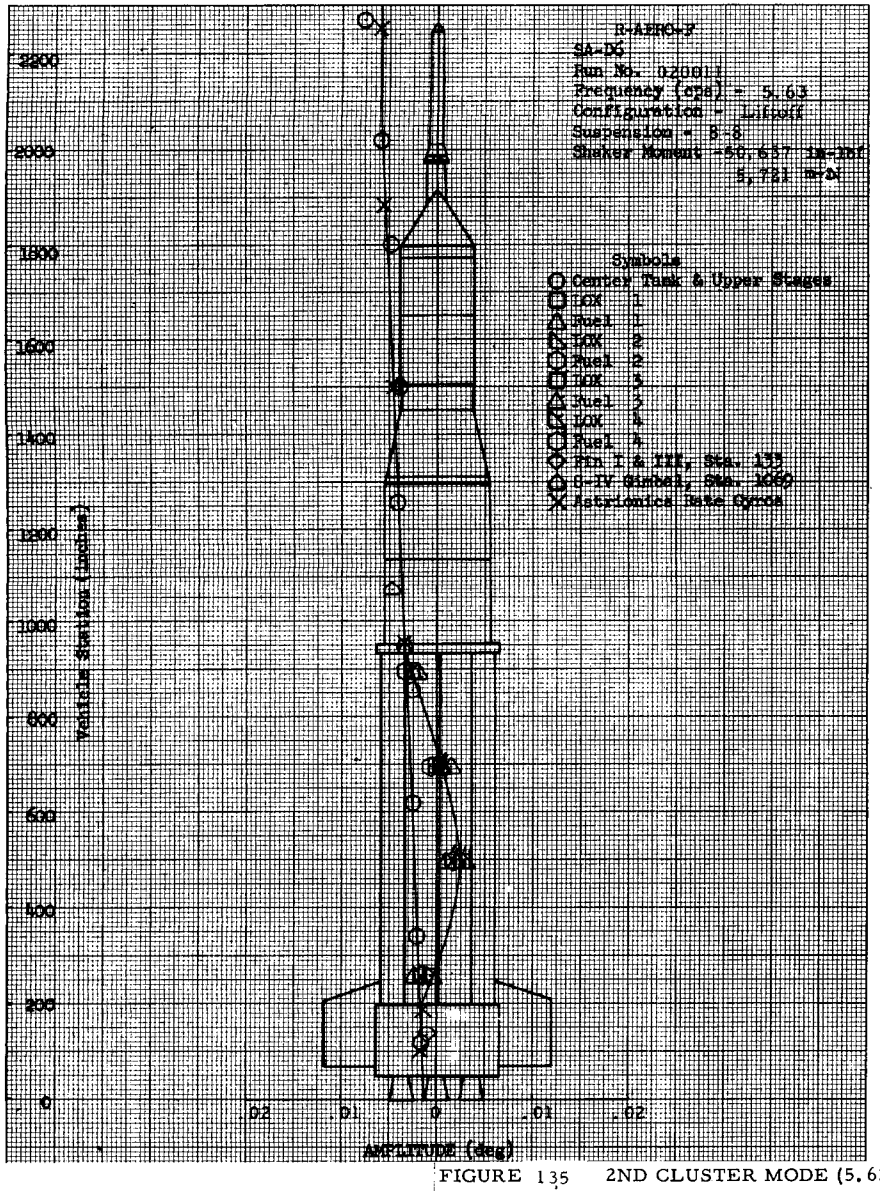


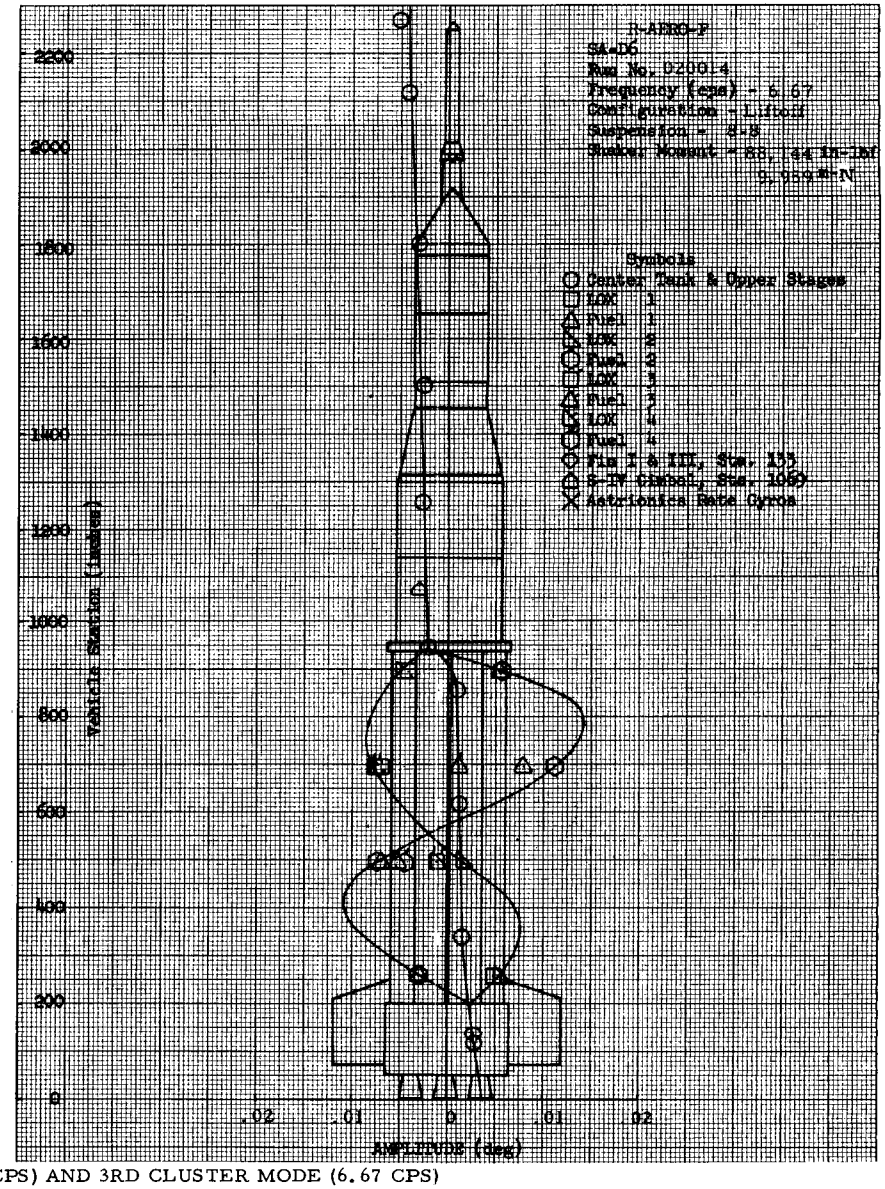


FIGURE 135 2ND CLUSTER MODE (5.63 CPS) AND 3RD CLUSTER MODE (6.67 CPS) AT LIFTOFF (TORSION)

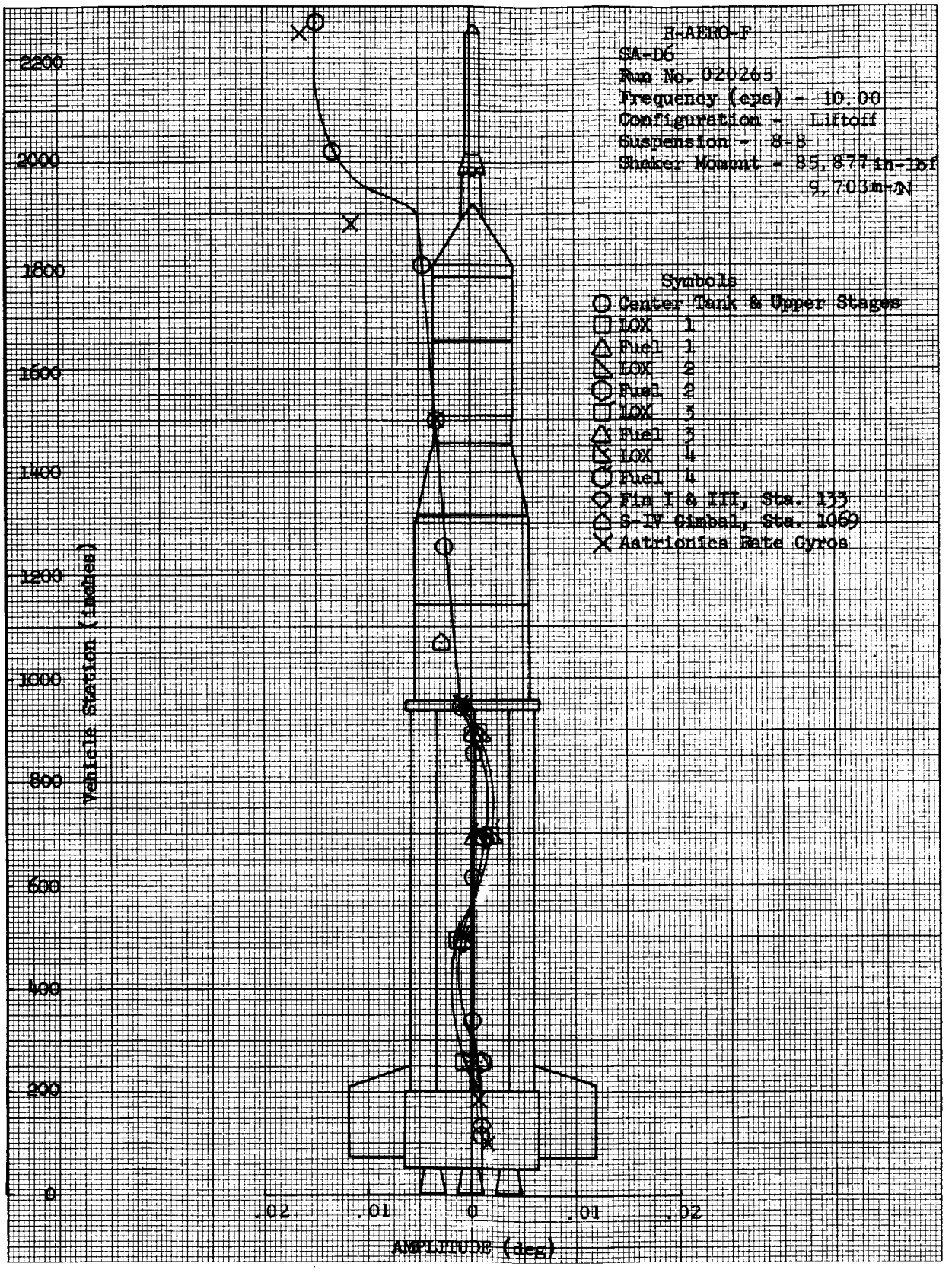


FIGURE 136 TOWER COUPLED WITH 4TH CLUSTER MODE (10.00 CPS) AT LIFTOFF (TORSION)

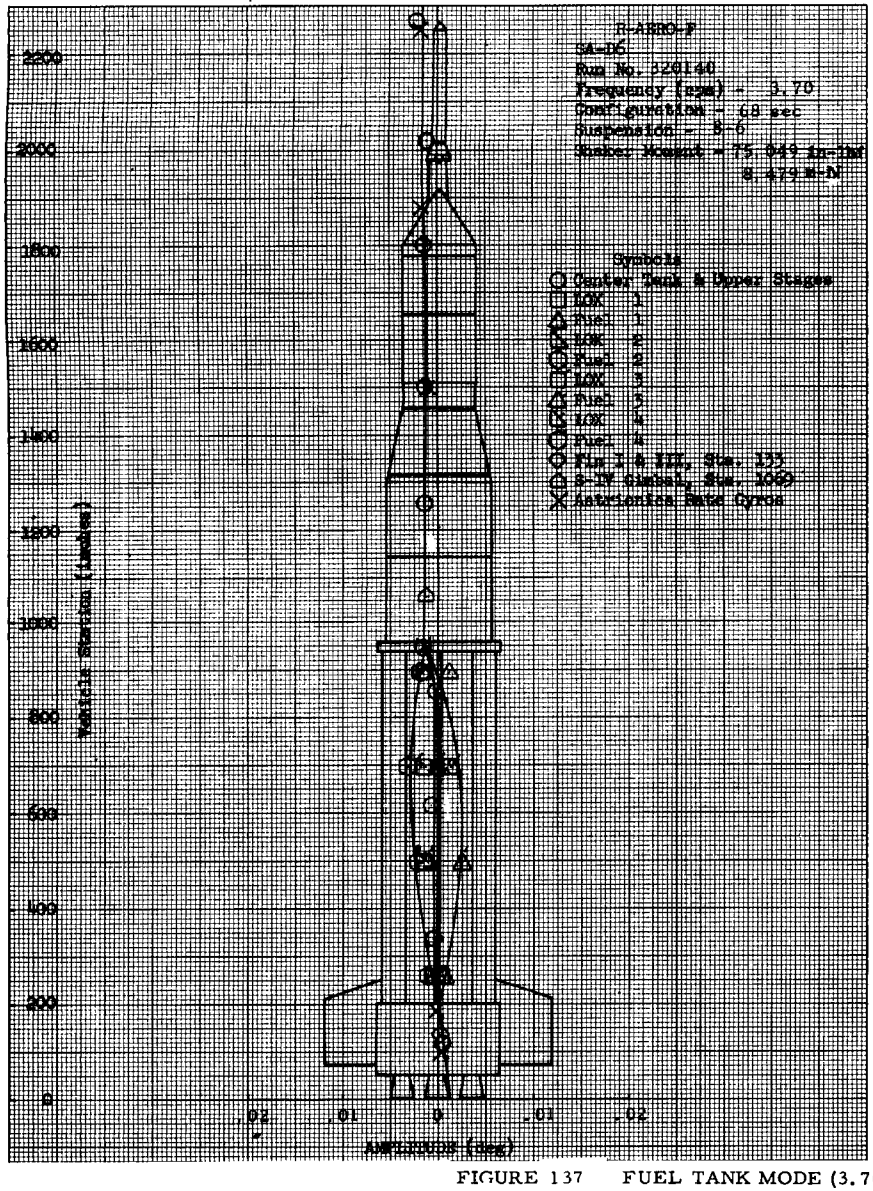


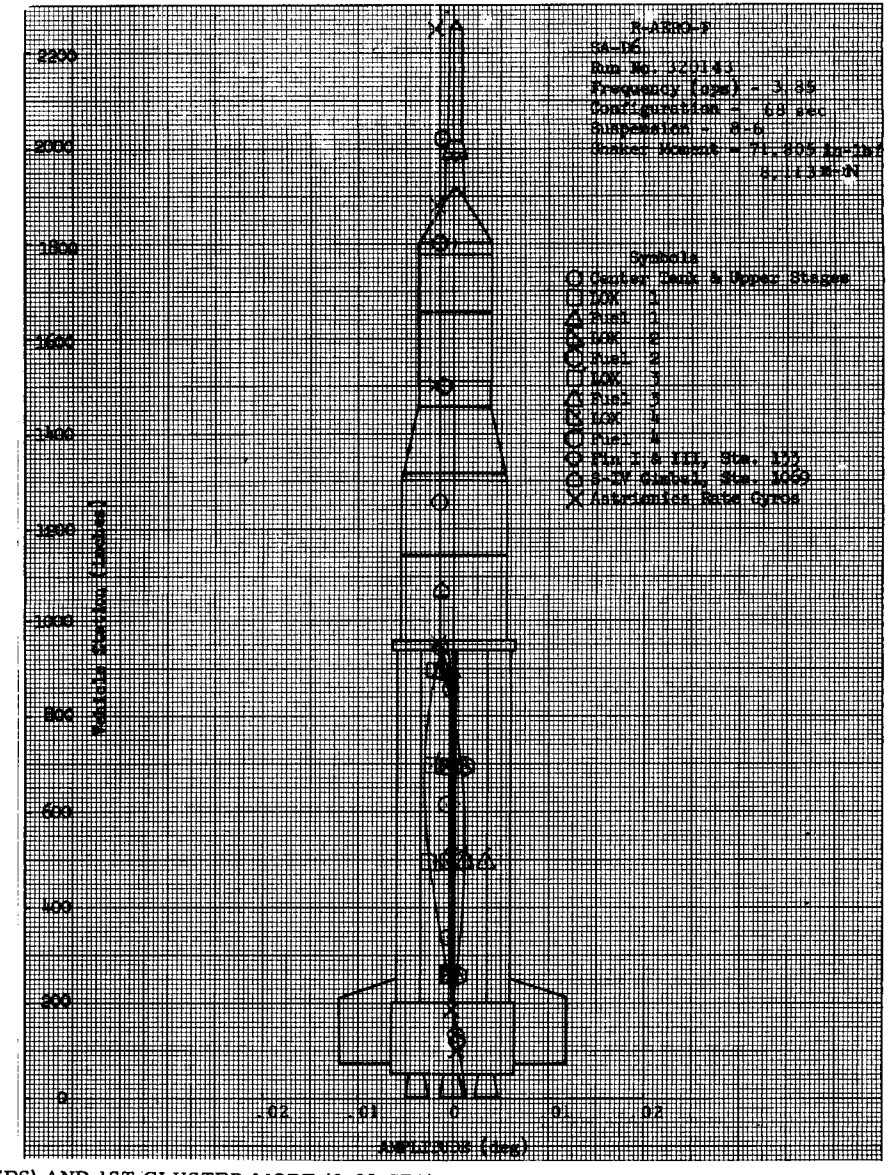


FIGURE 137 FUEL TANK MODE (3.70 CPS) AND 1ST CLUSTER MODE (3.85 CPS) AT 68 SEC (TORSION)

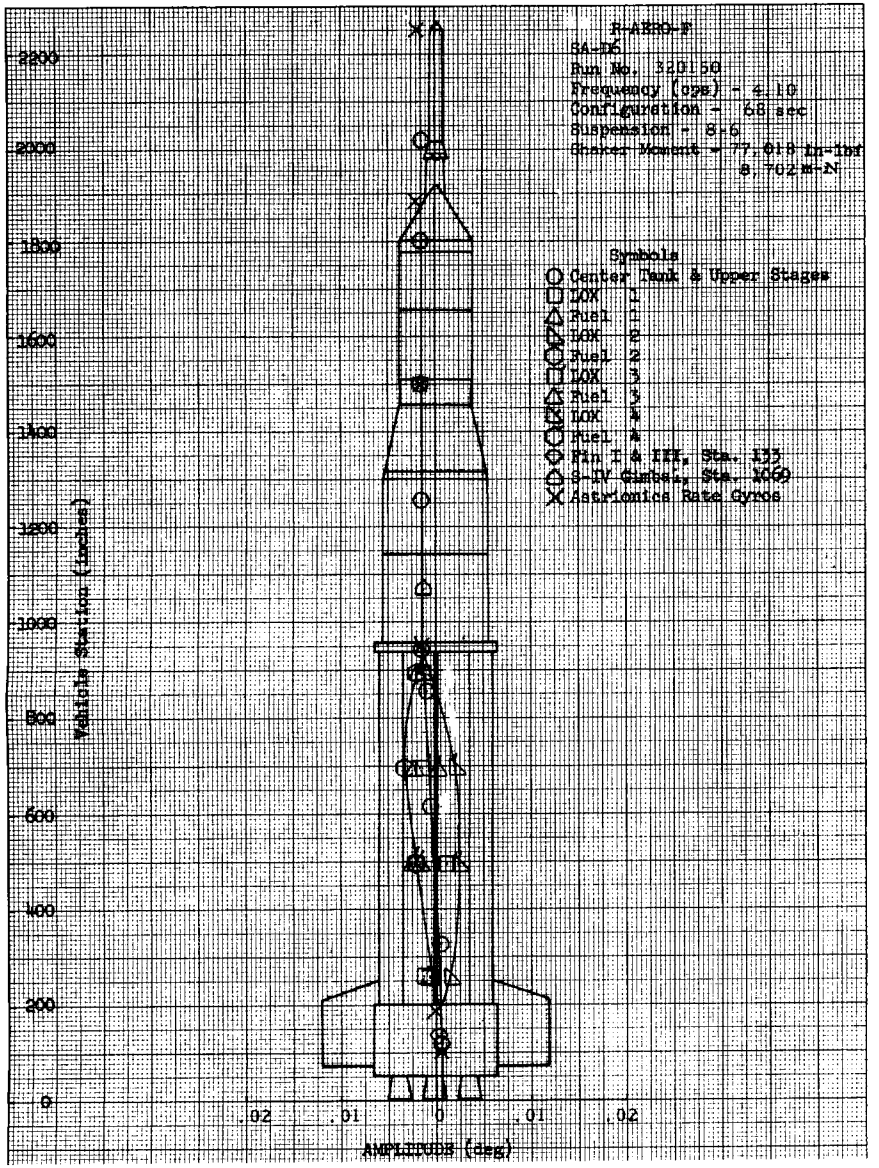


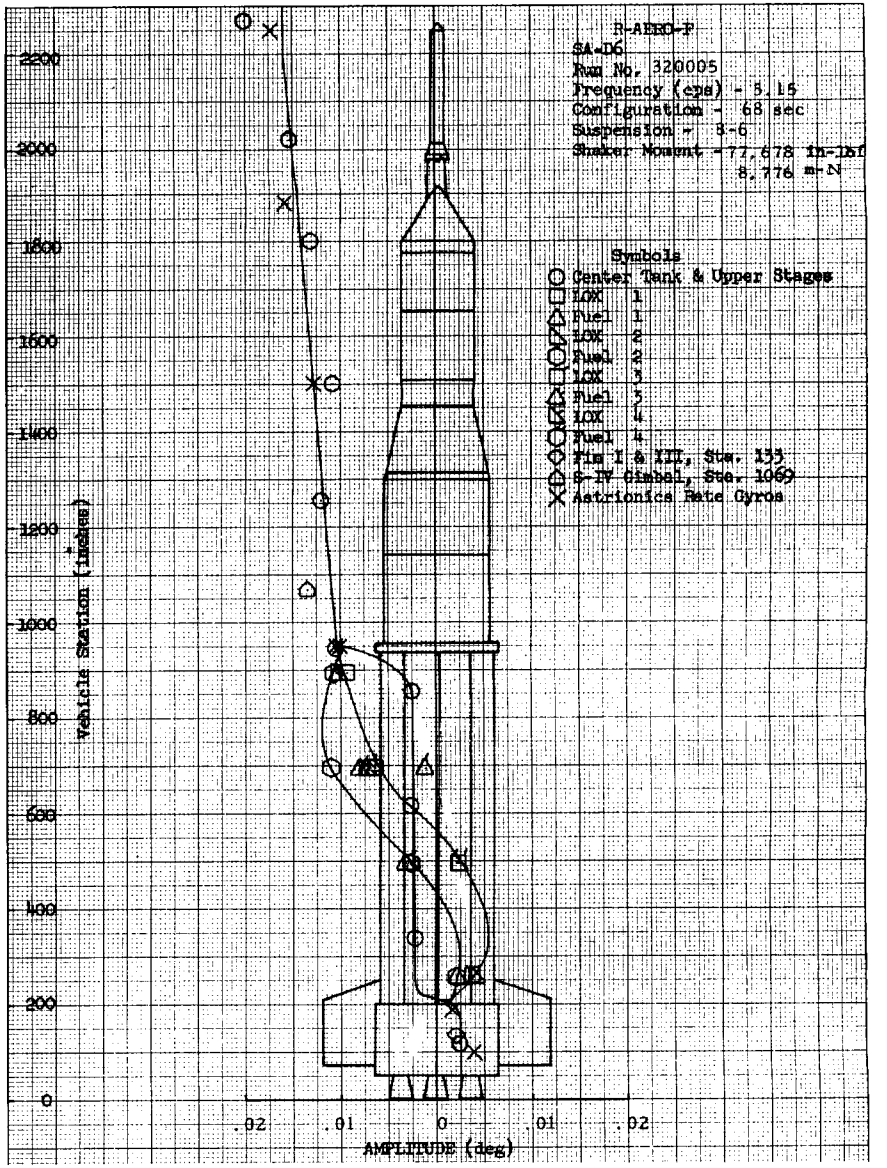


FIGURE 138 CLUSTER MODE COUPLED WITH 2ND BENDING (4.10 CPS) AND 1ST TORSIONAL MODE (5.15 CPS) AT 68 SEC (TORSION)

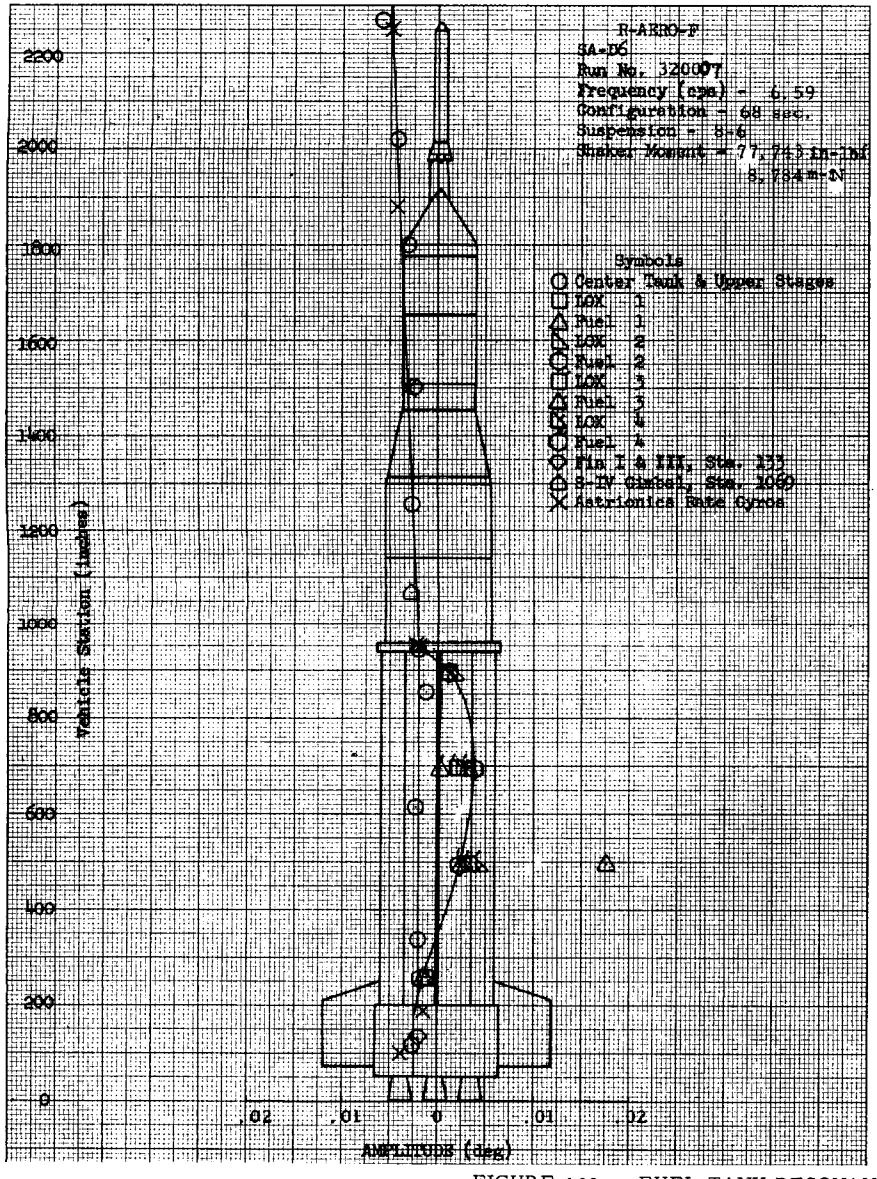


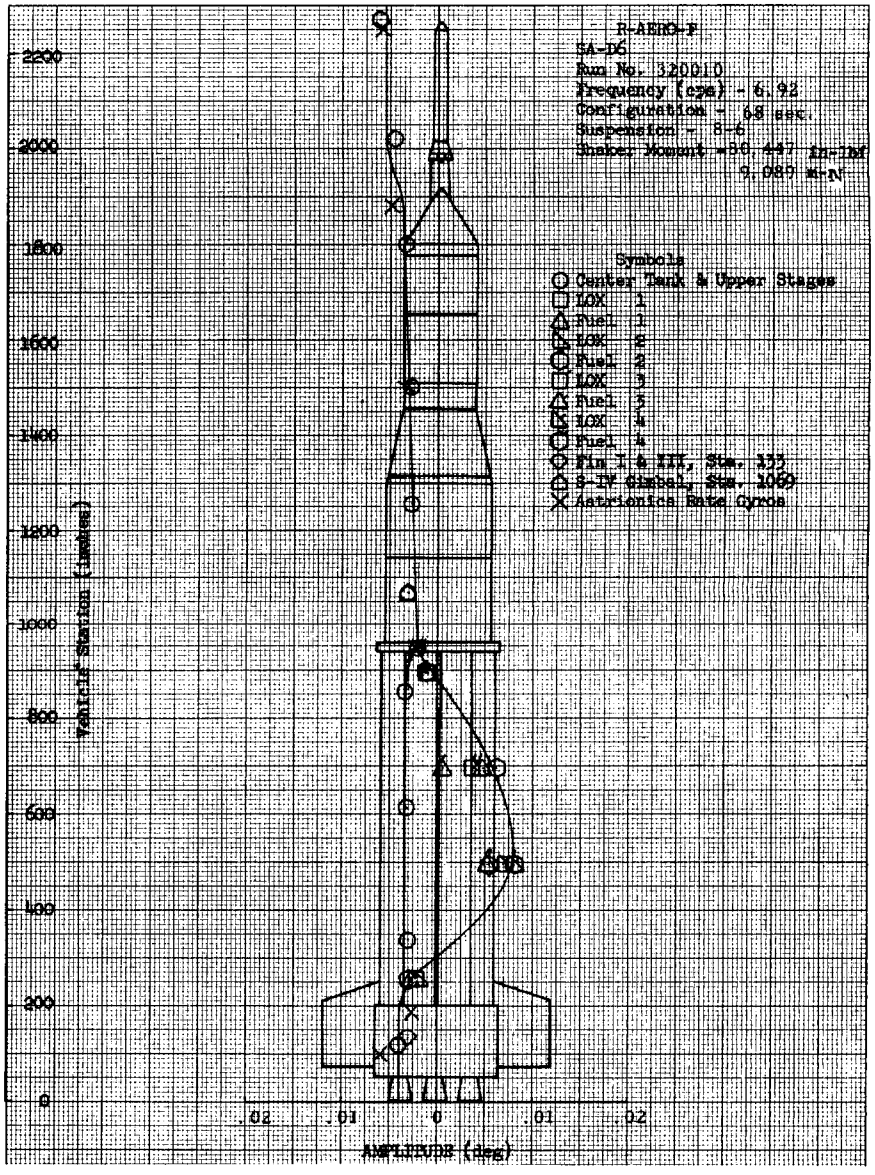


FIGURE 139 FUEL TANK RESONANCE (6.59 CPS) AND CLUSTER RESONANCE (6.92 CPS) FOR 2ND CLUSTER MODE AT 68 SEC (TORSION)

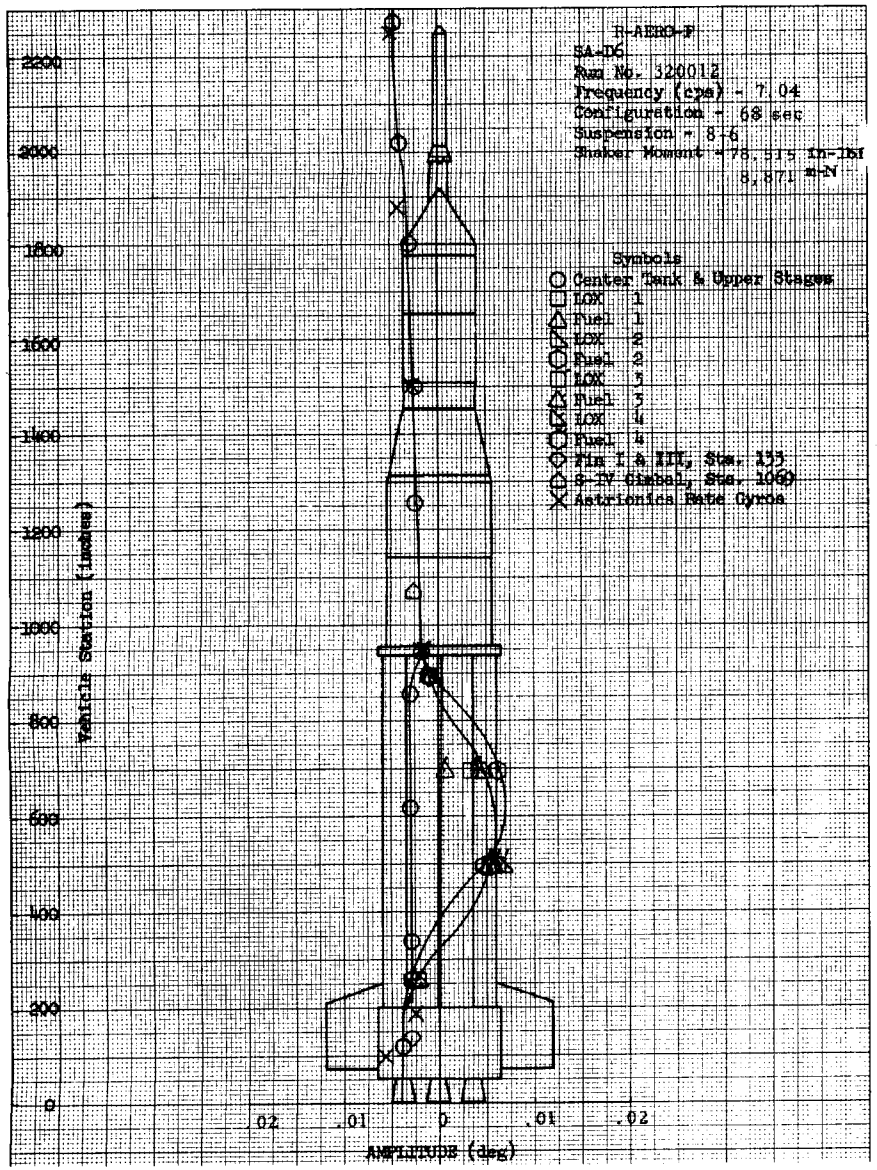


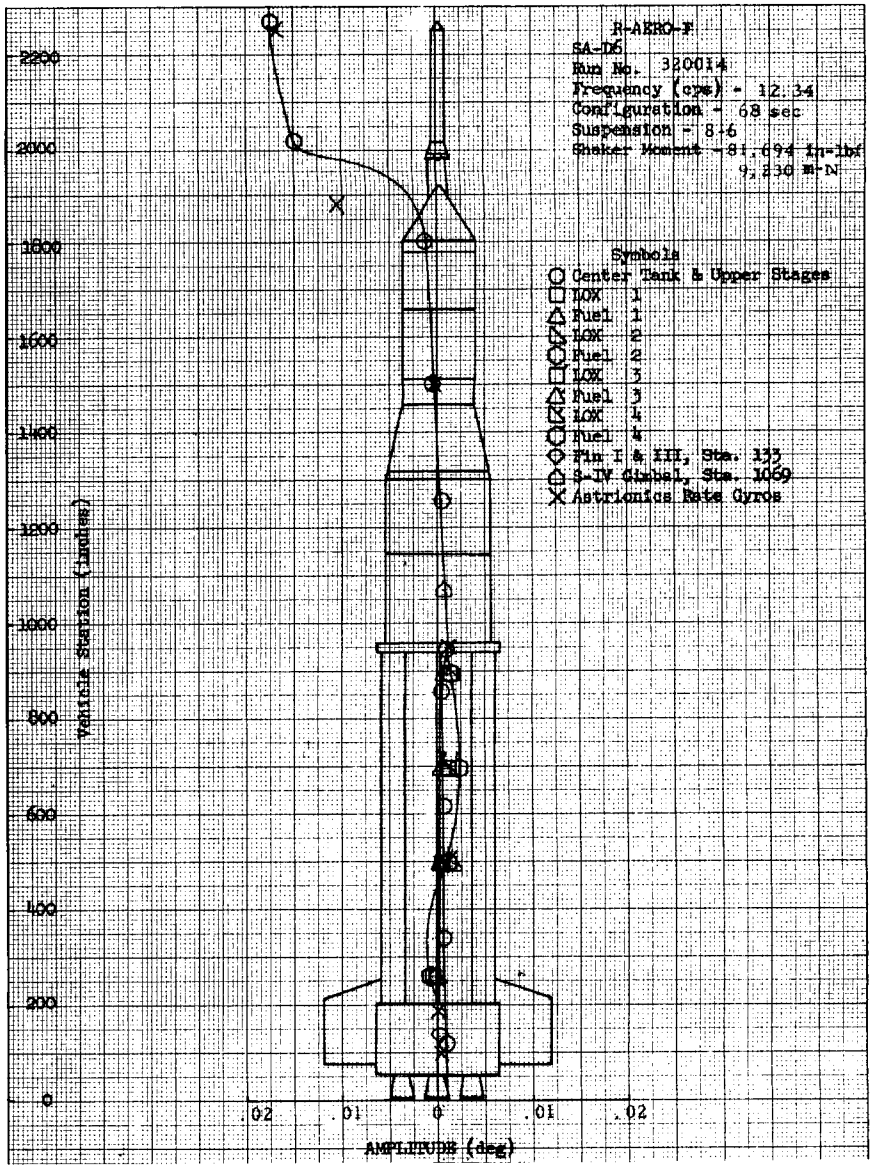


FIGURE 140 CENTER TANK RESONANCE (7.04 CPS) FOR 2ND CLUSTER MODE AND TOWER COUPLED WITH 4TH CLUSTER MODE (12.34 CPS) AT 68 SEC (TORSION)

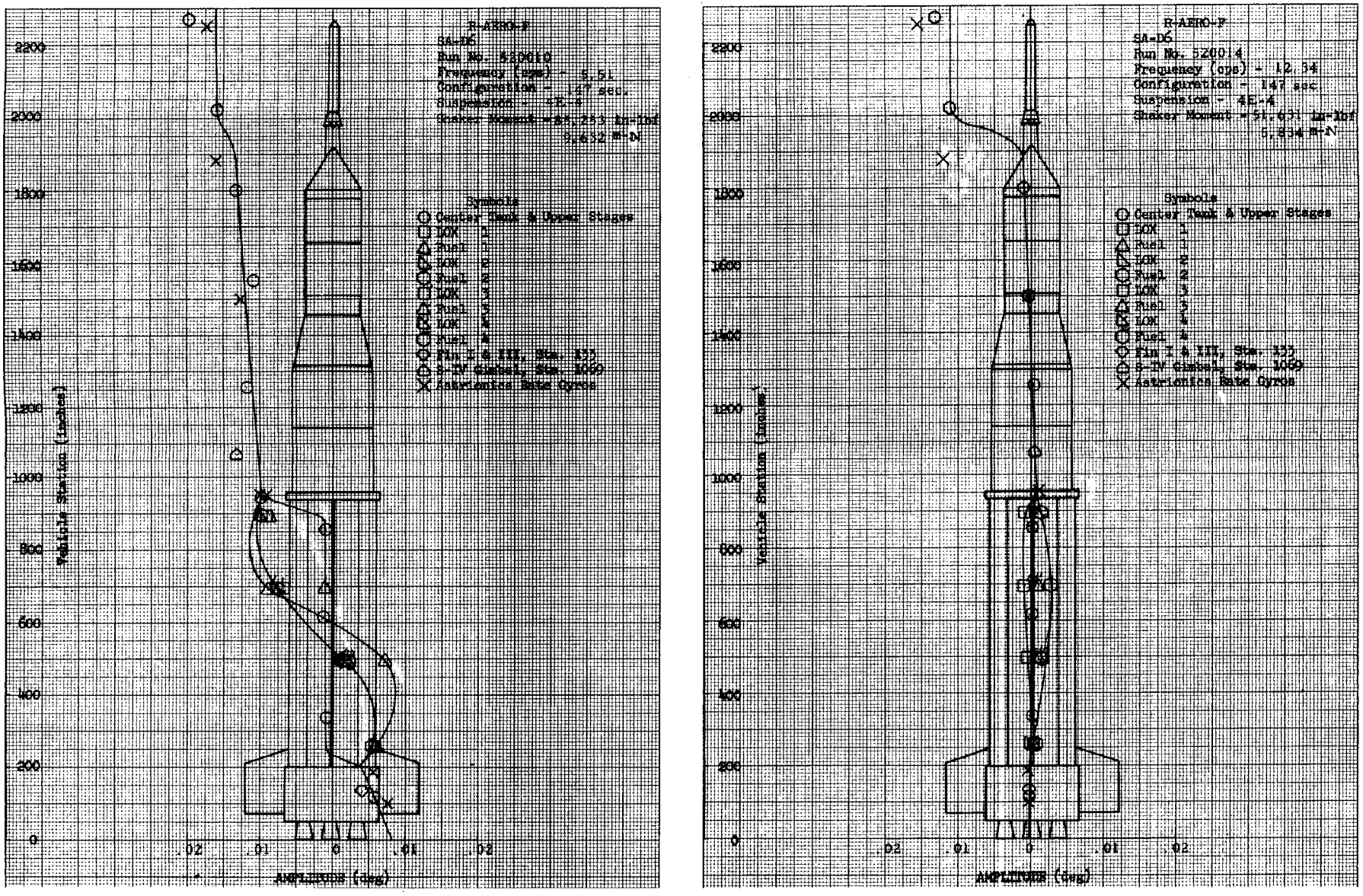


FIGURE 141 1ST TORSIONAL MODE (5.51 CPS) AND 1ST CLUSTER MODE (12.34 CPS) AT 147 SEC (TORSION)

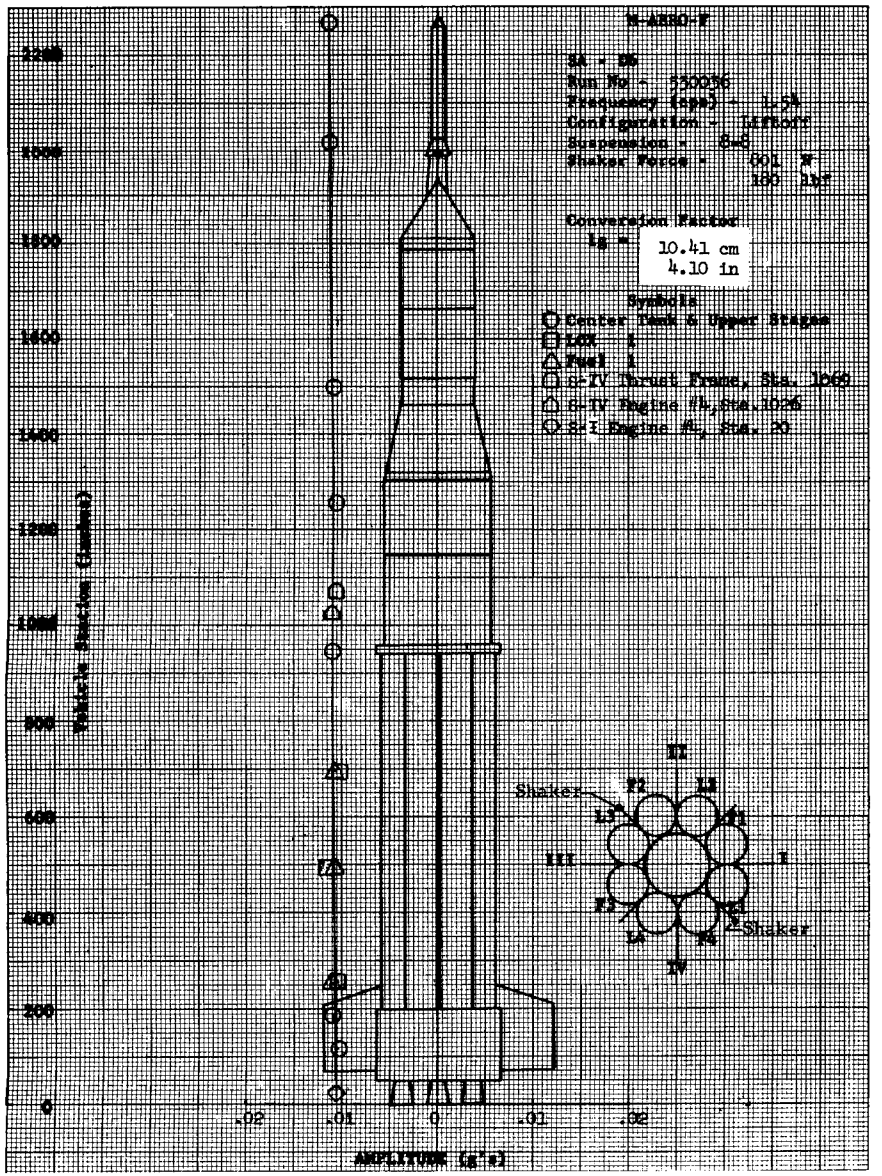


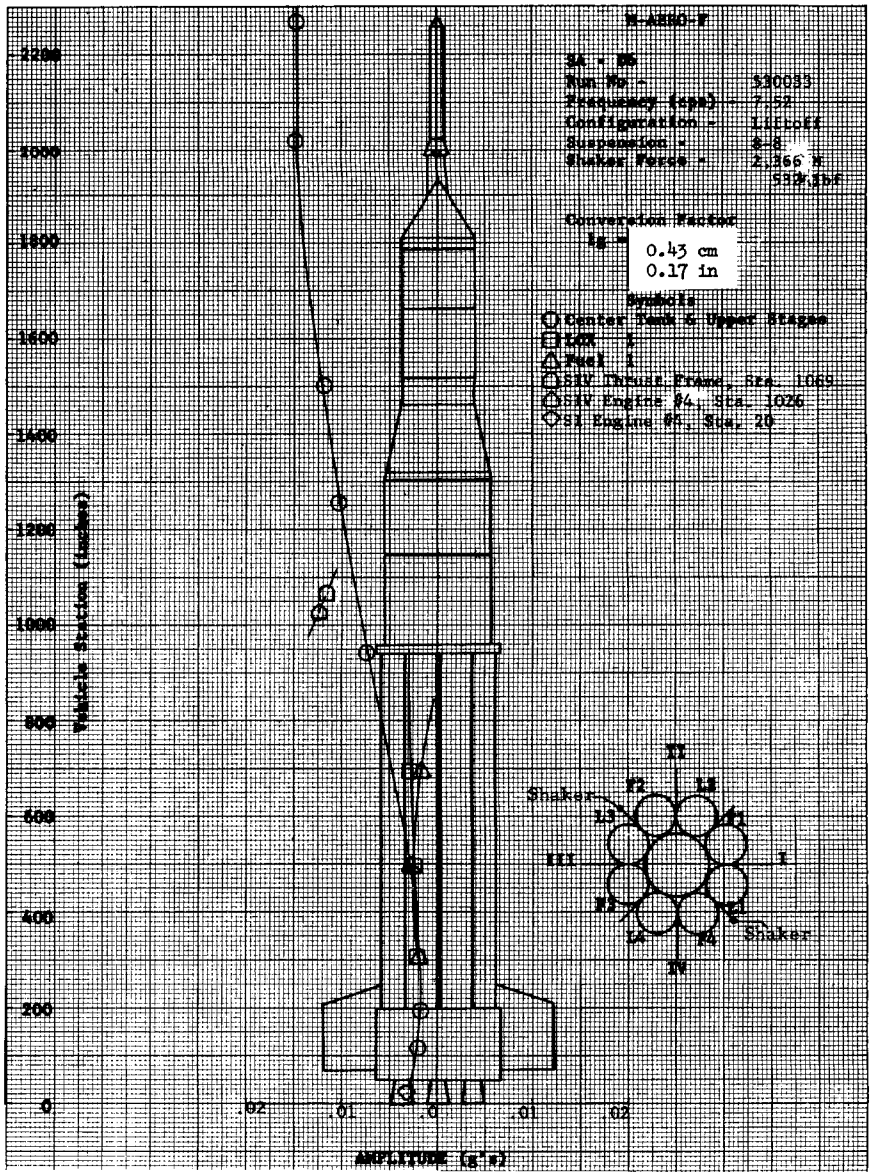


FIGURE 142 RIGID BODY MODE (1.54 CPS) AND CLUSTER MODE (7.52 CPS) AT LIFTOFF (LONGITUDINAL)

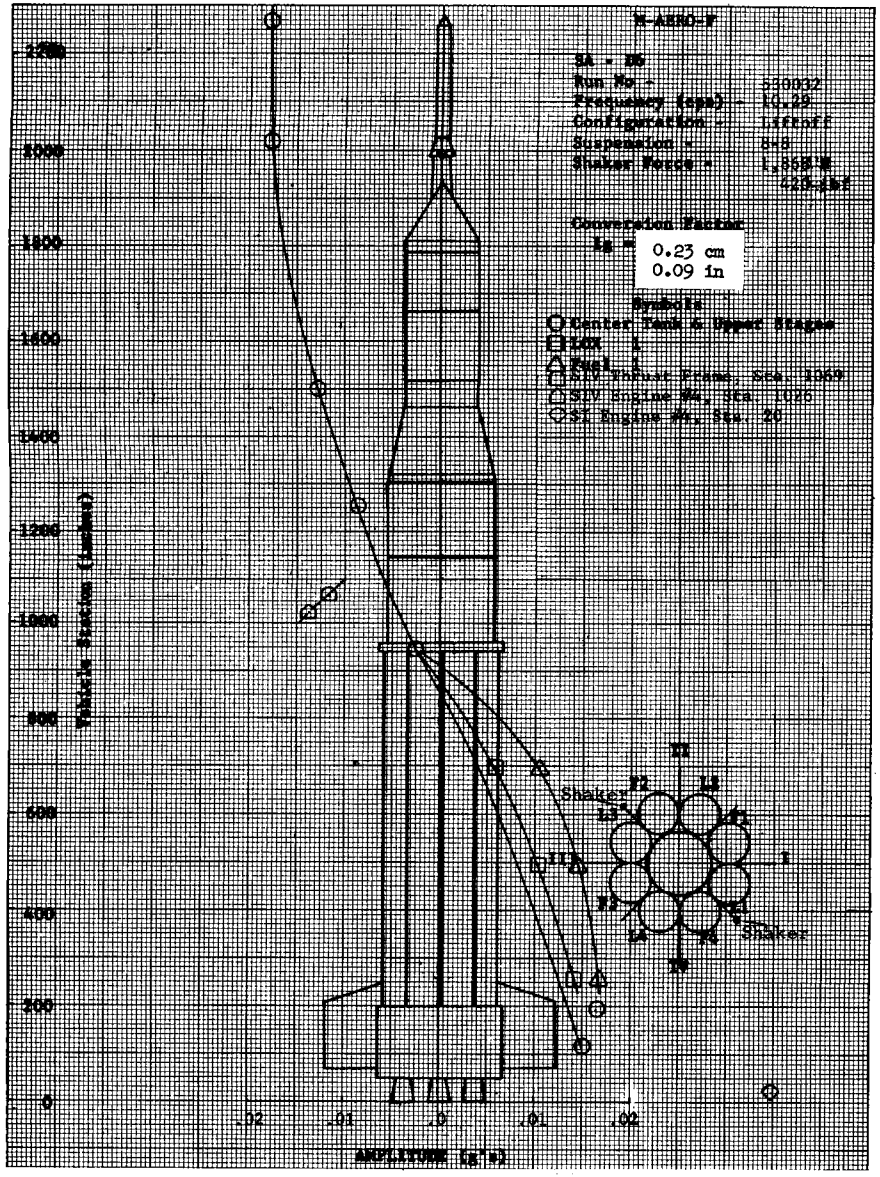


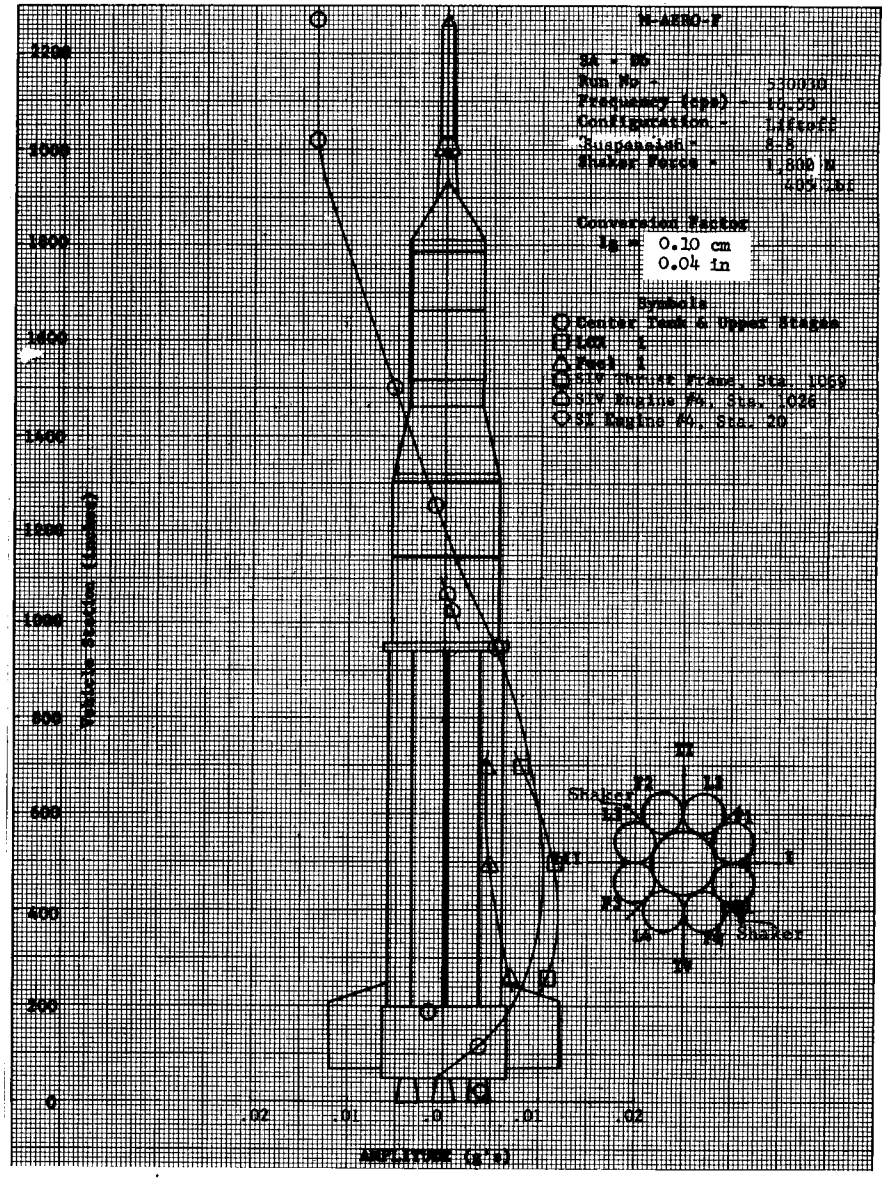


FIGURE 143 1ST LONGITUDINAL MODE (10.29 CPS) AND CLUSTER MODE (16.53 CPS) AT LIFTOFF (LONGITUDINAL)

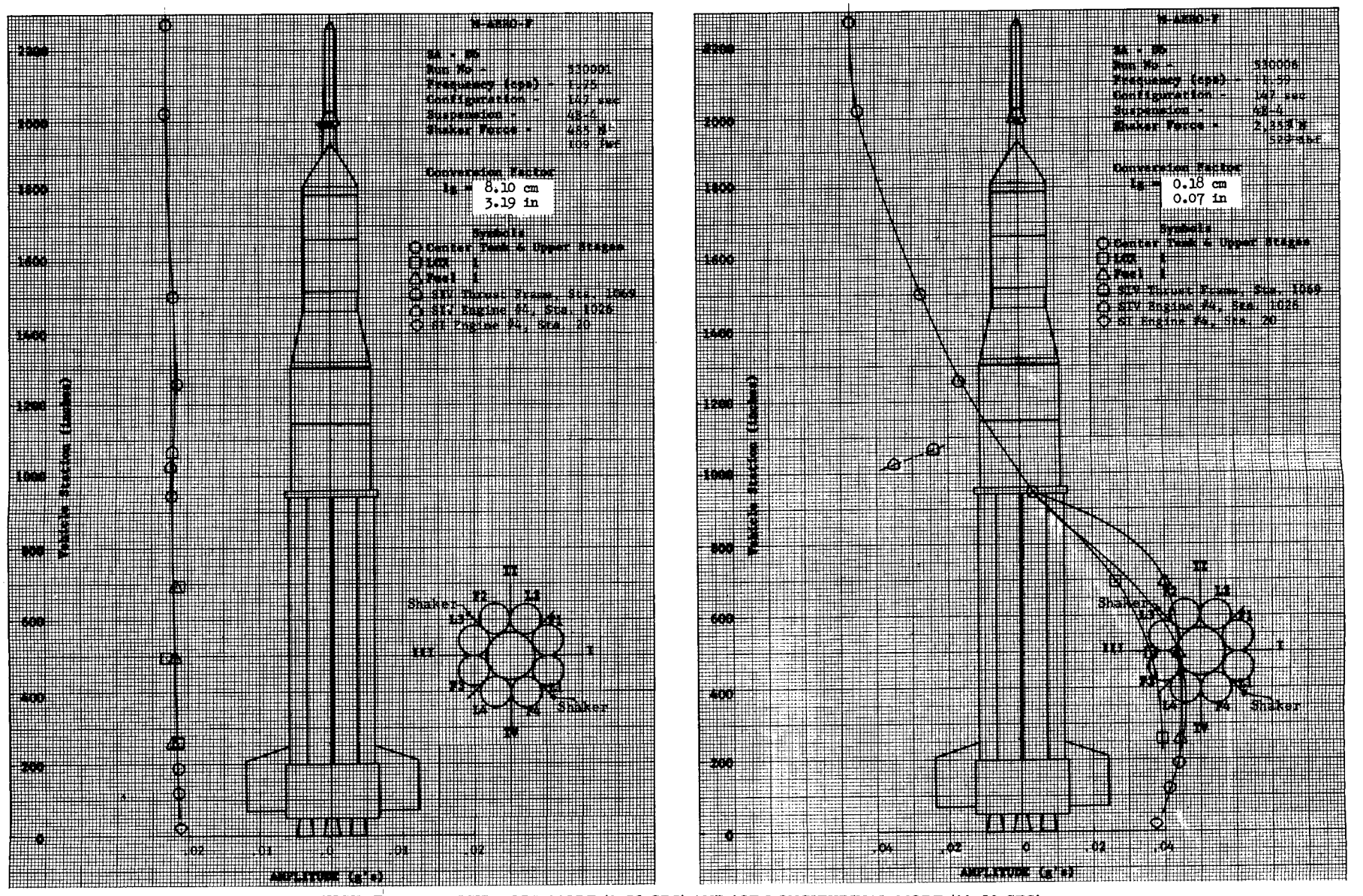


FIGURE 144 RIGID BODY MODE (1.75 CPS) AND 1ST LONGITUDINAL MODE (11.59 CPS) AT 147 SEC (LONGITUDINAL)

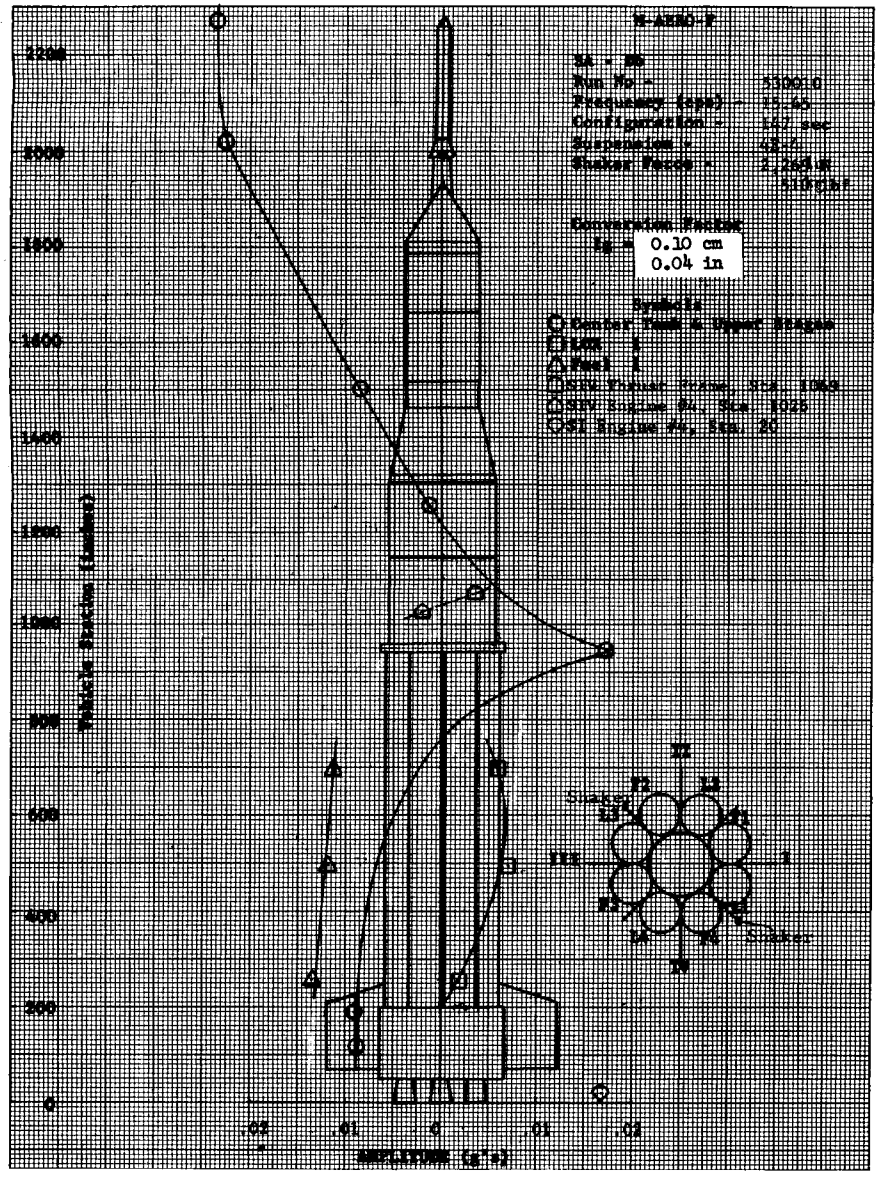


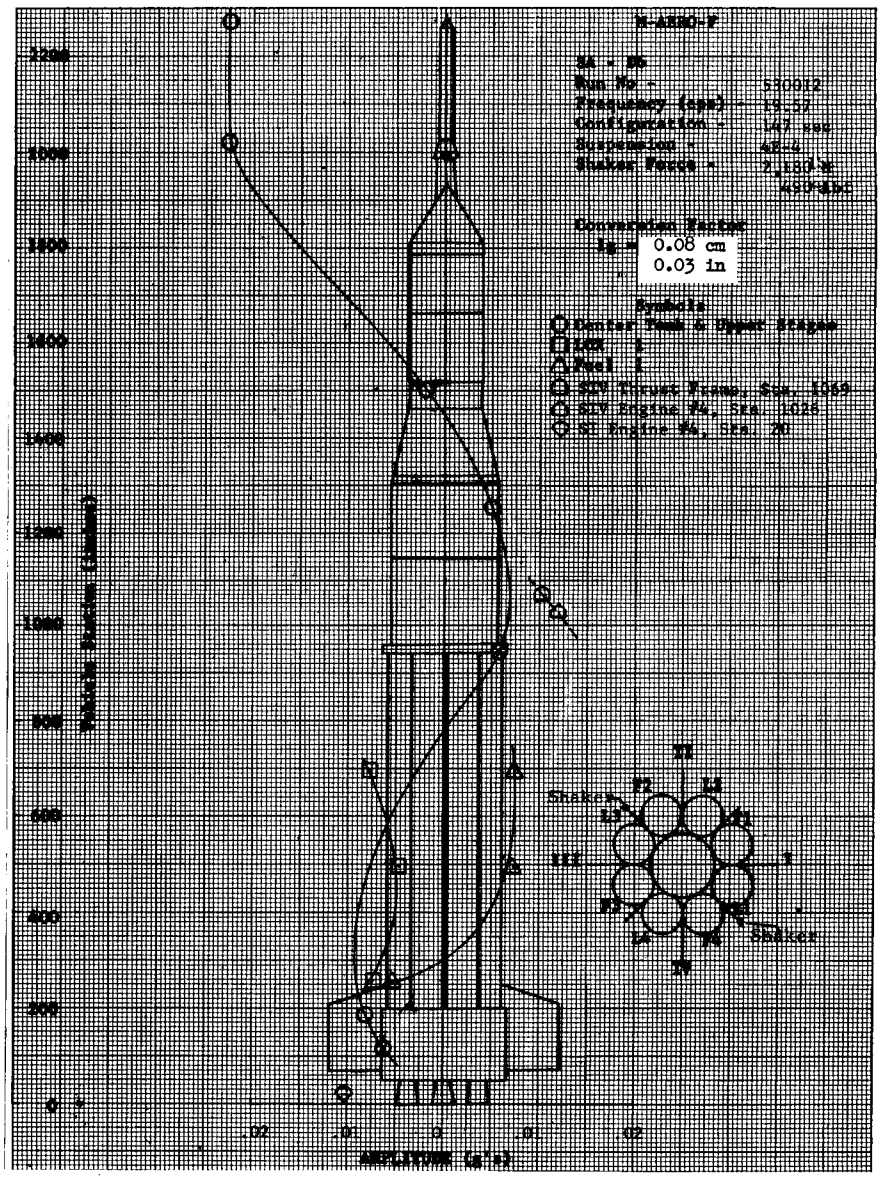


FIGURE 145 CLUSTER MODES (15.45 CPS AND 19.57 CPS) AT 147 SEC (LONGITUDINAL)

R-AERO-F

SAD-6 Phase II
Run Nos. 041006-041232
Ignition Pitch, 8-5 Susp.
Accel. No. 13, Sta. 2259
Accel. No. 10, Sta. 1886
Accel. No. 6, Sta. 1500

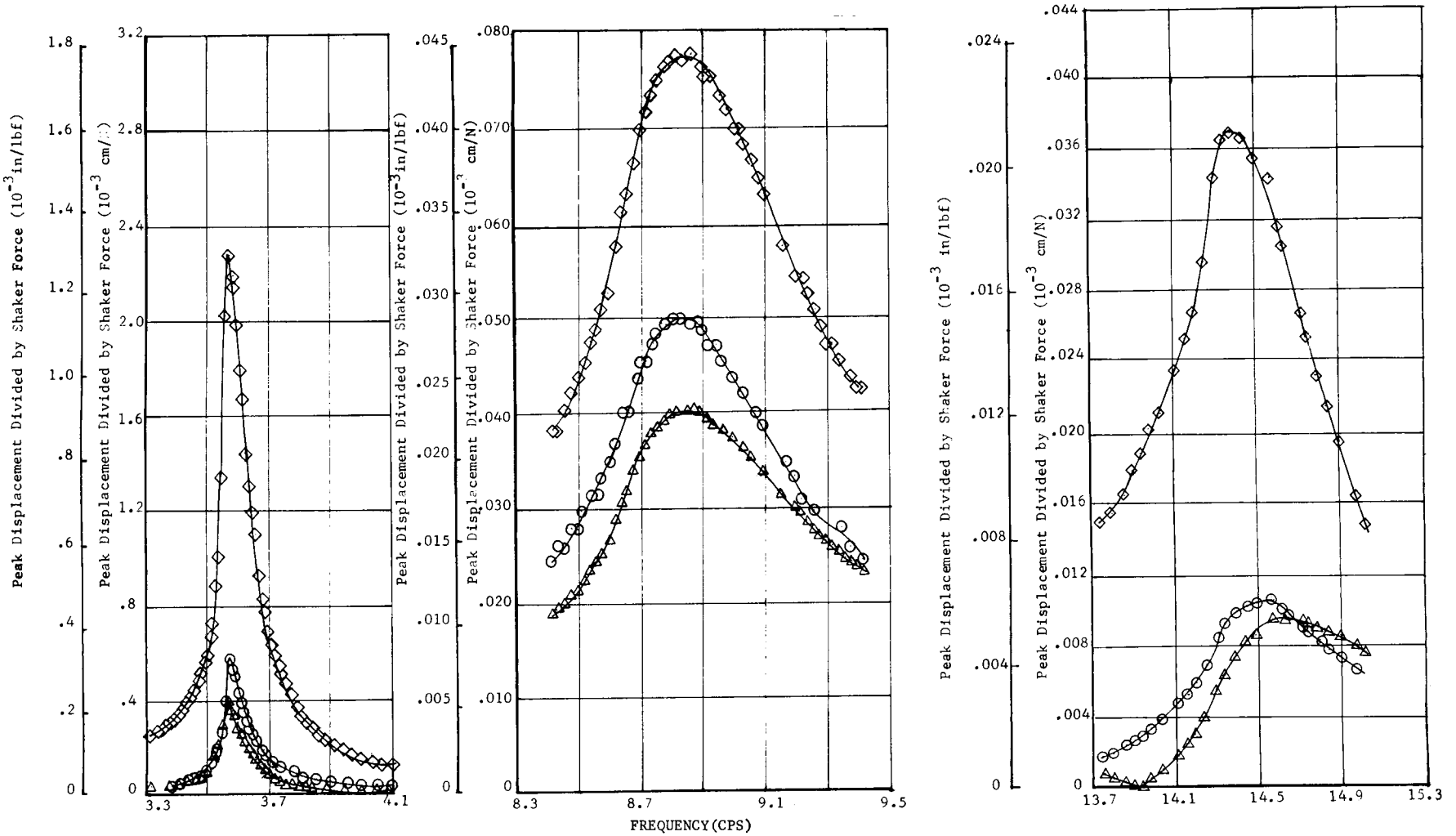


FIGURE 146 RESPONSE FOR PITCH EXCITATION, S-IV IGNITION (PHASE II)

SAD-6 Phase II
Run Nos. 051022-051257
Ignition Yaw, 8-5 Susp
Accel No. 13, Sta 2259
Accel No. 10, Sta 1886
Accel No. 6, Sta 1500

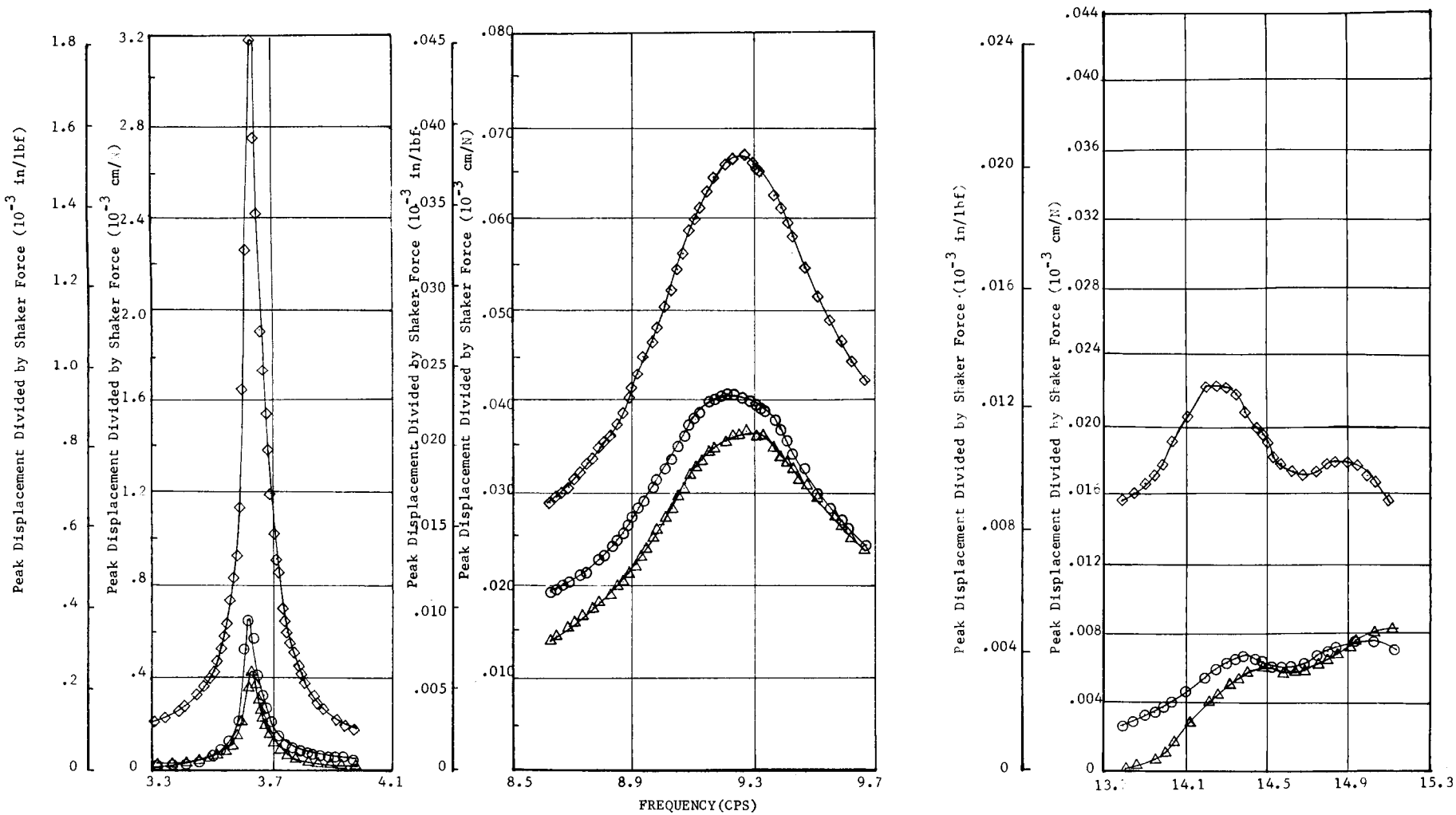


FIGURE 147 RESPONSE FOR YAW EXCITATION, S-IV IGNITION (PHASE II)

R-AERO-F

SAD-6 Phase II
Run Nos. 041006-041231
Ignition Pitch, 8-5 Susp.
Accel. No. 13, Sta. 2259
Accel. No. 10, Sta. 1886
Accel. No. 6, Sta. 1500

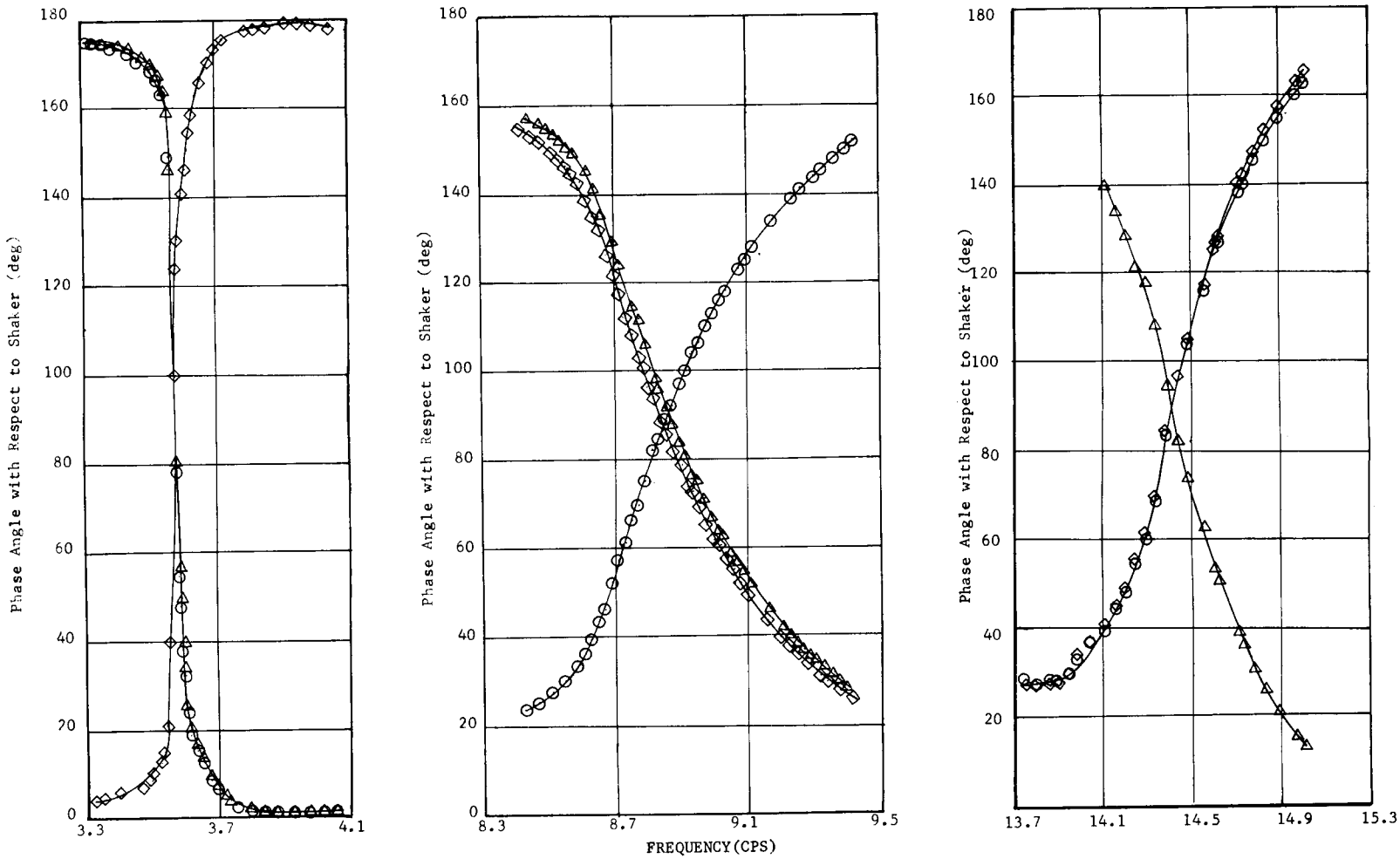


FIGURE 148 PHASE ANGLE FOR PITCH EXCITATION, S-IV IGNITION (PHASE II)

SAD-6 Phase II
Run Nos. 051022 - 051257
Ignition Yaw, 8-5 Susp.
Accel. No. 13, Sta. 2259
Accel. No. 10, Sta. 1886
Accel. No. 6, Sta. 1500

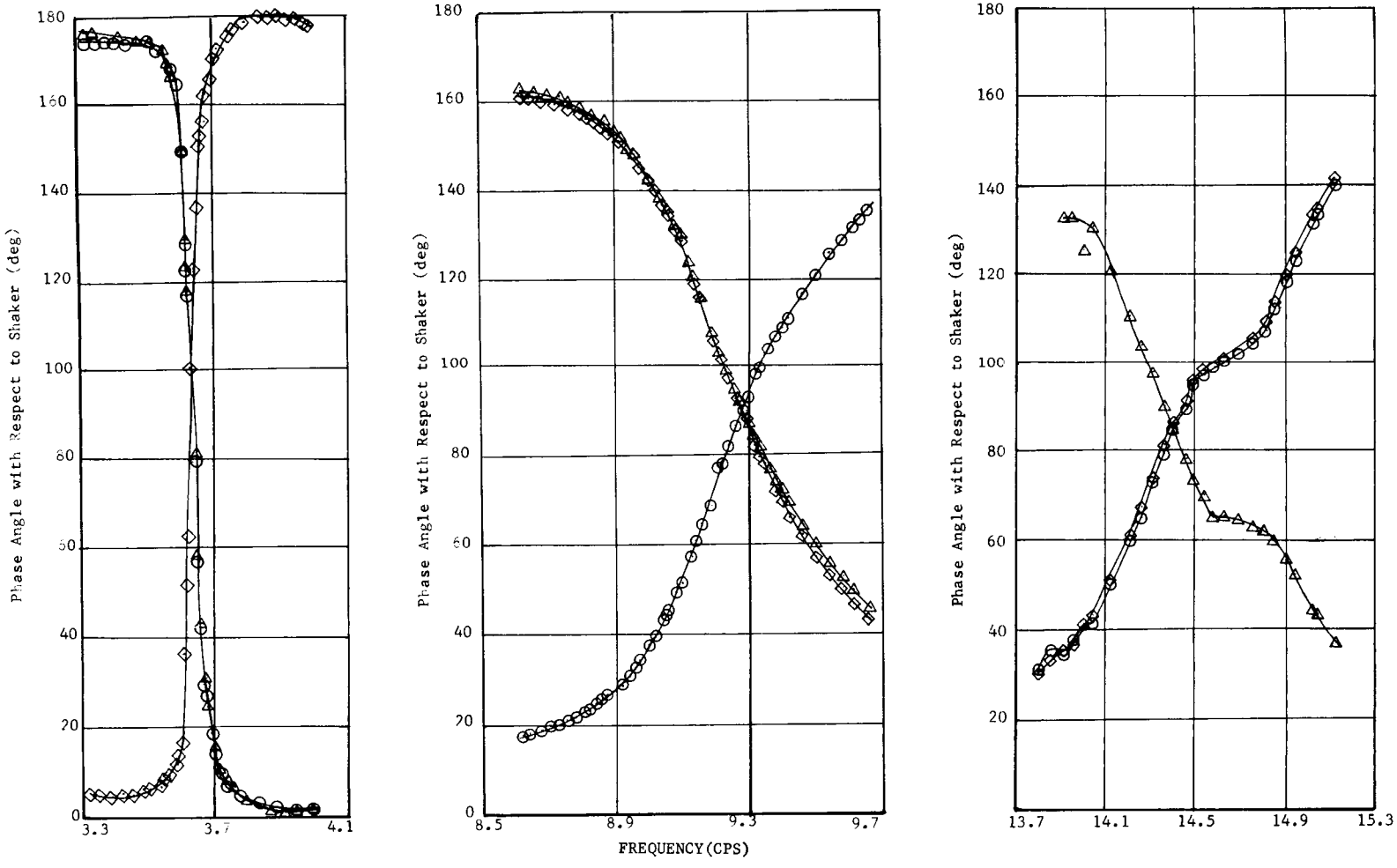


FIGURE 149 PHASE ANGLE FOR YAW EXCITATION, S-IV IGNITION (PHASE II)

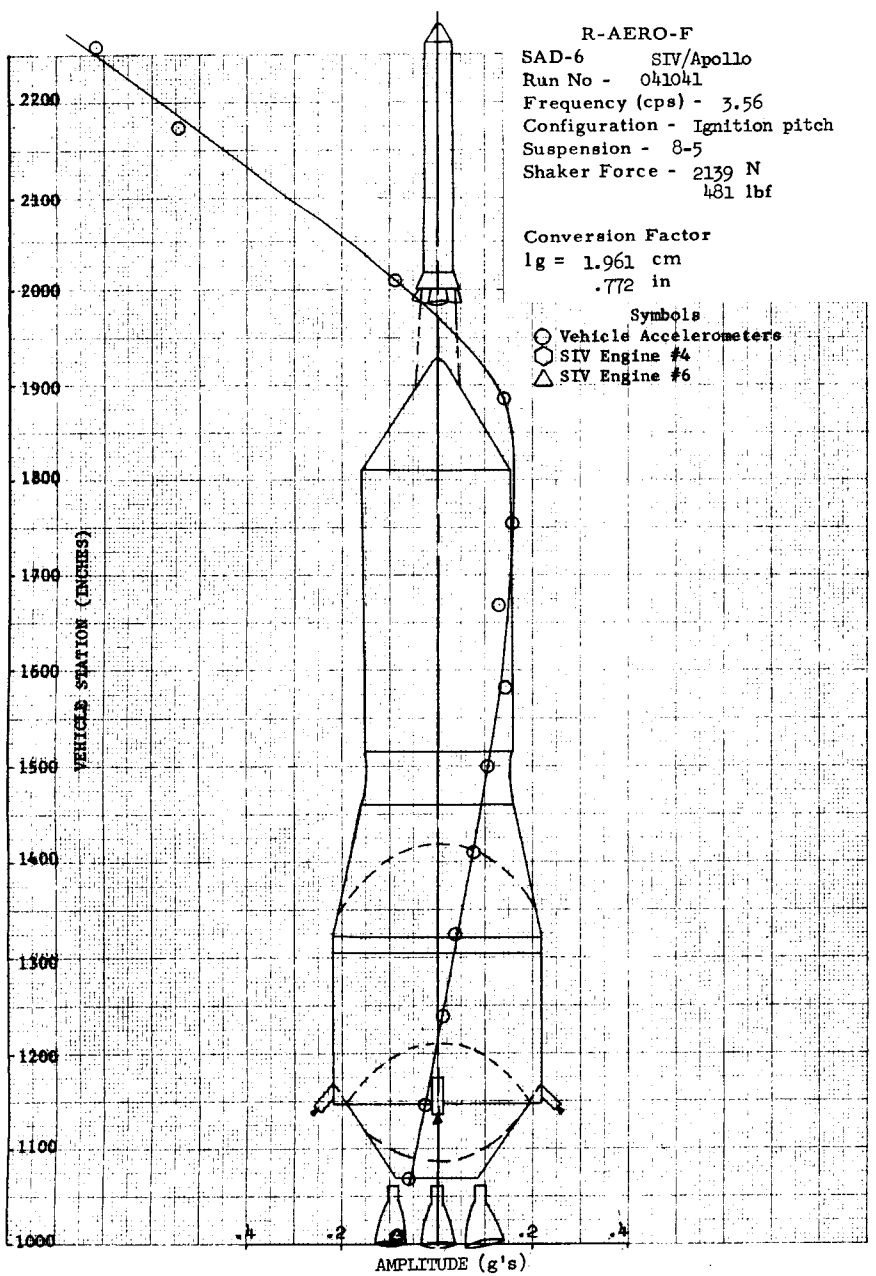


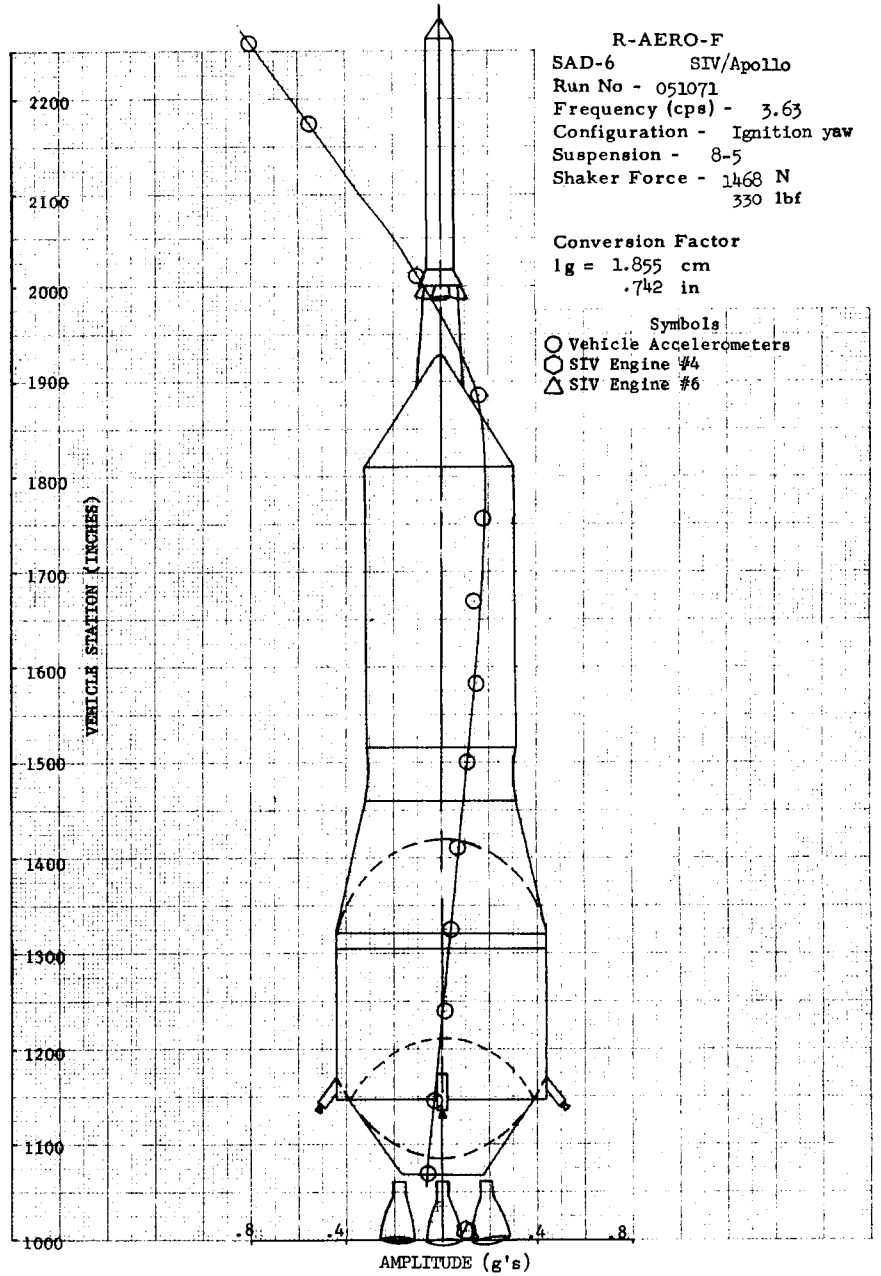


FIGURE 150 PITCH AND YAW 1ST BENDING MODES, S-IV IGNITION (PHASE II)

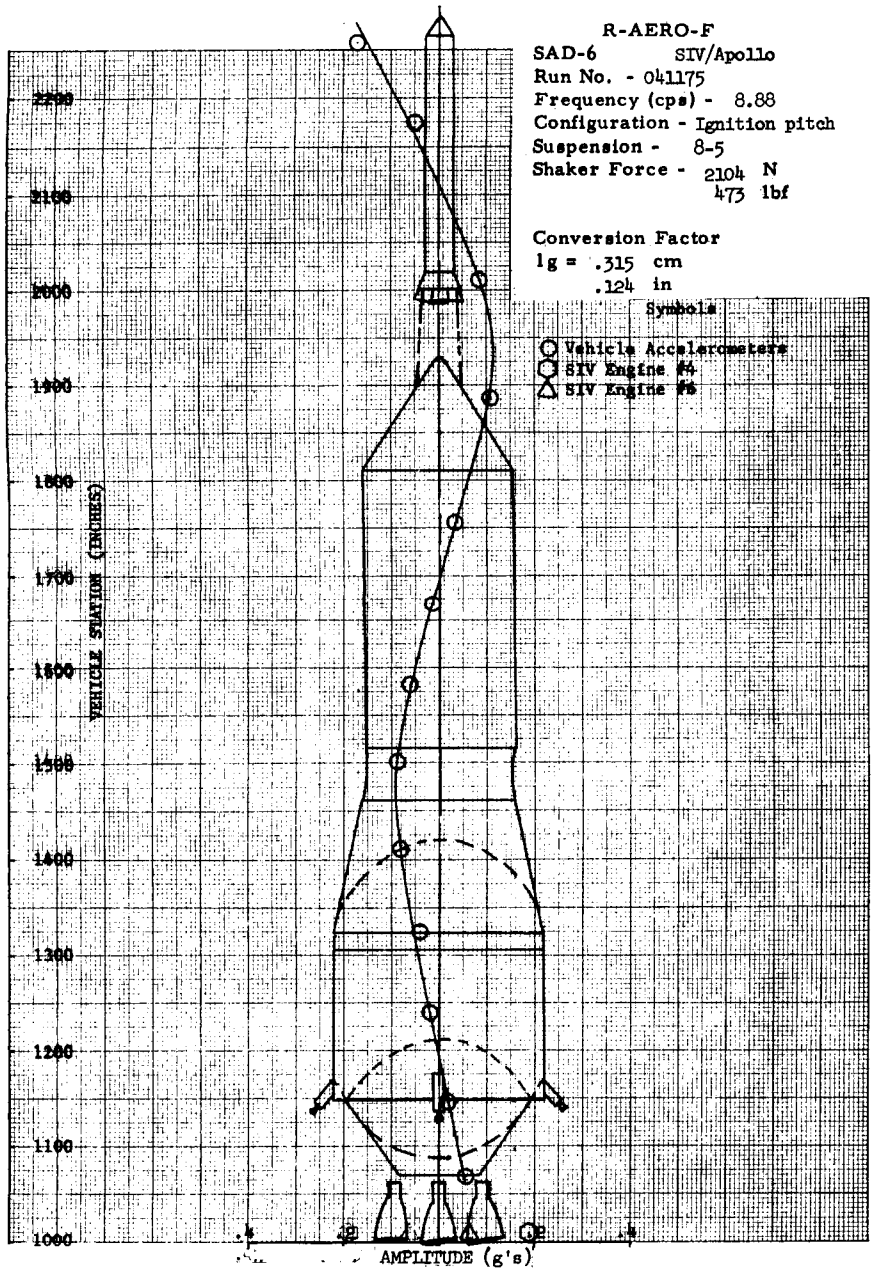


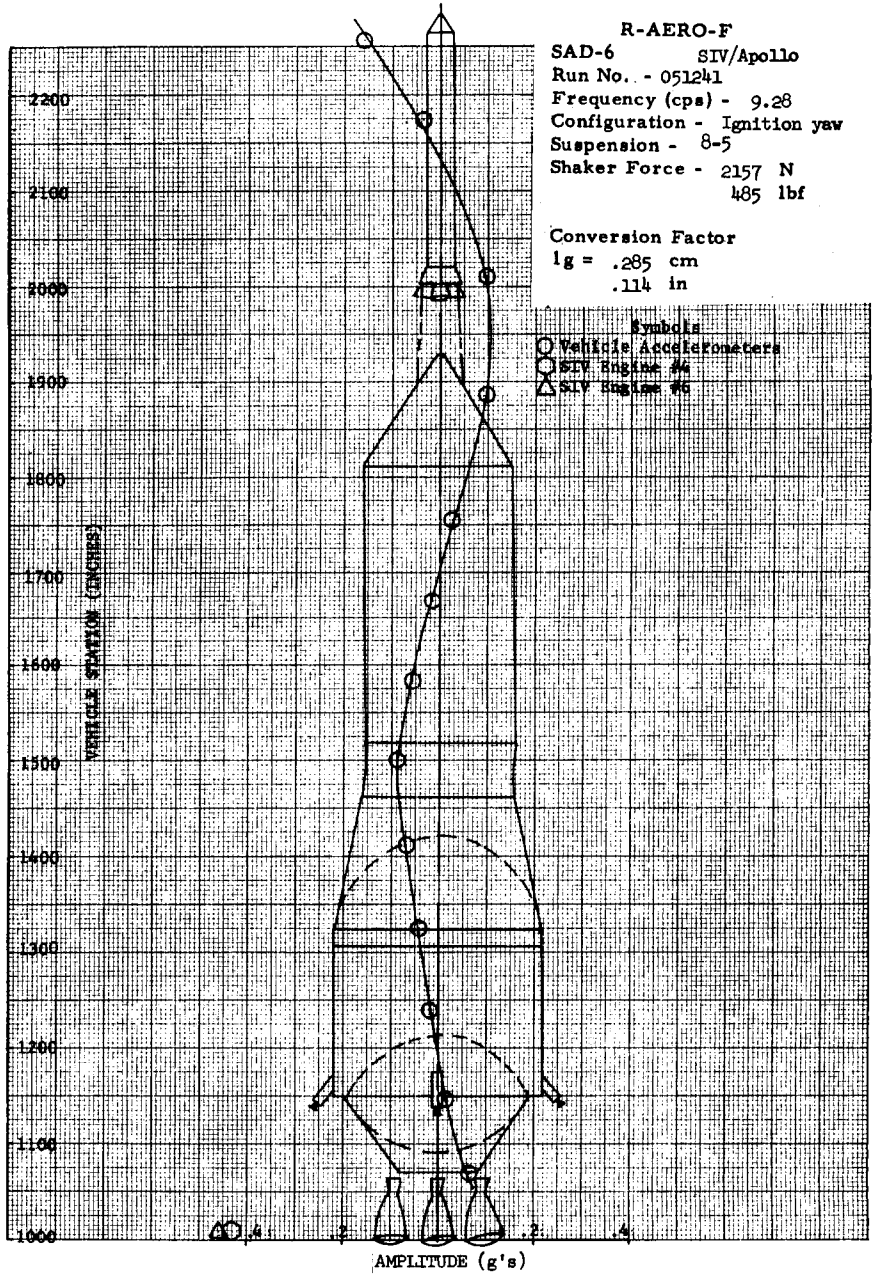


FIGURE 151 PITCH AND YAW 2ND BENDING MODES, S-IV IGNITION (PHASE II)

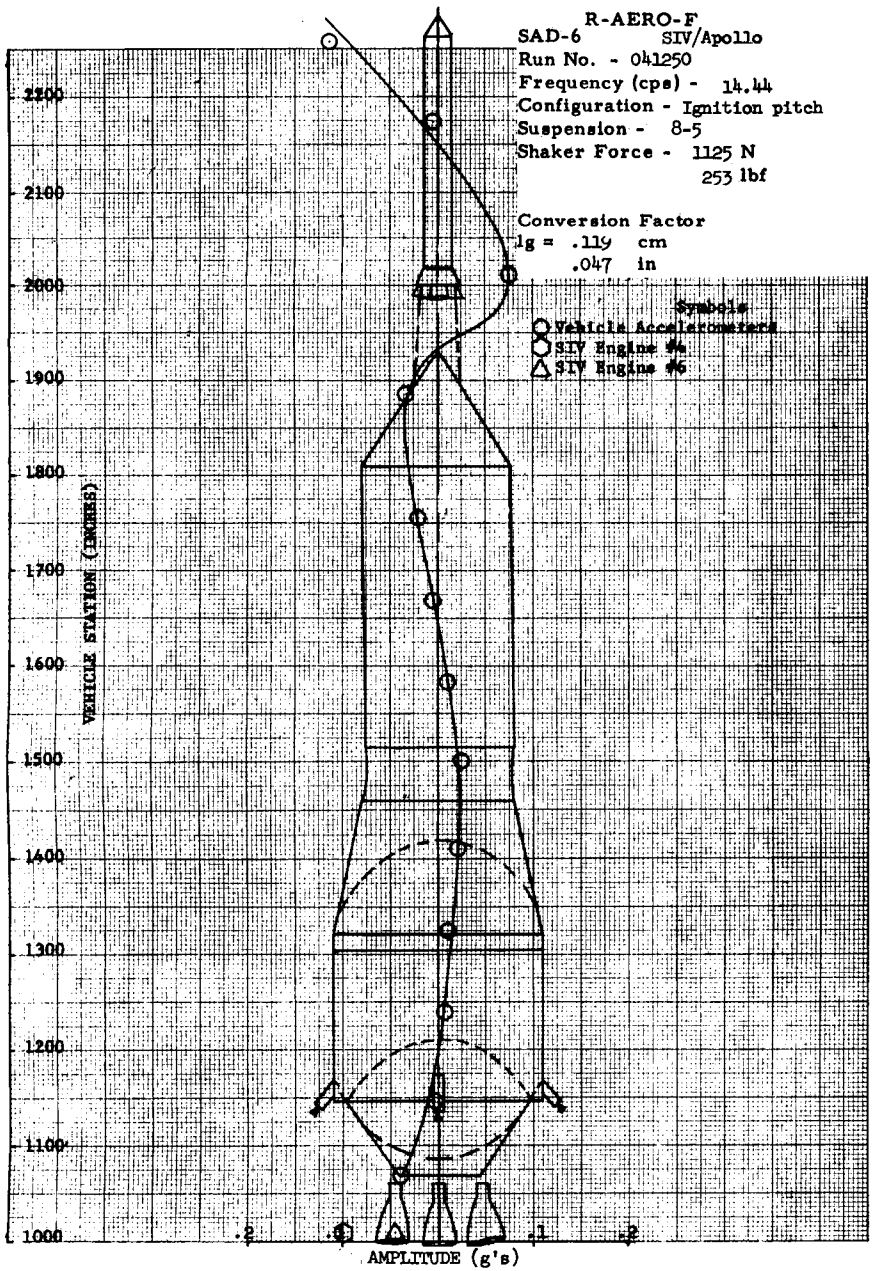


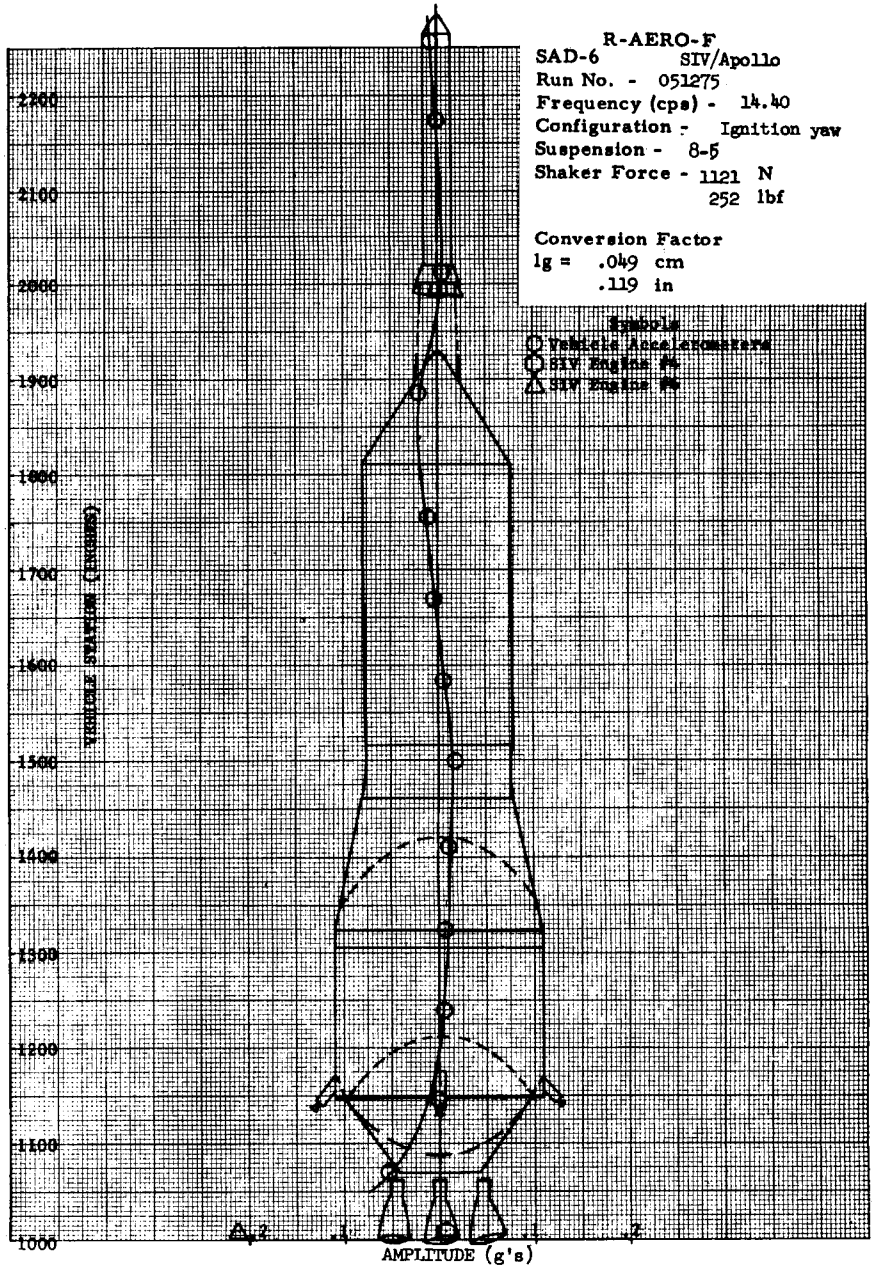


FIGURE 152 PITCH AND YAW 3RD BENDING MODES, S-IV IGNITION (PHASE II)

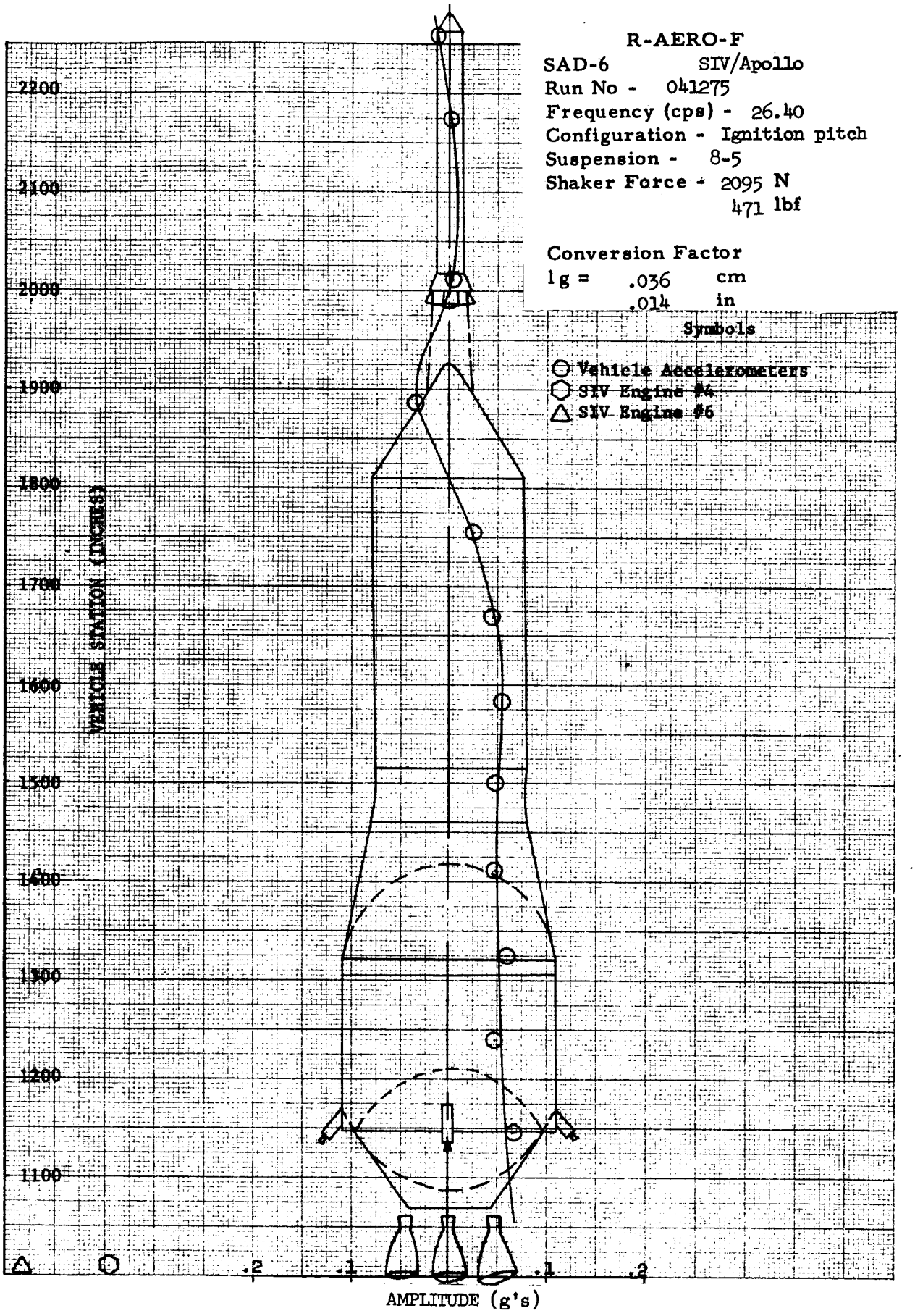


FIGURE 153 ENGINE MODE AT 26.40 CPS, S-IV IGNITION (PHASE II)

R-AERO-F
SAD-6 Phase II

Run Nos. 042017-042121
20 Sec. Pitch, 8-5 Susp.
Accel. No. 10, Sta. 1886
Accel. No. 6, Sta. 1500

Run Nos. 043012-043134
290 Sec. Pitch, 8-3 Susp.
Accel. No. 10, Sta. 1886
Accel. No. 6, Sta. 1500

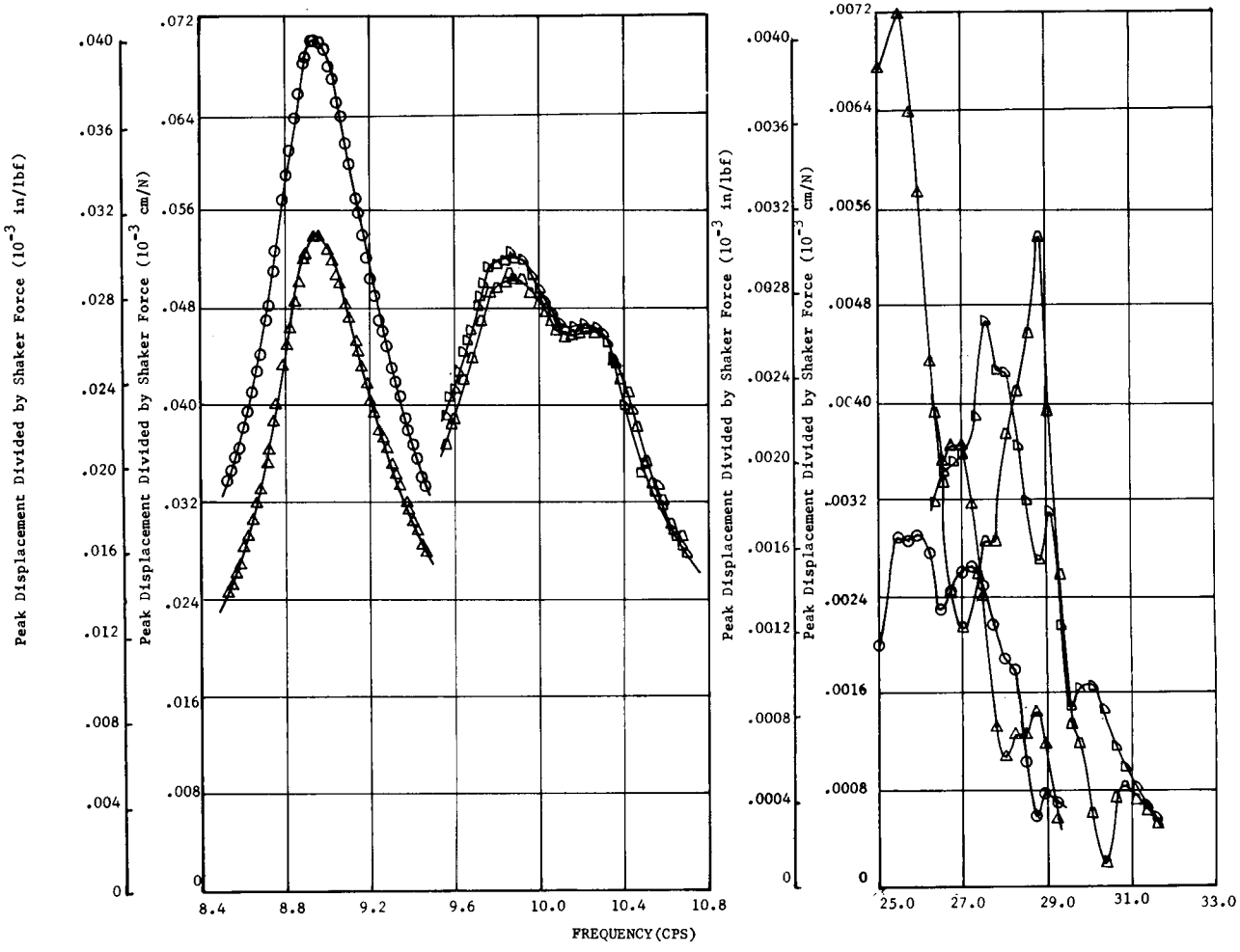


FIGURE 154 RESPONSE FOR PITCH EXCITATION AT 20 SEC AND 290 SEC (PHASE II)

R-AERO-F

SAD-6 Phase II

Run Nos. 042017-042121
20 Sec. Pitch, 8-5 Susp.
Accel. No. 10, Sta. 1886
Accel. No. 6, Sta. 1500

Run Nos. 043012-043134
290 Sec. Pitch, 8-3 Susp.
Accel. No. 10 Sta. 1886
Accel. No. 6, Sta. 1500

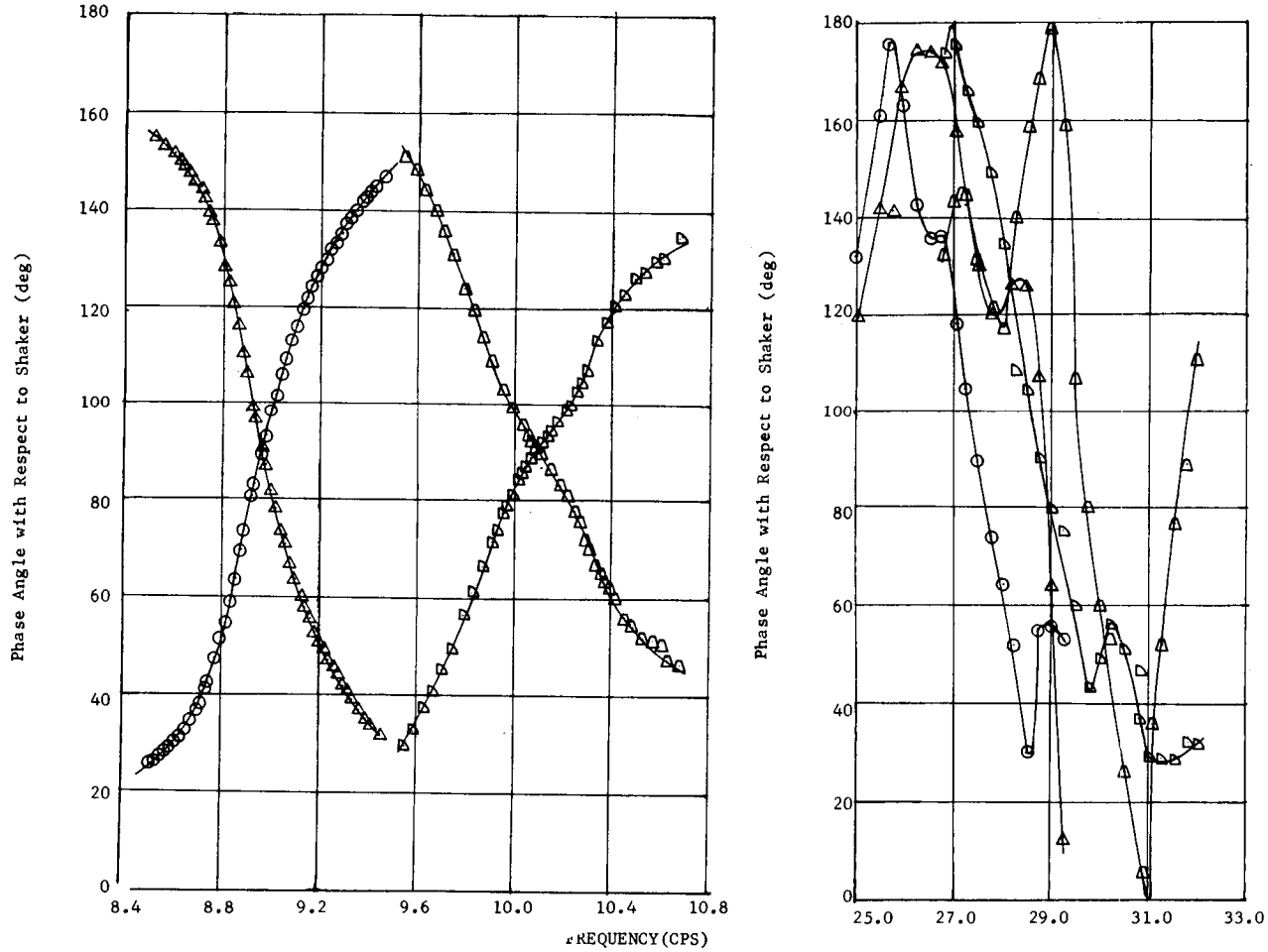


FIGURE 155 PHASE ANGLE FOR PITCH EXCITATION AT 20 SEC AND 290 SEC (PHASE II)

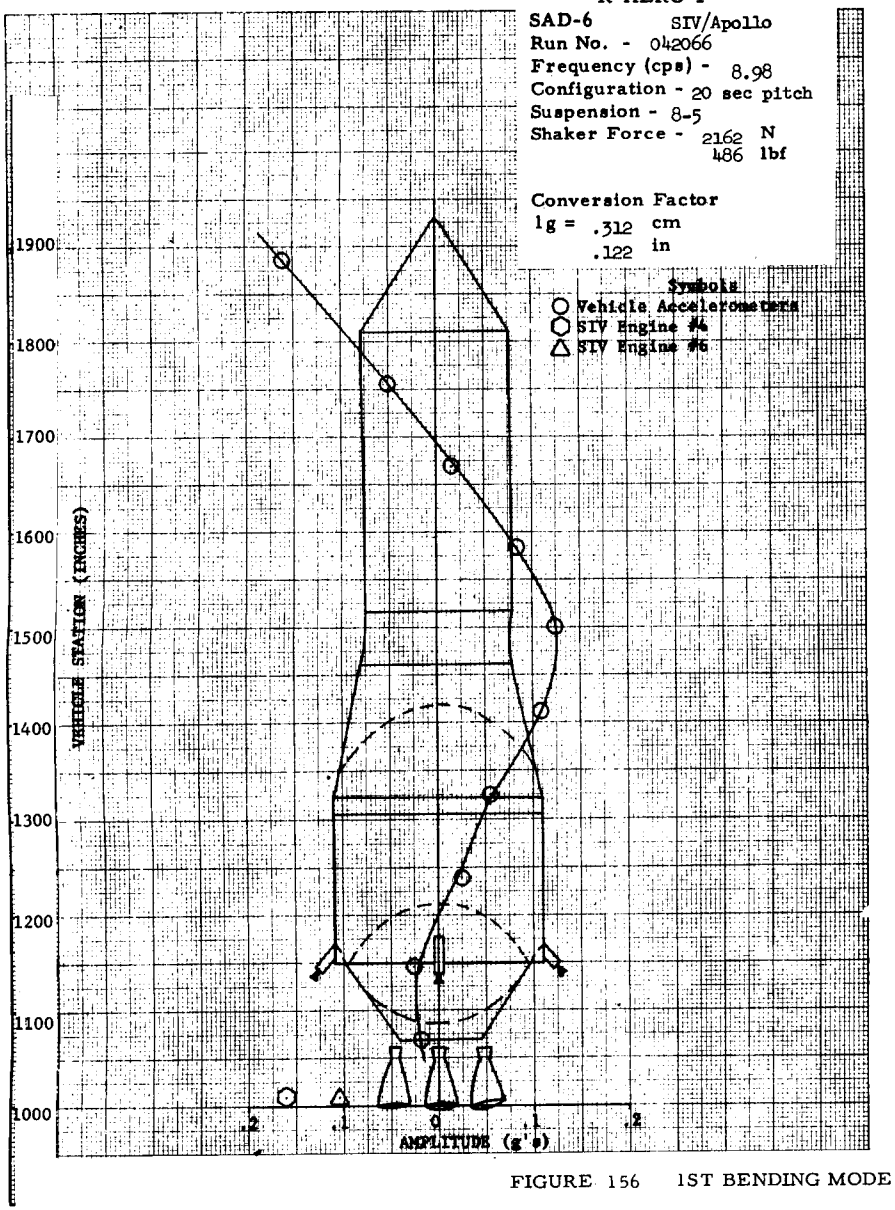


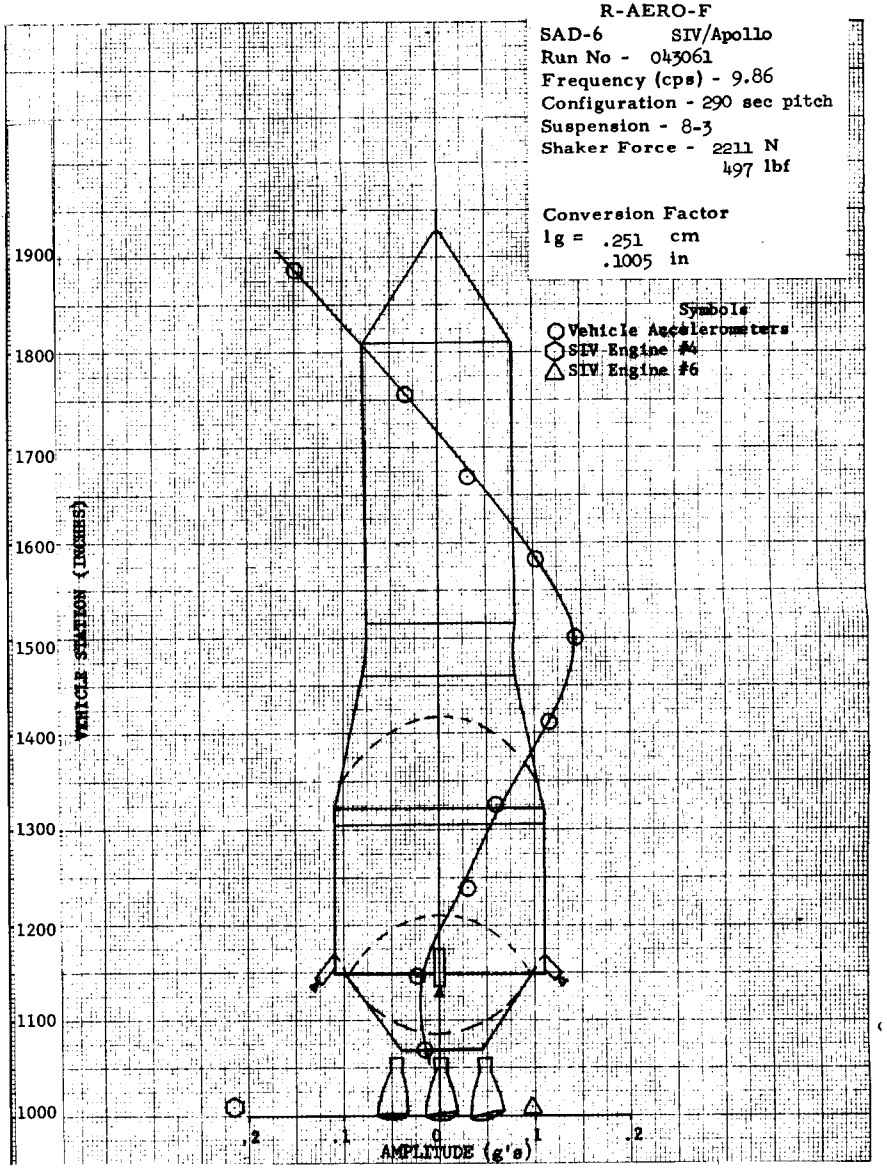


FIGURE 156 1ST BENDING MODE AT 20 SEC AND 290 SEC (PHASE II)

SAD-6 Phase II
Run Nos. 061011-061144
Ignition Roll, 8-5 Susp.
Accel. Nos. 13 & 26, Sta. 2259

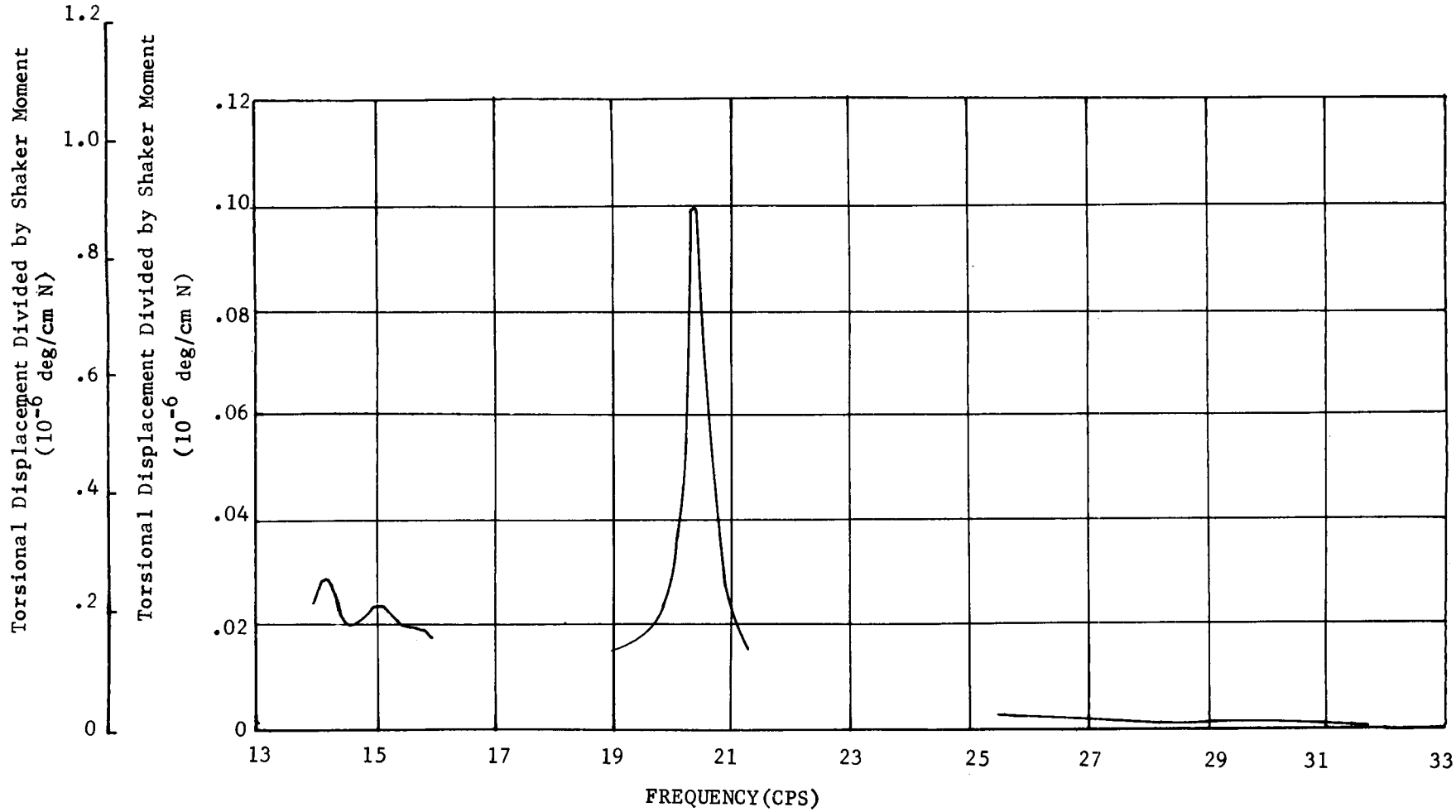


FIGURE 157 RESPONSE FOR TORSIONAL EXCITATION, S-IV IGNITION (PHASE II)

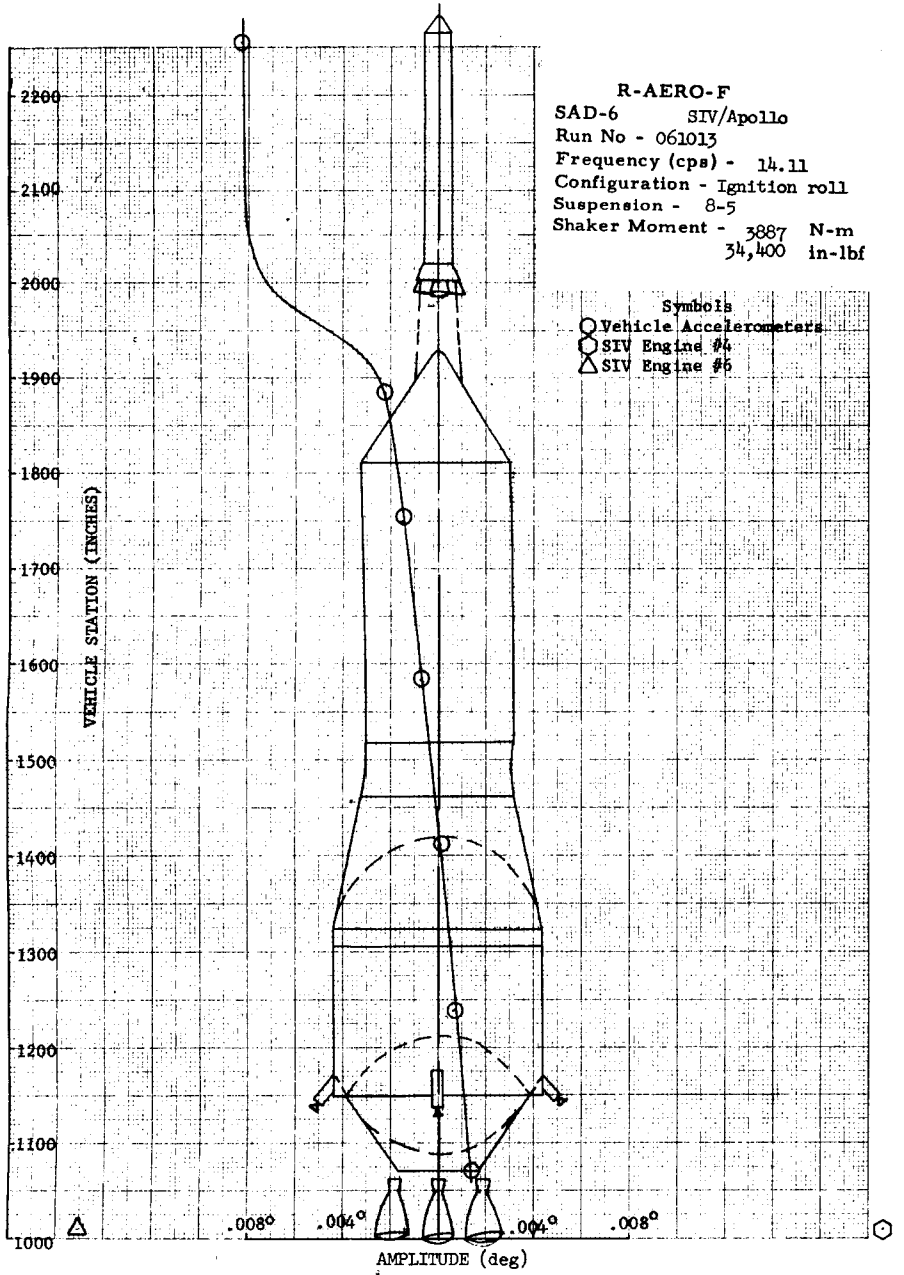


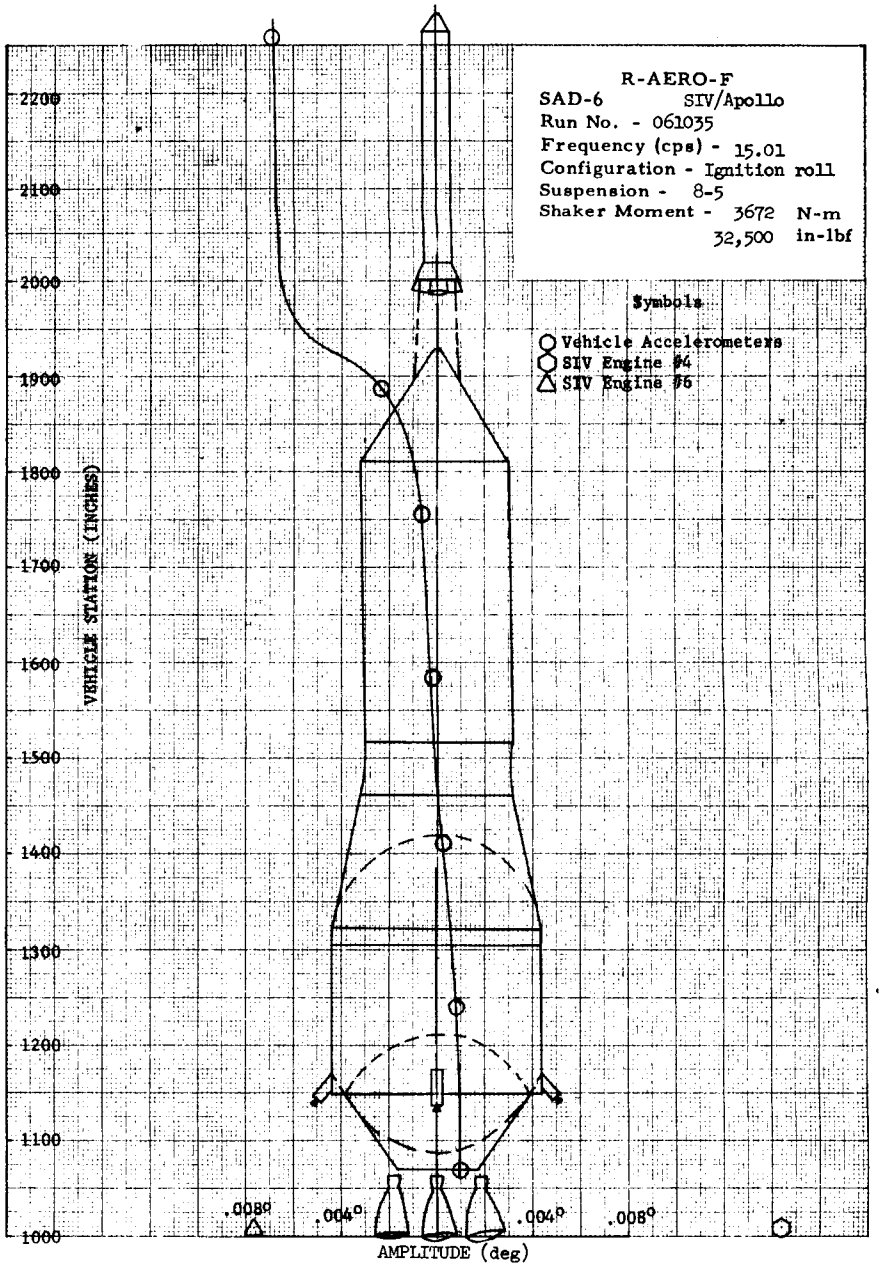


FIGURE 158 TORSIONAL MODES AT 14.11 CPS AND 15.01 CPS, S-IV IGNITION (PHASE II)

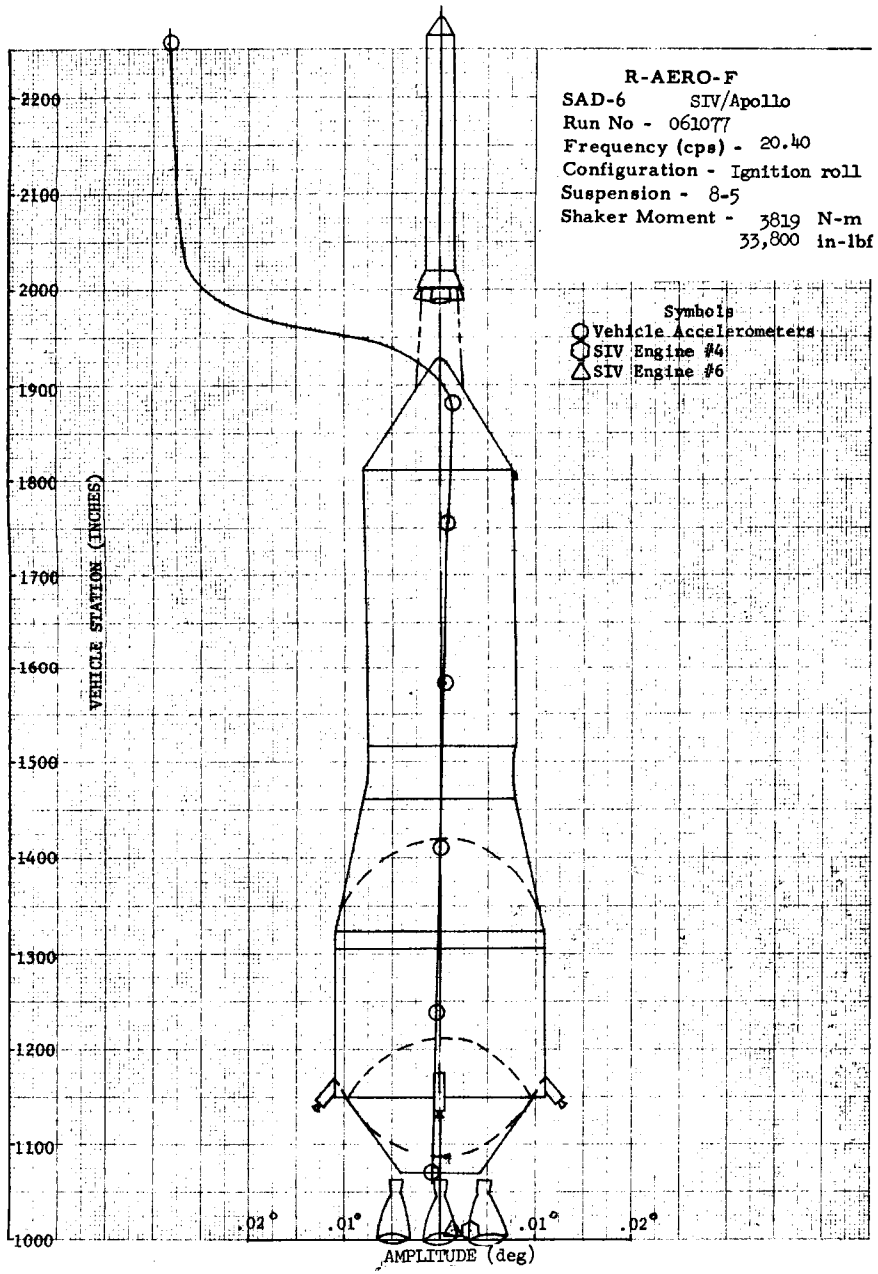


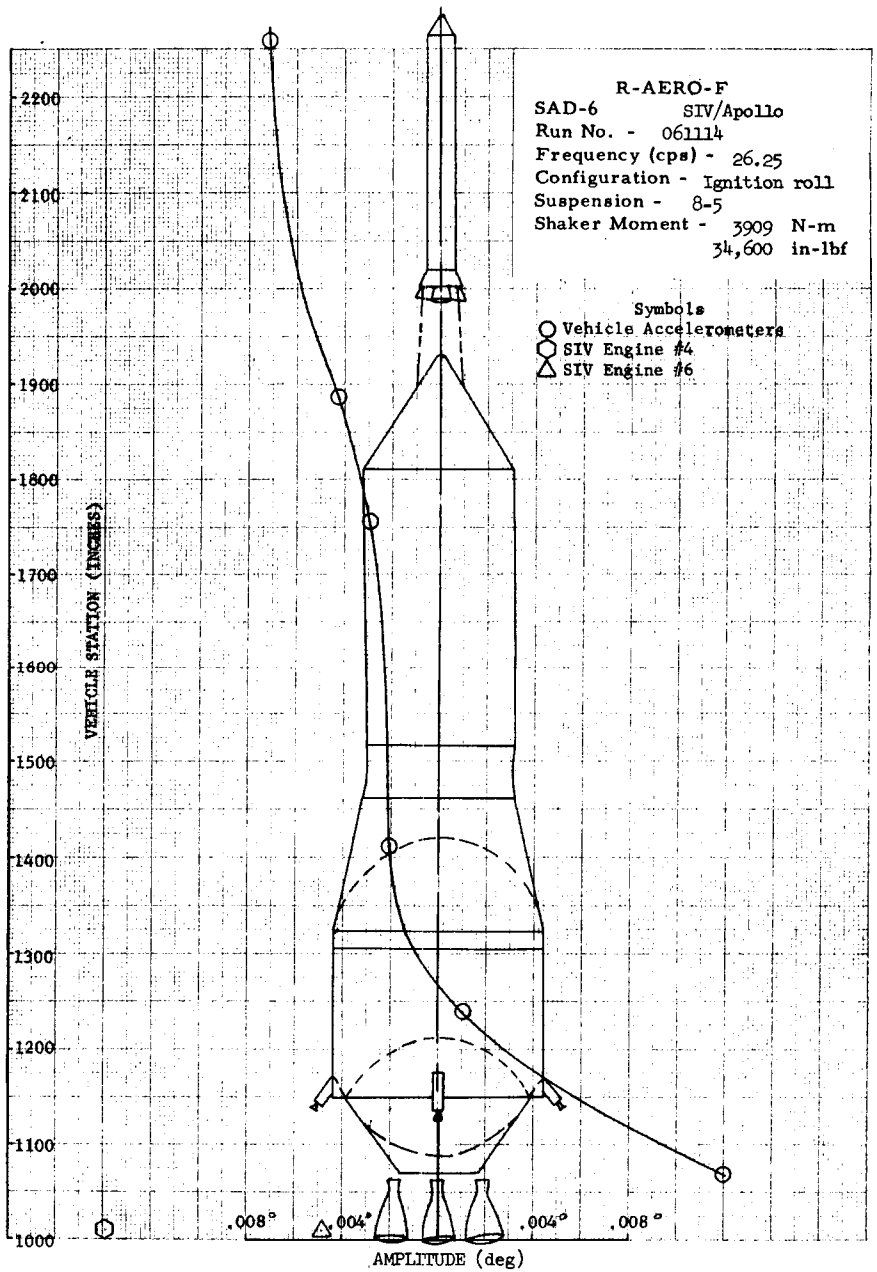


FIGURE 159 TORSIONAL MODES AT 20.40 CPS AND 26.25 CPS, S-IV IGNITION (PHASE II)

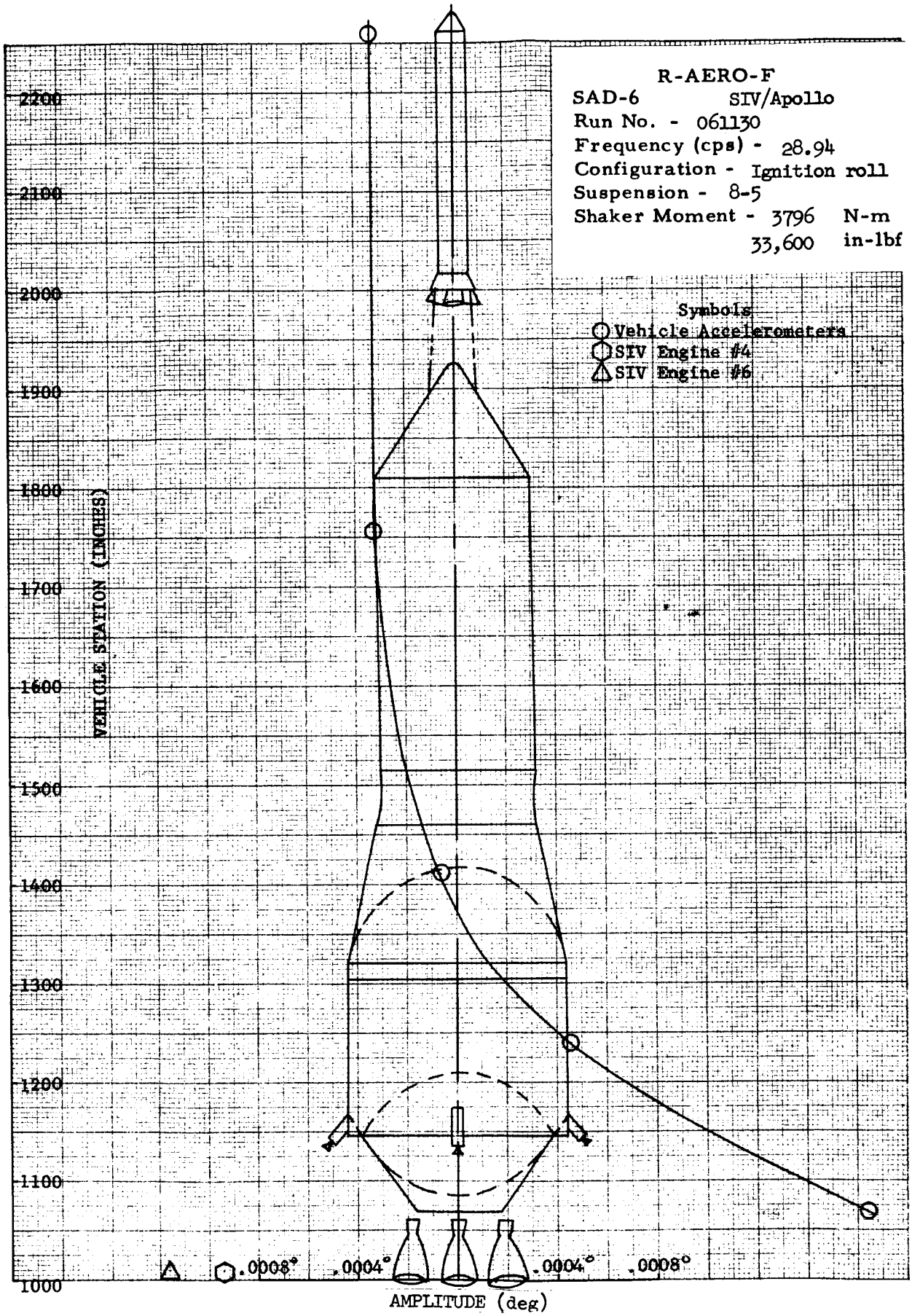


FIGURE 160 TORSIONAL MODE AT 28.94 CPS, S-IV IGNITION (PHASE II)

## REFERENCES


1. Papadopoulos, James G., "Dynamic Test Results of SAD-5," MTP-AERO-63-46, June 13, 1963, Unclassified.

2. Douglas, David G., "September 27, 1963, Minutes of the Control Dynamics and Structural Feedback Working Group," October 3, 1963, Unclassified.

3. Ernsberger, Gale R., "SAD-6, Dynamic Test Summary, R-AERO-FF-63-14, October 28, 1963, Unclassified.

NASA TM X-53029 APPROVAL April 6, 1964

# DYNAMIC TEST RESULTS OF SAD-6

By

Gale R. Ernsberger

The information in this report has been reviewed for security classification. Review of any information concerning Department of Defense or Atomic Energy Commission programs has been made by the MSFC Security Classification Officer. This report, in its entirety, has been determined to be unclassified.

James G. Papadopoulos

JAMES G. PAPADOPOULOS
Chief, Dynamics & Control Section

JAMES P. LINDBERG
Chief, Flight Evaluation Branch

F. Speer

FRIDTJOF A. SPEER
Chief, Flight Evaluation and
Operations Studies Division

E. D. Geissler

E. D. GEISSLER
Director, Aero-Astrodynamics
Laboratory

DISTRIBUTION

DEP-T, Dr. Rees

Aero-Astrodynamics Laboratory

R-AERO-DIR, Dr. Geissler
R-AERO-DIR, Mr. Jean
R-AERO-D, Mr. Horn
R-AERO-D, Mr. Douglas (5)
R-AERO-D, Mr. Rheinfurth
R-AERO-DD, Mr. Ryan
R-AERO-DD, Mr. McDonough
R-AERO-DD, Mr. Kiefling
R-AERO-F, Dr. Speer
R-AERO-FF, Mr. Lindberg
R-AERO-FFD, Mr. Papadopoulos (20)
R-AERO-FFD, Mr. Ernsberger (10)
R-AERO-G, Dr. Hoelker
R-AERO-P, Mr. McNair (6)
R-AERO-PS, Mr. McQueen
R-AERO-PS, Mr. Schmidt
R-AERO-PS, Mr. Thionnet
R-AERO-PS, Mr. Teague (20)
Mr. Vaughan, R-AERO-Y
Mr. Scoggins, R-AERO-Y

Astrionics Laboratory

R-ASTR-DIR, Dr. Haeussermann
R-ASTR-F, Mr. Hosenthien
R-ASTR-F, Mr. Lucas
R-ASTR-F, Mr. Blackstone
R-ASTR-F, Mr. George
R-ASTR-F, Mr. Landwehr
R-ASTR-F, Mr. Borelli
R-ASTR-M, Mr. Boehm
R-ASTR-M, Mr. Phillips
R-ASTR-N, Mr. Bridges
R-ASTR-N, Mr. Carter
R-ASTR-N, Mr. Cline
R-ASTR-N, Mr. Moore
R-ASTR-P, Mr. Angele

DISTRIBUTION (Cont'd)

Computation Laboratory

R-COMP-DIR, Dr. Hoelzer
R-COMP-RR, Mr. Hubbard
R-COMP-RRV, Mr. Jones
R-COMP-RRV, Mr. Newberry
R-COMP-RDC, Mr. Seija
R-COMP-RDC, Mrs. Cothran

Propulsion & Vehicle Engineering Laboratory

R-P&VE-DIR, Mr. Cline
R-P&VE-DIR, Mr. Hellebrand
R-P&VE-E, Mr. Prasthofer
R-P&VE-E, Mr. Brammeier
R-P&VE-S, Mr. Kroll
R-P&VE-S, Mr. Hunt
R-P&VE-S, Mr. Sterett
R-P&VE-SE, Mr. Sawyer
R-P&VE-SE, Mr. Flora
R-P&VE-SE, Mr. Watson
R-P&VE-SE, Mr. Slayden
R-P&VE-SE, Mr. Crow
R-P&VE-SD, Mr. Showers
R-P&VE-SD, Mr. Bullock
R-P&VE-ST, Mr. Farrow
R-P&VE-ST, Mr. Jewell
R-P&VE-SS, Mr. Fredericks

Test Laboratory

R-TEST-DIR, Mr. Heimburg
R-TEST-C, Mr. Grafton
R-TEST-CT, Mr. Perry
R-TEST-CT, Mr. Stone
R-TEST-M, Dr. Seiber
R-TEST-T, Mr. Driscoll
R-TEST-T, Mr. Kramer
R-TEST-D, Mr. Marsalis

R-SA, Mr. Barraza
R-SA, Mr. Germany
R-SA, Mr. Massey

DISTRIBUTION (Cont'd)

AST-S, Dr. Lange

I-I/IB, Col James
I-I/IB, Mr. Reinartz
I-I/IB, Mr. Vreuls
I-I/IB, Mr. Fikes
I-I/IB-T, Mr. Bender
I-I/IB-T, Mr. Ondocsin
II-B, Mr. Cooper

MS-IP
MS-IPL (8)
MS-H

M-PAT

M-HME-P

I-RM-A, Mr. Stein

External

Mr. John Windham (5)
Building 1218
Langley Research Center, NASA
Langley Air Force Base, Va.

Scientific and Technical Information Facility (25)
Attn: NASA Representative , (S-AK/RKT)
P. O. Box 5700
Bethesda, Maryland